

THE UNIVERSITY of ADELAIDE

Exploring Microglial Ageing: Insights from Human Genomic Data, Pre-Clinical Animal Models, and the Future of *In Vitro* Modelling

Laura Carr

A thesis submitted in fulfillment for the degree of

DOCTOR OF PHILOSOPHY

In

The Discipline of Anatomy and Pathology

School of Biomedicine

The University of Adelaide

December 2024

Copyright © 2024 – Laura Carr

All rights reserved

Thesis Abstract

Neurodegenerative diseases (NDs), including Alzheimer's disease (AD) and Parkinson's disease (PD), have profound global impacts that are expected to increase due to population aging. Understanding how age-related changes in brain cells contribute to susceptibility to ND is critical, specifically changes within the CNS immune system. Microglia, the resident immune cells of the brain, play a central role in initiating inflammatory responses and have been linked to ND pathology. Whilst microglia have diverse roles in development and neuroinflammation, the current understanding of microglial ageing is incomplete, and methods for assessing microglia remain inconsistent. Critically, research models of ND fail to consider age, potentially contributing to the poor translational ability of results.

The current thesis addresses these gaps in our understanding of aged microglia and the importance of considering age in ND research. Chapter 1 reviews existing literature on ageing models and the overall consideration of age in both *in vitro* and *in vivo* ND research and underscores the need to include age-appropriate models to recapitulate neurodegenerative environments in aged patients. Chapter 2 examines microglial ageing with specific reference to the 12 prescribed hallmarks of ageing, providing insight beyond inflammation into the cellular and molecular changes in microglia during ageing. Chapter 3 evaluates methods of microglial quantification in a human PD cohort and a rat TBI cohort. This chapter compares quantification performance of both the Halo automated microglia module and ImageJ automated analysis to manual analysis, demonstrating strong correlations between the methods in human post-mortem tissue, with Halo offering significant workflow efficiencies for microglial analysis over an automated ImageJ alternative. Chapter 4 presents a cross-species analysis of microglia across ageing in the lissencephalic rat brain compared to the gyrencephalic sheep brain. The animals utilised in this study reflect humans approximately around 45-50 years old, and thus, while not an exploration of aged microglia specifically, the findings of this study provide insight into subtle changes in microglia at a critical midlife period. Chapter 5 utilises a publicly available human gene expression database to analyse microglia-related gene expression across healthy aging, AD and traumatic brain injury (TBI). Findings suggest that TBI may exacerbate age-related changes in microglia, revealing a potential interaction between injury and ageing in microglia. Finally, Chapter 6 investigates phenotypic

changes in the BV2 microglial-like cell line, exploring the potential of immortalized cells to mimic the characteristics of aged microglia. This chapter explores a novel approach in modelling microglial aging in commonly used cell lines, offering an alternative avenue to animal models and primary cell culture models, where successfully obtaining an “aged” cohort may prove challenging.

Overall, this thesis expands our understanding of microglial ageing, emphasising the need for consistent methodologies and appropriate models in ND research. The insights into microglia across species has particular relevance for assessing the translation of research into humans and the exploration of potential *in vitro* models presents an efficient alternative for the study of molecular mechanisms in the aged brain. Ultimately, this work lays the foundation for future studies to explore the contribution of microglia in ageing and in NDs more broadly.

Thesis Declaration

I certify that this work contains no material which has been accepted for the award of any other degree or diploma in my name, in any university or other tertiary institution and, to the best of my knowledge and belief, contains no material previously published or written by another person, except where due reference has been made in the text. In addition, I certify that no part of this work will, in the future, be used in a submission in my name, for any other degree or diploma in any university or other tertiary institution without the prior approval of the University of Adelaide and where applicable, any partner institution responsible for the joint award of this degree.

I acknowledge that copyright of published works contained within this thesis resides with the copyright holder(s) of those works. I also give permission for the digital version of my thesis to be made available on the web, via the University's digital research repository, the Library Search and also through web search engines, unless permission has been granted by the University to restrict access for a period of time.

I acknowledge the support I have received for my research through the provision of an Australian Government Research Training Program Scholarship.

Laura May Carr

Acknowledgements

First and foremost, I would like to thank my supervisors Dr Andrew Care and Dr Ian Musgrave for their support and advice over the past three years. In particular, I'd like to thank my supervisor Dr Sanam Mustafa whose advice, both professional and personal, has been invaluable in helping me stay focused and calm throughout my degree but also making sure I remembered to enjoy the other things happening in my life. I am also deeply grateful for her hard work in the weeks leading up to my thesis submission to get me over the line.

I would also like to thank the University of Adelaide for the opportunity to undertake this program and the Australian Government Research Training Program Scholarship for funding my studies. I am particularly grateful for the funding which supported my research, the National Foundation for Medical Research and Innovation, Adelade Enterprise at the University of Adelaide: Commercial Acceleration Scheme and the NeuroSurgical Research Foundation. I would also like to give a special thank you to the School of Biomedicine Travel Award Grants for funding me to attend conferences and broaden my academic horizons.

I've had the privilege to meet some amazing people at the university, I think every person in the Translational Neuropathology Laboratory and Cognition Ageing and Neurodegenerative Disease Laboratory has supported me in completing this thesis, whether that be personally or at the lab bench. In particular, I'd like to thank Josh Woenig for all the support and advice you have given me and for putting up with my non-stop questions, and Shannon, Bella and Justin who I'm sure never want to see me knock on their door for help ever again.

I would like to especially thank the people who had to sit next to me every day. Olivia, my cell culture buddy, thank you for your help with my experiments but mostly for listening to my nonsense and for bringing me back down to earth when I was being unreasonable. Ben, you are genuinely the kindest person I've ever met, seeing you come into the office made my day one million times beer, I mean better. Thank you so much for always being there for me to bounce ideas off of and for giving me the emotional support I needed to get through the day, I don't know what I would have done without you.

Angus, I don't know where to start. From understanding every single one of my jokes, helping me with stats, with writing and just emotional support when I'm hysterical on a random Wednesday morning. I don't know how you had time to do your own work in between doing all of mine. You have all made the last three years bearable and have genuinely become my closest friends, I couldn't have picked a better group of people to go on this journey with.

Most of all I would like to thank my principal supervisor Associate Professor Lyndsey Collins-Praino. You've always been so patient and understanding with me and made me feel like it was all going to be fine. I am forever grateful for you taking me on in honours and giving me the opportunity to do this PhD, which was a journey for the both of us. Thank you for helping me to find an area I was passionate about and supporting me in following that pathway for the future.

To my best friends Amy and Tess. Amy, you almost managed to sneak into the thesis author list as well. One day soon well get there, that Green and Carr paper is on the horizon I know it. Thank you both for listening to all my issues over the past 3 years, whether it be about netball, my wedding, my experiments or just someone who upset me that day. I miss you both so so much.

To my husband Stefan you have been amazing, I'm so glad I married someone who can explain coding to me like I'm 5 years old without getting angry. Thank you for picking up the slack when it came to wedding planning and working on the house, and especially for being unbelievably patient with me at the end of every day. I'm not an easy person to live with but somehow, you've managed. I'm so excited to start the next chapter in my life with you.

Finally, I would like to thank my parents for giving me the opportunities that allowed me to achieve anything I wanted. Mum, words cannot describe how grateful I am for you and for your support. I genuinely could not have done half the work in this thesis without your help. I hope I have made you both proud.

Contributions made by co-authors

The following people have contributed to authorship of the manuscripts enclosed in this thesis (in alphabetical order): Isabella Bilecki, Andrew Care, Lyndsey Collins-Praino, Frances Corrigan, Bianca Guglietti, Aline Kunnel, Ian Musgrave, Claire Rennie, Sanam Mustafa, Shannon Stuckey, Reneé Turner, Ing Chee Wee

Conceptualisation of the work: LC, LCP, with advice from SM

Realisation of the work: LC, LCP, with experimental assistance from, AC, IW, CR, AK and advice from IB, RT, SS, IM and SM

Documentation of the work: LC, LCP, SM, IW, IB, AC

Editing and review of the work: LC, LCP, FC, AC, BG, IM, CR, AK, IB, SM, SS, RT

Publications and presentations arising from this thesis

Publications

Carr, L., Mustafa, S., Care, A., Collins-Praino, L.E. 2024. More than a number: Incorporating the aged phenotype to improve *in vitro* and *in vivo* modelling of neurodegenerative disease. *Brain, Behaviour, & Immunity.* 119, 554-571. DOI: 10.1016/j.bbi.2024.04.023

Conference presentations

1. **Carr, L.**, Guglietti, B., Mustafa, S., Corrigan, F., Collins-Praino, L.E., 'Optimisation of the HALO system for assessing microglial activation state in a Parkinson's cohort' Poster presentation at the Florey Postgraduate research conference, Adelaide, September 2021
2. **Carr, L.**, Mustafa, S., Musgrave, I., Care, A., Collins-Praino, L.E., 'The Potential of Immortalised Cell Lines as *in vitro* Tools for Aging and Neurodegenerative Disease Research' Poster presentation at the Florey Postgraduate Research conference, Adelaide, September 2022
3. **Carr, L.**, Mustafa, S., Musgrave, I., Care, A., Collins-Praino, L.E., 'The Potential of Immortalised Cell Lines as *in vitro* Tools for Aging and Neurodegenerative Disease Research' Poster presentation at the Australasian Neuroscience Society Annual Scientific Meeting, Melbourne, December 2022
4. **Carr, L.**, Mustafa, S., Musgrave, I., Care, A., Collins-Praino, L.E., 'The Potential of Immortalised Cell Lines as *in vitro* Tools for Aging and Neurodegenerative Disease Research' Poster presentation at the Cellular and Molecular Advances in Neurodegeneration conference, Brisbane, December 2023
5. **Carr, L.**, Mustafa, S., Musgrave, I., Care, A., Bilecki, I., Turner, R., Collins-Praino, L.E., 'Understanding Aged Microglia and their Role in Neurodegeneration' Poster presentation at the Australasian Neuroscience Society Annual Scientific Meeting, Brisbane, December 2023
6. **Carr, L.**, Guglietti, B., Wee, I., Mustafa, S., Collins-Praino, L.E., 'The Halo System as a Reliable Tool for Assessing Microglial Activation State' Poster presentation at the Light Microscopy Australia National Meeting, Melbourne, March 2024

7. **Carr, L.**, Mustafa, S., Musgrave, I., Care, A., Stuckey, S., Bilecki, I., Turner, R., Collins-Praino, L.E., 'Characterisation of phenotypic changes in aged microglia in the rodent and ovine brain' Oral presentation at the Australasian Winter Brain Conference, Queenstown September 2024.

Thesis explanation

Chapters 1 and 2 are introductory chapters detailing the background of this thesis. Chapter 1 is a published review paper (Carr et al., 2024) introducing how age is currently incorporated into models of neurodegenerative disease and highlighting paths by which this can be improved for future studies. Chapter 2 builds on this review and introduces microglial ageing and how these cells express key hallmarks of ageing, highlighting the need to understand how these cells change with age beyond the inflammatory response.

Chapter 3 assesses the consistency of two currently available automated methods of microglial analysis across human and rodent brain tissue compared to manual cell analysis. Chapter 4 explores how microglial ageing manifests in lissencephalic (rat) versus gyrencephalic (sheep) brains by conducting a detailed single cell approach to assess microglial morphology in cortical and subcortical regions. Chapter 5 explores how microglia change with age, during Alzheimer's Disease, and following Traumatic Brain Injury using publicly available RNA-Seq data from human post-mortem tissue. Chapter 6 details the development of an *in vitro* model to replicate microglial ageing in an immortalised cell line using a range of markers of cellular senescence. Finally, Chapter 7 presents a discussion of the work presented in this thesis.

All chapters presented in this thesis are prepared in publication format and preceded by a signed statement of authorship and experimental chapters are prefaced by a contextual statement to provide the reader with the context of the chapter.

List of Figures

Figure 1.1 Biological ageing 7
Figure 1.2 Pipeline for the incorporation of age into ND research models. 32
Figure 2.1: Microglial roles and morphologies during different stages of life. 60
Figure 2.2: Microglial classifications and accompanying morphology, functions and markers. 64
Figure 2.3:Pathways of microglial activation. a) PRR pathways of activation in microglia 71
Figure 2.4: Features of adult (left) and aged (right) microglia. 98
Figure 3.1 Representative images of IBA1 staining from each brain region in each dataset. 129
Figure 3.2 Examples of IBA1 stained microglia in human SN tissue identified by various methods. 130
Figure 3.3 Microglial counts in human tissue. 132
Figure 3.4 Correlation of microglial counts with Halo in human tissue. 134
Figure 3.5 Microglial counts in rat tissue. 137
Figure 3.6 Correlation of microglial counts with Halo in rat tissue. 139
Figure 4.1: Representative images of immunofluorescent staining in the aged rat and sheep cortex. 174
Figure 4.2 Microglial morphological analysis using ImageJ 176
Figure 4.3: Microglia counts in the rat brain. 180
Figure 4.4: Microglia counts in the sheep brain. 181
Figure 4.5: Visual representation of human ageing compared to the pre-clinical animal models used in the current study. 198
Figure 5.1: PLS-DA plot of samples in control and experimental groups. 241
Figure 5.2: Gene expression of microglial markers in the human brain. 245
Figure 5.3: Gene expression of microglial signalling genes in the human brain. 247
Figure 5.4: Expression of Klotho and Klotho-β in the human brain during ageing, AD and TBI. 249
Figure 6.1: Growth rate and metabolic activity of BV2 cells. 300
Figure 6.2: Inflammatory profile of BV2 cells. 302
Figure 6.3: Caspase-1 in BV2 cells analysed by Western blot. 303
Figure 6.4: K48 linked ubiquitination in BV2 cells analysed by Western blot. 304
Figure 6.5: Phagocytic activity of BV2 cells analysed by Vybrant Phagocytosis assay 305
Figure 6.6: Representative images of young and old BV2 cells at 4 hours following treatments. 307
Figure 6.7: Morphological analysis conducted at 20x magnification of BV2 cells 4-, 24-, and 48-hours following treatments. 308
Figure 6.8: Morphological analysis conducted at 40x magnification for adequate visualisation of BV2 processes 4-, 24-, and 48-hours following treatments 309
Figure 6.9: Image analysis conducted at 20x magnification of BV2 cells 4-, 24-, and 48-hours following treatments. 312
Figure 7.1: Examples of microglia provided by studies highlighting differences in description and visual examples provided by authors. 352
Figure 7.2: Considerations and future directions for microglial analysis. 370

List of Suplementary Figures

Supplementary Figure S 3.1 Examples of criteria for exclusion of images. 157
Supplementary Figure S 3.2 Accurate and inaccurate classification of microglia on Halo in rat tissue. 158
Supplementary Figure S 3.3 Correlation of microglial counts on ImageJ to manual counts in human tissue. 159
Supplementary Figure S 3.4 Correlation of microglial counts on ImageJ to manual counts in rat tissue. 160
Supplementary Figure S 4.1.3 Individual channels for representative images in Fig 4.3a. 217
Supplementary Figure S4.1.4 Individual channels for representative images in Fig 4.3a 218

Supplementary Figure S 4.1.5 Individual channels for representative images in Fig 4.3a. 219
Supplementary Figure S 4.1.6 Individual channels for representative images in Fig 4.3a. 220
Supplementary Figure S 4.1.7 Individual channels for representative images in Fig 4.3a. 221
Supplementary Figure S 4.1.8 Individual channels for representative images in Fig 4.3a. 222
Supplementary Figure S 4.1.9 Individual channels for representative images in Fig 4.3a. 223
Supplementary Figure S 4.1.10 Microglia in the sheep brain, grouped by age and sex. 224
Supplementary Figure S 6.1 Western blot replicates of K48-linked ubiquitination. 336
Supplementary Figure S 6.2 Western blot replicates of Caspase-1. 337
Supplementary Figure S 6.3 Representative images of immunofluorescent staining in BV2 cells after 24-hour incubation with treatments. 338
Supplementary Figure S 6.4 Representative images of immunofluorescent staining in BV2 cellsafter 48-hour incubation with treatments. 339
Supplementary Figure S 6.5 Photographs of MDA assay plates demonstrating intensity of colour change relative to standards. 340

List of Tables

Table 1.1: Strengths and weaknesses of *in vitro* methods to model CNS ageing 10
Table 1.2: Strengths and weaknesses of *in vivo* methods to model CNS ageing 20
Table 1.3: Summary of recommendations for improving the modelling of age both *in vitro* and *in vivo*. 37
Table 2.1: Definitions of the 12 hallmarks of ageing and their presentation during NDs 54
Table 2.2: Evidence of the hallmarks of ageing in microglia 91
Table 3.1: Study cohorts for human and rat datasets 124
Table 3.2: Antibody concentrations used in each dataset 126
Table 3.3: ImageJ Automated Microglial Analysis Parameter Summary 127
Table 3.4: HALO Microglial Detection Parameter Summary 128
Table 3.5: Summary of correlation analysis. 141
Table 4.1: Details of ethics approval and cohort details for murine and ovine datasets. 170
Table 4.2: Regions of interest in each dataset. 172
Table 4.3: Antibody concentrations used in each dataset 172
Table 4.4: Linear mixed effects modelling of microglial morphological analyses in rat brain tissue. 183
Table 4.5: Linear mixed effects models of Sholl analysis in rat brain tissue. 184
Table 4.6:Linear mixed effects modelling of microglial morphological analyses in sheep brain tissue. 188
Table 4.7: Linear mixed effects models of sholl analysis in sheep brain tissue. 190
Table 4.8: Changes observed in microglia in the current study. 193
Table 5.1: Regions of interest and sub structures included in analysis 236
Table 5.2: Demographic information for control and experimental groups 237
Table 5.3: GOI, Entrez ID and gene probe IDs used in the HBA and ADTS. 238
Table 5.4: Significant results from multiple comparison tests 242
Table 5.5: Summary of changes seen in GOI across ageing, AD and TBI. 250
Table 6.1: Antibodies and concentrations used for Western blots. 295
Table 6.2: Optimised signals for each of the fluorescent dyes used in imaging experiments 297
Table 6.3: Results of Tukey post-hoc tests following three-way ANOVA of TNF data 301
Table 6.4: Statistical results from Tukey post-hoc tests following three-way ANOVA of nucleus:cell ratio data. 306
Table 6.5: Summary of changes in high passage BV2 cells compared to low passage BV2 cells in each marker assessed in the current study 313

Table 7.1: Features, advantages and disadvantages of popular methods of *in vivo* microglia analysis. 347

List of Supplementary Tables

Supplementary Table S3.1 Clinicopathological data for human control and PD cases. 152
Supplementary Table S3.2 Summary of areas included in manual analysis and results per box for human tissue dataset. 153
Supplementary Table S3.3 Summary of areas included in manual analysis and results per image for rat tissue dataset. 153
Supplementary Table S4.1.1: Results from tukey post hoc testing conducted on sheep microglia data stratified into male and female groups. 225
Supplementary Table S4.1.2: Area analysed in microglial analysis in rat tissue. 226
Supplementary Table S4.1.3: Area analysed in microglial analysis in sheep tissue. 226
Supplementary Table S 5.0.1 All statistical results from linear regression models in the TCx. 273
Supplementary Table S 5.0.2 All statistical results from linear regression models in the PCx. 276
Supplementary Table S 5.0.3 All statistical results from linear regression models in the HIP 279
Supplementary Table S 6.1 Significant main effects and two-way interaction effects seen for each marker. 334

Financial Support

My doctoral studies were supported by funding from the Government of Australia (Research Training Scholarship).

Research carried out throughout the course of this thesis was supported by funding from the following funding bodies:

Chapter 1: National Foundation for Medical Research and Innovation (NFMRI)

Chapter 3: Adelade Enterprise at the University of Adelaide: Commercial Acceleration Scheme and the NeuroSurgical Research Foundation (NRF)

Chapter 4: NRF and Perpetual

Chapter 6: National Foundation for Medical Research and Innovation (NFMRI)

Statement of Authorship

Title of Paper	More than a number: Incorporating the aged phenotype to improve *in vitro* and *in vivo* modelling of neurodegenerative disease
Publication Status	☑ Published ☐ Accepted for Publication ☐ Submitted for Publication ☐ Unpublished and Unsubmitted w ork w ritten in manuscript style
Publication Details	Brain Behaviour and Immunity, 2024; 119

Principal Author

Name of Principal Author (Candidate)	Laura May Carr		
Contribution to the Paper	First author and main contributor. Concept, writer and formulation of manuscript. Reviewed prepared final draft following inputs from co-authors.		
Overall percentage (%)	70%		
Certification:	This paper is a narrative review I wrote during the period of my Higher Degree by Research candidature and is not subject to any obligations or contractual agreements with a third party that would constrain its inclusion in this thesis. I am the primary author of this paper.		
Signature		Date	30/11/2024

Co-Author Contributions

By signing the Statement of Authorship, each author certifies that:

i. the candidate's stated contribution to the publication is accurate (as detailed above);
ii. permission is granted for the candidate in include the publication in the thesis; and
iii. the sum of all co-author contributions is equal to 100% less the candidate's stated contribution.

Name of Co-Author	Sanam Mustafa		
Contribution to the Paper	Conceptualised, reviewed and drafted manuscript		
Signature		Date	01/12/24

Name of Co-Author	Andrew Care		
Contribution to the Paper	Reviewed and drafted manuscript		
Signature		Date	02-Dec-2024

Name of Co-Author	Lyndsey E. Collins-Praino		
Contribution to the Paper	Conceptualisation, reviewed and edited manuscript		
Signature		Date	2/12/24

Please cut and paste additional co-author panels here as required.

Chapter 1 : More Than a Number: Incorporating the Aged Phenotype to Improve *In Vitro* and *In Vivo* Modelling of Neurodegenerative Disease

***Laura M. Carr*[1], *Sanam Mustafa*[1,2,3], *Andrew Care*[4], *Lyndsey E. Collins-Praino*,[1,2]**

[1]School of Biomedicine, University of Adelaide, Adelaide, SA, Australia
[2]Australian Research Council Centre of Excellence for Nanoscale Biophotonics, The University of Adelaide, Adelaide, SA, Australia
[3]Davies Livestock Research Centre, The University of Adelaide, Roseworthy, SA, Australia
[4]School of Life Sciences, University of Technology Sydney, Sydney, NSW, Australia

1.1 Abstract

Age is the number one risk factor for developing a neurodegenerative disease (ND), such as Alzheimer's disease (AD) or Parkinson's disease (PD). With our rapidly ageing world population, there will be an increased burden of ND and need for disease-modifying treatments. Currently, however, translation of research from bench to bedside in NDs is poor. This may be due, at least in part, to the failure to account for the potential effect of ageing in preclinical modelling of NDs. While ageing can impact upon physiological response in multiple ways, only a limited number of preclinical studies of ND have incorporated ageing as a factor of interest. Here, we evaluate the aged phenotype and highlight the critical, but unmet, need to incorporate aspects of this phenotype into both the *in vitro* and *in vivo* models used in ND research. Given technological advances in the field over the past several years, we discuss how these could be harnessed to create novel models of ND that more readily incorporate aspects of the aged phenotype. This includes a recently described *in vitro* panel of ageing markers, which could help lead to more standardised models and improve reproducibility across studies. Importantly, we cannot assume that young cells or animals yield the same responses as seen in the context of ageing; thus, an improved understanding of the biology of ageing, and how to appropriately incorporate this into the modelling of ND, will ensure the best chance for successful translation of new therapies to the aged patient.

Keywords: Central nervous system ageing, *in vitro* models, mouse models, senescence, neurodegenerative disease, Parkinson's Disease, Alzheimer's Disease, ageing neuron

1.2 Introduction

1.2.1 Global ageing: Implications for neurodegenerative disease

Substantial scientific advancements have resulted in longer life expectancies. Global average life expectancy in 2019 was 9.8% higher than in 2000 and further increases are predicted, resulting in a significant aged population (Cao and Ho, 2020). For example, in Sweden, more than 50% of the 50,000 babies born in 2007 are expected to become centenarians, compared to ~750 people who turned 100 in 2007 (Vaupel, 2010). Concerningly, however, *healthy* average life expectancy (HALE) has not maintained this pace. In 2019, global HALE was 63.7, compared to the overall life expectancy of 73.4 years (Cao and Ho, 2020). This means that, while individuals may be living longer, they are not necessarily maintaining their health for this full period, resulting in increased prevalence of age-related diseases and demand for healthcare services (Chang et al., 2019). Particularly, incidence of neurodegenerative diseases (NDs), including Alzheimer's disease (AD) and Parkinson's disease (PD), which are highly prevalent in the >65 population, has increased dramatically (Hou et al., 2019).

This is significant, as these age-related NDs have long-term cumulative societal and economic impacts (Arafah et al., 2023). Analysis of the global burden of disease study 2019 revealed AD was responsible for 25.3 million disability adjusted life years (DALYs) and PD 6.2 million in 2019 (Ding et al., 2022). This represents a 161% and 128% increase in DALYs caused by AD and PD, respectively, since 1990 (Ding et al., 2022). Additionally, AD has an annual treatment cost of $305 billion USD (Wong, 2020) and PD around $52 billion (Yang et al., 2020a), with costs set to rise with the number of diagnoses. Current management focuses solely on symptomatic relief, as disease-modifying therapeutics are lacking (Kalia and Lang, 2015; Yiannopoulou and Papageorgiou, 2020). While symptomatic relief is critical for improving patient's daily lives, this does not address the underlying brain mechanisms of the disease, ultimately resulting in increased healthcare burden as the disease continues to progress and comorbidities arise (Arafah et al., 2023).

To develop disease-modifying treatments for NDs, there needs to be a better understanding not only of disease-specific pathophysiology, but also, the shared contribution of ageing across NDs (Mayne et al., 2020). Age is the primary risk for developing NDs (Hou et al., 2019), and it is well documented that

age-related cellular changes can impact physiological function and exacerbate disease pathology (González-Gualda et al., 2021). Despite this, while there are exceptions (DiMarco et al., 2023; Muñoz-Manchado et al., 2016), many preclinical ND studies are still conducted in young animals and *in vitro* studies are rarely carried out on the background of ageing. While this may be appropriate for certain study designs, for example where the focus is specifically on finding potential prophylactic therapeutic options for NDs (Yang et al., 2020b), this is nevertheless a considerable shortcoming for many investigations in the field. Assuming responses in young cohorts are reflective of older populations is inaccurate (Sun et al., 2020) and has the potential to impact translation of findings from preclinical therapeutic investigations to aged patients. With this in mind, here we first introduce the aged phenotype in mammals and then discuss how aspects of this phenotype may be better incorporated into both *in vitro* and *in vivo* modelling of NDs.

1.2.2 The aged phenotype

As ageing characterised by decline in function and is often described as a pathophysiological process, there is debate as to whether healthy ageing truly exists (Faragher, 2015). For this review, healthy ageing refers to the biological changes that occur in an organism later in life, after the growth and development period has ended and advanced adulthood has begun, and which are not associated with a diagnosed condition. There are a number of visible features commonly associated with natural ageing (Fig. 1.1A) which define an individual as aged. These include hair greying, skin changes (Halliwell and Dittmar, 2003) and musculoskeletal changes, including muscle wasting, joint immobility and decreased bone density (Azzolino et al., 2021). Functionally, ageing corresponds to changes in multiple systems, including digestive (Bhutto and Morley, 2008), reproductive (Kaufman et al., 2019; Shirasuna and Iwata, 2017), circulatory (Strait and Lakatta, 2012) and immunity (Wang et al., 2022), with the latter two contributing to increased vulnerability to infections and diseases (Strait and Lakatta, 2012). Cognitive function is also affected with natural ageing, with declines seen in several domains, including memory, processing speed and reasoning ability, although these changes are not as pronounced as mild cognitive impairment or AD (Moreira et al., 2019). Conversely, other aspects of cognition, such as vocabulary, are resistant to the effects of ageing and even increase until individuals are 60^{+} years old

(Hartshorne and Germine, 2015). Given the multiple systems impacted, ageing is clearly multifactorial, reflected by several theories being put forward to explain mechanisms of ageing (reviewed: (da Costa et al., 2016)). This has led to the formulation of 12 hallmarks of ageing by López-Otín and colleagues (López-Otín et al., 2023): genomic instability, telomere shortening, epigenetic alterations, loss of proteostasis, disabled macroautophagy, dysregulated nutrient sensing, mitochondrial dysfunction, cellular senescence, stem cell exhaustion, alterations in intracellular communication, chronic inflammation and dysbiosis. While an in-depth consideration of all of these hallmarks is outside the scope of the current work, below we discuss markers of ageing in the context of a senescent phenotype specifically those relevant to brain ageing. We direct the reader to López-Otín and colleagues excellent review on the topic (López-Otín et al., 2023) for further reading on the additional markers not discussed here. The markers discussed in aged cellular phenotype below are critical to take into account for age-related neurodegenerative diseases.

Central to ageing mechanisms are the defining features of a senescent cell, (Fig. 1.1B) with cellular senescence named as one of the hallmarks of ageing (López-Otín et al., 2023). Senescent cells are often physically distinguishable, with enlarged and flattened morphology compared to young cells (González-Gualda et al., 2021). A characteristic feature of cellular senescence is cell cycle arrest, with loss of proliferative capacity. Cellular senescence is commonly assessed by evaluating levels of cell cycle regulators, including P16 and P21, kinases which play crucial roles in the transition from G1 to S phase of the cell cycle and are upregulated in G1-phase cell cycle arrest (Serrano et al., 1997). DNA damage, measured by DNA double strand breaks (DSBs), and telomere shortening (Fig 1.1B (1-2)) are considered major drivers of cell cycle arrest and consequent senescent phenotype (Fumagalli et al., 2012), and accordingly were listed as two of the 12 hallmarks of ageing (López-Otín et al., 2023). Normally, the DNA damage response (DDR) counteracts DNA damage by either repairing damage or initiating apoptosis if the damage is beyond repair (reviewed: (Chatterjee and Walker, 2017). However, with ageing, rate of DNA damage overwhelms the capacity of the DDR, resulting in accumulated damage in both mitochondrial (mtDNA) and nuclear DNA, with subsequent altered gene expression, impaired cellular function and senescence (Victorelli et al., 2023).

Increased lysosome activity (Fig 1.1B (3)), measured by senescence-associated-beta-galactosidase (SA-β-gal) staining, is one of the most common markers of a senescent cell (López-Otín et al., 2023). While SA-β-gal increases have been shown in ageing cells, including mammalian neurons (Jurk et al., 2012) and fibroblasts (Yang and Hu, 2005), the presence of SA-β-gal is not exclusive to, or required for, senescence (de Mera-Rodríguez et al., 2021). In fact, SA-β-gal has been found to be upregulated in PD CSF (van Dijk et al., 2013) and AD plasma samples (Magini et al., 2015) compared to aged controls, indicating the presence of ND-related lysosomal dysfunction beyond ageing alone (van Dijk et al., 2013). A decrease in proteasome activity with age (Fig 1.1B (4)) is also widely reported (Ferrington et al., 2005; Kelmer Sacramento et al., 2020; Ponnappan et al., 1999), with dysfunctional proteostasis, identified as one of the 12 hallmarks of ageing (López-Otín et al., 2023), acting as a potential contributor to pathological protein accumulation in NDs (Kelmer Sacramento et al., 2020). Similarly, mitochondrial dysfunction is a major contributor to the senescent phenotype (Fig 1.1B (5)), leading to an altered metabolic phenotype (López-Otín et al., 2023). Damaged or dysfunctional mitochondria are a hallmark of ageing (López-Otín et al., 2023) and are major contributors to increased reactive oxygen species (ROS) production (Fig 1.1B (6)), which has been linked to both senescence (Nelson et al., 2018) and NDs (Gao et al., 2020). Increased ROS contributes to mitochondrial stress and damage, thereby exacerbating the senescent phenotype (Chakrabarti et al., 2011).

Inflamm-aging was a term first devised by Franceschi et al in 2000 to describe the concurrent decline in immune function and development of a chronic pro-inflammatory state with increasing age, in the absence of any external immune stimulation (Franceschi et al., 2000) and has since become a prominent theory of ageing (Xia et al., 2016). Fittingly, chronic inflammation is described as a hallmark of ageing (López-Otín et al., 2023) and is thought to be driven by the development of the senescence associated secretory phenotype (SASP) (Olivieri et al., 2018) (Fig 1.1B (8)), which is a key element of senescence discussed by López-Otín and colleagues (López-Otín et al., 2023). The SASP was observed to occur in multiple cell lines and *in vivo* in 2008 as a response to DNA damage (Coppé et al., 2008). This phenotype features high ongoing production of pro-inflammatory cytokines, such as interleukins (IL-6, IL-8, IL-1β) and Tumour Necrosis Factor (TNF, formerly known as TNF-α (Grimstad, 2016)), which

contribute to further immune activation (Coppé et al., 2008). In the brain, microglia are thought to be responsible for the emergence of this damaging inflammation in NDs and the SASP (Hu et al., 2021), with specific microglial pathways implicated in this process.

The shift toward an inflammatory phenotype in the brain is associated with changes in major signalling pathways involved in DNA-driven immune recognition responses (Gulen et al., 2023) (Fig 1.1C). For example, cyclic GMP-AMP synthase (cGAS) is a cytosolic DNA sensor, which, upon binding to DNA in the cytosol, initiates cyclic GMP-AMP (cGAMP) to bind with the stimulator of interferon genes (STING) located on the endoplasmic reticulum (Fig 1.1C (1)). This binding induces a signalling cascade leading to production of type-1 interferons and pro-inflammatory cytokines (Sun et al., 2013). During ageing, cGAS recognition of cytosolic DNA danger signals increases, potentially due to increased nuclear and mitochondrial damage, as outlined in Fig 1B (1-2 and 5)) (Gulen et al., 2023). The resulting increase in activation of this pathway is hypothesised to drive the ongoing low-grade inflammatory state seen in ageing (Gulen et al., 2023), a state which is also linked to neurodegenerative diseases (Guzman-Martinez et al., 2019) (Fig 1.1C (4)).

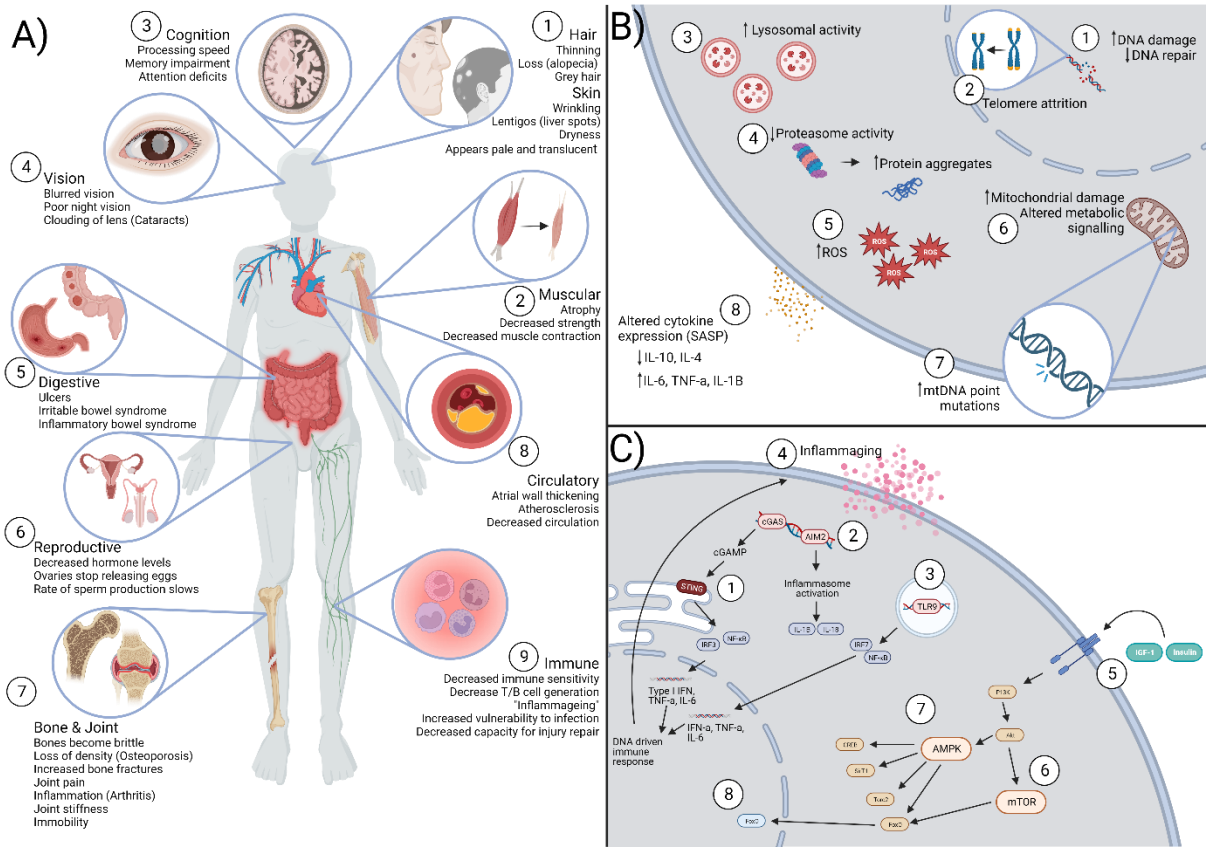


Figure 1.1 Biological ageing A) whole-body distinguishing features including changes in (1) hair and skin (2) muscle, (3) cognition, (4) vision, (5) digestion, (6) reproduction, (7) bones and joints, (8) circulation and (9) immunity. B) cells display aged/senescent features including (1) increased DNA damage and decreased DNA repair, (2) telomere shortening, (3) increased lysosomal presence and activity, (4) decreased proteasome activity causing an increase in intracellular protein aggregates, (5) increased production of reactive oxygen species (ROS), (6) mitochondrial damage, (7) increased mitochondrial DNA mutations and (8) the development of the senescence-associated secretory phenotype (SASP). C) functional changes to inflammation and metabolism driven by cell signalling changes with an increase in the DNA driven immune response influenced by the (1) cGAS-STING pathway, (2) AIM2 pathway and (3) the TLR9 pathway which all contribute to (4) increased inflammation termed 'inflammageing'. Metabolic signalling pathways are also altered with (5) altered insulin/IGF-1 binding and (6) mitochondrial damage both influencing changes in the (7) mTOR and (8) AMPK pathways. Both pathways can regulate transcription of factors important for cell cycle regulation, metabolism, and apoptosis such as (9) FoxO

Similarly, dysregulated intracellular metabolic processes are one of the hallmarks of ageing (López-Otín et al., 2023) and thus are critical in cellular and systems ageing. Key regulators of metabolism are insulin and insulin-like growth factor-1 (IGF-1), which both decline with age, as does binding to insulin/IGF-1 receptors (Fig 1.1C (5)) (Toth et al., 2022). Not only does decreased insulin/IGF-1 signalling impair cerebral blood flow and contribute to neuronal dysfunction (Toth et al., 2022), it also causes dysregulation in the mechanistic target of rapamycin (mTOR) and AMP-activated protein kinase (AMPK) metabolic pathways (Yang et al., 2018)(Fig. 1.1C (6-8)). The mTOR and AMPK pathways are major regulators of cell metabolism, mitochondrial function, cell growth and cell survival (Kazyken et al., 2019), and of the many signalling pathways involved in metabolism, these are the best described

and most closely linked to biological ageing (Morita et al., 2013). With age, there is a loss of sensitivity of the AMPK pathway, which normally has an inhibitory effect on mTOR signalling (Gwinn et al., 2008). This subsequently leads to an increase in mTOR signalling, which has been linked to the manifestation of age-related disorders (Bitto et al., 2016). Additionally, both AMPK and mTOR pathways induce transcription of genes related to mitochondrial function, in particular transcription of forkhead box class 0 (Fox0), a regulator of mitochondrial homeostasis (Davila et al., 2012). Dysregulation of these pathways with age may thus further exacerbate mitochondrial dysfunction. Interestingly, there is conflicting evidence regarding whether activation of the mTOR and AMPK pathways confers neuroprotective or damaging effects in ND (reviewed: (Querfurth and Lee, 2021)). Overall, however, it is evident that ND pathophysiology does not occur in isolation, but rather is concomitant with the complex and multifactorial physiological changes of ageing. It is thus imperative to consider these changes when modelling ND preclinically.

1.2.3 The aged phenotype may not only affect pathophysiology, but also directly influence drug response

Given that there is no single causative gene or pathway controlling ageing, but rather many changes contributing to the ageing process, results obtained in "young" models may not be translatable within an aged context. In fact, age-related differences in drug responses are widely recognised, with adverse drug reactions in elderly patients being twice as common compared to younger patients, particularly with drugs targeting the CNS (Beijer and de Blaey, 2002) .

Further, age-associated alterations have been reported for multiple (but not all) members of the cytochromes P450 family of drug-metabolising enzymes (CYPs) (reviewed: (Kinirons and O'Mahony, 2004)), suggesting that drug pharmacokinetics are altered in natural ageing. In line with this, a study that looked at the mRNA expression profile of 101 xenobiotic-processing genes in mice found that 44% of genes were altered with age in male mice and 64% changed with age in female mice (Zidong Donna et al., 2012). Interestingly, although it would be reasonable to hypothesise that these changes would be further exacerbated in NDs, to date, this has yet to be explored in the literature (Wu and Lin, 2019).

Although CYPs are abundantly expressed and studied in the liver, the primary site of drug metabolism, CYPs are also widely expressed in the brain, with some forms, such as CYP2D4 and CYP2D18, expressed exclusively, or at much higher levels, here than in other tissues (Kawashima and Strobel, 1995; Komori, 1993). Importantly, brain CYPs play a role in metabolising many drugs that act on the CNS (for review, see (Miksys and Tyndale, 2013)) and can alter response to CNS-acting drugs (Khokhar and Tyndale, 2011). This may have implications for the treatment of CNS disorders, including NDs. Intriguingly, there is great inter-individual variation in brain expression levels of CYP levels, and this can be affected by multiple factors, including age. For example, in humans, brain levels of the neuroprotective enzyme CYP2D6 gradually increase with age, reaching their highest levels in those aged 65+ (Mann et al., 2012). This gives further support to the idea that the response to centrally acting drugs may differ in younger versus older adults. This response may be further altered in those with NDs. In line with this, those with PD were shown to have ~40% lower levels of CYP2D6 within several brain regions, including the frontal cortex, cerebellum and hippocampus (although, interestingly, not in the substantia nigra or caudate), compared to age-matched controls (Mann et al., 2012).

These effects may be due, at least in part, to the increases in inflammation seen both with natural ageing (i.e. inflammageing) (Franceschi and Campisi, 2014) and in NDs (Guzman-Martinez et al., 2019). In support of this, pro-inflammatory factors are known to correspond to reduced activity of many drug metabolising enzymes (Aitken et al., 2008), including CYPs (reviewed: (de Jong et al., 2020)). A systematic review of 218 studies in adults by Lenoir et al. (2021) demonstrated that inflammation modulates the activity of multiple CYPs and thus alters drug pharmacokinetics, although the effect is dependent on the particular CYP isoform and source of inflammation considered (Lenoir et al., 2021). While the exact implications of this for understanding drug response in younger versus older individuals, as well as in individuals with a ND, remain to be explored, it nevertheless highlights that when testing potential therapeutics for NDs, either in *in vitro* or *in vivo* models, it is critical to account for the potential impact of age, in order to improve the translational relevance of the findings.

Table 1.1: Strengths and weaknesses of *in vitro* methods to model CNS ageing

Method of ageing	Model	Time to achieve phenotype	Aspects of the aged phenotype induced	Strengths	Weaknesses
Human donor derived cells	iPSC derived CNS cells	3wk-1mth	Astrocytes: Markers of mature astrocytes (GFAP, AQP4, ALDH1L1), presence of glutamate transporters, functional glutamate uptake (Voulgaris et al., 2022) Neurons: ↓yH2AX, ↓SA-B-gal, no impairment of nuclear organisation (Tang et al., 2017)	Reflective of primary cells from patients and of CNS origin Potential in regenerative therapy	Induction to pluripotency resets ageing Complex to establish Low production efficiency Single cells not complex model
	Induced neurons	4-6 wks	Impaired mitochondrial function, ↓oxidative phosphorylation (Kim et al., 2018) ↑yH2AX, ↑SA-B-gal, impaired nuclear organisation and compartmentalisation (Tang et al., 2017)	Reflective of primary cells from patients and of CNS origin Cells retain ageing and neurodegenerative pathology Preservation of epigenetic factors Potential in regenerative therapy	Limited time to be sustained in culture Complex to establish Low production efficiency Single cells not complex model
Replicative senescence	Primary cells (of peripheral or CNS origin)	40-60 population doublings	↑SA-B-gal (Boraldi et al., 2015; Caldeira et al., 2014; Deng et al., 2023; Kurz et al., 2000), ↑lysosomal mass (Kurz et al., 2000)	Ageing is not biased by manipulating a specific pathway	N/A for post-mitotic cells e.g., neurons.

		50-60 passages 10-20 days in culture	Activated morphology, ↑Matrix Metalloproteinase (MMP)-2, ↓NF-kB, ↓MMP-9, ↓TLR-2, ↓TLR-4, ↓autophagy, ↓migration and phagocytic capacity (Caldeira et al., 2014) Enlarged cells, vacuolated cytoplasm, aHDF: longer growth periods than nHDF (Boraldi et al., 2015) Enlarged nuclei, ↓proliferation, ↑P16/P21, ↑γH2AX, ↑uPAR, SASP (Deng et al., 2023)	Simple model to establish and maintain Insight into basic cell changes	Not practical for long term experiments. Variability in measurement of age Highly variable phenotype between cell populations Inconsistent markers assessed between studies makes it hard to compare results Not well understood in immortalised cell lines Single cells not complex model
Complex models	Co-culture primary neurons and glia	27 days	↑SA-B-gal, ↑γH2AX, ↑oxidative stress, ↑pro-inflammatory cytokine production (Bigagli et al., 2016)	Shows microRNA signature reflecting pathological ageing More complexity than single monolayer culture	difficult to establish successful co-cultures

			Resembles the brain environment	Complex to establish
Organoid models	45 days	SASP (↑IL-1β, TNF-a), ↑P16, P21 (Ao et al., 2022)	Demonstrates ageing phenotype without manipulating pathways	Stem cells have a young cellular phenotype inconsistent with ageing

1.3 Laboratory models of the aged phenotype

The mechanisms underpinning ageing are multifactorial and thus make modelling age-related NDs complex. In the following section, key laboratory models of ageing are described and critically examined for their applicability to NDs.

1.3.1 In vitro models of CNS ageing: Relevance for ND research

1.3.1.1 Cells derived from aged donors

In vitro studies are a critical tool in understanding how the aged brain functions at the cellular level. Primary cells from aged individuals are understandably regarded as one of the most accurate models, as they can capture the features of an aged cell and retain the genetic characteristics of the donor when harvested using specific techniques. However, for the human CNS, obtaining such cells directly can be difficult, relying on cultures produced from post-mortem brains or tissue removed during brain surgery. The advent of human induced pluripotent stem cells (iPSCs) in 2006 (Takahashi and Yamanaka, 2006) resolved some of these difficulties, allowing somatic cells to be induced to become pluripotent by expression of four reprogramming factors known as OKSM factors or Yamanaka factors (Takahashi and Yamanaka, 2006). These iPSCs can then be differentiated into CNS cells and used to model neurological disorders.

Using this method, both neurons (Miller et al., 2013) and glial cells (Abud et al., 2017; Voulgaris et al., 2022) derived from iPSCs have successfully been used as models of AD and PD (reviewed: (Pandey et al., 2022)). For example, utilising iPSCs derived from somatic cells of patients with familial PD, it is possible to generate dopaminergic neurons that express pathological PD mutations and show PD-like pathology in culture, including increased pathological α-synuclein aggregates (Kouroupi et al., 2017), neurite degeneration (Sánchez-Danés et al., 2012) and dysregulated dopamine pathways (Jiang et al., 2012). Cultures derived from iPSCs obtained from individuals with idiopathic PD also display PD-like impairment of neurite formation (Sánchez-Danés et al., 2012) and increased autophagy and mitophagy (Hsieh et al., 2016). Similarly, neurons derived from iPSCs of AD patients carrying the APP mutation display short fragments of amyloid-beta (Aβ) and increased Aβ42:40 ratios. Importantly, however, when using iPSCs to model ageing, studies have shown that the developmental reset induced by

treatment of the somatic cells with Yamanaka transcription factors erases senescent features in these cells (Kim et al., 2018; Tang et al., 2017). Table 1.1 summarises several studies where reset of the ageing phenotype has been demonstrated in iPSC-derived neurons and glia. Reset of telomeres, heterochromatin levels, mitochondrial health, nuclear organisation, and protein damage is widely thought to occur during induction to pluripotency (Miller et al., 2013) and has been reported across multiple studies on ageing iPSCs (Lapasset et al., 2011; Ocampo et al., 2016) (Prigione et al., 2011; Suhr et al., 2009). While iPSC technology has great potential for regenerative therapy in ND treatment (Limone et al., 2022), simply utilising iPSCs derived from older individuals may be insufficient to accurately replicate the aged phenotype of CNS cells.

Alternative to iPSCs, directly induced neurons (iNs) aim to achieve control over the phenotype of the induced cells. These are derived from somatic cells by lentiviral or microRNA-based expression of "BAM" factors and neurogenesis factors, such as NeuroD1 and Ngn2, similar to the expression of Yamanaka factors in the reprogramming iPSCs but bypassing the need to become pluripotent before differentiation (Vierbuchen et al., 2010). Promisingly, these cells display retention of age after differentiation, with epigenetic age of the original donor cell, measured by DNA methylation, displaying a high correlation with epigenetic age of the iN (Huh et al., 2016). Additionally, iNs derived from idiopathic PD patients maintain age-associated genetic signatures and α-syn pathology, which is not present in iPSC-neurons derived from these same patients (Drouin-Ouellet et al., 2022). Similarly, directly converted neural progenitor cells display ageing when further differentiated to astrocytes, with changes summarised in Table 1.1 (Gatto et al., 2021). Thus, skipping induction to pluripotency through direct conversion appears to avoid the senescence reset, allowing for a more robust model of ageing (Huh et al., 2016), as well as retention of sporadic neurodegenerative pathology (Drouin-Ouellet et al., 2022). While promising, protocols for direct cellular reprogramming into brain cells have been less extensively described than those for iPSCs. Additionally, there is a need for further validation regarding the neuronal phenotypes induced from differing cellular origin (Chouchane et al., 2017) and potential risks involved in using iNs for regenerative therapy (Kim et al., 2021).

Overall, it is important to note that the donor age does not consistently affect the lifespan of primary cells *in vitro* (Cristofalo et al., 1998; Kaji et al., 2009). This is exemplified from cultures generated from participants in the Baltimore Longitudinal Study of Ageing. This study compared the proliferative capacity of fibroblasts collected from young donors (20-29 years) versus old donors (65^{+}years) both cross-sectionally and longitudinally, with donor matched biopsies up to nine years apart (Smith et al., 2002). No difference in lifespan of fibroblasts was observed cross-sectionally, except when derived from female donors (Smith et al., 2002), where a reduced proliferative potential correlated with donor age. Comparison of cells from the same donor longitudinally demonstrated a trend to decrease in proliferative potential over time, but this was not statistically significant, potentially on account of considerable variation between cell lifespan from different donors (Smith et al., 2002). Conversely, a study comparing fibroblasts from donors aged 21-36 versus donors aged 63^{+} reported significant effect of donor age on the proliferative potential of cells in culture (Schneider and Mitsui, 1976), although large variability and overlapping data points between age groups was observed. These studies highlight that *in vivo* chronological age may not directly translate to reduced proliferative capacity and senescence *in vitro*, with variation between donors, combined with variations in cell isolation and culture protocols, leading to challenges in reproducibility (Qadan et al., 2018). While simply generating iPSCs or iNs from aged donor cells may not fully encapsulate an aged phenotype in the sense of proliferative capacity, the potential utility of these cells in ND research and therapy should not be understated. Further, other markers in addition to proliferation can be used to assess age and determine the age of a culture, as discussed in more detail below.

1.3.1.2 Replicative senescence

Other than utilising cells from aged donors, the most prominent method of inducing senescence *in vitro* is by culturing cells to a proliferative limit, termed replicative senescence, first proposed by Leonard Hayflick in 1965 (Hayflick, 1965). In these early studies, primary cells were cultured from human foetal tissue continually for up to 11mths or 55 passages. The "Hayflick limit" is widely accepted and is the basis for characterising serially cultured cells as a model of cellular ageing (Phipps et al., 2007). Passaging cells to this limit produces the characteristic cell cycle arrest and SASP seen in senescent cells, without researchers intentionally altering specific cellular pathways (Hayflick, 1965) and thus

may result in a more translationally relevant aged phenotype. In line with this, studies using peripheral cells (presented in table 1.1), including dermal fibroblasts and umbilical vein endothelial cells, display a senescent phenotype featuring the SASP (Deng et al., 2023), SA-β-gal (Boraldi et al., 2015; Caldeira et al., 2014; Kurz et al., 2000), increased cell cycle regulators (Deng et al., 2023), decreased proliferation (Boraldi et al., 2015) and increased markers of DNA damage (Deng et al., 2023), all key components of the aged phenotype (Fig1.1). When looking at CNS cells, similar results have been observed; however, the use of CNS cell types in studies of replicative senescence is sparce. Primary microglia have been shown to change from a reactive to a chronically active, age-like phenotype (Table 1.1) when kept in culture for a 16-day period (Caldeira et al., 2014). The lack of investigation of replicative senescence in neurons is due to the fact that they are post-mitotic, and thus do not replicate and cannot undergo replicative senescence (Hartmann et al., 2023), making this method less applicable for the modelling of NDs.

Replicative senescence as an *in vitro* model of ageing has been validated mostly in passaged primary cells, where replicative senescence occurs more readily than in immortalised cell lines. Recently, however, untransformed primary mouse T-cells have demonstrated the ability to continue to divide and remain functional in culture for 10 years, potentially challenging the idea of universal applicability of the Hayflick limit (Soerens et al., 2023). Additionally, a primary cell model of ageing is difficult to consistently reproduce due to variation between cell populations, presenting a challenge for widespread use and high throughput industry applications. Furthermore, there is limited capacity to conduct complex experiments or investigate long-term effects, due to the limited time primary cells can be sustained in culture (Hayflick, 1965). Alternatively, investigating passage number as a proxy for ageing in immortalised cell lines may offer the opportunity to study phenotypic or functional changes over time, rather than simply modelling cells at their proliferative end (Sapieha and Mallette, 2018). Although immortalised cells have been argued as unfit for a model of ageing due to their limitless proliferative capacity and resistance to replicative exhaustion (Bunc et al., 2019), it is a recommended laboratory practice to only culture cell lines for a limited passage range, beyond which the cells are assumed to have diverged from the original cell phenotype (Geraghty et al., 2014; Hughes et al., 2007).

Exactly what changes are induced in these cells with passage is not well characterised (Hughes et al., 2007), and, potentially, these changes may mirror some of the changes associated with the aged phenotype. Of particular relevance for NDs, it would be useful to characterise the phenotypic changes that occur in both immortalised glial cell lines (e.g. BV2 cells) and in neuronal-like cell lines (e.g., both differentiated and undifferentiated SH-SY5Y neuroblastoma cells, an *in vitro* model of PD (Xicoy et al., 2017)). If such immortalised cell lines do show alterations consistent with the aged phenotype with increased passage numbers, then this has significant implications for how these cells might be used to more appropriately model ND on an aged background *in vitro*.

1.3.1.3 Emerging methods and future directions

While single monolayer cultures provide a basic way to induce the senescence-related molecular changes associated with ageing, these models lack the complexity of co-culture and organoid brain models. This is particularly relevant for NDs, which are multifaceted, heterogenous diseases that involve interactions between multiple brain cell types (Luchena et al., 2022). In recent years, these alternative culture methods have been developed that provide an avenue to improve modelling of NDs. The use of co-culture models, which involve simultaneous expression of neuronal and glial cells, allows for examination of cellular interactions at the level of the tetrapartite synapse. Co-culture is being used to improve modelling of NDs and provide critical insights into cellular interactions in these diseases (see Table 1.1). For example, in a 2D triple co-culture model of murine astrocytes, microglia and neurons, exposure to oligomeric amyloid beta resulted in neuroinflammation and synaptic loss, providing a model that is more reflective of pathological processes associated with AD (Luchena et al., 2022). Similarly, using a co-culture model of LPS-stimulated macrophages and SH-SY5Y cells (model for dopaminergic neurons), reactive macrophages were shown to induce oxidative stress and consequent increased alpha-synuclein nitration and cell death in the SH-SY5Y cells (Shavali et al., 2006).

While allowing for complex interactions to be captured, it remains to be seen how the aged phenotype might be best incorporated into such co-cultures. One promising study by Bigagli and colleagues (2015) maintained primary neuronal/glial co-cultures up to 27 days *in vitro* and demonstrated that these cultures displayed multiple signs of cellular senescence, including increased levels of SA-β-gal, γ-

H2AX, oxidative stress and pro-inflammatory cytokines (Bigagli et al., 2016). Interestingly, however, analysis of 180 microRNAs showed a pattern of change more consistent with transgenic TgCRND8 mice (model of amyloid-β deposition) than with physiologically aged mice, suggesting that long-term maintenance of the co-culture model may more closely resemble the changes of pathological ageing than natural ageing. Nevertheless, this provides preliminary evidence that aspects of the aged phenotype can be incorporated in more complex co-culture models.

Similar to co-culture models, brain organoid models demonstrate potential to replicate the complexity of the aged brain. Organoid models are stem cell derived 3D tissue cultures comprised of multiple cell types aimed at recapitulating the complexity of whole systems, in a way that co-culture and single monolayer culture cannot (Shou et al., 2020). These models are generated by embedding embryoid bodies into extracellular matrix and inducing neural differentiation by supplementation with growth factors to support growth of specific brain structures (Shou et al., 2020). For NDs, these complex models have demonstrated utility in modelling ND pathology. Brain organoids have demonstrated pathological Aβ aggregation and Tau phosphorylation when derived from familial AD patients with cells overexpressing APP and PSEN1 (Choi et al., 2014; Raja et al., 2016). Similarly, organoids which have the LRRK2-G2019S mutations seen in familial PD display α-synuclein aggregation and altered neuronal morphology, as is seen in PD (Kim et al., 2019). Excitingly, organoids may also offer a way to incorporate an aged phenotype into models of ND. In support of this, a recent study by Ao and colleagues (2022) demonstrated that 45-day-old brain organoids show upregulation of key ageing markers, including cell cycle regulators and pro-inflammatory cytokines, in response to monocyte infiltration from aged patients compared to cultures infiltrated with young monocytes (Ao et al., 2022). Therefore, while embryonic stem cells, from which organoids are developed, naturally have a young cellular phenotype, with elongated telomeres not reflective of the senescent phenotype seen in the aged brain (Ao et al., 2022), long-term culture of organoids may produce a more translationally relevant model for studies of ND.

In addition to current model limitations, another major challenge in reproducing the aged phenotype *in vitro* is the inconsistency of markers used across studies, which can make it difficult to fully evaluate

models. This was recently addressed by Hartmann and colleagues (2023), who validated a biomarker-based panel to assess age *in vitro* in fibroblast cultures (Hartmann et al., 2023). This panel included many ageing markers discussed above, including DNA damage, telomere attrition, SA-β-gal, SASP, cell cycle arrest and morphological changes, as well as additional markers, such as histone modification and changes in nuclear lamina protein: Lamin B. Using these markers, an 'AgeScore' was derived, which correlated well with chronological donor age in both healthy individuals and donors with progeroid syndromes (diseases associated with accelerated ageing) (Hartmann et al., 2023). While not yet investigated, this AgeScore may also be translatable to CNS cells. However, neuronal populations are post-mitotic, meaning cell cycle arrest, the defining feature of replicative senescence, cannot define an aged neuron (Hartmann et al., 2023). Despite this, a recent study investigating senescence 1wk following repeated mild traumatic brain injury induced by closed skull controlled cortical impact in C57BL/6 mice identified 15 clusters of neurons in injured mice, all expressing at least one marker of senescence (Schwab et al., 2022). This study provides evidence that, while neurons are post-mitotic, they can still demonstrate traditional markers of a senescent phenotype following traumatic brain injury, hypothesised to accelerate brain ageing (Cole et al., 2015). Thus, a modified version of the "AgeScore" may have utility even in evaluating neuronal cultures and subsequent standardisation of modelling ageing *in vitro* between studies.

Overall, while there is a multitude of research on inducing and characterising age in cell culture models (reviewed: (González-Gualda et al., 2021)), there has been less implementation of these models in ND research. This may be due to the difficulties in replicating results from primary culture across laboratories and across studies (Hirsch and Schildknecht, 2019) or the complexity of modelling disease alongside brain ageing. While research using standard models has and will continue to make significant contributions to the ND research field, given the critical role of age in the risk of ND development, incorporating aspects of the aged phenotype *in vitro* has the potential to lead to more translationally relevant models of ND. This will enhance our understanding of the pathophysiological mechanisms that drive ND emergence and lend insight into the therapeutic effects of putative treatments.

Table 1.2: Strengths and weaknesses of *in vivo* methods to model CNS ageing

Method of ageing	Model	Age of phenotype presentation	Phenotype induced	Strengths	Weaknesses
Spontaneous accelerated ageing mice	SAMP8 (Takeda et al., 1981)	6-16mths	Shortened lifespan, hair loss, skin pigment changes, ↓light phase activity, cataract development, amyloidosis, lordokyphosis (spine curvature) (Takeda et al., 1981) ↓spine density in hippocampus, ↑axonal dystrophy in hippocampus, astrogliosis (Kawamata et al., 1998), Aβ aggregates, ↑Tau phosphorylation (Takeda, 2009), ↑microglia, dysfunctional mitochondria (Kawamata et al., 1998), DA neuron degeneration in SN, noradrenergic neuron degeneration in LC (Takeda et al., 1981) Decreased anxiety-like behaviour, disrupted sleep cycle (Miyamoto, 1997), impaired memory and learning (Takeda et al., 1981)	Ageing is not biased by manipulating a specific pathway. Mice widely available for purchase Compatible with other genetic models of disease	Longer time to achieve ageing (10 mths +) Cognitive and behavioural changes may confound results for NDs
	SAMP10 (Takeda et al., 1981)	6-16mths	Shortened lifespan, hair loss, skin pigment changes, ↓light phase activity, cataract development, amyloidosis, lordokyphosis (spine curvature) (Takeda et al., 1981) DNA damage (Shimada et al., 2002), cortical atrophy (Shimada et al., 1994), ↑microglial activation, ↑pro-inflammatory microglial signalling (Kumagai et al., 2007), ↑ubiquitinated inclusions (Shimada et al., 2008), ↓spine density and synapse density (Shimada et al., 2006) Depressive behaviour, emotional dysfunction (Miyamoto, 1997)		

	SAMP8-APP/PS1 (Lok et al., 2013)	6-9 mth (3mth earlier than SAMP8 control)	Aβ accumulation, neuronal loss, abnormal movement, anxiety, learning and memory deficits		
WRN protein deficiency	129/Sv/Black Swiss $WRN^{\Delta hel/\Delta hel}$ (Lebel and Leder, 1998)	4-6 mths old	Develop features of metabolic syndrome (↑blood insulin, cholesterol and triglyceride), ↑cardiac fibrosis, ↑ROS levels (Massip et al., 2006) ↓motor activity/coordination, ↓perception and memory, ↑ repetitive behaviour, ↑hyper ramified microglia, ↑ neuronal oxidative stress in PFC (Hui et al., 2018)	Wide range of ageing changes displayed including brain relevant changes.	Cognitive and behavioural changes may confound results for NDs.
	Mixed genetic background $Terc^{-/-}$ $WRN^{-/-}$ (Chang et al., 2004)	~7-mths old	Premature death, hair greying, alopecia, type-2 diabetes, osteoperosis, cataracts Cultured cells: ↑DNA damage markers, accelerated replicative senescence, ↑chromosomal instability		
LMNA mutation	C57BL/6 with HGS mutation: $LMNA^{G609G/G609G}$	3 wks	Growth retardation, ↑ cancer incidence, infertility, spine curvature	No neurological deficits to confound results	Variable timeframe for ageing to be induced (3wkss-16mths)
	Mice with HGS mutation: Tetop-LA^{G608G+}/Tetop-LA^{G608G-}	16 mths	Nuclear distortion, nuclear blebbing, nuclear invaginations No neurological deficits		
Terc deficiency	$Terc^{-/-}$ C57BL/6J	4-5 mths	Spatial learning and memory deficits, loss of neurons, loss of synaptic density, ↑CD11b+ microglia, ↑IBA1+ microglia, ↑microglial density Accelerated formation of a-synuclein aggregates in PD mice	Inflammatory ageing phenotype in the brain Compatible with other genetic ND models	Cognitive and behavioural changes may confound results for NDs
IL-10 deficiency	IL-$10^{-/-}$ C57BL/6J	10-15 mths	Alopecia, decreased muscle strength (Walston et al., 2008), ↑activation of pro-inflammatory pathways (IL-6, TNF-a, IL-1B) (Ko et al., 2012)	Brain relevant changes	Long time to achieve ageing

			↑Tau phosphorylation following neuroinflammatory stimulus (Weston et al., 2021)	Impacts ND pathology	
SIRT6 deficiency	$SIRT6^{-/-}$ C57BL/6J (Mostoslavsky et al., 2006)	4 wks	Genomic instability, development of altered glucose homeostasis, ↓body size, ↓B/T-cell generation Death at around 4 wks old	Brain specific KO does not significantly reduce lifespan and provides a short timeframe to achieve ageing	Overall KO causes significantly shortened lifespan. Cognitive and behavioural changes may confound results for NDs More reflective of an AD model than aged CNS model
	Brain specific $SIRT6^{-/-}$ C57BL/6J (Kaluski et al., 2017)	4 mths	Accumulated DNA damage, ↑hyperphosphorylated Tau, ↑locomotor activity, ↓non-associative learning		
Induced changes to the epigenome (ICE)	Targeted expression of an endonuclease I-Ppol (Yang et al., 2023)	10mths	↑muscle loss, alopecia, loss of skin pigment, ↑frailty, ↑glial activation in hippocampus	Visibly aged mice Can have direct control over ageing during studies	Long time to achieve ageing Neurological effects not characterised

1.3.2 In vivo models of ageing: Potential applications to ND research

1.3.2.1 Spontaneous and accelerated models of ageing

To date, research incorporating aged animals has shown differences in motor performance, cognition and pathology following induction of neurodegenerative models. Recently, in an intracerebroventricularly injected streptozotocin model of sporadic AD, aged rats at 23 months old demonstrated increased p-Tau/Tau levels compared to controls whereas this increase was not displayed in young AD rats compared to controls (Gáspár et al., 2022). Additionally, these aged rats showed increased susceptibility to toxicity following induction of the model compared to young rats. Similarly, age impacted the effect of 6-hydroxydopamine lesion on skilled motor function and TH positive neuronal loss in the substantia nigra (Barata-Antunes et al., 2020). The results from these studies, and others discussed at length by Sun and colleagues (Sun et al., 2020), highlight the importance of including age in pre-clinical models of NDs in order to fully recapitulate a disease phenotype relevant to those seen in aged patients in the clinic.

A natural model of ageing would be most accurate in recapitulating all elements of this phenotype *in vivo*. The naked mole rat has a lifespan upwards of 37 years and low incidence of age-related neurodegeneration (Delaney et al., 2021). This species has provided insight into the mechanisms of natural ageing and disease resistance; however, due to their long lifespan, the utilisation of naked mole rats in laboratory research is impractical (Delaney et al., 2021). Additionally, given their resistance to age-related neurodegenerative pathology, genetic or experimental manipulation is required to make them a relevant model for ND research. Instead, for an estimated 80% of ageing research, shorter lived rodent models are utilised (Andreollo et al., 2012), such as mice and rats, which live around 3 and 3.5 years, respectively, and, therefore, make it logistically feasible to house and obtain naturally aged animals within the time-frame of a reasonable research study (Andreollo et al., 2012).

Importantly, translating ageing across species is difficult due to differences in rate of maturation. In line with this, from birth to 1-month, mice mature approximately 150 times faster than humans, but this drops to 45 times faster in mice aged 1-6 months and to 25 times faster in mice aged 6-months or older (Flurkey et al., 2007). Despite this, some guidance has been put forward by Jackson Labs (Jackson

Laboratory, 2020). In brief, based on survival analyses in a large cohort of C57BL/6J mice, the most commonly used inbred strain, the following life stages have been proposed: (1) mature adult from 3-6 months of age, roughly equivalent to 20-30 years of age in humans; (2) middle age from 10-15 months of age, which corresponds to approximately 38-47 years of age in humans and (3) old age from 18-24 months+, which is comparable to humans from 56 to 69 years of age (Jackson Laboratory, 2020). Interestingly, given that the old age period in mice is approximately equivalent to the period when age-related neurodegenerative diseases typically begin to arise in humans (Hou et al., 2019), while mice at 18-24 months old may not fully encapsulate the full aged phenotype of humans 70+ years of age, they can still provide valuable insights into the impact of ageing on disease pathophysiology and vulnerability to age-related diseases. It is important to investigate, however, how these age equivalents might vary as a factor of mouse strain, or indeed in other species, such as rats. In line with this, allele variation has been shown to result in both phenotypic differences (Simon et al., 2013) and disparities in response to an intervention (Liao et al., 2010), even in closely related strains.

Overall, the use of aged rodents comes with caveats, such as the presence of comorbidities, leading to many animals meeting ethical criteria for euthanasia prior to becoming aged (Brayton et al., 2012). While this may reflect population morbidities in humans, a portion of the study cohort is lost prior to reaching the experimental starting point (Toth, 2018). Further, the portion of the cohort that remains is arguably biased. In addition, long-term housing of rodents can often be prohibitively expensive and may be limited by potential space constraints of animal holding facilities. Additionally, when animals are housed long-term under so-called standard conditions, it can also lead to chronic stress, behavioural abnormalities and increased risk of health conditions (Cait et al., 2022; Pinelli et al., 2017) , requiring alterations to conventional housing protocols when maintaining animals for months at a time. To counter these practical and ethical difficulties, inbred and genetic models of accelerated ageing have been developed and are discussed below as alternatives to naturally ageing animals in research. Such models, particularly when crossed with well-established genetic models of ND, such as the APP/PS1 mouse model of AD, may allow for accelerated investigations, overcoming the practical challenges

associated with long-term rodent investigations, while also modelling disease pathophysiology on a more translationally relevant aged phenotype background.

Mice are the most common model of accelerated ageing, due to their well characterised ageing phenotype and genome (Cai et al., 2022). The senescence accelerated prone mouse (SAMP) model is widely used and was created by selectively inbreeding mice from the AKR/J strain that showed spontaneous age-related changes between 2 and 12mths, such as shortened lifespan and decreased activity, as well as physical features of ageing, including alopecia, cataracts and musculoskeletal changes (Takeda et al., 1981). One strength of SAMP mice is that, as opposed to genetically modified models, acquisition of the aged phenotype is spontaneous and not induced by manipulation of a specific gene or pathway. As biological ageing has no known single cause, inducing models via specific pathways may over-simplify the complexity of natural ageing. In this sense, the SAMP mouse model may be more reflective of the heterogenous nature of human ageing.

A number of sub-strains of the SAMP mouse were generated displaying different phenotypes, two of which (SAMP8 and SAMP10) are particularly relevant to ND (reviewed: (Takeda, 2009)). SAMP8 is widely utilised in AD research, as these mice display both the cognitive deficits seen in AD and AD-specific pathology. Behaviourally, SAMP8 mice have deficits in learning and memory and show decreased anxiety-like behaviours and disrupted sleep cycles (Miyamoto et al., 1992). Summarised in Table 1.2, the brains of these mice show age-related changes (Takeda et al., 1981), as well as amyloid beta aggregates and tau hyperphosphorylation (Takemura et al., 1993). Additionally, SAMP8 mice have shown evidence of a dysregulated immune response, which, as discussed above, has been linked to both ageing and neurodegeneration (Molina-Martínez et al., 2020). Thus, the SAMP8 mouse combines ageing with the presence of relevant neurodegenerative brain pathology (del Valle et al., 2010) and has been used to test the therapeutic potential of multiple agents, including lithium (Malerba et al., 2021; Toricelli et al., 2021), fatty acids (Vela et al., 2019), acupuncture (Wang et al., 2018; Zhang et al., 2013) and both natural (Igarashi et al., 2022; Kim et al., 2023; Shih et al., 2010) and conventional (Lian et al., 2021) medicines. In addition, SAMP8 mice have also furthered our understanding of the role that an array of factors may play in the pathophysiology of AD, including protein chaperones (Akbor et al.,

2021b), protein (Liu et al., 2010) and histone deacetylases (Fontán-Lozano et al., 2008) and candidate AD genes, such as SLC24A4 polymorphism (Akbor et al., 2021a).

Interestingly, combining the SAMP8 mouse strain with a mouse model of AD may better represent both the natural ageing changes occurring in these mice, as well as disease pathology. In line with this, the SAMP8 mouse was crossed with the widely used APP/PS1 model of AD (SAMP8-APP/PS1) by Lok and colleagues in 2013 (Lok et al., 2013). The APP/PS1 transgenic model mimics amyloid pathology in the brain and the combined SAMP8-APP/PS1 model demonstrates earlier presentation of pathology, with Aβ immunoreactivity manifesting at 6-mths, compared to 9-mths in control mice. Further, an increased number of Aβ deposits were present in the hippocampus in SAMP8-APP/PS1 mice at 9-mths. Acquisition of the AD behavioural phenotype was also more pronounced in SAMP8-APP/PS1 mice, with more severe learning and memory deficits and decreased anxiety at 9-mths of age (Lok et al., 2013). While this suggests that it is feasible to generate a combined model to investigate AD in the context of an aged phenotype, outside of this initial report a decade ago, this model has not been used in further studies and no other combined models have been produced, representing a potential underutilised opportunity to more quickly and accurately model AD. Additionally, despite the presence of relevant pathology, including degeneration of DA neurons in the substantia nigra and noradrenergic neurons in the locus coeruleus in SAMP mice (Karasawa et al., 1997), SAMP8 mice are rarely used for PD research.

In contrast to SAMP8 mice, SAMP10 mice display primarily age-related changes in the brain and lack the Aβ deposition and tau hyperphosphorylation seen in SAMP8 (see Table 1.2). There are also behavioural differences between the two strains. While SAMP8 mice show a pronounced decrease in anxiety-like behaviour, SAMP10 mice display increased emotional dysfunction and depressive behaviour (Shimada and Hasegawa-Ishii, 2011). This is thought to be due to a number of changes in the dopamine and serotonin systems of SAMP10 mice, with changes in DA and serotonin receptor sensitivity (Onodera et al., 2000) and altered DA metabolism present in these mice (Takahashi et al., 2004). Interestingly, however, despite these observed changes in the dopaminergic pathway, SAMP10 mice are also underutilised as a model in PD research.

1.3.2.2 Genetic mouse models of ageing

In contrast to the spontaneous ageing models, genetic models, which involve knockout, mutation, or overexpression of particular genes, are widespread methods in many areas of research, including both ageing and ND. In the context of ageing research specifically, these models involve manipulating a specific pathway or factor to induce premature ageing, which allows for the study of how this pathway/factor contributes to the neurobiological process of natural ageing. An understanding of this is critical for understanding the mechanisms of normal ageing, which lays the foundation for how this may be further altered in the context of age-related ND. Mouse models of the aged CNS have been reviewed previously (Heng et al., 2017), including transgenic models based on genetic changes in progeroid syndromes and specific age-related pathways, including IL-10 and SIRT6. While multiple genetic models of ageing are available, Sharma et al., (2018) recommended the use of progeroid mouse models particularly to study AD, in order to combine the rapid ageing seen in the progeroid models with the disease phenotype induced by AD models (Sharma et al., 2018). Progeroid mouse models are based on accelerated ageing diseases with a known genetic cause, such as the LMNA gene in Hutchinson Gilford syndrome (HGS), which results in a partially processed pre-lamin A protein, termed progerin (Inesta-Vaquera et al., 2022), and the WRN gene in Werner syndrome (WS), which causes dysregulation in DNA repair systems (Massip et al., 2006). These progeroid syndromes are characterised by early onset of ageing and age-related disease (Ding and Shen, 2008). HGS mice with a mutation in the LMNA gene ($LMNA^{G609G/G609G}$) display ageing at three wks, including increased cancer incidence, infertility and curvature of the spine (Osorio et al., 2011). Importantly, however, the brains of these mice do not demonstrate neurodegenerative change, with neurons appearing to not be sensitive to increased progerin expression (Baek et al., 2015). In line with this, HGS mice do not display deficits on tests of reference or spatial memory (Baek et al., 2015) and individuals with HGS do not exhibit deficits in mental or intellectual abilities. This makes the HGS mouse model itself unsuitable for studying ND; however, it may have utility for crossing with established genetic models of ND (e.g., the APP/PS1 model of AD) to produce ND changes in combination with an accelerated aged phenotype.

In contrast, WS mice, which are deficient in part of the helicase domain of the WRN protein ($WRN^{\Delta hel/\Delta hel}$), show an ageing phenotype with onset at 5 mths, including insulin resistance, increased

ROS, DNA damage and increased cancer incidence (Massip et al., 2006). Additionally, both motor (loss of activity and coordination) and cognitive (deficits in spatial and social novelty memory) changes, concomitant with signs of cellular ageing and enhanced oxidative stress and neuroinflammation, have been described in this model (Hui et al., 2018) (Table 1.2). This suggests that these mice may have utility in their own right for the study of ND, with studies needed to examine markers associated with neurodegenerative change (e.g., tau hyperphosphorylation). It is also important to note, however, that this potentially limits the ability to cross WRN mice with established genetic models of ND (e.g., the APP/PS1 model of AD) to produce mixed models, as the presence of such behavioural impairments may confound interpretation of results.

This has not, however, prevented the generation of a mouse model with a combined complete KO of both WRN and telomerase RNA component (Terc), a ribonucleoprotein polymerase that maintains telomere length, ($Terc^{-/-}WRN^{-/-}$) (Chang et al., 2004). $Terc^{-/-}$ mice display accelerated ageing at just 4-8 mths old, as well as upregulation of SASP related genes, increased oxidative stress response and apoptotic markers in the brain (Yang et al., 2022). To date, $Terc^{-/-}WRN^{-/-}$ mice have not been assessed for neurological or behavioural effects, but since both $Terc^{-/-}$ (Khan et al., 2015) and WRN modified ($WRN^{\Delta hel/\Delta hel}$) (Hui et al., 2018) mice have neurological impairments and cellular brain changes (Yang et al., 2022), it is reasonable to predict that $Terc^{-/-}WRN^{-/-}$ mice may display exacerbated behavioural change and a greater extent of age-related pathophysiological change, compared to either model alone. This may make this model particularly useful for ND research, although this has yet to be evaluated. Nevertheless, Terc knockout mice have previously been utilised to study PD. Scheffold and colleagues (2016) crossed C57/BL6/J $Terc^{-/-}$mice with C57/BL6/J mice expressing the human mutant α-synuclein (A3oP) to model PD in the context of telomere shortening (Scheffold et al., 2016). Results demonstrated that telomere shortening accelerated the formation of α-synuclein aggregates and impaired responses of brainstem microglia (Scheffold et al., 2016). This study provided evidence that age-related changes in the brain, such as telomere shortening, impact the progression of degenerative pathology in PD, further highlighting the importance of accounting for the effects of ageing when modelling ND.

In addition to progeroid and telomere shortening, genetic models based on inflammatory and metabolic theories of ageing have also been utilised, including IL-10 (Walston et al., 2008) and SIRT6 deficiency (Kaluski et al., 2017). Mice deficient in the anti-inflammatory cytokine IL-10 (IL-10$^{-/-}$) had previously been established as a model of human frailty, showing alopecia and decreased muscle strength at 11mths (Walston et al., 2008), low-grade activation of inflammatory signalling pathways, including IL-6, TNF-α and IL-1β, at 15mths (Ko et al., 2012), and increased neuroinflammation and Tau phosphorylation at 6mths old following an inflammatory stimulus (Weston et al., 2021). While IL-10$^{-/-}$ mice display brain changes similar to those in AD (Richwine et al., 2009), however, they are currently not widely used in ND research.

Similarly, SIRT6, a member of the Sirtuin family of signalling proteins, is important for maintaining normal DNA repair (Mostoslavsky et al., 2006) and has been the basis for modelling ageing in C57BL/6 mice (Mostoslavsky et al., 2006). SIRT6$^{-/-}$ mice demonstrated genomic instability, altered metabolic homeostasis and immune cell generation and decreased size (Mostoslavsky et al., 2006). While these changes demonstrate key elements of the mammalian aged phenotype discussed above, SIRT6$^{-/-}$ mice develop degenerative progeroid pathology and do not survive beyond 4wks (Mostoslavsky et al., 2006), limiting the ability of researchers to conduct experiments. However, mice with a neuronal specific SIRT6 deficiency survive longer and demonstrate ageing, measured by DNA damage and cell death, at 4mths of age (Kaluski et al., 2017) (Table 1.2). Considering the deficits in non-associative learning and increases in locomotor activity in this model are similar to those in AD models, and that SIRT6 expression in the brain is reduced in AD patients compared to aged controls (Kaluski et al., 2017), SIRT6$^{-/-}$ mice may be useful for modelling AD in the context of an accelerated aged phenotype. Of note, SIRT6$^{-/-}$ embryonic stem cells have previously been used as an *in vitro* model of age-related cellular changes (Mostoslavsky et al., 2006) (Table 1.1).

Of potential relevance, a new genetic rodent model of ageing was reported in January 2023, the inducible changes to the epigenome (ICE) mouse. This mouse was created by tamoxifen-controlled expression of the endonuclease I-PpoI at 20 canonical sites in the mouse genome, causing DSBs without mutations in the genome (Yang et al., 2023). When I-Ppol was activated at 4-6mths, an aged phenotype

was observed by 10-12mths. This featured muscle loss, alopecia, loss of skin pigment and premature frailty, similar to that of 24mo controls (Yang et al., 2023). Additionally, higher levels of activated glial cells in the hippocampus suggest potential applications in modelling the brain changes seen in NDs. The researchers additionally investigated the ability to reverse these changes by treatment with Yamanaka factors, which are used to differentiate somatic cells to iPSCs. Ageing changes observed in ICE mice were able to be reversed *in vitro*, demonstrating the potential usefulness of the Yamanaka factors beyond iPSC differentiation. It is important to note, however, that there have been a number of major issues identified with the design of this study (Timmons and Brenner, 2023), most notably that genotoxicity due to the expression of I-Ppol appears to potentially play a role in development of the ageing phenotype in ICE mice through p53 signalling (Kim et al., 2016), which has not been accounted for in controls of this study. However, while the specific mechanisms driving ageing in this model are yet to be fully validated, this method presents a potentially significant contribution to the research field by providing an inducible rodent model of ageing that could be crossed with established genetic models of ND disease. Regardless, further characterisation of the neurobiological changes in these mice needs to be undertaken to understand the utility of this model in age-related research, as well as for CNS research more generally.

While potentially promising, particularly with regard to their ability to overcome the practical challenges associated with the long-term investigations needed to investigate spontaneous ageing, it is important to note that accelerated ageing models are not without their own limitations and challenges. Namely, there are important questions about how closely these models mirror the changes associated with natural ageing. In line with this, it has been observed that the histopathologic lesions associated with these accelerated ageing models often don't overlap completely with those seen in natural ageing (Gurkar and Niedernhofer, 2015), and that accelerated ageing models often exhibit features not typical of normal ageing (Kõks et al., 2016). Similarly, none of the progeria models reviewed here are able to mimic all of the complex aspects associated with the aged phenotype in mammals due to the fact that they were created to specifically model the changes seen in certain diseases (Gurkar and Niedernhofer, 2015). It is also important to note that the morphologic changes observed in these models are often

segmental in nature, meaning that multiple different models would be required in order to fully explore the complex changes that contribute to the aged phenotype within a particular tissue or organ system (Harkema et al., 2016).

1.4 Considering age in NDs moving forward- Recommendations for researchers

A major gap in ND research currently is the lack of consideration given in current disease models to the typical changes associated with the aged phenotype that occur alongside disease-specific pathology. Fig. 1.2 outlines a proposed research pipeline to integrate ageing into ND research both *in vitro* and *in vivo* using currently available models. First, the aged phenotype is induced in either a relevant cell or animal model (Fig 2 step1), in order to simulate the complex cellular environment present in the aged individual. Once this has been established, a disease model can then be induced on this background using an inflammatory (Hoban et al., 2013; Mutemberezi et al., 2018), chemical (Sherer et al., 2003) or protein stimulus *in vitro (Ross et al., 2020)* and, additionally, genetic (Flood et al., 2002) or neurotoxic methods (Ungerstedt, 1968) *in vivo* (Fig 1.2 step 2). This more translationally relevant model can then be used to undertake the desired investigations (Fig 1.2 step 3). The incorporation of this pipeline would benefit both the understanding of disease pathogenesis, by providing insight into the contribution of biological ageing to NDs, and additionally would assist in the development of disease treatments by providing more accurate screening of potential therapies. Major drawbacks of this pipeline include not only the time needed to establish the combined ageing and ND model, but that the complexity of the generated model introduces the need for extra validation and requires a more multifaceted interpretation of results. To address the issue of time, utilising the accelerated *in vivo* ageing models reviewed here would alleviate some of this cost compared to using naturally ageing animals; however, none of these models individually can capture all the age-related changes described above. Establishing such models *in vitro* is far less costly and time consuming; for example, inducing replicative senescence in primary cells, which have a limited lifespan, would be considerably faster and cheaper than housing mice for 18 months or longer. Modelling the complex processes seen in both ageing and NDs presents significant challenges for researchers both *in vitro* and *in vivo*. Below we present a discussion of these challenges,

and in Table 1.3, we offer some recommendations to consider when designing both *in vitro* and *in vivo* ND studies.

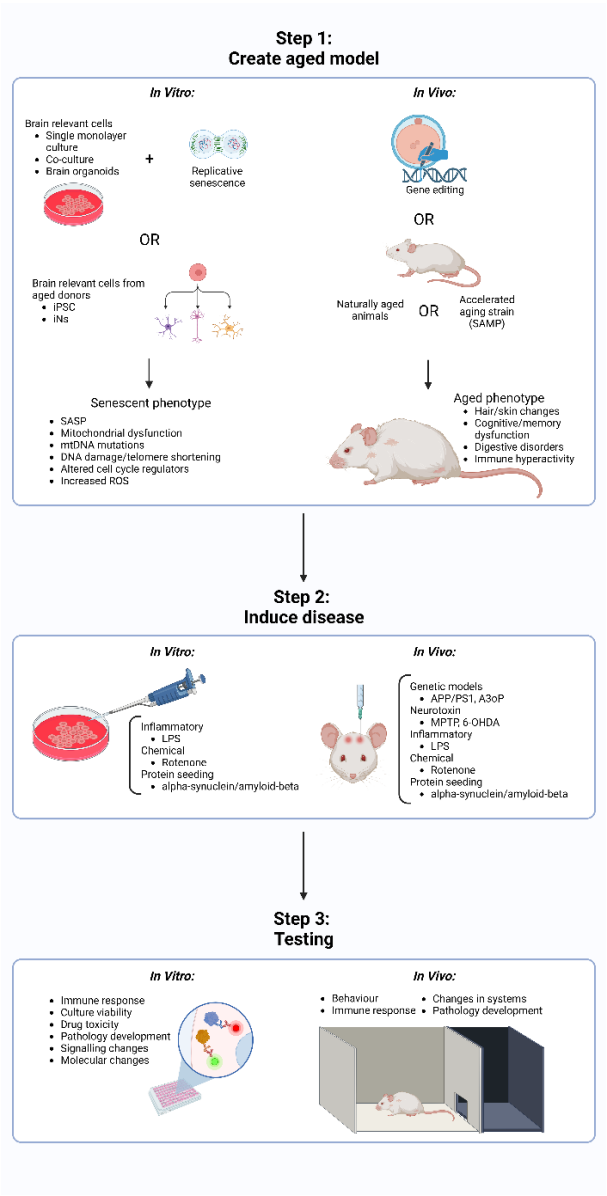


Figure 1.2 Pipeline for the incorporation of age into ND research models.Step 1: Either *in vitro* or *in vivo*, studies need to induce the senescent phenotype in cells or ageing in animals. Step 2: Once ageing has been induced, disease can then be modelled within those animals/cultures. Types of models to induce disease include genetic, inflammatory, seeding, or neurotoxic models Step 3: biological responses of cells/tissue and behavioural responses of animals can then be tested to develop treatments and understand disease pathology.

As reviewed above, despite the array of techniques used to induce and quantify ageing *in vitro* and *in vivo,* there is yet untapped potential for incorporating the aged phenotype in preclinical ND research. First, when it comes to *in vitro* work, current models are often over-simplified and fail to recapitulate the complex 3D interactions amongst different types of brain cells in the tetrapartite synapse. Moving forward, use of co-culture and organoid models kept for longer periods of time in culture (i.e. 27 day old co-cultures (Bigagli et al., 2016) or 45 day old brain organoids (Ao et al., 2022) displaying ageing markers) can be drawn upon, in combination with iN technology, to produce sophisticated "aged" *in vitro* models that allow for investigation of disease mechanisms or treatment efficacy in more representative models. In order to validate such models, use of a standardised "aged phenotype" marker panel, inspired by the 'AgeScore' panel of Hartmann and colleagues (2023) (Hartmann et al., 2023), should be developed and consistently applied across studies in order to improve reproducibility and allow for more ready comparison between labs. By utilising cells which meet a minimum criterion on this panel, or a minimum 'AgeScore', ageing can be equally accounted for across experiments and between lab groups. While this panel needs further validation across cell types, we suggest that for a culture to be considered 'aged,' cells must show changes in major cellular ageing markers discussed as part of the aged cellular phenotype above and identified as a hallmark of ageing. For ND models, the acquisition of the SASP is particularly important, as chronic inflammation has well established links to neurodegenerative pathology (Guzman-Martinez et al., 2019) and ageing (Franceschi and Campisi, 2014) and should serve as a major marker of ageing in any potential aged ND model. This could serve a similar function to the ARRIVE guidelines (Animal Research: Reporting of *In Vivo* Experiments), which have sought to improve reporting of research in animal studies (Percie du Sert et al., 2020), and could also be used for validation of *in vivo* models. The generation of such well-validated, sophisticated "aged" *in vitro* models will provide a powerful tool on which to model ND and could be used in combination with exciting advances in bioengineering technologies, such as microfluidic devices (Fernandes et al., 2016) (e.g. brain-on chip) and 3D tissue engineering (Lam et al., 2019) (e.g. extracellular matrix decellularization) to take our understanding of disease mechanisms and drug development to new heights.

From an *in vivo* perspective, despite recent improvements in animal models of ageing, there is an overall lack of consideration of age in ND study design. In a survey of 297 researchers on the use of rodents in biomedical research conducted by the National Centre for the Replacement, Refinement and Reduction of Animals in Research (NC3R), the most common age of use is 8-12 weeks (Jackson et al., 2017) (with 6-20 weeks being reported as "adult" animals). This is problematic, as this is a stage in which many developmental processes are still ongoing, including, importantly, both development of the immune system (Holladay and Smialowicz, 2000) and brain maturation (Downes and Mullins, 2014) and myelination (Fu et al., 2013). Further, as discussed extensively above, the physiological changes that occur with ageing differ significantly in young versus old animals. Concerningly, however, only ten percent of respondents to the survey reported using rodents over 16 weeks of age, with just 24% of these in in rats (Jackson et al., 2017). This is regardless of whether age is a significant risk factor for the disease being modelled (e.g. NDs) and in spite of a growing number of studies showing the moderating effect of age on disease presentation and pathophysiology (e.g. older rats have increased susceptibility (Yager and Thornhill, 1997) to and take longer to recover from (Brown et al., 2003) ischaemic insults).

To improve upon this, animal age must be carefully considered when designing studies. For NDs, this means planning for either the long-term use of animals (i.e. 18-months or longer) or the use of an accelerated ageing model, such as those reviewed above. In selecting an accelerated ageing model, particularly those based on progeroid syndromes, researchers must consider the different pathophysiological changes that occur in each model, when these changes occur and how this may impact their interpretation of findings (e.g. cognitive impairment seen in WRN mice may confound behavioural results in a mixed model of AD). Due to the difficulties in interpretation of results and the limited hallmarks of ageing displayed by any one accelerated model, using naturally aged animals is the ideal base model to use in step 1 (Fig 1.2). However, when using naturally aged animals, there are important financial and practical difficulties associated with maintaining rodent colonies long term. For example, a comparison by NC3R of the cost of obtaining animals at six versus 12-weeks of age from a major commercial supplier in the US and UK demonstrated that 12-week animals cost at least 50%

more per animal, and sometimes as much as 100% more (Jackson et al., 2017), and this is without accounting for increases in agistment costs associated with ageing rodents in-house. Improvements in the availability and accessibility of aged animals, such as better commercial availability, local/national networks for aged animal sharing or improved banking of tissues or findings into biobanks/data repositories for secondary analyses, would help to offset the significant costs, challenges and, most importantly, variability associated with individual research groups housing animals for extended periods of time within their own housing facilities, in order to obtain aged cohorts. Some efforts have already been made in this direction via the Shared Ageing Research Models (ShARM) initiative (Duran et al., 2013) and the Aging Rodent Colonies project at the National Institute on Aging (Jackson et al., 2017). Additionally, researchers must work together to advocate to government and philanthropic bodies to provide adequate funding to allow for the increased costs associated with the use of aged animals within grant applications, where appropriately justified.

The field would also benefit from the development of guidelines for animal care and use specifically tailored towards older animals, given the unique challenges associated with these cohorts. For example, rats have been shown to develop multiple diseases and alterations in organ function in conjunction with ageing, including renal disease (Roncal-Jimenez et al., 2016), respiratory disease/infections (Carthew et al., 1989), increased tumour presentation (Sandusky et al., 1988) and atrophy of lumbar/hindlimb muscles (Ibebunjo et al., 2013). Further, such age-related changes may be strain specific, which also must be accounted for when working with aged animals. In support of this, C57BL/6J mice have missense mutation in the nicotinamide nucleotide transhydrogenase gene, which leads to impaired glucose tolerance (Toye et al., 2005) and age-related declines in mitochondrial function (Ghosh et al., 2014). Researchers would thus benefit from sharing experiences of working with aged cohorts and from working closely with laboratory animal servicers and veterinary staff at the time of experimental design, to anticipate challenges that may arise and appropriately plan how to manage these. Importantly, there are also several extraneous factors not discussed in this review which can influence ageing markers and potentially contribute to heterogeneity in human populations, including stress (Yegorov et al., 2020), exercise (Carapeto and Aguayo-Mazzucato, 2021) and diet (Longo et al., 2021); however, these factors

need to be considered and controlled for in the study design phase, keeping in mind that the needs of older animals may not be equivalent to those of younger animals.

Finally, in accordance with 8a of the Essential 10 of the ARRIVE guidelines, increased emphasis needs to be placed on appropriate reporting of animal age. This includes both summary statistics (mean +/- SD, as well as range) for each experimental group and, importantly, values for individual animals in the supplementary materials (Percie du Sert et al., 2020). This is critical, given that animal age is often poorly reported, or even unreported, in preclinical studies, with poor justifications offered for age choices (e.g. monetary costs, supply/availability and maintaining comparability with historical data) (Jackson et al., 2017). This leads to wide discrepancy in the age of animals being used by different labs, with an investigation of this by NC3R showing that, within the same model paradigm, the age of the animal used could vary over a range of up to 20 weeks (Jackson et al., 2017). Such inconsistencies in age choice and reporting can lead to variability between animals within a given study, as well as between studies using the same model from different laboratories, negatively impacting data quality and study outcomes (Jackson et al., 2017). Additionally, there needs to be greater consensus in the field about what constitutes specific age ranges of interest in a given species (e.g. younger adult versus middle-age versus older adult) and how this relates to human ageing.

To assist with this, as discussed above, recommendations have been put forward by the Jackson Laboratory, proposing three life stages in mice: mature adult from 3-6 months of age (~ 20-30 human years), middle age from 10-15 months of age (~38-47 human years) and old age from 18-24 months (~56-69 human years) (Jackson Laboratory, 2020). Researchers can use these as a guide when designing studies which utilise aged mice; however, potential strain and species differences also need to be considered. In order to facilitate this, additional tools have been developed to help determine equivalent human age in mice (Geifman and Rubin, 2013) and rats (Quinn, 2005), as well as other species (Clancy et al., 2007). Ideally, researchers should aim to utilise animals at the higher end of the defined "old age" range (e.g. 24-months of age in C57BL/6J mice), although potential health concerns for animals of this age, as well as practical and financial concerns associated with long-term housing, also need to be considered.

Table 1.3: Summary of recommendations for improving the modelling of age both *in vitro* and *in vivo*.

***In vitro* recommendations**
Develop more sophisticated *in vitro* models as a background on which to model NDs using advances in co-culture and organoid technology
Validate "aged" models using a standard marker panel and use this to develop reporting guidelines (in line with the ARRIVE guidelines for *in vivo* research
Harness advances from bioengineering (e.g. brain on a chip and extracellular metric decellularization) to use in combination with aged *in vitro* models in order to allow for deeper investigation of disease mechanisms
***In vivo* recommendations**
When designing studies, utilise models which include changes relevant to the disease of interest (e.g. pathological protein deposition in ND studies)
Advocate for improvements in the availability and accessibility of aged animals, including better commercial availability, local/national networks for aged animal sharing or improved banking of tissues or findings into biobanks and data repositories for secondary analyses
Educate governmental and philanthropic bodies about the importance of incorporating aged animals into research and the need for increased funding to allow for this, where justified
Develop guidelines for animal care and use specifically tailored towards older animals that also account for strain-specific differences
Work closely with laboratory animal services and veterinary staff when designing experiments, in order to anticipate challenges that may arise and develop strategies to manage these.
Adhere to the ARRIVE guidelines for the appropriate reporting of animal age in peer-reviewed literature, reporting both summary statistics for each experimental group and, where possible, age data for individual animals in the supplementary data
Utilise tools developed to determine human equivalent age when selecting the age of animals to be used in a given study, in order to facilitate the development of a field-specific consensus about age of animals to be used in a given model moving forward

1.5 Conclusions

Overall, there is a critical need to incorporate ageing into studies of neurodegeneration, which is currently often overlooked by researchers, despite age being the most significant risk factor for ND development. Whilst we highlight that it is critical to include age in ND research to improve translatability, we acknowledge that all models have limitations and no one model can recapitulate all elements of human disease. ND research conducted without specific consideration of age still presents

an invaluable contribution, as evidenced by the multiple advances made in the field to date. Nevertheless, moving forward, effort should be made to account for ageing in study design or consider it in the interpretation of results. This is particularly critical given how age may alter not only pathophysiology, but also potentially the response to therapeutic interventions. Therefore, whilst we also recognise the difficulties involved in analysing such convoluted data, the interactions between NDs and ageing make the diseases themselves complex. Thus, a complex model is more reflective of the naturally occurring disease environment. Here, we have summarised what constitutes the aged phenotype in humans and critically evaluated several major methods to induce ageing in a laboratory setting, with a particular focus on the significant under-utilisation of these models to date in ND research. Emerging *in vitro* technologies could help to improve this, broadening the landscape of available models and allowing for more sophisticated investigations of disease mechanisms and therapeutic response in the context of a complex environment more reflective of the CNS. Similarly, the advent of *in vivo* models of ageing that are both inducible and reversible may help us to probe the contribution of ageing to the emergence of the ND-phenotype in a way never before possible. In spite of these advancements, however, it is critical that ND researchers prioritise including age as a critical component of their models moving forward. With this in mind, and in the spirit of overcoming current practical challenges, we have offered here specific recommendations for improving the incorporation of the aged phenotype into both *in vitro* and *in vivo* experimental models. Taken together, it is hoped that more widespread use of these models, in conjunction with our recommendations, will improve the quality and reproducibility of the data produced, ultimately helping to ensure that results can translate to effective treatments for neurodegeneration.

1.6 Acknowledgements

LC is supported by an Australian Government Research Training Program Scholarship. This work was supported by grants to LCP and AC by the National Foundation for Medical Research and Innovation. Figures created in BioRender.

1.7 Conflict of interest statement

The authors declare no competing financial interests.

1.8 References

Abud, E.M., Ramirez, R.N., Martinez, E.S., Healy, L.M., Nguyen, C.H.H., Newman, S.A., Yeromin, A.V., Scarfone, V.M., Marsh, S.E., Fimbres, C., Caraway, C.A., Fote, G.M., Madany, A.M., Agrawal, A., Kayed, R., Gylys, K.H., Cahalan, M.D., Cummings, B.J., Antel, J.P., Mortazavi, A., Carson, M.J., Poon, W.W., Blurton-Jones, M., 2017. iPSC-Derived Human Microglia-like Cells to Study Neurological Diseases. Neuron 94, 278-293.e279.

Aitken, A.E., Lee, C.M., Morgan, E.T., 2008. Roles of nitric oxide in inflammatory downregulation of human cytochromes P450. Free Radic Biol Med 44, 1161-1168.

Akbor, M.M., Kim, J., Nomura, M., Sugioka, J., Kurosawa, N., Isobe, M., 2021a. A candidate gene of Alzheimer diseases was mutated in senescence-accelerated mouse prone (SAMP) 8 mice. Biochemical and Biophysical Research Communications 572, 112-117.

Akbor, M.M., Kurosawa, N., Nakayama, H., Nakatani, A., Tomobe, K., Chiba, Y., Ueno, M., Tanaka, M., Nomura, Y., Isobe, M., 2021b. Polymorphic SERPINA3 prolongs oligomeric state of amyloid beta. PLoS One 16, e0248027.

Andreollo, N.A., Santos, E.F., Araújo, M.R., Lopes, L.R., 2012. Rat's age versus human's age: what is the relationship? Arq Bras Cir Dig 25, 49-51.

Ao, Z., Song, S., Tian, C., Cai, H., Li, X., Miao, Y., Wu, Z., Krzesniak, J., Ning, B., Gu, M., Lee, L.P., Guo, F., 2022. Understanding Immune-Driven Brain Aging by Human Brain Organoid Microphysiological Analysis Platform. Advanced Science 9, 2200475.

Arafah, A., Khatoon, S., Rasool, I., Khan, A., Rather, M.A., Abujabal, K.A., Faqih, Y.A.H., Rashid, H., Rashid, S.M., Bilal Ahmad, S., Alexiou, A., Rehman, M.U., 2023. The Future of Precision Medicine in the Cure of Alzheimer's Disease. Biomedicines 11.

Azzolino, D., Spolidoro, G.C.I., Saporiti, E., Luchetti, C., Agostoni, C., Cesari, M., 2021. Musculoskeletal Changes Across the Lifespan: Nutrition and the Life-Course Approach to Prevention. Frontiers in Medicine 8.

Baek, J.H., Schmidt, E., Viceconte, N., Strandgren, C., Pernold, K., Richard, T.J., Van Leeuwen, F.W., Dantuma, N.P., Damberg, P., Hultenby, K., Ulfhake, B., Mugnaini, E., Rozell, B., Eriksson, M., 2015. Expression of progerin in aging mouse brains reveals structural nuclear abnormalities without detectible significant alterations in gene expression, hippocampal stem cells or behavior. Hum Mol Genet 24, 1305-1321.

Barata-Antunes, S., Teixeira, F.G., Mendes-Pinheiro, B., Domingues, A.V., Vilaça-Faria, H., Marote, A., Silva, D., Sousa, R.A., Salgado, A.J., 2020. Impact of Aging on the 6-OHDA-Induced Rat Model of Parkinson's Disease. International Journal of Molecular Sciences.

Beijer, H.J., de Blaey, C.J., 2002. Hospitalisations caused by adverse drug reactions (ADR): a meta-analysis of observational studies. Pharm World Sci 24, 46-54.

Bhutto, A., Morley, J.E., 2008. The clinical significance of gastrointestinal changes with aging. Curr Opin Clin Nutr Metab Care 11, 651-660.

Bigagli, E., Luceri, C., Scartabelli, T., Dolara, P., Casamenti, F., Pellegrini-Giampietro, D.E., Giovannelli, L., 2016. Long-term Neuroglial Cocultures as a Brain Aging Model: Hallmarks of Senescence, MicroRNA Expression Profiles, and Comparison With In Vivo Models. The Journals of Gerontology: Series A 71, 50-60.

Bitto, A., Ito, T.K., Pineda, V.V., LeTexier, N.J., Huang, H.Z., Sutlief, E., Tung, H., Vizzini, N., Chen, B., Smith, K., Meza, D., Yajima, M., Beyer, R.P., Kerr, K.F., Davis, D.J., Gillespie, C.H., Snyder, J.M., Treuting, P.M., Kaeberlein, M., 2016. Transient rapamycin treatment can increase lifespan and healthspan in middle-aged mice. Elife 5.

Boraldi, F., Bartolomeo, A., Di Bari, C., Cocconi, A., Quaglino, D., 2015. Donor's age and replicative senescence favour the in-vitro mineralization potential of human fibroblasts. Experimental Gerontology 72, 218-226.

Brayton, C.F., Treuting, P.M., Ward, J.M., 2012. Pathobiology of Aging Mice and GEM: Background Strains and Experimental Design. Vet Pathol 49, 85-105.

Brown, A.W., Marlowe, K.J., Bjelke, B., 2003. Age effect on motor recovery in a post-acute animal stroke model. Neurobiol Aging 24, 607-614.

Bunc, M., Hanning, S., Prieto, J., Kristl, J., Orlu, M., 2019. Characterisation of an in vitro aged cell culture model. Farmacia 67.

Cai, N., Wu, Y., Huang, Y., 2022. Induction of Accelerated Aging in a Mouse Model. Cells 11.
Cait, J., Cait, A., Scott, R.W., Winder, C.B., Mason, G.J., 2022. Conventional laboratory housing increases morbidity and mortality in research rodents: results of a meta-analysis. BMC Biol 20, 15.
Caldeira, C., Oliveira, A.F., Cunha, C., Vaz, A.R., Falcão, A.S., Fernandes, A., Brites, D., 2014. Microglia change from a reactive to an age-like phenotype with the time in culture. Front Cell Neurosci 8, 152.
Cao, B., Ho, J., 2020. WHO methods and data sources for life tables 1990-2019. World Health Organization (WHO), Geneva.
Carapeto, P.V., Aguayo-Mazzucato, C., 2021. Effects of exercise on cellular and tissue aging. Aging (Albany NY) 13, 14522-14543.
Carthew, P., Aldred, P., Hill, R.J., Riley, J., Edwards, R.E., 1989. Dyspnea in aging rats due to disseminated intravascular coagulation (DIC). Vet Pathol 26, 505-509.
Chakrabarti, S., Munshi, S., Banerjee, K., Thakurta, I.G., Sinha, M., Bagh, M.B., 2011. Mitochondrial Dysfunction during Brain Aging: Role of Oxidative Stress and Modulation by Antioxidant Supplementation. Aging Dis 2, 242-256.
Chang, A.Y., Skirbekk, V.F., Tyrovolas, S., Kassebaum, N.J., Dieleman, J.L., 2019. Measuring population ageing: an analysis of the Global Burden of Disease Study 2017. The Lancet Public Health 4, e159-e167.
Chang, S., Multani, A.S., Cabrera, N.G., Naylor, M.L., Laud, P., Lombard, D., Pathak, S., Guarente, L., DePinho, R.A., 2004. Essential role of limiting telomeres in the pathogenesis of Werner syndrome. Nature Genetics 36, 877-882.
Chatterjee, N., Walker, G.C., 2017. Mechanisms of DNA damage, repair, and mutagenesis. Environmental and Molecular Mutagenesis 58, 235-263.
Choi, S.H., Kim, Y.H., Hebisch, M., Sliwinski, C., Lee, S., D'Avanzo, C., Chen, H., Hooli, B., Asselin, C., Muffat, J., Klee, J.B., Zhang, C., Wainger, B.J., Peitz, M., Kovacs, D.M., Woolf, C.J., Wagner, S.L., Tanzi, R.E., Kim, D.Y., 2014. A three-dimensional human neural cell culture model of Alzheimer's disease. Nature 515, 274-278.
Chouchane, M., Melo de Farias, A.R., Moura, D.M.S., Hilscher, M.M., Schroeder, T., Leão, R.N., Costa, M.R., 2017. Lineage Reprogramming of Astroglial Cells from Different Origins into Distinct Neuronal Subtypes. Stem Cell Reports 9, 162-176.
Clancy, B., Kersh, B., Hyde, J., Darlington, R.B., Anand, K.J., Finlay, B.L., 2007. Web-based method for translating neurodevelopment from laboratory species to humans. Neuroinformatics 5, 79-94.
Cole, J.H., Leech, R., Sharp, D.J., 2015. Prediction of brain age suggests accelerated atrophy after traumatic brain injury. Ann Neurol 77, 571-581.
Coppé, J.-P., Patil, C.K., Rodier, F., Sun, Y., Muñoz, D.P., Goldstein, J., Nelson, P.S., Desprez, P.-Y., Campisi, J., 2008. Senescence-Associated Secretory Phenotypes Reveal Cell-Nonautonomous Functions of Oncogenic RAS and the p53 Tumor Suppressor. PLOS Biology 6, e301.
Cristofalo, V.J., Allen, R.G., Pignolo, R.J., Martin, B.G., Beck, J.C., 1998. Relationship between donor age and the replicative lifespan of human cells in culture: a reevaluation. Proc Natl Acad Sci U S A 95, 10614-10619.
da Costa, J.P., Vitorino, R., Silva, G.M., Vogel, C., Duarte, A.C., Rocha-Santos, T., 2016. A synopsis on aging-Theories, mechanisms and future prospects. Ageing research reviews 29, 90-112.
Davila, D., Connolly, N.M.C., Bonner, H., Weisová, P., Dussmann, H., Concannon, C.G., Huber, H.J., Prehn, J.H.M., 2012. Two-step activation of FOXO3 by AMPK generates a coherent feed-forward loop determining excitotoxic cell fate. Cell Death & Differentiation 19, 1677-1688.
de Jong, L.M., Jiskoot, W., Swen, J.J., Manson, M.L., 2020. Distinct Effects of Inflammation on Cytochrome P450 Regulation and Drug Metabolism: Lessons from Experimental Models and a Potential Role for Pharmacogenetics. Genes (Basel) 11.
de Mera-Rodríguez, J.A., Álvarez-Hernán, G., Gañán, Y., Martín-Partido, G., Rodríguez-León, J., Francisco-Morcillo, J., 2021. Is Senescence-Associated β-Galactosidase a Reliable in vivo Marker of Cellular Senescence During Embryonic Development? Frontiers in Cell and Developmental Biology 9, 36.
del Valle, J., Duran-Vilaregut, J., Manich, G., Casadesús, G., Smith, M.A., Camins, A., Pallàs, M., Pelegrí, C., Vilaplana, J., 2010. Early Amyloid Accumulation in the Hippocampus of SAMP8 Mice. Journal of Alzheimer's Disease 19, 1303-1315.

Delaney, M.A., Imai, D.M., Buffenstein, R., 2021. Spontaneous Disease and Pathology of Naked Mole-Rats. In: Buffenstein, R., Park, T.J., Holmes, M.M. (Eds.), The Extraordinary Biology of the Naked Mole-Rat. Springer International Publishing, Cham, pp. 353-380.
Deng, W., Jo, J.-i., Morikuni, H., Sasayama, S., Hashimoto, Y., Matsumoto, N., Honda, Y., 2023. Senescence-associated secretory phenotypes in rat-derived dedifferentiated fat cells with replicative senescence. Dental Materials Journal advpub.
DiMarco, G.M., Harris, B.N., Savonenko, A.V., Soto, P.L., 2023. Acute stressors do not impair short-term memory or attention in an aged mouse model of amyloidosis. Frontiers in Behavioral Neuroscience 17.
Ding, C., Wu, Y., Chen, X., Chen, Y., Wu, Z., Lin, Z., Kang, D., Fang, W., Chen, F., 2022. Global, regional, and national burden and attributable risk factors of neurological disorders: The Global Burden of Disease study 1990–2019. Frontiers in Public Health 10.
Ding, S.-L., Shen, C.-Y., 2008. Model of human aging: recent findings on Werner's and Hutchinson-Gilford progeria syndromes. Clin Interv Aging 3, 431-444.
Downes, N., Mullins, P., 2014. The development of myelin in the brain of the juvenile rat. Toxicol Pathol 42, 913-922.
Drouin-Ouellet, J., Legault, E.M., Nilsson, F., Pircs, K., Bouquety, J., Petit, F., Shrigley, S., Birtele, M., Pereira, M., Storm, P., Sharma, Y., Bruzelius, A., Vuono, R., Kele, M., Stoker, T.B., Ottosson, D.R., Falk, A., Jakobsson, J., Barker, R.A., Parmar, M., 2022. Age-related pathological impairments in directly reprogrammed dopaminergic neurons derived from patients with idiopathic Parkinson's disease. Stem Cell Reports 17, 2203-2219.
Duran, A.L., Potter, P., Wells, S., Kirkwood, T., von Zglinicki, T., McArdle, A., Scudamore, C., Meng, Q.J., de Haan, G., Corcoran, A., Bellantuono, I., 2013. Shared Ageing Research Models (ShARM): a new facility to support ageing research. Biogerontology 14, 789-794.
Faragher, R.G., 2015. Should we treat aging as a disease? The consequences and dangers of miscategorisation. Front Genet 6, 171.
Fernandes, J.T., Chutna, O., Chu, V., Conde, J.P., Outeiro, T.F., 2016. A Novel Microfluidic Cell Co-culture Platform for the Study of the Molecular Mechanisms of Parkinson's Disease and Other Synucleinopathies. Front Neurosci 10, 511.
Ferrington, D.A., Husom, A.D., Thompson, L.V., 2005. Altered proteasome structure, function, and oxidation in aged muscle. Faseb j 19, 644-646.
Flood, D.G., Reaume, A.G., Dorfman, K.S., Lin, Y.G., Lang, D.M., Trusko, S.P., Savage, M.J., Annaert, W.G., De Strooper, B., Siman, R., Scott, R.W., 2002. FAD mutant PS-1 gene-targeted mice: increased A beta 42 and A beta deposition without APP overproduction. Neurobiol Aging 23, 335-348.
Flurkey, K., M. Currer, J., Harrison, D.E., 2007. Chapter 20 - Mouse Models in Aging Research. In: Fox, J.G., Davisson, M.T., Quimby, F.W., Barthold, S.W., Newcomer, C.E., Smith, A.L. (Eds.), The Mouse in Biomedical Research (Second Edition). Academic Press, Burlington, pp. 637-672.
Fontán-Lozano, Á., Romero-Granados, R., Troncoso, J., Múnera, A., Delgado-García, J.M., Carrión, Á.M., 2008. Histone deacetylase inhibitors improve learning consolidation in young and in KA-induced-neurodegeneration and SAMP-8-mutant mice. Molecular and Cellular Neuroscience 39, 193-201.
Franceschi, C., Bonafè, M., Valensin, S., Olivieri, F., De Luca, M., Ottaviani, E., De Benedictis, G., 2000. Inflamm-aging. An evolutionary perspective on immunosenescence. Annals of the New York Academy of Sciences, pp. 244-254.
Franceschi, C., Campisi, J., 2014. Chronic inflammation (inflammaging) and its potential contribution to age-associated diseases. J Gerontol A Biol Sci Med Sci 69 Suppl 1, S4-9.
Fu, Y., Rusznák, Z., Herculano-Houzel, S., Watson, C., Paxinos, G., 2013. Cellular composition characterizing postnatal development and maturation of the mouse brain and spinal cord. Brain Struct Funct 218, 1337-1354.
Fumagalli, M., Rossiello, F., Clerici, M., Barozzi, S., Cittaro, D., Kaplunov, J.M., Bucci, G., Dobreva, M., Matti, V., Beausejour, C.M., Herbig, U., Longhese, M.P., d'Adda di Fagagna, F., 2012. Telomeric DNA damage is irreparable and causes persistent DNA-damage-response activation. Nat Cell Biol 14, 355-365.

Gao, Y., Tu, D., Yang, R., Chu, C.H., Hong, J.S., Gao, H.M., 2020. Through Reducing ROS Production, IL-10 Suppresses Caspase-1-Dependent IL-1β Maturation, thereby Preventing Chronic Neuroinflammation and Neurodegeneration. Int J Mol Sci 21.
Gáspár, A., Hutka, B., Ernyey, A.J., Tajti, B.T., Varga, B.T., Zádori, Z.S., Gyertyán, I., 2022. Performance of the intracerebroventricularly injected streptozotocin Alzheimer's disease model in a translationally relevant, aged and experienced rat population. Sci Rep 12, 20247.
Gatto, N., Dos Santos Souza, C., Shaw, A.C., Bell, S.M., Myszczynska, M.A., Powers, S., Meyer, K., Castelli, L.M., Karyka, E., Mortiboys, H., Azzouz, M., Hautbergue, G.M., Márkus, N.M., Shaw, P.J., Ferraiuolo, L., 2021. Directly converted astrocytes retain the ageing features of the donor fibroblasts and elucidate the astrocytic contribution to human CNS health and disease. Aging Cell 20, e13281.
Geifman, N., Rubin, E., 2013. The Mouse Age Phenome Knowledgebase and Disease-Specific Inter-Species Age Mapping. PLOS ONE 8, e81114.
Geraghty, R.J., Capes-Davis, A., Davis, J.M., Downward, J., Freshney, R.I., Knezevic, I., Lovell-Badge, R., Masters, J.R., Meredith, J., Stacey, G.N., Thraves, P., Vias, M., 2014. Guidelines for the use of cell lines in biomedical research. Br J Cancer 111, 1021-1046.
Ghosh, D., Levault, K.R., Brewer, G.J., 2014. Relative importance of redox buffers GSH and NAD(P)H in age-related neurodegeneration and Alzheimer disease-like mouse neurons. Aging Cell 13, 631-640.
González-Gualda, E., Baker, A.G., Fruk, L., Muñoz-Espín, D., 2021. A guide to assessing cellular senescence in vitro and in vivo. The FEBS Journal 288, 56-80.
Grimstad, Ø., 2016. Tumor Necrosis Factor and the Tenacious α. JAMA Dermatology 152, 557-557.
Gulen, M.F., Samson, N., Keller, A., Schwabenland, M., Liu, C., Glück, S., Thacker, V.V., Favre, L., Mangeat, B., Kroese, L.J., Krimpenfort, P., Prinz, M., Ablasser, A., 2023. cGAS–STING drives ageing-related inflammation and neurodegeneration. Nature 620, 374-380.
Gurkar, A.U., Niedernhofer, L.J., 2015. Comparison of mice with accelerated aging caused by distinct mechanisms. Exp Gerontol 68, 43-50.
Guzman-Martinez, L., Maccioni, R.B., Andrade, V., Navarrete, L.P., Pastor, M.G., Ramos-Escobar, N., 2019. Neuroinflammation as a Common Feature of Neurodegenerative Disorders. Frontiers in Pharmacology 10, 1008.
Gwinn, D.M., Shackelford, D.B., Egan, D.F., Mihaylova, M.M., Mery, A., Vasquez, D.S., Turk, B.E., Shaw, R.J., 2008. AMPK phosphorylation of raptor mediates a metabolic checkpoint. Mol Cell 30, 214-226.
Halliwell, E., Dittmar, H., 2003. A Qualitative Investigation of Women's and Men's Body Image Concerns and Their Attitudes Toward Aging. Sex Roles 49, 675-684.
Harkema, L., Youssef, S.A., de Bruin, A., 2016. Pathology of Mouse Models of Accelerated Aging. Vet Pathol 53, 366-389.
Hartmann, C., Herling, L., Hartmann, A., Köckritz, V., Fuellen, G., Walter, M., Hermann, A., 2023. Systematic estimation of biological age of in vitro cell culture systems by an age-associated marker panel. Frontiers in Aging 4.
Hartshorne, J.K., Germine, L.T., 2015. When Does Cognitive Functioning Peak? The Asynchronous Rise and Fall of Different Cognitive Abilities Across the Life Span. Psychological Science 26, 433-443.
Hayflick, L., 1965. The limited in vitro lifetime of human diploid cell strains. Experimental Cell Research 37, 614-636.
Heng, Y., Eggen, B.J.L., Boddeke, E.W.G.M., Kooistra, S.M., 2017. Mouse models of central nervous system ageing. Drug Discovery Today: Disease Models 25-26, 21-34.
Hirsch, C., Schildknecht, S., 2019. In Vitro Research Reproducibility: Keeping Up High Standards. Frontiers in Pharmacology 10.
Hoban, D.B., Connaughton, E., Connaughton, C., Hogan, G., Thornton, C., Mulcahy, P., Moloney, T.C., Dowd, E., 2013. Further characterisation of the LPS model of Parkinson's disease: a comparison of intra-nigral and intra-striatal lipopolysaccharide administration on motor function, microgliosis and nigrostriatal neurodegeneration in the rat. Brain Behav Immun 27, 91-100.
Holladay, S.D., Smialowicz, R.J., 2000. Development of the murine and human immune system: differential effects of immunotoxicants depend on time of exposure. Environ Health Perspect 108 Suppl 3, 463-473.

Hou, Y., Dan, X., Babbar, M., Wei, Y., Hasselbalch, S.G., Croteau, D.L., Bohr, V.A., 2019. Ageing as a risk factor for neurodegenerative disease. Nature Reviews Neurology 15, 565-581.
Hsieh, C.H., Shaltouki, A., Gonzalez, A.E., Bettencourt da Cruz, A., Burbulla, L.F., St Lawrence, E., Schüle, B., Krainc, D., Palmer, T.D., Wang, X., 2016. Functional Impairment in Miro Degradation and Mitophagy Is a Shared Feature in Familial and Sporadic Parkinson's Disease. Cell Stem Cell 19, 709-724.
Hu, Y., Fryatt, G.L., Ghorbani, M., Obst, J., Menassa, D.A., Martin-Estebane, M., Muntslag, T.A.O., Olmos-Alonso, A., Guerrero-Carrasco, M., Thomas, D., Cragg, M.S., Gomez-Nicola, D., 2021. Replicative senescence dictates the emergence of disease-associated microglia and contributes to Aβ pathology. Cell Reports 35.
Hughes, P., Marshall, D., Reid, Y., Parkes, H., Gelber, C., 2007. The costs of using unauthenticated, over-passaged cell lines: how much more data do we need? BioTechniques 43, 575-586.
Huh, C.J., Zhang, B., Victor, M.B., Dahiya, S., Batista, L.F.Z., Horvath, S., Yoo, A.S., 2016. Maintenance of age in human neurons generated by microRNA-based neuronal conversion of fibroblasts. Elife 5, e18648.
Hui, C.W., St-Pierre, M.-K., Detuncq, J., Aumailley, L., Dubois, M.-J., Couture, V., Skuk, D., Marette, A., Tremblay, J.P., Lebel, M., Tremblay, M.-È., 2018. Nonfunctional mutant Wrn protein leads to neurological deficits, neuronal stress, microglial alteration, and immune imbalance in a mouse model of Werner syndrome. Brain, Behavior, and Immunity 73, 450-469.
Ibebunjo, C., Chick, J.M., Kendall, T., Eash, J.K., Li, C., Zhang, Y., Vickers, C., Wu, Z., Clarke, B.A., Shi, J., Cruz, J., Fournier, B., Brachat, S., Gutzwiller, S., Ma, Q., Markovits, J., Broome, M., Steinkrauss, M., Skuba, E., Galarneau, J.R., Gygi, S.P., Glass, D.J., 2013. Genomic and proteomic profiling reveals reduced mitochondrial function and disruption of the neuromuscular junction driving rat sarcopenia. Mol Cell Biol 33, 194-212.
Igarashi, K., Takagi, M., Fukushima, Y., 2022. The Effects of Matcha and Decaffeinated Matcha on Learning, Memory and Proteomics of Hippocampus in Senescence-Accelerated (SAMP8) Mice. Nutrients 14.
Inesta-Vaquera, F., Weiland, F., Henderson, C.J., Wolf, C.R., 2022. In vivo stress reporters as early biomarkers of the cellular changes associated with progeria. J Cell Mol Med 26, 5463-5472.
Jackson Laboratory, T., 2020. Aged C57BL/6J Mice for Research Studies. Bar Harbor, Maine.
Jackson, S.J., Andrews, N., Ball, D., Bellantuono, I., Gray, J., Hachoumi, L., Holmes, A., Latcham, J., Petrie, A., Potter, P., Rice, A., Ritchie, A., Stewart, M., Strepka, C., Yeoman, M., Chapman, K., 2017. Does age matter? The impact of rodent age on study outcomes. Lab Anim 51, 160-169.
Jiang, H., Ren, Y., Yuen, E.Y., Zhong, P., Ghaedi, M., Hu, Z., Azabdaftari, G., Nakaso, K., Yan, Z., Feng, J., 2012. Parkin controls dopamine utilization in human midbrain dopaminergic neurons derived from induced pluripotent stem cells. Nat Commun 3, 668.
Jurk, D., Wang, C., Miwa, S., Maddick, M., Korolchuk, V., Tsolou, A., Gonos, E.S., Thrasivoulou, C., Saffrey, M.J., Cameron, K., von Zglinicki, T., 2012. Postmitotic neurons develop a p21-dependent senescence-like phenotype driven by a DNA damage response. Aging Cell 11, 996-1004.
Kaji, K., Ohta, T., Horie, N., Naru, E., Hasegawa, M., Kanda, N., 2009. Donor age reflects the replicative lifespan of human fibroblasts in culture. Human Cell 22, 38-42.
Kalia, L.V., Lang, A.E., 2015. Parkinson's disease. The Lancet 386, 896-912.
Kaluski, S., Portillo, M., Besnard, A., Stein, D., Einav, M., Zhong, L., Ueberham, U., Arendt, T., Mostoslavsky, R., Sahay, A., Toiber, D., 2017. Neuroprotective Functions for the Histone Deacetylase SIRT6. Cell Reports 18, 3052-3062.
Karasawa, N., Nagatsu, I., Sakai, K., Nagatsu, T., Watanabe, K., Onozuka, M., 1997. Immunocytochemical study of catecholaminergic neurons in the senescence-accelerated mouse (SAM-P8) brain. Journal of Neural Transmission 104, 1267-1275.
Kaufman, J.-M., Lapauw, B., Mahmoud, A., T'Sjoen, G., Huhtaniemi, I.T., 2019. Aging and the Male Reproductive System. Endocrine Reviews 40, 906-972.
Kawamata, T., Akiguchi, I., Maeda, K., Tanaka, C., Higuchi, K., Hosokawa, M., Takeda, T., 1998. Age-related changes in the brains of senescence-accelerated mice (SAM): Association with glial and endothelial reactions. Microscopy Research and Technique 43, 59-67.
Kawashima, H., Strobel, H.W., 1995. cDNA cloning of a novel rat brain cytochrome P450 belonging to the CYP2D subfamily. Biochem Biophys Res Commun 209, 535-540.

Kazyken, D., Magnuson, B., Bodur, C., Acosta-Jaquez, H.A., Zhang, D., Tong, X., Barnes, T.M., Steinl, G.K., Patterson, N.E., Altheim, C.H., Sharma, N., Inoki, K., Cartee, G.D., Bridges, D., Yin, L., Riddle, S.M., Fingar, D.C., 2019. AMPK directly activates mTORC2 to promote cell survival during acute energetic stress. Sci Signal 12.
Kelmer Sacramento, E., Kirkpatrick, J.M., Mazzetto, M., Baumgart, M., Bartolome, A., Di Sanzo, S., Caterino, C., Sanguanini, M., Papaevgeniou, N., Lefaki, M., Childs, D., Bagnoli, S., Terzibasi Tozzini, E., Di Fraia, D., Romanov, N., Sudmant, P.H., Huber, W., Chondrogianni, N., Vendruscolo, M., Cellerino, A., Ori, A., 2020. Reduced proteasome activity in the aging brain results in ribosome stoichiometry loss and aggregation. Mol Syst Biol 16, e9596.
Khan, A.M., Babcock, A.A., Saeed, H., Myhre, C.L., Kassem, M., Finsen, B., 2015. Telomere dysfunction reduces microglial numbers without fully inducing an aging phenotype. Neurobiology of Aging 36, 2164-2175.
Khokhar, J.Y., Tyndale, R.F., 2011. Drug metabolism within the brain changes drug response: selective manipulation of brain CYP2B alters propofol effects. Neuropsychopharmacology 36, 692-700.
Kim, H., Park, H.J., Choi, H., Chang, Y., Park, H., Shin, J., Kim, J., Lengner, C.J., Lee, Y.K., Kim, J., 2019. Modeling G2019S-LRRK2 Sporadic Parkinson's Disease in 3D Midbrain Organoids. Stem Cell Reports 12, 518-531.
Kim, H.L., Lee, S.K., Min, D.E., Bastola, T., Chang, B.Y., Bae, J.H., Lee, D.R., 2023. Effects of Scrophularia buergeriana Extract (Brainon®) on Aging-Induced Memory Impairment in SAMP8 Mice. Current Issues in Molecular Biology, pp. 1287-1305.
Kim, J., Sturgill, D., Tran, A.D., Sinclair, D.A., Oberdoerffer, P., 2016. Controlled DNA double-strand break induction in mice reveals post-damage transcriptome stability. Nucleic Acids Res 44, e64.
Kim, K.M., Thaqi, M., Peterson, D.A., Marr, R.A., 2021. Induced Neurons for Disease Modeling and Repair: A Focus on Non-fibroblastic Cell Sources in Direct Reprogramming. Frontiers in Bioengineering and Biotechnology 9.
Kim, Y., Zheng, X., Ansari, Z., Bunnell, M.C., Herdy, J.R., Traxler, L., Lee, H., Paquola, A.C.M., Blithikioti, C., Ku, M., Schlachetzki, J.C.M., Winkler, J., Edenhofer, F., Glass, C.K., Paucar, A.A., Jaeger, B.N., Pham, S., Boyer, L., Campbell, B.C., Hunter, T., Mertens, J., Gage, F.H., 2018. Mitochondrial Aging Defects Emerge in Directly Reprogrammed Human Neurons due to Their Metabolic Profile. Cell Rep 23, 2550-2558.
Kinirons, M.T., O'Mahony, M.S., 2004. Drug metabolism and ageing. Br J Clin Pharmacol 57, 540-544.
Ko, F., Yu, Q., Xue, Q.L., Yao, W., Brayton, C., Yang, H., Fedarko, N., Walston, J., 2012. Inflammation and mortality in a frail mouse model. Age (Dordr) 34, 705-715.
Kõks, S., Dogan, S., Tuna, B.G., González-Navarro, H., Potter, P., Vandenbroucke, R.E., 2016. Mouse models of ageing and their relevance to disease. Mechanisms of Ageing and Development 160, 41-53.
Komori, M., 1993. A novel P450 expressed at the high level in rat brain. Biochem Biophys Res Commun 196, 721-728.
Kouroupi, G., Taoufik, E., Vlachos, I.S., Tsioras, K., Antoniou, N., Papastefanaki, F., Chroni-Tzartou, D., Wrasidlo, W., Bohl, D., Stellas, D., Politis, P.K., Vekrellis, K., Papadimitriou, D., Stefanis, L., Bregestovski, P., Hatzigeorgiou, A.G., Masliah, E., Matsas, R., 2017. Defective synaptic connectivity and axonal neuropathology in a human iPSC-based model of familial Parkinson's disease. Proc Natl Acad Sci U S A 114, E3679-e3688.
Kumagai, N., Chiba, Y., Hosono, M., Fujii, M., Kawamura, N., Keino, H., Yoshikawa, K., Ishii, S., Saitoh, Y., Satoh, M., Shimada, A., Hosokawa, M., 2007. Involvement of pro-inflammatory cytokines and microglia in an age-associated neurodegeneration model, the SAMP10 mouse. Brain Research 1185, 75-85.
Kurz, D.J., Decary, S., Hong, Y., Erusalimsky, J.D., 2000. Senescence-associated (beta)-galactosidase reflects an increase in lysosomal mass during replicative ageing of human endothelial cells. Journal of Cell Science 113, 3613-3622.
Lam, D., Enright, H.A., Cadena, J., Peters, S.K.G., Sales, A.P., Osburn, J.J., Soscia, D.A., Kulp, K.S., Wheeler, E.K., Fischer, N.O., 2019. Tissue-specific extracellular matrix accelerates the formation of neural networks and communities in a neuron-glia co-culture on a multi-electrode array. Scientific Reports 9, 4159.

Lapasset, L., Milhavet, O., Prieur, A., Besnard, E., Babled, A., Aït-Hamou, N., Leschik, J., Pellestor, F., Ramirez, J.M., De Vos, J., Lehmann, S., Lemaitre, J.M., 2011. Rejuvenating senescent and centenarian human cells by reprogramming through the pluripotent state. Genes Dev 25, 2248-2253.
Lebel, M., Leder, P., 1998. A deletion within the murine Werner syndrome helicase induces sensitivity to inhibitors of topoisomerase and loss of cellular proliferative capacity. Proceedings of the National Academy of Sciences 95, 13097-13102.
Lenoir, C., Rollason, V., Desmeules, J.A., Samer, C.F., 2021. Influence of Inflammation on Cytochromes P450 Activity in Adults: A Systematic Review of the Literature. Frontiers in Pharmacology 12.
Lian, W.W., Zhou, W., Zhang, B.Y., Jia, H., Xu, L.J., Liu, A.L., Du, G.H., 2021. DL0410 ameliorates cognitive disorder in SAMP8 mice by promoting mitochondrial dynamics and the NMDAR-CREB-BDNF pathway. Acta Pharmacol Sin 42, 1055-1068.
Liao, C.Y., Rikke, B.A., Johnson, T.E., Diaz, V., Nelson, J.F., 2010. Genetic variation in the murine lifespan response to dietary restriction: from life extension to life shortening. Aging Cell 9, 92-95.
Limone, F., Klim, J.R., Mordes, D.A., 2022. Pluripotent stem cell strategies for rebuilding the human brain. Front Aging Neurosci 14, 1017299.
Liu, W., Liu, C., Zhu, J.X., Li, A.H., Zhao, Z.Q., Yin, B., Peng, X.Z., 2010. D-Tyr-tRNA(Tyr) deacylase, a new role in Alzheimer's-associated disease in SAMP8 mice. Chin Med Sci J 25, 90-94.
Lok, K., Zhao, H., Shen, H., Wang, Z., Gao, X., Zhao, W., Yin, M., 2013. Characterization of the APP/PS1 mouse model of Alzheimer's disease in senescence accelerated background. Neuroscience Letters 557, 84-89.
Longo, V.D., Di Tano, M., Mattson, M.P., Guidi, N., 2021. Intermittent and periodic fasting, longevity and disease. Nature Aging 1, 47-59.
López-Otín, C., Blasco, M.A., Partridge, L., Serrano, M., Kroemer, G., 2023. Hallmarks of aging: An expanding universe. Cell 186, 243-278.
Luchena, C., Zuazo-Ibarra, J., Valero, J., Matute, C., Alberdi, E., Capetillo-Zarate, E., 2022. A Neuron, Microglia, and Astrocyte Triple Co-culture Model to Study Alzheimer's Disease. Frontiers in Aging Neuroscience 14.
Magini, A., Polchi, A., Tozzi, A., Tancini, B., Tantucci, M., Urbanelli, L., Borsello, T., Calabresi, P., Emiliani, C., 2015. Abnormal cortical lysosomal β-hexosaminidase and β-galactosidase activity at post-synaptic sites during Alzheimer's disease progression. Int J Biochem Cell Biol 58, 62-70.
Malerba, H.N., Pereira, A.A.R., Pierrobon, M.F., Abrao, G.S., Toricelli, M., Akamine, E.H., Buck, H.S., Viel, T.A., 2021. Combined Neuroprotective Strategies Blocked Neurodegeneration and Improved Brain Function in Senescence-Accelerated Mice. Front Aging Neurosci 13, 681498.
Mann, A., Miksys, S.L., Gaedigk, A., Kish, S.J., Mash, D.C., Tyndale, R.F., 2012. The neuroprotective enzyme CYP2D6 increases in the brain with age and is lower in Parkinson's disease patients. Neurobiol Aging 33, 2160-2171.
Massip, L., Garand, C., Turaga, R.V.N., Deschênes, F., Thorin, E., Lebel, M., 2006. Increased insulin, triglycerides, reactive oxygen species, and cardiac fibrosis in mice with a mutation in the helicase domain of the Werner syndrome gene homologue. Experimental Gerontology 41, 157-168.
Mayne, K., White, J.A., McMurran, C.E., Rivera, F.J., de la Fuente, A.G., 2020. Aging and Neurodegenerative Disease: Is the Adaptive Immune System a Friend or Foe? Frontiers in Aging Neuroscience 12.
Miksys, S., Tyndale, R.F., 2013. Cytochrome P450-mediated drug metabolism in the brain. J Psychiatry Neurosci 38, 152-163.
Miller, J.D., Ganat, Y.M., Kishinevsky, S., Bowman, R.L., Liu, B., Tu, E.Y., Mandal, P.K., Vera, E., Shim, J.W., Kriks, S., Taldone, T., Fusaki, N., Tomishima, M.J., Krainc, D., Milner, T.A., Rossi, D.J., Studer, L., 2013. Human iPSC-based modeling of late-onset disease via progerin-induced aging. Cell Stem Cell 13, 691-705.
Miyamoto, M., 1997. Characteristics of age-related behavioral changes in senescence-accelerated mouse SAMP8 and SAMP10. Experimental Gerontology 32, 139-148.
Miyamoto, M., Kiyota, Y., Nishiyama, M., Nagaoka, A., 1992. Senescence-accelerated mouse (SAM): age-related reduced anxiety-like behavior in the SAM-P/8 strain. Physiol Behav 51, 979-985.
Molina-Martínez, P., Corpas, R., García-Lara, E., Cosín-Tomás, M., Cristòfol, R., Kaliman, P., Solà, C., Molinuevo, J.L., Sánchez-Valle, R., Antonell, A., Lladó, A., Sanfeliu, C., 2020. Microglial

Hyperreactivity Evolved to Immunosuppression in the Hippocampus of a Mouse Model of Accelerated Aging and Alzheimer's Disease Traits. Front Aging Neurosci 12, 622360.
Moreira, H.S., Costa, A.S., Machado, Á., Castro, S.L., Lima, C.F., Vicente, S.G., 2019. Distinguishing mild cognitive impairment from healthy aging and Alzheimer's Disease: The contribution of the INECO Frontal Screening (IFS). PLoS One 14, e0221873.
Morita, M., Gravel, S.-P., Chénard, V., Sikström, K., Zheng, L., Alain, T., Gandin, V., Avizonis, D., Arguello, M., Zakaria, C., McLaughlan, S., Nouet, Y., Pause, A., Pollak, M., Gottlieb, E., Larsson, O., St-Pierre, J., Topisirovic, I., Sonenberg, N., 2013. mTORC1 Controls Mitochondrial Activity and Biogenesis through 4E-BP-Dependent Translational Regulation. Cell Metab 18, 698-711.
Mostoslavsky, R., Chua, K.F., Lombard, D.B., Pang, W.W., Fischer, M.R., Gellon, L., Liu, P., Mostoslavsky, G., Franco, S., Murphy, M.M., Mills, K.D., Patel, P., Hsu, J.T., Hong, A.L., Ford, E., Cheng, H.-L., Kennedy, C., Nunez, N., Bronson, R., Frendewey, D., Auerbach, W., Valenzuela, D., Karow, M., Hottiger, M.O., Hursting, S., Barrett, J.C., Guarente, L., Mulligan, R., Demple, B., Yancopoulos, G.D., Alt, F.W., 2006. Genomic Instability and Aging-like Phenotype in the Absence of Mammalian SIRT6. Cell 124, 315-329.
Muñoz-Manchado, A.B., Villadiego, J., Romo-Madero, S., Suárez-Luna, N., Bermejo-Navas, A., Rodríguez-Gómez, J.A., Garrido-Gil, P., Labandeira-García, J.L., Echevarría, M., López-Barneo, J., Toledo-Aral, J.J., 2016. Chronic and progressive Parkinson's disease MPTP model in adult and aged mice. J Neurochem 136, 373-387.
Mutemberezi, V., Buisseret, B., Masquelier, J., Guillemot-Legris, O., Alhouayek, M., Muccioli, G.G., 2018. Oxysterol levels and metabolism in the course of neuroinflammation: insights from in vitro and in vivo models. J Neuroinflammation 15, 74.
Nelson, G., Kucheryavenko, O., Wordsworth, J., von Zglinicki, T., 2018. The senescent bystander effect is caused by ROS-activated NF-κB signalling. Mechanisms of Ageing and Development 170, 30-36.
Ocampo, A., Reddy, P., Martinez-Redondo, P., Platero-Luengo, A., Hatanaka, F., Hishida, T., Li, M., Lam, D., Kurita, M., Beyret, E., Araoka, T., Vazquez-Ferrer, E., Donoso, D., Roman, J.L., Xu, J., Rodriguez Esteban, C., Nuñez, G., Nuñez Delicado, E., Campistol, J.M., Guillen, I., Guillen, P., Izpisua Belmonte, J.C., 2016. In Vivo Amelioration of Age-Associated Hallmarks by Partial Reprogramming. Cell 167, 1719-1733.e1712.
Olivieri, F., Prattichizzo, F., Grillari, J., Balistreri, C.R., 2018. Cellular Senescence and Inflammaging in Age-Related Diseases. Mediators Inflamm 2018, 9076485.
Onodera, T., Watanabe, R., Tha, K.K., Hayashi, Y., Murayama, T., Okuma, Y., Ono, C., Oketani, Y., Hosokawa, M., Nomura, Y., 2000. Depressive Behavior and Alterations in Receptors for Dopamine and 5-Hydroxytryptamine in the Brain of the Senescence Accelerated Mouse (SAM)-P10. Japanese Journal of Pharmacology 83, 312-318.
Osorio, F.G., Navarro, C.L., Cadiñanos, J., López-Mejía, I.C., Quirós, P.M., Bartoli, C., Rivera, J., Tazi, J., Guzmán, G., Varela, I., Depetris, D., de Carlos, F., Cobo, J., Andrés, V., De Sandre-Giovannoli, A., Freije, J.M.P., Lévy, N., López-Otín, C., 2011. Splicing-Directed Therapy in a New Mouse Model of Human Accelerated Aging. Sci Transl Med 3, 106ra107-106ra107.
Pandey, S., Jirásko, M., Lochman, J., Chvátal, A., Chottova Dvorakova, M., Kučera, R., 2022. iPSCs in Neurodegenerative Disorders: A Unique Platform for Clinical Research and Personalized Medicine. J Pers Med 12.
Percie du Sert, N., Hurst, V., Ahluwalia, A., Alam, S., Avey, M.T., Baker, M., Browne, W.J., Clark, A., Cuthill, I.C., Dirnagl, U., Emerson, M., Garner, P., Holgate, S.T., Howells, D.W., Karp, N.A., Lazic, S.E., Lidster, K., MacCallum, C.J., Macleod, M., Pearl, E.J., Petersen, O.H., Rawle, F., Reynolds, P., Rooney, K., Sena, E.S., Silberberg, S.D., Steckler, T., Würbel, H., 2020. The ARRIVE guidelines 2.0: Updated guidelines for reporting animal research. PLOS Biology 18, e3000410.
Phipps, S.M.O., Berletch, J.B., Andrews, L.G., Tollefsbol, T.O., 2007. Aging cell culture: methods and observations. Methods Mol Biol 371, 9-19.
Pinelli, C.J., Leri, F., Turner, P.V., 2017. Long Term Physiologic and Behavioural Effects of Housing Density and Environmental Resource Provision for Adult Male and Female Sprague Dawley Rats. Animals (Basel) 7.
Ponnappan, U., Zhong, M., Trebilcock, G.U., 1999. Decreased proteasome-mediated degradation in T cells from the elderly: A role in immune senescence. Cell Immunol 192, 167-174.

Prigione, A., Hossini, A.M., Lichtner, B., Serin, A., Fauler, B., Megges, M., Lurz, R., Lehrach, H., Makrantonaki, E., Zouboulis, C.C., Adjaye, J., 2011. Mitochondrial-associated cell death mechanisms are reset to an embryonic-like state in aged donor-derived iPS cells harboring chromosomal aberrations. PLoS One 6, e27352.
Qadan, M.A., Piuzzi, N.S., Boehm, C., Bova, W., Moos, M., Jr., Midura, R.J., Hascall, V.C., Malcuit, C., Muschler, G.F., 2018. Variation in primary and culture-expanded cells derived from connective tissue progenitors in human bone marrow space, bone trabecular surface and adipose tissue. Cytotherapy 20, 343-360.
Querfurth, H., Lee, H.-K., 2021. Mammalian/mechanistic target of rapamycin (mTOR) complexes in neurodegeneration. Molecular Neurodegeneration 16, 44.
Quinn, R., 2005. Comparing rat's to human's age: how old is my rat in people years? Nutrition 21, 775-777.
Raja, W.K., Mungenast, A.E., Lin, Y.T., Ko, T., Abdurrob, F., Seo, J., Tsai, L.H., 2016. Self-Organizing 3D Human Neural Tissue Derived from Induced Pluripotent Stem Cells Recapitulate Alzheimer's Disease Phenotypes. PLoS One 11, e0161969.
Richwine, A.F., Sparkman, N.L., Dilger, R.N., Buchanan, J.B., Johnson, R.W., 2009. Cognitive deficits in interleukin-10-deficient mice after peripheral injection of lipopolysaccharide. Brain Behav Immun 23, 794-802.
Roncal-Jimenez, C.A., Ishimoto, T., Lanaspa, M.A., Milagres, T., Hernando, A.A., Jensen, T., Miyazaki, M., Doke, T., Hayasaki, T., Nakagawa, T., Marumaya, S., Long, D.A., Garcia, G.E., Kuwabara, M., Sánchez-Lozada, L.G., Kang, D.H., Johnson, R.J., 2016. Aging-associated renal disease in mice is fructokinase dependent. Am J Physiol Renal Physiol 311, F722-f730.
Ross, A., Xing, V., Wang, T.T., Bureau, S.C., Link, G.A., Fortin, T., Zhang, H., Hayley, S., Sun, H., 2020. Alleviating toxic α-Synuclein accumulation by membrane depolarization: evidence from an in vitro model of Parkinson's disease. Molecular Brain 13, 108.
Sánchez-Danés, A., Richaud-Patin, Y., Carballo-Carbajal, I., Jiménez-Delgado, S., Caig, C., Mora, S., Di Guglielmo, C., Ezquerra, M., Patel, B., Giralt, A., Canals, J.M., Memo, M., Alberch, J., López-Barneo, J., Vila, M., Cuervo, A.M., Tolosa, E., Consiglio, A., Raya, A., 2012. Disease-specific phenotypes in dopamine neurons from human iPS-based models of genetic and sporadic Parkinson's disease. EMBO Mol Med 4, 380-395.
Sandusky, G.E., Van Pelt, C.S., Todd, G.C., Wightman, K., 1988. An immunocytochemical study of pituitary adenomas and focal hyperplasia in old Sprague-Dawley and Fischer 344 rats. Toxicol Pathol 16, 376-380.
Sapieha, P., Mallette, F.A., 2018. Cellular Senescence in Postmitotic Cells: Beyond Growth Arrest. Trends in Cell Biology 28, 595-607.
Scheffold, A., Holtman, I.R., Dieni, S., Brouwer, N., Katz, S.-F., Jebaraj, B.M.C., Kahle, P.J., Hengerer, B., Lechel, A., Stilgenbauer, S., Boddeke, E.W.G.M., Eggen, B.J.L., Rudolph, K.-L., Biber, K., 2016. Telomere shortening leads to an acceleration of synucleinopathy and impaired microglia response in a genetic mouse model. Acta Neuropathologica Communications 4, 87.
Schneider, E.L., Mitsui, Y., 1976. The relationship between in vitro cellular aging and in vivo human age. Proc Natl Acad Sci U S A 73, 3584-3588.
Schwab, N., Taskina, D., Leung, E., Innes, B.T., Bader, G.D., Hazrati, L.-N., 2022. Neurons and glial cells acquire a senescent signature after repeated mild traumatic brain injury in a sex-dependent manner. Frontiers in Neuroscience 16.
Serrano, M., Lin, A.W., McCurrach, M.E., Beach, D., Lowe, S.W., 1997. Oncogenic ras Provokes Premature Cell Senescence Associated with Accumulation of p53 and p16INK4a. Cell 88, 593-602.
Sharma, K., Darvas, M., Keene, C.D., Niedernhofer, L.J., Ladiges, W., 2018. Modeling Alzheimer's disease in progeria mice. An age-related concept. Pathobiol Aging Age Relat Dis 8, 1524815.
Shavali, S., Combs, C.K., Ebadi, M., 2006. Reactive Macrophages Increase Oxidative Stress and Alpha-Synuclein Nitration During Death of Dopaminergic Neuronal Cells in Co-Culture: Relevance to Parkinson's Disease. Neurochemical Research 31, 85-94.
Sherer, T.B., Betarbet, R., Testa, C.M., Seo, B.B., Richardson, J.R., Kim, J.H., Miller, G.W., Yagi, T., Matsuno-Yagi, A., Greenamyre, J.T., 2003. Mechanism of toxicity in rotenone models of Parkinson's disease. J Neurosci 23, 10756-10764.

Shih, P.H., Chan, Y.C., Liao, J.W., Wang, M.F., Yen, G.C., 2010. Antioxidant and cognitive promotion effects of anthocyanin-rich mulberry (Morus atropurpurea L.) on senescence-accelerated mice and prevention of Alzheimer's disease. J Nutr Biochem 21, 598-605.
Shimada, A., Hasegawa-Ishii, S., 2011. Senescence-accelerated Mice (SAMs) as a Model for Brain Aging and Immunosenescence. Aging Dis 2, 414-435.
Shimada, A., Hosokawa, M., Ohta, A., Akiguchi, I., Takeda, T., 1994. Localization of atrophy-prone areas in the aging mouse brain: Comparison between the brain atrophy model SAM-P/10 and the normal control SAM-R/1. Neuroscience 59, 859-869.
Shimada, A., Keino, H., Kawamura, N., Chiba, Y., Hosokawa, M., 2008. Limbic structures are prone to age-related impairments in proteasome activity and neuronal ubiquitinated inclusions in SAMP10 mouse: a model of cerebral degeneration. Neuropathol Appl Neurobiol 34, 33-51.
Shimada, A., Keino, H., Satoh, M., Kishikawa, M., Seriu, N., Hosokawa, M., 2002. Age-Related Progressive Neuronal DNA Damage Associated With Cerebral Degeneration in a Mouse Model of Accelerated Senescence. The Journals of Gerontology: Series A 57, B415-B421.
Shimada, A., Tsuzuki, M., Keino, H., Satoh, M., Chiba, Y., Saitoh, Y., Hosokawa, M., 2006. Apical vulnerability to dendritic retraction in prefrontal neurones of ageing SAMP10 mouse: a model of cerebral degeneration. Neuropathology and Applied Neurobiology 32, 1-14.
Shirasuna, K., Iwata, H., 2017. Effect of aging on the female reproductive function. Contracept Reprod Med 2, 23.
Shou, Y., Liang, F., Xu, S., Li, X., 2020. The Application of Brain Organoids: From Neuronal Development to Neurological Diseases. Frontiers in Cell and Developmental Biology 8.
Simon, M.M., Greenaway, S., White, J.K., Fuchs, H., Gailus-Durner, V., Wells, S., Sorg, T., Wong, K., Bedu, E., Cartwright, E.J., Dacquin, R., Djebali, S., Estabel, J., Graw, J., Ingham, N.J., Jackson, I.J., Lengeling, A., Mandillo, S., Marvel, J., Meziane, H., Preitner, F., Puk, O., Roux, M., Adams, D.J., Atkins, S., Ayadi, A., Becker, L., Blake, A., Brooker, D., Cater, H., Champy, M.-F., Combe, R., Danecek, P., di Fenza, A., Gates, H., Gerdin, A.-K., Golini, E., Hancock, J.M., Hans, W., Hölter, S.M., Hough, T., Jurdic, P., Keane, T.M., Morgan, H., Müller, W., Neff, F., Nicholson, G., Pasche, B., Roberson, L.-A., Rozman, J., Sanderson, M., Santos, L., Selloum, M., Shannon, C., Southwell, A., Tocchini-Valentini, G.P., Vancollie, V.E., Westerberg, H., Wurst, W., Zi, M., Yalcin, B., Ramirez-Solis, R., Steel, K.P., Mallon, A.-M., de Angelis, M.H., Herault, Y., Brown, S.D.M., 2013. A comparative phenotypic and genomic analysis of C57BL/6J and C57BL/6N mouse strains. Genome Biology 14, R82.
Smith, J.R., Venable, S., Roberts, T.W., Metter, E.J., Monticone, R., Schneider, E.L., 2002. Relationship Between In Vivo Age and In Vitro Aging: Assessment of 669 Cell Cultures Derived From Members of The Baltimore Longitudinal Study of Aging. The Journals of Gerontology: Series A 57, B239-B246.
Soerens, A.G., Künzli, M., Quarnstrom, C.F., Scott, M.C., Swanson, L., Locquiao, J.J., Ghoneim, H.E., Zehn, D., Youngblood, B., Vezys, V., Masopust, D., 2023. Functional T cells are capable of supernumerary cell division and longevity. Nature 614, 762-766.
Strait, J.B., Lakatta, E.G., 2012. Aging-associated cardiovascular changes and their relationship to heart failure. Heart Fail Clin 8, 143-164.
Suhr, S.T., Chang, E.A., Rodriguez, R.M., Wang, K., Ross, P.J., Beyhan, Z., Murthy, S., Cibelli, J.B., 2009. Telomere dynamics in human cells reprogrammed to pluripotency. PLoS One 4, e8124.
Sun, L., Wu, J., Du, F., Chen, X., Chen, Z.J., 2013. Cyclic GMP-AMP synthase is a cytosolic DNA sensor that activates the type I interferon pathway. Science 339, 786-791.
Sun, M., McDonald, S.J., Brady, R.D., Collins-Praino, L., Yamakawa, G.R., Monif, M., O'Brien, T.J., Cloud, G.C., Sobey, C.G., Mychasiuk, R., Loane, D.J., Shultz, S.R., 2020. The need to incorporate aged animals into the preclinical modeling of neurological conditions. Neuroscience & Biobehavioral Reviews 109, 114-128.
Takahashi, H., Sakamoto, J., Ohta, H., Miyamoto, M., 2004. Age-related decrease in spontaneity observed in senescence-accelerated mice (SAMP10) and the involvement of the dopaminergic system in behavioral disorders. International Congress Series 1260, 309-314.
Takahashi, K., Yamanaka, S., 2006. Induction of pluripotent stem cells from mouse embryonic and adult fibroblast cultures by defined factors. Cell 126, 663-676.

Takeda, T., 2009. Senescence-Accelerated Mouse (SAM) with Special References to Neurodegeneration Models, SAMP8 and SAMP10 Mice. Neurochemical Research 34, 639-659.
Takeda, T., Hosokawa, M., Takeshita, S., Irino, M., Higuchi, K., Matsushita, T., Tomita, Y., Yasuhira, K., Hamamoto, H., Shimizu, K., Ishii, M., Yamamuro, T., 1981. A new murine model of accelerated senescence. Mechanisms of Ageing and Development 17, 183-194.
Takemura, M., Nakamura, S., Akiguchi, I., Ueno, M., Oka, N., Ishikawa, S., Shimada, A., Kimura, J., Takeda, T., 1993. Beta/A4 proteinlike immunoreactive granular structures in the brain of senescence-accelerated mouse. Am J Pathol 142, 1887-1897.
Tang, Y., Liu, M.L., Zang, T., Zhang, C.L., 2017. Direct Reprogramming Rather than iPSC-Based Reprogramming Maintains Aging Hallmarks in Human Motor Neurons. Front Mol Neurosci 10, 359.
Timmons, J., Brenner, C., 2023. Matters Arising: The Information Theory of Aging Has Not Been Tested.
Toricelli, M., Evangelista, S.R., Buck, H.S., Viel, T.A., 2021. Microdose Lithium Treatment Reduced Inflammatory Factors and Neurodegeneration in Organotypic Hippocampal Culture of Old SAMP-8 Mice. Cellular and Molecular Neurobiology 41, 1509-1520.
Toth, L., Czigler, A., Hegedus, E., Komaromy, H., Amrein, K., Czeiter, E., Yabluchanskiy, A., Koller, A., Orsi, G., Perlaki, G., Schwarcz, A., Buki, A., Ungvari, Z., Toth, P.J., 2022. Age-related decline in circulating IGF-1 associates with impaired neurovascular coupling responses in older adults. GeroScience 44, 2771-2783.
Toth, L.A., 2018. Identifying and Implementing Endpoints for Geriatric Mice. Comp Med 68, 439-451.
Toye, A.A., Lippiat, J.D., Proks, P., Shimomura, K., Bentley, L., Hugill, A., Mijat, V., Goldsworthy, M., Moir, L., Haynes, A., Quarterman, J., Freeman, H.C., Ashcroft, F.M., Cox, R.D., 2005. A genetic and physiological study of impaired glucose homeostasis control in C57BL/6J mice. Diabetologia 48, 675-686.
Ungerstedt, U., 1968. 6-Hydroxy-dopamine induced degeneration of central monoamine neurons. Eur J Pharmacol 5, 107-110.
van Dijk, K.D., Persichetti, E., Chiasserini, D., Eusebi, P., Beccari, T., Calabresi, P., Berendse, H.W., Parnetti, L., van de Berg, W.D., 2013. Changes in endolysosomal enzyme activities in cerebrospinal fluid of patients with Parkinson's disease. Mov Disord 28, 747-754.
Vaupel, J.W., 2010. Biodemography of human ageing. Nature 464, 536-542.
Vela, S., Sainz, N., Moreno-Aliaga, M.J., Solas, M., Ramirez, M.J., 2019. DHA Selectively Protects SAMP-8-Associated Cognitive Deficits Through Inhibition of JNK. Mol Neurobiol 56, 1618-1627.
Victorelli, S., Salmonowicz, H., Chapman, J., Martini, H., Vizioli, M.G., Riley, J.S., Cloix, C., Hall-Younger, E., Machado Espindola-Netto, J., Jurk, D., Lagnado, A.B., Sales Gomez, L., Farr, J.N., Saul, D., Reed, R., Kelly, G., Eppard, M., Greaves, L.C., Dou, Z., Pirius, N., Szczepanowska, K., Porritt, R.A., Huang, H., Huang, T.Y., Mann, D.A., Masuda, C.A., Khosla, S., Dai, H., Kaufmann, S.H., Zacharioudakis, E., Gavathiotis, E., LeBrasseur, N.K., Lei, X., Sainz, A.G., Korolchuk, V.I., Adams, P.D., Shadel, G.S., Tait, S.W.G., Passos, J.F., 2023. Apoptotic stress causes mtDNA release during senescence and drives the SASP. Nature 622, 627-636.
Vierbuchen, T., Ostermeier, A., Pang, Z.P., Kokubu, Y., Südhof, T.C., Wernig, M., 2010. Direct conversion of fibroblasts to functional neurons by defined factors. Nature 463, 1035-1041.
Voulgaris, D., Nikolakopoulou, P., Herland, A., 2022. Generation of Human iPSC-Derived Astrocytes with a mature star-shaped phenotype for CNS modeling. Stem Cell Rev Rep 18, 2494-2512.
Walston, J., Fedarko, N., Yang, H., Leng, S., Beamer, B., Espinoza, S., Lipton, A., Zheng, H., Becker, K., 2008. The physical and biological characterization of a frail mouse model. J Gerontol A Biol Sci Med Sci 63, 391-398.
Wang, X., Wang, Y., Yu, S., Ren, L., 2018. Effect of Electroacupuncture on Levels of β-amyloid and Neprilysin Proteins in the Cerebral Cortex of Alzheimer's Disease Mice Based on "Mutual Assistance of Kidney and Brain" Theory. Zhen Ci Yan Jiu 43, 20-24.
Wang, Y., Dong, C., Han, Y., Gu, Z., Sun, C., 2022. Immunosenescence, aging and successful aging. Front Immunol 13, 942796.
Weston, L.L., Jiang, S., Chisholm, D., Jantzie, L.L., Bhaskar, K., 2021. Interleukin-10 deficiency exacerbates inflammation-induced tau pathology. J Neuroinflammation 18, 161.
Wong, W., 2020. Economic burden of Alzheimer disease and managed care considerations. Am J Manag Care 26, S177-s183.

Wu, K.-C., Lin, C.-J., 2019. The regulation of drug-metabolizing enzymes and membrane transporters by inflammation: Evidences in inflammatory diseases and age-related disorders. Journal of Food and Drug Analysis 27, 48-59.
Xia, S., Zhang, X., Zheng, S., Khanabdali, R., Kalionis, B., Wu, J., Wan, W., Tai, X., 2016. An Update on Inflamm-Aging: Mechanisms, Prevention, and Treatment. J Immunol Res 2016, 8426874.
Xicoy, H., Wieringa, B., Martens, G.J.M., 2017. The SH-SY5Y cell line in Parkinson's disease research: a systematic review. Molecular Neurodegeneration 12, 10.
Yager, J.Y., Thornhill, J.A., 1997. The effect of age on susceptibility to hypoxic-ischemic brain damage. Neurosci Biobehav Rev 21, 167-174.
Yang, C., Pang, Y., Huang, Y., Ye, F., Chen, X., Gao, Y., Zhang, C., Yao, L., Gao, J., 2022. Single-cell transcriptomics identifies premature aging features of TERC-deficient mouse brain and bone marrow. Geroscience 44, 2139-2155.
Yang, J.-H., Hayano, M., Griffin, P.T., Amorim, J.A., Bonkowski, M.S., Apostolides, J.K., Salfati, E.L., Blanchette, M., Munding, E.M., Bhakta, M., Chew, Y.C., Guo, W., Yang, X., Maybury-Lewis, S., Tian, X., Ross, J.M., Coppotelli, G., Meer, M.V., Rogers-Hammond, R., Vera, D.L., Lu, Y.R., Pippin, J.W., Creswell, M.L., Dou, Z., Xu, C., Mitchell, S.J., Das, A., O'Connell, B.L., Thakur, S., Kane, A.E., Su, Q., Mohri, Y., Nishimura, E.K., Schaevitz, L., Garg, N., Balta, A.-M., Rego, M.A., Gregory-Ksander, M., Jakobs, T.C., Zhong, L., Wakimoto, H., El Andari, J., Grimm, D., Mostoslavsky, R., Wagers, A.J., Tsubota, K., Bonasera, S.J., Palmeira, C.M., Seidman, J.G., Seidman, C.E., Wolf, N.S., Kreiling, J.A., Sedivy, J.M., Murphy, G.F., Green, R.E., Garcia, B.A., Berger, S.L., Oberdoerffer, P., Shankland, S.J., Gladyshev, V.N., Ksander, B.R., Pfenning, A.R., Rajman, L.A., Sinclair, D.A., 2023. Loss of epigenetic information as a cause of mammalian aging. Cell 186, 305-326.e327.
Yang, M., Wen, T., Chen, H., Deng, J., Yang, C., Zhang, Z., 2018. Knockdown of insulin-like growth factor 1 exerts a protective effect on hypoxic injury of aged BM-MSCs: role of autophagy. Stem Cell Research & Therapy 9, 284.
Yang, N.-C., Hu, M.-L., 2005. The limitations and validities of senescence associated-β-galactosidase activity as an aging marker for human foreskin fibroblast Hs68 cells. Experimental Gerontology 40, 813-819.
Yang, W., Hamilton, J.L., Kopil, C., Beck, J.C., Tanner, C.M., Albin, R.L., Ray Dorsey, E., Dahodwala, N., Cintina, I., Hogan, P., Thompson, T., 2020a. Current and projected future economic burden of Parkinson's disease in the U.S. npj Parkinson's Disease 6, 15.
Yang, Y., He, Z., Xing, Z., Zuo, Z., Yuan, L., Wu, Y., Jiang, M., Qi, F., Yao, Z., 2020b. Influenza vaccination in early Alzheimer's disease rescues amyloidosis and ameliorates cognitive deficits in APP/PS1 mice by inhibiting regulatory T cells. J Neuroinflammation 17, 65.
Yegorov, Y.E., Poznyak, A.V., Nikiforov, N.G., Sobenin, I.A., Orekhov, A.N., 2020. The Link between Chronic Stress and Accelerated Aging. Biomedicines 8.
Yiannopoulou, K.G., Papageorgiou, S.G., 2020. Current and Future Treatments in Alzheimer Disease: An Update. J Cent Nerv Syst Dis 12, 1179573520907397-1179573520907397.
Zhang, Y.F., Yu, J.C., Zhang, X.Z., Han, J.X., 2013. Effect of acupuncture intervention on hippocampal neuron loss and astrocytosis in SAMP 8 mice. Zhen Ci Yan Jiu 38, 358-364.
Zidong Donna, F., Iván, L.C., Curtis, D.K., 2012. Effects of Aging on mRNA Profiles for Drug-Metabolizing Enzymes and Transporters in Livers of Male and Female Mice. Drug Metabolism and Disposition 40, 1216.

Statement of Authorship

Title of Paper	The Hallmarks of Ageing in Microglia
Publication Status	☐ Published ☐ Accepted for Publication ☐ Submitted for Publication ☑ Unpublished and Unsubmitted work written in manuscript style
Publication Details	

Principal Author

Name of Principal Author (Candidate)	Laura Carr		
Contribution to the Paper	First author and main contributor. Concept, writer and formulation of manuscript. Reviewed prepared final draft following inputs from co-authors.		
Overall percentage (%)	70%		
Certification:	This paper is a narrative review I wrote during the period of my Higher Degree by Research candidature and is not subject to any obligations or contractual agreements with a third party that would constrain its inclusion in this thesis. I am the primary author of this paper		
Signature		Date	30/11/2024

Co-Author Contributions

By signing the Statement of Authorship, each author certifies that:

i. the candidate's stated contribution to the publication is accurate (as detailed above);
ii. permission is granted for the candidate in include the publication in the thesis; and
iii. the sum of all co-author contributions is equal to 100% less the candidate's stated contribution.

Name of Co-Author	Sanam Mustafa		
Contribution to the Paper	Reviewed and edited manuscript, project supervision		
Signature		Date	01/12/24

Name of Co-Author	Lyndsey E. Collins-Praino		
Contribution to the Paper	Conceptualised paper, reviewed and edited manuscript, project supervision		
Signature		Date	2/12/24

Chapter 2 : The Hallmarks of Ageing in Microglia

***Laura M. Carr*[1], *Sanam Mustafa*[1,2,3], *Lyndsey E. Collins-Praino*[1, 2]**

[1]School of Biomedicine, University of Adelaide, Adelaide, SA, Australia
[2]Australian Research Council Centre of Excellence for Nanoscale Biophotonics, The University of Adelaide, Adelaide, SA, Australia

2.1 Abstract

Due to the known link between ageing and the development of neurodegenerative diseases (NDs), such as Alzheimer's Disease and Parkinson's Disease, it is important to disentangle the independent effect of age-related changes from those due to disease processes. To do so, changes to central nervous system (CNS) cells as a function of advanced age need better characterisation and consideration. When investigating ageing in NDs, microglia are of particular interest due to their proposed to be links to the development and progression of NDs through control of the CNS immune response. Therefore, understanding the extent to which this microglial dysfunction is related to normal ageing rather than a disease process is of critical importance. As microglia age, they are believed to take on a pro-inflammatory phenotype with a distinct dystrophic morphology, but a clear description of the functional changes that occur in microglia during older adulthood is yet to be definitively established. While established hallmarks of ageing have been investigated across a range of cell types, such as macrophages, microglia have not been given the same detailed consideration. Here, we describe the dynamic phenotypes of microglia and evaluate the current state of understanding regarding how microglia change with advanced age, with a particular focus on the recently updated twelve hallmarks of ageing. Understanding how these hallmarks present in microglia represents a step towards better characterisation of microglial ageing which is essential in the development of more representative models of NDs.

Keywords: Microglia, Ageing, Morphology, Neuroinflammation, Inflammageing, Immunosenescence

2.2 Introduction

2.2.1 Brain changes with age

As our population ages, healthy ageing and the ability to maintain an independent lifestyle in the later years of life is becoming increasingly relevant (Dlima et al., 2024). Globally, the number of individuals over the age of 60 is projected to double by 2050 (Rudnicka et al., 2020), and, thus, as more people enter their later stages of life, the demand for interventions to stave off frailty and age-related diseases will increase. Ageing is the number one risk factor for developing neurodegenerative diseases (ND), such as Alzheimer's Disease (AD) and Parkinson's Disease (PD) (Hou et al., 2019), and it has been widely recognised that the prevalence of these diseases will increase dramatically as the population ages (Hou et al., 2019; Pallas et al., 2008). This increase has already been observed, with the number of global AD cases increasing 160.84% from 1990-2019 (Nichols et al., 2019) and the number of PD cases rising 155.5% within the same period (Ou et al., 2021). This relationship suggests a role of age-related biological changes in the pathophysiology of NDs. In line with this, both advanced age and NDs are known to share alterations in several common underlying physiological processes, which can impact the function of central nervous system (CNS) cells. López-Otín and colleagues (López-Otín et al., 2023) outlined 12 hallmarks of ageing, many of which show overlapping patterns of change with NDs. In fact, recent reviews have focused on these 12 hallmarks in AD (Liu et al., 2024b; Zhao and Huai, 2023), and the presence of a number of these hallmarks in PD (Coleman and Martin, 2022). These 12 hallmarks are: genomic instability, telomere attrition, epigenetic changes, loss of proteostasis, disabled macroautophagy, dysregulated nutrient sensing, mitochondrial dysfunction, cellular senescence, stem cell exhaustion, altered intercellular communication, chronic inflammation and dysbiosis. These are described further in Table 2.1, with direction provided for further reading on the presentation of each of these in age-related neurodegenerative disease.

Table 2.1: Definitions of the 12 hallmarks of ageing and their presentation during NDs

Hallmark	Definition and main features as described by López-Otín and colleagues (López-Otín et al., 2023)	Presentation in age related NDs	
		AD	**PD**
Genomic instability	The accumulation of genetic damage throughout the lifespan • Loss of DNA repair mechanisms • Accumulation of DNA damage • Increased frequency of DNA double strand breaks	Reviewed: (Hou et al., 2017) Accumulation of damaged DNA in neurons and astrocytes in the post-mortem frontal cortex of AD and mild cognitive impairment (MCI) cases (Shanbhag et al., 2019) ↓ in DNA repair factor BRCA1 in dentate gyrus of post-mortem AD brains and hAPP-J20 mice (Suberbielle et al., 2015)	Recent review: (Wang et al., 2023) Increased oxidative DNA damage is present in dopaminergic neurons in the substantia nigra of PD post-mortem tissue (Alam et al., 1997) ↑ DNA damage foci in C57BL/6 mice following stereotaxic injection of α-synuclein pre-formed-fibrils (Milanese et al., 2018)
Telomere attrition	The progressive shortening of telomeres • ↓telomerase activation • ↓telomerase reverse transcriptase (TERT) and telomerase RNA component (TERC) expression • Overall loss of telomere maintenance mechanisms	Recent review: (Kuan et al., 2023) Upregulation of TERT is neuroprotective against Aβ neurotoxicity in culture (Baruch-Eliyahu et al., 2019) Telomeres in leukocytes of AD patients are shorter than aged matched controls and length correlates with disease status (Panossian et al., 2003)	Recent review: (Vellingiri et al., 2023) <u>No evidence for telomere changes in PD</u> 2016 Meta-analysis reports no association between telomere shortening and PD (Forero et al., 2016) Telomere lengthening shown in peripheral blood monocytes of PD patients but not in the substantia nigra (Hudson et al., 2011) Telomere shortening in leukocytes of PD patients (Wu et al., 2020) Telomere lengthening in leukocytes of male PD patients (Schürks et al., 2014)
Epigenetic changes	Changes in epigenetic pathways • Histone modifications • DNA methylation • Chromatin remodelling	Recent review: (Gao et al., 2022) ↑ DNA methylation in post-mortem AD middle frontal gyrus and middle temporal gyrus (Coppieters et al., 2014)	Recent review: (Sharma et al., 2024) ↓ expression of DNA methylation regulating enzymes in post-mortem tissue from the frontal cortex of PD patients and in α-syn over expressing mice (Desplats et al., 2011)

	• Altered gene expression without changes to DNA sequences	Abnormal localisation of H3k4me3 is associated with Tau pathology and increasing Braak staging in human post-mortem AD brains (Mastroeni et al., 2015)	Hypermethylation of DNA measured by whole genome DNA bisulfite sequencing in iPSC derived dopaminergic neurons from PD patients (Fernández-Santiago et al., 2019) ↑ H3 acetylation in the primary motor cortex of PD post-mortem brains (Gebremedhin and Rademacher, 2016)
Loss of proteostasis	De-regulation of protein homeostasis • ↑ oxidative protein damage • Failure of protein quality control • Production of misfolded and incomplete proteins • Changes in proteasome capacity	Recent review: (Cozachenco et al., 2023) Polymorphism in Ubiquilin 1 gene (UBQ-8i polymorphism) associated with increased AD risk (Zhang and Jia, 2014) ↑eEF2 (a mediator of protein synthesis) phosphorylation in hippocampal lysates of AD patients (Beckelman et al., 2019) Ubiquitinated and hyperphosphorylated Tau accumulates in oligomers at synapses in cortical grey matter from AD patients (Tai et al., 2012)	Review: (Lehtonen et al., 2019) Co-localisation of 20 S proteasome components and α-synuclein in Lewy bodies inhibits proteasome activity (Lindersson et al., 2004) 20 S proteasome subunits are lost in dopaminergic neurons of the substantia nigra of PD post-mortem tissue (McNaught et al., 2002) α-synuclein oligomers inhibit the 26 S proteasome in PC12 cells (Emmanouilidou et al., 2010)
Disabled macroautophagy	Impairment of autophagic recycling of damaged organelles and proteins • ↓ in degradation and recycling of cytoplasmic components	Recent review: (Liu and Li, 2019) Induction of macroautophagy precedes Aβ pathology development in APP/PS1 mice (Yu et al., 2005) Autophagic vacuoles accumulate in dystrophic processes close to Aβ plaques (Nixon et al., 2005)	Recent review: (Nechushtai et al., 2023) Neuronal degeneration and mitochondrial loss is caused by activation of macroautophagy in primary cortical mouse neurons overexpressing A53T α-synuclein (Choubey et al., 2011) ↑macroautophagic pathways are observed in prefrontal cortex homogenate from patients with Lewy body dementia, but this is not sufficient to clear α-synuclein aggregates (Yu et al., 2009)

			The presence of mutant human α-synuclein in the substantia nigra of mice upregulated macroautophagic pathways (Yu et al., 2009)
Deregulated nutrient sensing	Dysregulation of metabolic pathways involved in nutrient sensing • ↑activity of mTOR pathway • Dysregulated Insulin sensing • ↓AMPK and sirtuin pathways	mTOR pathway reviewed: (Perluigi et al., 2021) insulin pathways reviewed: (Gabbouj et al., 2019) AMPK pathway reviewed: (Cai et al., 2012) Phosphorylation of P70 S6 kinase (part of the MAPK/P13K nutrient sensing pathways) is associated with Braak staging in post-mortem human brain tissue (An et al., 2003) ↑Akt activation in post-mortem AD temporal cortex (Griffin et al., 2005) P13k/Akt/mTOR pathway is hyperactivated in the inferior parietal lobule of AM and MCI brains (Tramutola et al., 2015)	mTOR pathway reviewed: (Lan et al., 2017) Insulin pathway reviewed: (Castilla-Cortázar et al., 2020) Levels of insulin-like growth factor 1 (IGF1) in serum of newly diagnosed PD patients was increased compared to controls (Godau et al., 2011) IGF1 levels in PD CSF was increased compared to controls (Mashayekhi et al., 2010) Inhibition of mTORC1 is neuroprotective against dopaminergic neuron loss in mice 6-months following injection of α-synuclein pre-formed fibrils (Khan et al.)
Mitochondrial dysfunction	Dysfunctional mitochondrial homeostasis and decline in mitochondrial function • ↓mitochondrial turnover • ↑ROS production • ↑mitochondrial membrane permeability	Recent reviews: (Bhatia et al., 2022; Leuner et al., 2012) Aβ treatment increases fragmented mitochondria in hippocampal neurons isolated from day 1 C57BL/6 pups (Calkins and Reddy, 2011) Mitochondrial complex 1 deficient mice show increased $A\beta_{1\text{-}40}$ levels in the cerebellum (Leuner et al., 2012)	Recent review: (Henrich et al., 2023) Reduced mitochondrial complex 1 activity in the substantia nigra of PD patient tissue (Schapira et al., 1989) α-synuclein aggregates are associated with mitochondria in post-mortem PD tissue and α-synuclein fibril binding to mitochondria *in vitro* impairs cellular respiration (Wang et al., 2019)
Cellular senescence	A state of irreversible growth arrest to prevent proliferation of damaged cells • Cell cycle arrest (↑$p16^{INK4A}$, ↑ $p21^{Cip1/Waf1}$)	Recent review: (Liu, 2022) Clearance of senescent glia from Ps19 mice prevents development of Tau pathology in hippocampal and cortical neurons (Bussian et al., 2018)	Recent review: (Miller et al., 2022) ↑ senescent astrocytes in the substantia nigra of PD patients post-mortem (Chinta et al., 2018)

	• Formation of senescence associated heterochromatin foci (SAHF) • ↑ Inflammatory profile (acquisition of the SASP)	↑proportion of senescent cells in the human AD prefrontal cortex (Herdy et al., 2022) ↑ senescent astrocytes in post -mortem human AD frontal cortex (Bhat et al., 2012)	Paraquat induces astrocytic senescence in p16-3MR C57BL6/J mice and removal of senescent astrocytes is neuroprotective against paraquat (Chinta et al., 2018) C57BL/6 mice overexpressing human A53T α-synuclein show a senescence associated secretory phenotype and ↑ levels of senescence markers (SA-β-gal, p16, p21 and γ-H2A.X) (Shen et al., 2024)
Stem cell exhaustion	Decline in number and function of stem cells • ↓Tissue renewal/impaired repair	Adult male APP mice and standard C57BL/6 mice injected with Aβ peptide display disrupted neurogenesis in the subventricular zone (Haughey et al., 2002) Aβ oligomer exposure in human neural stem cells decreased cell proliferative potential and impaired neurogenesis (Lee et al., 2013) Aβ plaque associated oligodendrocyte progenitor cells in the human post-mortem inferior parietal cortex of AD patients, and the hippocampus and entorhinal cortex of APP/PS1 mice exhibit a senescence-like phenotype (Zhang et al., 2019)	MPTP, used to induce animal models of PD, induces a premature senescent phenotype and autophagic function in human neural stem cells (Zhu et al., 2015)
Altered intercellular communication	Changes in signalling between cells • Altered activity of neural and hormonal pathways • Changes in extracellular molecules and cytokines • Changes in junction mediated cell-to-cell communication	Reviewed: (Gadhave et al., 2021) Human snRNA-seq dataset analysis of pathway changes (Liu et al., 2024a)	Recent review: (Dong-Chen et al., 2023) Analysis of multiple human single-cell/single-nucleus transcriptomic datasets reveal selective alterations in substantia nigra dopaminergic neuronal signalling with other cells in PD (Huang et al., 2022)

Chronic inflammation	Low-grade, persistent inflammation • ↑inflammatory responses • ↓immune function • Overexpression of proinflammatory cytokines (like in SASP)	Recent review: (Wong-Guerra et al., 2023) Administration of LPS to the 4th ventricle of male 3-mo Fisher-344 rats for 4 weeks and increased inflammatory markers and amyloid precursor protein mRNA levels in the hippocampus and basal forebrain (Hauss-Wegrzyniak et al., 1998) ↑ markers of microglial activation across studies of human post-mortem AD tissue (Hopperton et al., 2018) ↑ astrocyte activation in post-mortem AD tissue but no changes in NLRP3 inflammasome activation (Tang and Harte, 2021)	Recent review: (Tansey et al., 2022) ↑ inflammatory cytokines in the plasma of PD, PD-dementia, and Lewy body dementia patients compared to controls (Usenko et al., 2020) ↑microglial activation in the PD-dementia amygdala and ↑ infiltration of CD4+ T-lymphocytes in PD and PD-dementia cases (Kouli et al., 2020) NLRP3 inflammasome is associated with progression of PD symptomology (Fan et al., 2020)
Dysbiosis	Imbalance of the gut microbiome • ↓microbial diversity • ↑harmful microbes	Recent review: (Liu et al., 2020) Microbiome of AD participants has ↓microbial diversity and a distinct composition compared to age matched and young controls (Vogt et al., 2017; Zhuang et al., 2018) Dysregulation of the gut-brain-axis occurs in the Tg2576 mouse model of AD prior to cerebral Aβ aggregation (Honarpisheh et al., 2020)	Recent systematic review: (Li et al., 2023b) Altered gut microbiome composition in early PD, REM sleep behaviour disorder (RBD) and RBD relatives compared to healthy controls (Huang et al., 2023a)

The pathological commonalities between ageing hallmarks and ND underscores the need to disentangle the independent effect of normal age-related changes from those due to disease processes. One commonality across the above hallmarks of ageing is the presence of increased pro-inflammatory cytokines and their interaction with multiple other hallmarks. For example, dysbiosis has been shown to impact inflammatory signals in the brain (Huang et al., 2023b), causing an increase in pro-inflammatory cytokines (Henry et al., 2009) and oxidative stress (Tse, 2017) (features of both chronic inflammation and cellular senescence (Sobhon et al., 2023)). Pro-inflammatory cytokines have downstream effects on proteostasis (Sonninen et al., 2020), intercellular signalling (Turner et al., 2014) and nutrient sensing (Mancini et al., 2017). Reactive oxygen species (ROS) and other oxidative products further have effects on the genome (causing DNA damage (Renaudin, 2021)) and organelle health, particularly mitochondria, which are sensitive to oxidative damage (Guo et al., 2013).

Understanding each of these hallmarks on a molecular level is crucial in improving our ability to replicate the true environment that occurs in NDs. However, these changes may present differently in different CNS cell types. For example, cell cycle arrest is a defining characteristic of cellular senescence, a hallmark of ageing (López-Otín et al., 2023). However, in post-mitotic cells, such as neurons, the classical hallmark cell cycle arrest does not function as a marker of an aged cell (Sapieha and Mallette, 2018). Conversely, microglia and astrocytes are capable of division (Joya and Martín, 2021) and thus have the potential to express this element of cellular senescence. Given the particular role of glial cells in supporting neuronal health (Rahman et al., 2022), characterising aging in these support cells is critical. While both microglia and astrocytes are important in immune functions in the CNS (see reviews (Borst et al., 2021), (Giovannoni and Quintana, 2020) respectively), microglia are considered the primary drivers of the immune response (Ginhoux et al., 2013) and are the focus of the current review.

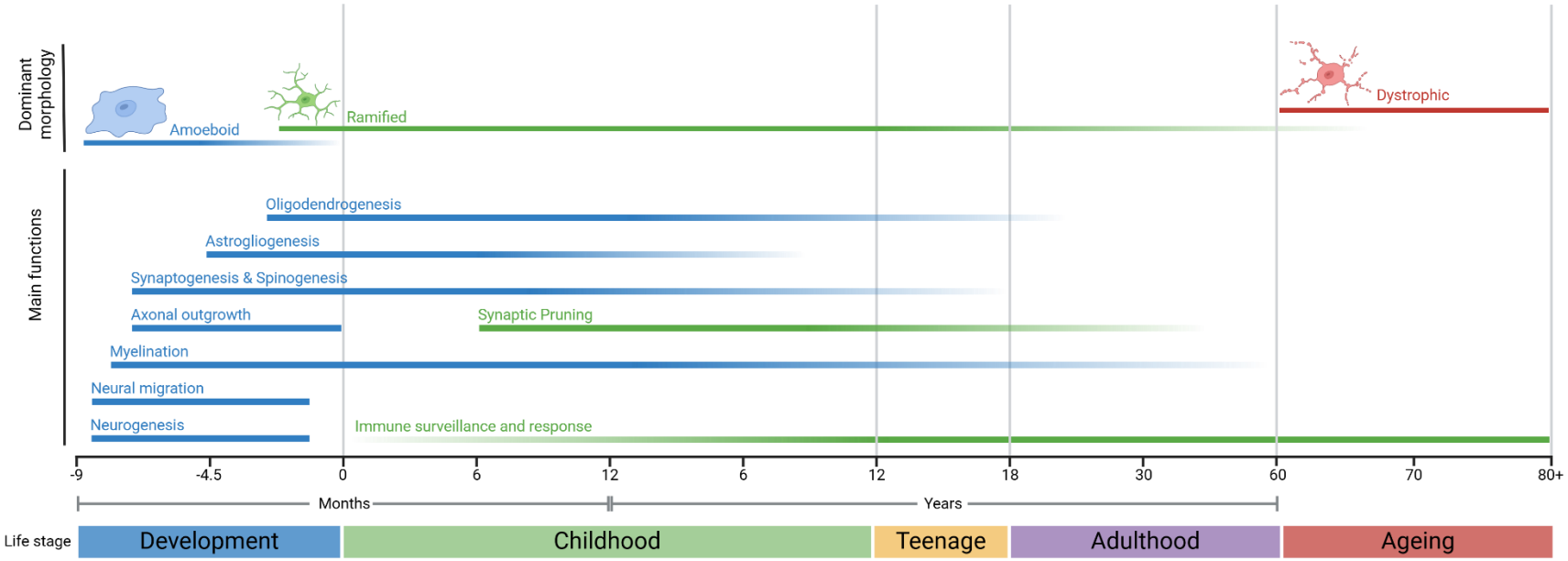


Figure 2.1: Microglial roles and morphologies during different stages of life.During development and early childhood, microglia have major roles in supporting the development of the CNS. Before birth, microglia display an amoeboid morphology. Ramified morphology begins to become the dominant morphology at the time of birth and remains so until late adulthood. During childhood, microglia maintain developmental roles through synaptic pruning, but transition to their major immune role around adolescence. During ageing, microglia acquire a dystrophic morphology; however, the functional changes at this stage remain unclear. Figure created in BioRender.

2.2.2 Microglial function during development and adulthood

Microglia are the tissue resident macrophages in the CNS, accounting for 5-20% of the total cell population in the brain (Hugh Perry, 1998). Whereas peripheral macrophages originate from hematopoietic stem cells in bone marrow (van Furth and Cohn, 1968), microglia arise from progenitor cells in the yolk sac during early development (Alliot et al., 1999; Cuadros et al., 1993) where they are responsible for facilitating cell migration, neurogenesis and gliogenesis (Menassa and Gomez-Nicola, 2018). While they have responsibilities in CNS maintenance, including synaptic pruning and phagocytosis of apoptotic cells (Borst et al., 2021), their major role in the adult CNS is the initiation of an adequate immune response to injury or infection (Ginhoux et al., 2013). Due to their dual role in both homeostasis and immune functions, microglia are highly dynamic cells, with constantly changing morphologies and functional phenotypes (Fig 2.1). Across the lifespan, the main function of microglia adapts to meet the needs of the developing brain and, thus, at different stages of life, different phenotypes are more dominant. Figure 2.1 shows the different roles and morphologies of human microglia present throughout the lifespan. During prenatal development in humans, microglia have diverse morphologies, ranging from amoeboid and migratory to ramified; however, amoeboid is the most dominant morphology until just before birth, when resting/ramified microglia begin to emerge as the more dominant phenotype (Fig. 2.1) (Menassa et al., 2022). Functionally, during prenatal development, microglia regulate neurogenesis, neuronal migration, synaptic connections and axon growth (Squarzoni et al., 2014) (Fig. 2.1). During neurogenesis, microglia are important for promotion or inhibition of the differentiation of neural stem cells to neurons (Matsui and Mori, 2018). By facilitating the removal of apoptotic or damaged cells, microglia help to maintain the correct trajectory of neuronal development (Cunningham et al., 2013). Additionally, microglia act to guide newly formed neurons to their correct locations, ensuring correct establishment of neural circuits essential for brain function (Ueno and Yamashita, 2014). This is additionally facilitated by microglia supporting axonal outgrowth and guidance (Squarzoni et al., 2014), as well as the differentiation of astrocytes and oligodendrocytes from progenitor cells (Reemst et al., 2016). The latter function, in particular, is essential in ensuring the development of a fully functioning CNS and limiting the likelihood of glia-related disorders down the track.

Microglia continue to release growth factors and cytokines to support the differentiation of astrocytes and oligodendrocytes throughout childhood and into the late teenage years (Fig. 2.1) (Borst et al., 2021), ensuring successful ongoing brain development and facilitating CNS plasticity during these critical developmental periods (Mallya et al., 2019). Microglial support during synaptogenesis is also a crucial function, to ensure that neural circuits are formed in an optimal manner (Miyamoto et al., 2016). Specifically, during development, the contact of microglial processes with dendrites leads to the development of filopodia, protrusions which later establish synaptic connections with surrounding cells (Miyamoto et al., 2016). In addition to supporting synapse formation, microglia ensure neural circuits are further refined through pruning of excess synapses, allowing for maintenance of optimal brain function (Paolicelli et al., 2011). This continues throughout the late teenage/young adult years, helping to maintain network plasticity; however, it is most critical during early development and childhood (Mastenbroek et al., 2024). The functions of microglia are reflected in their morphology. For example, during embryonic stages, microglia present with an amoeboid shape (Swinnen et al., 2013). However, when initiating synapse formation, microglia shift to a primitive ramified shape before transitioning to a fully ramified morphology to facilitate synapse elimination (Miyamoto et al., 2016). During most of early and middle adulthood, microglia maintain a surveillant, non-inflammatory phenotype, with much of their population displaying resting/ramified morphology (Harry and Kraft, 2012) (Fig. 2.1).

During ageing (i.e. 60+ years of age), microglia typically display a dystrophic morphology (Greenwood and Brown, 2021), also called "senescent microglia," featuring marked de-ramification, with remaining processes fragmented or swollen (Neumann et al., 2023). These cells have been mainly characterised in aged human post-mortem tissue (Lopes et al., 2008; Streit et al., 2004), and studied to a lesser extent in aged mice (d'Avila et al., 2018; St-Pierre et al., 2022). Such microglial dystrophy appears to be reflective of a disease associated phenotype, rather than ageing itself (Shahidehpour et al., 2021; Streit et al., 2009). Further, it is well documented that, with advancing age, microglia have a decreased ability to perform homeostatic functions and exhibit an altered immune response (Niraula et al., 2017). This includes a shift towards a more reactive phenotype, with microglia existing in a primed state, featuring heightened immune responses and longer time to resolve the response following activation (Norden et

al., 2015). In line with this, microglia in 22-month-old (mo) male Sprague Dawley rats maintained an inflammatory response for longer than microglia in 3-to 4-mo rats following intracerebral haemorrhage induced by collagenase injection to the striatum, with aged rats showing higher numbers of activated microglia (Wasserman et al., 2008). Similarly, 18-to 20-mo male BALB/c mice had a hyperactive microglial response to lipopolysaccharide (LPS) stimulation compared to 3-to 4-mo mice (Henry et al., 2009). Thus, experimental evidence demonstrates that aged microglia exist in a primed state, with the ability to sustain immune responses following injury. While ageing changes in microglial activation state are relatively well investigated, the exact phenotype of aged microglia at a molecular level is still largely unknown.

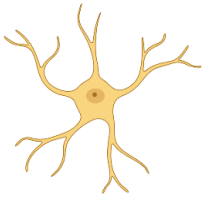
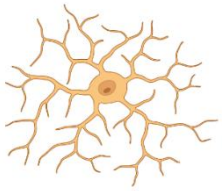
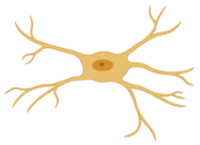
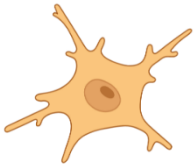
	a)	b)	c)	d)	e)	f)	g)
Class	**Resting/surveillant**	**Hyper-ramified**	**Reactive**	**Bushy**	**Rod**	**Amoeboid/activated**	**Dystrophic**
Morphology (Green and Rowe, 2024)	 Small cell body Multiple extending processes	 Small cell body Dense network of fine processes	 Enlarged cell body Decreased number and branching of processes	 Enlarged cell body "bushy" in appearance Shorter/thicker processes	 Elongated cell body Fewer processes stretching in one direction	 Rounded cell body Few to no processes	 Irregular cell body Swollen/fragmented processes
Function	**Functionally resting (Paolicelli et al., 2022)** Motile processes to monitor the CNS for damage or infection Support neuronal circuits Synaptic pruning Clearing cellular debris	**Conflicting reports on function** Primed and hyperactive response to stimuli (Maras et al., 2022; Ziebell et al., 2015) **OR** Static state with impaired physiological responses associated with chronic stress (Smith et al., 2019)	**Initiation of immune response (Gao et al., 2023; Soltys et al., 2001)** Production of inflammatory cytokines Migration to injury sites and pathology Phagocytosis of cellular debris	**Intermediate state of activation (Green and Rowe, 2024; Soltys et al., 2001)** Reactive proliferation and cytokine production Associated with brain injuries	**Associated with infection and disease (Bachstetter et al., 2017)** Potentially acting as scaffolding for damaged neurons	**Function as an active macrophage (Giulian and Baker, 1986)** Mainly scavenging and phagocytic activity Secretion of pro-inflammatory and toxic factors	**Associated with injury, neurodegeneration and ageing (Green and Rowe, 2024; Solito and Sastre, 2012)** Impaired ability to perform normal functions Less effective at clearing debris and pathogens
Markers (Jurga et al., 2020; Paolicelli et al., 2022)	IBA1, P2RY12, TMEM119 **Inflammatory cytokines:** Low levels of cytokines to maintain homeostasis	IBA1, ↑P2RY12, ↑TMTM119 **Inflammatory cytokines:** ↑IL-10	IBA1, MHCII, CD68, CD86, CD40 **Inflammatory cytokines:** ↑TNF, ↑ IL-6, ↑IL-1β	IBA1, CD68 **Inflammatory cytokines:** ↑TNF, ↑IL-6, ↑ IL-1β	IBA1, CD68 **Inflammatory cytokines:** ↑TNF, ↑IL-1β, ↑IFN-γ	IBA1, CD68, CD11b, MHCII **Inflammatory cytokines:** ↑TNF, ↑IL-1β, ↑IFN-γ **↑Reactive oxygen species** **↑Nitric oxide**	IBA1, FTL (Shahidehpour et al., 2021) **Inflammatory cytokines:** ↑TNF, ↑IL-6, ↑IL-1β (Sierra et al., 2007)

Figure 2.2: Microglial classifications and accompanying morphology, functions and markers. Green: Phenotypes present under physiological conditions, Yellow: Phenotypes present following induction of immune response (i.e. response to injury/infection), Red: Phenotypes present under dysregulated or pathological conditions a) Resting/ramified microglia are in a state of CNS surveillance, with low baseline levels of inflammatory cytokine release. b) Hyper-ramified microglia functionally have either a heightened or an impaired response to stimuli. c) Reactive microglia initiate the immune response. d) Bushy microglia are semi-activated and have some phagocytic and inflammatory functions. e) Rod microglia are associated with degeneration and injury, with potential roles in structural support of neurons. f) Activated/amoeboid microglia are active macrophages, with main roles in

phagocytosis and secretion of pro-inflammatory factors. g) Dystrophic microglia are associated with neurodegeneration and ageing and have a diminished capacity to perform normal resting functions. Images from BioRender.

2.2.3 Microglial activation: Morphology and mechanisms

In response to injury or infection, microglia become activated, shifting their morphology to suit the functional needs of the immune stimulus. The classical definition of microglial activation is displaying a mobile, amoeboid morphology, increased phagocytosis and increased release of pro-inflammatory cytokines (Giulian and Baker, 1986) (Fig 2.2f). It should be noted, however, that microglial classification throughout the literature is inconsistent, with morphological terms being used interchangeably (e.g. bushy and hyper-ramified (Reddaway et al., 2023; Ziebell et al., 2015)), and less characterised morphologies, such as rod microglia, being vaguely described, with little understanding of their functional phenotype (Giordano et al., 2021).

The classical state of microglial activation has often been shown to occur in the presence of protein aggregation, as occurs during ageing and in age-related NDs (Barger and Harmon, 1997; Gao et al., 2023; Scheiblich et al., 2021). This activation occurs largely through pattern recognition receptors (PRRs), which allow the recognition of pathogenic signals such as damage associated molecular patterns (DAMPs), and pathogen associated molecular patterns (PAMPs), causing microglia to acquire this classical activated phenotype (Glezer et al., 2007; Kigerl et al., 2014). The microglial PRR pathways are shown in Figure 2.3a. Toll-like receptors (TLRs), present on the cell surface, are the main initiator of microglial activation, activating a cascade which ultimately triggers the release of pro-inflammatory factors, such as IL-6, TNF-α, IL-1β and IL-8, IFNγ. Intracellular PRRs, including Nod-like receptors (NLRs) and RIG-1-like receptors (RLRs), are also capable of activating microglia through recognition of cytosolic PAMPs/DAMPs or viral RNA, respectively (Kigerl et al., 2014) Additionally, activation of NLR protein 3 (NLRP3) is essential in the formation of the NLRP3 inflammasome, a multiprotein complex which drives the release of pro-inflammatory signals from cells, specifically IL-1β and IL-18.

Microglia can also undergo inflammatory activation driven by intracellular DNA sensing mechanisms (Fig 2.3b). Specifically, activation of the cGAS-STING pathway in microglia leads to the production and release of pro-inflammatory cytokines. In mixed primary glial cultures, administration of pre-formed α-synuclein fibrils (α-syn PFF) caused increased DNA damage (measured by γ-H2A.X staining)

within 24hrs, and upregulation of 2'3'-cGAMP, a key component of the cGAS-STING pathway (Hinkle et al., 2022). When this mechanism was further probed in a C57BL/6 mouse model of α-synucleinopathy induced by intrastriatal inoculation of α-syn PFF, increased expression of the STING product pTBK1 was detected in microglia, along with increased γ-H2A.X expression (Hinkle et al., 2022). Given the presence of DNA damage and dysregulated proteostasis during ageing, the demonstrated exacerbating effect of pathological proteins suggests a potential link between these mechanisms in microglial ageing.

In addition to the classic amoeboid morphology of activated microglia, another morphological presentation of microglial activation is rod-shaped microglia, often observed following TBI (Giordano et al., 2021). These cells have an elongated soma, with less complex branching than ramified microglia, and are often organised in trains aligning with dendrites of damaged neurons. The function of rod microglia is largely unknown, but placement relative to neuronal dendrites has suggested a role in either supporting neuronal repair following injury or exacerbating axonal injuries (Giordano et al., 2021). It is suggested that these microglia may provide a scaffolding to support remodelling following injury. These microglia express typical markers of microglial activation, including OX6 (Ziebell et al., 2012), a marker of MHCII, but no specific marker is available to distinctly identify rod microglia. This suggests that these are a morphological variant of activated microglia and may occupy similar molecular functioning, and thus are likely to undergo the same mechanisms of activation outlined in Figure 2.3.

Of note, microglia can also exist in an intermittent reactive state, referred to as reactive or primed microglia. Reactive microglia are cells which have been previously exposed to an immune stimulus and maintain a level of innate immune memory, leading to a lower threshold for becoming activated and an exaggerated immune response following activation (Norden et al., 2015). In 3-mo APP23 transgenic C57BL/6J female mice, which develop Aβ pathology at 6-mo, two kinds of innate immune memory have been demonstrated in microglia: training (one 500μg/kg LPS IP injection) and tolerance (four 500μg/kg LPS IP injections) (Wendeln et al., 2018). Following priming by training or tolerance at 3-mo, neuropathology was assessed at 9-mo. Plaque load and levels of Aβ were increased in the training group, but decreased in the tolerance group, when compared to both wild-type littermates and APP

control mice. This suggests that a single inflammatory event can shift microglia towards a primed state where, in the presence of pathology, microglia will show an exacerbated immune response. Only a single exposure in necessary to prime microglia however over a lifetime, due to communication with peripheral immune cells and effects of systemic infections, microglia will be exposed to more than one immune challenge (Düsedau et al., 2021), suggesting that the tolerant microglial phenotype observed in the above study may be more relevant and aged microglia may in fact have decreased response to pathology.

2.2.4 Consequences of microglial activation

When acute and adequately regulated, microglial activation and immune responses are beneficial, promoting repair and maintaining neuronal health (Morgan et al., 2004; Ziv et al., 2006). However, when this response persists unregulated, it can be detrimental to the surrounding cells (Tang et al., 2014). Specifically, chronic activation of microglia is hypothesised to be one of the major drivers of neuronal death in NDs (Jeohn et al., 1998; Mander and Brown, 2005; Tang et al., 2014). However, activated microglia contribute to neuronal death either by direct actions on neurons or by indirect actions of pro-inflammatory factors released by microglia. In line with this, LTA (TLR2 agonist) administration to primary rat neuronal cultures caused inflammatory activation of microglia, enhanced microglial phagocytic activity and exposure of phosphatidylserine (PS) on the processes of neurons, a phospholipid which acts as an "eat me" signal to phagocytic cells (Neher et al., 2011). Peroxynitrite, a byproduct of the interaction of nitric oxide (NO) and superoxide radicals released from microglia during activation, was determined to be the cause of PS exposure on these neurons (Neher et al., 2011). In contrast, activating microglial phagocytosis by non-inflammatory pathways (i.e. administration of GM-CSF) did not lead to neuron loss in culture (Neher et al., 2011). When Aβ-42 was administered by the same authors, to mixed glial cultures from the cortex of OFA/SPF rat pups, an increase in microglial inflammation and phagocytic capacity was accompanied by an increased phagocytosis of neurons by microglia (Neniskyte et al., 2011). These results indicate that activation of microglia by pathological proteins, such as Aβ, causes a loss of neurons *in vitro.* In support of this,, progranulin (pgrn-1), a gene which is inactivated in frontotemporal lobular degeneration (FTLD), is important in preventing the

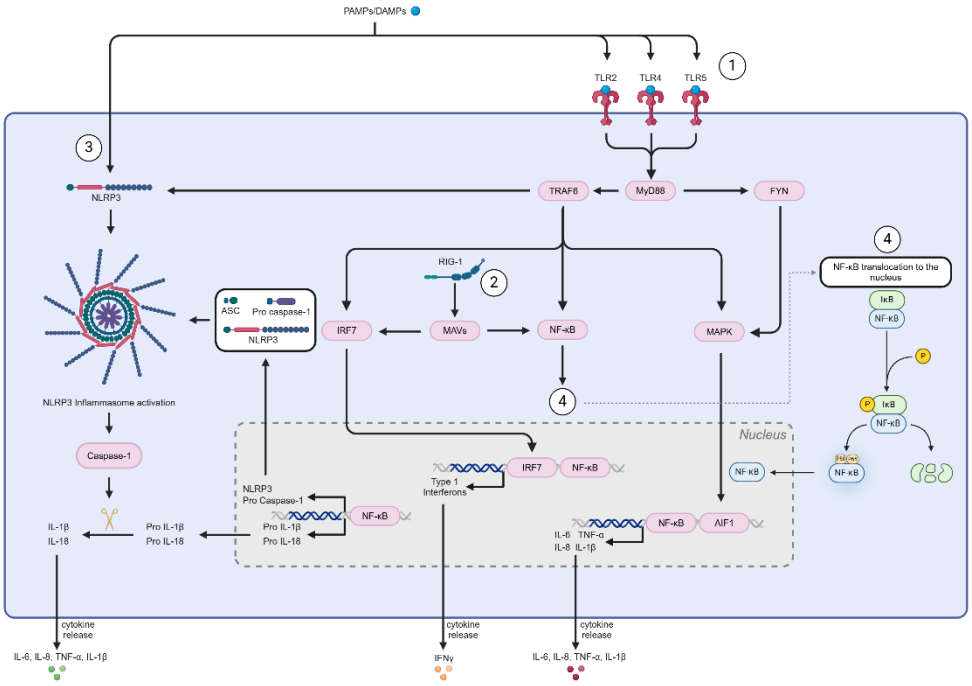
phagocytosis of PS-exposed neurons in pgrn-1 mutant *C.elegans* (Kao et al., 2011), and in *pgrn*$^{-/-}$ mice. In both species, pgrn-1 mutants showed increased microglia and astrocyte reactivity compared to wild-type following LPS administration (Yin et al., 2010). Taken together these results directly implicate inflammatory activation of microglial phagocytosis in neuronal loss.

Indirectly, release of pro-inflammatory factors from microglia impacts nearby neurons. Specifically, the production of microglial reactive oxygen species (ROS), NO, and pro-inflammatory cytokines affect mitochondrial health of neighbouring neurons (Lull and Block, 2010). Following production and release by microglia, the binding of the pro-inflammatory cytokine TNF-α to receptors on neurons promotes the induction of inflammatory signals intracellularly (Zou and Crews, 2005). Similarly, in an LPS induced model of hypoxic-ischemic injury, TNF has been demonstrated as a regulator of the apoptotic JNK pathway in neurons and microglia of C57BL/6 mouse pups, with downregulation of TNF receptor-1 attenuating inflammation and reducing JNK activation (Wang et al., 2014). Similarly, TNF-α upregulation of AMPA receptors at neuronal synapses additionally contributes to glutamate excitotoxicity and neuronal cell death in the spinal cords of male Sprague Dawley rats (Hermann et al., 2001). Other products of microglial activation, including the generation of NO and ROS, also impact neuronal functioning and have a role in neuron death through the induction of oxidative stress. By diffusing into neighbouring neurons, ROS and NO cause oxidative damage to proteins, DNA and, particularly, organelles like mitochondria (Guo et al., 2013; Renaudin, 2021). Mitochondrial stress and damage have a major link to neuronal apoptosis in neurodegenerative conditions (see review: (Sivagurunathan et al., 2023)). Mitochondria and mtDNA are particularly susceptible to damage and damaged mitochondria themselves further produce superoxide radicals and release damaged mtDNA, activating DNA driven immune responses (Piantadosi, 2020). These results highlight the downstream effects of microglial activation in neuronal death. Additionally, the death of neurons by these mechanisms drives microglia to become further activated, with neuronal debris and pathological proteins released from dead/dying neurons activating PRR on microglia (Hsieh et al., 2009). This leads to a pernicious cycle, where enhanced activation of microglia drives further neuronal death, leading to even greater microglial activation (Lull and Block, 2010). This positive feedback loop raises a chicken

and egg-like dilemma, whereby either neurodegenerative processes or microglial activation itself could be the initiating factor of this cycle, a matter of great debate within the field (Lull and Block, 2010).

Considering the aged background on which NDs, such as AD and PD, occur, it is reasonable to infer that age-related alterations in microglia are a major contributor to disease pathophysiology in NDs (Gamage et al., 2023; Zhang et al., 2023). Given this link, the importance of including age as a factor in the preclinical modelling of NDs cannot be understated; however, there is a clear lack of consideration of age in current preclinical studies of NDs (reviewed: (Carr et al., 2024; Sun et al., 2020)). In order to better model the age-related changes occurring in CNS cells, there needs to be broader understanding of how the CNS immune response changes with advancing age (Angelova and Brown, 2019), particularly the role of microglia in this process.

a) PRR pathways of microglial activation



b) DNA driven pathways of microglial activation

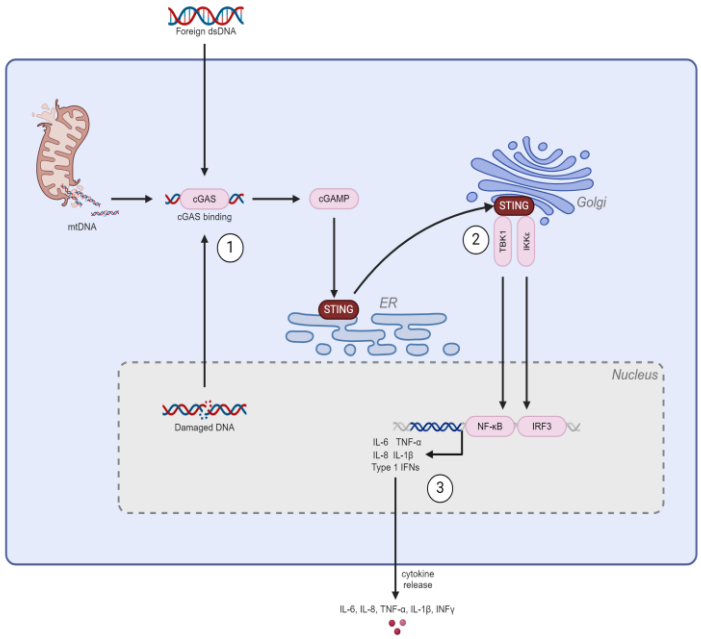


Figure 2.3:Pathways of microglial activation. a) PRR pathways of activation in microgliaPRRs, such as 1. TLRs, 2. RLRs, and 3. NLRs, recognise PAMPs/DAMPs and trigger signalling cascades, including 4. Exposure of NF-κB subunits by degradation if IκB and translocation of NF-κB to the nucleus. These cascades cause microglial activation and the downstream release of inflammatory cytokines. b) DNA driven immune responses in microglia. 1. cGAS binds to free DNA in the cytosol (mtDNA, nuclear DNA, foreign DNA), which activates the cGAS-STING pathway, causing the transcription of proinflammatory genes and release of proinflammatory cytokines. Figure was created using BioRender.

2.3 Understanding molecular changes in microglia through the hallmarks of ageing

As described above, changes in microglial activation and morphology with age are well described; however, there has been little characterisation of microglia with reference to the known hallmarks of ageing. As outlined in Table 2.1, the hallmarks of ageing (López-Otín et al., 2023) represent specific patterns of change in critical systems which can be used to distinguish an aged phenotype. These hallmarks have been described in peripheral macrophages (Guimarães et al., 2021), but are less well investigated in microglia, with studies instead focusing on how microglial production and release of pro-inflammatory factors and activation state changes with age. Below, we review the studies to date that have explored the presentation of these hallmarks in microglia with advancing age, with a focus on how these changes may be relevant in the context of neurodegeneration, as well as on gaps in the current literature.

2.3.1 Genomic instability

Genomic instability as a hallmark of ageing is defined by an accumulation of damaged DNA and loss of or alterations in DNA repair pathways (Chen et al., 2022). In microglia, this has been studied both preclinically and in human-post mortem tissue. In 24-month-old (mo) C57BL/6 male and female mice, microglia have been shown to accumulate damaged DNA fragments as identified by γ-H2A.X staining and an increase in the percentage of pSTING+/CD11b+ cells compared to 2-mo animals (Arvanitaki et al., 2024). These changes indicate activation of the DNA driven immune response, contributing to the acquisition of a pro-inflammatory phenotype in microglia. Similarly, the *Ercc1*$^{\Delta/-}$ mouse is deficient in DNA repair mechanisms and displays features of accelerated ageing. In *Ercc1*$^{\Delta/-}$ mice at 16-weeks-old, following peripheral LPS injection microglia displayed hypertrophied processes and an increase in cell body size, along with increased proliferation, phagocytosis and ROS production compared to WT controls (Raj et al., 2014). In addition, *Ercc1*$^{\Delta/-}$mice showed evidence of microglial priming, as indicated by an enhanced inflammatory response, following peripheral LPS challenge, a result which has also been replicated in *Ercc1*$^{\Delta/-}$mice at older ages (4-, 8-, and 14-mo) (Zhang et al., 2021). While DNA damage itself was not explicitly measured in microglia in either of these studies, these results

implicate a loss of DNA repair mechanisms in driving microglial ageing and pro-inflammatory activation.

Conversely, in human post-mortem tissue from 14 healthy controls (6M:8F) aged 65-96 years old, dystrophic microglia did not show positive γ-H2A.X staining (Neumann et al., 2023), but were strongly correlated with increased ferritin expression, a marker also known to increase with ageing. Nevertheless, another human post-mortem study in older adults (mean age 94.07 years ± 0.95) investigating microglial transcriptomics identified 1054 genes which made up an aged microglial signature (Olah et al., 2018). DNA damage associated pathways were enriched in these genes, along with telomere maintenance and phagocytosis (Olah et al., 2018). These results together suggest that while γ-H2A.X expression is not associated with aged microglia in humans, alterations in DNA damage pathways are indeed present in aged human microglia; however, the specific changes which occur as a consequence of alterations in these pathways are yet to be identified. These results should be interpreted with caution, however, as they are derived from only two studies, with the former containing a relatively small sample size and no young control cohort. This represents a wider issue in the field, with young healthy brain tissue difficult to obtain (Bell et al., 2008), making human post-mortem studies challenging, and questions remaining about how well age-related changes observed in pre-clinical rodent models reflect those seen in the in human brain. While large animal models, which are arguably more translational, can be used to investigate microglia alterations (Sorby-Adams et al., 2018), to our knowledge, none have yet been used to investigate changes that occur in the microglial genome with age. This necessitates further research into this area to uncover the extent to which typical markers of senescence, such as accumulated DNA damage, can be observed in aged microglia across species.

2.3.2 Telomere shortening

Telomere shortening is one of the most widely recognised and accepted hallmarks of ageing (Fasching, 2018). Telomeres, protective DNA sequences which cap the end of chromosomes, function to stabilise the ends of chromosomes and protect genomic material from degradation (Vaiserman and Krasnienkov, 2021). However, with each cell division, telomeres become progressively shorter due to the inability of DNA polymerase to fully replicate the end of the C-rich lagging strand (Vaiserman and Krasnienkov,

2021). This effect is referred to as the end replication problem, where telomeres will shorten until reaching a critical length where they can no longer protect the chromosome (Vaiserman and Krasnienkov, 2021). This triggers cell cycle arrest and cells either enter a senescent state or undergo apoptosis. Telomere length has been widely utilised as a biomarker of ageing (Sanders and Newman, 2013); however, there is debate as to whether these pre-clinical results have translational relevance for human ageing, where there have been conflicting results regarding the association of telomere length and age. While a full discussion of this debate is beyond the scope of this review, for detailed information regarding the validity of telomere shortening as a marker of ageing, see: (Mather et al., 2011; Vaiserman and Krasnienkov, 2021).

The evidence for telomere length as a marker of ageing has come primarily from peripheral blood leukocytes and fibroblasts. In line with this, a 2022 systematic review and meta-analysis of 27 studies reported that longer leukocyte telomeres were associated with lower levels of age-related structural change (brain volume loss) and cognitive decline in non-demented cases (Gampawar et al., 2022). Telomere alterations in the brain itself, however, have been less well investigated. Nevertheless, some studies in isolated rat microglia demonstrate telomere shortening with age. The first study to investigate glial telomeres was conducted by Flanary and Streit in 2003 (Flanary and Streit, 2004), who found telomeres in microglia from neonatal rat cortices shorten over 32 days in culture when measured using flow cytometry fluorescent *in situ* hybridization (flow-FISH). Telomerase activity in these microglia declined steadily until day 24 but increased dramatically until the end of the 32-day culture period. This study also investigated astrocyte telomeres and found no overall changes in telomere length, with a steady increase, followed by a decrease, in telomerase activity, the opposite pattern to that found in microglia (Flanary and Streit, 2004). Similarly, in a 2007 study by the same authors, microglia isolated from 30-mo male Fisher-344 rats were found to have shorter telomeres than microglia isolated from 3-mo rats when measured using flow-FISH (Flanary et al., 2007). These aged microglia also had decreased telomerase activity compared to young microglia, indicating both a decline in telomere length and telomere maintenance with age in rodent microglia (Flanary et al., 2007). Of note, the authors also investigated microglial telomere length in human post-mortem tissue from AD patients in this study.

Microglia were isolated from the superior frontal gyrus/frontal pole region of 4 AD (86-years-old ± 2.54) and one non-dementia case (86-years-old), and microglial telomere length and telomerase activity were measured. Telomeres in AD microglia were significantly shorter than the non-dementia case; however, no changes in telomerase activity were observed (Flanary et al., 2007). Notably, there was no investigation of microglial telomere length compared to young human tissue, likely due to limitations associated with obtaining post-mortem tissue from young donors, as discussed above.

Several other studies have also investigated telomere shortening in the context of ND. For example, one study utilised a cross between the APP23 transgenic mouse model of AD and the Telomerase RNA component (Terc) knockout model of telomere shortening ($G3Terc^{-/-}APP23^{+}$) to investigate AD pathology on the background of shortened telomeres (Rolyan et al., 2011). Interestingly, at 12-mo of age, $G3Terc^{-/-}APP23^{+}$ mice actually had reduced Aβ pathology in the frontal cortex, as well as improved spatial memory, compared to $APP23^{+}$ mice. Additionally, $G3Terc^{-/-}APP23^{+}$ mice showed no increase in microglial activation ($MHCII^{+}$ microglia) in the vicinity of Aβ plaques. Similarly, a cross between a preclinical model of PD, the Thy-1[A30P] α-synuclein transgenic mouse model, and $Terc^{-/-}$ mice ($\alpha SYN^{tg/tg}G3Terc^{-/-}$) showed decreased microglial Il-1β gene expression and reductions in expression of the microglial activation marker MHCII in the brainstem of 17-mo $\alpha SYN^{tg/tg}G3Terc^{-/-}$ mice compared to $\alpha SYN^{tg/tg}$ mice (Scheffold et al., 2016). Taken together, these results surprisingly seem to suggest that telomere shortening is protective against microglial activation, however in these animals this correlated with accelerated disease phenotype and early death of PD mice. This suggests that loss of telomere maintenance inhibits a protective response by microglia and ultimately leads to worsened disease phenotypes however, further research is required to unravel potential mechanisms that may underlie these processes. Additionally, as telomere shortening was artificially induced via Terc knockout in both of these previous studies, it is important to investigate how this may differ from changes that occur with physiological ageing.

2.3.3 Epigenetic changes

Epigenetic changes encompass a range of heritable changes that cause alterations in gene expression, without directly changing DNA sequences (la Torre et al., 2023). Some of the main epigenetic

alterations studied with regard to ageing are chromatin remodelling, histone modifications and DNA methylation (see review: (la Torre et al., 2023)), and these are thought to be major contributors to the ageing process (Horvath, 2013). Changes in all of these processes have been reported to occur in microglia with advancing age. Chromatin remodelling refers to alterations in the structure and organisation of chromatin and includes altered chromatin accessibility (CA), a measure of how easily genes may be accessed for transcription (Li et al., 2023a). One study, which conducted mapping of CA by ATAC-seq in the microglia of female and male C57BL/6J mice at 3-, 14- and 24-mo of age, described a number of genes differentially expressed with age, termed age-dependent microglia genes (ADEM genes) (Li et al., 2023a). Genes which positively correlated with age were termed P-ADEM genes (notably genes related to phagocytosis, IFN signalling, ROS production and antigen presentation), while genes that negatively correlated with age were designated as N-ADEM genes (including chemokine suppression and iron transportation genes). P-ADEM genes had a higher CA than N-ADEM genes in promoter regions, indicating that alterations in CA of ADEM genes may dictate the emergence of specific microglial phenotypes during ageing (Li et al., 2023a). For example, the increased CA of ROS production genes (*Cybb* and *Hp*) and IFN signalling genes (*Ifitm3, Ifi204, Cxcl16, Xaf1, Gas6* and *Tgtp2)* suggests a shift towards a more pro-inflammatory phenotype in microglia, potentially leading to increased inflammation and microglial activation with age.

Histone modifications have also been shown to occur in microglia with advancing age. In line with this, an age-related decrease in the histone demethylase Jumonji domain-containing protein-3 (JMJD3) has been observed in microglia of male C57BL/6 mice aged 16-18-mo compared to 2- to 3-mo mice (Tang et al., 2014). JMJD3 is suggested to be necessary for microglia to switch to an active, anti-inflammatory state (Tang et al., 2014). Thus, its decrease with age is potentially representative of a shift towards a pro-inflammatory phenotype with advancing age. This study also found an increased level of the histone H3K27me3 in the midbrain of aged mice. H3K27me3 is the trimethylation of lysine 27 on histone H3, a histone modification which is associated with reduced transcriptional activity, which can be reduced by JMJD3. Thus, this increase in H3K27me3 may be a consequence of the decrease in JMJD3 seen in microglia with advanced age and may further contribute to imbalances in microglial responses.

Finally, DNA methylation refers to the addition of a methyl group to a DNA molecule, typically associated with silencing of genes. In microglia isolated from young adult (4- to 6-mo) and aged (24- to 26-mo) C57BL/6 mice exposed to LPS, an increase in IL-1β expression was observed with age (Matt et al., 2016). When probed further, IL-1β promoter DNA in aged microglia from older animals showed decreased methylation compared to that seen in younger animals (Matt et al., 2016). This suggests that, with age, silencing of proinflammatory cytokine genes is reduced following an inflammatory stimulus, potentially leading to an overactive microglial response. Overall, changes in CA and DNA methylation in microglia suggest a shift towards pro-inflammatory secretory phenotype, with histone modifications contributing to a reduced likelihood of taking on an anti-inflammatory phenotype. Taken together, this provides compelling evidence that microglia undergo a number of epigenetic changes with advancing age which cause an enhanced pro-inflammatory response, which may be further exacerbated in the presence of ND-associated pathological proteins, such as Aβ in AD or α-synuclein in PD.

2.3.4 Loss of proteostasis

López-Otín and colleagues describe the hallmark loss of proteostasis as dysregulation of the intracellular mechanisms responsible for the degradation of proteins (López-Otín et al., 2023). A decline of proteostasis is often related to the aggregation and accumulation of proteins, a hallmark of neurodegenerative diseases such as AD and PD. Thus, the study of microglial proteostasis with age is critical in order to understand the mechanisms by which pathology may be targeted. Proteomic analysis of microglia isolated from young (3- to 5-mo) and aged (20- to 24-mo) mice revealed differential expression in a number of proteins, including downregulation of proteasome complex subunits PSMB4, PSMA6, and PSMC1 (Flowers et al., 2017). Downregulation of these subunits would likely impair the ability of microglia to degrade damaged or misfolded proteins, leading to ineffective protein clearance in aged tissues. In AD for example, microglia are important for degradation of Aβ (Qiu et al., 1997). However, if their capacity for proteasomal degradation is impaired, this may lead to accumulation of pathological Aβ within microglia, further disrupting proteostasis and protein degradation ability (Pomilio et al., 2020). In APP/PS1 mice also deficient in the immunoproteasome component LMP7, microglial immunoreactivity was decreased at 8-mo when compared to APP/PS1 mice with LMP7 of

the same age. Interestingly, this change in microglial state did not alter the presence of Aβ pathology in these mice at any age (Wagner et al., 2017). Notably, however, this was only assessed at 8-mo, relatively young compared to other studies on microglial ageing, and results may differ in older animals. In line with this, in 22-mo transgenic mice with a C57BL/6N background, deletion of COP1 E3 ubiquitin ligase by tamoxifen administration at ~2-mo of age resulted in an increased expression of microglial genes involved in IFN signalling, and APOE, a major AD risk factor gene, compared to WT mice (Ndoja et al., 2020).

Such effects may also be sex specific, at least to some extent. For example, in 18-mo old C57BL/6 mice, microglia showed sex dependent alterations in proteostasis. Microglia in female mice demonstrated a decreased ability to phagocytose Aβ42, while microglia from male mice showed a decrease in proteolytic gene expression but no change in phagocytic abilities. Of note, microglia from both sexes at 22-mo had decreased expression of the phagocytic receptor TREM2 (Thomas et al., 2022), suggesting a potential alteration in recognition of pathological proteins in aged microglia. Overall, there is mounting evidence that there is a de-regulation of the protein degradation pathways within microglia with advancing age, which may have significant implications for the pathogenesis of diseases like AD and PD, where an inability of microglia to combat pathological protein aggregation may contribute to the spread of pathology throughout the brain (Gao et al., 2023).

2.3.5 Disabled macroautophagy

Macroautophagy is defined as the recycling of large cargo and cellular contents by lysosomes, with cargo packaged into specialised vesicles called autophagosomes (Nieto-Torres and Hansen, 2021). With age, the efficiency of cellular autophagy declines, resulting in a decreased turnover of organelles, protein and lipid degradation and reduced ability to dispose of pathogens (Nieto-Torres and Hansen, 2021). In microglia, age-related autophagic changes are understudied, with most research to date focused on these changes in neurons. However, there has been some investigation of changes with age in microglial degradation pathways. Disruptions in macroautophagy have been investigated *in vitro* via knockout of ATG7, a key autophagic gene, in both primary microglia and BV2 microglia-like cells. ATG7 knockout has been shown to increase expression of NLRP3 inflammasome components CASP-

1 and ASC following administration and uptake of Aβ (Cho et al., 2014). Thus, disruption of microglial autophagy may cause expression of pro-inflammatory factors and priming of microglia for expression of the NLRP3 inflammasome upon NLRP3 activation. Although this mechanism has not been specifically investigated in the context ageing, disruption of Aβ receptor turnover in microglia from aged animals, combined with evidence of macroautophagic disruption in peripheral macrophages, strengthens the possibility that dysregulated receptor turnover occurs with age and impairs microglial responses. For example, in bone marrow derived macrophages isolated from 23-mo C57BL/6 mice, there was reduced expression of autophagic genes (ATG-6 and ATG-7) and impaired autophagic flux measured by LC3 (Stranks et al., 2015). Of note, like the above results seen in ATG7 deficient primary microglia, ATG7 deficient macrophages in this study demonstrated a pro-inflammatory phenotype. This suggests a role of dysregulated autophagy in macrophage-driven inflammation and solidifies the theory that similar processes may occur in microglia with age, potentially predisposing these cells to an inadequate response to ND pathology. While distinct from macroautophagy, microglia also rely on distinct endocytic pathways to process extracellular material which have been shown to change with age. LC3-associated endocytosis (LANDO) is critical in the turnover of Aβ receptors (including TLR4 and TREM2) on microglia, ensuring correct recognition of the Aβ protein (Heckmann et al.). Microglia isolated from 24-mo mice lacking the WD domain of Atg16L, which is necessary for LANDO recycling of Aβ receptors, demonstrated decreases in uptake of Aβ in culture compared to aged-matched WT controls, suggesting a role for Aβ receptor turnover in dysfunctional proteostasis with age (Heckmann et al., 2020). This suggests that turnover of microglial surface receptors is crucial to ensure that microglia can respond adequately to pathological proteins, and loss of these mechanism may occur with age and limit the ability of microglia to respond to pathological proteins. Further investigation is necessary to determine whether macroautophagic and endocytic pathways interact in aged microglia and how potential changes in these pathways may influence microglial ageing as a whole.

2.3.6 Dysregulated nutrient sensing

In the brain, nutrient pathways and signalling cascades are critical in maintaining CNS homeostasis, which can be disrupted by microglia during ageing. Key pathways affected by microglial signalling

specifically include: the mechanistic target or rapamycin (mTOR), the 5'AMP-activated protein kinase (AMPK), and insulin/Insulin-like growth factor-1 (IGF-1) signalling pathways. Each of these pathways exert effects on one another and have been implicated in both ageing and NDs.

The mTOR pathway acts as a cellular energy sensor, responding to amino acids glucose, oxygen and growth factors including IGF-1 (Garza-Lombó et al., 2018). Dysregulated mTOR signalling with age can lead to overactive nutrient sensing, where excessive activation may contribute to the chronic, low-grade inflammation observed during ageing (reviewed: (Stallone et al., 2019)). This overaction could stem from persistently elevated levels of IGF-1 or other growth factors, as observed in C57BL/6J mice where mTOR activation was significantly increased at 23-mo compared to 6-mo in microglial isolated from female mice following analysis by phospho-flow cytometry (Keane et al., 2021). Studies in model organisms such as *Saccharomyces cerevisiae* and *Caenorhabditis elegans* (*C. elegans*) have supported the link between mTOR activity and ageing, where reduced mTOR activity has been shown to extend the lifespan (Fabrizio et al., 2001; Vellai et al., 2003). However, the specific analysis of mTOR pathway components in microglia remains sparce, and this gap underscores the need for further investigation into how nutrient signalling dysregulation in microglia might contribute to CNS ageing and NDs

Insulin/IGF-1 signalling, closely linked to mTOR activation, has also been linked with longevity in multiple species including *C. elegans, Drosophila melanogaster* and laboratory mouse strains (see review: (van Heemst, 2010)). In aged $APP_{SWE}/PS1_{\Delta E9}$ mice (24-mo), a model of AD, IGF-1 mRNA and TNF mRNA levels were both increased in the hippocampus compared to age matched WT mice. This was suggested to be due to the increase in IGF-1 mRNA-expressing microglia in the subgranular zone of the dentate gyrus (Myhre et al., 2019). These results suggest that increased IGF-1 signalling is a key component of microglial pro-inflammatory activation in AD during advanced ageing but whether this represents a point of difference to the inflammatory response in young animals needs further investigation.

The AMPK pathway serves as a central regulator of energy homeostasis, maintaining balance by counteracting mTOR activity (Garza-Lombó et al., 2018). AMPK responds to energy depletion (low ATP) by inhibiting anabolic processes and activating catabolic pathways (Garza-Lombó et al., 2018).

These functions highlight the role of AMPK as a critical controller of aging processes by modulating metabolism, oxidative stress and inflammation (Salminen and Kaarniranta, 2012). APMK activity has been shown to increase with age in the brain whereby phosphorylation of AMPK in young male C57BL/6 mice (2- to 3-mo) has been observed to be lower than in aged 16- to 18-mo mice, suggesting more activation of AMPK in the brain during healthy ageing (Liu et al., 2012). However, in this same study, activation of AMPK following reversible middle cerebral artery occlusion is decreased in aged mice compared to young mice (Liu et al., 2012), indicating decreased responsiveness of AMPK during ageing which may contribute to worsened outcomes following injury or pathology. The understanding of these changes during the neuroinflammatory response is thus critical in understanding AMPK pathway roles in neuroinflammation with ageing however the AMPK pathway has not been explored specifically in microglia with ageing. However, BV2 microglia-like cells have been used to demonstrate the anti-inflammatory effects of AMPK activation in microglia. For instance, activation of the AMPK pathway by administration of 80μM of ENERGI-F704, a small molecule drug which causes phosphorylation and activation of AMPK, reduced the pro-Il-6 and TNF response of BV2 cells following LPS stimulation (Chen et al., 2014). This suggests an ameliorating effect and potentially beneficial role of this pathway in reducing microglial inflammation (Chen et al., 2014). It is not yet known if and how levels of AMPK pathway activation are altered in microglia with advanced age, with further investigation needed to probe these changes.

2.3.7 Mitochondrial dysfunction

Mitochondria are responsible for regulating a host of different cellular processes but are mainly involved in energy production and oxidative balance. They are a critical component of the free radical theory of ageing due to their high production of and vulnerability to ROS. Additionally, damaged or dysfunctional mitochondria are involved in inflammatory processes, particularly by activation of the DNA driven immune response by mtDNA damage or by free mtDNA released from damaged mitochondria (Fig 2.3b). With age, mitochondrial function declines, leading to increased production of ROS and ROS-induced inflammatory responses (Amorim et al., 2022). Mitochondrial transcription factor A (TFAM) is a promotor of mtDNA transcription and is critical in maintaining correct mtDNA

transcription and regulating degradation of damaged mtDNA (Xu et al., 2019). In a study of male C57BL/6 mice overexpressing TFAM at 24-mo, microglia demonstrated a decrease in malondialdehyde levels, a product of lipid peroxidation and oxidative stress, compared to young WT mice, but in aged WT mice (24-mo), lipid peroxidation was increased (Hayashi et al., 2008). This suggests a decline in TFAM regulation of mtDNA transcription with age, which may, in turn, lead to increased oxidative stress in microglia. In addition, TFAM mice demonstrated no changes in mitochondrial complex 1 activity, measured by the reduction of decylubiquinone (a product of mitochondrial complex 1 catalysation), with age, whereas aged WT mice did. A decrease in mitochondrial complex 1 activity has been shown to cause increased in ROS production in bovine aortic endothelial cells (Hernansanz-Agustín et al., 2017).

As well as damaged mtDNA accumulation with age, mtDNA can also move into the cytosol, caused during ageing by altered mitophagy, leading to the escape of both damaged and undamaged mtDNA from mitochondria and stimulating the DNA driven immune response (Pérez-Treviño et al., 2020). In line with this, microglia from 20-mo C57BL/6J mice have shown an increased amount of cytosolic mtDNA compared to microglia from 2- to 3-mo mice (Gulen et al., 2023). This stimulated the cGAS-STING pathway in these animals, leading to the acquisition of a pro-inflammatory phenotype (Gulen et al., 2023). Taken together, these studies suggest that, with age, a loss of TFAM control of mtDNA leads to increased ROS production, with dysfunctional mitophagy further contributing to the accumulation of mtDNA within the cytosol of microglia. Combined, these mechanisms increase the pro-inflammatory nature of aged microglia, and the increased ROS production likely causes further damage to mitochondria, feeding the cycle of continued inflammation and oxidative stress which is characteristic of both ageing and NDs.

2.3.8 Cellular senescence

Cellular senescence is the term used to refer to cells which have undergone an irreversible cell cycle arrest (Gorgoulis et al., 2019) and is commonly associated with ageing, as senescent cells are known to accumulate in aged tissues (López-Otín et al., 2023). There are many features of senescence (reviewed: (González-Gualda et al., 2021)), but the characteristic cell cycle arrest is the most defining feature.

Indeed, microglia demonstrate changes in the senescence associated markers of cell cycle arrest, $p16^{INK4A}$ and $p21^{Cip1/Waf1}$, with advancing age. In 18-mo male C57BL/6 mice, expression of $p16^{INK4A}$, but not $p21^{Cip1/Waf1}$, was observed in microglia (Ritzel et al., 2019). This study also reported an increase in DNA damage (H2A.X stain) and lipofuscin accumulation in microglia in these mice. Lipofuscin progressively accumulates within aged cells and is considered to be involved in a number of age-related pathologies (Jung et al., 2007). Indeed, an increase in lipofuscin accumulation has been demonstrated within microglia in 24mo C57BL/6J mice of both sexes, although this was low in comparison to the levels that accumulated within neurons (Stillman et al., 2023).

Lipofuscin accumulation is often investigated in conjunction with senescence associated β Galactosidase (SA-β-Gal), as the presence of both has been shown to be related to lysosomal dysfunction with age (Georgakopoulou et al., 2013). In microglia, SA-β-Gal has been utilised to identify senescent microglia for further analysis. For example, to assess the proximity of senescent microglia to Aβ plaques, microglia in 8-mo 5XFAD mice, a model of AD pathology, and C57BL/6J WT mice were compared. Sagittal brain sections were stained for SA-β-Gal by overnight incubation in SA-β-Gal detection solution before undergoing 3,3'-diaminobenzidine (DAB) staining with IBA1 for microglial detection. Co-localisation of DAB (IBA1) with SA-β-Gal pigment demonstrated that the microglia surrounding pathological plaques were SA-β-Gal positive (Shin et al., 2024). SA-β-Gal staining has also been used to identify senescent microglia *in vitro*, identifying senescence in BV2 microglia-like cells following three or six treatments with the endotoxin LPS (Yu et al., 2012). Further, these BV2 cells demonstrated the acquisition of another well described marker of senescence, Senescence associated heterochromatin foci (SAHF). SAHF are regions of highly condensed chromatin formed in response to stresses, such as DNA damage and telomere dysfunction (Aird and Zhang, 2013). These formations are seen in LPS-induced ageing in BV2 cells (Borgonetti and Galeotti, 2023; Yu et al., 2012), but have not been assessed in *in vivo* studies looking at microglia change with advancing age.

Another marker of cellular senescence previously assessed in microglia is the acquisition of the senescence associated secretory phenotype (SASP), characterised by an increase in the production and release of pro-inflammatory cytokines and chemokines (Rim et al., 2024). Microglia are known for their

increased secretion of pro-inflammatory factors in NDs and indeed take on a similar phenotype during normal ageing. Microglia in 18-mo transgenic p7.2*fms*-EGFP mice on a C57BL6/6XCBA background have shown an increased release of pro- (IL-6, TNFα, IL-1β) and anti- (IL-10) inflammatory cytokines compared to mice at 2-mo of age (Sierra et al., 2007). Additionally, microglia from the spinal cords of C57BL/6J male mice at 22-mo show an increase in inflammatory cytokine release (TNFα, IL-1β), coupled with increased ROS-induced oxidative stress and microglial phagocytic ability (Ritzel et al., 2015). Taken together, there is significant evidence to show microglia display multiple markers of cellular senescence with advancing age. Given that senescence is associated with pro-inflammatory factors, microglia acquiring a senescent phenotype with age implicates ageing itself as a factor in the development of chronic inflammation, which is hypothesised to underly ND development.

2.3.9 Stem cell exhaustion

As a hallmark of ageing, stem cell exhaustion describes the decline in regenerative potential of adult stem cells, defined by López-Otín and colleagues (López-Otín et al., 2013, 2023) as the reduction of cell cycle activity of hematopoietic stem cells, contributing to the lack of capacity for tissue regeneration with age. Microglia have been shown to have great capacity for regeneration following mass depletion of their population, indicating that they are capable of proliferation and self-renewal (Bruttger et al., 2015; Elmore et al., 2014; Huang et al., 2018). Despite this, however, previous studies in mice have shown that microglia are generally long lived, with half the microglial population lasting the entire lifespan of an animal (Füger et al., 2017). In line with this, a study in human post-mortem tissue from young (20- to 35-years-old) and old (58- to 79-years-old) adults showed no changes in the number of microglia positive for the proliferative marker Ki67 between groups, supporting the hypothesis of slow maintained turnover across the lifespan (Askew et al., 2017). Interestingly, in the presence of amyloid pathology in a triple-transgenic CD11b-CreERT2;R26-tdTomato;APP/PS1 mouse model of AD, microglia increased their proliferation at 10-mo compared to wild-type animals of the same age, with these new microglia proliferating from existing mature microglia, rather than microglial precursor cells (Füger et al., 2017). Overall, the literature reports microglial renewal as a slow steady process

throughout the lifespan, however in the presence of pathology at older timepoints, microglial proliferation may increase.

2.3.10 Altered intercellular signalling

Changes in intercellular communication are an indicator of ageing, with alterations in cell signalling pathways potentially leading to an increased pro-inflammatory environment and loss of homeostatic processes (López-Otín et al., 2023). During ageing, there is dysregulation in a number of mechanisms of intercellular communication, including loss of gap junctions and changes in pro-inflammatory signalling pathways. For microglia in particular, intrinsic changes in pathways such as the NF-κB/NLRP3, Fyn kinase and MAPK pathways lead to altered release of key signalling molecules, including cytokines. The NLRP3 inflammasome is expressed by both microglia (Cho et al., 2014) and astrocytes (Lu et al., 2014) in the CNS; however, it is primarily associated with microglia (Chiarini et al., 2023). Under physiological conditions, NLRP3 is expressed at low levels; however, during the inflammatory response, microglia have increased activation of the NLRP3 inflammasome complex (Fig 2.3a) (Song et al., 2017). This leads to the release of IL-1β, in turn activating neighbouring cells, including other microglia, further perpetuating the inflammatory response (Kamo et al., 2013). With age, the NLRP3 inflammasome becomes overactive, indicating a potential contribution to the chronic pro-inflammatory state seen in microglia with advancing age (Liang et al., 2024). In line with this, in 18-mo old male BALB/c mice, multiple NLRP3 pathway proteins, including ASC, caspase-1, IL-18 and NLRC4, were increased in the hippocampus and cortex compared to 3-mo mice (Mejias et al., 2018). Additionally, there was an increase in pyroptosis in these regions, indicating a role for increased NLRP3 signalling in pyroptotic cell death. Of note, microglial activation in the dentate gyrus has been shown to be decreased in 23-mo NLRP3$^{-/-}$ mice compared to aged matched genetic controls, as well as relative to 2-mo NLRP3$^{-/-}$ mice, suggesting that NLRP3 activation may play a larger role in microglial activation with advancing age (Youm et al., 2013).

NF-κB signalling is involved in activation of the NLRP3 inflammasome by causing the transcription of pro-IL-1β, pro-caspase-1 and NLRP3 (Liu et al., 2017) (Figure 2.3a). Age-related increases in NF-κB signalling and nuclear translocation lead to an increase in both NLRP3 inflammasome formation and

secretion of pro-inflammatory cytokines (Liu et al., 2017). Figure 2.3a.4 shows the mechanisms by which NF-κB is translocated to the nucleus. IκB is normally bound to NF-κB in the cytoplasm and prevents NF-κB activation. IκB phosphorylation and degradation by the proteasome exposes NF-κB localisation subunits including P50 and P65, leading to translocation of NF-κB to the nucleus where it then triggers various gene expression (Liu et al., 2017). Alterations in these NF-κB subunits, specifically ablation of the p50 subunit in C57BL/6J mice ($p50^{-/-}$), has been shown to increase the inflammatory response of microglia to LPS administration (Taetzsch et al., 2019). This response was exacerbated in $p50^{-/-}$ mice at 16-18-mo compared to both $p50^{+/+}$ age-matched controls, and young $p50^{-/-}$ mice (3-weeks-old), suggesting that NF-κB disruption may be particularly detrimental in the context of ageing (Taetzsch et al., 2019).

Fyn kinase and MAPK pathways are upstream regulators of both NLRP3 and NF-κB, with increased Fyn and p38 MAPK signalling promoting pro-inflammatory signals within microglia (Bachstetter et al., 2011; Panicker et al., 2015). Previous literature indicates that activation of both pathways may be impacted by ageing, although in differential ways. In line with this, a previous study in 1-year-old C57BL/6J mice has shown reductions in Fyn signalling in both pre- and post-synaptic density protein fractions in the frontal cortex compared to 2-mo mice three days following traumatic stress induced by dorsomyotomy and exploratory laparotomy (Zhao et al., 2012). Conversely, in male C57BL/6J mice at 20-mo of age, phosphorylated-p38 MAPK protein levels in the brain were increased compared to 2-mo mice (Li et al., 2011). While neither Fyn nor MAPK pathways have yet been studied specifically in microglia during ageing, given the link between these signalling pathways and the changes seen in the brain overall with age, it is reasonable to hypothesise that dysregulation in these key pathways within microglia themselves may be responsible for the upregulation in pro-inflammatory signalling seen with increased age.

2.3.11 Chronic inflammation

Evidence for chronic inflammation in the aged brain has previously been extensively reviewed (Andronie-Cioara et al., 2023; Jin et al., 2022; Moyse et al., 2022). Given their critical role in regulating the inflammatory response, microglia are likely a major driver of this response. Of note, microglia in

aged mice remain activated for longer following brain injury than their young counterparts. For example, following a controlled cortical impact (CCI), microglia in the hippocampus of male 24-mo C57BL/6 mice showed increased markers of activation and took a longer time to resolve their response compared to mice at 5- to 6-mo (Sandhir et al., 2008). Additionally, aged C57BL/6 male mice displayed a propensity to acquire a pro-inflammatory phenotype at 24-months of age following CCI, with a decreased ability to mount an anti-inflammatory response compared to 3-mo mice (Kumar et al., 2013). Similar results have also been seen in stroke models, where, following intracerebral haemorrhage induced by collagenase injection to the striatum, male Sprague-Dawley rats at 22-mo showed a slower microglial response and prolonged activation around the hematoma compared to 3- to 4-mo rats following injury (Wasserman et al., 2008). This study additionally demonstrated morphological differences in microglia of naïve animals with age, with microglia from 24-mo rats demonstrating shorter and thicker processes, characteristic of bushy morphology, compared to the ramified morphology in 3- to 4-mo rats (Figure 2.2).

The population of microglia is also altered with age however, there appear to be clear sex differences in these changes. For example, in the hippocampus of male C57BL/6 mice, microglial number was stable throughout the lifespan, with no changes observed from young (4- to 5-mo), middle-aged (13- to 14-mo) to aged (27- to 28-mo) mice in the dentate gyrus, CA1 or Hilus (Long et al., 1998). Additionally, no changes in microglial density in these regions were observed, nor were there differences in the number of astrocytes present, indicating that glial numbers are stable with age, at least within hippocampal regions. Conversely, in a separate study by the same authors, in the CA1 region of female C57BL/6 mice, microglial numbers increased steadily across young (3- to 4-mo), middle-aged (13- to 14-mo) and aged (20- to 24-mo) cohorts (Mouton et al., 2002). Importantly, at each timepoint, the microglial counts in female mice were significantly higher than CA1 counts in the equivalent male cohort from the previous study. These differences are also seen in human post-mortem brains, where for example, the number of microglia in the female neocortex (age range: 18-93 years) increased with age; however, in these regions in males, no such changes were observed (age range: 19-87 years) (Pelvig

et al., 2008). Taken together, these results indicate an effect of biological sex on microglial dynamics with age, and thus highlight the importance of including sex balanced cohorts in ageing research.

Beyond population dynamic, the activation state of microglia is also altered with increased age. In line with this, the number of activated microglia measured by MHCII positivity increase with age in both mouse and non-human primate tissue. In male C57BL/6 mice, the number of MHCII positive microglia at 22- to 24-mo was increased compared to in 3- to 5-mo mice (Garner et al., 2018). Similarly, when investigated in macaque brains, microglial MHCII expression increased at 10- to 18-years-old compared to at 2- to 5-years-old (Sheffield and Berman, 1998). In humans, microglial activation with age has been studied by utilising the positron emission tomography (PET) ligand (R)-[^{11}c]PK111955, which specifically binds to activated microglia expressing the 18 kDa translocator protein (TSPO) (Shah et al., 1994). One study using this ligand in a cohort of 33 subjects (22M:11F) aged 19- to 79-years-old found an association between increasing age and enhanced ligand binding throughout the brain. This data suggests that microglial activation is associated with increasing age in healthy living subjects (Schuitemaker et al., 2012). Taken together, these data support a pattern of increased microglial activation with age, regardless of species and sex. This enhanced activation may contribute to the ongoing chronic inflammation seen in age-related NDs.

Age-related intrinsic changes within microglia are thought to drive the chronic inflammatory environment observed in the aged brain. Nuclear and mtDNA damage is thought to play a key role in this through the DNA driven immune response (Pérez-Treviño et al., 2020). In line with this, in 20-mo C57BL/6J mice, STING activity was shown to be upregulated in microglia, suggesting heightened cytosolic DNA sensing in these cells (Gulen et al., 2023). Indeed, the increased stimulation of the cGAS-STING pathway, described in the mitochondrial dysfunction section above, is thought to drive the shift towards a pro-inflammatory phenotype with age, contributing to ongoing inflammation in microglia (Gulen et al., 2023). These studies support the idea that microglia are a driver of the chronic inflammation observed with advancing age which potentially underlies and likely exacerbates ND pathology.

2.3.12 Dysbiosis

Dysbiosis as a hallmark of ageing refers to the imbalance of bacteria in the gut (López-Otín et al., 2023). A 2022 review identified two groups of taxa associated with ageing (Ghosh et al., 2022). The first group consisted of mainly pro-inflammatory taxa and was associated with unhealthy ageing, defined by shortened lifespans, whereas the second group consisted of beneficial taxa and was associated with healthy ageing but were also decreased in unhealthy ageing compared to the first group (Ghosh et al., 2022). This result suggests that longevity and healthy ageing may be associated with higher levels of beneficial taxa in the gut, while pro-inflammatory taxa may lead to an accelerated ageing process. Links between changes in the composition of the gut microbiome and CNS conditions are becoming increasingly apparent (Abdel-Haq et al., 2019), and the gut-brain-axis is an important pathway of regulation of glial function (Loh et al., 2024). Microglia appear to be the most vulnerable CNS cell type to changes in the gut microbiome (Huang et al., 2023b). In 2-mo Kun Ming mice, gene expression in microglia in response to altered gut microbiome was altered more than any other cell type (Huang et al., 2023b). Specifically, differential expression of inflammasome genes, genes associated with mitochondrial dysfunction and oxidative phosphorylation genes, have shown alterations in the prefrontal cortex and hippocampus (Huang et al., 2023b). Thus, microglial function and maturation can be influenced by changes in the gut microbiota, which, when considering the increase of pro-inflammatory taxa in the gut with age, has implications for phenotypic changes in microglia (Abdel-Haq et al., 2019). Indirect modulation of microglia via interactions of pro-inflammatory bacteria with peripheral immune cells has additionally been demonstrated in aged mice. Peripheral administration of LPS in 20-mo male BALB/c mice induced a hyperactive microglial response, as measured by increased mRNA expression of IL-1β, IL-10 and TLR-2 in isolated microglia (Henry et al., 2009). Given that LPS is often released as a signalling byproduct by microbes in the gut (Mohr et al., 2022) and that during ageing, increased gut permeability allows LPS to cross into blood circulation (Thevaranjan et al., 2017), this study further implicates pro-inflammatory changes in the gut with age as a potential driver of microglial ageing. Further, interactions between gut microbiota and microglial phenotypes have also previously been demonstrated and reviewed (Abdel-Haq et al., 2019; Zhou et al., 2022). Thus,

the gut dysbiosis seen with advancing age can reasonably be expected to impact microglia, likely promoting a pro-inflammatory phenotype and contributing to vulnerability to neurological dysfunction.

Table 2.2: Evidence of the hallmarks of ageing in microglia

Hallmark	Features seen in aged microglia				
	Model	**Sex**	**Ages compared** Age of observed change is underlined	**Changes observed**	**Ref**
Genomic instability	C57BL/6 mice	Not specified	24mo compared to 2mo	↑accumulation of DNA damage measured by γ-H2A.X staining ↑ percentage of microglia positive for pSTING and CD11b	(Arvanitaki et al., 2024)
	Ercc1$^{\Delta/-}$mice on C57BL6J/FVB background	Male and female	16wo compared to age/sex matched genetic controls	Hypertrophy of processes and ↑ cell body size ↑proliferation, ↑phagocytosis, ↑ROS production	(Raj et al., 2014)
	Ercc1$^{\Delta/-}$mice induced by tamoxifen administration at 6- to 8-wo on C57BL6J/FVB background	Male and female	2-, 6-, and 12-months following tamoxifen administration (approx. 4-, 6-, and 14-mo) compared to age/sex matched genetic controls	↓microglial number at 6- and 12-month timepoints	(Zhang et al., 2021)
	Human post-mortem tissue from the: temporal cortex, hippocampus, entorhinal cortex, substantia nigra, superior colliculi, locus coeruleus and inferior colliculi	6M:8F	65-96 years old (80.42±9.07)	Dystrophic microglia associated with ↑ferritin but not γ-H2A.X staining	(Neumann et al., 2023)
	Microglia isolated from human mid-frontal gyrus (n=10)	2M:8F	94.07 years ±0.95 compared to published middle age microglial transcriptomic dataset (53 years ± 5.29)	Identified 1060 upregulated, and 1174 downregulated genes with ageing	(Olah et al., 2018)
Telomere attrition	Microglia isolated from cortex of neonatal rats	Not specified	Aged by replicative senescence over 32 days in culture	↓telomere length measured by flow-FISH Steady decline and then rapid increase in telomerase activity during culture	(Flanary and Streit, 2004)
	Microglial isolated from Fisher-344 rats	Male	30-mo compared to 3-mo	↓telomere length measured by flow-FISH ↓telomerase activity	(Flanary et al., 2007)

	Microglia isolated from human superior frontal gyrus/frontal pole region	AD = 3M:1F ND = M	4 AD cases (86-years-old ± 2.54) One non-dementia case (86-years-old)	↓telomere length measured by flow-FISH No change in telomerase activity	(Flanary et al., 2007)
	Terc knockout mice with AD pathology: G3Terc$^{-/-}$APP23^{+} mice	Not specified	12-mo compared to age matched genetic controls	↓Aβ pathology in frontal cortex Improved spatial memory No microglial activation near Aβ plaques	(Rolyan et al., 2011)
	Terc knockout mice with PD pathology: αSYN$^{tg/tg}$G3Terc$^{-/-}$ mice	Not specified	75-wo compared to age matched genetic controls	↓microglial IL-1β and MHCII in the brainstem	(Scheffold et al., 2016)
Epigenetic changes	C57BL/6J mice	Male	16- to 18-mo compared to 2- to 3-mo	↑ iNOS, IL-6 and TNFα ↑ H3K27me3 in the midbrain ↓ JMJD3	ang et al., 2014)
	Microglia isolated from C57BL/6J mice following LPS exposure	Not specified	24- to 26-mo compared to 4- to 6-mo	↓ methylation of IL-1β promoter DNA leading to increased IL-1β production	(Matt et al., 2016)
	C57BL/6J mice	Male and female	24-mo compared to 3- and 14-mo	↑ chromatin accessibility of phagocytosis, IFN signalling, ROS production and antigen presentation genes ↓ chromatin accessibility of chemokine suppression and iron transportation genes	(Li et al., 2023a)
Loss of proteostasis	Microglia isolated from C57BL/6N mice	Not specified	20- to 24-mo compared to 3- to 5-mo	↓ proteasomal subunits PSMB4, PSMA6, PSMC1	(Flowers et al., 2017)
	APP/PS1 mice lacking the LMP7 immunoproteasome component	Not specified	8-mo compared to age matched genetic controls	↓ microglial immunoreactivity No change in Aβ pathology	(Wagner et al., 2017)
	Deletion of E3 ubiquitin ligase COP1 in C57BL/6N mice by tamoxifen administration	Male and female	22-mo compared to young WT mice	↑ microglial IFN signalling gene expression ↑APOE expression	(Ndoja et al., 2020)

	C57BL/6 mice	Male and female	Sex differences at 18-mo compared to 3-mo Both sexes differences at 22-mo compared to 3-mo	Female mice: ↓ microglial phagocytic action on Aβ42 Male mice: ↓ proteolytic gene expression Both sexes: ↓ expression of phagocytic receptor TREM2	(Thomas et al., 2022)
Disabled macroautophagy	Microglia isolated from mice with deletion of WD domain of Atg16L on a mixed 129/C57BL/6 background	Male and female	24-mo compared to age matched genetic controls	↓ uptake of Aβ	(Heckmann et al., 2020)
	Bone marrow derived macrophages isolated from C56BL/6 mice**	Male	23-mo compared to 6- to 8-wo	↓expression of autophagic genes ATF7 and ATG6 Impaired autophagic flux	(Stranks et al., 2015)
Deregulated nutrient sensing	Microglia isolated from C57BL/6N mice	Not specified	20- to 24-mo compared to 3- to 5-mo	↓ mTORC2-dependent AKT D473 phosphorylation ↑IL-6, IL-1β, TNFα at baseline and in response to TNFα	(Flowers et al., 2017)
	Wistar rats treated with insulin for 5 days	Male	22-mo compared to 3-mo	↓microglial activation in hippocampus	(Haas et al., 2020)
	Microglia isolated from C57BL/6J mice	Female	23-mo	mTOR dysregulation	(Keane et al., 2021)
	$APP_{SWE}/PS1_{\Delta E9}$ mice	Female	24-mo compared to age matched genetic controls	↑IGF-1 and TNF mRNA in hippocampus ↑IGF-1 mRNA expressing microglia in subgranular zone of dentate gyrus	(Myhre et al., 2019)
Mitochondrial dysfunction	WT C57BL/6 mice and C57BL/6 mice overexpressing TFAM	Male	24-mo WT compared to 2-mo WT 24-mo TFAM compared to 2-mo WT	24-mo WT: ↑lipid peroxidation 24-mo TFAM: ↓ lipid peroxidation	(Hayashi et al., 2008)
	Microglia isolated from C57BL/6 mice	Not specified	20-mo compared to 8- to 12-wo	↑cytosolic mtDNA	
Cellular senescence	C57BL/6 mice	Male	18-mo compared to 3-mo	↑ expression of $p16^{INK4A}$ but no change in $p21^{Cip1/Waf1}$ Accumulated lipofuscin	(Ritzel et al., 2019)

				↑ DNA damage measured by γ-H2A.X staining	
	C57BL/6 mice	Male and Female	24-mo	Accumulated lipofuscin	(Stillman et al., 2023)
	5XFAD mice and C57BL/6J WT mice	Male and female	8-mo compared to 4-mo	↑presence of SA-β-Gal^{+} microglia proximal to Aβ plaques	(Shin et al., 2024)
	BV2 microglia-like cells	N/A	Cells aged by repetitive (6x) LPS administration	↑SA-β-Gal and ↑SAHF formation	(Yu et al., 2012)
	Transgenic p7.2*fms*-EGFP mice on a C57BL6/6XCBA background	Male and female	18-mo compared to 2-mo	↑pro- ((IL-6, TNFα, IL-1β) and anti- (IL-10) inflammatory cytokines	(Sierra et al., 2007)
	Microglia isolated from spinal cords of C57BL/6J mice	Male	22-mo compared to 3-mo	↑TNFα, IL-1β release ↑ ROS induced oxidative stress ↑microglia phagocytic ability	(Ritzel et al., 2015)
Stem cell exhaustion	Cd11b-CreERT2 transgenic mice on a C57BL/6J x C3Hej background	Male and female	15-mo compared to 4-mo	Microglial cells are long lived and stable across life	(Füger et al., 2017)
	C57BL/6 mice	Not specified	18- to 20-mo compared to 4- to 6-mo	No changes in microglial number in hippocampus or cortex but ↑ in the thalamus	(Askew et al., 2017)
	Human post-mortem tissue	Not specified	58- to 79-yo compared to 20- to 35-yo	No changes in number of proliferating (Ki67^{+}) cells	(Askew et al., 2017)
Altered intercellular communication	BALB/c mice	Male	18-mo compared to 3-mo	↑ NLRP3 pathway proteins in hippocampus and cortex ↑pyroptosis in hippocampus and cortex	(Mejias et al., 2018)
	NLRP3$^{-/-}$ mice	Male and female	23-mo compared to 2-mo and to aged matched genetic controls	Loss of NLRP3 caused ↓ in microglial activation in dentate gyrus ↓in IL-1β and TNF mRNA expression	(Youm et al., 2013)
	C57BL/6J mice deficient in the p50 NF-κB subunit	Not specified	16- to 18-mo compared to 3-wo and age matched genetic controls	↑inflammatory response of microglia to LPS administration	(Taetzsch et al., 2019)

	C57BL/6J mice	Not specified	12-mo compared to 2-mo	↓Fyn in pre- and post-synaptic protein fractions from the frontal cortex following traumatic stress	(Zhao et al., 2012)
	C57BL/6J mice	Male	20-mo compared to 2-mo	↑phospho-p38 MAPK in brain tissue	(Li et al., 2011)
Chronic inflammation	C57BL/6 mice following a moderate controlled cortical impact (CCI)	Male	21- to 24-mo compared to 5- to 6-mo	↑ inflammatory response in the hippocampus following injury ↑ time to resolve response	(Sandhir et al., 2008)
	C57BL/6 mice following CCI	Male	24-mo compared to 3-mo	↑pro- and ↓ anti-inflammatory markers of activation	(Kumar et al., 2013)
	Sprague-Dawley rats following collagenase-induced intracerebral haemorrhage	Male	22-mo compared to 3- to 4-mo	Slower microglial response to injury Prolonged activation around hematoma	(Wasserman et al., 2008)
	C57BL/6J mice	Male	27- to 28-mo compared to 13- to 14-mo and 4- to 5-mo	No change in microglial number in hippocampal regions across ageing	(Long et al., 1998)
	C57BL/6J mice	Female	20- to 24-mo compared to 13- to 14-mo and 3- to 4-mo	Increase in microglial numbers with age in CA1 region Increased numbers at each age group compared to equivalent cohort in males (study above (253))	(Mouton et al., 2002)
	Human post-mortem neocortex	Males and females	Age range females 18-93 years Age range males 19-87 years	Number of microglia increased with age in females but not males	(Pelvig et al., 2008)
	C57BL/6 mice	Male	22- to 24-mo compared to 3- to 5-mo	↑ MHCII positive microglia	(Garner et al., 2018)
	Macaca nemestrina	Females	10- to 18-yo compared to 2- to 5-yo	↑ MHCII positive microglia	(Sheffield and Berman, 1998)
	In vivo human brain (PET imaging)	Males and females (22M:11F)	19 to 79-years-old	↑ (R)-[^{11}c]PK111955 ligand binding associated with ↑ age	(Schuitemaker et al., 2012)

	C57BL/6J mice	Not specified	20-mo compared to 3-mo	↑ STING activity	(Gulen et al., 2023)
Dysbiosis	BALB/c mice	Male	18- to 20-mo compared to 3- to 4-mo	Peripheral administration of LPS leads to hyperactive immune response ↑mRNA expression of IL-1β, IL-10 and TLR2	(Henry et al., 2009)

2.4 The functional phenotype of microglia beyond activation

Overall, the dystrophic morphology of aged microglia is accompanied by the acquisition of a senescent state with increased pro-inflammatory signalling. The aged phenotype of microglia as related to the twelve hallmarks of ageing is outlined in Figure 2.4. Microglia display a decreased capacity for homeostatic functions, including phagocytosis, and an increased production and release of pro-inflammatory factors, resulting in increased pro-inflammatory signalling. In general, this decreased capacity of microglia to maintain homeostatic immune functions may contribute to the vulnerability of the brain to age-related diseases, including the development of NDs (Koellhoffer et al., 2017). However, these changes may not be the sole cause of NDs, and indeed age-related changes in neurons also appear to be major drivers of disease pathophysiology (Höhn et al., 2020).

While the studies discussed above highlight significant features of aged microglia, this is still a relatively understudied area. Research on ageing in peripheral macrophages have garnered more attention, with the hallmarks of ageing in macrophages reviewed recently (Guimarães et al., 2021). However, microglia have not received equivalent focus, a notable gap likely due to the challenges of accurately replicating aged CNS cells in research models (Carr et al., 2024). This is also reflective that ageing more generally is often not considered in preclinical modelling studies of ND, a critical consideration to improve translational potential (Carr et al., 2024). Therefore, studies should seek to investigate ageing at an individual cell level to uncover changes which may drive changes overall changes in the brain.

Additionally, there is an underappreciation of sex-specific differences in microglial ageing and immune activation. Previous literature has highlighted sex differences in microglia with age and in neuroinflammation more generally. For instance, in female Fischer 344 rats, microglial number in the dentate gyrus increases with age at 18-mo compared to in rats at 3-mo but no difference is observed in male rats (Perkins et al., 2018). Similarly, in human post-mortem tissue, no changes in the number of microglia in the neocortex has been observed with age in males (19- to 87-years) but increased numbers have been seen in females (18- to 93-years) (Pelvig et al., 2008). These studies suggest sex specific differences in microglial dynamics which have been further explored and reviewed (Cyr and de Rivero

Vaccari, 2023; Lynch, 2022) and have been suggested as a driving mechanism for broader sex differences seen in ND susceptibility (Lynch, 2022). This is of concern as only 20% of neuroscience studies using both sexes and 25% not reporting the sex of subjects (Beery, 2018). Future research should therefore endeavour to consistently include and report both female and male animals in order to better understand differences in microglia during disease and ageing.

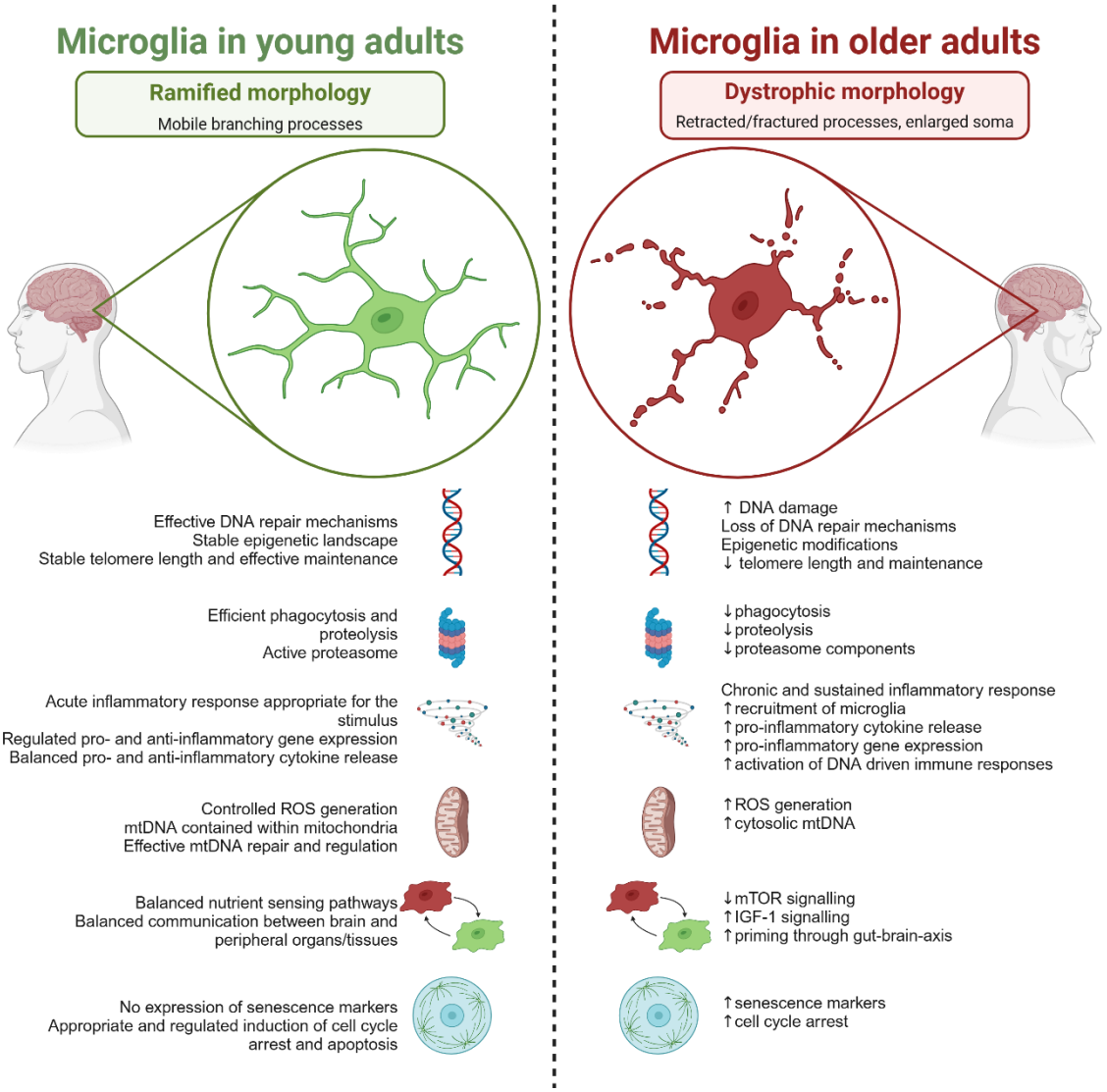


Figure 2.4: Features of adult (left) and aged (right) microglia.Left: Normal young adult microglia are highly motile with a ramified morphology and can perform homeostatic and immune functions without inducing hostile environmental conditions. Right: Aged microglia display enlarged dystrophic morphology and present with many of the hallmarks of ageing.

2.5 Conclusions

As the major immune cells of the brain, microglia have a critical role in maintaining brain health and responding to immune challenges. Ageing has a profound impact on microglial function and intrinsic changes within these cells are suggested to contribute to vulnerability of the brain to age-related disorders, including processes. Currently, the literature defines aged microglia as pro-inflammatory and dystrophic, with a similar phenotype to that seen in disease. However, studies on microglial morphology may benefit from consistency of terminology and clear definition of microglial phenotypes. Additionally, studies have largely focused on pro-inflammatory processes linked to microglia in NDs or following injury. However, understanding the changes which occur in microglia with ageing alone is critical in understanding the contribution of the ageing process to disease susceptibility and progression.

Here, a consideration of alterations in the 12 hallmarks of ageing (López-Otín et al., 2023) within microglia highlights clear gaps in our knowledge of how these processes change in microglia with increasing age. Many of these processes have been investigated in the context of disease (e.g. NDs), but studies have only rarely investigated the impact of ageing alone on these hallmarks. For example, both chronic inflammation and changes in proteostasis within microglia have been extensively studied in the context of ND. Conversely, other hallmarks not as clearly associated with ND pathophysiology, such as gut dysbiosis and stem cell exhaustion, have been investigated in aged microglia in only a handful of studies presented above. Thus, the full phenotype of aged microglia remains poorly characterised and needs to be better understood in both older age and late-middle age brains in order to improve our ability to capture these changes in research models. Investigating microglial ageing in older adults will contribute to understanding of the background environment upon which NDs occur whereas understanding microglia in late-middle age will help to elucidate potential changes happening prior to disease onset. As such, a comprehensive characterisation of microglia at different points across the lifespan is needed to understand how these cells contribute to vulnerability to disease and the potential to target microglial ageing to benefit NDs.

2.6 References

Abdel-Haq, R., Schlachetzki, J.C.M., Glass, C.K., Mazmanian, S.K., 2019. Microbiome-microglia connections via the gut-brain axis. J Exp Med 216, 41-59.

Aird, K.M., Zhang, R., 2013. Detection of senescence-associated heterochromatin foci (SAHF). Methods Mol Biol 965, 185-196.

Alam, Z.I., Jenner, A., Daniel, S.E., Lees, A.J., Cairns, N., Marsden, C.D., Jenner, P., Halliwell, B., 1997. Oxidative DNA Damage in the Parkinsonian Brain: An Apparent Selective Increase in 8-Hydroxyguanine Levels in Substantia Nigra. Journal of Neurochemistry 69, 1196-1203.

Alliot, F., Godin, I., Pessac, B., 1999. Microglia derive from progenitors, originating from the yolk sac, and which proliferate in the brain. Brain Res Dev Brain Res 117, 145-152.

Amorim, J.A., Coppotelli, G., Rolo, A.P., Palmeira, C.M., Ross, J.M., Sinclair, D.A., 2022. Mitochondrial and metabolic dysfunction in ageing and age-related diseases. Nature Reviews Endocrinology 18, 243-258.

An, W.L., Cowburn, R.F., Li, L., Braak, H., Alafuzoff, I., Iqbal, K., Iqbal, I.G., Winblad, B., Pei, J.J., 2003. Up-regulation of phosphorylated/activated p70 S6 kinase and its relationship to neurofibrillary pathology in Alzheimer's disease. Am J Pathol 163, 591-607.

Andronie-Cioara, F.L., Ardelean, A.I., Nistor-Cseppento, C.D., Jurcau, A., Jurcau, M.C., Pascalau, N., Marcu, F., 2023. Molecular Mechanisms of Neuroinflammation in Aging and Alzheimer's Disease Progression. Int J Mol Sci 24.

Angelova, D.M., Brown, D.R., 2019. Microglia and the aging brain: are senescent microglia the key to neurodegeneration? Journal of Neurochemistry 151, 676-688.

Arvanitaki, E.S., Goulielmaki, E., Gkirtzimanaki, K., Niotis, G., Tsakani, E., Nenedaki, E., Rouska, I., Kefalogianni, M., Xydias, D., Kalafatakis, I., Psilodimitrakopoulos, S., Karagogeos, D., Schumacher, B., Stratakis, E., Garinis, G.A., 2024. Microglia-derived extracellular vesicles trigger age-related neurodegeneration upon DNA damage. Proceedings of the National Academy of Sciences 121, e2317402121.

Askew, K., Li, K., Olmos-Alonso, A., Garcia-Moreno, F., Liang, Y., Richardson, P., Tipton, T., Chapman, M.A., Riecken, K., Beccari, S., Sierra, A., Molnár, Z., Cragg, M.S., Garaschuk, O., Perry, V.H., Gomez-Nicola, D., 2017. Coupled Proliferation and Apoptosis Maintain the Rapid Turnover of Microglia in the Adult Brain. Cell Reports 18, 391-405.

Bachstetter, A.D., Ighodaro, E.T., Hassoun, Y., Aldeiri, D., Neltner, J.H., Patel, E., Abner, E.L., Nelson, P.T., 2017. Rod-shaped microglia morphology is associated with aging in 2 human autopsy series. Neurobiology of Aging 52, 98-105.

Bachstetter, A.D., Xing, B., de Almeida, L., Dimayuga, E.R., Watterson, D.M., Van Eldik, L.J., 2011. Microglial p38α MAPK is a key regulator of proinflammatory cytokine up-regulation induced by toll-like receptor (TLR) ligands or beta-amyloid (Aβ). J Neuroinflammation 8, 79.

Barger, S.W., Harmon, A.D., 1997. Microglial activation by Alzheimer amyloid precursor protein and modulation by apolipoprotein E. Nature 388, 878-881.

Baruch-Eliyahu, N., Rud, V., Braiman, A., Priel, E., 2019. Telomerase increasing compound protects hippocampal neurons from amyloid beta toxicity by enhancing the expression of neurotrophins and plasticity related genes. Sci Rep 9, 18118.

Beckelman, B.C., Yang, W., Kasica, N.P., Zimmermann, H.R., Zhou, X., Keene, C.D., Ryazanov, A.G., Ma, T., 2019. Genetic reduction of eEF2 kinase alleviates pathophysiology in Alzheimer's disease model mice. The Journal of Clinical Investigation 129, 820-833.

Beery, A.K., 2018. Inclusion of females does not increase variability in rodent research studies. Curr Opin Behav Sci 23, 143-149.

Bell, J.E., Alafuzoff, I., Al-Sarraj, S., Arzberger, T., Bogdanovic, N., Budka, H., Dexter, D.T., Falkai, P., Ferrer, I., Gelpi, E., Gentleman, S.M., Giaccone, G., Huitinga, I., Ironside, J.W., Klioueva, N., Kovacs, G.G., Meyronet, D., Palkovits, M., Parchi, P., Patsouris, E., Reynolds, R., Riederer, P., Roggendorf, W., Seilhean, D., Schmitt, A., Schmitz, P., Streichenberger, N., Schwalber, A., Kretzschmar, H., 2008. Management of a twenty-first century brain bank: experience in the BrainNet Europe consortium. Acta Neuropathologica 115, 497-507.

Bhat, R., Crowe, E.P., Bitto, A., Moh, M., Katsetos, C.D., Garcia, F.U., Johnson, F.B., Trojanowski, J.Q., Sell, C., Torres, C., 2012. Astrocyte senescence as a component of Alzheimer's disease. PLoS One 7, e45069.
Bhatia, S., Rawal, R., Sharma, P., Singh, T., Singh, M., Singh, V., 2022. Mitochondrial Dysfunction in Alzheimer's Disease: Opportunities for Drug Development. Curr Neuropharmacol 20, 675-692.
Borgonetti, V., Galeotti, N., 2023. Microglia senescence is related to neuropathic pain-associated comorbidities in the spared nerve injury model. Pain 164, 1106-1117.
Borst, K., Dumas, A.A., Prinz, M., 2021. Microglia: Immune and non-immune functions. Immunity 54, 2194-2208.
Bruttger, J., Karram, K., Wörtge, S., Regen, T., Marini, F., Hoppmann, N., Klein, M., Blank, T., Yona, S., Wolf, Y., Mack, M., Pinteaux, E., Müller, W., Zipp, F., Binder, H., Bopp, T., Prinz, M., Jung, S., Waisman, A., 2015. Genetic Cell Ablation Reveals Clusters of Local Self-Renewing Microglia in the Mammalian Central Nervous System. Immunity 43, 92-106.
Bussian, T.J., Aziz, A., Meyer, C.F., Swenson, B.L., van Deursen, J.M., Baker, D.J., 2018. Clearance of senescent glial cells prevents tau-dependent pathology and cognitive decline. Nature 562, 578-582.
Cai, Z., Yan, L.J., Li, K., Quazi, S.H., Zhao, B., 2012. Roles of AMP-activated protein kinase in Alzheimer's disease. Neuromolecular Med 14, 1-14.
Calkins, M.J., Reddy, P.H., 2011. Amyloid beta impairs mitochondrial anterograde transport and degenerates synapses in Alzheimer's disease neurons. Biochim Biophys Acta 1812, 507-513.
Carr, L.M., Mustafa, S., Care, A., Collins-Praino, L.E., 2024. More than a number: Incorporating the aged phenotype to improve in vitro and in vivo modeling of neurodegenerative disease. Brain, Behavior, and Immunity 119, 554-571.
Castilla-Cortázar, I., Aguirre, G.A., Femat-Roldán, G., Martín-Estal, I., Espinosa, L., 2020. Is insulin-like growth factor-1 involved in Parkinson's disease development? J Transl Med 18, 70.
Chen, C.C., Lin, J.T., Cheng, Y.F., Kuo, C.Y., Huang, C.F., Kao, S.H., Liang, Y.J., Cheng, C.Y., Chen, H.M., 2014. Amelioration of LPS-induced inflammation response in microglia by AMPK activation. Biomed Res Int 2014, 692061.
Chen, M., Linstra, R., van Vugt, M.A.T.M., 2022. Genomic instability, inflammatory signaling and response to cancer immunotherapy. Biochimica et Biophysica Acta (BBA) - Reviews on Cancer 1877, 188661.
Chiarini, A., Gui, L., Viviani, C., Armato, U., Dal Prà, I., 2023. NLRP3 Inflammasome's Activation in Acute and Chronic Brain Diseases-An Update on Pathogenetic Mechanisms and Therapeutic Perspectives with Respect to Other Inflammasomes. Biomedicines 11.
Chinta, S.J., Woods, G., Demaria, M., Rane, A., Zou, Y., McQuade, A., Rajagopalan, S., Limbad, C., Madden, D.T., Campisi, J., Andersen, J.K., 2018. Cellular Senescence Is Induced by the Environmental Neurotoxin Paraquat and Contributes to Neuropathology Linked to Parkinson’s Disease. Cell Reports 22, 930-940.
Cho, M.-H., Cho, K., Kang, H.-J., Jeon, E.-Y., Kim, H.-S., Kwon, H.-J., Kim, H.-M., Kim, D.-H., Yoon, S.-Y., 2014. Autophagy in microglia degrades extracellular β-amyloid fibrils and regulates the NLRP3 inflammasome. Autophagy 10, 1761-1775.
Choubey, V., Safiulina, D., Vaarmann, A., Cagalinec, M., Wareski, P., Kuum, M., Zharkovsky, A., Kaasik, A., 2011. Mutant A53T alpha-synuclein induces neuronal death by increasing mitochondrial autophagy. J Biol Chem 286, 10814-10824.
Coleman, C., Martin, I., 2022. Unraveling Parkinson’s Disease Neurodegeneration: Does Aging Hold the Clues? J Parkinsons Dis 12, 2321-2338.
Coppieters, N., Dieriks, B.V., Lill, C., Faull, R.L.M., Curtis, M.A., Dragunow, M., 2014. Global changes in DNA methylation and hydroxymethylation in Alzheimer's disease human brain. Neurobiology of Aging 35, 1334-1344.
Cozachenco, D., Ribeiro, F.C., Ferreira, S.T., 2023. Defective proteostasis in Alzheimer's disease. Ageing Res Rev 85, 101862.
Cuadros, M.A., Martin, C., Coltey, P., Almendros, A., Navascués, J., 1993. First appearance, distribution, and origin of macrophages in the early development of the avian central nervous system. Journal of Comparative Neurology 330, 113-129.
Cunningham, C.L., Martínez-Cerdeño, V., Noctor, S.C., 2013. Microglia Regulate the Number of Neural Precursor Cells in the Developing Cerebral Cortex. The Journal of Neuroscience 33, 4216.

Cyr, B., de Rivero Vaccari, J.P., 2023. Sex Differences in the Inflammatory Profile in the Brain of Young and Aged Mice. Cells 12.
d'Avila, J.C., Siqueira, L.D., Mazeraud, A., Azevedo, E.P., Foguel, D., Castro-Faria-Neto, H.C., Sharshar, T., Chrétien, F., Bozza, F.A., 2018. Age-related cognitive impairment is associated with long-term neuroinflammation and oxidative stress in a mouse model of episodic systemic inflammation. J Neuroinflammation 15, 28.
Desplats, P., Spencer, B., Coffee, E., Patel, P., Michael, S., Patrick, C., Adame, A., Rockenstein, E., Masliah, E., 2011. Alpha-synuclein sequesters Dnmt1 from the nucleus: a novel mechanism for epigenetic alterations in Lewy body diseases. J Biol Chem 286, 9031-9037.
Dlima, S.D., Hall, A., Aminu, A.Q., Akpan, A., Todd, C., Vardy, E.R.L.C., 2024. Frailty: a global health challenge in need of local action. BMJ Global Health 9, e015173.
Dong-Chen, X., Yong, C., Yang, X., Chen-Yu, S., Li-Hua, P., 2023. Signaling pathways in Parkinson's disease: molecular mechanisms and therapeutic interventions. Signal Transduction and Targeted Therapy 8, 73.
Düsedau, H.P., Steffen, J., Figueiredo, C.A., Boehme, J.D., Schultz, K., Erck, C., Korte, M., Faber-Zuschratter, H., Smalla, K.H., Dieterich, D., Kröger, A., Bruder, D., Dunay, I.R., 2021. Influenza A Virus (H1N1) Infection Induces Microglial Activation and Temporal Dysbalance in Glutamatergic Synaptic Transmission. mBio 12, e0177621.
Elmore, M.R., Najafi, A.R., Koike, M.A., Dagher, N.N., Spangenberg, E.E., Rice, R.A., Kitazawa, M., Matusow, B., Nguyen, H., West, B.L., Green, K.N., 2014. Colony-stimulating factor 1 receptor signaling is necessary for microglia viability, unmasking a microglia progenitor cell in the adult brain. Neuron 82, 380-397.
Emmanouilidou, E., Stefanis, L., Vekrellis, K., 2010. Cell-produced α-synuclein oligomers are targeted to, and impair, the 26S proteasome. Neurobiology of Aging 31, 953-968.
Fabrizio, P., Pozza, F., Pletcher, S.D., Gendron, C.M., Longo, V.D., 2001. Regulation of Longevity and Stress Resistance by Sch9 in Yeast. Science 292, 288-290.
Fan, Z., Pan, Y.T., Zhang, Z.Y., Yang, H., Yu, S.Y., Zheng, Y., Ma, J.H., Wang, X.M., 2020. Systemic activation of NLRP3 inflammasome and plasma α-synuclein levels are correlated with motor severity and progression in Parkinson's disease. J Neuroinflammation 17, 11.
Fasching, C.L., 2018. Telomere length measurement as a clinical biomarker of aging and disease. Critical Reviews in Clinical Laboratory Sciences 55, 443-465.
Fernández-Santiago, R., Merkel, A., Castellano, G., Heath, S., Raya, Á., Tolosa, E., Martí, M.-J., Consiglio, A., Ezquerra, M., 2019. Whole-genome DNA hyper-methylation in iPSC-derived dopaminergic neurons from Parkinson's disease patients. Clinical Epigenetics 11, 108.
Flanary, B.E., Sammons, N.W., Nguyen, C., Walker, D., Streit, W.J., 2007. Evidence That Aging And Amyloid Promote Microglial Cell Senescence. Rejuvenation Res 10, 61-74.
Flanary, B.E., Streit, W.J., 2004. Progressive telomere shortening occurs in cultured rat microglia, but not astrocytes. Glia 45, 75-88.
Flowers, A., Bell-Temin, H., Jalloh, A., Stevens, S.M., Bickford, P.C., 2017. Proteomic analysis of aged microglia: shifts in transcription, bioenergetics, and nutrient response. J Neuroinflammation 14, 96.
Forero, D.A., González-Giraldo, Y., López-Quintero, C., Castro-Vega, L.J., Barreto, G.E., Perry, G., 2016. Telomere length in Parkinson's disease: A meta-analysis. Exp Gerontol 75, 53-55.
Füger, P., Hefendehl, J.K., Veeraraghavalu, K., Wendeln, A.-C., Schlosser, C., Obermüller, U., Wegenast-Braun, B.M., Neher, J.J., Martus, P., Kohsaka, S., Thunemann, M., Feil, R., Sisodia, S.S., Skodras, A., Jucker, M., 2017. Microglia turnover with aging and in an Alzheimer's model via long-term in vivo single-cell imaging. Nature Neuroscience 20, 1371-1376.
Gabbouj, S., Ryhänen, S., Marttinen, M., Wittrahm, R., Takalo, M., Kemppainen, S., Martiskainen, H., Tanila, H., Haapasalo, A., Hiltunen, M., Natunen, T., 2019. Altered Insulin Signaling in Alzheimer's Disease Brain – Special Emphasis on PI3K-Akt Pathway. Frontiers in Neuroscience 13.
Gadhave, K., Kumar, D., Uversky, V.N., Giri, R., 2021. A multitude of signaling pathways associated with Alzheimer's disease and their roles in AD pathogenesis and therapy. Medicinal Research Reviews 41, 2689-2745.
Gamage, R., Rossetti, I., Niedermayer, G., Münch, G., Buskila, Y., Gyengesi, E., 2023. Chronic neuroinflammation during aging leads to cholinergic neurodegeneration in the mouse medial septum. J Neuroinflammation 20, 235.

Gampawar, P., Schmidt, R., Schmidt, H., 2022. Telomere length and brain aging: A systematic review and meta-analysis. Ageing Research Reviews 80, 101679.
Gao, C., Jiang, J., Tan, Y., Chen, S., 2023. Microglia in neurodegenerative diseases: mechanism and potential therapeutic targets. Signal Transduction and Targeted Therapy 8, 359.
Gao, X., Chen, Q., Yao, H., Tan, J., Liu, Z., Zhou, Y., Zou, Z., 2022. Epigenetics in Alzheimer's Disease. Frontiers in Aging Neuroscience 14.
Garner, K.M., Amin, R., Johnson, R.W., Scarlett, E.J., Burton, M.D., 2018. Microglia priming by interleukin-6 signaling is enhanced in aged mice. Journal of Neuroimmunology 324, 90-99.
Garza-Lombó, C., Schroder, A., Reyes-Reyes, E.M., Franco, R., 2018. mTOR/AMPK signaling in the brain: Cell metabolism, proteostasis and survival. Curr Opin Toxicol 8, 102-110.
Gebremedhin, K.G., Rademacher, D.J., 2016. Histone H3 acetylation in the postmortem Parkinson's disease primary motor cortex. Neuroscience Letters 627, 121-125.
Georgakopoulou, E.A., Tsimaratou, K., Evangelou, K., Fernandez Marcos, P.J., Zoumpourlis, V., Trougakos, I.P., Kletsas, D., Bartek, J., Serrano, M., Gorgoulis, V.G., 2013. Specific lipofuscin staining as a novel biomarker to detect replicative and stress-induced senescence. A method applicable in cryo-preserved and archival tissues. Aging (Albany NY) 5, 37-50.
Ghosh, T.S., Shanahan, F., O'Toole, P.W., 2022. The gut microbiome as a modulator of healthy ageing. Nature Reviews Gastroenterology & Hepatology 19, 565-584.
Ginhoux, F., Lim, S., Hoeffel, G., Low, D., Huber, T., 2013. Origin and differentiation of microglia. Frontiers in Cellular Neuroscience 7.
Giordano, K.R., Denman, C.R., Dubisch, P.S., Akhter, M., Lifshitz, J., 2021. An update on the rod microglia variant in experimental and clinical brain injury and disease. Brain Commun 3, fcaa227.
Giovannoni, F., Quintana, F.J., 2020. The Role of Astrocytes in CNS Inflammation. Trends in Immunology 41, 805-819.
Giulian, D., Baker, T.J., 1986. Characterization of ameboid microglia isolated from developing mammalian brain. J Neurosci 6, 2163-2178.
Glezer, I., Simard, A.R., Rivest, S., 2007. Neuroprotective role of the innate immune system by microglia. Neuroscience 147, 867-883.
Godau, J., Knauel, K., Weber, K., Brockmann, K., Maetzler, W., Binder, G., Berg, D., 2011. Serum Insulinlike Growth Factor 1 as Possible Marker for Risk and Early Diagnosis of Parkinson Disease. Archives of Neurology 68, 925-931.
González-Gualda, E., Baker, A.G., Fruk, L., Muñoz-Espín, D., 2021. A guide to assessing cellular senescence in vitro and in vivo. The FEBS Journal 288, 56-80.
Gorgoulis, V., Adams, P.D., Alimonti, A., Bennett, D.C., Bischof, O., Bishop, C., Campisi, J., Collado, M., Evangelou, K., Ferbeyre, G., Gil, J., Hara, E., Krizhanovsky, V., Jurk, D., Maier, A.B., Narita, M., Niedernhofer, L., Passos, J.F., Robbins, P.D., Schmitt, C.A., Sedivy, J., Vougas, K., von Zglinicki, T., Zhou, D., Serrano, M., Demaria, M., 2019. Cellular Senescence: Defining a Path Forward. Cell 179, 813-827.
Green, T.R.F., Rowe, R.K., 2024. Quantifying microglial morphology: an insight into function. Clinical and Experimental Immunology 216, 221-229.
Greenwood, E.K., Brown, D.R., 2021. Senescent Microglia: The Key to the Ageing Brain? , International Journal of Molecular Sciences.
Griffin, R.J., Moloney, A., Kelliher, M., Johnston, J.A., Ravid, R., Dockery, P., O'Connor, R., O'Neill, C., 2005. Activation of Akt/PKB, increased phosphorylation of Akt substrates and loss and altered distribution of Akt and PTEN are features of Alzheimer's disease pathology. Journal of Neurochemistry 93, 105-117.
Guimarães, G.R., Almeida, P.P., de Oliveira Santos, L., Rodrigues, L.P., de Carvalho, J.L., Boroni, M., 2021. Hallmarks of Aging in Macrophages: Consequences to Skin Inflammaging. Cells 10.
Gulen, M.F., Samson, N., Keller, A., Schwabenland, M., Liu, C., Glück, S., Thacker, V.V., Favre, L., Mangeat, B., Kroese, L.J., Krimpenfort, P., Prinz, M., Ablasser, A., 2023. cGAS–STING drives ageing-related inflammation and neurodegeneration. Nature 620, 374-380.
Guo, C., Sun, L., Chen, X., Zhang, D., 2013. Oxidative stress, mitochondrial damage and neurodegenerative diseases. Neural Regen Res 8, 2003-2014.

Haas, C.B., de Carvalho, A.K., Muller, A.P., Eggen, B.J.L., Portela, L.V., 2020. Insulin activates microglia and increases COX-2/IL-1β expression in young but not in aged hippocampus. Brain Research 1741, 146884.
Harry, G.J., Kraft, A.D., 2012. Microglia in the developing brain: a potential target with lifetime effects. Neurotoxicology 33, 191-206.
Haughey, N.J., Liu, D., Nath, A., Borchard, A.C., Mattson, M.P., 2002. Disruption of neurogenesis in the subventricular zone of adult mice, and in human cortical neuronal precursor cells in culture, by amyloid β-peptide. NeuroMolecular Medicine 1, 125-135.
Hauss-Wegrzyniak, B., Dobrzanski, P., Stoehr, J.D., Wenk, G.L., 1998. Chronic neuroinflammation in rats reproduces components of the neurobiology of Alzheimer's disease. Brain Research 780, 294-303.
Hayashi, Y., Yoshida, M., Yamato, M., Ide, T., Wu, Z., Ochi-Shindou, M., Kanki, T., Kang, D., Sunagawa, K., Tsutsui, H., Nakanishi, H., 2008. Reverse of age-dependent memory impairment and mitochondrial DNA damage in microglia by an overexpression of human mitochondrial transcription factor a in mice. J Neurosci 28, 8624-8634.
Heckmann, B.L., Teubner, B.J.W., Boada-Romero, E., Tummers, B., Guy, C., Fitzgerald, P., Mayer, U., Carding, S., Zakharenko, S.S., Wileman, T., Green, D.R., 2020. Noncanonical function of an autophagy protein prevents spontaneous Alzheimer's disease. Science Advances 6, eabb9036.
Henrich, M.T., Oertel, W.H., Surmeier, D.J., Geibl, F.F., 2023. Mitochondrial dysfunction in Parkinson's disease – a key disease hallmark with therapeutic potential. Molecular Neurodegeneration 18, 83.
Henry, C.J., Huang, Y., Wynne, A.M., Godbout, J.P., 2009. Peripheral lipopolysaccharide (LPS) challenge promotes microglial hyperactivity in aged mice that is associated with exaggerated induction of both pro-inflammatory IL-1beta and anti-inflammatory IL-10 cytokines. Brain Behav Immun 23, 309-317.
Herdy, J.R., Traxler, L., Agarwal, R.K., Karbacher, L., Schlachetzki, J.C.M., Boehnke, L., Zangwill, D., Galasko, D., Glass, C.K., Mertens, J., Gage, F.H., 2022. Increased post-mitotic senescence in aged human neurons is a pathological feature of Alzheimer's disease. Cell Stem Cell 29, 1637-1652.e1636.
Hermann, G.E., Rogers, R.C., Bresnahan, J.C., Beattie, M.S., 2001. Tumor Necrosis Factor-α Induces cFOS and Strongly Potentiates Glutamate-Mediated Cell Death in the Rat Spinal Cord. Neurobiology of Disease 8, 590-599.
Hernansanz-Agustín, P., Ramos, E., Navarro, E., Parada, E., Sánchez-López, N., Peláez-Aguado, L., Cabrera-García, J.D., Tello, D., Buendia, I., Marina, A., Egea, J., López, M.G., Bogdanova, A., Martínez-Ruiz, A., 2017. Mitochondrial complex I deactivation is related to superoxide production in acute hypoxia. Redox Biology 12, 1040-1051.
Hinkle, J.T., Patel, J., Panicker, N., Karuppagounder, S.S., Biswas, D., Belingon, B., Chen, R., Brahmachari, S., Pletnikova, O., Troncoso, J.C., Dawson, V.L., Dawson, T.M., 2022. STING mediates neurodegeneration and neuroinflammation in nigrostriatal α-synucleinopathy. Proc Natl Acad Sci U S A 119, e2118819119.
Höhn, A., Tramutola, A., Cascella, R., 2020. Proteostasis Failure in Neurodegenerative Diseases: Focus on Oxidative Stress. Oxid Med Cell Longev 2020, 5497046.
Honarpisheh, P., Reynolds, C.R., Blasco Conesa, M.P., Moruno Manchon, J.F., Putluri, N., Bhattacharjee, M.B., Urayama, A., McCullough, L.D., Ganesh, B.P., 2020. Dysregulated Gut Homeostasis Observed Prior to the Accumulation of the Brain Amyloid-β in Tg2576 Mice. Int J Mol Sci 21.
Hopperton, K.E., Mohammad, D., Trépanier, M.O., Giuliano, V., Bazinet, R.P., 2018. Markers of microglia in post-mortem brain samples from patients with Alzheimer's disease: a systematic review. Mol Psychiatry 23, 177-198.
Horvath, S., 2013. DNA methylation age of human tissues and cell types. Genome Biology 14, 3156.
Hou, Y., Dan, X., Babbar, M., Wei, Y., Hasselbalch, S.G., Croteau, D.L., Bohr, V.A., 2019. Ageing as a risk factor for neurodegenerative disease. Nature Reviews Neurology 15, 565-581.
Hou, Y., Song, H., Croteau, D.L., Akbari, M., Bohr, V.A., 2017. Genome instability in Alzheimer disease. Mechanisms of Ageing and Development 161, 83-94.
Hsieh, C.L., Koike, M., Spusta, S.C., Niemi, E.C., Yenari, M., Nakamura, M.C., Seaman, W.E., 2009. A role for TREM2 ligands in the phagocytosis of apoptotic neuronal cells by microglia. J Neurochem 109, 1144-1156.

Huang, B., Chau, S.W.H., Liu, Y., Chan, J.W.Y., Wang, J., Ma, S.L., Zhang, J., Chan, P.K.S., Yeoh, Y.K., Chen, Z., Zhou, L., Wong, S.H., Mok, V.C.T., To, K.F., Lai, H.M., Ng, S., Trenkwalder, C., Chan, F.K.L., Wing, Y.K., 2023a. Gut microbiome dysbiosis across early Parkinson's disease, REM sleep behavior disorder and their first-degree relatives. Nature Communications 14, 2501.
Huang, M., Xu, L., Liu, J., Huang, P., Tan, Y., Chen, S., 2022. Cell–Cell Communication Alterations via Intercellular Signaling Pathways in Substantia Nigra of Parkinson's Disease. Frontiers in Aging Neuroscience 14.
Huang, Y., Wu, J., Zhang, H., Li, Y., Wen, L., Tan, X., Cheng, K., Liu, Y., Pu, J., Liu, L., Wang, H., Li, W., Perry, S.W., Wong, M.L., Licinio, J., Zheng, P., Xie, P., 2023b. The gut microbiome modulates the transformation of microglial subtypes. Mol Psychiatry 28, 1611-1621.
Huang, Y., Xu, Z., Xiong, S., Sun, F., Qin, G., Hu, G., Wang, J., Zhao, L., Liang, Y.X., Wu, T., Lu, Z., Humayun, M.S., So, K.F., Pan, Y., Li, N., Yuan, T.F., Rao, Y., Peng, B., 2018. Repopulated microglia are solely derived from the proliferation of residual microglia after acute depletion. Nat Neurosci 21, 530-540.
Hudson, G., Faini, D., Stutt, A., Eccles, M., Robinson, L., Burn, D.J., Chinnery, P.F., 2011. No evidence of substantia nigra telomere shortening in Parkinson's disease. Neurobiology of Aging 32, 2107.e2103-2107.e2105.
Hugh Perry, V., 1998. A revised view of the central nervous system microenvironment and major histocompatibility complex class II antigen presentation. Journal of Neuroimmunology 90, 113-121.
Jeohn, G.-H., Kong, L.-Y., Wilson, B., Hudson, P., Hong, J.-S., 1998. Synergistic neurotoxic effects of combined treatments with cytokines in murine primary mixed neuron/glia cultures. Journal of Neuroimmunology 85, 1-10.
Jin, R., Chan, A.K.Y., Wu, J., Lee, T.M.C., 2022. Relationships between Inflammation and Age-Related Neurocognitive Changes. Int J Mol Sci 23.
Joya, A., Martín, A., 2021. Evaluation of glial cell proliferation with non-invasive molecular imaging methods after stroke. Neural Regen Res 16, 2209-2210.
Jung, T., Bader, N., Grune, T., 2007. Lipofuscin: formation, distribution, and metabolic consequences. Ann N Y Acad Sci 1119, 97-111.
Jurga, A.M., Paleczna, M., Kuter, K.Z., 2020. Overview of General and Discriminating Markers of Differential Microglia Phenotypes. Front Cell Neurosci 14, 198.
Kamo, N., Ke, B., Ghaffari, A.A., Shen, X.D., Busuttil, R.W., Cheng, G., Kupiec-Weglinski, J.W., 2013. ASC/caspase-1/IL-1β signaling triggers inflammatory responses by promoting HMGB1 induction in liver ischemia/reperfusion injury. Hepatology 58, 351-362.
Kao, A.W., Eisenhut, R.J., Martens, L.H., Nakamura, A., Huang, A., Bagley, J.A., Zhou, P., de Luis, A., Neukomm, L.J., Cabello, J., Farese, R.V., Jr., Kenyon, C., 2011. A neurodegenerative disease mutation that accelerates the clearance of apoptotic cells. Proc Natl Acad Sci U S A 108, 4441-4446.
Keane, L., Antignano, I., Riechers, S.P., Zollinger, R., Dumas, A.A., Offermann, N., Bernis, M.E., Russ, J., Graelmann, F., McCormick, P.N., Esser, J., Tejera, D., Nagano, A., Wang, J., Chelala, C., Biederbick, Y., Halle, A., Salomoni, P., Heneka, M.T., Capasso, M., 2021. mTOR-dependent translation amplifies microglia priming in aging mice. J Clin Invest 131.
Khan, M.R., Yin, X., Kang, S.-U., Mitra, J., Wang, H., Ryu, T., Brahmachari, S., Karuppagounder, S.S., Kimura, Y., Jhaldiyal, A., Kim, H.H., Gu, H., Chen, R., Redding-Ochoa, J., Troncoso, J., Na, C.H., Ha, T., Dawson, V.L., Dawson, T.M., 2023. Enhanced mTORC1 signaling and protein synthesis in pathologic α-synuclein cellular and animal models of Parkinson's disease. Sci Transl Med 15, eadd0499.
Kigerl, K.A., de Rivero Vaccari, J.P., Dietrich, W.D., Popovich, P.G., Keane, R.W., 2014. Pattern recognition receptors and central nervous system repair. Exp Neurol 258, 5-16.
Koellhoffer, E.C., McCullough, L.D., Ritzel, R.M., 2017. Old Maids: Aging and Its Impact on Microglia Function. Int J Mol Sci 18.
Kouli, A., Camacho, M., Allinson, K., Williams-Gray, C.H., 2020. Neuroinflammation and protein pathology in Parkinson's disease dementia. Acta Neuropathologica Communications 8, 211.
Kuan, X.-Y., Fauzi, N.S.A., Ng, K.Y., Bakhtiar, A., 2023. Exploring the Causal Relationship Between Telomere Biology and Alzheimer's Disease. Mol Neurobiol 60, 4169-4183.

Kumar, A., Stoica, B.A., Sabirzhanov, B., Burns, M.P., Faden, A.I., Loane, D.J., 2013. Traumatic brain injury in aged animals increases lesion size and chronically alters microglial/macrophage classical and alternative activation states. Neurobiol Aging 34, 1397-1411.
la Torre, A., Lo Vecchio, F., Greco, A., 2023. Epigenetic Mechanisms of Aging and Aging-Associated Diseases. Cells.
Lan, A.P., Chen, J., Zhao, Y., Chai, Z., Hu, Y., 2017. mTOR Signaling in Parkinson's Disease. Neuromolecular Med 19, 1-10.
Lee, I.S., Jung, K., Kim, I.S., Park, K.I., 2013. Amyloid-β oligomers regulate the properties of human neural stem cells through GSK-3β signaling. Exp Mol Med 45, e60.
Lehtonen, Š., Sonninen, T.M., Wojciechowski, S., Goldsteins, G., Koistinaho, J., 2019. Dysfunction of Cellular Proteostasis in Parkinson's Disease. Front Neurosci 13, 457.
Leuner, K., Müller, W.E., Reichert, A.S., 2012. From Mitochondrial Dysfunction to Amyloid Beta Formation: Novel Insights into the Pathogenesis of Alzheimer's Disease. Mol Neurobiol 46, 186-193.
Li, X., Li, Y., Jin, Y., Zhang, Y., Wu, J., Xu, Z., Huang, Y., Cai, L., Gao, S., Liu, T., Zeng, F., Wang, Y., Wang, W., Yuan, T.-F., Tian, H., Shu, Y., Guo, F., Lu, W., Mao, Y., Mei, X., Rao, Y., Peng, B., 2023a. Transcriptional and epigenetic decoding of the microglial aging process. Nature Aging 3, 1288-1311.
Li, Z., Li, J., Bu, X., Liu, X., Tankersley, C.G., Wang, C., Huang, K., 2011. Age-induced augmentation of p38 MAPK phosphorylation in mouse lung. Experimental Gerontology 46, 694-702.
Li, Z., Liang, H., Hu, Y., Lu, L., Zheng, C., Fan, Y., Wu, B., Zou, T., Luo, X., Zhang, X., Zeng, Y., Liu, Z., Zhou, Z., Yue, Z., Ren, Y., Li, Z., Su, Q., Xu, P., 2023b. Gut bacterial profiles in Parkinson's disease: A systematic review. CNS Neuroscience & Therapeutics 29, 140-157.
Liang, R., Qi, X., Cai, Q., Niu, L., Huang, X., Zhang, D., Ling, J., Wu, Y., Chen, Y., Yang, P., Liu, J., Zhang, J., Yu, P., 2024. The role of NLRP3 inflammasome in aging and age-related diseases. Immun Ageing 21, 14.
Lindersson, E., Beedholm, R., Højrup, P., Moos, T., Gai, W., Hendil, K.B., Jensen, P.H., 2004. Proteasomal Inhibition by α-Synuclein Filaments and Oligomers*. Journal of Biological Chemistry 279, 12924-12934.
Liu, A., Fernandes, B.S., Citu, C., Zhao, Z., 2024a. Unraveling the intercellular communication disruption and key pathways in Alzheimer's disease: an integrative study of single-nucleus transcriptomes and genetic association. Alzheimers Res Ther 16, 3.
Liu, F., Benashski, S.E., Persky, R., Xu, Y., Li, J., McCullough, L.D., 2012. Age-related changes in AMP-activated protein kinase after stroke. Age (Dordr) 34, 157-168.
Liu, J., Li, L., 2019. Targeting Autophagy for the Treatment of Alzheimer's Disease: Challenges and Opportunities. Frontiers in Molecular Neuroscience 12.
Liu, R.M., 2022. Aging, Cellular Senescence, and Alzheimer's Disease. Int J Mol Sci 23.
Liu, S., Gao, J., Zhu, M., Liu, K., Zhang, H.L., 2020. Gut Microbiota and Dysbiosis in Alzheimer's Disease: Implications for Pathogenesis and Treatment. Mol Neurobiol 57, 5026-5043.
Liu, T., Zhang, L., Joo, D., Sun, S.-C., 2017. NF-κB signaling in inflammation. Signal Transduction and Targeted Therapy 2, 17023.
Liu, Y., Tan, Y., Zhang, Z., Yi, M., Zhu, L., Peng, W., 2024b. The interaction between ageing and Alzheimer's disease: insights from the hallmarks of ageing. Translational Neurodegeneration 13, 7.
Loh, J.S., Mak, W.Q., Tan, L.K.S., Ng, C.X., Chan, H.H., Yeow, S.H., Foo, J.B., Ong, Y.S., How, C.W., Khaw, K.Y., 2024. Microbiota–gut–brain axis and its therapeutic applications in neurodegenerative diseases. Signal Transduction and Targeted Therapy 9, 37.
Long, J.M., Kalehua, A.N., Muth, N.J., Calhoun, M.E., Jucker, M., Hengemihle, J.M., Ingram, D.K., Mouton, P.R., 1998. Stereological analysis of astrocyte and microglia in aging mouse hippocampus. Neurobiology of Aging 19, 497-503.
Lopes, K.O., Sparks, D.L., Streit, W.J., 2008. Microglial dystrophy in the aged and Alzheimer's disease brain is associated with ferritin immunoreactivity. Glia 56, 1048-1060.
López-Otín, C., Blasco, M.A., Partridge, L., Serrano, M., Kroemer, G., 2013. The hallmarks of aging. Cell 153, 1194-1217.
López-Otín, C., Blasco, M.A., Partridge, L., Serrano, M., Kroemer, G., 2023. Hallmarks of aging: An expanding universe. Cell 186, 243-278.

Lu, M., Sun, X.-L., Qiao, C., Liu, Y., Ding, J.-H., Hu, G., 2014. Uncoupling protein 2 deficiency aggravates astrocytic endoplasmic reticulum stress and nod-like receptor protein 3 inflammasome activation. Neurobiology of Aging 35, 421-430.
Lull, M.E., Block, M.L., 2010. Microglial Activation and Chronic Neurodegeneration. Neurotherapeutics 7, 354-365.
Lynch, M.A., 2022. Exploring Sex-Related Differences in Microglia May Be a Game-Changer in Precision Medicine. Front Aging Neurosci 14, 868448.
Mallya, A.P., Wang, H.D., Lee, H.N.R., Deutch, A.Y., 2019. Microglial Pruning of Synapses in the Prefrontal Cortex During Adolescence. Cereb Cortex 29, 1634-1643.
Mancini, S.J., White, A.D., Bijland, S., Rutherford, C., Graham, D., Richter, E.A., Viollet, B., Touyz, R.M., Palmer, T.M., Salt, I.P., 2017. Activation of AMP-activated protein kinase rapidly suppresses multiple pro-inflammatory pathways in adipocytes including IL-1 receptor-associated kinase-4 phosphorylation. Mol Cell Endocrinol 440, 44-56.
Mander, P., Brown, G.C., 2005. Activation of microglial NADPH oxidase is synergistic with glial iNOS expression in inducing neuronal death: a dual-key mechanism of inflammatory neurodegeneration. J Neuroinflammation 2, 20.
Maras, P.M., Hebda-Bauer, E.K., Hagenauer, M.H., Hilde, K.L., Blandino, P., Watson, S.J., Akil, H., 2022. Differences in microglia morphological profiles reflect divergent emotional temperaments: insights from a selective breeding model. Translational Psychiatry 12, 105.
Mashayekhi, F., Mirzajani, E., Naji, M., Azari, M., 2010. Expression of insulin-like growth factor-1 and insulin-like growth factor binding proteins in the serum and cerebrospinal fluid of patients with Parkinson's disease. Journal of Clinical Neuroscience 17, 623-627.
Mastenbroek, L.J.M., Kooistra, S.M., Eggen, B.J.L., Prins, J.R., 2024. The role of microglia in early neurodevelopment and the effects of maternal immune activation. Seminars in Immunopathology 46, 1.
Mastroeni, D., Delvaux, E., Nolz, J., Tan, Y., Grover, A., Oddo, S., Coleman, P.D., 2015. Aberrant intracellular localization of H3k4me3 demonstrates an early epigenetic phenomenon in Alzheimer's disease. Neurobiology of Aging 36, 3121-3129.
Mather, K.A., Jorm, A.F., Parslow, R.A., Christensen, H., 2011. Is telomere length a biomarker of aging? A review. J Gerontol A Biol Sci Med Sci 66, 202-213.
Matsui, T.K., Mori, E., 2018. Microglia support neural stem cell maintenance and growth. Biochemical and Biophysical Research Communications 503, 1880-1884.
Matt, S.M., Lawson, M.A., Johnson, R.W., 2016. Aging and peripheral lipopolysaccharide can modulate epigenetic regulators and decrease IL-1β promoter DNA methylation in microglia. Neurobiology of Aging 47, 1-9.
McNaught, K.S.P., Belizaire, R., Jenner, P., Olanow, C.W., Isacson, O., 2002. Selective loss of 20S proteasome α-subunits in the substantia nigra pars compacta in Parkinson's disease. Neuroscience Letters 326, 155-158.
Mejias, N.H., Martinez, C.C., Stephens, M.E., de Rivero Vaccari, J.P., 2018. Contribution of the inflammasome to inflammaging. Journal of Inflammation 15, 23.
Menassa, D.A., Gomez-Nicola, D., 2018. Microglial dynamics during human brain development. Frontiers in Immunology 9.
Menassa, D.A., Muntslag, T.A.O., Martin-Estebané, M., Barry-Carroll, L., Chapman, M.A., Adorjan, I., Tyler, T., Turnbull, B., Rose-Zerilli, M.J.J., Nicoll, J.A.R., Krsnik, Z., Kostovic, I., Gomez-Nicola, D., 2022. The spatiotemporal dynamics of microglia across the human lifespan. Developmental Cell 57, 2127-2139.e2126.
Milanese, C., Cerri, S., Ulusoy, A., Gornati, S.V., Plat, A., Gabriels, S., Blandini, F., Di Monte, D.A., Hoeijmakers, J.H., Mastroberardino, P.G., 2018. Activation of the DNA damage response in vivo in synucleinopathy models of Parkinson's disease. Cell Death Dis 9, 818.
Miller, S.J., Campbell, C.E., Jimenez-Corea, H.A., Wu, G.H., Logan, R., 2022. Neuroglial Senescence, α-Synucleinopathy, and the Therapeutic Potential of Senolytics in Parkinson's Disease. Front Neurosci 16, 824191.
Miyamoto, A., Wake, H., Ishikawa, A.W., Eto, K., Shibata, K., Murakoshi, H., Koizumi, S., Moorhouse, A.J., Yoshimura, Y., Nabekura, J., 2016. Microglia contact induces synapse formation in developing somatosensory cortex. Nature Communications 7, 12540.

Mohr, A.E., Crawford, M., Jasbi, P., Fessler, S., Sweazea, K.L., 2022. Lipopolysaccharide and the gut microbiota: considering structural variation. FEBS Lett 596, 849-875.
Morgan, S.C., Taylor, D.L., Pocock, J.M., 2004. Microglia release activators of neuronal proliferation mediated by activation of mitogen-activated protein kinase, phosphatidylinositol-3-kinase/Akt and delta–Notch signalling cascades. Journal of Neurochemistry 90, 89-101.
Mouton, P.R., Long, J.M., Lei, D.-L., Howard, V., Jucker, M., Calhoun, M.E., Ingram, D.K., 2002. Age and gender effects on microglia and astrocyte numbers in brains of mice. Brain Research 956, 30-35.
Moyse, E., Krantic, S., Djellouli, N., Roger, S., Angoulvant, D., Debacq, C., Leroy, V., Fougere, B., Aidoud, A., 2022. Neuroinflammation: A Possible Link Between Chronic Vascular Disorders and Neurodegenerative Diseases. Frontiers in Aging Neuroscience 14.
Myhre, C.L., Thygesen, C., Villadsen, B., Vollerup, J., Ilkjær, L., Krohn, K.T., Grebing, M., Zhao, S., Khan, A.M., Dissing-Olesen, L., Jensen, M.S., Babcock, A.A., Finsen, B., 2019. Microglia Express Insulin-Like Growth Factor-1 in the Hippocampus of Aged APP(swe)/PS1(ΔE9) Transgenic Mice. Front Cell Neurosci 13, 308.
Ndoja, A., Reja, R., Lee, S.-H., Webster, J.D., Ngu, H., Rose, C.M., Kirkpatrick, D.S., Modrusan, Z., Chen, Y.-J.J., Dugger, D.L., Gandham, V., Xie, L., Newton, K., Dixit, V.M., 2020. Ubiquitin Ligase COP1 Suppresses Neuroinflammation by Degrading c/EBPβ in Microglia. Cell 182, 1156-1169.e1112.
Nechushtai, L., Frenkel, D., Pinkas-Kramarski, R., 2023. Autophagy in Parkinson's Disease. Biomolecules 13.
Neher, J.J., Neniskyte, U., Zhao, J.-W., Bal-Price, A., Tolkovsky, A.M., Brown, G.C., 2011. Inhibition of Microglial Phagocytosis Is Sufficient To Prevent Inflammatory Neuronal Death. The Journal of Immunology 186, 4973-4983.
Neniskyte, U., Neher, J.J., Brown, G.C., 2011. Neuronal death induced by nanomolar amyloid β is mediated by primary phagocytosis of neurons by microglia. J Biol Chem 286, 39904-39913.
Neumann, P., Lenz, D.E., Streit, W.J., Bechmann, I., 2023. Is microglial dystrophy a form of cellular senescence? An analysis of senescence markers in the aged human brain. Glia 71, 377-390.
Nichols, E., Szoeke, C.E.I., Vollset, S.E., Abbasi, N., Abd-Allah, F., Abdela, J., Aichour, M.T.E., Akinyemi, R.O., Alahdab, F., Asgedom, S.W., Awasthi, A., Barker-Collo, S.L., Baune, B.T., Béjot, Y., Belachew, A.B., Bennett, D.A., Biadgo, B., Bijani, A., Bin Sayeed, M.S., Brayne, C., Carpenter, D.O., Carvalho, F., Catalá-López, F., Cerin, E., Choi, J.-Y.J., Dang, A.K., Degefa, M.G., Djalalinia, S., Dubey, M., Duken, E.E., Edvardsson, D., Endres, M., Eskandarieh, S., Faro, A., Farzadfar, F., Fereshtehnejad, S.-M., Fernandes, E., Filip, I., Fischer, F., Gebre, A.K., Geremew, D., Ghasemi-Kasman, M., Gnedovskaya, E.V., Gupta, R., Hachinski, V., Hagos, T.B., Hamidi, S., Hankey, G.J., Haro, J.M., Hay, S.I., Irvani, S.S.N., Jha, R.P., Jonas, J.B., Kalani, R., Karch, A., Kasaeian, A., Khader, Y.S., Khalil, I.A., Khan, E.A., Khanna, T., Khoja, T.A.M., Khubchandani, J., Kisa, A., Kissimova-Skarbek, K., Kivimäki, M., Koyanagi, A., Krohn, K.J., Logroscino, G., Lorkowski, S., Majdan, M., Malekzadeh, R., März, W., Massano, J., Mengistu, G., Meretoja, A., Mohammadi, M., Mohammadi-Khanaposhtani, M., Mokdad, A.H., Mondello, S., Moradi, G., Nagel, G., Naghavi, M., Naik, G., Nguyen, L.H., Nguyen, T.H., Nirayo, Y.L., Nixon, M.R., Ofori-Asenso, R., Ogbo, F.A., Olagunju, A.T., Owolabi, M.O., Panda-Jonas, S., Passos, V.M.d.A., Pereira, D.M., Pinilla-Monsalve, G.D., Piradov, M.A., Pond, C.D., Poustchi, H., Qorbani, M., Radfar, A., Reiner, R.C., Jr., Robinson, S.R., Roshandel, G., Rostami, A., Russ, T.C., Sachdev, P.S., Safari, H., Safiri, S., Sahathevan, R., Salimi, Y., Satpathy, M., Sawhney, M., Saylan, M., Sepanlou, S.G., Shafieesabet, A., Shaikh, M.A., Sahraian, M.A., Shigematsu, M., Shiri, R., Shiue, I., Silva, J.P., Smith, M., Sobhani, S., Stein, D.J., Tabarés-Seisdedos, R., Tovani-Palone, M.R., Tran, B.X., Tran, T.T., Tsegay, A.T., Ullah, I., Venketasubramanian, N., Vlassov, V., Wang, Y.-P., Weiss, J., Westerman, R., Wijeratne, T., Wyper, G.M.A., Yano, Y., Yimer, E.M., Yonemoto, N., Yousefifard, M., Zaidi, Z., Zare, Z., Vos, T., Feigin, V.L., Murray, C.J.L., 2019. Global, regional, and national burden of Alzheimer's disease and other dementias, 1990-2016: a systematic analysis for the Global Burden of Disease Study 2016. The Lancet Neurology 18, 88-106.
Nieto-Torres, J.L., Hansen, M., 2021. Macroautophagy and aging: The impact of cellular recycling on health and longevity. Mol Aspects Med 82, 101020.
Niraula, A., Sheridan, J.F., Godbout, J.P., 2017. Microglia Priming with Aging and Stress. Neuropsychopharmacology 42, 318-333.

Nixon, R.A., Wegiel, J., Kumar, A., Yu, W.H., Peterhoff, C., Cataldo, A., Cuervo, A.M., 2005. Extensive Involvement of Autophagy in Alzheimer Disease: An Immuno-Electron Microscopy Study. Journal of Neuropathology & Experimental Neurology 64, 113-122.
Norden, D.M., Muccigrosso, M.M., Godbout, J.P., 2015. Microglial priming and enhanced reactivity to secondary insult in aging, and traumatic CNS injury, and neurodegenerative disease. Neuropharmacology 96, 29-41.
Olah, M., Patrick, E., Villani, A.-C., Xu, J., White, C.C., Ryan, K.J., Piehowski, P., Kapasi, A., Nejad, P., Cimpean, M., Connor, S., Yung, C.J., Frangieh, M., McHenry, A., Elyaman, W., Petyuk, V., Schneider, J.A., Bennett, D.A., De Jager, P.L., Bradshaw, E.M., 2018. A transcriptomic atlas of aged human microglia. Nature Communications 9, 539.
Ou, Z., Pan, J., Tang, S., Duan, D., Yu, D., Nong, H., Wang, Z., 2021. Global Trends in the Incidence, Prevalence, and Years Lived With Disability of Parkinson's Disease in 204 Countries/Territories From 1990 to 2019. Front Public Health 9, 776847.
Pallas, M., Camins, A., Smith, M.A., Perry, G., Lee, H.-g., Casadesus, G., 2008. From Aging to Alzheimer's Disease: Unveiling "The Switch" with the Senescence-Accelerated Mouse Model (SAMP8). Journal of Alzheimer's Disease 15, 615-624.
Panicker, N., Saminathan, H., Jin, H., Neal, M., Harischandra, D.S., Gordon, R., Kanthasamy, K., Lawana, V., Sarkar, S., Luo, J., Anantharam, V., Kanthasamy, A.G., Kanthasamy, A., 2015. Fyn Kinase Regulates Microglial Neuroinflammatory Responses in Cell Culture and Animal Models of Parkinson's Disease. J Neurosci 35, 10058-10077.
Panossian, L.A., Porter, V.R., Valenzuela, H.F., Zhu, X., Reback, E., Masterman, D., Cummings, J.L., Effros, R.B., 2003. Telomere shortening in T cells correlates with Alzheimer's disease status. Neurobiology of Aging 24, 77-84.
Paolicelli, R.C., Bolasco, G., Pagani, F., Maggi, L., Scianni, M., Panzanelli, P., Giustetto, M., Ferreira, T.A., Guiducci, E., Dumas, L., Ragozzino, D., Gross, C.T., 2011. Synaptic Pruning by Microglia Is Necessary for Normal Brain Development. Science 333, 1456-1458.
Paolicelli, R.C., Sierra, A., Stevens, B., Tremblay, M.-E., Aguzzi, A., Ajami, B., Amit, I., Audinat, E., Bechmann, I., Bennett, M., Bennett, F., Bessis, A., Biber, K., Bilbo, S., Blurton-Jones, M., Boddeke, E., Brites, D., Brône, B., Brown, G.C., Butovsky, O., Carson, M.J., Castellano, B., Colonna, M., Cowley, S.A., Cunningham, C., Davalos, D., De Jager, P.L., de Strooper, B., Denes, A., Eggen, B.J.L., Eyo, U., Galea, E., Garel, S., Ginhoux, F., Glass, C.K., Gokce, O., Gomez-Nicola, D., González, B., Gordon, S., Graeber, M.B., Greenhalgh, A.D., Gressens, P., Greter, M., Gutmann, D.H., Haass, C., Heneka, M.T., Heppner, F.L., Hong, S., Hume, D.A., Jung, S., Kettenmann, H., Kipnis, J., Koyama, R., Lemke, G., Lynch, M., Majewska, A., Malcangio, M., Malm, T., Mancuso, R., Masuda, T., Matteoli, M., McColl, B.W., Miron, V.E., Molofsky, A.V., Monje, M., Mracsko, E., Nadjar, A., Neher, J.J., Neniskyte, U., Neumann, H., Noda, M., Peng, B., Peri, F., Perry, V.H., Popovich, P.G., Pridans, C., Priller, J., Prinz, M., Ragozzino, D., Ransohoff, R.M., Salter, M.W., Schaefer, A., Schafer, D.P., Schwartz, M., Simons, M., Smith, C.J., Streit, W.J., Tay, T.L., Tsai, L.-H., Verkhratsky, A., von Bernhardi, R., Wake, H., Wittamer, V., Wolf, S.A., Wu, L.-J., Wyss-Coray, T., 2022. Microglia states and nomenclature: A field at its crossroads. Neuron 110, 3458-3483.
Pelvig, D.P., Pakkenberg, H., Stark, A.K., Pakkenberg, B., 2008. Neocortical glial cell numbers in human brains. Neurobiology of Aging 29, 1754-1762.
Pérez-Treviño, P., Velásquez, M., García, N., 2020. Mechanisms of mitochondrial DNA escape and its relationship with different metabolic diseases. Biochimica et Biophysica Acta (BBA) - Molecular Basis of Disease 1866, 165761.
Perkins, A.E., Piazza, M.K., Deak, T., 2018. Stereological Analysis of Microglia in Aged Male and Female Fischer 344 Rats in Socially Relevant Brain Regions. Neuroscience 377, 40-52.
Perluigi, M., Di Domenico, F., Barone, E., Butterfield, D.A., 2021. mTOR in Alzheimer disease and its earlier stages: Links to oxidative damage in the progression of this dementing disorder. Free Radic Biol Med 169, 382-396.
Piantadosi, C.A., 2020. Mitochondrial DNA, oxidants, and innate immunity. Free Radical Biology and Medicine 152, 455-461.
Pomilio, C., Gorojod, R.M., Riudavets, M., Vinuesa, A., Presa, J., Gregosa, A., Bentivegna, M., Alaimo, A., Alcon, S.P., Sevlever, G., Kotler, M.L., Beauquis, J., Saravia, F., 2020. Microglial

autophagy is impaired by prolonged exposure to β-amyloid peptides: evidence from experimental models and Alzheimer's disease patients. Geroscience 42, 613-632.
Qiu, W.Q., Ye, Z., Kholodenko, D., Seubert, P., Selkoe, D.J., 1997. Degradation of Amyloid β-Protein by a Metalloprotease Secreted by Microglia and Other Neural and Non-neural Cells Journal of Biological Chemistry 272, 6641-6646.
Rahman, M.M., Islam, M.R., Yamin, M., Islam, M.M., Sarker, M.T., Meem, A.F.K., Akter, A., Emran, T.B., Cavalu, S., Sharma, R., 2022. Emerging Role of Neuron-Glia in Neurological Disorders: At a Glance. Oxid Med Cell Longev 2022, 3201644.
Raj, D.D.A., Jaarsma, D., Holtman, I.R., Olah, M., Ferreira, F.M., Schaafsma, W., Brouwer, N., Meijer, M.M., de Waard, M.C., van der Pluijm, I., Brandt, R., Kreft, K.L., Laman, J.D., de Haan, G., Biber, K.P.H., Hoeijmakers, J.H.J., Eggen, B.J.L., Boddeke, H.W.G.M., 2014. Priming of microglia in a DNA-repair deficient model of accelerated aging. Neurobiology of Aging 35, 2147-2160.
Reddaway, J., Richardson, P.E., Bevan, R.J., Stoneman, J., Palombo, M., 2023. Microglial morphometric analysis: so many options, so little consistency. Frontiers in Neuroinformatics 17.
Reemst, K., Noctor, S.C., Lucassen, P.J., Hol, E.M., 2016. The Indispensable Roles of Microglia and Astrocytes during Brain Development. Frontiers in Human Neuroscience 10.
Renaudin, X., 2021. Chapter Three - Reactive oxygen species and DNA damage response in cancer. In: Weyemi, U., Galluzzi, L. (Eds.), International Review of Cell and Molecular Biology. Academic Press, pp. 139-161.
Rim, C., You, M.-J., Nahm, M., Kwon, M.-S., 2024. Emerging role of senescent microglia in brain aging-related neurodegenerative diseases. Translational Neurodegeneration 13, 10.
Ritzel, R.M., Doran, S.J., Glaser, E.P., Meadows, V.E., Faden, A.I., Stoica, B.A., Loane, D.J., 2019. Old age increases microglial senescence, exacerbates secondary neuroinflammation, and worsens neurological outcomes after acute traumatic brain injury in mice. Neurobiol Aging 77, 194-206.
Ritzel, R.M., Patel, A.R., Pan, S., Crapser, J., Hammond, M., Jellison, E., McCullough, L.D., 2015. Age- and location-related changes in microglial function. Neurobiology of Aging 36, 2153-2163.
Rolyan, H., Scheffold, A., Heinrich, A., Begus-Nahrmann, Y., Langkopf, B.H., Hölter, S.M., Vogt-Weisenhorn, D.M., Liss, B., Wurst, W., Lie, D.C., Thal, D.R., Biber, K., Rudolph, K.L., 2011. Telomere shortening reduces Alzheimer's disease amyloid pathology in mice. Brain 134, 2044-2056.
Rudnicka, E., Napierała, P., Podfigurna, A., Męczekalski, B., Smolarczyk, R., Grymowicz, M., 2020. The World Health Organization (WHO) approach to healthy ageing. Maturitas 139, 6-11.
Salminen, A., Kaarniranta, K., 2012. AMP-activated protein kinase (AMPK) controls the aging process via an integrated signaling network. Ageing Research Reviews 11, 230-241.
Sanders, J.L., Newman, A.B., 2013. Telomere length in epidemiology: a biomarker of aging, age-related disease, both, or neither? Epidemiol Rev 35, 112-131.
Sandhir, R., Onyszchuk, G., Berman, N.E., 2008. Exacerbated glial response in the aged mouse hippocampus following controlled cortical impact injury. Exp Neurol 213, 372-380.
Sapieha, P., Mallette, F.A., 2018. Cellular Senescence in Postmitotic Cells: Beyond Growth Arrest. Trends in Cell Biology 28, 595-607.
Schapira, A.H.V., Cooper, J.M., Dexter, D., Jenner, P., Clark, J.B., Marsden, C.D., 1989. MITOCHONDRIAL COMPLEX I DEFICIENCY IN PARKINSON'S DISEASE. The Lancet 333, 1269.
Scheffold, A., Holtman, I.R., Dieni, S., Brouwer, N., Katz, S.-F., Jebaraj, B.M.C., Kahle, P.J., Hengerer, B., Lechel, A., Stilgenbauer, S., Boddeke, E.W.G.M., Eggen, B.J.L., Rudolph, K.-L., Biber, K., 2016. Telomere shortening leads to an acceleration of synucleinopathy and impaired microglia response in a genetic mouse model. Acta Neuropathologica Communications 4, 87.
Scheiblich, H., Bousset, L., Schwartz, S., Griep, A., Latz, E., Melki, R., Heneka, M.T., 2021. Microglial NLRP3 Inflammasome Activation upon TLR2 and TLR5 Ligation by Distinct α-Synuclein Assemblies. J Immunol 207, 2143-2154.
Schuitemaker, A., van der Doef, T.F., Boellaard, R., van der Flier, W.M., Yaqub, M., Windhorst, A.D., Barkhof, F., Jonker, C., Kloet, R.W., Lammertsma, A.A., Scheltens, P., van Berckel, B.N.M., 2012. Microglial activation in healthy aging. Neurobiology of Aging 33, 1067-1072.
Schürks, M., Buring, J., Dushkes, R., Gaziano, J.M., Zee, R.Y., Kurth, T., 2014. Telomere length and Parkinson's disease in men: a nested case-control study. Eur J Neurol 21, 93-99.

Shah, F., Hume, S.P., Pike, V.W., Ashworth, S., McDermott, J., 1994. Synthesis of the enantiomers of [N-methyl-11C]PK 11195 and comparison of their behaviours as radioligands for PK binding sites in rats. Nuclear Medicine and Biology 21, 573-581.
Shahidehpour, R.K., Higdon, R.E., Crawford, N.G., Neltner, J.H., Ighodaro, E.T., Patel, E., Price, D., Nelson, P.T., Bachstetter, A.D., 2021. Dystrophic microglia are associated with neurodegenerative disease and not healthy aging in the human brain. Neurobiol Aging 99, 19-27.
Shanbhag, N.M., Evans, M.D., Mao, W., Nana, A.L., Seeley, W.W., Adame, A., Rissman, R.A., Masliah, E., Mucke, L., 2019. Early neuronal accumulation of DNA double strand breaks in Alzheimer's disease. Acta Neuropathol Commun 7, 77.
Sharma, R., Bisht, P., Kesharwani, A., Murti, K., Kumar, N., 2024. Epigenetic modifications in Parkinson's disease: A critical review. European Journal of Pharmacology 975, 176641.
Sheffield, L.G., Berman, N.E.J., 1998. Microglial Expression of MHC Class II Increases in Normal Aging of Nonhuman Primates. Neurobiology of Aging 19, 47-55.
Shen, Q.-q., Jv, X.-h., Ma, X.-z., Li, C., Liu, L., Jia, W.-t., Qu, L., Chen, L.-l., Xie, J.-x., 2024. Cell senescence induced by toxic interaction between α-synuclein and iron precedes nigral dopaminergic neuron loss in a mouse model of Parkinson's disease. Acta Pharmacologica Sinica 45, 268-281.
Shin, H.J., Kim, I.S., Choi, S.G., Lee, K., Park, H., Shin, J., Kim, D., Beom, J., Yi, Y.Y., Gupta, D.P., Song, G.J., Chung, W.-S., Lee, C.J., Kim, D.W., 2024. Rejuvenating aged microglia by p16ink4a-siRNA-loaded nanoparticles increases amyloid-β clearance in animal models of Alzheimer's disease. Molecular Neurodegeneration 19, 25.
Sierra, A., Gottfried-Blackmore, A.C., McEwen, B.S., Bulloch, K., 2007. Microglia derived from aging mice exhibit an altered inflammatory profile. Glia 55, 412-424.
Sivagurunathan, N., Gnanasekaran, P., Calivarathan, L., 2023. Mitochondrial Toxicant-Induced Neuronal Apoptosis in Parkinson's Disease: What We Know so Far. Degener Neurol Neuromuscul Dis 13, 1-13.
Smith, K.L., Kassem, M.S., Clarke, D.J., Kuligowski, M.P., Bedoya-Pérez, M.A., Todd, S.M., Lagopoulos, J., Bennett, M.R., Arnold, J.C., 2019. Microglial cell hyper-ramification and neuronal dendritic spine loss in the hippocampus and medial prefrontal cortex in a mouse model of PTSD. Brain, Behavior, and Immunity 80, 889-899.
Sobhon, P., Savedvanich, G., Weerakiet, S., 2023. Oxidative stress and inflammation: the root causes of aging. Exploration of Medicine 4, 127-156.
Solito, E., Sastre, M., 2012. Microglia Function in Alzheimer's Disease. Frontiers in Pharmacology 3.
Sołtys, Z., Ziaja, M., Pawliński, R., Setkowicz, Z., Janeczko, K., 2001. Morphology of reactive microglia in the injured cerebral cortex. Fractal analysis and complementary quantitative methods. Journal of Neuroscience Research 63, 90-97.
Song, L., Pei, L., Yao, S., Wu, Y., Shang, Y., 2017. NLRP3 Inflammasome in Neurological Diseases, from Functions to Therapies. Frontiers in Cellular Neuroscience 11.
Sonninen, T.M., Goldsteins, G., Laham-Karam, N., Koistinaho, J., Lehtonen, Š., 2020. Proteostasis Disturbances and Inflammation in Neurodegenerative Diseases. Cells 9.
Sorby-Adams, A.J., Vink, R., Turner, R.J., 2018. Large animal models of stroke and traumatic brain injury as translational tools. American Journal of Physiology-Regulatory, Integrative and Comparative Physiology 315, R165-R190.
Squarzoni, P., Oller, G., Hoeffel, G., Pont-Lezica, L., Rostaing, P., Low, D., Bessis, A., Ginhoux, F., Garel, S., 2014. Microglia Modulate Wiring of the Embryonic Forebrain. Cell Reports 8, 1271-1279.
St-Pierre, M.-K., Carrier, M., González Ibáñez, F., Šimončičová, E., Wallman, M.-J., Vallières, L., Parent, M., Tremblay, M.-È., 2022. Ultrastructural characterization of dark microglia during aging in a mouse model of Alzheimer's disease pathology and in human post-mortem brain samples. J Neuroinflammation 19, 235.
Stallone, G., Infante, B., Prisciandaro, C., Grandaliano, G., 2019. mTOR and Aging: An Old Fashioned Dress. Int J Mol Sci 20.
Stillman, J.M., Mendes Lopes, F., Lin, J.P., Hu, K., Reich, D.S., Schafer, D.P., 2023. Lipofuscin-like autofluorescence within microglia and its impact on studying microglial engulfment. Nat Commun 14, 7060.

Stranks, A.J., Hansen, A.L., Panse, I., Mortensen, M., Ferguson, D.J., Puleston, D.J., Shenderov, K., Watson, A.S., Veldhoen, M., Phadwal, K., Cerundolo, V., Simon, A.K., 2015. Autophagy Controls Acquisition of Aging Features in Macrophages. J Innate Immun 7, 375-391.
Streit, W.J., Braak, H., Xue, Q.-S., Bechmann, I., 2009. Dystrophic (senescent) rather than activated microglial cells are associated with tau pathology and likely precede neurodegeneration in Alzheimer's disease. Acta Neuropathologica 118, 475-485.
Streit, W.J., Sammons, N.W., Kuhns, A.J., Sparks, D.L., 2004. Dystrophic microglia in the aging human brain. Glia 45, 208-212.
Suberbielle, E., Djukic, B., Evans, M., Kim, D.H., Taneja, P., Wang, X., Finucane, M., Knox, J., Ho, K., Devidze, N., Masliah, E., Mucke, L., 2015. DNA repair factor BRCA1 depletion occurs in Alzheimer brains and impairs cognitive function in mice. Nat Commun 6, 8897.
Sun, M., McDonald, S.J., Brady, R.D., Collins-Praino, L., Yamakawa, G.R., Monif, M., O'Brien, T.J., Cloud, G.C., Sobey, C.G., Mychasiuk, R., Loane, D.J., Shultz, S.R., 2020. The need to incorporate aged animals into the preclinical modeling of neurological conditions. Neuroscience & Biobehavioral Reviews 109, 114-128.
Swinnen, N., Smolders, S., Avila, A., Notelaers, K., Paesen, R., Ameloot, M., Brône, B., Legendre, P., Rigo, J.-M., 2013. Complex invasion pattern of the cerebral cortex bymicroglial cells during development of the mouse embryo. Glia 61, 150-163.
Taetzsch, T., Benusa, S., Levesque, S., Mumaw, C.L., Block, M.L., 2019. Loss of NF-κB p50 function synergistically augments microglial priming in the middle-aged brain. J Neuroinflammation 16, 60.
Tai, H.-C., Serrano-Pozo, A., Hashimoto, T., Frosch, M.P., Spires-Jones, T.L., Hyman, B.T., 2012. The Synaptic Accumulation of Hyperphosphorylated Tau Oligomers in Alzheimer Disease Is Associated With Dysfunction of the Ubiquitin-Proteasome System. The American Journal of Pathology 181, 1426-1435.
Tang, H., Harte, M., 2021. Investigating Markers of the NLRP3 Inflammasome Pathway in Alzheimer's Disease: A Human Post-Mortem Study. Genes (Basel) 12.
Tang, Y., Li, T., Li, J., Yang, J., Liu, H., Zhang, X.J., Le, W., 2014. Jmjd3 is essential for the epigenetic modulation of microglia phenotypes in the immune pathogenesis of Parkinson's disease. Cell Death Differ 21, 369-380.
Tansey, M.G., Wallings, R.L., Houser, M.C., Herrick, M.K., Keating, C.E., Joers, V., 2022. Inflammation and immune dysfunction in Parkinson disease. Nature Reviews Immunology 22, 657-673.
Thevaranjan, N., Puchta, A., Schulz, C., Naidoo, A., Szamosi, J.C., Verschoor, C.P., Loukov, D., Schenck, L.P., Jury, J., Foley, K.P., Schertzer, J.D., Larché, M.J., Davidson, D.J., Verdú, E.F., Surette, M.G., Bowdish, D.M.E., 2017. Age-Associated Microbial Dysbiosis Promotes Intestinal Permeability, Systemic Inflammation, and Macrophage Dysfunction. Cell Host & Microbe 21, 455-466.e454.
Thomas, A.L., Lehn, M.A., Janssen, E.M., Hildeman, D.A., Chougnet, C.A., 2022. Naturally-aged microglia exhibit phagocytic dysfunction accompanied by gene expression changes reflective of underlying neurologic disease. Sci Rep 12, 19471.
Tramutola, A., Triplett, J.C., Di Domenico, F., Niedowicz, D.M., Murphy, M.P., Coccia, R., Perluigi, M., Butterfield, D.A., 2015. Alteration of mTOR signaling occurs early in the progression of Alzheimer disease (AD): analysis of brain from subjects with pre-clinical AD, amnestic mild cognitive impairment and late-stage AD. Journal of Neurochemistry 133, 739-749.
Tse, J.K.Y., 2017. Gut Microbiota, Nitric Oxide, and Microglia as Prerequisites for Neurodegenerative Disorders. ACS Chemical Neuroscience 8, 1438-1447.
Turner, M.D., Nedjai, B., Hurst, T., Pennington, D.J., 2014. Cytokines and chemokines: At the crossroads of cell signalling and inflammatory disease. Biochimica et Biophysica Acta (BBA) - Molecular Cell Research 1843, 2563-2582.
Ueno, M., Yamashita, T., 2014. Bidirectional tuning of microglia in the developing brain: from neurogenesis to neural circuit formation. Current Opinion in Neurobiology 27, 8-15.
Usenko, T.S., Nikolaev, M.A., Miliukhina, I.V., Bezrukova, A.I., Senkevich, K.A., Gomzyakova, N.A., Beltceva, Y.A., Zalutskaya, N.M., Gracheva, E.V., Timofeeva, A.A., Petrova, O.A., Semenov, A.V., Lubimova, N.E., Totolyan, A.A., Pchelina, S.N., 2020. Plasma cytokine profile in synucleinophaties with dementia. Journal of Clinical Neuroscience 78, 323-326.

Vaiserman, A., Krasnienkov, D., 2021. Telomere Length as a Marker of Biological Age: State-of-the-Art, Open Issues, and Future Perspectives. Frontiers in Genetics 11.
van Furth, R., Cohn, Z.A., 1968. The origin and kinetics of mononuclear phagocytes. J Exp Med 128, 415-435.
van Heemst, D., 2010. Insulin, IGF-1 and longevity. Aging Dis 1, 147-157.
Vellai, T., Takacs-Vellai, K., Zhang, Y., Kovacs, A.L., Orosz, L., Müller, F., 2003. Influence of TOR kinase on lifespan in C. elegans. Nature 426, 620-620.
Vellingiri, B., Balasubramani, K., Iyer, M., Raj, N., Elangovan, A., Song, K., Yeo, H.-C., Jayakumar, N., Kinoshita, M., Thangarasu, R., Narayanasamy, A., Dayem, A.A., Prajapati, V.K., Gopalakrishnan, A.V., Cho, S.-G., 2023. Role of Telomeres and Telomerase in Parkinson's Disease—A New Theranostics? Advanced Biology 7, 2300097.
Vogt, N.M., Kerby, R.L., Dill-McFarland, K.A., Harding, S.J., Merluzzi, A.P., Johnson, S.C., Carlsson, C.M., Asthana, S., Zetterberg, H., Blennow, K., Bendlin, B.B., Rey, F.E., 2017. Gut microbiome alterations in Alzheimer's disease. Sci Rep 7, 13537.
Wagner, L.K., Gilling, K.E., Schormann, E., Kloetzel, P.M., Heppner, F.L., Krüger, E., Prokop, S., 2017. Immunoproteasome deficiency alters microglial cytokine response and improves cognitive deficits in Alzheimer's disease-like APPPS1 mice. Acta Neuropathologica Communications 5, 52.
Wang, L.-W., Chang, Y.-C., Chen, S.-J., Tseng, C.-H., Tu, Y.-F., Liao, N.-S., Huang, C.-C., Ho, C.-J., 2014. TNFR1-JNK signaling is the shared pathway of neuroinflammation and neurovascular damage after LPS-sensitized hypoxic-ischemic injury in the immature brain. J Neuroinflammation 11, 215.
Wang, X., Becker, K., Levine, N., Zhang, M., Lieberman, A.P., Moore, D.J., Ma, J., 2019. Pathogenic alpha-synuclein aggregates preferentially bind to mitochondria and affect cellular respiration. Acta Neuropathologica Communications 7, 41.
Wang, Z.X., Li, Y.L., Pu, J.L., Zhang, B.R., 2023. DNA Damage-Mediated Neurotoxicity in Parkinson's Disease. Int J Mol Sci 24.
Wasserman, J.K., Yang, H., Schlichter, L.C., 2008. Glial responses, neuron death and lesion resolution after intracerebral hemorrhage in young vs. aged rats. European Journal of Neuroscience 28, 1316-1328.
Wendeln, A.-C., Degenhardt, K., Kaurani, L., Gertig, M., Ulas, T., Jain, G., Wagner, J., Häsler, L.M., Wild, K., Skodras, A., Blank, T., Staszewski, O., Datta, M., Centeno, T.P., Capece, V., Islam, M.R., Kerimoglu, C., Staufenbiel, M., Schultze, J.L., Beyer, M., Prinz, M., Jucker, M., Fischer, A., Neher, J.J., 2018. Innate immune memory in the brain shapes neurological disease hallmarks. Nature 556, 332-338.
Wong-Guerra, M., Calfio, C., Maccioni, R.B., Rojo, L.E., 2023. Revisiting the neuroinflammation hypothesis in Alzheimer's disease: a focus on the druggability of current targets. Frontiers in Pharmacology 14.
Wu, Y., Pei, Y., Yang, Z., Li, K., Lou, X., Cui, W., 2020. Accelerated telomere shortening independent of LRRK2 variants in Chinese patients with Parkinson's disease. Aging (Albany NY) 12, 20483-20492.
Xu, W., Boyd, R.M., Tree, M.O., Samkari, F., Zhao, L., 2019. Mitochondrial transcription factor A promotes DNA strand cleavage at abasic sites. Proceedings of the National Academy of Sciences 116, 17792-17799.
Yin, F., Banerjee, R., Thomas, B., Zhou, P., Qian, L., Jia, T., Ma, X., Ma, Y., Iadecola, C., Beal, M.F., Nathan, C., Ding, A., 2010. Exaggerated inflammation, impaired host defense, and neuropathology in progranulin-deficient mice. J Exp Med 207, 117-128.
Youm, Y.-H., Grant, Ryan W., McCabe, Laura R., Albarado, Diana C., Nguyen, Kim Y., Ravussin, A., Pistell, P., Newman, S., Carter, R., Laque, A., Münzberg, H., Rosen, Clifford J., Ingram, Donald K., Salbaum, J.M., Dixit, Vishwa D., 2013. Canonical Nlrp3 Inflammasome Links Systemic Low-Grade Inflammation to Functional Decline in Aging. Cell Metab 18, 519-532.
Yu, H.-M., Zhao, Y.-M., Luo, X.-G., Feng, Y., Ren, Y., Shang, H., He, Z.-Y., Luo, X.-M., Chen, S.-D., Wang, X.-Y., 2012. Repeated Lipopolysaccharide Stimulation Induces Cellular Senescence in BV2 Cells. Neuroimmunomodulation 19, 131-136.
Yu, W.H., Cuervo, A.M., Kumar, A., Peterhoff, C.M., Schmidt, S.D., Lee, J.-H., Mohan, P.S., Mercken, M., Farmery, M.R., Tjernberg, L.O., Jiang, Y., Duff, K., Uchiyama, Y., Näslund, J., Mathews, P.M., Cataldo, A.M., Nixon, R.A., 2005. Macroautophagy—a novel β-amyloid peptide-generating pathway activated in Alzheimer's disease. Journal of Cell Biology 171, 87-98.

Yu, W.H., Dorado, B., Figueroa, H.Y., Wang, L., Planel, E., Cookson, M.R., Clark, L.N., Duff, K.E., 2009. Metabolic activity determines efficacy of macroautophagic clearance of pathological oligomeric alpha-synuclein. Am J Pathol 175, 736-747.
Zhang, P., Kishimoto, Y., Grammatikakis, I., Gottimukkala, K., Cutler, R.G., Zhang, S., Abdelmohsen, K., Bohr, V.A., Misra Sen, J., Gorospe, M., Mattson, M.P., 2019. Senolytic therapy alleviates Aβ-associated oligodendrocyte progenitor cell senescence and cognitive deficits in an Alzheimer's disease model. Nat Neurosci 22, 719-728.
Zhang, T., Jia, Y., 2014. Meta-analysis of Ubiquilin1 gene polymorphism and Alzheimer's disease risk. Med Sci Monit 20, 2250-2255.
Zhang, W., Xiao, D., Mao, Q., Xia, H., 2023. Role of neuroinflammation in neurodegeneration development. Signal Transduction and Targeted Therapy 8, 267.
Zhang, X., Heng, Y., Kooistra, S.M., van Weering, H.R.J., Brummer, M.L., Gerrits, E., Wesseling, E.M., Brouwer, N., Nijboer, T.W., Dubbelaar, M.L., Boddeke, E.W.G.M., Eggen, B.J.L., 2021. Intrinsic DNA damage repair deficiency results in progressive microglia loss and replacement. Glia 69, 729-745.
Zhao, H., Zhao, X., Cao, X., Wu, G., 2012. Age-Dependent Neuroimmune Modulation of IGF-1R in the Traumatic Mice. Immunity & Ageing 9, 12.
Zhao, J., Huai, J., 2023. Role of primary aging hallmarks in Alzheimer´s disease. Theranostics 13, 197-230.
Zhou, R., Qian, S., Cho, W.C.S., Zhou, J., Jin, C., Zhong, Y., Wang, J., Zhang, X., Xu, Z., Tian, M., Chan, L.W.C., Zhang, H., 2022. Microbiota-microglia connections in age-related cognition decline. Aging Cell 21, e13599.
Zhu, L., Dong, C., Sun, C., Ma, R., Yang, D., Zhu, H., Xu, J., 2015. Rejuvenation of MPTP-induced human neural precursor cell senescence by activating autophagy. Biochemical and Biophysical Research Communications 464, 526-533.
Zhuang, Z.Q., Shen, L.L., Li, W.W., Fu, X., Zeng, F., Gui, L., Lü, Y., Cai, M., Zhu, C., Tan, Y.L., Zheng, P., Li, H.Y., Zhu, J., Zhou, H.D., Bu, X.L., Wang, Y.J., 2018. Gut Microbiota is Altered in Patients with Alzheimer's Disease. J Alzheimers Dis 63, 1337-1346.
Ziebell, J.M., Adelson, P.D., Lifshitz, J., 2015. Microglia: dismantling and rebuilding circuits after acute neurological injury. Metab Brain Dis 30, 393-400.
Ziebell, J.M., Taylor, S.E., Cao, T., Harrison, J.L., Lifshitz, J., 2012. Rod microglia: elongation, alignment, and coupling to form trains across the somatosensory cortex after experimental diffuse brain injury. J Neuroinflammation 9, 247.
Ziv, Y., Avidan, H., Pluchino, S., Martino, G., Schwartz, M., 2006. Synergy between immune cells and adult neural stem/progenitor cells promotes functional recovery from spinal cord injury. Proceedings of the National Academy of Sciences 103, 13174-13179.
Zou, J.Y., Crews, F.T., 2005. TNFα potentiates glutamate neurotoxicity by inhibiting glutamate uptake in organotypic brain slice cultures: neuroprotection by NFκB inhibition. Brain Research 1034, 11-24.

Contextual statement: Chapter 3

Chapter 3 is presented in manuscript format intended to be submitted for publication. This chapter presents a comparison of automated and manual methods to assess microglia in histological tissue sections. Typically, the first microglial analysis to be conducted in tissue is counting of total and activated microglia. The gold standard method for this is by manual identification of microglia and while objective antibodies for activation exist, classification of amoeboid microglia as activated is a widely accepted and published metric however this is time consuming and is subjective to the judgement of the researcher. Automated software to conduct this analysis thus presents an avenue to save time and avoid biased microglial classification. Therefore, in the following chapter we aimed to assess whether the novel microglial analysis module on Halo, a software originally designed for pathology diagnoses, is comparable to manual assessment of microglia. Analysis of microglia using an ImageJ code was also included as an additional automated method for comparison. This chapter represents the first study to assess the accuracy of the Halo microglia analysis module in the literature.

Statement of Authorship

Title of Paper	Comparison of Automated and Manual Approaches for Microglial Quantification and Classification: A Focus on The Halo Digital Pathology Platform
Publication Status	☐ Published ☐ Accepted for Publication ☐ Submitted for Publication ☑ Unpublished and Unsubmitted w ork w ritten in manuscript style
Publication Details	

Principal Author

Name of Principal Author (Candidate)	Laura Carr		
Contribution to the Paper	First author and main contributor. Conceptualised paper, conducted analysis, writer and formulation of manuscript. Reviewed prepared final draft following inputs from co-authors.		
Overall percentage (%)	70%		
Certification:	This paper reports on original research I conducted during the period of my Higher Degree by Research candidature and is not subject to any obligations or contractual agreements with a third party that would constrain its inclusion in this thesis. I am the primary author of this paper.		
Signature		Date	31/10/24

Co-Author Contributions

By signing the Statement of Authorship, each author certifies that:

i. the candidate's stated contribution to the publication is accurate (as detailed above);
ii. permission is granted for the candidate in include the publication in the thesis; and
iii. the sum of all co-author contributions is equal to 100% less the candidate's stated contribution.

Name of Co-Author	Bianca Guglietti		
Contribution to the Paper	Conceptualised, reviewed and edited manuscript		
Signature		Date	1/11/24

Name of Co-Author	Ing Chee Wee
Contribution to the Paper	Tissue generation and analysis, reviewed and edited manuscript

Signature		Date	5/11/24

Name of Co-Author	Sanam Mustafa		
Contribution to the Paper	Conceptualised paper, reviewed and edited manuscript, Project supervision		
Signature		Date	1.11.24

Name of Co-Author	Ian Musgrave		
Contribution to the Paper	Reviewed and edited manuscript, Project supervision		
Signature		Date	7/11/2024

Name of Co-Author	Frances Corrigan		
Contribution to the Paper	Tissue generation, reviewed and edited manuscript		
Signature		Date	1/11/2024

Name of Co-Author	Lyndsey E. Collins-Praino		
Contribution to the Paper	Conceptualised paper, reviewed and edited manuscript, Project supervision		
Signature		Date	31/10/24

Please cut and paste additional co-author panels here as required.

Chapter 3 : Comparison of Automated and Manual Approaches for Microglial Quantification and Classification: A Focus on The Halo Digital Pathology Platform

Laura M. Carr[1], Bianca Guglietti[1], Ing Chee Wee[1], Ian Musgrave[1], Sanam Mustafa[1,2,3], Frances Corrigan[1], Lyndsey E. Collins-Praino[1,2]

[1]School of Biomedicine, University of Adelaide, Adelaide, SA, Australia
[2]Australian Research Council Centre of Excellence for Nanoscale Biophotonics, The University of Adelaide, Adelaide, SA, Australia
[3]Davies Livestock Research Centre, The University of Adelaide, Roseworthy, SA, Australia

3.1 Abstract

In the central nervous system, microglia act as the brain's resident macrophages. Phenotypic changes in microglia have been linked to multiple neurological conditions, such as dementia, Parkinson's Disease (PD), stroke and traumatic brain injury (TBI). Consistent identification and classification of microglial phenotypes is essential in understanding the link between microglia and neurological diseases. Currently, there are several ways by which microglial population and morphology are assessed, including manually, or using open-source image analysis platforms, such as ImageJ. A microglial classification module for the Halo digital pathology platform has been developed for this purpose but has not yet been validated within the literature. The current study therefore conducted a comparison of the performance of this Halo module to the gold standard manual microglial analysis and an automated analysis code on ImageJ using human and rat brain tissue. In 5µm thick human tissue, the number of total and activated microglia detected by Halo correlated well with both manual and ImageJ methods and showed limited differences in raw numbers. In 20µm thick rat tissue, total counts correlated reasonably well however activated counts were not correlated with any method. To our knowledge this is the first study to systematically compare the Halo module to other common methods of analysis. Findings suggest that the Halo module is as accurate as other open-source automated methods when applied to 5µm tissue. However, when analysing thicker tissue, a more in-depth analysis and consideration of parameters must be taken to combat the variation in staining signal.

3.2 Introduction

It is now understood that a variety of immune cells exist in the CNS under homeostatic conditions (Prinz and Priller, 2017) however microglia are considered the resident tissue macrophages in the brain (van Furth and Cohn, 1968). Though microglia have diverse roles in development, homeostasis and disease, their primary roles are regulating immune responses and maintenance of CNS tissues (Collins et al., 2012; Hope et al., 2020; Leng and Edison, 2021), where they take on various phenotypes characterised by diverse morphological profiles. Under normal physiological conditions, ramified microglia actively survey the CNS, expanding and contracting their processes to monitor the surrounding environment (Nimmerjahn et al., 2005). Microglia are morphologically diverse with resting microglia presenting with long branching processes and a small cell soma (summarised in a recent review: (Lier et al., 2021)). Upon recognition of tissue damage or pathogens, microglia undergo functional and morphological changes to respond to the perceived immunological threat, by retracting their branches and switching to an amoeboid, phagocytic phenotype (Ransohoff and Brown, 2012; Reddaway et al., 2023). Functionally, microglial activation involves increased release of pro-inflammatory cytokines and phagocytosis of pathogens and debris (Kettenmann et al., 2011). While acute inflammation driven by microglia is crucial in maintaining overall CNS health, chronic activation of microglia and resulting chronic CNS inflammation is associated with many neurological conditions (Vidal-Itriago et al., 2022). Abnormal increases in activated microglia have been observed in neurodegenerative diseases, such as Alzheimer's disease (AD) and Parkinson's disease (PD), and in cases of neurotrauma, such as following traumatic brain injury (TBI) and stroke (For reviews see : (Donat et al., 2017; Gao et al., 2023; Zhang, 2019)).

Given the role of aberrant microglial activation across many different neurological disorders, identifying and classifying microglia within brain tissue in a consistent manner is critical. To date, however, significant variation exists between laboratory groups in terms of how this is conducted (Reddaway et al., 2023). Quantifying the total number of microglia in regions of interest is often the first point of call in assessing microglia, as cells migrate to an affected location to initiate a response (Davalos et al., 2005). This is achieved by immunohistochemical staining for general microglial

markers, including ionized calcium-binding adapter molecule 1 (IBA1). Despite not being microglia specific, also staining macrophages in addition to microglia (Uff et al., 2022), IBA1 is one of the most commonly utilised general microglia markers (Jurga et al., 2020). Additional assessment of the activation state of microglia is often performed by measuring markers of activation or by assessing cell morphology (Fernández-Arjona et al., 2017; Leng and Edison, 2021; Moehle and West, 2015). Extensive lists of markers for activated microglia exist in the literature (reviewed: (Jurga et al., 2020; Lier et al., 2021)), with the most common inclusions on these being major histocompatibility complex II (MHCII) (Jimenez-Ferrer et al., 2021) and various cluster of differentiation (CD) molecules, including CD11b (Ritzel et al., 2023) and CD68 (Bido et al., 2021). However, such staining for activation markers requires optimisation of antibodies and extensive use of tissue samples. Instead, morphological analysis in tissue stained for general microglia markers, such as IBA1, offer a reliable alternative, and allow visualisation of the entire population of microglia rather than staining for activation alone.

Currently, there are several ways by which images of stained microglia are assessed for morphology. The gold standard method to conduct microglial analysis is using unbiased stereological assessment (Yurt et al., 2018). This method requires 3D images and applies random sampling to isolate specific areas of tissue in a structured way so as to avoid selection bias (Brown, 2017). Stereology assesses multiple focal planes to count only cells which appear in a defined three-dimensional space, avoiding overcounting cells which may be cut in a thin section of tissue. Mathematical models are then applied to determine the total estimated number of cells in the whole region of interest (Brown, 2017; Yurt et al., 2018). Stereological analysis critically avoids bias and accounts for the 3D structure of microglia which limits analyses conducted in 2D tissue sections. While this analysis is the most rigorous method for an unbiased approach, the use of this is reliant on the availability of thicker tissue sections and specialised software, such as Stereo Investigator (MBF Bioscience), which may not always be feasible. Additionally, many studies will often rely on archival tissue to reduce the use of additional animals, but such tissue is often prepared as single-plane sections rather than thick sections suitable for 3D imaging. In these cases, alternate methods are necessary. These include manually counting and analysing

microglia, or using open-source image analysis platforms, such as ImageJ (Schneider et al., 2012). Visualising tissue sections and manually recording the number of activated and non-activated microglia is one of the most common methods of microglial identification (de Gracia et al., 2015; Gallego and de Gracia, 2016). In this method, sections of tissue are isolated and cells within that area are counted and classified based on their morphology. The results of this type of analysis are then expressed as a number of microglia per mm^2 for total number of microglia, or as a percentage out of 100 for the ratio of activated microglia to total number of microglia. Such manual counting can be extremely time consuming. Further, this manual analysis introduces a degree of subjectivity, as researchers manually decide which classification a cell belongs to, with this opinion subject to change between researchers, or even as the researcher moves through the dataset (Reddaway et al., 2023). Additionally, as manual counting is done on a randomised number of images within a region, it may not be reflective of the entire population of cells within the area of interest. Therefore, to assess larger areas, without significantly increasing the time needed for analysis, automated analysis of entire sections of tissue is desirable.

Image analysis programs, including ImageJ (Arganda-Carreras et al., 2010; Arshadi et al., 2021), have the potential to fill this gap. Similar to manual counts, ImageJ is commonly used to conduct analysis on a subsection of cells within a given region, but optimising the batch analysis function within the program can allow for quantification of a larger area (Klemm and Miura, 2022). This requires understanding of the Java coding language used by ImageJ to perform a batch analysis on multiple folders. However, there are a large number of microglial analysis protocols available online for ImageJ, and resources to write scripts are relatively easy to locate (Schroeder et al., 2021). Once set up and optimised, a script to analyse a batch of images takes very little time to complete the analysis. However, the use of ImageJ for whole tissue analysis requires many smaller images to be exported and processed as it cannot handle the original full slide images (Ishikawa et al., 2015). This process can be time consuming, introducing further subjectivity to the analysis. Additionally, for images with low contrast, separating microglia from background for analysis by thresholding can be subjective and image

information, including cell morphology, may be lost (Tajima and Kato, 2011). Recent reports on microglial analysis in ImageJ have assisted in validating existing single cell methods and provide a detailed resource for conducting morphological analysis on individual cells (Green et al., 2022; Young and Morrison, 2018). However, there is no standardised method to automate these analyses, and methods to do this are highly dependent on imaging protocols and file formats. While there is an abundance of community resources available for ImageJ and other open-source software (Schroeder et al., 2021), these methods are not always user friendly and can be difficult to navigate and troubleshoot. Thus, a user friendly, automated method of microglial analysis, requiring limited pre-processing of images, would greatly contribute to improving study reproducibility (Reddaway et al., 2023).

Halo is an image analysis software developed by Indica Labs (Albuquerque, New Mexico, USA) for fast, high throughput image analysis. It includes a number of purpose developed modules which have been widely utilised, including cytonuclear and multiplex immunohistochemistry (IHC) (Kayagaki et al., 2023; Zhang et al., 2023) and *in situ* hybridisation (ISH) (Gioia et al., 2023; Vore et al., 2022) analysis modules. A module for the quantification of activated microglia has also been developed (Indica Labs, 2024), which uses basic morphological parameters to not only assess microglial number, but also to distinguish between activated and resting cells. Halo calculates the number of activated microglia, non-activated microglia and non-microglial cells, as well as morphological data, including average process length, total process length and process thickness. Further, this analysis can be conducted for the entire area of tissue, giving researchers data on thousands of cells, rather than limiting analysis to a relatively small area within a given tissue section (Horai et al., 2019). Additionally, Halo can generate data on cell characteristics for specific cells, providing the potential for a more detailed analysis of individual microglial morphology. With the ability to perform automated batch analysis, Halo presents a potential step forward in improving consistency of microglial analysis across studies (Horai et al., 2019); however, to our knowledge, the Halo microglial analysis module has not previously been validated against other analysis methods. Accordingly, the current study aimed to assess the ability

of the Halo microglial analysis module to identify and classify microglia by comparing its performance to both manual counting and automated counting using ImageJ across human and rat datasets.

3.3 Materials and methods

3.3.1 Study cohorts

Human post-mortem brain tissue from Parkinson's disease patients or neurologically healthy age-matched controls was provided by the South Australian Brain Bank for the human dataset. Ages ranged from 61 to 86 in controls (71.33 ± 3.56) and 73 to 88 in PD (78.2 ± 1.63) cases. Previously generated archival tissue from adult male Sprague-Dawley rats at 12- months-old was utilised for the rat dataset. Animals received either a sham surgery, a single mild TBI, repetitive mild TBI or moderate-severe TBI utilising the Marmarou impact-acceleration injury protocol, with the protocol for injury and post-operative care descry ibed extensively previously (Marmarou et al., 1994). Male to female ratios of human subjects and final numbers included in each cohort are presented in Table 3.1. For correlation analyses, as differences between groups were not of interest in the present study, groups were combined. Specific inclusion criteria and demographic data for human subjects can be found in Supplementary Table S3.1, and injury protocols for rat tissue can be found in Supplementary Methods 1.

Table 3.1: Study cohorts for human and rat datasets

Parameter	Human dataset	Rat dataset
Control/Sham	6 (3M:3F)	6
PD	10 (5M:5F)	-
Mild-TBI (mTBI)	-	6
Repetitive mild TBI (rmTBI)	-	7
Moderate-severe TBI (msTBI)	-	8
Total n	**16**	**27**

3.3.2 Tissue Collection and Processing

The post-mortem human brains were bisected at autopsy, with one half immersion fixed in buffered formalin and the other half coronally sectioned, frozen on a bed of dry ice and stored at -80ºC. Fixed tissues were processed and embedded in paraffin wax. For the current study, 5µm coronal sections of regions of interest (ROIs) were prepared from embedded tissue (n = 16), mounted on silane coated slides and dried overnight at 37°C. Animals in the rat cohort (n=27) were transcardially perfused with

0.2mL heparin + 10% formalin, following which brain samples were post-fixed in 10% formalin at room temperature for a minimum of 7 days. For immunohistochemistry, brains were transferred through a series of sucrose solutions with a gradual concentration increase (10% to 20% to 30%) over 5-7 days for cryoprotection. Following this, 2-3mm thick coronal sections were collected, spanning the frontal lobe to the SN, and embedded in Optimal Cutting Temperature compound (Tissue-Tek O.C.T. compound, Proscitech, Ref 4583) in −80°C freezing isopentane (2-methylbutane, Sigma Aldrich, M32631). 20µm coronal sections were taken from ROIs of each animal and mounted on microscope slides. Frozen sections mounted on slides were stored in -20°C freezer. The prefrontal cortex (PFC), striatum (ST) and substantia nigra (SN) were chosen as ROIs in both datasets, to allow for investigation across multiple brain regions. In human tissue, the specific areas were identified and sectioned by the SA Brain Bank and are summarised in supplementary table S3.2. In rat tissue, regions were sectioned to include: the prelimbic area, anterior cingulate area and infralimbic area of the PFC; the caudate nucleus and putamen of the ST; and the *pars compacta* and *pars reticulata* regions of the SN. These regions are summarised in supplementary table S3.3.

3.3.3 Immunohistochemistry

Immunohistochemical (IHC) staining was performed similarly across the two datasets, according to standard protocols. Briefly, human tissue slides were prepared by deparaffinisation in xylene and washed in ethanol, where-as rat tissue slides were prepared by air-drying overnight and rehydrating in ethanol. Following this, both datasets underwent the same protocol. Endogenous peroxidases were blocked using methanol with 0.5% hydrogen peroxide. Slides were then washed twice with phosphate buffered saline (PBS). Antigen retrieval was performed (citrate) and sections were blocked in 3% normal horse serum (NHS) for 30min, before overnight incubation at room temperature with the primary antibody (see Table 3.2 for all antibody details). On the following day, slides were again washed twice in 0.1% Triton-X-100 in PBS and incubated with secondary antibodies for 30 minutes at room temperature, followed by two more washes with PBS and incubation with streptavidin peroxidase conjugate for 1 hour. Following a final wash with PBS, the chromogen 3,3-Diaminobenzidine tetrahydrochloride was applied for 7 minutes. Human tissue was counterstained with haematoxylin,

dehydrated in ethanol and cleared with xylene. Rat tissue was not counterstained. Slides were mounted with coverslips using DPX mountant (Sigma Aldrich) and air-dried in the fume hood for 2 days. Representative staining from each brain region in each dataset is shown in Figure 3.1. The experimenter was blinded to the group in all following analyses.

Table 3.2: Antibody concentrations used in each dataset

Antibody	Species	Source	Human	Rat
Ionized Calcium Binding adaptor molecule 1 (IBA1)	Rabbit	Wako – 019-19741	1:800	1:20,000
Anti-Rabbit IgG secondary antibody	Goat (human) Horse (rat)	Vector Human: BA-1000 Rat: BA-1100	1:250	1:250
Streptavidin Peroxidase Conjugate (SPC)	N/A	Vector - SA-5004	1:1000	1:1000
3,3-Diaminobenzidine tetrahydrochloride (DAB)	N/A	Vector (human) Sigma Aldrich (rat)	1:50	1:50

3.3.4 Image acquisition

IBA1 stained slides in both datasets were scanned using a Nanozoomer slide scanner (Hamamatsu, Shizouka, Japan). Human tissue was scanned in a single plane, with 5 fine focus points set per image to achieve 228nm/pixel (111403 DPI). For rat tissue, seven 1µm layers of the 20µm thick slides were scanned, starting at the clearest layer and extending ±3µm in either direction, for a total scan covering 7µm of tissue. Using ImageJ, areas of interest were isolated using 'The Rat Brain in Stereotaxic Coordinates' atlas for reference (Paxinos and Watson, 2007) at 20x zoom and z-stacks of each area of interest were created for subsequent analysis. Images were analysed according to the methods described below.

3.3.5 Manual Quantification

Manual counting was conducted by a single assessor using QuPath (v0.4.4) (Bankhead et al., 2017). While conducting automated counts on QuPath is possible using the pixel classifier function, here, the program was utilised only for manual counting and exporting images to ImageJ as below. For human tissue, six boxes of equal size (2.8mm^2) were annotated on each slide (16.8mm^2) and cells within boxes were manually counted. For rat tissue, cells in each stacked image were counted. The number of boxes or images analysed for each animal and the average number of microglia counted is summarised in supplementary tables 3.2 and S3.3. Number of resting microglia and number of activated microglia

were counted in each box or image. Total microglia count was calculated as resting + activated cells. Total area analysed for each case was used to calculate cells per mm^2 (cell count / total area). Microglia were identified by the presence of positive DAB staining. Activated microglia were distinguished based on a high soma circularity (amoeboid morphology) and shortened or no processes.

3.3.6 Automated batch analysis

For human tissue, QuPath was used to export the entire tissue into tiles at 13.3x zoom for screen dimensions 1920x1088 using the batch macro function (Supplementary Methods 2). Some tiles were excluded based on criteria that would likely impact automated count (e.g. blurry image, tissue artifacts, large vessels visible, <75% of tile containing tissue). See Supplementary Fig S3.1 for examples of excluded images. For rat tissue, each Z-stacked image was analysed in its entirety, as artifacts and tissue edges were avoided when creating Z-stacks. Images were analysed in ImageJ using the batch macro function (Supplementary Methods 3). ImageJ 'color deconvolution' (Ruifrok and Johnston, 2001) was used, and parameters were set as outlined in Table 3.3. ImageJ automated analysis was chosen over pixel classification using QuPath as ImageJ is widely utilised for automated cell analysis (Schroeder et al., 2021). As regions were stained separately, thresholds were altered between regions, but pixel size and circularity for activated analysis were kept consistent within each dataset. Area calculations and cells/cm^2 were conducted as for the manual counts above.

Table 3.3: ImageJ Automated Microglial Analysis Parameter Summary

Parameter	**Human tissue**				**Rat tissue**		
	PFC	**ST**	**SN**	**HIPP**	**PFC**	**ST**	**SN**
Threshold	0, 90	0, 80	0, 50	0, 70	0, 40	0, 70	0, 50
Pixels (range)	50-2000				100-2000		
Circularity (activated)	0.80-1.00				0.80-1.00		

3.3.7 HALO Quantification

IBA1 stained slides were analysed using the Halo image analysis platform (Indica Labs, Albuquerque, New Mexico, USA). Analysis settings were based on the microglial activation module (v1.2) for

automated counting. Parameters for human tissue were optimised for each slide and for rat tissue were optimised for each region to capture 80-90% of microglial morphology accurately (Supplementary Fig S3.2) across 10 test images, before being applied to the full analysis. The range of parameters for each dataset is indicated in Table 3.4. Microglial and nuclear stain selection varied between each slide/image. For consistency, morphological parameters (i.e. cell size, process radius, fragmentation length and activation process thickness) were kept consistent, while parameters that varied due to staining (i.e. contrast threshold and process optical density (OD)) were optimised between images/slides. Total microglial population and activation state were determined based on morphological parameters of $IBA1^+$ cells (see Table 3.5) across the entire slide for human tissue, and within each stacked image for rat tissue. Microglial count was divided by total area to determine cells per mm^2.

Table 3.4: HALO Microglial Detection Parameter Summary

Parameter	Human tissue	Rat tissue
Min Microglia Cell Body Diameter	3.2µm	3.3µm
Microglia Contrast Threshold	0.1-0.55	0
Min Microglial Process OD	0.14-0.35	0.15-0.40
Max Microglia Process Radius	12µm	15µm
Microglia Max Fragmentation Length	1.1µm	7µm
Activation Process Thickness	2.4µm	2.3µm

3.4 Statistical Methods

Outliers with a Q value of 0.1% were identified in GraphPad Prism version 9.0.0 for Windows (GraphPad Software, San Diego, California USA) using the Robust Regression and Outlier Removal (ROUT) method (Motulsky and Brown, 2006). All subsequent statistical analysis was conducted using IBM SPSS® Statistics (Version 29.0.1.0), with the exception of Kruskal Wallis tests for non-parametric data, conducted in R (version 1.4.1717) (Dalgaard, 2010). Shapiro-Wilk test was used to explore data normality within each region. Normally distributed data were analysed using a two-way analysis of variance (ANOVA), with Tukey post-hoc, and Pearson's correlation analysis. Non-normally distributed data were analysed using a Kruskal Wallis test and Spearman's correlational analysis. For both normal and non-normal data, alpha was set to 0.05. Data were graphed using GraphPad Prism.

Figure 3.1 Representative images of IBA1 staining from each brain region in each dataset.Sections from Human control tissue and Rat sham tissue were stained for IBA1 and imaged using a nanozoomer slide scanner, as described in materials and methods. IBA1+ microglia are stained brown; black arrows indicate activated microglia. The hippocampus was not sectioned from rats and thus, no representative image is available. Scale bar = 50µm

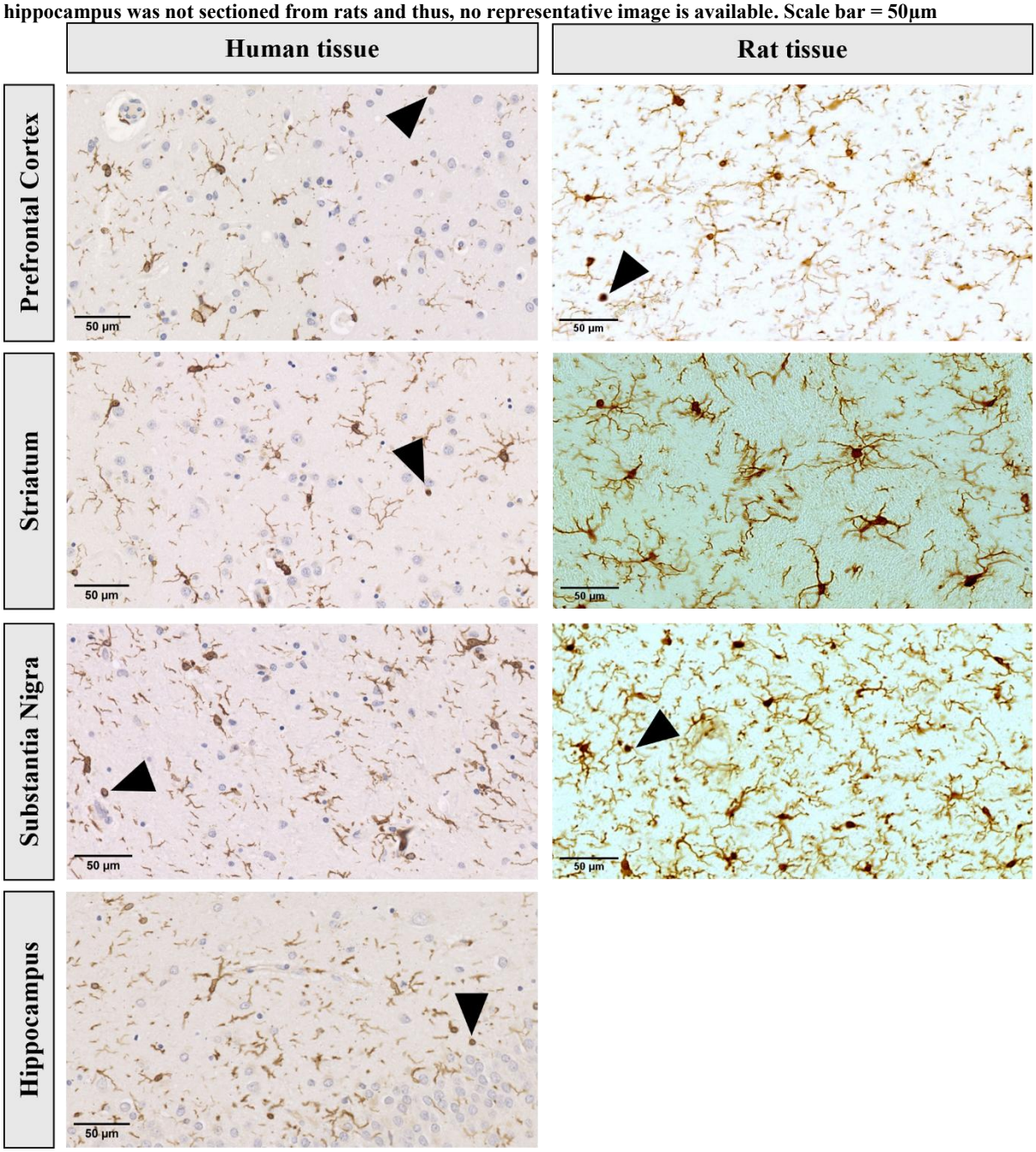
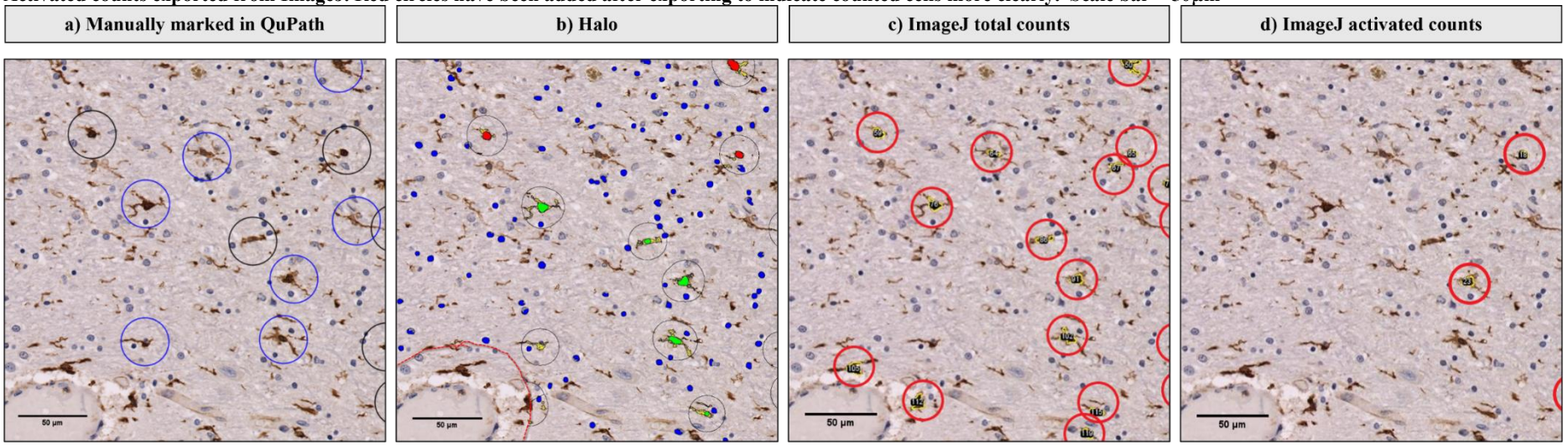


Figure 3.2 Examples of IBA1 stained microglia in human SN tissue identified by various methods.a) Microglia counted manually. Blue circles indicate non-activated microglia and black circles indicate activated microglia. b) Microglia counted using Halo. Areas contained within red dotted circles are manually marked to be excluded from analysis. Green cells indicate non-activated microglia and red cells indicate activated microglia. Nuclei of surrounding cells are identified by Halo in blue c) Total counts exported from ImageJ and d) Activated counts exported from ImageJ. Red circles have been added after exporting to indicate counted cells more clearly. Scale bar = 50µm



3.5 Results

3.5.1 Human post-mortem tissue:

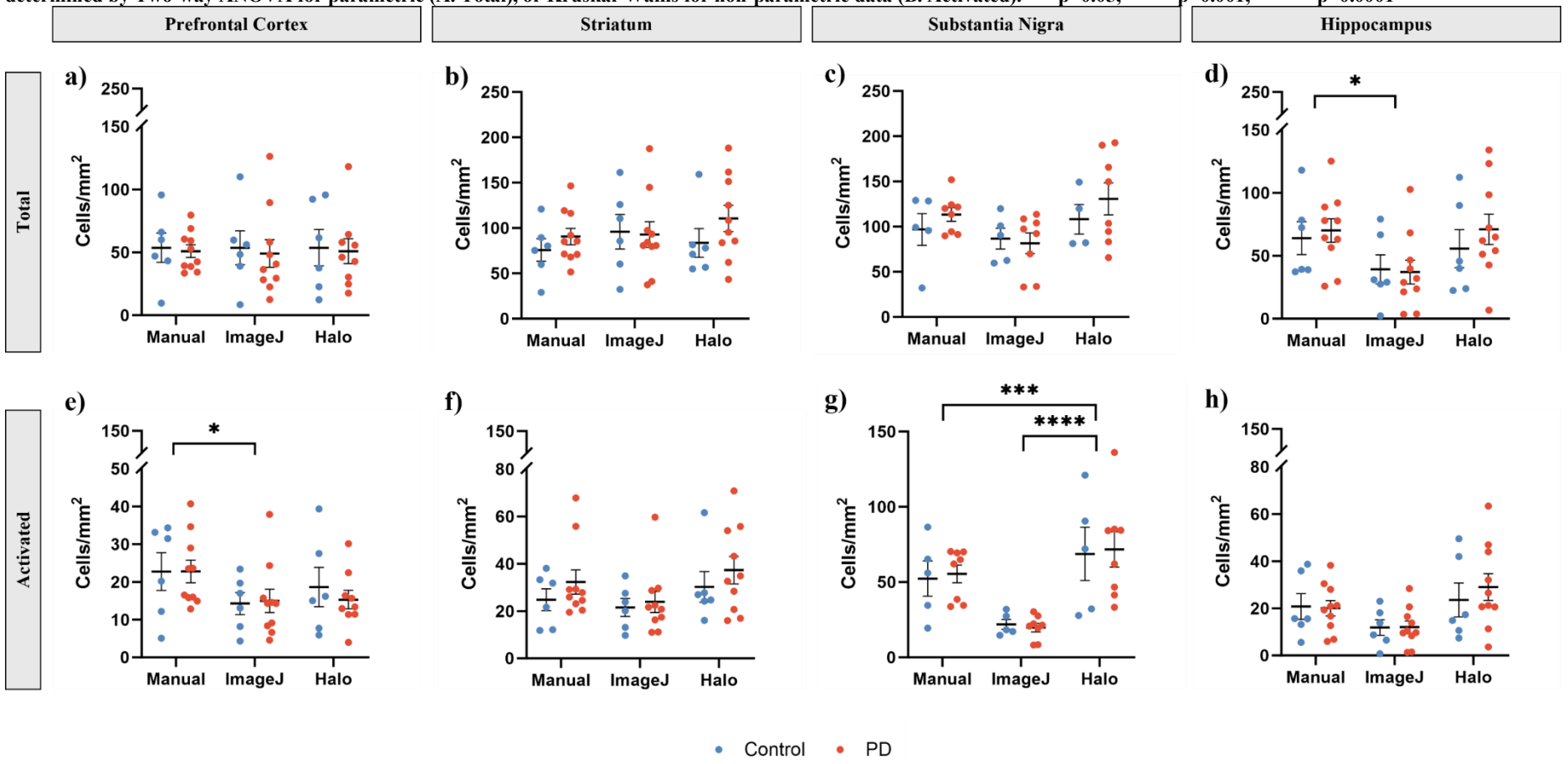
3.5.1.1 Total microglia count did not differ between groups or between methods, except in the hippocampus of 5µm human brain tissue.

Human tissue was stained for IBA1, and both total and activated microglial number were analysed using manual, ImageJ and Halo counting methods. Representative images and examples of tissue within each region in this dataset are shown (Fig 3.1). Figure 3.2 shows the output from the different counting methods utilised in this study on one section of SN tissue, highlighting the differences in counts between methods (Fig 3.2). When total microglia counts were analysed using a two-way ANOVA, a significant main effect of method was detected in the HIPP *(F(2,42) = 3.45, p = 0.04)* (Fig 3.3d), but not in the PFC *(F(2,41) = 0.005, p = 0.1),* ST *(F(2,42) = 0.505, p = 0.61)* or SN *(F(2,32) = 2.912, p = 0.07)* (Fig 3.3a-c). Tukey post hoc test demonstrated that ImageJ detected fewer total microglia than manual counting within the HIPP *(37.92±28.47* vs *67.85±29.61, p = 0.035).* Neither a significant group effect (PFC *(F(1,41) = 0.141, p = 0.71)*; ST *(F(1,42) = 1.152, p = 0.29)*; HIPP *(F(1,42) = 0.428, p = 0.52)*; SN *(F(1,32) = 0.902, p = 0.35)*) or interaction effect (PFC *(F(2,41) = 0.004, p = 0.99)*; ST (F(2,42) = 0.539, *p* = 0.59); HIPP *(F(2,42) = 0.267, p = 0.77)*; SN *(F(2,32) = 0.497, p = 0.61)*) was seen in any of the brain regions analysed.

3.5.1.2 Activated microglia count differed between methods in the PFC and SN of 5µm human brain tissue.

When analysing activated microglial counts, significant main effects of method were seen in the PFC *(H(2) = 6.74, p = 0.035)* (Fig 3.3E) and SN *(H(2) = 23.5, p = <0.0001)* (Fig 3.3g), but not in the ST *(H(2) = 4.82, p = 0.089)* or HIPP *(H(2) = 5.40, p = 0.067)* (Fig 3.3f, h). Post-hoc Dunn test revealed that there were fewer activated microglia detected by ImageJ compared to manual counting in the PFC *(13.18±6.31* vs *22.76±10.15, p = 0.036),* and more activated microglia detected by Halo compared to both ImageJ *(70.54±34.19* vs *20.6±7.5, p = <0.0001)* and manual counts *(70.54±34.19* vs *54.27±19.86, p = <0.001)* in the SN.

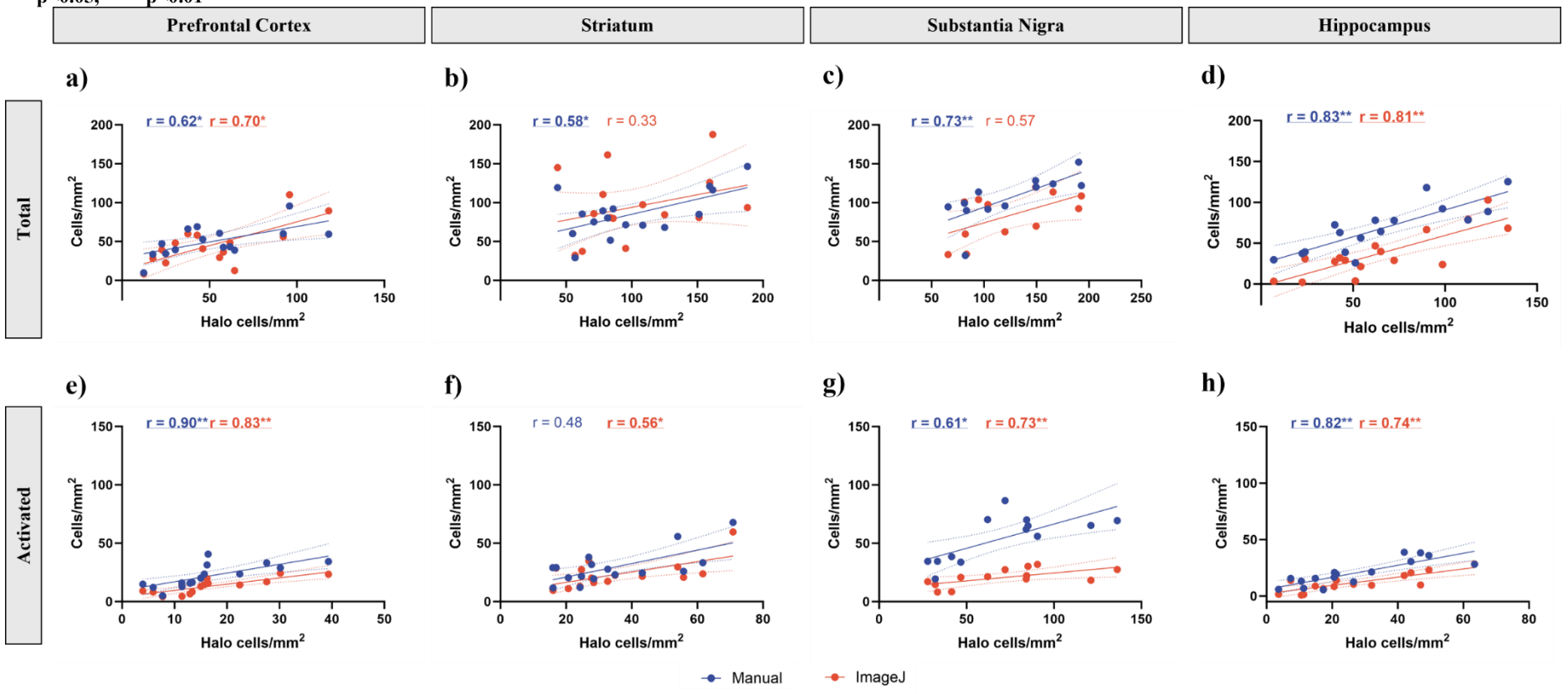
Figure 3.3 Microglial counts in human tissue.Microglia were quantitated in control and PD brain tissue across 4 ROIs by manual counting, ImageJ automated counting and Halo software. Microglia identified as a-d. Total, by IBAI positive staining; e-h. Activated, by IBAI positive and ameboid morphology. Individual values from controls (blue, n=5-6), and PD (red, n=8-10) were quantitated as described in materials and methods, with each dot point representing a single case. Mean±SEM are plotted and significant differences determined by Two-way ANOVA for parametric (A. Total), or Kruskal-Wallis for non-parametric data (B. Activated). * = p<0.05, *** = p<0.001, **** = p<0.0001



3.5.1.3 Significant correlations between total and activated microglia counts obtained using Halo and those obtained via other methods were detected in all regions for 5µm human tissue.

For both total and activated microglial counts, correlation analysis detected significant positive correlations between Halo and the other analysis methods across multiple brain regions. Total Halo counts were significantly correlated with manual counts in the PFC *(r = 0.62, n = 15, p = 0.014)*, ST *(r = 0.58, n = 16, p = 0.018)*, SN *(r = 0.73, n = 12, p = 0.007)*, and HIPP *(r = 0.83, n = 16, p = <0.001)* (Fig 3.4a-d), and with ImageJ counts in both the PFC *(r = 0.70, n = 15, p = 0.004)* and HIPP *(r = 0.81, n = 16, p = <0.001)* (Fig 3.4a, d), but not in the ST *(r = 0.33, n = 16, p = 0.21)* or SN *(r = 0.57, n = 12, p = 0.051)* (Fig 3.4b,c). Activated counts on Halo were significantly correlated with manual counts in the PFC *(r_s (13) = 0.90, p = <0.001)*, SN *(r_s (11) = 0.61, p = 0.027)* and HIPP *(r_s (14) = 0.82, p = <0.001)* (Fig 3.4e, g, h) but not the ST *(r_s (16) = 0.48, p = 0.058)* (Fig 3.4f), and with ImageJ counts in all brain regions analysed (PFC *(r_s (13) = 0.83, p = <0.001),* ST *(r_s (14) = 0.56, p = 0.024),* SN *(r_s (11) = 0.73, p = 0.005),* HIPP *(r_s (14) = 0.74, p = <0.001)*) (Fig 3.4 e-h).

Figure 3.4 Correlation of microglial counts with Halo in human tissue. Microglia were quantitated and identified as a-d. Total and e-h. Activated, as described in Fig 3.3. Individual values from both groups as quantitated by manual counting (blue) or ImageJ (red) were correlated with Halo counts and plotted, with each dot point representing a single case. Pearson r values (total counts) and Spearman r_s (non-parametric activated counts) are displayed. Halo showed significant correlations with manual counts in all regions, except activated counts in the ST, and with ImageJ in all regions, except total counts in the ST and SN. Significant correlations are bolded and underlined, with significance levels indicated, * = p<0.05, ** = p<0.01



3.5.2 Rat tissue:

3.5.2.1 Total microglia count differed with method in every brain region analysed in 20µm rat tissue.

Rat brain tissue was stained for IBA1 and both total and activated microglial number was analysed using manual, ImageJ and Halo counting methods. When total microglia counts in the ST were analysed using a two-way ANOVA, significant main effects of both method *(F(2,63) = 16.944, p = <0.001)* and group *(F(3,63) = 12.004, p = <0.001)* were detected, as well as an interaction between group and method *(F(6,63) = 2.997, p = 0.012).* Tukey post-hoc tests showed that ImageJ detected fewer microglia than both manual counting *(96.96±59.05* vs *123.49±23.41, p = 0.009)* and Halo *(96.96±59.05* vs *145±22.10, p = <0.001).* Additionally, Halo detected more microglia than manual counting *(145±22.10* vs *123.49±23.41, p = 0.039*). Post-hoc tests also identified significant differences between msTBI and sham *(155.22±37.42* vs *120.55±38.89, p = 0.006),* mTBI *(155.22±37.42* vs *106.1±35.18, p = <0.001),* and rmTBI *(155.22±37.42* vs *102.81±43.33, p = <0.001)* groups in the ST. The interaction effect of group and method suggested that there were differences between groups detected by one method and not another. Indeed, ImageJ detected more microglia in the msTBI group compared to the other groups, an effect that was undetectable by manual counting or using Halo.

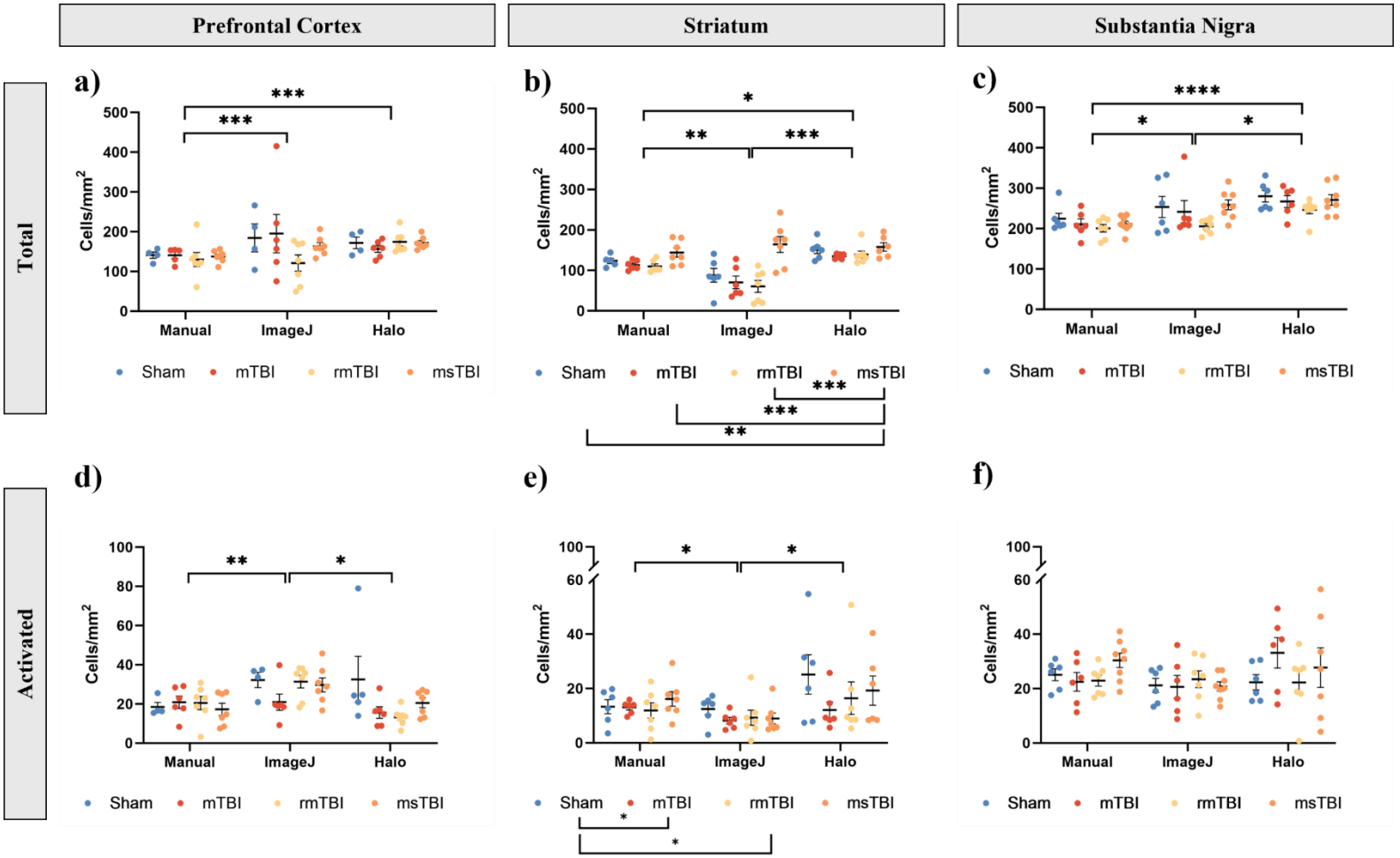
Conversely, Kruskal Wallis tests identified an effect of method in the PFC *(H(2) = 14.0, p = <0.001)* and SN *(H(2) = 20.2, p = <0.0001),* but no effects of group in either region (PFC *(H(3) = 1.49, p = 0.685),* SN *(H(3) = 7.32, p = 0.062).* Post-hoc Dunn tests identified that, in the PFC, manual counting identified fewer total microglia than both ImageJ (*136.48±15* vs *162.58±70.03, p* = 0.04) and Halo *(136.48±15* vs *168.21±23.12, p = <0.001)*. In the SN Halo detected more microglia than manual counting *(268.17±31.42* vs *208.42±22.09, p = <0.001)* and ImageJ *(268.17±31.42* vs *234.76±43.03, p = 0.032).* Additionally, ImageJ detected more microglia than manual counting *(234.76±43.03* vs *208.42±22.09, p = 0.032).*

3.5.2.2 Activated microglial count differed between methods in the PFC and ST of 20µm rat tissue.

When analysing activated microglial counts, significant main effects of method were seen in the PFC *(F(2,61) = 5.650, p = 0.006)* (Fig 3.3e), but not in the SN *(F(2,68) = 1.760, p = 0.18),* when analysed using a two-way ANOVA. In the PFC, ImageJ detected higher numbers of activated microglia than both manual counting *(28.41±9.61* vs *19.3±7.56, p = 0.008)* and Halo *(28.41±9.61* vs *19.37±13.85, p*

= 0.011). No significant interaction effects or main effects of group were identified in either the PFC *(*group*: F(3,61) = 1.838, p = 0.1;,* interaction:*(F(6,61) = 1.752, p = 0.124*) or SN (group: *F(3.68) = 0.673, p = 0.571;* interaction*: F(6,68) = 1.113, p = 0.364*). Within the striatum, main effects of both method *(H(2) = 8.65, p = 0.013)* and group *(H(3) = 9.84, p = 0.019)* were identified, with ImageJ detecting less activated microglia than both manual counting *(28.41±9.61* vs *19.37±13.85, p = 0.045)* and Halo *(28.41±9.61* vs *19.37±13.85, p = 0.018)*. Further, there were more activated microglia in shams compared to mTBI *(16.99±12.16 vs 9.94±5.79, p = 0.028)* and mTBI *(16.99±12.16* vs *11.11±4.95, p = 0.026).*

Figure 3.5 Microglial counts in rat tissue. Microglia were quantitated in Sham and TBI brain tissue across 3 ROIs by manual counting, ImageJ automated counting and Halo software. Microglia identified as a-c. Total, by IBAI positive staining; d-f. Activated, by IBAI positive and ameboid morphology. Individual values from Sham (blue, n=4-6), mTBI (red, n=5-6), rmTBI (yellow, n=6-7) and msTBI (orange, n=6-8) were quantitated as described in materials and methods, with each dot point representing a single case. Mean±SEM are plotted and significant differences determine by Two-way ANOVA for parametric (b total ST, d. activated PFC, f. activated SN), or Kruskal-Wallis for non-parametric data (a. total PFC, c. total SN, e. activated ST). * = p<0.05, *** = p<0.001, **** = p<0.0001

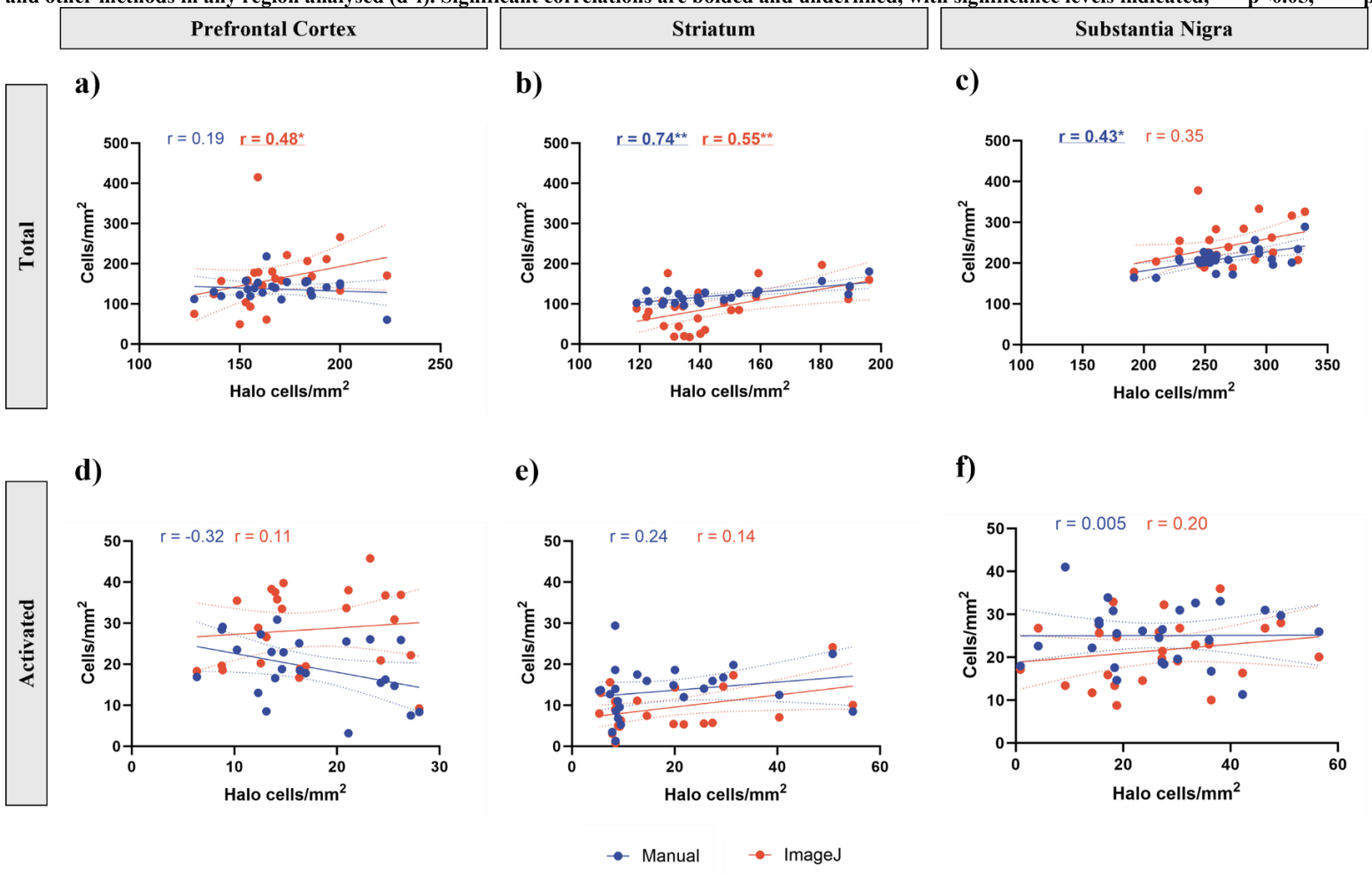


3.5.2.3 Significant correlations between total microglia counts on Halo and other methods were detected in all regions, but no correlations were detected between activated counts.

For total microglial counts in rat tisssue, correlation analysis detected significant positive correlations between Halo and other methods. Total Halo counts were significantly correlated with manual counts in the ST *($r = 0.74$, $n = 23$, $p = <0.001$)* and SN *($r_s(25) = 0.43$, $p = 0.026$)* (Fig 3.6b, c), but not in the PFC *($r_s(21) = 0.19$, $p = 0.387$)* (Fig 3.6a), and with ImageJ counts in the PFC *($r_s(22) = 0.48$, $p = 0.018$)* and ST *($r = 0.55$, $n = 25$, $p = 0.004$)* (Fig 3.6a,b), but not in the SN *($r_s(25) = 0.35$, $p = 0.070$)* (Fig 3.6c)

Of note, no correlations were observed between activated counts on Halo and manual counts (PFC *($r = -0.32$, $n = 24$, $p = 0.59$),* ST *($r_s(23) = 0.24$, $p = 0.248$)*, SN *($r = 0.005$, $n = 26$, $p = 0.979$)*) or between Halo and ImageJ counts (PFC *($r = 0.11$, $n = 24$, $p = 0.622$)*, ST *($r_s(23) = 0.14$, $p = 0.507$)*, SN *($r = 0.20$, $n = 26$, $p = 0.335$)*) in any region analysed (Fig 3.6d-f).

Figure 3.6 Correlation of microglial counts with Halo in rat tissue. Microglia were quantitated and identified as a-c. Total and d-f. Activated, as described in Figure 3.1. Individual values from all groups (n=24-26) as quantitated by manual counting (blue) or ImageJ (red) were correlated with Halo counts and plotted, with each dot point representing a single case. Pearson r values (b. total ST, d. activated PFC, f. activated SN), and Spearman r_s (a. total PFC, c. total SN, e. activated ST) are displayed. Total counts on Halo correlated significantly with manual counts in the b. ST and c. SN, and with ImageJ counts in the a. PFC and b. ST. No significant correlations were observed in activated counts between Halo and other methods in any region analysed (d-f). Significant correlations are bolded and underlined, with significance levels indicated, * = p<0.05, ** = p<0.01



3.6 Discussion

Accurate identification and classification of microglia is key in understanding how these cells contribute to brain health and disease. The commercially available Indica Labs Halo microglia analysis module presents an opportunity for researchers to automate this process, saving time and improving objectivity of results, including comparability across study sites. Since the development of the microglial analysis module, to date only eight publications have utilised it (Dinh et al., 2024; George et al., 2021; Guglietti et al., 2024; Kloske et al., 2023; Krieg et al., 2023; Kritzinger et al., 2018; Naseer et al., 2022; Smith et al., 2022). However, to the best of our knowledge, no validation of this module has yet been peer reviewed and published. The datasets utilised in this study have been utilised in previously published analyses (for human tissue analysis see (Guglietti et al., 2024), for rat tissue analysis see (Wee et al., 2024)), and thus discussion and interpretation of group differences are not included in the current manuscript. This research aimed to examine the ability of the Halo microglia module to identify and classify $IBA1^+$ microglia in IHC stained tissue across different species and regions of the brain, in both healthy and diseased states. Manual analysis is the most commonly employed method when it comes to assessing microglial number and morphology (Gallego and de Gracia, 2016) though several studies have acknowledged its limitations (Chan et al., 2023; de Gracia et al., 2015; Gallego and de Gracia, 2016; Horai et al., 2019). Thus, here manual analysis was employed as the benchmark positive standard against which we assessed the accuracy of the Halo microglial activation module, relative to an additional widely available automated counting method on ImageJ. Here, we demonstrate that Halo, despite showing high variability in the detection of activated microglia, is largely comparable to both manual counting and automated batch analysis using ImageJ.

Table 3.5: Summary of correlation analysis. Green = strong correlation (r>0.6, p<0.05); yellow = moderate correlation (r 0.3-0.6, p>0.05); red = no significant correlation (r<0.3 or p>0.05)

	Human tissue				Rat tissue		
	PFC	ST	SN	HIPP	PFC	ST	SN
Manual vs Halo							
Total							
Activated							
Image J vs Halo							
Total							
Activated							

In 5µm sectioned human post-mortem tissue, there were minimal differences between Halo and other quantitation methods (Table 3.5). Of note, in the ST of human tissue, Halo correlated only moderately with both total manual counts and activated ImageJ counts and showed no significant correlation with either activated manual or total ImageJ counts. This may be reflective of the fact that areas of high microglial density, such as the striatum (Keller et al., 2018), present additional challenges when classifying microglia as the overlapping cell bodies and processes makes image segmentation by automated methods difficult. Microglia counts obtained in the present study are notably lower than those reported in previous studies. In rodent brains, prior research has estimated microglial densities of around 400-600 microglia/mm^2 in the mouse SN (George et al., 2021; Shaerzadeh et al., 2020). Whereas here, we report 100-300 microglia/mm^2 depending on the group and method utilised. However, in human tissue, previous studies have reported microglial densities in the SN ranging from <50-200 microglia/mm^2 (Kouli et al., 2020), and here we observed similar values of 50-200 microglia/mm^2. This discrepancy in the rat tissue compared to other rodents may be attributed to species differences, variations in tissue preparation, or differences in methodologies. However, as this lower microglia density was observed consistently across all methods used in our study, it does not impact the comparative outcomes. Instead, the observed differences may reflect technical factors such as user variability, differences in section thickness, staining, or image analysis parameters when compared to prior studies. Additionally, the different methods may produce less agreement due to the differing ways

in which they classify microglia, with regions of high density or highly variable microglial morphology further exacerbating these effects.

Conversely, while strong correlations between Halo and both manual counts and ImageJ counts were seen within the 5µm sectioned human post-mortem tissue, this same pattern was not observed for the 20µm sectioned rat tissue. In fact, in this dataset, significant differences between methods in raw counts for both total and activated microglia were detected in every region analysed, except for between activated counts in the SN. Notably, correlations between Halo and other methods were particularly weak for activated microglia, with no significant correlations noted in any of the three brain regions analysed in rat tissue. Taken together, these findings suggest that the Halo module may be optimised for thinner tissue and significant adjustments might need to be made when inputting parameters for thicker or z-stacked tissue sections. Given that the focus of Indica Labs, the maker of the Halo system, is to provide clinical pathology tools, one of which recently received FDA clearance for primary diagnosis in the USA ((FDA), 2024), it is perhaps unsurprising that the system should be optimised for thinner tissue sections of around 4-5µm, the recommended thickness for pathology sections (Lott et al., 2015).

In comparison to manual counting, the batch automated thresholding approach conducted in ImageJ presented with similar discrepancies, consistently underestimating numbers of total and activated microglia. Where manually a researcher can delineate positive staining as a cell, in ImageJ, nuances in staining intensity mean the blanket thresholding parameters will likely cause the program to either miss particles or count processes as whole cells, as thresholding is an incredibly sensitive process (Hemel et al., 2021). Both automated methods struggled to account for the added depth within the rat images, necessitating adjustments to parameters, in order to handle overlapping cells and elongated processes. Precise adjustments of parameters are therefore needed to account for optical aberrations in thick tissue sections as the finer cell details blur with increasing depth (Ji et al., 2012). Existing literature has shown microglial analysis in full photomicrographs is unable to detect morphological changes that were

observed at a single cell level (Green et al., 2022), suggesting that noise from background cells may have an impact on the overall results from these images. This suggests that, in the case of thicker tissue where optical aberrations make thresholding difficult, single cell analysis of microglial morphology may be a more appropriate method of analysis. To account for the different depths of tissue sections which can alter signal strength especially when processes are thinner or more distant from the focal plane, setting a specific OD for processes allows Halo to determine whether detections are classed as a process, or a cell body. Although this becomes difficult in thicker sections where the signal is highly varied, in thinner tissue sections this parameter is useful in overcoming background signal alterations. These challenges with thicker tissue suggest that when using automated methods additional adjustments to parameters must be made.

While ImageJ and Halo appear to be comparable in terms of performance, the goal of automation is not only to ensure the reliability of the quantitation but should also benefit workflow. A recent review on different methods to analyse microglial morphology highlighted the limited number of studies currently using automated high throughput methods, and, additionally, outlined the need to provide a simple, automated process, with a friendly user interface (Reddaway et al., 2023). In this regard, Halo offers a few advantages over ImageJ in terms of the workflow. For the ImageJ analysis conducted here, workflow involved scanned slides, processed into tiles using a third-party program, which then underwent a manual exclusion process for artefacts. This is a very time-consuming process for large datasets. Further, the macro used for quantitation is a counting protocol and to count both total cells and activated cells, the protocol must be applied to each image twice: once without any parameters for circularity (total microglia), and once with a circularity parameter set (activated microglia). Subsequently, there is additional work in processing the outputs from ImageJ counting, which take the form of an individual .csv file for each case, requiring significant time to compile results into a workable document to perform statistics. Conversely, use of the Halo microglial module involves uploading of images directly to the program, where the researcher then draws inclusion and exclusion zones on each image, sets parameters for microglial detection and applies the program to the full image set. When the program is first utilised, there is some optimisation of parameters required; however, overall, this

process is far more streamlined than ImageJ analysis. Halo identifies activated and non-activated cells simultaneously, eliminating the need to run the module multiple times and thus, analysis on Halo is far less time consuming and complex than analysis using ImageJ for batch analysis. Similarly, the workflow benefits of using Halo compared to manual counting, a laborious and time-consuming undertaking, are clear. In Halo, in addition to the built-in outputs of average cell measurements across the whole tissue section, there is the function to save individual object measurements, allowing bulk analysis of single cell data, that would otherwise be time consuming to analyse using ImageJ. This feature makes Halo a useful tool in more advanced automated microglial analysis (Green et al., 2022). For example, one study utilising the Halo microglial activation module in 12-week-old C57BL/6J mice undergoing a stereotactic injection of human preformed α-synuclein fibrils, researchers chose to report only the total cell count/mm^2, and the area:perimeter index to indicate activated microglia, forgoing the activated count provided by the Halo microglial activation module (George et al., 2021). This reporting of more detailed morphological analysis is in line with the current direction of the literature, where assigning microglia to either activated or resting is not considered to be reflective of the full picture of microglial phenotypes in tissue (Lier et al., 2021; Reddaway et al., 2023; Torres-Platas et al., 2014). Although a full discussion of microglial phenotypes is beyond the scope of the current paper, it is now well understood that microglial activation is a spectrum and different morphological phenotypes of microglia reflect different functional states during ageing, disease, and injury (for reviews see: (Reddaway et al., 2023; Vidal-Itriago et al., 2022)). ImageJ analysis is unable to conduct this kind of morphological analysis in an automated fashion. Rather, in order to conduct this analysis within ImageJ, isolation and analysis of single cells is needed, rather than assessing these features at a population level (Green et al., 2022). However, single cell morphological analysis of microglia is time consuming and falls victim to the same difficulties at the thresholding stages, where incorrectly thresholded images can lead to inaccurate measurement of cells (Young and Morrison, 2018).

Given the strong correlations shown here of Halo with manual counting for both total and activated microglia, particularly for 5µm tissue, the Halo module represents a significant contribution to the field. AI-driven approaches are increasingly integrated into modern image analysis platforms and offer

powerful tools for segmentation, classification and quantification of cellular features (Möhle et al., 2021). Although, not utilised in the current study, Halo software now integrates AI and deep-learning networks into specific licenses, increasing the usefulness of the software for automated analysis of microglia. However, cost-benefit also needs to be considered. The Halo module as a method of analysis has a high cost of purchase and on-going licencing maintenance costs, which can be significant over the life of the machine. Nevertheless, for laboratories where microglial staining and analysis are conducted on a regular basis, institutions where central facilities can offer specialised services, or research studies where fine delineation of microglial numbers and activation state are of primary interest, then the beneficial outputs and workflow likely outweigh the cost for the Halo module.

3.7 Conclusions

This study presents, to our knowledge, the first standardised evaluation of the Halo microglial activation module compared to other methods of microglial analysis. Compared to manual assessments which are time consuming and subjective, and automated analysis on ImageJ, which is limited by sensitivity of thresholding parameters, the Halo platform provides an automated high throughput method to analyse microglia in a time and user-friendly manner. The Halo output provides researchers with the ability to both quantify microglial morphology on larger sections and gain a detailed understanding of morphological characteristics of a microglial population. However, as the field moves towards characterisation of microglia using thicker tissue to visualise morphology, it is of critical importance that the imaging of these sections be correctly adjusted to reduce loss of resolution and the analysis of these sections be optimised for accuracy. Currently, using Halo to analyse these sections requires extensive optimisation and tailored parameters to combat staining variability and imaging artifacts. Despite these challenges, the value of automated tools to better improve our knowledge of microglia, such as Halo, cannot be understated and the benefits of further developing these tools will allow for advancements in the overall understanding of microglia in neurological diseases.

3.8 Acknowledgements

The authors would like to thank Dr Rebecca Ormsby and the South Australian Brain Bank for preparing and providing the post-mortem tissue used in the current study

3.9 Declarations

3.9.1 Ethics

Human tissue collection and subsequent analyses were carried out in accordance with the National Statement on Ethical Conduct in Human Research (2018) and approved by the University of Adelaide Human Research Ethics Committee (H-2016-174). All experimental procedures associated with the collection of rat tissue were approved by the University of Adelaide Animal Ethics Committee (S-2019-019) and were conducted in accordance with the Australian Code for the Care and Use of Animals for Scientific Purposes, 8th Edition, 2013 guidelines.

3.9.2 Funding

LC, BG and ICW were supported by Australian Government Research Training Program Scholarships provided by the Department of Education and Training, Canberra, Australia. This work was supported by grants to LCP from the Commercial Acceleration Scheme by Adelade Enterprise at the University of Adelaide, Adelaide Australia as well as to LCP and FC by the Neurosurgical Research Foundation, Australia.

3.9.3 Competing interests

The authors declare that they have no known conflicts of interest

1

3.10 References

(FDA), U.S.F.a.D.A., 2024. FDA 510(k) Clearance for Whole Slide Imaging System (K232833).

Arganda-Carreras, I., Fernández-González, R., Muñoz-Barrutia, A., Ortiz-De-Solorzano, C., 2010. 3D reconstruction of histological sections: Application to mammary gland tissue. Microscopy Research and Technique 73, 1019-1029.

Arshadi, C., Günther, U., Eddison, M., Harrington, K.I.S., Ferreira, T.A., 2021. SNT: a unifying toolbox for quantification of neuronal anatomy. Nature Methods 18, 374-377.

Bankhead, P., Loughrey, M.B., Fernández, J.A., Dombrowski, Y., McArt, D.G., Dunne, P.D., McQuaid, S., Gray, R.T., Murray, L.J., Coleman, H.G., James, J.A., Salto-Tellez, M., Hamilton, P.W., 2017. QuPath: Open source software for digital pathology image analysis. Scientific Reports 7, 16878.

Bido, S., Muggeo, S., Massimino, L., Marzi, M.J., Giannelli, S.G., Melacini, E., Nannoni, M., Gambarè, D., Bellini, E., Ordazzo, G., Rossi, G., Maffezzini, C., Iannelli, A., Luoni, M., Bacigaluppi, M., Gregori, S., Nicassio, F., Broccoli, V., 2021. Microglia-specific overexpression of α-synuclein leads to severe dopaminergic neurodegeneration by phagocytic exhaustion and oxidative toxicity. Nature Communications 12, 6237.

Brown, D.L., 2017. Bias in image analysis and its solution: unbiased stereology. J Toxicol Pathol 30, 183-191.

Chan, N.R., Hwang, B., Waworuntu, R.L., Tran, A.J., Ratner, B.D., Bryers, J.D., 2023. Novel HALO® image analysis to determine cell phenotype in porous precision-templated scaffolds. Journal of Biomedical Materials Research Part A 111, 1459-1467.

Collins, L.M., Toulouse, A., Connor, T.J., Nolan, Y.M., 2012. Contributions of central and systemic inflammation to the pathophysiology of Parkinson's disease. Neuropharmacology 62, 2154-2168.

Dalgaard, P., 2010. R Development Core Team (2010): R: A language and environment for statistical computing.

Davalos, D., Grutzendler, J., Yang, G., Kim, J.V., Zuo, Y., Jung, S., Littman, D.R., Dustin, M.L., Gan, W.-B., 2005. ATP mediates rapid microglial response to local brain injury in vivo. Nature Neuroscience 8, 752-758.

de Gracia, P., Gallego, B.I., Rojas, B., Ramírez, A.I., de Hoz, R., Salazar, J.J., Triviño, A., Ramírez, J.M., 2015. Automatic Counting of Microglial Cells in Healthy and Glaucomatous Mouse Retinas. PLoS One 10, e0143278.

Dinh, D.D., Wan, H., Lidington, D., Bolz, S.-S., 2024. Female mice display sex-specific differences in cerebrovascular function and subarachnoid haemorrhage-induced injury. eBioMedicine 102.

Donat, C.K., Scott, G., Gentleman, S.M., Sastre, M., 2017. Microglial Activation in Traumatic Brain Injury. Front Aging Neurosci 9, 208.

Fernández-Arjona, M.d.M., Grondona, J.M., Granados-Durán, P., Fernández-Llebrez, P., López-Ávalos, M.D., 2017. Microglia Morphological Categorization in a Rat Model of Neuroinflammation by Hierarchical Cluster and Principal Components Analysis. Frontiers in Cellular Neuroscience 11, 235.

Gallego, B.I., de Gracia, P., 2016. Automatic counting of microglial cell activation and its applications. Neural Regen Res 11, 1212-1215.

Gao, C., Jiang, J., Tan, Y., Chen, S., 2023. Microglia in neurodegenerative diseases: mechanism and potential therapeutic targets. Signal Transduction and Targeted Therapy 8, 359.

George, S., Tyson, T., Rey, N.L., Sheridan, R., Peelaerts, W., Becker, K., Schulz, E., Meyerdirk, L., Burmeister, A.R., von Linstow, C.U., Steiner, J.A., Galvis, M.L.E., Ma, J., Pospisilik, J.A., Labrie, V.,

Brundin, L., Brundin, P., 2021. T Cells Limit Accumulation of Aggregate Pathology Following Intrastriatal Injection of α-Synuclein Fibrils. J Parkinsons Dis 11, 585-603.

Gioia, U., Tavella, S., Martínez-Orellana, P., Cicio, G., Colliva, A., Ceccon, M., Cabrini, M., Henriques, A.C., Fumagalli, V., Paldino, A., Presot, E., Rajasekharan, S., Iacomino, N., Pisati, F., Matti, V., Sepe, S., Conte, M.I., Barozzi, S., Lavagnino, Z., Carletti, T., Volpe, M.C., Cavalcante, P., Iannacone, M., Rampazzo, C., Bussani, R., Tripodo, C., Zacchigna, S., Marcello, A., d'Adda di Fagagna, F., 2023. SARS-CoV-2 infection induces DNA damage, through CHK1 degradation and impaired 53BP1 recruitment, and cellular senescence. Nature Cell Biology 25, 550-564.

Green, T.R.F., Murphy, S.M., Rowe, R.K., 2022. Comparisons of quantitative approaches for assessing microglial morphology reveal inconsistencies, ecological fallacy, and a need for standardization. Sci Rep 12, 18196.

Guglietti, B., Mustafa, S., Corrigan, F., Collins-Praino, L.E., 2024. Anatomical distribution of Fyn kinase in the human brain in Parkinson's disease. Parkinsonism & Related Disorders 118.

Hemel, I.M.G.M., Engelen, B.P.H., Luber, N., Gerards, M., 2021. A hitchhiker's guide to mitochondrial quantification. Mitochondrion 59, 216-224.

Hope, K.T., Hawes, I.A., Moca, E.N., Bonci, A., De Biase, L.M., 2020. Maturation of the microglial population varies across mesolimbic nuclei. European Journal of Neuroscience 52, 3689-3709.

Horai, Y., Mizukawa, M., Nishina, H., Nishikawa, S., Ono, Y., Takemoto, K., Baba, N., 2019. Quantification of histopathological findings using a novel image analysis platform. J Toxicol Pathol 32, 319-327.

Indica Labs, I., 2024. HALO Microglial Activation Module.

Ishikawa, T., Takahashi, J., Kasai, M., Shiina, T., Iijima, Y., Takemura, H., Mizoguchi, H., Kuwata, T., 2015. Support system for pathologists and researchers. J Pathol Inform 6, 34.

Ji, N., Sato, T.R., Betzig, E., 2012. Characterization and adaptive optical correction of aberrations during in vivo imaging in the mouse cortex. Proceedings of the National Academy of Sciences 109, 22-27.

Jimenez-Ferrer, I., Bäckström, F., Dueñas-Rey, A., Jewett, M., Boza-Serrano, A., Luk, K.C., Deierborg, T., Swanberg, M., 2021. The MHC class II transactivator modulates seeded alpha-synuclein pathology and dopaminergic neurodegeneration in an in vivo rat model of Parkinson's disease. Brain, Behavior, and Immunity 91, 369-382.

Jurga, A.M., Paleczna, M., Kuter, K.Z., 2020. Overview of General and Discriminating Markers of Differential Microglia Phenotypes. Front Cell Neurosci 14, 198.

Kayagaki, N., Stowe, I.B., Alegre, K., Deshpande, I., Wu, S., Lin, Z., Kornfeld, O.S., Lee, B.L., Zhang, J., Liu, J., Suto, E., Lee, W.P., Schneider, K., Lin, W., Seshasayee, D., Bhangale, T., Chalouni, C., Johnson, M.C., Joshi, P., Mossemann, J., Zhao, S., Ali, D., Goldenberg, N.M., Sayed, B.A., Steinberg, B.E., Newton, K., Webster, J.D., Kelly, R.L., Dixit, V.M., 2023. Inhibiting membrane rupture with NINJ1 antibodies limits tissue injury. Nature 618, 1072-1077.

Keller, D., Erö, C., Markram, H., 2018. Cell Densities in the Mouse Brain: A Systematic Review. Frontiers in Neuroanatomy 12.

Kettenmann, H., Hanisch, U.-K., Noda, M., Verkhratsky, A., 2011. Physiology of Microglia. Physiological Reviews 91, 461-553.

Klemm, A., Miura, K., 2022. Batch Processing Methods in ImageJ. In: Miura, K., Sladoje, N. (Eds.), Bioimage Data Analysis Workflows – Advanced Components and Methods. Springer International Publishing, Cham, pp. 7-27.

Kloske, C.M., Gearon, M.D., Weekman, E.M., Rogers, C., Patel, E., Bachstetter, A., Nelson, P.T., Wilcock, D.M., 2023. Association between APOE genotype and microglial cell morphology. Journal of Neuropathology & Experimental Neurology 82, 620-630.

Kouli, A., Camacho, M., Allinson, K., Williams-Gray, C.H., 2020. Neuroinflammation and protein pathology in Parkinson's disease dementia. Acta Neuropathologica Communications 8, 211.

Krieg, J.L., Leonard, A.V., Tuner, R.J., Corrigan, F., 2023. Characterization of Traumatic Brain Injury in a Gyrencephalic Ferret Model Using the Novel Closed Head Injury Model of Engineered Rotational Acceleration (CHIMERA). Neurotrauma Reports 4, 761-780.

Kritzinger, A., Ferger, B., Gillardon, F., Stierstorfer, B., Birk, G., Kochanek, S., Ciossek, T., 2018. Age-related pathology after adenoviral overexpression of the leucine-rich repeat kinase 2 in the mouse striatum. Neurobiology of Aging 66, 97-111.

Leng, F., Edison, P., 2021. Neuroinflammation and microglial activation in Alzheimer disease: where do we go from here? Nature Reviews Neurology 17, 157-172.

Lier, J., Streit, W.J., Bechmann, I., 2021. Beyond Activation: Characterizing Microglial Functional Phenotypes. Cells 10.

Lott, R., Tunncliffe, J., Sheppard, E., Santiago, J., Hladik, C., Nasim, M., Zeitner, K., Haas, T., Kohl, S., Movahedi-Lankarani, S., 2015. practical guide to specimen handling in surgical pathology. College of American Pathologists, Northfield, IL.

Marmarou, A., Foda, M.A., van den Brink, W., Campbell, J., Kita, H., Demetriadou, K., 1994. A new model of diffuse brain injury in rats. Part I: Pathophysiology and biomechanics. J Neurosurg 80, 291-300.

Moehle, M.S., West, A.B., 2015. M1 and M2 immune activation in Parkinson's Disease: Foe and ally? Neuroscience 302, 59-73.

Möhle, L., Bascuñana, P., Brackhan, M., Pahnke, J., 2021. Development of deep learning models for microglia analyses in brain tissue using DeePathology™ STUDIO. Journal of Neuroscience Methods 364, 109371.

Motulsky, H.J., Brown, R.E., 2006. Detecting outliers when fitting data with nonlinear regression – a new method based on robust nonlinear regression and the false discovery rate. BMC Bioinformatics 7, 123.

Naseer, S., Abelleira-Hervas, L., Savani, D., de Burgh, R., Aleksynas, R., Donat, C.K., Syed, N., Sastre, M., 2022. Traumatic Brain Injury Leads to Alterations in Contusional Cortical miRNAs Involved in Dementia. Biomolecules.

Nimmerjahn, A., Kirchhoff, F., Helmchen, F., 2005. Resting Microglial Cells Are Highly Dynamic Surveillants of Brain Parenchyma in Vivo. Science 308, 1314-1318.

Paxinos, G., Watson, C., 2007. The Rat Brain in Stereotaxic Coordinates. Elsevier.

Prinz, M., Priller, J., 2017. The role of peripheral immune cells in the CNS in steady state and disease. Nature Neuroscience 20, 136-144.

Ransohoff, R.M., Brown, M.A., 2012. Innate immunity in the central nervous system. J Clin Invest 122, 1164-1171.

Reddaway, J., Richardson, P.E., Bevan, R.J., Stoneman, J., Palombo, M., 2023. Microglial morphometric analysis: so many options, so little consistency. Frontiers in Neuroinformatics 17.

Ritzel, R.M., Li, Y., Jiao, Y., Lei, Z., Doran, S.J., He, J., Shahror, R.A., Henry, R.J., Khan, R., Tan, C., Liu, S., Stoica, B.A., Faden, A.I., Szeto, G., Loane, D.J., Wu, J., 2023. Brain injury accelerates the onset

of a reversible age-related microglial phenotype associated with inflammatory neurodegeneration. Sci Adv 9, eadd1101.

Ruifrok, A.C., Johnston, D.A., 2001. Quantification of histochemical staining by color deconvolution. Anal Quant Cytol Histol 23, 291-299.

Schneider, C.A., Rasband, W.S., Eliceiri, K.W., 2012. NIH Image to ImageJ: 25 years of image analysis. Nature Methods 9, 671-675.

Schroeder, A.B., Dobson, E.T.A., Rueden, C.T., Tomancak, P., Jug, F., Eliceiri, K.W., 2021. The ImageJ ecosystem: Open-source software for image visualization, processing, and analysis. Protein Sci 30, 234-249.

Shaerzadeh, F., Phan, L., Miller, D., Dacquel, M., Hachmeister, W., Hansen, C., Bechtle, A., Tu, D., Martcheva, M., Foster, T.C., Kumar, A., Streit, W.J., Khoshbouei, H., 2020. Microglia senescence occurs in both substantia nigra and ventral tegmental area. Glia 68, 2228-2245.

Smith, A.M., Davey, K., Tsartsalis, S., Khozoie, C., Fancy, N., Tang, S.S., Liaptsi, E., Weinert, M., McGarry, A., Muirhead, R.C.J., Gentleman, S., Owen, D.R., Matthews, P.M., 2022. Diverse human astrocyte and microglial transcriptional responses to Alzheimer's pathology. Acta Neuropathologica 143, 75-91.

Tajima, R., Kato, Y., 2011. Comparison of threshold algorithms for automatic image processing of rice roots using freeware ImageJ. Field Crops Research 121, 460-463.

Torres-Platas, S.G., Comeau, S., Rachalski, A., Bo, G.D., Cruceanu, C., Turecki, G., Giros, B., Mechawar, N., 2014. Morphometric characterization of microglial phenotypes in human cerebral cortex. J Neuroinflammation 11, 12.

Uff, C.E.G., Patel, K., Yeung, C., Yip, P.K., 2022. Advances in Visualizing Microglial Cells in Human Central Nervous System Tissue. Biomolecules 12.

van Furth, R., Cohn, Z.A., 1968. The origin and kinetics of mononuclear phagocytes. J Exp Med 128, 415-435.

Vidal-Itriago, A., Radford, R.A.W., Aramideh, J.A., Maurel, C., Scherer, N.M., Don, E.K., Lee, A., Chung, R.S., Graeber, M.B., Morsch, M., 2022. Microglia morphophysiological diversity and its implications for the CNS. Front Immunol 13, 997786.

Vore, A.S., Barney, T.M., Deak, M.M., Varlinskaya, E.I., Deak, T., 2022. Adolescent intermittent ethanol exposure produces Sex-Specific changes in BBB Permeability: A potential role for VEGFA. Brain, Behavior, and Immunity 102, 209-223.

Wee, I.C., Arulsamy, A., Corrigan, F., Collins-Praino, L., 2024. Long-Term Impact of Diffuse Traumatic Brain Injury on Neuroinflammation and Catecholaminergic Signaling: Potential Relevance for Parkinson's Disease Risk. Molecules.

Young, K., Morrison, H., 2018. Quantifying Microglia Morphology from Photomicrographs of Immunohistochemistry Prepared Tissue Using ImageJ. J Vis Exp.

Yurt, K.K., Kivrak, E.G., Altun, G., Mohamed, H., Ali, F., Gasmalla, H.E., Kaplan, S., 2018. A brief update on physical and optical disector applications and sectioning-staining methods in neuroscience. Journal of Chemical Neuroanatomy 93, 16-29.

Zhang, R., Yang, Y., Hu, C., Huang, M., Cen, W., Ling, D., Long, Y., Yang, X.-H., Xu, B., Peng, J., Wang, S., Zhu, W., Wei, M., Yang, J., Xu, Y., Zhang, X., Ma, J., Wang, F., Zhang, H., Ma, P., Zhu, X., Song, G., Sun, L.-Y., Wang, D.-S., Wang, F.-H., Li, Y.-H., Santagata, S., Li, Q., Feng, Y.-F., Du, Z., 2023. Comprehensive analysis reveals potential therapeutic targets and an integrated risk stratification model for solitary fibrous tumors. Nature Communications 14, 7479.

Zhang, S., 2019. Microglial activation after ischaemic stroke. Stroke and Vascular Neurology 4, 71.

3.11 Supporting Information

Comparison of Automated and Manual Approaches for Microglial Quantification and Classification: A Focus on The Halo Digital Pathology Platform

Laura Carr[1], Bianca Guglietti[1], Ing Chee Wee[1], Ian Musgrave[1], Sanam Mustafa[1,2,3], Frances Corrigan[1], Lyndsey E Collins-Praino[1,2]

[1]School of Biomedicine, University of Adelaide, Adelaide, Australia

[2]Australian Research Council Centre of Excellence for Nanoscale Biophotonics, The University of Adelaide, Adelaide, SA, Australia

[3]Davies Livestock Research Centre, The University of Adelaide, Roseworthy, SA, Australia

A/Professor Lyndsey Collins-Praino

Email: Lyndsey.collins-praino@adelaide.edu.au

This document includes

Tables S3.1-S3.3

Supplementary Methods

Figures S3.1-S3.4

Supplementary Table S3.1 Clinicopathological data for human control and PD cases. Male:Female ratios are presented. Values presented as: range (mean±SEM). Pathological findings required for inclusion/exclusion in each group are listed

	Sex	Age (years)	Post-mortem interval (hours)	Years since diagnosis	Inclusion pathology	Notes
Control	3M:3F	61-86 (71.33 ± 3.56)	6-48 (22.43 ± 6.69)	N/A	No clinical history of PD/AD No evidence of neurological pathology post-mortem	
Parkinson's disease	5M:5F	73-88 (78.2 ± 1.63)	3-28 (14.61 ± 2.61)	3-16 (6 ± 2.53) *	Clinical PD diagnosis Post-mortem PD diagnosis No other neurological conditions present	*Years since diagnosis only available for 5/10 of cases

Supplementary Table S3.2 Summary of areas included in manual analysis and results per box for human tissue dataset. SNpc = Substantia Nigra *Pars Compacta*, SNpr = Substantia Nigra *Pars Reticulata.*

Human Dataset												
	PFC			ST			SN			HIPP		
	Sub regions	# of boxes per animal	Average # of microglia per box	Sub regions	# of boxes per animal	Average # of microglia per box	Sub regions	# of boxes per animal	Average # of microglia per box	Sub regions	# of boxes per animal	Average # of microglia per box
Control	Unknown	6	126.87	Caudate nucleus Putamen	6	187.1	SNpc, SNpr	6	313.77	Dentate gyrus CA1 CA2 CA3	6	149.10
PD		6	153.02		6	255.08		6	372.07		6	194.37

Supplementary Table S3.3 Summary of areas included in manual analysis and results per image for rat tissue dataset. SNpc = Substantia Nigra *Pars Compacta*, SNpr = Substantia *Nigra Pars Reticulata.*

Rat Dataset									
	PFC			ST			SN		
	Sub regions	# of images per animal	Average # of microglia per image	Sub regions	# of images per animal	Average # of microglia per image	Sub regions	# of images per animal	Average # of microglia per image
Sham	Prelimbic area Anterior cingulate area Infralimbic area	6	56.07	Caudoputamen	1-8	52.66	SNpc SNpr	5-6	89.34
mTBI		3-6	86.16		5-8	53.43		6	91.72
rmTBI		3-6	59.53		1-8	49.71		6	79.69
msTBI		3-6	62.05		3-10	55.49		6	84.04

Supplementary methods

1. Rat experimental groups and surgical/injury procedures

Experimental groups

Animals were randomly allocated to one of four experimental groups: (1) sham surgery, (2) a single mild TBI (mTBI), (3) repetitive mild TBI (rmTBI) or (4) moderate-severe TBI (msTBI). Sham animals received procedures identical to those of their experimental counterparts to account for anaesthesia and analgesia exposure, e.g. repetitive sham animals underwent the surgical incision three times, with 5-day intervals between each incision. 12 months following the final TBI or sham surgery, animals were transcardially perfused with 0.2mL heparin + 10% formalin and brains were taken for immunohistochemical analysis

Injury protocol

Injury procedures were performed using the Marmarou impact-acceleration injury method. Briefly, a 450kg weight was released from 2m (msTBI) or 0.75m (mTBI, rmTBI) onto a metal disc fixed centrally to the skull of the animal. To ensure a single direct hit with no rebound hits, the impact was carefully monitored. A single impact was given to the mTBI and msTBI animals, while rmTBI animals received three hits. 5-day intervals were adhered to between each hit in order to allow for sufficient recovery time between injury events providing greater relevance for clinical scenarios.

msTBI animals were additionally exposed to 10 minutes of hypoxic conditions (2L/min nitrogen;0.2L/min oxygen) to better mimic the clinic effects of severe head trauma. All remaining groups were kept under normoxic ventilation via nose cone after injury.

2. Tile export macro used in QuPath

```
// SCRIPT TO EXPORT IMAGE TILES (CAN BE CUSTOMISED IN VARIOUS WAYS)


// Get the current image (supports 'Run for project')
def imageData = getCurrentImageData()


// Define output path (here, relative to project)
def name =
GeneralTools.getNameWithoutExtension(imageData.getServer().getMetadata().getName())
def pathOutput = buildFilePath(PROJECT_BASE_DIR, 'TILES_IBA1_ST', name)
mkdirs(pathOutput)


// Define output resolution in calibrated units (e.g. µm if available)
double requestedPixelSize = 5.0


// Convert output resolution to a downsample factor
```

```
double pixelSize = imageData.getServer().getPixelCalibration().getAveragedPixelSize()
double downsample = requestedPixelSize / pixelSize

// Create an exporter that requests corresponding tiles from the original & labelled image servers
new TileExporter(imageData)
    .downsample(3)   // Define export resolution
    .imageExtension('.jpg')   // Define file extension for original pixels (often .tif, .jpg, '.png' or '.ome.tif')
    .tileSize(1920,1088)            // Define size of each tile, in pixels
    .annotatedTilesOnly(true) // If true, only export tiles if there is a (classified) annotation present
    .overlap(0)              // Define overlap, in pixel units at the export resolution
    .writeTiles(pathOutput)   // Write tiles to the specified directory

print 'Done!'
```

3. Macro used for automated microglial analysis on ImageJ

Highlighted parameters were optimised for datasets as in table 3.4.

```
//NAME MACRO-change name as required
macro "Automated-Particle-Analysis" {

//CHOOSE INPUT AND OUTPUT FOLDERS
inputFolder = getDirectory("Choose input folder ");
outputFolder = getDirectory("Choose output folder for images and results ");

//RUN BATCH MODE
list = getFileList(inputFolder);
setBatchMode(true);
for (i=0; i<list.length; i++) {
showProgress(i+1, list.length);
open(inputFolder+list[i]);

//DUPLICATE ORIGINAL IMAGE
imgName=getTitle();
run("Duplicate...", imgName);
selectWindow(imgName);
```

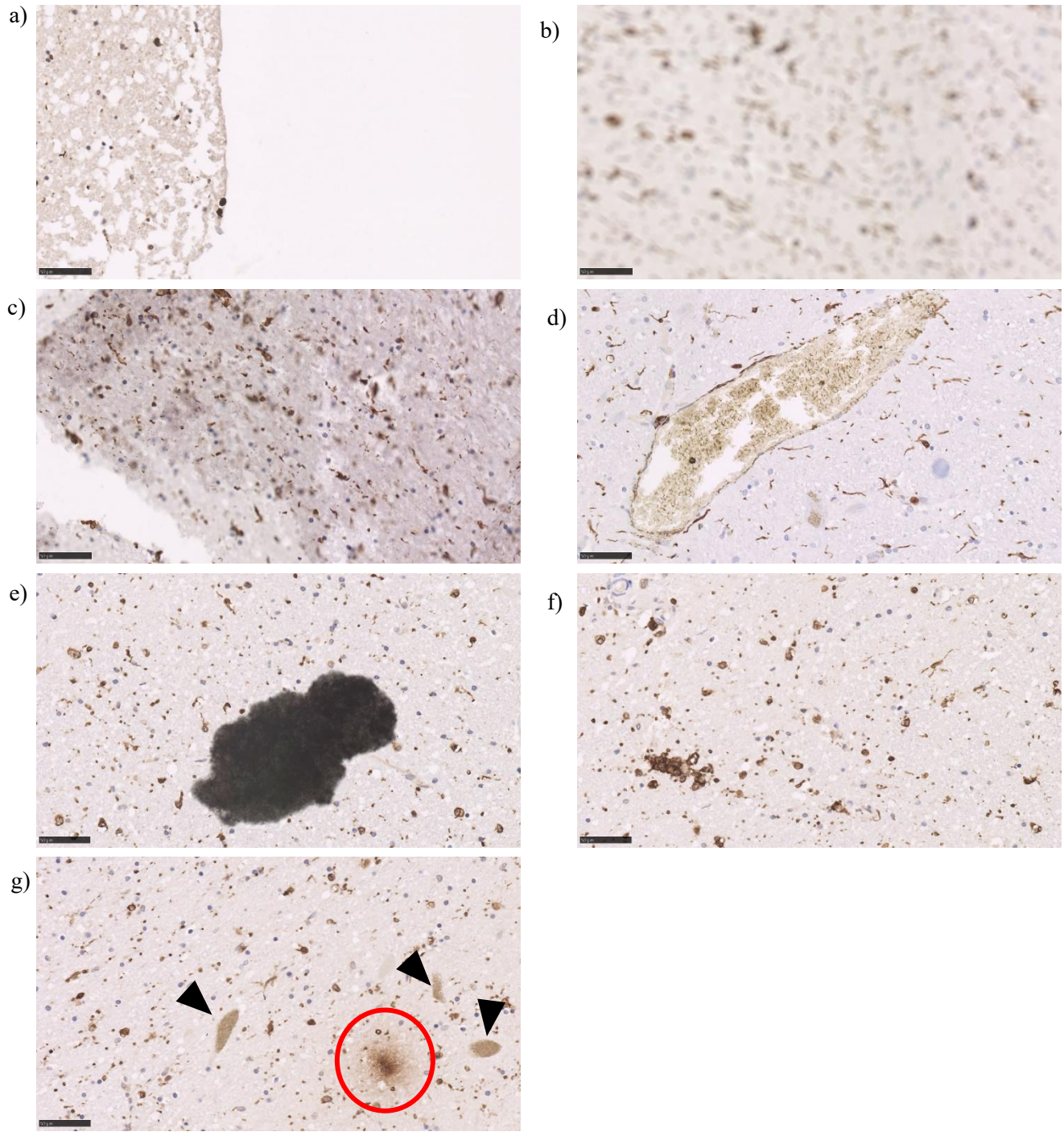
```
//RUN COLOUR DECONVOLUTION-change vector as required
run("Colour Deconvolution", "vectors=[H DAB]");
//close Images we don't need
selectWindow(imgName + "-(Colour_3)");
close();
selectWindow(imgName +"-(Colour_1)");
close();
selectWindow(imgName + "-(Colour_2)");
title = getTitle();

//THRESHOLDING-change threshold values as required
setAutoThreshold("Default");
//run("Threshold...");
setThreshold(0, 90);
run("Despeckle");
run("Despeckle");

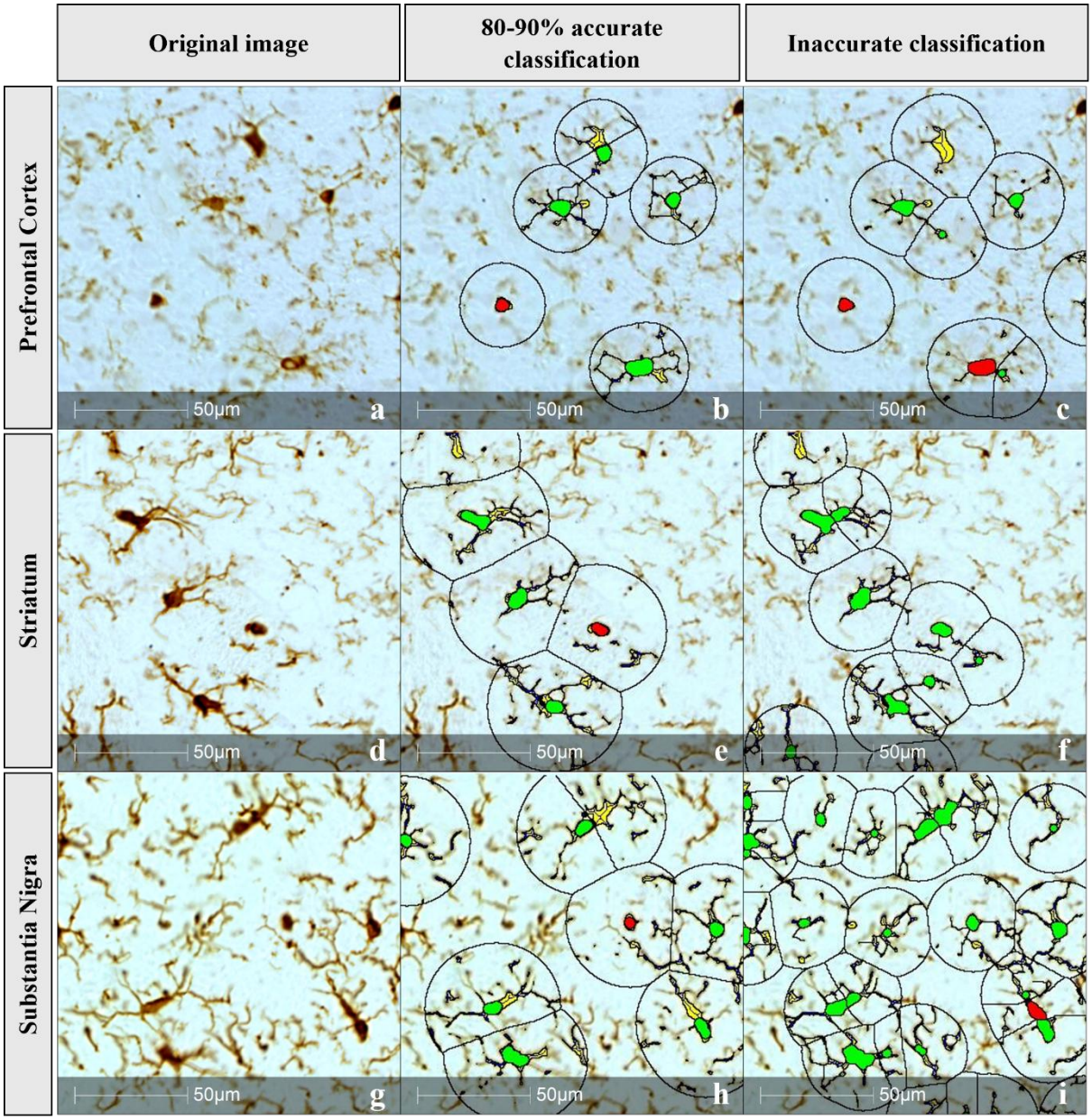
//PARTICLE ANALYSIS-change particle size as required
run("Analyze Particles...", "size=50-2000 circularity=0.80-1.00 show=[Outlines] display clear summarize add");
title = getTitle();
saveAs("JPEG", outputFolder + title);

//OVERLAY PARTICLES ON ORIGINAL IMAGE
selectWindow(imgName);
roiManager("Show All with labels");
run("Flatten");
saveAs("JPEG", outputFolder+title+"_overlay");
close();
}

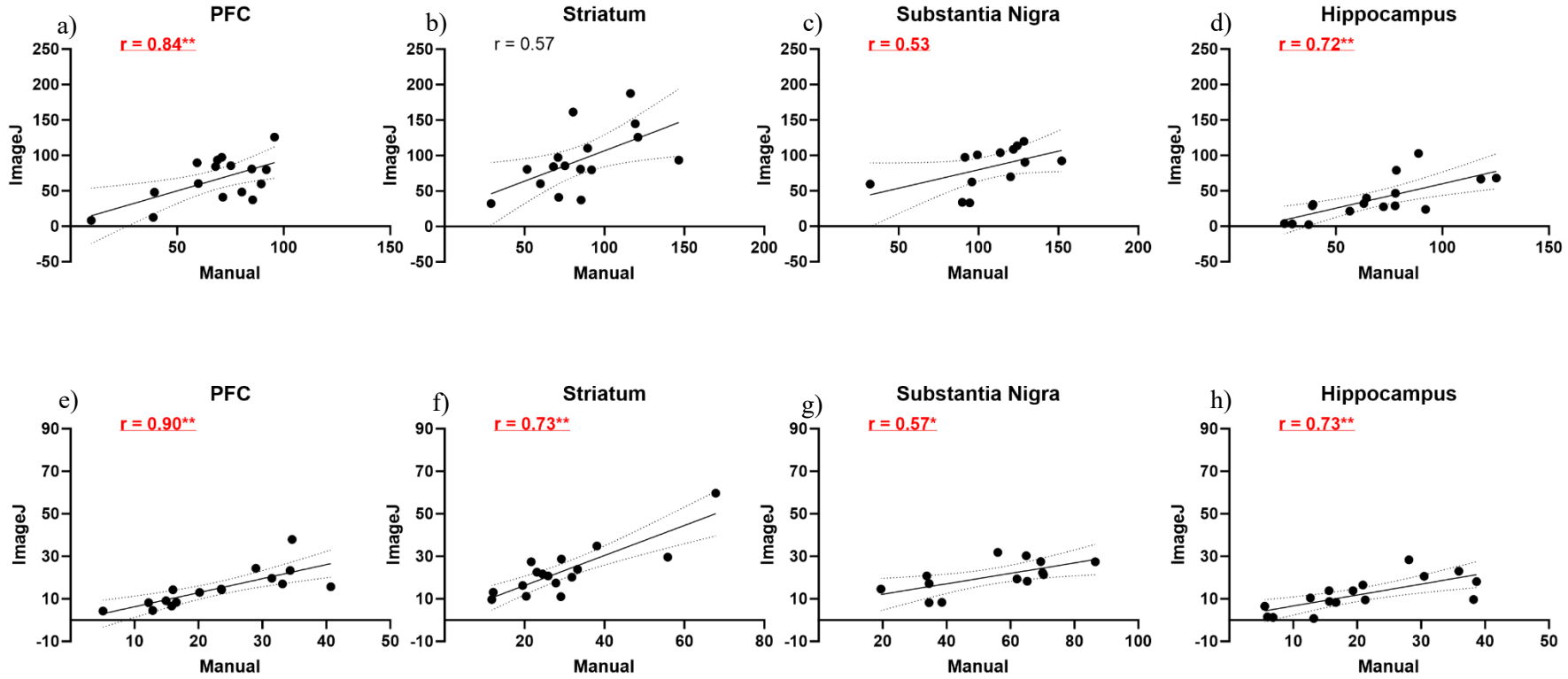
//SAVE ALL RESULTS-change filename as necessary
selectWindow("Summary");
saveAs("Results", outputFolder+"Results_Particle_Analysis_IBA1.csv");
close();
}
```



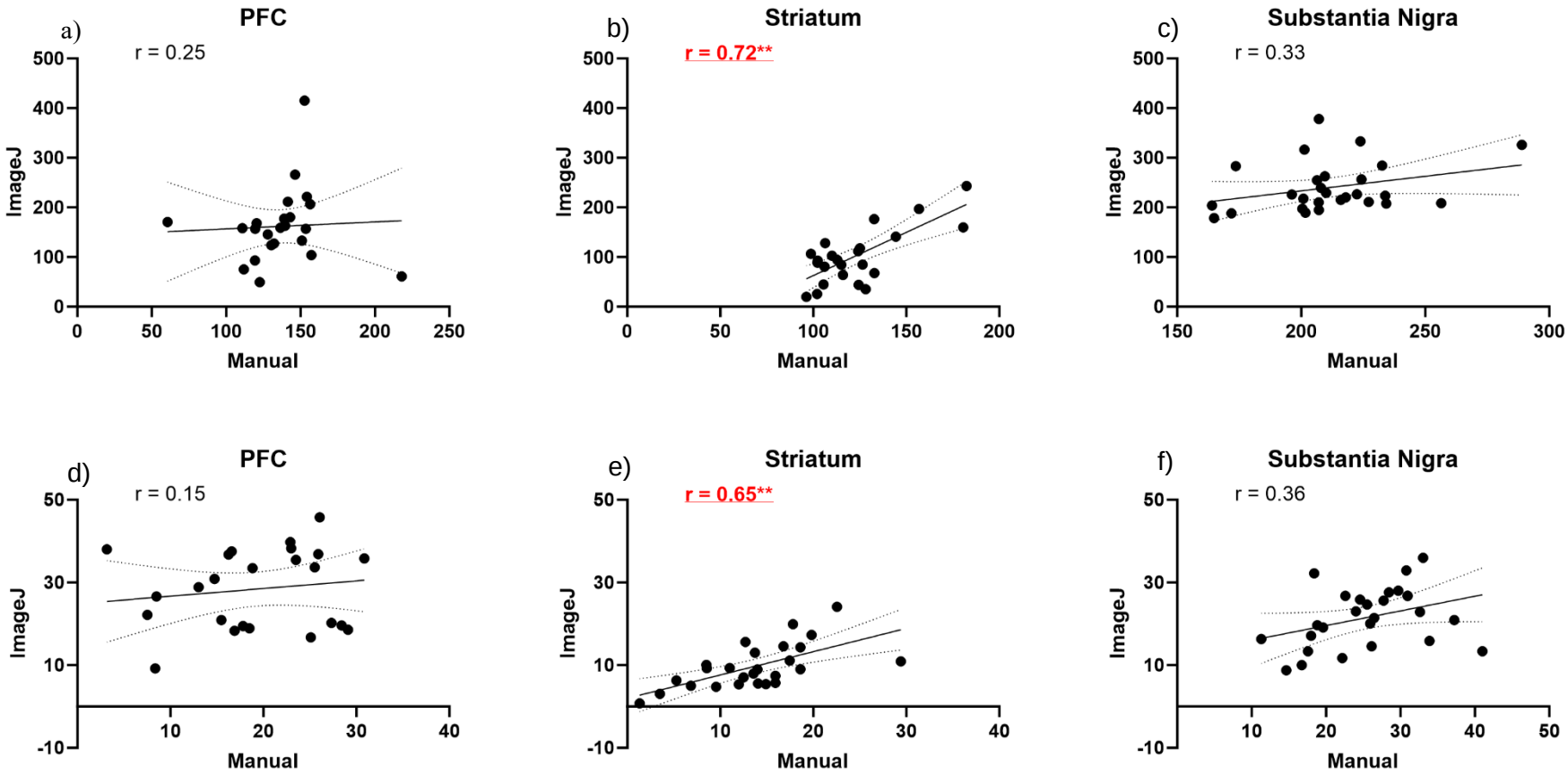
Supplementary Figure S 3.1 Examples of criteria for exclusion of images. In ImageJ analysis entire tiles were excluded. In Halo, artifacts were directly excluded by manual tracing of the exclusion area. Images were excluded if: a) <50% of the image included tissue, b) the image was blurry, c) the tissue was folded over or damaged, d) blood vessels were stained indiscriminately, e) black artifacts were present, f) big clumps of stained cells were present and were likely to impact the count, g) (circled) indiscriminate staining was present or (arrows) neuromelanin staining from neurons in the SN was likely to impact the automated count



Supplementary Figure S 3.2 Accurate and inaccurate classification of microglia on Halo in rat tissue. Example images from each region are shown to illustrate differences in Halo classification in each region. Accurate classification was determined when Halo correctly identified the activation state of the cell (GREEN = non-activated, RED = activated, YELLOW = microglial processes), and correctly captured the processes belonging to that cell. Identical settings were applied to the images in panel c, f and i. In panel c, Halo identifies additional activated microglia and picks up a cell as just processes. With the same parameters applied to the ST image in panel f, Halo does not correctly classify the activated microglia and picks up processes as individual cells. In panel i, Halo both misclassifies cells, and identifies processes as individual cells.



Supplementary Figure S 3.3 Correlation of microglial counts on ImageJ to manual counts in human tissue. Microglia were quantitated and identified as a-d. Total and e-h. Activated, as described in Fig 3.3. Individual values from both groups, as quantitated by manual counting (x-axis) or ImageJ (y-axis) were correlated and plotted, with each dot point representing a single case. Pearson r values (a. total counts) and Spearman r_s (b. non-parametric activated counts) are displayed. ImageJ showed significant correlations with manual counts in all regions, except total counts in the ST. Significant correlations are in red, bolded and underlined, with significance levels indicated, * = $p<0.05$, ** = $p<0.01$.



Supplementary Figure S 3.4 Correlation of microglial counts on ImageJ to manual counts in rat tissue. Microglia were quantitated and identified as a-c. Total and d-f. Activated, as described in Fig 3.3. Individual values from both groups, as quantitated by manual counting (x-axis) or ImageJ (y-axis) were correlated and plotted, with each dot point representing a single case. Pearson r values (b total ST, d. activated PFC, f. activated SN) and Spearman r_s (a. total PFC, c. total SN, e. activated ST) are displayed. ImageJ showed significant correlations with manual counts only in the ST. Significant correlations are in red, bolded and underlined, with significance levels indicated, * = $p<0.05$, ** = $p<0.01$.)

Contextual statement: Chapter 4

Chapter 4 is an experimental chapter presented in manuscript format for publication. This chapter presents a cross-species comparison of microglial ageing. The majority of neurodegenerative disease studies are conducted in mice and rats leaving a gap in translation from rodent models into clinical human work. Large animal models of the brain are thought to be more translatable due to their neuroanatomical similarities to human brains however they are expensive to work with and to not have as many established cognitive assessments as exist for small rodents. In order to assess the relevance of findings in aged rodents to the environment in aged humans, pre-clinical gyrencephalic models of the aged brain are needed to bridge this gap. Therefore, in chapter 4, archival tissue was sourced from previous studies in our laboratory using Sprague Dawley rats (aged 3-, 13-, 15-, and 19-months-old) and a study using sheep (aged 1-1.5-, 3-3.5-, and 5-6-years-old) and analysed using immunofluorescence for markers of microglia. As microglial analysis using morphology alone does not fully capture the states of microglia in tissue, here we utilised both number and percentage activated as in chapter 3, paired with a detailed analysis of microglia morphometrics at a single-cell level. Additionally, counts were paired with a marker of proliferation, in order to understand the dynamics of microglia at the population level. This basic microglial analysis conducted across multiple age groups of two pre-clinical models provides important baseline information about microglial population and morphological phenotypes with age in currently used models which can be used to inform future analysis in human post-mortem tissue or in creating better models of aged microglia.

Statement of Authorship

Title of Paper	Cross-species characterisation of microglial morphology and proliferation during ageing
Publication Status	☐ Published ☐ Accepted for Publication ☐ Submitted for Publication ☑ Unpublished and Unsubmitted work written in manuscript style
Publication Details	

Principal Author

Name of Principal Author (Candidate)	Laura Carr		
Contribution to the Paper	First author and main contributor. Concept, writer and formulation of manuscript. Reviewed prepared final draft following inputs from co-authors.		
Overall percentage (%)	70%		
Certification:	This paper reports on original research I conducted during the period of my Higher Degree by Research candidature and is not subject to any obligations or contractual agreements with a third party that would constrain its inclusion in this thesis. I am the primary author of this paper.		
Signature		Date	30/11/2024

Co-Author Contributions

By signing the Statement of Authorship, each author certifies that:

i. the candidate's stated contribution to the publication is accurate (as detailed above);

ii. permission is granted for the candidate in include the publication in the thesis; and

iii. the sum of all co-author contributions is equal to 100% less the candidate's stated contribution.

Name of Co-Author	Shannon Stuckey		
Contribution to the Paper	Assistance with tissue generation and experimental advice, reviewed and edited manuscript		
Signature		Date	01/12/24

Name of Co-Author	Isabella Bilecki
Contribution to the Paper	Generated tissue, provided experimental advice, reviewed and edited manuscript

Signature		Date	01/12/24

Name of Co-Author	Sanam Mustafa		
Contribution to the Paper	Reviewed and edited manuscript, project supervision		
Signature		Date	01/12/24

Name of Co-Author	Renée J. Turner		
Contribution to the Paper	Conceptualisation, tissue generation, reviewed and edited manuscript		
Signature		Date	02/12/2024

Name of Co-Author	Lyndsey E. Collins-Praino		
Contribution to the Paper	Conceptualisation, experimental advice, reviewed and edited manuscript, project supervision		
Signature		Date	01/12/24

Please cut and paste additional co-author panels here as required.

Chapter 4 : A Cross-Species Characterisation of Microglial Morphology and Proliferation During Ageing

Laura M. Carr[1], Shannon Stuckey[1], Isabella Bilecki[1], Sanam Mustafa[1,23], Renée J. Turner[1], Lyndsey E. Collins-Praino[1,2]

[1] School of Biomedicine, University of Adelaide, Adelaide, SA, Australia
[2]Australian Research Council Centre of Excellence for Nanoscale Biophotonics, The University of Adelaide, Adelaide, SA, Australia

4.1 Abstract

By 2050, one-fifth of the global population is expected to be over 60 years old [1], a fact which is predicted to cause the burden of age-related neurological conditions, such as Alzheimer's Disease, Parkinson's Disease and stroke, to dramatically increase. The translation of treatments for neurological conditions, however, has remained notoriously slow. To improve this, it is important to ensure that research models best reflect the conditions of the disease of interest, including the incorporation of aged backgrounds in models of neurodegenerative disease, which is currently lacking [2].

The current study presents a cross-species characterisation of microglia, the key regulator of the brain's immune response, during ageing. Microglial number, activation state, proliferation and morphology were assessed in Sprague Dawley rats and merino sheep. Manual quantification of microglia in rats revealed decreased numbers of activated microglia and increased numbers of proliferating microglia, in the cortex and hippocampus aged compared to young rats, but no change in total microglial numbers were observed. Microglia in these regions also demonstrated morphological changes with age. In sheep, the total number of microglia in subcortical regions decreased with age, and no changes in activation were detected, but microglial proliferation in the dentate gyrus and cortex was with age. Morphological changes in microglia were only observed in striatal regions of sheep. Species-specific differences in both when microglia begin to change with age and the regions in which this occurs was observed, which has implications for the use of these pre-clinical models for the investigation of age-related neurological disease.

4.2 Introduction

Neurological diseases currently affect millions of people globally. In 2021, despite pandemic conditions increasing the effect of COVID-19 related deaths, stroke and Alzheimer's disease (AD) remained among the top 10 leading causes of death globally, occupying 3rd and 7th place, respectively (Naghavi et al., 2024). Increasing age is the leading non-modifiable risk factor for stroke (Boehme et al., 2017) and is the number one risk factor for developing AD (Hou et al., 2019). With one-fifth of the global population expected to be over 60 years old by 2050 (Mathews, 2024), the burden of these age-related neurological conditions is expected to increase dramatically. The effect of population ageing on Parkinson's disease (PD) is already evident. In 2016, PD was the fastest growing neurological disorder (Dorsey et al., 2018), with the crude prevalence rate increased by 74% compared to 1990 (Dorsey et al., 2018). Additionally, the age-standardised prevalence during this time increased by 22%, demonstrating that, while other factors may contribute to increasing PD prevalence, our ageing population is a major factor. Neurological disorders remain difficult to treat, and the translation of potential treatments for neurodegenerative diseases to the clinic, in particular, is notoriously slow, with 99.6% of clinical trials for AD failing (Asher and Priefer, 2022). To improve these translation rates and successfully develop effective treatments for age-related neurological conditions, it is critical that experimental models incorporate the aged phenotype, in order to best reflect the physiological conditions that occur in disease states (Carr et al., 2024; Sun et al., 2020). To do so, it is important to understand how key hallmarks of ageing (López-Otín et al., 2023) are altered throughout the lifespan in animal models commonly used in preclinical research.

Mice and rats comprise the majority of animal models utilised in neurological disease research (Keifer and Summers, 2016). These small rodents are preferred not only for the logistical benefits, including their small size, ease of handling, low cost of housing and husbandry, short lifespan and rapid reproduction (Jaramillo and Zador, 2014), but also for well-established batteries of behavioural tests and well characterised genomes and techniques for genetic manipulation (Jaramillo and Zador, 2014). Nevertheless, small rodent models have key neuroanatomical differences when compared to humans, which may impact the ability to directly translate results both across species and clinically (Sorby-

Adams et al., 2018). For example, rat brains are lissencephalic, which may lead to important translational differences when compared to the gyrencephalic human brain (Krieg et al., 2023). In line with this, in traumatic brain injury research, animals with gyrencephalic brains are preferred for the enhanced ability to transmit mechanical forces (Krieg et al., 2023; Sorby-Adams et al., 2018). Additionally, in stroke research, the use of animals with gyrencephlaic brains, such as sheep, may better mimic the anatomical vasculature of humans and thus improve the translatability of stroke treatments (Sorby-Adams et al., 2018). In generating an ovine model of middle cerebral artery occlusion (MCAO) in adult merino rams one study has demonstrated similarities to the pathology in humans following stroke (Boltze et al., 2008). Post-mortem neuropathologic evaluation of ovine brains following MCAO, revealed lesions similar to those in humans at a macroscopic level and additionally, neuronal loss, macrophage recruitment and cavitation in lesion areas at a microscopic level, demonstrating the pathological relevance of ovine models for human stroke beyond anatomical similarities (Boltze et al., 2008).

Similarly, the immune system in the mouse brain shows marked differences to that of humans. In line with this, when investigating mouse and human neuroinflammatory models built using Biological Expression Language, differences between species were found at both molecular and cellular levels (Kodamullil et al., 2017). Molecularly, only 27% of cytokine interactions were conserved across species, with 58% unique to humans. Of note, interactions between microglia and astrocytes, which both contribute to immune responses in the central nervous system (CNS), showed high similarity between species (62% similar interactions); however 28% of interactions seen in humans were not observed in mice (Kodamullil et al., 2017). Considering these discrepancies, over reliance on rodent models could be a contributing factor to the high failure rate seen in neurological disease clinical trials (Kodamullil et al., 2017; Żakowski, 2020). This has certainly been the case in stroke which led to the publication of the updated Stroke Therapy Academy Industry Roundtable (STAIR) recommendations in 2009 which outlined potential reasons for the translational failings of stroke therapeutics (Fisher et al., 2009). A multi-species approach was suggested in order to ensure pre-clinical research is conducted with rigor and to allow for enhanced clinical translation of therapeutics (Turner and Farr, 2024). While

sheep present with highly similar brain anatomy to that of humans (reviewed: (Murray and Mitchell, 2022)), the immune system in the brain has not been directly compared to that in humans. However, one study comparing immune factors in blood samples from sheep and human following *ex vivo* stimulation with 1μg/ml LPS or 10μg/ml monophosphoryl lipid A (MPLA) found that gene expression of key pro-inflammatory factors, including IL-6, TNF and NF-κB, were similarly upregulated in response to stimulation in both species. This result, though not specific to the brain, suggests that immune responses in sheep are much like those seen in humans, thus supporting the use of sheep in translational immune research (Enkhbaatar et al., 2015).

In understanding potential species-specific differences, it is particularly crucial to understand differences in the population and response of CNS immune cells specifically, in particular understanding how these cells contribute to neuroinflammation in age-related NDs. The role of neuroinflammation in NDs has been extensively reviewed (Leng and Edison, 2021; Troncoso-Escudero et al., 2018) and is of significant interest in both AD and PD as neuroinflammatory processes have strong links to disease pathology and progression (Zhang et al., 2023). Neuroinflammation is characterised by chronic and sustained activation of immune cells in the brain including microglia, which drive the initiation of the neuroinflammatory immune response (Ginhoux et al., 2013). Microglia are derived from progenitor cells in the embryonic yolk sac, with their origin first described in chick embryo-quail yolk sac chimeras (Cuadros et al., 1992; Cuadros et al., 1993) and subsequently demonstrated across other species, including mice (Alliot et al., 1999; Ginhoux et al., 2010) and humans (Monier et al., 2007). Once established, the microglial population is capable of self-renewal (Bruttger et al., 2015), with the population of microglia undergoing regular remodelling (Askew et al., 2017). Microglia under physiological conditions are motile cells, routinely surveying the CNS microenvironment for tissue damage or potential pathogens (Nimmerjahn et al., 2005). As part of their resting phenotype, microglia display a ramified structure. The complexity of these ramifications has been observed to vary slightly between species, with humans showing less complex morphology than other primates, but more than other high-order vertebrates, such as the whale (Geirsdottir et al., 2019). The acute immune response initiated by microglia is critical in responding to a perceived immunological

threat and helps to maintain a healthy and functional CNS (Vidal-Itriago et al., 2022). During this response there is a shift in microglial morphology, with responsive or activated microglia taking on an amoeboid shape, with thicker and shorter processes (Vidal-Itriago et al., 2022). This morphology has been associated with an activated state in humans (Torres-Platas et al., 2014), mice (Leyh et al., 2021; Takagi et al., 2019), rats (Schwarz et al., 2012), marmosets (Philippens et al., 2017) and sheep (Finnie et al., 2024; Zhou et al., 2022). While diversities in microglial morphology across species have previously been characterised (Geirsdottir et al., 2019) and reviewed (Sharma et al., 2021), species specific differences in microglia throughout the lifespan, including with increased age, have not been widely investigated. This knowledge would greatly contribute to the ability to assess translatability of results across different models to ensure that therapeutic strategies are accurately targeted. This approach not only aids in validating models of NDs in the context of age, but also improves the relevance of pre-clinical studies for advancing treatments.

Aged microglia have been described as having an activated and hyper-inflammatory phenotype, with studies reporting a heightened response to inflammatory stimuli. In aged (22- to 24-months-old) C57BL/6 male mice, microglia showed upregulation of soluble interleukin (IL) -6 receptors compared to mice at 3- to 5-months-old (Garner et al., 2018). Additionally, these aged mice demonstrated upregulation of the pro-inflammatory cytokines IL-1β and IL-6, as well as major histocompatibility complex II (MHCII), a marker of immune activation (Garner et al., 2018). Similarly, microglia in pigmented Lister Hooded rats at 25-30 months of age have shown upregulation in the number of microglia positive for MHCII compared to 3- to 6-month-old rats (Perry et al., 1993). Of note, microglia maintain a stable population, with a steady rate of proliferation across ageing, which has been demonstrated in both mice and in post-mortem human tissue (Askew et al., 2017). In line with this, the microglia of aged mice (18- to 24-months-old) demonstrated no changes in proliferation, as measured using BrdU, except for in the dentate gyrus, compared to microglia of mice aged 4- to 6-months-old (Askew et al., 2017). Similarly, no changes in the number of microglia or percentage of proliferating microglia (i.e. $Ki67^{+}$) were observed in aged brains (58-79 years) compared to young brains (20-35 years) in human post-mortem tissue from the temporal cortex (Askew et al., 2017). This study is one of

the only studies conducted to date that performed a cross-species analysis of microglial ageing, but it focused exclusively on microglial proliferation. In order to improve understanding of how microglial ageing differs across species, multiple indicators and multiple regions need to be considered to provide a comprehensive understanding of microglial ageing. Additionally, a comparison of species-specific differences between models commonly used for pre-clinical modelling of neurological disease (e.g. rodents vs sheep) is essential for the informed use of appropriate animal models that best fit the research question, and to drive improved clinical translation for neurological disorder treatments.

Thus, the present study aimed to investigate changes in the microglial population and microglial morphology in the context of ageing across both rodent and ovine cohorts. Specifically, changes in the number of microglia, their activation state and proliferative rate were assessed across multiple neuroanatomical regions known to demonstrate vulnerability in neurological disease.

4.3 Methods

4.3.1 Ethics

All tissue used within this study was sourced from archival sources, and both datasets contained tissue that had been stored for similar lengths of time. Ethics approval and cohort details are shown in Table 4.1. All experiments were performed in accordance with the Animal Welfare Act (1985) and the National Health and Medical Research Council (NHMRC) *Australian Code for the Care and Use of Animals for Scientific Purposes* (8th edition, 2013).

4.3.2 Animal details

For the rodent dataset, sham tissue was sourced from previously conducted stroke studies. Male Sprague-Dawley rats (aged 3-19 months; male n=37, weight 370±20.37g) were housed under conventional laboratory conditions with a 12-hour light/dark cycle and access to standard rodent chow and water *ad libitum*. Tissue for the ovine dataset was sourced from a previously conducted lifespan study, where animals were not subjected to any experimental conditions beyond anaesthesia and tissue collection. Merino adult sheep (male wethers n=18, weight 65.2±12.4kg; female ewes n=24, weight 58.4±7.3kg) were obtained and housed at the South Australian Health and Medical Research Institute (SAHMRI) Large Animal Research and Imaging Facility (LARIF) 2 weeks prior to study involvement.

Table 4.1: Details of ethics approval and cohort details for murine and ovine datasets.

Approving body	Ethics approval	Dataset	Ages	Number of animals		Total
				Male	Female	
The University of Adelaide Animal Ethics Committee	M-2015-11b	Young rat	3-month-old (3mth)	8	0	37
	M-2019-103	Aged rat	13-month-old (13mth)	9	0	
			15-month-old (15mth)	10	0	
			19-month-old (19mth)	10	0	
The South Australian Health and Medical Research Institute Animal Ethics Committee	SAM402.19	Sheep	1-1.5 years-old (1-1.5y)	8	8	42
			3-3.5 years-old (3-3.5y)	8	8	
			5-6 years-old (5-6y)	2	8	

4.3.3 Murine tissue collection and processing

Both the young and aged rat cohorts underwent anaesthesia and tissue perfusion via direct cardiac perfusion and exsanguination prior to brain tissue collection. Briefly, animals were anaesthetised (5%

inhalational isoflurane with 2L/min normoxic air mix) in the supine position and a thoracotomy was performed horizontally below the sternum. Transcardiac perfusion was then performed with 100µl of heparin (5,000IU/ml; Pfizer, USA), which was prepared in water for injection. This was followed by perfusion using 10% neutral buffered formalin (NBF) (POCD Healthcare, Australia), which contained 3.7% formaldehyde in PBS. Formalin was pumped at a consistent rate (12rpm gradually increased to 24rpm) for 8 minutes or until the perfusate ran clear. Administration of formalin was then ceased. To reduce perfusion artifacts, animals were left in place for 30 minutes prior to decapitation and brain removal.

After decapitation, and brain extraction, brain tissue was submerged in 10% NBF (POCD Healthcare, Australia) for 10 days and processed within 14 days of extraction. 2mm thick coronal slices were prepared and processed through changes of ethanol (75%-100%), xylene and paraffin over a 16-hour cycle, before being embedded in paraffin wax. Using the rat brain atlas for reference (Paxinos and Watson, 2007), 5µm sections were cut using a microtome at the levels of the striatum and hippocampus to obtain key regions of interest (Table 4.2), mounted on glass histology slides and stored at room temperature (RT) until histological staining was performed.

4.3.4 Ovine tissue collection

Animals were weighed and anaesthetised via intravenous injection of ketamine (1mL/20kg, Ceva Animal Health Pty Ltd, Australia) and diazepam (2mL/20kg, Ceva Animal Health Pty Ltd, Australia). Anaesthesia was maintained using inhalational isoflurane (2-3%, Provet Pty Ltd, Australia) while animals were euthanised through common carotid artery perfusion and exsanguination. Whilst anaesthetised, animals were intubated and ventilated for tissue extraction and perfusion. Animals were placed to the supine position and a partial tracheostomy was performed laterally to the tracheae down the midline of the neck to expose the carotid arteries. Heparin (25,000IU, Pfizer, USA) was administered intravenously into the jugular and perfusion PE tubing lines were inserted rostrally into both carotid arteries and secured in place. Cold Tris-saline (2L) was pumped through the carotid lines at 120mmHg and both jugular veins and incised to allow for free exsanguination, following which the jugular perfusate ran clear, following which decapitation and brain extraction was performed. Whole

brains were sectioned into 10mm coronal slices for embedding and histological staining. Sections were submerged in 10% NBF (POCD, Healthcare, Australia) before being processed through changes of ethanol (75-100%), xylene and paraffin over a 69-hour cycle and embedded in paraffin wax. Using a sheep brain atlas (Johnson et al., 2024), 5µm thick sections of single hemispheres (left or right randomly allocated within age and sex groups) were prepared using a microtome from embedded tissue at the levels of the striatum and hippocampus to obtain key regions of interest (Table 4.2), mounted on microscope slides and stored at RT until undergoing histological staining.

Table 4.2: Regions of interest in each dataset. Hippocampal and striatal regions were further split into sub regions in sheep tissue where delineations between regions were well defined.

Rat	Sheep
Cortex	Cortex
Hippocampus	Dentate Gyrus (DG)
	Hippocampus Proper (HP)
Striatum	Caudate Nucleus (CN)
	Putamen (PUT)

4.3.5 Immunofluorescence and imaging

Immunofluorescent (IF) staining was performed according to standard protocols. Briefly, slides were deparaffinised in xylene and washed in 100% ethanol. Following this, slides were washed twice in phosphate buffered saline (PBS) and heat-induced antigen retrieval was conducted (in citrate solution). Slides were then washed in 0.1% triton-X-100 (Sigma Aldrich T8787) and PBS (PBS-T) and blocked in 3% normal goat serum (NGS, Gibco #16210064) for 1 hour at RT before being incubated overnight at RT in the primary antibodies (See Table 4.3 for all antibody details). On the following day, slides were washed three times in PBS and incubated for 1 hour at RT in secondary antibodies protected from light. Following this, slides were then washed twice in PBS and incubated with DAPI (Sigma Aldrich #D9542) for 5 minutes before being mounted on coverslips using Fluoromount-G mounting medium (Thermofisher, 00-4958-02). Slides were left to dry at RT protected from light for at least 2 hours before being cleaned and imaged using a Zeiss AxioScan.Z1 at 20x magnification (Zeiss Microscopy).

Table 4.3: Antibody concentrations used in each dataset

Antibody	Host species	Source	Murine concentration	Ovine concentration
		Primary antibodies		
Ionized Calcium Binding adaptor molecule 1 (IBA1)	Mouse	Thermofisher: MA5-27726	1:1000	1:1000

Ki67	Rabbit	Abcam: ab15580	1:1000	1:1000
		Secondary antibodies		
Alexa Fluor 647 Goat anti-mouse IgG (H+L)	Goat	Thermofisher: A32728	1:400	1:400
Alexa Fluor 488 Goat anti-rabbit IgG (H+L)	Goat	Thermofisher: A32731	1:400	1:400
DAPI	N/A	Sigma-Aldrich: D9542	1:10,000	1:10,000

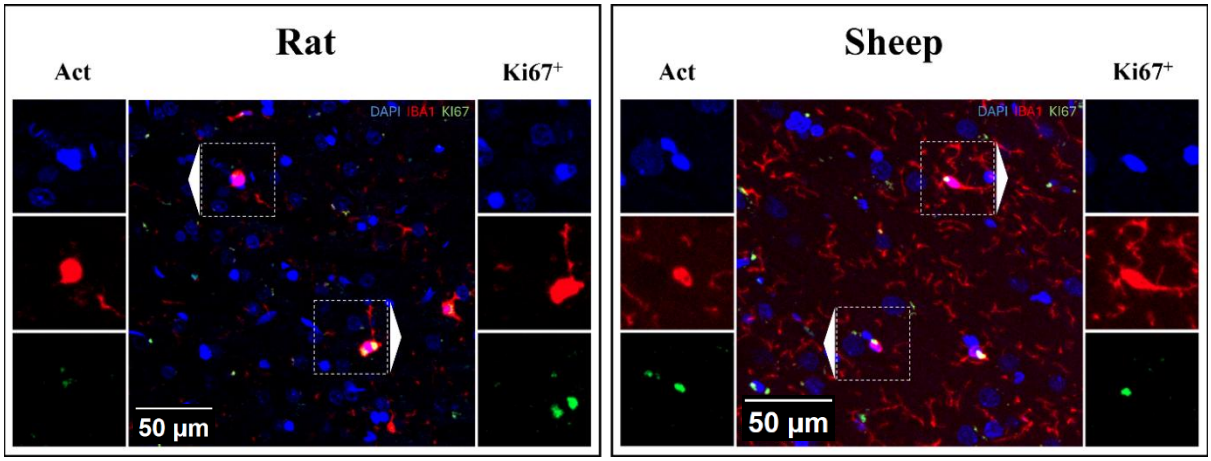


Figure 4.1: Representative images of immunofluorescent staining in the aged rat and sheep cortex.Microglia were counted by identifying colocalised DAPI and IBA1. Microglia with an amoeboid morphology were classified as activated (Act) (left columns). Microglia were classified as Ki67$^+$ when both DAPI, IBA1 and Ki67 signal overlapped (right columns). Number of non-activated, activated and Ki67$^+$ microglia were counted manually.

4.3.6 Image analysis

4.3.6.1 Cell counting

Microglial cell counts were conducted manually in QuPath on IBA1 stained images with assessors blinded to age groups. Six boxes of equal size were annotated in each region, and microglia (those with a visible nucleus only) within the boxes were manually counted. The specific areas analysed, and average numbers counted for each group and region are summarised in Supplementary Tables S4.1.2 (rats) and S4.1.3 (Sheep) located in the Supporting Information document. Within these boxes, the number of activated microglia was also counted, with microglia classified as activated based on morphology, where cells with high soma circularity and shortened processes or no processes were counted as activated. Representative images of non-activated and activated microglia are shown in Figure 4.1. Cells/mm^2 (total cell count/total area analysed) and percentage of activated microglia (activated count/total count x 100) were calculated for analysis.

4.3.6.2 Positive Ki67 cell detection

Colocalisation of DAPI and IBA1 was used to identify microglia and cells were counted as above. Microglia positive for Ki67, a marker of cell proliferation, were manually counted and analysed as a percentage of the total microglial population. Cells were counted as positive for Ki67 when Ki67 signal was visible in the cell soma. Representative images of Ki67$^+$ microglia are shown in Figure 4.1.

4.3.6.3 Single cell morphological analysis

Morphology of microglia was assessed using the IBA1 stained images. For each animal, 10 cells from each region were randomly extracted for morphological analysis using ImageJ (Schneider et al., 2012). Briefly, cells were isolated to individual images and converted to binary (Fig4.2 a/b). Background pixels were then removed and sections of the cell that had been fragmented in the processing stages were connected using the paintbrush tool and the original image for reference (Fig 4.2c). Four copies of the image were saved, one for each of the analyses illustrated in Fig 4.2. For skeleton analysis (Fig 4.2d), binary images were skeletonized and analysed using the AnalyzeSkeleton plugin (Arganda-Carreras et al., 2010) to obtain the number of branches per cell and mean branch length per cell. Cell area (Fig 4.2e) was assessed using the second binary image on ImageJ. Soma area (Fig 4.2f) was assessed by isolating the soma within the binary image of the cell and running area analysis on ImageJ. Sholl analysis was conducted using the Sholl analysis plugin (Ferreira et al., 2014). The centre point and maximum radius of each cell was first defined by the assessor using the line tool in ImageJ (Fig 4.2g). From this point, concentric circles were drawn at 5µm increments starting 5µm from the centre point. The number of branches intercepting each concentric circle was counted for a measure of branching complexity.

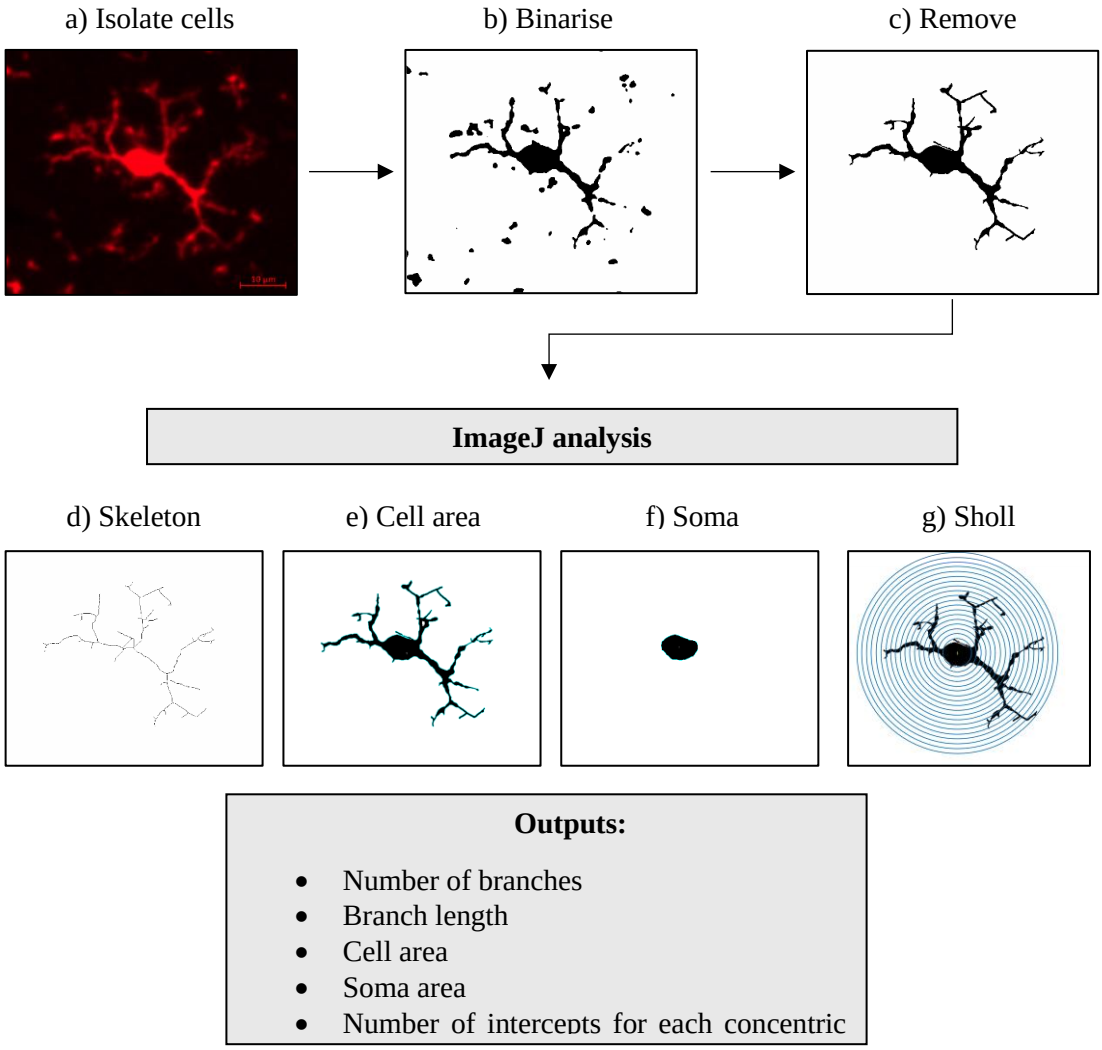


Figure 4.2 Microglial morphological analysis using ImageJa) 10 cells in each region were isolated for analysis. b) Images were binarised and c) background pixels were removed. d) Cells were then skeletonised to obtain number of branches and average branch length. e) Whole cell and f) soma area were measured. g) Sholl analysis was conducted to obtain the number of times microglial branches intercepted each concentric circle

4.3.7 Statistical analysis

Outliers with a Q value of 0.1% were identified in GraphPad Prism version 10.0.0 for Windows (GraphPad Software, San Diego, California USA) using the Robust Regression and Outlier Removal (ROUT) method (Motulsky and Brown, 2006) and were removed. All subsequent statistical analysis was conducted in R (version 1.4.1717) (Dalgaard, 2010). Data from manual counts were analysed using a one-way analysis of variance (ANOVA), with Tukey post-hoc, to investigate the effect of age within each region of the brain. Single cell morphological data were analysed using linear mixed effects models using the *lme4* package (Bates et al., 2015). As the variable of interest was age, this acted as the fixed

effect in the model. A random intercept for animal ID was included to account for individual variability in the data, and for Sholl analysis, an additional random intercept of distance was also included to account for repeated measures across distances. These models were based on a similar published analysis on single cell microglia data (Green et al., 2022), where distance from cell body was included as a continuous variable. In the present study, given that random effects are traditionally categorical, distance from cell body was operationalised as increments of 10µm. For all analyses, the significance level was set a $p < 0.05$.

4.4 Results

4.4.1 Microglia in rat and sheep show opposing changes in number and activation with age

Rat (n=37) and sheep (n=42) brain tissue was fluorescently stained for IBA1 and DAPI and by identifying colocalization of these markers, total and activated microglia were counted. When analysing total microglia counts in rat brain tissue (Fig 4.3b), one-way ANOVA detected a significant effect of age in the hippocampus *(F(3,32)= 5.708, p = 0.003).* Tukey post-hoc test showed a significant increase in total microglia at 15mths compared to at 3mths *(93.79±13.26 vs 72.59±11.37, p = 0.007)* and a decrease at 19mths compared to 15mths *(72.09±17.17 vs 93.79±13.26, p = 0.009).* No differences between total microglia counts at 3mths and 19mths were detected *(72.59±11.37 vs 72.09±17.17*, *p = 1).* No significant effect of age was detected in either the striatum *(F(3,34)= 1.369, p = 0.26)* or the cortex *(F(3,36)= 2.184, p = 0.052).*

When analysing percent activated microglia in the rat brain (Fig 4.3c), one-way ANOVA detected a significant effect of age in the hippocampus *(F(3,32)= 5.985, p = 0.002)*, striatum *(F(3,36)= 4.335, p = 0.010)* and cortex *(F(3,37= 5.91, p = 0.002)*. Specifically, there was a decrease in the percentage of activated microglia at 13mths compared to 3mths in both the cortex *(5.79±1.4 vs 9.59±3.42, p = 0.009)* and striatum *(5.47±2.08 vs 9.63±4.17, p = 0.02),* and a decrease at 19mths compared to 3mths in both the hippocampus *(3.82±1.67 vs 8.96±4.17, p = 0.001)* and cortex *(5.51±1.75 vs 9.59±3.42, p = 0.003).* In the striatum at 19mths, there was an increase in percent activated microglia compared to at 13mths *(9.62±2.42 vs 5.47±2.08, p = 0.02)*, but no differences detected between 3mths and 19mths *(9.63±4.17 vs 9.62±2.42*, p = *1)*.

Conversely, when total microglia counts in sheep brain tissue (Fig 4.4b) were analysed using one-way ANOVA, an effect of age was seen in the DG *(F(2,31)= 4.667, p = 0.01),* CN *(F(2,35)= 5.719, p = 0.007),* PUT*(F(2,36)= 3.84, p = 0.03*) and cortex*(F(2,36)= 3.611, p = 0.03)*, but not in the HP *(F(2,32)= 0.81, p = 0.45).* Specifically, there was a decrease in total microglia in 5-6yo sheep compared to 1-1.5yo sheep in the DG *(95.58±9.54 vs 116.35±19.31, p = 0.01)*, CN *(104.91±15.78 vs 126.73±17.37, p = 0.005)* and PUT *(126±16.24 vs 154.72±28.51, p = 0.02),* with no significant differences detected by post-hoc testing in the cortex *(p = >0.05 for all comparisons)*. When analysing

percent activated microglia in sheep brains (Fig 4.4c), no effect of age was detected in any region (DG*: F(2,32)= 0.195, p = 0.824*; HP: *F(2,31)= 1.942, p = 0.16;* CN*: F(2,35) 0.138, p = 0.872*; PUT*: F(2,36)= 0.495, p = 0.614*; cortex*: F(2,35)= 0.842, p = 0.439)*.

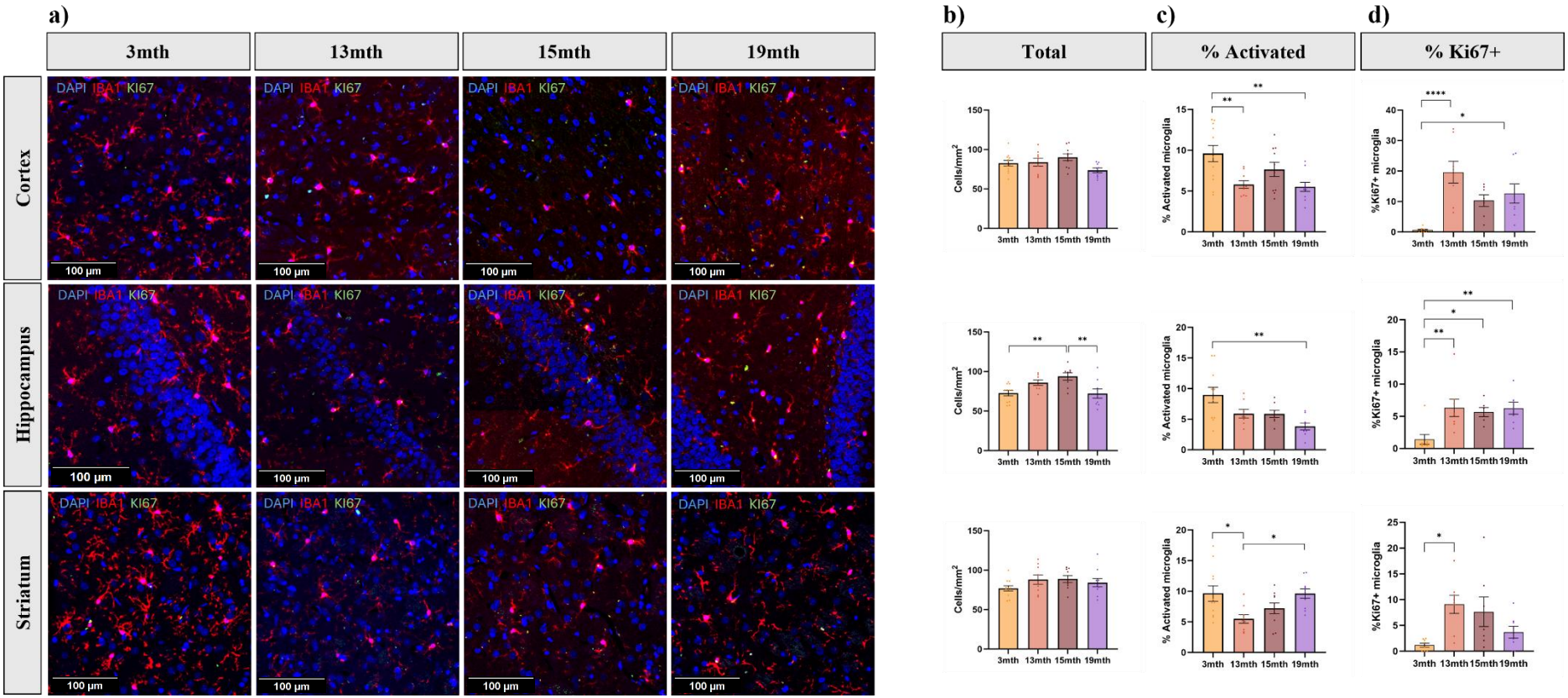


Figure 4.3: Microglia counts in the rat brain. a) Representative merged images of microglia (red) in different regions of the rat brain at each age. IBA1$^+$ cells with a strong Ki67 signal (green) were classified as Ki67$^+$ microglia. Individual channels are shown in figures S4.1.2, 4.1.3 and 4.1.4. b) Total number of microglia c) percentage of activated microglia and d) percentage of Ki67$^+$ microglia were manually counted and graphed as mean±SEM. Significant differences were determined by one-way ANOVA and Tukey post hoc testing. * = p<0.05, ** = p<0.01. Scale bar = 100µ

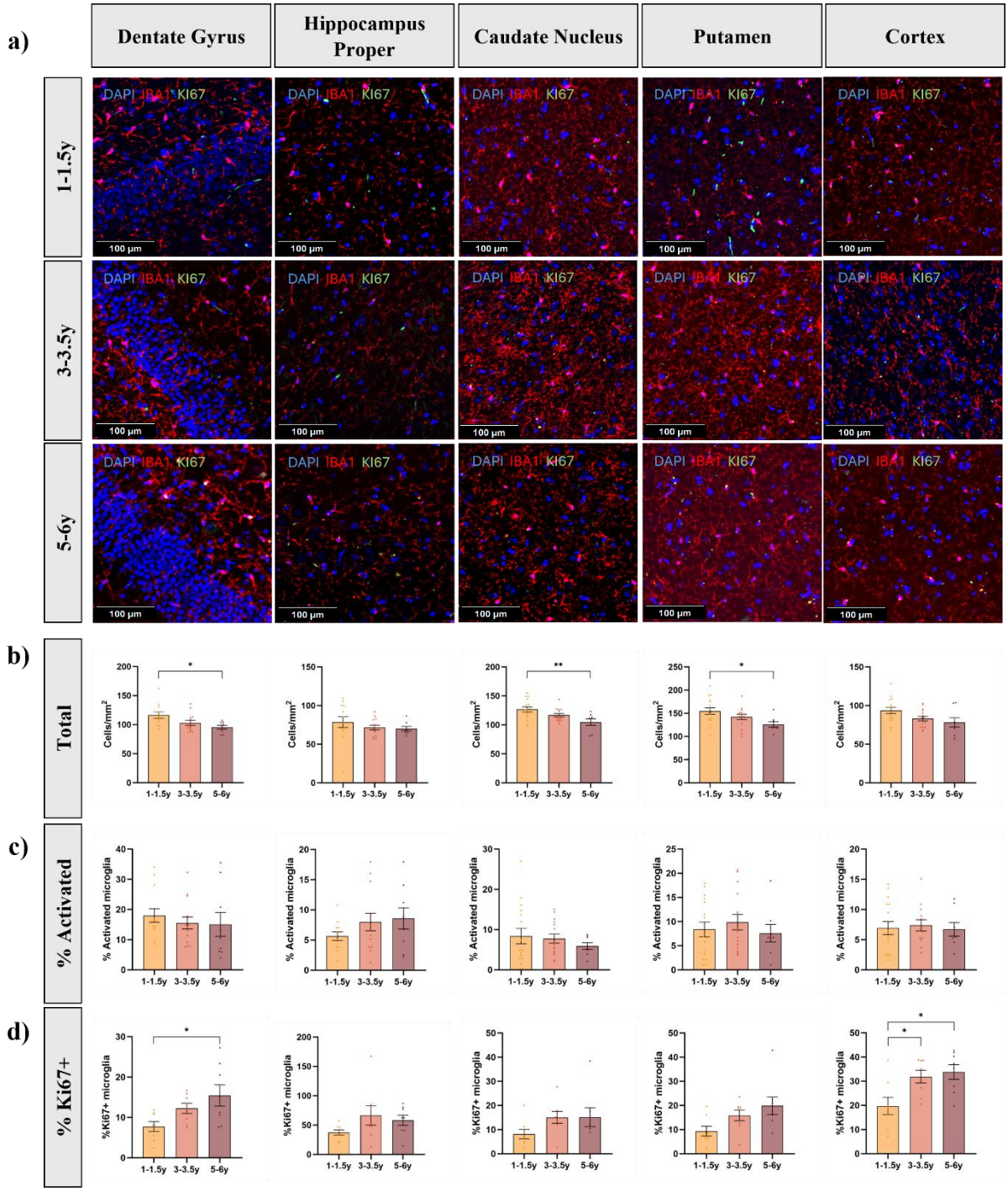


Figure 4.4: Microglia counts in the sheep brain. a) Representative merged images of microglia (red) in different regions of the sheep brain at each age. IBA1$^+$ cells with a strong Ki67 signal (green) were classified as Ki67$^+$ microglia. Individual channels are shown in S4.1.5, 4.1.6, 4.1.7, 4.1.8, 4.1.9. b) Total number of microglia c) percentage of activated microglia and d) percentage of Ki67$^+$ microglia were manually counted and graphed as mean±SEM. Significant differences determined by one-way ANOVA and Tukey post hoc testing. * = p<0.05, ** = p<0.01.

4.4.2 Microglial proliferation increases with age in the hippocampus of rats, and the cortex of both species

Brain tissue from rats (n=24) and sheep (n=24) were fluorescently stained for DAPI, IBA1 and Ki67. By colocalising these three markers, proliferating microglia were identified and manually counted. Analysis of the percentage of the microglia population positive for Ki67 in rat tissue by one-way ANOVA revealed a significant effect of age in the cortex *(F(3,27)= 9.317, p = <0.001),* hippocampus *(F(3,25)= 5.886, p = 0.003)* and striatum *(F(3,27)= 4.639, p = 0.009).* Tukey post-hoc testing revealed a significant increase in the percentage of $Ki67^+$ microglia from 3mths to 13mths in the striatum *(1.17±1.1 vs 9.09±5.02, p = 0.01),* to both 13mths *(0.60±0.79 vs 19.59±10.09, p = >0.0001)*, and 19mths *(0.60±0.79 vs 12.62±8.92, p = 0.01)* in the cortex, and at all three timepoints in the hippocampus (13mth*: 1.4±2.13 vs 6.3±3.76, p = 0.006*; 15mths: *1.4±2.13 vs 10.31±5.04, p = 0.03*; 19mths: *1.4±2.13 vs 6.26±2.48, p = 0.009)* (Fig 4.3d).

Analysis of percentage $Ki67^+$ microglia in sheep tissue by one-way ANOVA revealed a significant effect of age in the cortex *(F(2,21)= 6.104, p = 0.008),* the DG *(F(2,21)= 4.483, p = 0.023),* and the PUT*(F(2,20)= 3.916, p = 0.036),* but not in either the HP *(F(2,21)= 1.338, p = 0.284)* or CN *(F(2,18)= 3.158, p = 0.066).* Tukey post-hoc testing revealed no significant differences between groups in the PUT. But there was a significant increase compared to 1-1.5y at both 3-3.5y *(19.72±10.10 vs 31.9±7.4. p = 0.028)* and 5-6y *(19.72±10.10 vs 33.78±8.5, p = 0.011)* in the cortex, and at 5-6y *(7.74±3.43 vs 15.44±7.46, p = 0.018)* in the DG (Fig 4.4d).

Table 4.4: Linear mixed effects modelling of microglial morphological analyses in rat brain tissue. Individual microglia were isolated from each animal (n=10 per region) and analysed on ImageJ as described in Figure 4.2 to obtain cell area, number of branches, mean branch length per cell and soma area. Individual cell data were analysed using linear mixed effects modelling within the cortex, hippocampus and striatum. Models contained a fixed effect of age, and a random intercept of animal ID. 3mth groups were used as a baseline comparison group (indicated by *), alpha was set at 0.05, significant values are bolded. Graphical representations of data are shown in S3.

Cortex

	Cell Area (µm)			**Mean Number of Branches**			**Mean Branch Length (µm)**			**Soma Area (µm)**		
Predictors	*Estimates*	*CI*	*p*	*Estimates*	*CI*	*p*	*Estimates*	*CI*	*p*	*Estimates*	*CI*	*p*
3-Months *	189.52	170.01 – 209.02	**<0.001**	21.67	19.95 – 23.38	**<0.001**	6.12	5.55 – 6.69	**<0.001**	77.94	70.86 – 85.03	**<0.001**
13-Months	-16.20	-46.00 – 13.60	0.286	-6.86	-9.47 – -4.24	**<0.001**	1.58	0.71 – 2.45	**<0.001**	0.88	-9.94 – 11.71	0.872
15-Months	-58.12	-87.06 – -29.19	**<0.001**	-10.95	-13.49 – -8.40	**<0.001**	1.84	0.99 – 2.69	**<0.001**	-6.43	-16.94 – 4.08	0.230
19-Months	14.04	-14.89 – 42.98	0.341	-6.53	-9.07 – -3.98	**<0.001**	1.96	1.11 – 2.80	**<0.001**	18.97	8.45 – 29.48	**<0.001**
Random Effects												
σ^2	2905.70			50.43			5.25			512.72		
τ_{00}	891.22_{ID}			4.08_{ID}			0.49_{ID}			104.72_{ID}		
ICC	0.23			0.07			0.08			0.17		
N	41_{ID}			41_{ID}			41_{ID}			41_{ID}		
Observations	410			410			410			410		
Marginal R^2 / Conditional R^2	0.161 / 0.358			0.235 / 0.292			0.107 / 0.183			0.124 / 0.273		

Hippocampus

	Cell Area (µm)			**Mean Number of Branches**			**Mean Branch Length (µm)**			**Soma Area (µm)**		
Predictors	*Estimates*	*CI*	*p*	*Estimates*	*CI*	*p*	*Estimates*	*CI*	*p*	*Estimates*	*CI*	*p*
3-Months *	183.50	155.65 – 211.35	**<0.001**	19.10	16.89 – 21.31	**<0.001**	6.59	6.08 – 7.10	**<0.001**	75.56	65.15 – 85.97	**<0.001**
13-Months	34.71	-6.81 – 76.23	0.101	0.23	-3.06 – 3.53	0.889	0.11	-0.65 – 0.87	0.779	12.02	-3.50 – 27.54	0.128
15-Months	-24.86	-67.78 – 18.06	0.255	-3.90	-7.31 – -0.49	**0.025**	0.34	-0.45 – 1.12	0.400	-2.99	-19.03 – 13.05	0.714

19-Months	34.68	-5.68 – 75.04	0.092	0.81	-2.40 – 4.02	0.620	0.11	-0.63 – 0.84	0.776	9.40	-5.69 – 24.49	0.221
Random Effects												
σ^2	4222.72			72.75			4.47			609.49		
τ_{00}	1784.68 $_{ID}$			6.65 $_{ID}$			0.29 $_{ID}$			247.40 $_{ID}$		
ICC	0.30			0.08			0.06			0.29		
N	38 $_{ID}$			38 $_{ID}$			38 $_{ID}$			38 $_{ID}$		
Observations	380			380			380			380		
Marginal R^2 / Conditional R^2	0.089 / 0.360			0.037 / 0.118			0.003 / 0.063			0.042 / 0.319		

Striatum

	Cell Area (µm)			**Mean Number of Branches**			**Mean Branch Length (µm)**			**Soma Area (µm)**		
Predictors	*Estimates*	*CI*	*p*	*Estimates*	*CI*	*p*	*Estimates*	*CI*	*p*	*Estimates*	*CI*	*p*
3-Months *	188.15	169.65 – 206.64	**<0.001**	22.80	20.98 – 24.62	**<0.001**	6.17	5.69 – 6.65	**<0.001**	72.82	66.64 – 79.01	**<0.001**
13-Months	-11.87	-38.74 – 15.00	0.386	-6.34	-9.00 – -3.69	**<0.001**	0.84	0.14 – 1.54	**0.018**	1.88	-7.10 – 10.87	0.681
15-Months	-42.43	-68.59 – -16.28	**0.002**	-8.15	-10.73 – -5.57	**<0.001**	0.91	0.23 – 1.59	**0.009**	-6.95	-15.70 – 1.80	0.119
19-Months	-2.63	-28.79 – 23.52	0.843	-5.66	-8.24 – -3.08	**<0.001**	1.21	0.53 – 1.89	**0.001**	6.66	-2.08 – 15.41	0.135
Random Effects												
σ^2	3189.51			65.49			6.00			416.67		
τ_{00}	565.78 $_{ID}$			2.06 $_{ID}$			0.00 $_{ID}$			57.29 $_{ID}$		
ICC	0.15			0.03						0.12		
N	39 $_{ID}$			39 $_{ID}$			39 $_{ID}$			39 $_{ID}$		
Observations	390			390			390			390		
Marginal R^2 / Conditional R^2	0.072 / 0.212			0.123 / 0.150			0.033 / NA			0.049 / 0.164		

Table 4.5: Linear mixed effects models of Sholl analysis in rat brain tissue. Individual microglia were isolated from each animal (n=10 per region) and images underwent Sholl analysis on ImageJ, as described in Figure 4.2, to obtain a metric of branching complexity. Individual cell data were analysed using linear mixed effects modelling within the cortex,

hippocampus and striatum. Models contained a fixed effect of age, random intercepts of animal ID and distance from cell body. 3mth groups were used as a baseline comparison group, (indicated by *), alpha was set at 0.05, significant values are bolded. Graphical representations of data are shown in S3.

	Cortex			**Hippocampus**			**Striatum**		
Predictors	*Estimates*	*CI*	*p*	*Estimates*	*CI*	*p*	*Estimates*	*CI*	*p*
3-Months *	2.23	1.42 – 3.05	**<0.001**	1.98	1.07 – 2.89	**<0.001**	2.36	1.42 – 3.31	**<0.001**
13-Months	-0.46	-0.76 – -0.17	**0.002**	0.07	-0.22 – 0.36	0.626	-0.26	-0.59 – 0.07	0.126
15-Months	-0.85	-1.14 – -0.56	**<0.001**	-0.16	-0.46 – 0.14	0.307	-0.57	-0.89 – -0.26	**<0.001**
19-Months	-0.32	-0.61 – -0.04	**0.027**	0.09	-0.19 – 0.37	0.527	-0.09	-0.40 – 0.23	0.582
Random Effects									
σ^2	1.76			2.22			2.19		
τ_{00}	0.10_{ID}			0.09_{ID}			0.11_{ID}		
	1.05_{Radius}			1.29_{Radius}			1.24_{Radius}		
ICC	0.40			0.38			0.38		
N	7_{Radius}			7_{Radius}			6_{Radius}		
	41_{ID}			38_{ID}			38_{ID}		
Observations	4241			3975			3815		
Marginal R^2 / Conditional R^2	0.030 / 0.414			0.002 / 0.384			0.014 / 0.390		

4.4.3 Microglia in the rat brain display altered branch dynamics in the cortex and striatum, but not the hippocampus, with age

Linear mixed effects models were employed to understand the effect of age on microglial morphology. Results from models are presented in Table 4.4 for area and skeletal analyses, and Table 4.5 for Sholl analysis. Models used the 3mth group as a baseline category and included a fixed effect of age and random intercepts for animal ID, and in Sholl analysis, distance, which was operationalised as increments of 10µm.

Microglia in the cortex of 15mth animals were significantly smaller than those from 3mth animals *(Est = -58.12, 95% CI [-87.06, -29.19], p = <0.001).* However, the total area of microglia in 13mth *(Est = 14, 95% CI [-14.89, 42.98], p = 0.341)* and 19mth *(Est = 14.04, 95% CI [-14.89, 42.98], p = 0.341)* animals did not differ from 3mths. No changes were observed in soma area at 13mth *(Est = 0.88, 95% CI [-9.94, 11.71], p = 0.872)* or 15mth *(Est = -6.43, 95% CI [-16.94, 4.08], p = 0.230),* but at 19mth, soma area was increased compared to 3mth *(Est = 18.97, 95% CI [8.45, 29.48], p = <0.001)*. The number of branches decreased in 13mth *(Est = -6.86, 95% CI [-9.47, -4.24], p = <0.001)*, 15mth *(Est = -10.95, 95% CI [-13.49, -8.40], p = <0.001)* and 19mth *(Est = -6.53, 95% CI [-9.07, -3.98], p = <0.001)* animals compared to in 3mth animals, while the length of microglial branches increased at all timepoints compared to 3mths (13mth *(Est = 1.58, 95% CI [0.71, 2.45], p = <0.001);* 15mth *(Est = 1.84, 95% CI [0.99, 2.69], p = <0.001);* 19mth *(Est = 1.96, 95% CI [1.11, 2.80], p = <0.001)*). Sholl analysis demonstrated that the number of intercepts at each concentric circle was decreased at 13mths *(Est = -0.46, 95% CI [-0.76, -0.17], p = 0.002),* 15mths *(Est = -0.85, 95% CI [-1.17, -0.56], p = <0.001)* and 19mths *(Est = -0.32, 95% CI [-0.61, -0.04], p = 0.027)* compared to 3mth animals, suggesting a decrease in branching complexity within the cortex with age.

In the hippocampus, no morphological changes were observed at any age (Tables 4.4 and 4.5), with the exception of the number of branches, which decreased at 15mths compared to 3mths *(Est = -3.90, 95% CI [-7.31, -0.49], p = 0.025)*.

In the striatum, no changes in soma area were observed at any age (Table 4.4) and while a decrease in total cell area was seen at 15mths *(Est = -42.43, 95% CI [-68.59, -16.28], p = 0.002),* no changes were

seen at either 13mths *(Est = -11.87, 95% CI [-38.74, 15], p = 0.386)* or 19mths *(Est = -2.63, 95% CI [-28.79, 23.52], p = 0.843)* compared to 3mths. The number of branches was decreased at all timepoints compared to 3mths (13mth *(Est = -6.34, 95% CI [-9, -3.69], p = <0.001);* 15mth *(Est = -8.15, 95% CI [-10.73, -5.57], p = <0.001);* 19mth *(Est = -5.66, 95% CI [-8.24, -3.08], p = <0.001)*), whilst branch length was increased at all timepoints (13mth *(Est = 0.84, 95% CI [014, 1.54], p = 0.018),* 15mth *(Est = 0.91, 95% CI [0.23, 1.59], p = 0.009);* 19mth *(Est = 1.21, 95% CI [0.53, 1.89], p = 0.001)*). Sholl analysis demonstrated that the number of intercepts at each concentric circle, and, thus branching complexity, was decreased at 15mths *(Est = -0.46, 95% CI [-0.76, -0.17], p = 0.002),* compared to at 3mths. However, no significant changes were observed at either 13mths *(Est = -0.26, 95% CI [-0.59, 0.07], p = 0.126)* or 19mths *(Est = -0.09, 95% CI [-0.40, 0.23], p = 0.582)*. Graphical representations of all morphological data are presented in S3.

Table 4.6:Linear mixed effects modelling of microglial morphological analyses in sheep brain tissue. Individual microglia were isolated from each animal (n=10 per region) and analysed on ImageJ, as described in Figure 4.2, to obtain cell area, number of branches, mean branch length per cell and soma area. Individual cell data were analysed using linear mixed effects modelling within the cortex, dentate gyrus, hippocampus proper, caudate nucleus and putamen. Models contained a fixed effect of age, and a random intercept of animal ID. 1-1.5y groups were used as a baseline comparison group, (indicated by *), alpha was set at 0.05, significant values are bolded. Graphical representations of data are shown in Supplementary figure S4.1.4.

Cortex

	Cell Area (µm)			**Mean Number of Branches**			**Mean Branch Length (µm)**			**Soma Area (µm)**		
Predictors	*Estimates*	*CI*	*p*	*Estimates*	*CI*	*p*	*Estimates*	*CI*	*p*	*Estimates*	*CI*	*p*
1-1.5 Years *	144.12	131.12 – 157.12	**<0.001**	9.57	8.22 – 10.92	**<0.001**	8.45	7.54 – 9.35	**<0.001**	70.76	60.39 – 81.14	**<0.001**
3-3.5 Years	1.18	-17.35 – 19.72	0.900	0.11	-1.81 – 2.04	0.907	0.70	-0.60 – 2.00	0.288	7.10	-7.29 – 21.49	0.333
5-6 Years	12.51	-10.02 – 35.04	0.276	-0.57	-2.91 – 1.77	0.630	1.13	-0.44 – 2.70	0.156	7.72	-10.57 – 26.01	0.407
Random Effects												
σ^2	2740.66			33.01			27.18			383.19		
τ_{00}	426.87_{ID}			4.25_{ID}			0.67_{ID}			430.97_{ID}		
ICC	0.13			0.11			0.02			0.53		
N	39_{ID}			39_{ID}			39_{ID}			39_{ID}		
Observations	390			390			390			390		
Marginal R^2 / Conditional R^2	0.007 / 0.141			0.002 / 0.116			0.007 / 0.031			0.016 / 0.537		

Dentate Gyrus

	Cell Area (µm)			**Mean Number of Branches**			**Mean Branch Length (µm)**			**Soma Area (µm)**		
Predictors	*Estimates*	*CI*	*p*	*Estimates*	*CI*	*p*	*Estimates*	*CI*	*p*	*Estimates*	*CI*	*p*
1-1.5 Years *	164.87	149.67 – 180.07	**<0.001**	15.14	13.26 – 17.02	**<0.001**	7.63	6.79 – 8.47	**<0.001**	64.66	59.48 – 69.84	**<0.001**
3-3.5 Years	4.03	-17.08 – 25.14	0.708	1.51	-1.10 – 4.12	0.255	0.01	-1.16 – 1.18	0.983	-1.09	-8.28 – 6.10	0.766
5-6 Years	15.48	-8.25 – 39.21	0.200	1.44	-1.49 – 4.37	0.334	-0.30	-1.61 – 1.02	0.657	1.08	-7.00 – 9.17	0.792
Random Effects												

σ^2	4276.08	82.94	19.14	320.24
τ_{00}	349.31 $_{ID}$	3.58 $_{ID}$	0.47 $_{ID}$	58.09 $_{ID}$
ICC	0.08	0.04	0.02	0.15
N	36 $_{ID}$	36 $_{ID}$	36 $_{ID}$	36 $_{ID}$
Observations	361	361	361	361
Marginal R^2 / Conditional R^2	0.008 / 0.083	0.006 / 0.047	0.001 / 0.025	0.002 / 0.155

Hippocampus Proper

	Cell Area (µm)			Mean Number of Branches			Mean Branch Length (µm)			Soma Area (µm)		
Predictors	*Estimates*	*CI*	*p*	*Estimates*	*CI*	*p*	*Estimates*	*CI*	*p*	*Estimates*	*CI*	*p*
1-1.5 Years *	178.50	160.84 – 196.16	**<0.001**	16.58	14.05 – 19.10	**<0.001**	7.45	6.86 – 8.04	**<0.001**	67.86	63.39 – 72.33	**<0.001**
3-3.5 Years	0.18	-22.97 – 23.33	0.988	0.54	-2.73 – 3.80	0.747	0.02	-0.77 – 0.80	0.965	1.00	-4.91 – 6.90	0.740
5-6 Years	6.31	-20.53 – 33.16	0.644	-0.06	-3.87 – 3.75	0.975	0.08	-0.82 – 0.98	0.860	1.75	-5.07 – 8.57	0.614
Random Effects												
σ^2	4405.12			79.55			5.96			308.91		
τ_{00}	746.37 $_{ID}$			17.01 $_{ID}$			0.67 $_{ID}$			43.54 $_{ID}$		
ICC	0.14			0.18			0.10			0.12		
N	36 $_{ID}$			36 $_{ID}$			36 $_{ID}$			36 $_{ID}$		
Observations	360			360			360			360		
Marginal R^2 / Conditional R^2	0.001 / 0.146			0.001 / 0.177			0.000 / 0.101			0.001 / 0.125		

Caudate Nucleus

	Cell Area (µm)			Mean Number of Branches			Mean Branch Length (µm)			Soma Area (µm)		
Predictors	*Estimates*	*CI*	*p*	*Estimates*	*CI*	*p*	*Estimates*	*CI*	*p*	*Estimates*	*CI*	*p*
1-1.5 Years *	178.99	122.67 – 235.31	**<0.001**	17.73	15.04 – 20.42	**<0.001**	6.63	6.03 – 7.23	**<0.001**	68.39	1.38 – 135.40	**0.046**
3-3.5 Years	-9.22	-90.18 – 71.74	0.823	0.57	-3.30 – 4.44	0.773	-0.62	-1.48 – 0.25	0.160	-1.62	-97.96 – 94.71	0.974
5-6 Years	106.17	8.62 – 203.71	**0.033**	0.07	-4.59 – 4.73	0.977	-0.02	-1.06 – 1.02	0.968	112.61	-3.46 – 228.68	0.057

Random Effects				
σ^2	131271.88	76.64	6.18	185856.80
τ_{00}	0.00 $_{ID}$	22.29 $_{ID}$	0.87 $_{ID}$	0.00 $_{ID}$
ICC		0.23	0.12	
N	39 $_{ID}$	39 $_{ID}$	39 $_{ID}$	39 $_{ID}$
Observations	390	390	390	390
Marginal R^2 / Conditional R^2	0.015 / NA	0.001 / 0.226	0.012 / 0.134	0.011 / NA

Putamen

	Cell Area (µm)			**Mean Number of Branches**			**Mean Branch Length (µm)**			**Soma Area (µm)**		
Predictors	*Estimates*	*CI*	*p*	*Estimates*	*CI*	*p*	*Estimates*	*CI*	*p*	*Estimates*	*CI*	*p*
1-1.5 Years *	163.29	150.69 – 175.89	**<0.001**	16.39	14.16 – 18.61	**<0.001**	6.54	5.94 – 7.13	**<0.001**	64.10	59.60 – 68.60	**<0.001**
3-3.5 Years	-18.61	-36.72 – -0.50	**0.044**	-3.35	-6.55 – -0.15	**0.040**	0.50	-0.35 – 1.35	0.247	2.84	-3.63 – 9.30	0.389
5-6 Years	18.60	-3.23 – 40.42	0.095	-1.77	-5.63 – 2.08	0.366	1.08	0.05 – 2.10	**0.040**	9.19	1.40 – 16.98	**0.021**
Random Effects												
σ^2	3041.67			61.04			8.51			235.30		
τ_{00}	352.97 $_{ID}$			14.42 $_{ID}$			0.60 $_{ID}$			60.14 $_{ID}$		
ICC	0.10			0.19			0.07			0.20		
N	39 $_{ID}$			39 $_{ID}$			39 $_{ID}$			39 $_{ID}$		
Observations	390			390			390			390		
Marginal R^2 / Conditional R^2	0.054 / 0.152			0.029 / 0.214			0.018 / 0.082			0.038 / 0.234		

Table 4.7: Linear mixed effects models of sholl analysis in sheep brain tissue. Individual microglia were isolated from each animal (n=10 per region) and images underwent Sholl analysis on ImageJ, as described in Figure 4.2, to obtain a metric of branching complexity. Individual cell data were analysed using linear mixed effects modelling within the cortex, dentate gyrus, hippocampus proper, caudate nucleus and putamen. Models contained a fixed effect of age, random intercepts of animal ID and distance from cell body. 1-1.5y groups were used as a baseline comparison group, (indicated by *), alpha was set at 0.05, significant values are bolded. Graphical representations of data are shown in Supplementary Figure 4.1.4.

Cortex	**Dentate Gyrus**	**Hippocampus Proper**	**Caudate Nucleus**	**Putamen**

Predictors	*Estimates*	*CI*	*p*	*Estimates*	*CI*	*p*	*Estimates*	*CI*	*p*	*Estimates*	*CI*	*p*	*Estimates*	*CI*	*p*
1-1.5 Years *	1.05	0.01 – 2.09	**0.047**	0.98	0.08 – 1.88	**0.033**	1.24	0.25 – 2.23	**0.014**	1.06	-0.19 – 2.30	0.097	1.04	-0.16 – 2.25	0.089
3-3.5 Years	-0.05	-0.30 – 0.21	0.718	0.07	-0.16 – 0.29	0.570	-0.05	-0.37 – 0.28	0.772	0.04	-0.30 – 0.39	0.802	0.28	-0.03 – 0.59	0.081
5-6 Years	-0.06	-0.27 – 0.15	0.585	-0.20	-0.41 – 0.00	0.053	-0.23	-0.52 – 0.07	0.129	0.09	-0.20 – 0.37	0.548	0.25	-0.01 – 0.50	0.056
Random Effects															
σ^2	1.28			1.52			1.68			1.72			1.59		
τ_{00}	0.08_{ID}			0.07_{ID}			0.14_{ID}			0.15_{ID}			0.12_{ID}		
	1.36_{Radius}			1.64_{Radius}			1.69_{Radius}			2.36_{Radius}			1.84_{Radius}		
ICC	0.53			0.53			0.52			0.59			0.55		
N	5_{Radius}			8_{Radius}			7_{Radius}			6_{Radius}			5_{Radius}		
	39_{ID}			36_{ID}			36_{ID}			39_{ID}			39_{ID}		
Observations	5282			6541			6664			6190			5688		
Marginal R^2 / Conditional R^2	0.000 / 0.530			0.004 / 0.530			0.003 / 0.523			0.000 / 0.594			0.004 / 0.554		

4.4.4 Microglial morphology in the sheep brain is altered with age in striatal regions but remains stable in the hippocampus and cortex

Linear mixed effects models were employed to investigate the effect of age on microglial morphology in sheep tissue. Results from models are presented in Table 4.6 for area and skeletal analyses, and Table 4.7 for Sholl analysis. These models used the 1-1.5y group as a baseline category and included a fixed effect of age and a random intercept for animal ID. In Sholl analysis, distance, operationalised as increments of 10μm, was included as an additional random intercept.

Overall, morphological differences were significantly more restricted than those observed in the rat cohort. No significant changes in total microglial area, soma area, number of branches or branch length were observed in the cortex, DG or HP (Table 4.6). Similarly, there were no differences in branching complexity in any region analysed (Table 4.7). In the CN, microglia had a larger cell area in the 5-6y group compared to the 1-1.5y group *(Est = 106.17, 95% CI [8.62, 203.71], p = 0.033),* but no significant differences were seen between groups for soma size, number of branches or branch length. Within the PUT, microglia at 3-3.5y were smaller *(Est = -18.61, 95% CI [-36.72, -0.50], p = 0.044)* and had fewer branches *(Est = -3.35, 95% CI [-6.55, -0.15], p = 0.04)* than microglia at 1-1.5y. However, at 5-6y, both microglial size *(Est = 18.60, 95% CI [-3.23, 40.42], p = 0.095)* and number of branches *(Est = -1.77, 95% CI [-5.63, 2.08], p = 0.366)* were unchanged compared to 1-1.5y animals. There were, however, some differences noted at this timepoint compared to 1-1.5y animals. Specifically, at 5-6y, microglia had an increased branch length *(Est = 1.08, 95% CI [0.05, 2.10], p = 0.040)* and soma area *(Est = 9.19, 95% CI [1.40, 16.98], p = 0.021)*. Graphical representations of sheep morphological data are shown in Supplementary Figure S4.1.1. Table 4.8 summarises the observed changes from baseline (youngest age group) for each species at each age.

Table 4.8: Changes observed in microglia in the current study. Significant changes between age groups for each marker assessed are summarised below. Changes listed are in reference to the youngest age group for that species (3mths in rats, 1-1.5y in sheep). Changes between intermediate age groups are not included in this summary. hipp = hippocampus, ST = striatum, green shading with a ↑ indicates an increase, red shading with a ↓ indicates a decrease, and no shading with a dash (-) indicates no change from the youngest age group

	Rat			Sheep	
	13mth	15mth	19mth	3-3.5y	5-6y
Total number	-	↑ hipp	-	-	↓ DG, CN & PUT
% activated	↓ cortex & ST	-	↓ cortex & hipp	-	-
% Ki67^{+}	↑ cortex, hipp & ST	↑ hipp	↑ cortex & hipp	↑ cortex	↑ DG & cortex
Cell area	-	↓ cortex & ST	-	↓ PUT	↑ CN
Soma area	-	-	↑ cortex	-	↑ PUT
Number of branches	↓ cortex & ST	↓ cortex, hipp & ST	↓ cortex & ST	↓ PUT	-
Branch length	↑ cortex & ST	↑ cortex & ST	↑ cortex & ST	-	↑ PUT
Branching complexity	↓ cortex	↓ cortex & ST	↓ cortex	-	-

4.5 Discussion

The current study conducted a cross-species comparison of changes in the microglial population and morphology with age in naïve animals. To do this, archival tissue from a commonly used lissencephalic model (rat) and a large gyrencephalic model (sheep) was utilised. In the cortex and hippocampus of 19-month-old rats compared to 3-month-old rats, numbers of activated microglia decreased, but numbers of proliferating microglia increased. However, no change in total microglial numbers were observed between these groups. Cortical microglia in 19-month-old rats had a larger soma area and longer branches, but less complexity and number of branches. Conversely, in the dentate gyrus, caudate nucleus and putamen of aged sheep compared to young sheep, the total number of microglia decreased, with no changes in numbers of activated microglia detected in any region. Further, more proliferating microglia were observed in the dentate gyrus and cortex in 5-6y sheep compared to 1-1.5y. Morphological changes in microglia were only observed in striatal regions of sheep, with microglia in the putamen showing increased soma size and branch length, and microglia in the caudate nucleus showing an increase in overall size. Overall, species-specific differences were seen in both when microglia begin to acquire an aged phenotype and the regions in which this occurs, highlighting the potential translational differences of these pre-clinical models for the investigation of neuroinflammation in age-related neurological disease.

The current study found limited evidence of alterations in total number of microglia with age in the rodent brain, limited to upregulation of IBA1 in the hippocampus at 15-months compared to 3-months of age, with no differences seen at the oldest time point (i.e. 19 months of age). This is despite an increase proliferation (Ki67) observed, primarily in the hippocampus and cortex, in all older age groups compared to 3-month-old animals. Previous literature looking at the number of $IBA1^{+}$ microglia in the rat brain with age has been inconsistent. For example, one study reported that there was a 65% increase in microglial number in the auditory cortex of 30-month-old male Sprague-Dawley rats compared to 3-month-old rats (Vaughan and Peters, 1974).Conversely, microglial number in the striatum of male C57BL/6 mice has been observed to decrease at both 18mths and 24mths compared to 12mths, with no differences seen compared to 3 month-old animals (Sharaf et al., 2013), suggesting that effects may be

region specific. Age of the animals at time of assessment may also be a key contributing factor, as even the oldest cohort in this study was notably younger, at 19mths, than those used in these previous studies. This highlights an inherent limitation of using archival tissue, where research questions and data are limited by the available samples. In the case of the current study, the available tissue was not aged beyond 19mths for rats, and 6 years for sheep, limiting the ability to draw conclusions beyond this middle age timepoint. Thus, it is possible that changes in number of microglia may be more pronounced in older animals however sex-specific differences may also contribute. In line with this, in human post-mortem tissue, while an increase in number of microglia in the neocortex has been shown to occur with increasing age in females (range: 18-93 years), the same effect was not seen in males (range: 19-87 years) (Pelvig et al., 2008). Similarly, an increase in the number of $IBA1^+$ microglia has been reported in the dentate gyrus only, not in regions of the hippocampus proper, in female Fischer 344 (F344) rats at 18mths of age compared to at 3mths, differences not observed in males (Perkins et al., 2018). As the current study utilised archival tissue from a study which included only male rats, examination of sex differences in could not be assessed in this rat cohort but is an important avenue for future investigations.

To the best of our knowledge, changes in microglia in the sheep brain across the lifespan have not previously reported. Markers of AD have previously been investigated in aged sheep (n=4 8-year-old; n=1 14-year-old), where $A\beta_{1-42}$ and total/phosphorylated Tau proteins were detectable in sheep CSF, and Aβ plaques and Tau neurofibrillary tangles were present within the brain (Reid et al., 2017). This study did not investigate glial reactivity and neuroinflammatory mechanisms in these sheep, nor were these pathologies compared to sheep at younger ages (Reid et al., 2017). Nevertheless, the presence of AD pathological hallmarks in sheep at these ages, speaks to the homology of sheep and human brains in patterns of protein accumulation with age. In the current study, we observed a decrease in the number of microglia in multiple regions (i.e. the DG, CN and PUT) at 5-6y compared to 1-1.5y of age. Given that studies in rats and humans have shown sex differences in the number of microglia with age, it is conceivable that the imbalance of sex in our 5-6y sheep may have impacted these results. Although, based on previous studies in rats and human tissue discussed above (Pelvig et al., 2008; Perkins et al.,

2018), the high proportion of females to males might be expected to lead to higher, not lower, numbers of total microglia within the 5-6y group. Analysis of data stratified into male, and females is presented in the Supporting Information document (see Supplementary Figure S4.1.10 and Supplementary Table S4.1.1), however due to the aforementioned imbalance of sex in the oldest age group (2M:8F for IBA1 analysis and 0M:8F in the Ki67 analysis) no conclusions regarding the effect of sex on microglia can be drawn from these results. Of note, the male to female ratio in the Ki67 analysis (0M:8F) was due to the quality of tissue from male sheep causing these animals to be excluded from this analysis. Regardless, the pattern of change observed in sheep was unexpected, as microglia are known to increase in number and take on a more surveillant phenotype, as they age (Perry and Holmes, 2014). This is also surprising, given that a marker of proliferation (Ki67) was increased in sheep within the dentate gyrus (and cortex), although not within the caudate and putamen, at the same timepoint. It is unclear what might account for the differences observed here between rats and sheep, but future studies should seek to investigate the mechanisms that may underlie this discrepancy and probe what the translational significance of this might be for preclinical modelling.

A discrepancy in the percentage of activated microglia was also observed between rats and sheep in the current work. Specifically, while a decrease was noted in several regions in both 13- and 19-month-old rats compared to 3-month-old animals, there were no differences seen between any age groups in sheep. This is in contrast to previous literature, where microglial activation, as measured by MHCII induction, has been reported to increase with age in multiple species, including C57BL/6 mice (22- to 24-months-old compared to mice at 3- to 5-months-old) (Garner et al., 2018), Lister Hooded rats (25- to 30-months-old compared to 3- to 6-months-old) (Perry et al., 1993), macaques (11- to 19-years old compared to juveniles (2- to 5-years)) (Sheffield and Berman, 1998). Additionally, in humans the positron emission tomography (PET) ligand (R)-[^{11}c]PK111955, which specifically binds to activated microglia expressing the 18 kDa translocator protein (TSPO) has shown an association between increasing age and enhanced ligand binding throughout the brain in a cohort aged 19- to 79-years-old (22M:11F) (Shah et al., 1994). Similarly, previous studies determining activation state based on the presence of amoeboid morphology, have also reported increases in the dentate gyrus of aged female Wistar rats at 23-months-

old (Viana et al., 2013), as well as in cultured microglia harvested from the cortex of 30-month-old male F344 rats (Rozovsky et al., 1998). Amoeboid/reactive microglia have also been shown to be the dominant microglial phenotype in the aged brain in human post-mortem tissue (Franco-Bocanegra et al., 2021). It may be that the animals used in the current study were simply too young to see any age-related changes. Though given their different rates of development human age is not linear with rat or sheep age, approximate equivalent ages can be discerned based on female reproductive milestones in each species. Figure 4.5 displays an estimation of comparable ages across species based on these milestones in humans (Liu and Gao, 2023), rats (Sengupta, 2013) and sheep (Creveling et al., 2018; Lévy et al., 2017). Based on these estimates, the 19-month-old rats and 5-6-year-old sheep used in the current study were roughly equivalent to 55-year-old humans. Further, the 13-month-old rats and 3-3.5-year-old sheep were roughly equivalent late 20s or early 30s in humans. Thus, the results of the current study may be more reflective of changes associated with "middle age" (or even earlier) than those associated with older adulthood. Of note, studying these processes in animals at older ages is logistically and financially difficult, particularly for large animals such as sheep or for groups where access to aged rodent colonies is not readily available. Further, region-specific differences may be reflective either of natural regional variation throughout the lifespan or could indicate regions of particular vulnerability. In line with this, previous literature has suggested that both the striatum and hippocampus are both vulnerable to a variety of insults, including the effects of microglial driven neuroinflammation (Choi et al., 2009; Davidson and Stevenson, 2024; Mitchell et al., 1999; Nishino et al., 2000; Pearson-Leary et al., 2017). Alternatively, it is possible that some of the discrepancy observed could be attributable to the way in which microglia were classified. Manual counting of activated microglia based on morphology has been shown to vary greatly, making it hard to generalise results across studies (Khakpour et al., 2022). Here, a strict criterion for activation was used, with only cells showing an amoeboid morphology counted as activated. In contrast, other studies have classified cells as activated based on size and process measurements (Torres-Platas et al., 2014), which could potentially contribute to the differences observed. Additionally, the use of image-based manual cell counting in the current study introduces subjectiveness to the analysis and may impact the ability to compare results to previous

studies utilising more objective measures such as AI driven (Choi et al., 2022; Möhle et al., 2021) or stereological analysis (Long et al., 1998; Perkins et al., 2018).

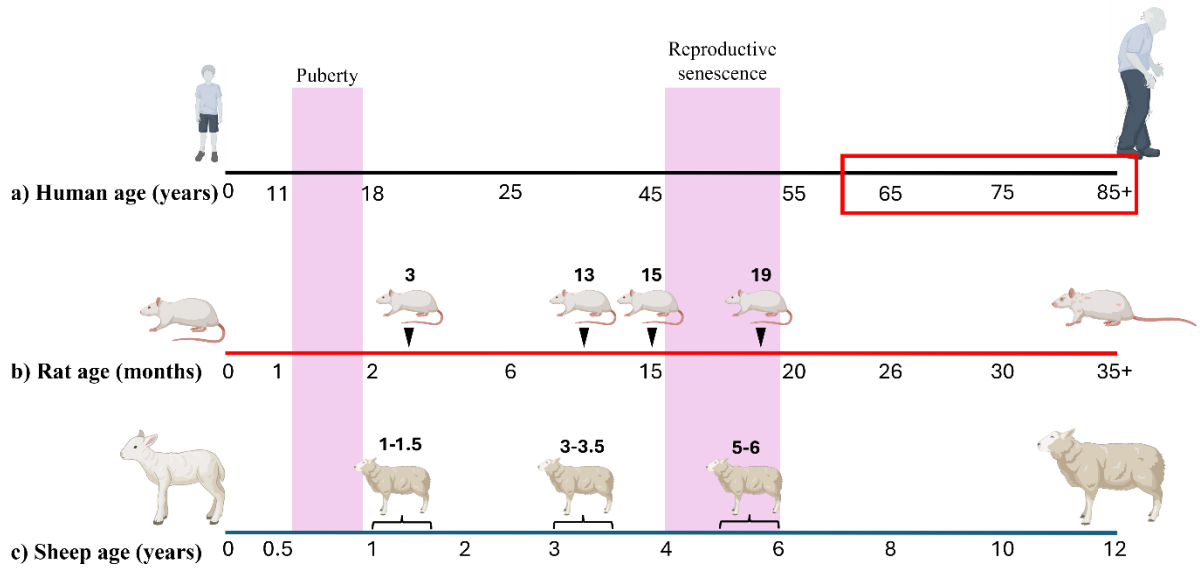


Figure 4.5: Visual representation of human ageing compared to the pre-clinical animal models used in the current study.The red box indicates the age at which neurodegenerative diseases are most prominent. Comparative ages are estimates based on female reproductive milestones in each species. Ages utilised in the current cohort are indicated for b) rats and c) sheep.

Unlike the species-specific differences observed for both total number and percent of activated microglia, the morphometric changes observed in microglia across timepoints were largely consistent between rats and sheep. One exception to this was for cell area- while a decrease was seen in both 15-month-old rats in the cortex and striatum and in 3-3.5y sheep in the putamen, an increase was seen in the caudate nucleus of 5–6-year-old sheep, compared to the youngest age group for each species. Similarly, while decreases in branching complexity were seen, mainly within the cortex, in rats of all three older age groups compared to 3-month-old animals, no significant differences were observed in either 3-3.5- or 5–6-year-old sheep when compared to 1-1.5-year-old sheep. As discussed above, the mechanisms that might account for these species-specific differences are unclear, and these may be reflective of normal variation across the lifespan between the two species, rather than specific age-related effects. A similar pattern was observed between species for soma area, where an increase in size was seen in the oldest group of rats and sheep, albeit in different regions (cortex for rats vs. putamen for sheep). This is in line with previous literature, which has shown that an increase in microglial soma area occurs with age in the CA3 region of 18-month-old male and female F344 rats (Perkins et al.,

2018), although it is important to note that we did not observe any overall changes in soma size in the hippocampus here. Conversely, a decrease in the number of branches, and a concomitant increase in branch length, was found in the cortex and striatum of rats and in the putamen in sheep. This in in contrast with a previous study by Viana et al., which reported that the number of trees (branching structures) per cell were increased in the molecular layer of the dentate gyrus of 23-month-old male Wistar rats compared to rats at 4-months-old (Viana et al., 2013). This discrepancy may be accounted for by the differences in methods of microglial reconstruction and analysis. Here a manual method of microglia isolation from 5µm thick tissue was utilised and measurements conducted in ImageJ. However, Viana et al., used tissue cut at 70µm allowing for 3D reconstruction of the microglia on using software for cell reconstruction. While the morphological characterisation in the current study likely does not capture the full picture of microglia due to limitations of the tissue thickness and simple 2D analysis, these results still provide insight into the dynamics of microglia with age. Thus, it is important to keep this in mind when comparing these results to previous studies which have utilised 3D reconstruction or other differing analytical approaches. Overall, the morphology observed here was more reflective of a reactive/intermediate morphology of microglia, with fewer (but longer) branches and less complex branching structure (Green and Rowe, 2024). This is interesting, especially as there was a region-specific decrease in the percentage of activated microglia in rats, and no change in percentage of activated microglia in sheep.

In the current study, an increase in proliferation, as measured by Ki67, was reported across all older age groups of both rats and sheep. These changes were largely confined to the cortex and hippocampus, with an increase in proliferation in the striatum only noted in 13-month-old rats. While this increase in proliferation in conjunction with largely unchanged numbers of total microglia (and indeed decreases in total number in the dentate gyrus, caudate and putamen of 5–6-year-old sheep) seems contradictory, a potential mechanism behind this may reflect vulnerability of these regions to microglial pyroptosis. Pyroptosis is a form of cell death referring specifically to cell death due to inflammatory mechanisms (Zhou et al., 2023), often associated with activation of the NLRP3 inflammasome pathway, with pyroptotic signalling occurring mainly through caspase pathway activation (Zhou et al., 2023). Multiple

NLRP3 pathway proteins, including ASC, caspase-1, IL-18 and NLRC4, were increased in the hippocampus and cortex of 18-mo old male BALB/c mice compared to 3-mo mice (Mejias et al., 2018). In these regions there was also an increase in microglial pyroptosis, supporting the notion of a role for increased NLRP3 signalling in pyroptotic cell death (Mejias et al., 2018). Further, loss of NLRP3 signalling appears to attenuate microglial activation during ageing. This is evidenced by a study demonstrating decreased microglial activation in the DG of 23-mo NLRP3$^{-/-}$ mice, compared to aged matched genetic controls and to 2-mo NLRP3$^{-/-}$ mice (Youm et al., 2013). Further, microglial pyroptosis has been suggested to contribute to the development of multiple age-related neurological conditions, including AD (Friker et al., 2020), PD (Mao et al., 2017) and stroke (Xu et al., 2019) (see review: (Wu et al., 2022)), it is possible that pyroptosis could affect the results of the current study. This could lead to seemingly maintained (or even decreased) numbers of total microglia, even in the face of ongoing proliferation, with the potential that these proliferation rates may be increased in relation to younger animals in a compensatory fashion. In order to assess this, future studies should assess markers of both key neuroinflammatory pathways (e.g. NLRP3 inflammasome activation), as well as markers of microglial cell death such as cleaved caspase-3 or cytokeratin-18 (Ward et al., 2008).

Of note, regional differences in microglia were evident between species. With the exception of proliferation, changes in sheep were restricted to subcortical regions and were not seen in the cortex itself. In contrast, microglial alterations in rats were observed both subcortically and cortically. This may indicate that age-related alterations in microglia progress more rapidly in small animals compared to large animals, which is likely given the length of the rat lifespan compared to that of sheep or humans (Fig 4.5). Alternatively, differences in the structure of the cortex between species may play a role, for example, in addition to being lissencephalic, the rat cortex is much thinner, with less a complex cortical architecture (Haghir et al., 2024) than sheep (Peruffo et al., 2019) and humans (Cho et al., 2016). Further, the overall size of the rat brain (1-2g) is smaller than that of sheep (130-140g) and humans (1.3-1.4kg) (Murray and Mitchell, 2022), and thus the connectivity and composition of each cortical layer is different to that seen in gyrencephalic brains (Xu et al., 2022). For example, the rat cortex consists mainly of mesocortical areas, whereas in humans and rhesus macaques, isocortical areas make

up a significant portion of the cortex (García-Cabezas et al., 2023). When comparing the sheep isocortex to that in humans, sheep appear to lack a defined layer 4, a region important for receiving thalamic input (Peruffo et al., 2019). Such differences may drive the variations observed in the current study whereby differential structure of neuronal layers in the cortex, could impact the scale of microglial recruitment to the area and by analysing inconsistent cortical areas in sheep, may therefore yield results inconsistent with literature. Whether this is reflective of actual differences between species, however, or simply an experimental artifact, requires further investigation of microglial distribution within the cortex across species.

Beyond anatomical differences, it is also important to note that the different sizes of the rat versus sheep brain contributed to a difference in the percentage of total area analysed in the present study. While, overall, a larger area in the sheep cortex was analysed, this represented a smaller percentage of the overall cortical area compared to rats. This could have led to the results not capturing the full extent of microglia number and morphology in the cortex. For example, when placing boxes for counting, it was prioritised that they be from a range of areas (i.e. not all from the base of the sulci). Although this was done to gain a wider representation of microglia within the cortex, there may be subtle changes within specific areas with age that were not captured using this method. For example, changes in microglia in chronic traumatic encephalopathy (CTE) have been shown to be most evident at the depths of the sulci, with more activated microglia in this area in the vicinity of pathological inclusions (Cherry et al., 2016). Such regional variation would be underestimated using our current method. To overcome this, future studies could perform a full analysis of the entire region of interest, but the benefits of this must be weighed against the time-consuming nature of such an intensive analysis method.

Investigating what stages in life microglia begin to acquire a more inflammatory phenotype is crucial in understanding the biological mechanisms that underlie age-related neurological disorders. By examining the time course of microglial change across the lifespan in different species, future models can work to incorporate these features, improving their translatability. Taken together, the data from the current study indicate that microglia in rats begin to develop an altered phenotype as early as 13mths of age, at least within the cortex and striatum. In sheep, decreases in cell area and number of branches

in the putamen appear to reflect the dynamic states of microglia, as these remain unchanged out to 5-6y in sheep. Instead, changes in morphology similar to those seen in the cortex of rats (increased size and branch length) are seen in the putamen and caudate nucleus in older (5-6y) sheep. This suggests that age-related changes in microglia may occur earlier in rodent models compared to in large animal models which is likely considering that rodents age approximately 26.7 times faster than humans (Agoston, 2017). While this would have significant implications for the use of such models to investigate the role of neuroinflammation in the pathophysiology of age-related neurological disorders, further research is required to validate these findings. This should include the assessment of age-related microglial changes in additional small and large animal species, as well as a more thorough characterisation of microglial changes throughout the lifespan, rather than at the relatively restricted time periods assessed here. Of note, even in the oldest age groups in the current study, animals were still only around the equivalent of 55 years of age in humans. This is significant, as many age-related disorders do not manifest until around 55+ years of age, or even later (Oliveira et al., 2017), suggesting that the results of this study likely do not reflect the actions and phenotypes of microglia in these vulnerable aged populations. Instead, these results are potentially reflective of the state of microglia prior to disease diagnosis. Thus, an investigation of microglial changes between species at older ages should be a particular area of focus for future research in this area.

4.6 Conclusions

The current study presents a detailed cross-species comparison of microglial ageing across regions of the rat and sheep brain, demonstrating species specific differences in when and where microglia begin to acquire an aged phenotype. This knowledge not only presents evidence that microglial phenotype is altered with age, but also advances understanding of when such changes start to occur, providing insight into when targeting microglia driven neuroinflammation may be effective for the treatment of age-related neurological disease. Importantly the results reported here suggest that species specific differences vary by region, with microglia in the cortex remaining relatively unaffected by age in sheep, whereas prominent changes were seen in rats. This emphasises the need to investigate the cellular changes that occur with advanced age under normal physiological conditions across species, to better

understand the pathophysiological basis of age-related neurological disease and, subsequently, improve the preclinical models used to investigate disease mechanisms and treatment. Future work should also seek to compare these results to alterations in microglia that occur in both healthy ageing and neurological disease in humans to further elucidate the role of microglial ageing in the brains susceptibility to neurological disease.

4.7 Acknowledgements

This work was supported, in part, by funding from the NeuroSurgical Research Foundation and Perpetual.

4.8 References

Agoston, D.V., 2017. How to Translate Time? The Temporal Aspect of Human and Rodent Biology. Front Neurol 8, 92.

Alliot, F., Godin, I., Pessac, B., 1999. Microglia derive from progenitors, originating from the yolk sac, and which proliferate in the brain. Brain Res Dev Brain Res 117, 145-152.

Arganda-Carreras, I., Fernández-González, R., Muñoz-Barrutia, A., Ortiz-De-Solorzano, C., 2010. 3D reconstruction of histological sections: Application to mammary gland tissue. Microscopy Research and Technique 73, 1019-1029.

Asher, S., Priefer, R., 2022. Alzheimer's disease failed clinical trials. Life Sciences 306, 120861.

Askew, K., Li, K., Olmos-Alonso, A., Garcia-Moreno, F., Liang, Y., Richardson, P., Tipton, T., Chapman, M.A., Riecken, K., Beccari, S., Sierra, A., Molnár, Z., Cragg, M.S., Garaschuk, O., Perry, V.H., Gomez-Nicola, D., 2017. Coupled Proliferation and Apoptosis Maintain the Rapid Turnover of Microglia in the Adult Brain. Cell Reports 18, 391-405.

Bates, D., Mächler, M., Bolker, B., Walker, S., 2015. Fitting Linear Mixed-Effects Models Using lme4. Journal of Statistical Software 67, 1 - 48.

Boehme, A.K., Esenwa, C., Elkind, M.S., 2017. Stroke Risk Factors, Genetics, and Prevention. Circ Res 120, 472-495.

Boltze, J., Förschler, A., Nitzsche, B., Waldmin, D., Hoffmann, A., Boltze, C.M., Dreyer, A.Y., Goldammer, A., Reischauer, A., Hartig, W., Geiger, K.D., Barthel, H., Emmrich, F., Gille, U., 2008. Permanent Middle Cerebral Artery Occlusion in Sheep: A Novel Large Animal Model of Focal Cerebral Ischemia. Journal of Cerebral Blood Flow & Metabolism 28, 1951-1964.

Bruttger, J., Karram, K., Wörtge, S., Regen, T., Marini, F., Hoppmann, N., Klein, M., Blank, T., Yona, S., Wolf, Y., Mack, M., Pinteaux, E., Müller, W., Zipp, F., Binder, H., Bopp, T., Prinz, M., Jung, S., Waisman, A., 2015. Genetic Cell Ablation Reveals Clusters of Local Self-Renewing Microglia in the Mammalian Central Nervous System. Immunity 43, 92-106.

Carr, L.M., Mustafa, S., Care, A., Collins-Praino, L.E., 2024. More than a number: Incorporating the aged phenotype to improve in vitro and in vivo modeling of neurodegenerative disease. Brain, Behavior, and Immunity 119, 554-571.

Cherry, J.D., Tripodis, Y., Alvarez, V.E., Huber, B., Kiernan, P.T., Daneshvar, D.H., Mez, J., Montenigro, P.H., Solomon, T.M., Alosco, M.L., Stern, R.A., McKee, A.C., Stein, T.D., 2016. Microglial neuroinflammation contributes to tau accumulation in chronic traumatic encephalopathy. Acta Neuropathol Commun 4, 112.

Cho, Y.T., Fudge, J.L., Ross, D.A., 2016. The Architecture of Cortex-in Illness and in Health. Biol Psychiatry 80, e95-e97.

Choi, D.Y., Liu, M., Hunter, R.L., Cass, W.A., Pandya, J.D., Sullivan, P.G., Shin, E.J., Kim, H.C., Gash, D.M., Bing, G., 2009. Striatal neuroinflammation promotes Parkinsonism in rats. PLoS One 4, e5482.

Choi, S., Hill, D., Guo, L., Nicholas, R., Papadopoulos, D., Cordeiro, M.F., 2022. Automated characterisation of microglia in ageing mice using image processing and supervised machine learning algorithms. Scientific Reports 12, 1806.

Creveling, C.J., Colter, J., Coats, B., 2018. Changes in Vitreoretinal Adhesion With Age and Region in Human and Sheep Eyes. Frontiers in Bioengineering and Biotechnology 6.

Cuadros, M.A., Coltey, P., Carmen Nieto, M., Martin, C., 1992. Demonstration of a phagocytic cell system belonging to the hemopoietic lineage and originating from the yolk sac in the early avian embryo. Development 115, 157-168.

Cuadros, M.A., Martin, C., Coltey, P., Almendros, A., Navascués, J., 1993. First appearance, distribution, and origin of macrophages in the early development of the avian central nervous system. Journal of Comparative Neurology 330, 113-129.

Dalgaard, P., 2010. R Development Core Team (2010): R: A language and environment for statistical computing.

Davidson, T.L., Stevenson, R.J., 2024. Vulnerability of the Hippocampus to Insults: Links to Blood–Brain Barrier Dysfunction. International Journal of Molecular Sciences.

Dorsey, E.R., Elbaz, A., Nichols, E., Abbasi, N., Abd-Allah, F., Abdelalim, A., Adsuar, J.C., Ansha, M.G., Brayne, C., Choi, J.-Y.J., Collado-Mateo, D., Dahodwala, N., Do, H.P., Edessa, D., Endres, M.,

Fereshtehnejad, S.-M., Foreman, K.J., Gankpe, F.G., Gupta, R., Hamidi, S., Hankey, G.J., Hay, S.I., Hegazy, M.I., Hibstu, D.T., Kasaeian, A., Khader, Y., Khalil, I., Khang, Y.-H., Kim, Y.J., Kokubo, Y., Logroscino, G., Massano, J., Mohamed Ibrahim, N., Mohammed, M.A., Mohammadi, A., Moradi-Lakeh, M., Naghavi, M., Nguyen, B.T., Nirayo, Y.L., Ogbo, F.A., Owolabi, M.O., Pereira, D.M., Postma, M.J., Qorbani, M., Rahman, M.A., Roba, K.T., Safari, H., Safiri, S., Satpathy, M., Sawhney, M., Shafieesabet, A., Shiferaw, M.S., Smith, M., Szoeke, C.E.I., Tabarés-Seisdedos, R., Truong, N.T., Ukwaja, K.N., Venketasubramanian, N., Villafaina, S., weldegwergs, K.g., Westerman, R., Wijeratne, T., Winkler, A.S., Xuan, B.T., Yonemoto, N., Feigin, V.L., Vos, T., Murray, C.J.L., 2018. Global, regional, and national burden of Parkinson's disease, 1990-2016: a systematic analysis for the Global Burden of Disease Study 2016. The Lancet Neurology 17, 939-953.

Enkhbaatar, P., Nelson, C., Salsbury, J.R., Carmical, J.R., Torres, K.E., Herndon, D., Prough, D.S., Luan, L., Sherwood, E.R., 2015. Comparison of Gene Expression by Sheep and Human Blood Stimulated with the TLR4 Agonists Lipopolysaccharide and Monophosphoryl Lipid A. PLoS One 10, e0144345.

Ferreira, T.A., Blackman, A.V., Oyrer, J., Jayabal, S., Chung, A.J., Watt, A.J., Sjöström, P.J., van Meyel, D.J., 2014. Neuronal morphometry directly from bitmap images. Nature Methods 11, 982-984.

Finnie, J., Hemsley, K., Manavis, J., Beard, H., Brealey, J., Robertson, T., Blumbergs, P., 2024. Striking and widespread microglial activation in the brains of Southdown lambs with type II glucocerebrosidosis (neuronopathic Gaucher disease). Journal of Comparative Pathology 215, 10-13.

Fisher, M., Feuerstein, G., Howells, D.W., Hurn, P.D., Kent, T.A., Savitz, S.I., Lo, E.H., 2009. Update of the Stroke Therapy Academic Industry Roundtable Preclinical Recommendations. Stroke 40, 2244-2250.

Franco-Bocanegra, D.K., Gourari, Y., McAuley, C., Chatelet, D.S., Johnston, D.A., Nicoll, J.A.R., Boche, D., 2021. Microglial morphology in Alzheimer's disease and after Aβ immunotherapy. Scientific Reports 11, 15955.

Friker, L.L., Scheiblich, H., Hochheiser, I.V., Brinkschulte, R., Riedel, D., Latz, E., Geyer, M., Heneka, M.T., 2020. β-Amyloid Clustering around ASC Fibrils Boosts Its Toxicity in Microglia. Cell Rep 30, 3743-3754.e3746.

García-Cabezas, M., Hacker, J.L., Zikopoulos, B., 2023. Homology of neocortical areas in rats and primates based on cortical type analysis: an update of the Hypothesis on the Dual Origin of the Neocortex. Brain Struct Funct 228, 1069-1093.

Garner, K.M., Amin, R., Johnson, R.W., Scarlett, E.J., Burton, M.D., 2018. Microglia priming by interleukin-6 signaling is enhanced in aged mice. Journal of Neuroimmunology 324, 90-99.

Geirsdottir, L., David, E., Keren-Shaul, H., Weiner, A., Bohlen, S.C., Neuber, J., Balic, A., Giladi, A., Sheban, F., Dutertre, C.-A., Pfeifle, C., Peri, F., Raffo-Romero, A., Vizioli, J., Matiasek, K., Scheiwe, C., Meckel, S., Mätz-Rensing, K., van der Meer, F., Thormodsson, F.R., Stadelmann, C., Zilkha, N., Kimchi, T., Ginhoux, F., Ulitsky, I., Erny, D., Amit, I., Prinz, M., 2019. Cross-Species Single-Cell Analysis Reveals Divergence of the Primate Microglia Program. Cell 179, 1609-1622.e1616.

Ginhoux, F., Greter, M., Leboeuf, M., Nandi, S., See, P., Gokhan, S., Mehler, M.F., Conway, S.J., Ng, L.G., Stanley, E.R., Samokhvalov, I.M., Merad, M., 2010. Fate mapping analysis reveals that adult microglia derive from primitive macrophages. Science 330, 841-845.

Ginhoux, F., Lim, S., Hoeffel, G., Low, D., Huber, T., 2013. Origin and differentiation of microglia. Frontiers in Cellular Neuroscience 7.

Green, T.R.F., Murphy, S.M., Rowe, R.K., 2022. Comparisons of quantitative approaches for assessing microglial morphology reveal inconsistencies, ecological fallacy, and a need for standardization. Sci Rep 12, 18196.

Green, T.R.F., Rowe, R.K., 2024. Quantifying microglial morphology: an insight into function. Clinical and Experimental Immunology 216, 221-229.

Haghir, H., Kuckertz, A., Zhao, L., Hami, J., Palomero-Gallagher, N., 2024. A new map of the rat isocortex and proisocortex: cytoarchitecture and M2 receptor distribution patterns. Brain Structure and Function 229, 1795-1822.

Hou, Y., Dan, X., Babbar, M., Wei, Y., Hasselbalch, S.G., Croteau, D.L., Bohr, V.A., 2019. Ageing as a risk factor for neurodegenerative disease. Nature Reviews Neurology 15, 565-581.

Jaramillo, S., Zador, A.M., 2014. Mice and rats achieve similar levels of performance in an adaptive decision-making task. Frontiers in Systems Neuroscience 8.

Johnson, J.I., Sudheimer, K.D., Davis, K.K., Kerndt, G.M., Winn, B.M., 2024. Sheep Brain Atlas.
Keifer, J., Summers, C.H., 2016. Putting the "Biology" Back into "Neurobiology": The Strength of Diversity in Animal Model Systems for Neuroscience Research. Frontiers in Systems Neuroscience 10.
Khakpour, M., Ibáñez, F.G., Bordeleau, M., Picard, K., McKee-Reid, L., Ben-Azu, B., Maggi, L., Tremblay, M.-È., 2022. Manual versus automatic analysis of microglial density and distribution: a comparison in the hippocampus of healthy and lipopolysaccharide-challenged mature male mice. Micron 161, 103334.
Kodamullil, A.T., Iyappan, A., Karki, R., Madan, S., Younesi, E., Hofmann-Apitius, M., 2017. Of Mice and Men: Comparative Analysis of Neuro-Inflammatory Mechanisms in Human and Mouse Using Cause-and-Effect Models. J Alzheimers Dis 59, 1045-1055.
Krieg, J.L., Leonard, A.V., Tuner, R.J., Corrigan, F., 2023. Characterization of Traumatic Brain Injury in a Gyrencephalic Ferret Model Using the Novel Closed Head Injury Model of Engineered Rotational Acceleration (CHIMERA). Neurotrauma Reports 4, 761-780.
Leng, F., Edison, P., 2021. Neuroinflammation and microglial activation in Alzheimer disease: where do we go from here? Nature Reviews Neurology 17, 157-172.
Lévy, F., Batailler, M., Meurisse, M., Migaud, M., 2017. Adult Neurogenesis in Sheep: Characterization and Contribution to Reproduction and Behavior. Frontiers in Neuroscience 11.
Leyh, J., Paeschke, S., Mages, B., Michalski, D., Nowicki, M., Bechmann, I., Winter, K., 2021. Classification of Microglial Morphological Phenotypes Using Machine Learning. Frontiers in Cellular Neuroscience 15.
Liu, Y., Gao, J., 2023. Reproductive aging: biological pathways and potential interventive strategies. Journal of Genetics and Genomics 50, 141-150.
Long, J.M., Kalehua, A.N., Muth, N.J., Calhoun, M.E., Jucker, M., Hengemihle, J.M., Ingram, D.K., Mouton, P.R., 1998. Stereological analysis of astrocyte and microglia in aging mouse hippocampus. Neurobiology of Aging 19, 497-503.
López-Otín, C., Blasco, M.A., Partridge, L., Serrano, M., Kroemer, G., 2023. Hallmarks of aging: An expanding universe. Cell 186, 243-278.
Mao, Z., Liu, C., Ji, S., Yang, Q., Ye, H., Han, H., Xue, Z., 2017. The NLRP3 Inflammasome is Involved in the Pathogenesis of Parkinson's Disease in Rats. Neurochem Res 42, 1104-1115.
Mathews, C., 2024. Population Ageing in Lower- and Middle-income Countries. Celebrating 40 Years of HelpAge International. Journal of Population Ageing 17, 1-4.
Mejias, N.H., Martinez, C.C., Stephens, M.E., de Rivero Vaccari, J.P., 2018. Contribution of the inflammasome to inflammaging. Journal of Inflammation 15, 23.
Mitchell, I.J., Cooper, A.J., Griffiths, M.R., 1999. The selective vulnerability of striatopallidal neurons. Progress in Neurobiology 59, 691-719.
Möhle, L., Bascuñana, P., Brackhan, M., Pahnke, J., 2021. Development of deep learning models for microglia analyses in brain tissue using DeePathology™ STUDIO. Journal of Neuroscience Methods 364, 109371.
Monier, A., Adle-Biassette, H., Delezoide, A.L., Evrard, P., Gressens, P., Verney, C., 2007. Entry and distribution of microglial cells in human embryonic and fetal cerebral cortex. J Neuropathol Exp Neurol 66, 372-382.
Motulsky, H.J., Brown, R.E., 2006. Detecting outliers when fitting data with nonlinear regression – a new method based on robust nonlinear regression and the false discovery rate. BMC Bioinformatics 7, 123.
Murray, S.J., Mitchell, N.L., 2022. The Translational Benefits of Sheep as Large Animal Models of Human Neurological Disorders. Frontiers in Veterinary Science 9.
Naghavi, M., Ong, K.L., Aali, A., Ababneh, H.S., Abate, Y.H., Abbafati, C., Abbasgholizadeh, R., Abbasian, M., Abbasi-Kangevari, M., Abbastabar, H., Abd ElHafeez, S., Abdelmasseh, M., Abd-Elsalam, S., Abdelwahab, A., Abdollahi, M., Abdollahifar, M.-A., Abdoun, M., Abdulah, D.M., Abdullahi, A., Abebe, M., Abebe, S.S., Abedi, A., Abegaz, K.H., Abhilash, E.S., Abidi, H., Abiodun, O., Aboagye, R.G., Abolhassani, H., Abolmaali, M., Abouzid, M., Aboye, G.B., Abreu, L.G., Abrha, W.A., Abtahi, D., Abu Rumeileh, S., Abualruz, H., Abubakar, B., Abu-Gharbieh, E., Abu-Rmeileh, N.M.E., Aburuz, S., Abu-Zaid, A., Accrombessi, M.M.K., Adal, T.G., Adamu, A.A., Addo, I.Y., Addolorato, G., Adebiyi, A.O., Adekanmbi, V., Adepoju, A.V., Adetunji, C.O., Adetunji, J.B., Adeyeoluwa, T.E., Adeyinka, D.A., Adeyomoye, O.I., Admass, B.A.A., Adnani, Q.E.S., Adra, S.,

Afolabi, A.A., Afzal, M.S., Afzal, S., Agampodi, S.B., Agasthi, P., Aggarwal, M., Aghamiri, S., Agide, F.D., Agodi, A., Agrawal, A., Agyemang-Duah, W., Ahinkorah, B.O., Ahmad, A., Ahmad, D., Ahmad, F., Ahmad, M.M., Ahmad, S., Ahmad, S., Ahmad, T., Ahmadi, K., Ahmadzade, A.M., Ahmed, A., Ahmed, A., Ahmed, H., Ahmed, L.A., Ahmed, M.S., Ahmed, M.S., Ahmed, M.B., Ahmed, S.A., Ajami, M., Aji, B., Akara, E.M., Akbarialiabad, H., Akinosoglou, K., Akinyemiju, T., Akkaif, M.A., Akyirem, S., Al Hamad, H., Al Hasan, S.M., Alahdab, F., Alalalmeh, S.O., Alalwan, T.A., Al-Aly, Z., Alam, K., Alam, M., Alam, N., Al-amer, R.M., Alanezi, F.M., Alanzi, T.M., Al-Azzam, S., Albakri, A., Albashtawy, M., AlBataineh, M.T., Alcalde-Rabanal, J.E., Aldawsari, K.A., Aldhaleei, W.A., Aldridge, R.W., Alema, H.B., Alemayohu, M.A., Alemi, S., Alemu, Y.M., Al-Gheethi, A.A.S., Alhabib, K.F., Alhalaiqa, F.A.N., Al-Hanawi, M.K., Ali, A., Ali, A., Ali, L., Ali, M.U., Ali, R., Ali, S., Ali, S.S.S., Alicandro, G., Alif, S.M., Alikhani, R., Alimohamadi, Y., Aliyi, A.A., Aljasir, M.A.M., Aljunid, S.M., Alla, F., Allebeck, P., Al-Marwani, S., Al-Maweri, S.A.A., Almazan, J.U., Al-Mekhlafi, H.M., Almidani, L., Almidani, O., Alomari, M.A., Al-Omari, B., Alonso, J., Alqahtani, J.S., Alqalyoobi, S., Alqutaibi, A.Y., Al-Sabah, S.K., Altaany, Z., Altaf, A., Al-Tawfiq, J.A., Altirkawi, K.A., Aluh, D.O., Alvis-Guzman, N., Alwafi, H., Al-Worafi, Y.M., Aly, H., Aly, S., Alzoubi, K.H., Amani, R., Amare, A.T., Amegbor, P.M., Ameyaw, E.K., Amin, T.T., Amindarolzarbi, A., Amiri, S., Amirzade-Iranaq, M.H., Amu, H., Amugsi, D.A., Amusa, G.A., Ancuceanu, R., Anderlini, D., Anderson, D.B., Andrade, P.P., Andrei, C.L., Andrei, T., Angus, C., Anil, A., Anil, S., Anoushiravani, A., Ansari, H., Ansariadi, A., Ansari-Moghaddam, A., Antony, C.M., Antriyandarti, E., Anvari, D., Anvari, S., Anwar, S., Anwar, S.L., Anwer, R., Anyasodor, A.E., Aqeel, M., Arab, J.P., Arabloo, J., Arafat, M., Aravkin, A.Y., Areda, D., Aremu, A., Aremu, O., Ariffin, H., Arkew, M., Armocida, B., Arndt, M.B., Ärnlöv, J., Arooj, M., Artamonov, A.A., Arulappan, J., Aruleba, R.T., Arumugam, A., Asaad, M., Asadi-Lari, M., Asgedom, A.A., Asghariahmadabad, M., Asghari-Jafarabadi, M., Ashraf, M., Aslani, A., Astell-Burt, T., Athar, M., Athari, S.S., Atinafu, B.T.T., Atlaw, H.W., Atorkey, P., Atout, M.M.d.W., Atreya, A., Aujayeb, A., Ausloos, M., Avan, A., Awedew, A.F., Aweke, A.M., Ayala Quintanilla, B.P., Ayatollahi, H., Ayuso-Mateos, J.L., Ayyoubzadeh, S.M., Azadnajafabad, S., Azevedo, R.M.S., Azzam, A.Y., B, D.B., Babu, A.S., Badar, M., Badiye, A.D., Baghdadi, S., Bagheri, N., Bagherieh, S., Bah, S., Bahadorikhalili, S., Bahmanziari, N., Bai, R., Baig, A.A., Baker, J.L., Bako, A.T., Bakshi, R.K., Balakrishnan, S., Balasubramanian, M., Baltatu, O.C., Bam, K., Banach, M., Bandyopadhyay, S., Banik, P.C., Bansal, H., Bansal, K., Barbic, F., Barchitta, M., Bardhan, M., Bardideh, E., Barker-Collo, S.L., Bärnighausen, T.W., Barone-Adesi, F., Barqawi, H.J., Barrero, L.H., Barrow, A., Barteit, S., Barua, L., Basharat, Z., Bashiri, A., Basiru, A., Baskaran, P., Basnyat, B., Bassat, Q., Basso, J.D., Basting, A.V.L., Basu, S., Batra, K., Baune, B.T., Bayati, M., Bayileyegn, N.S., Beaney, T., Bedi, N., Beghi, M., Behboudi, E., Behera, P., Behnoush, A.H., Behzadifar, M., Beiranvand, M., Bejarano Ramirez, D.F., Béjot, Y., Belay, S.A., Belete, C.M., Bell, M.L., Bello, M.B., Bello, O.O., Belo, L., Beloukas, A., Bender, R.G., Bensenor, I.M., Beran, A., Berezvai, Z., Berhie, A.Y., Berice, B.N., Bernstein, R.S., Bertolacci, G.J., Bettencourt, P.J.G., Beyene, K.A., Bhagat, D.S., Bhagavathula, A.S., Bhala, N., Bhalla, A., Bhandari, D., Bhangdia, K., Bhardwaj, N., Bhardwaj, P., Bhardwaj, P.V., Bhargava, A., Bhaskar, S., Bhat, V., Bhatti, G.K., Bhatti, J.S., Bhatti, M.S., Bhatti, R., Bhutta, Z.A., Bikbov, B., Bishai, J.D., Bisignano, C., Bisulli, F., Biswas, A., Biswas, B., Bitaraf, S., Bitew, B.D., Bitra, V.R., Bjørge, T., Boachie, M.K., Boampong, M.S., Bobirca, A.V., Bodolica, V., Bodunrin, A.O., Bogale, E.K., Bogale, K.A., Bohlouli, S., Bolarinwa, O.A., Boloor, A., Bonakdar Hashemi, M., Bonny, A., Bora, K., Bora Basara, B., Borhany, H., Borzutzky, A., Bouaoud, S., Boustany, A., Boxe, C., Boyko, E.J., Brady, O.J., Braithwaite, D., Brant, L.C., Brauer, M., Brazinova, A., Brazo-Sayavera, J., Breitborde, N.J.K., Breitner, S., Brenner, H., Briko, A.N., Briko, N.I., Britton, G., Brown, J., Brugha, T., Bulamu, N.B., Bulto, L.N., Buonsenso, D., Burns, R.A., Busse, R., Bustanji, Y., Butt, N.S., Butt, Z.A., Caetano dos Santos, F.L., Calina, D., Cámera, L.A., Campos, L.A., Campos-Nonato, I.R., Cao, C., Cao, Y., Capodici, A., Cárdenas, R., Carr, S., Carreras, G., Carrero, J.J., Carugno, A., Carvalheiro, C.G., Carvalho, F., Carvalho, M., Castaldelli-Maia, J.M., Castañeda-Orjuela, C.A., Castelpietra, G., Catalá-López, F., Catapano, A.L., Cattaruzza, M.S., Cederroth, C.R., Cegolon, L., Cembranel, F., Cenderadewi, M., Cercy, K.M., Cerin, E., Cevik, M., Chadwick, J., Chahine, Y., Chakraborty, C., Chakraborty, P.A., Chan, J.S.K., Chan, R.N.C., Chandika, R.M., Chandrasekar, E.K., Chang, C.-K., Chang, J.-C., Chanie, G.S., Charalampous, P., Chattu, V.K., Chaturvedi, P., Chatzimavridou-Grigoriadou, V., Chaurasia, A., Chen, A.W., Chen, A.-T., Chen, C.S., Chen, H., Chen, M.X., Chen, S., Cheng, C.-Y., Cheng, E.T.W., Cherbuin, N., Cheru, W.A., Chien, J.-H., Chimed-Ochir, O., Chimoriya, R., Ching, P.R., Chirinos-

Caceres, J.L., Chitheer, A., Cho, W.C.S., Chong, B., Chopra, H., Choudhari, S.G., Chowdhury, R., Christopher, D.J., Chukwu, I.S., Chung, E., Chung, E., Chung, E., Chung, S.-C., Chutiyami, M., Cindi, Z., Cioffi, I., Claassens, M.M., Claro, R.M., Coberly, K., Cogen, R.M., Columbus, A., Comfort, H., Conde, J., Cortese, S., Cortesi, P.A., Costa, V.M., Costanzo, S., Cousin, E., Couto, R.A.S., Cowden, R.G., Cramer, K.M., Criqui, M.H., Cruz-Martins, N., Cuadra-Hernández, S.M., Culbreth, G.T., Cullen, P., Cunningham, M., Curado, M.p., Dadana, S., Dadras, O., Dai, S., Dai, X., Dai, Z., Dalli, L.L., Damiani, G., Darega Gela, J., Das, J.K., Das, S., Das, S., Dascalu, A.M., Dash, N.R., Dashti, M., Dastiridou, A., Davey, G., Dávila-Cervantes, C.A., Davis Weaver, N., Davletov, K., De Leo, D., de Luca, K., Debele, A.T., Debopadhaya, S., Degenhardt, L., Dehghan, A., Deitesfeld, L., Del Bo, C., Delgado-Enciso, I., Demessa, B.H., Demetriades, A.K., Deng, K., Deng, X., Denova-Gutiérrez, E., Deravi, N., Dereje, N., Dervenis, N., Dervišević, E., Des Jarlais, D.C., Desai, H.D., Desai, R., Devanbu, V.G.C., Dewan, S.M.R., Dhali, A., Dhama, K., Dhimal, M., Dhingra, S., Dhulipala, V.R., Dias da Silva, D., Diaz, D., Diaz, M.J., Dima, A., Ding, D.D., Ding, H., Dinis-Oliveira, R.J., Dirac, M.A., Djalalinia, S., Do, T.H.P., do Prado, C.B., Doaei, S., Dodangeh, M., Dodangeh, M., Dohare, S., Dokova, K.G., Dolecek, C., Dominguez, R.-M.V., Dong, W., Dongarwar, D., D'Oria, M., Dorostkar, F., Dorsey, E.R., dos Santos, W.M., Doshi, R., Doshmangir, L., Dowou, R.K., Driscoll, T.R., Dsouza, H.L., Dsouza, V., Du, M., Dube, J., Duncan, B.B., Duraes, A.R., Duraisamy, S., Durojaiye, O.C., Dwyer-Lindgren, L., Dzianach, P.A., Dziedzic, A.M., E'Mar, A.R., Eboreime, E., Ebrahimi, A., Echieh, C.P., Edinur, H.A., Edvardsson, D., Edvardsson, K., Efendi, D., Efendi, F., Effendi, D.E., Eikemo, T.A., Eini, E., Ekholuenetale, M., Ekundayo, T.C., El Sayed, I., Elbarazi, I., Elema, T.B., Elemam, N.M., Elgar, F.J., Elgendy, I.Y., ElGohary, G.M.T., Elhabashy, H.R., Elhadi, M., El-Huneidi, W., Elilo, L.T., Elmeligy, O.A.A., Elmonem, M.A., Elshaer, M., Elsohaby, I., Emeto, T.I., Engelbert Bain, L., Erkhembayar, R., Esezobor, C.I., Eshrati, B., Eskandarieh, S., Espinosa-Montero, J., Esubalew, H., Etaee, F., Fabin, N., Fadaka, A.O., Fagbamigbe, A.F., Fahim, A., Fahimi, S., Fakhri-Demeshghieh, A., Falzone, L., Fareed, M., Farinha, C.S.e.S., Faris, M.E.M., Faris, P.S., Faro, A., Fasanmi, A.O., Fatehizadeh, A., Fattahi, H., Fauk, N.K., Fazeli, P., Feigin, V.L., Feizkhah, A., Fekadu, G., Feng, X., Fereshtehnejad, S.-M., Feroze, A.H., Ferrante, D., Ferrari, A.J., Ferreira, N., Fetensa, G., Feyisa, B.R., Filip, I., Fischer, F., Flavel, J., Flood, D., Florin, B.T., Foigt, N.A., Folayan, M.O., Fomenkov, A.A., Foroutan, B., Foroutan, M., Forthun, I., Fortuna, D., Foschi, M., Fowobaje, K.R., Francis, K.L., Franklin, R.C., Freitas, A., Friedman, J., Friedman, S.D., Fukumoto, T., Fuller, J.E., Fux, B., Gaal, P.A., Gadanya, M.A., Gaidhane, A.M., Gaihre, S., Gakidou, E., Galali, Y., Galles, N.C., Gallus, S., Ganbat, M., Gandhi, A.P., Ganesan, B., Ganiyani, M.A., Garcia-Gordillo, M.A., Gardner, W.M., Garg, J., Garg, N., Gautam, R.K., Gbadamosi, S.O., Gebi, T.G., Gebregergis, M.W., Gebrehiwot, M., Gebremeskel, T.G., Georgescu, S.R., Getachew, T., Gething, P.W., Getie, M., Ghadiri, K., Ghahramani, S., Ghailan, K.Y., Ghasemi, M.-R., Ghasempour Dabaghi, G., Ghasemzadeh, A., Ghashghaee, A., Ghassemi, F., Ghazy, R.M., Ghimire, A., Ghoba, S., Gholamalizadeh, M., Gholamian, A., Gholamrezanezhad, A., Gholizadeh, N., Ghorbani, M., Ghorbani Vajargah, P., Ghoshal, A.G., Gill, P.S., Gill, T.K., Gillum, R.F., Ginindza, T.G., Girmay, A., Glasbey, J.C., Gnedovskaya, E.V., Göbölös, L., Godinho, M.A., Goel, A., Golchin, A., Goldust, M., Golechha, M., Goleij, P., Gomes, N.G.M., Gona, P.N., Gopalani, S.V., Gorini, G., Goudarzi, H., Goulart, A.C., Goulart, B.N.G., Goyal, A., Grada, A., Graham, S.M., Grivna, M., Grosso, G., Guan, S.-Y., Guarducci, G., Gubari, M.I.M., Gudeta, M.D., Guha, A., Guicciardi, S., Guimarães, R.A., Gulati, S., Gunawardane, D.A., Gunturu, S., Guo, C., Gupta, A.K., Gupta, B., Gupta, M.K., Gupta, M., Gupta, R.D., Gupta, R., Gupta, S., Gupta, V.B., Gupta, V.K., Gupta, V.K., Gurmessa, L., Gutiérrez, R.A., Habibzadeh, F., Habibzadeh, P., Haddadi, R., Hadei, M., Hadi, N.R., Haep, N., Hafezi-Nejad, N., Hailu, A., Haj-Mirzaian, A., Halboub, E.S., Hall, B.J., Haller, S., Halwani, R., Hamadeh, R.R., Hameed, S., Hamidi, S., Hamilton, E.B., Han, C., Han, Q., Hanif, A., Hanifi, N., Hankey, G.J., Hanna, F., Hannan, M.A., Haque, M.N., Harapan, H., Hargono, A., Haro, J.M., Hasaballah, A.I., Hasan, I., Hasan, M.T., Hasani, H., Hasanian, M., Hashi, A., Hasnain, M.S., Hassan, I., Hassanipour, S., Hassankhani, H., Haubold, J., Havmoeller, R.J., Hay, S.I., He, J., Hebert, J.J., Hegazi, O.E., Heidari, G., Heidari, M., Heidari-Foroozan, M., Helfer, B., Hendrie, D., Herrera-Serna, B.Y., Herteliu, C., Hesami, H., Hezam, K., Hill, C.L., Hiraike, Y., Holla, R., Horita, N., Hossain, M.M., Hossain, S., Hosseini, M.-S., Hosseinzadeh, H., Hosseinzadeh, M., Hosseinzadeh Adli, A., Hostiuc, M., Hostiuc, S., Hsairi, M., Hsieh, V.C.-r., Hsu, R.L., Hu, C., Huang, J., Hultström, M., Humayun, A., Hundie, T.G., Hussain, J., Hussain, M.A., Hussein, N.R., Hussien, F.M., Huynh, H.-H., Hwang, B.-F., Ibitoye, S.E., Ibrahim, K.S., Iftikhar, P.M., Ijo, D., Ikiroma, A.I., Ikuta, K.S., Ikwegbue, P.C., Ilesanmi, O.S., Ilic,

I.M., Ilic, M.D., Imam, M.T., Immurana, M., Inamdar, S., Indriasih, E., Iqhrammullah, M., Iradukunda, A., Iregbu, K.C., Islam, M.R., Islam, S.M.S., Islami, F., Ismail, F., Ismail, N.E., Iso, H., Isola, G., Iwagami, M., Iwu, C.C.D., Iyamu, I.O., Iyer, M., J, L.M., Jaafari, J., Jacob, L., Jacobsen, K.H., Jadidi-Niaragh, F., Jafarinia, M., Jafarzadeh, A., Jaggi, K., Jahankhani, K., Jahanmehr, N., Jahrami, H., Jain, N., Jairoun, A.A., Jaiswal, A., Jamshidi, E., Janko, M.M., Jatau, A.I., Javadov, S., Javaheri, T., Jayapal, S.K., Jayaram, S., Jebai, R., Jee, S.H., Jeganathan, J., Jha, A.K., Jha, R.P., Jiang, H., Jin, Y., Johnson, O., Jokar, M., Jonas, J.B., Joo, T., Joseph, A., Joseph, N., Joshua, C.E., Joshy, G., Jozwiak, J.J., Jürisson, M., K, V., Kaambwa, B., Kabir, A., Kabir, Z., Kadashetti, V., Kadir, D.H., Kalani, R., Kalankesh, L.R., Kalankesh, L.R., Kaliyadan, F., Kalra, S., Kamal, V.K., Kamarajah, S.K., Kamath, R., Kamiab, Z., Kamyari, N., Kanagasabai, T., Kanchan, T., Kandel, H., Kanmanthareddy, A.R., Kanmiki, E.W., Kanmodi, K.K., Kannan S, S., Kansal, S.K., Kantar, R.S., Kapoor, N., Karajizadeh, M., Karanth, S.D., Karasneh, R.A., Karaye, I.M., Karch, A., Karim, A., Karimi, S.E., Karimi Behnagh, A., Kashoo, F.Z., Kasnazani, Q.H.A., Kasraei, H., Kassebaum, N.J., Kassel, M.B., Kauppila, J.H., Kaur, N., Kawakami, N., Kayode, G.A., Kazemi, F., Kazemian, S., Kazmi, T.H., Kebebew, G.M., Kebede, A.D., Kebede, F., Keflie, T.S., Keiyoro, P.N., Keller, C., Kelly, J.T., Kempen, J.H., Kerr, J.A., Kesse-Guyot, E., Khajuria, H., Khalaji, A., Khalid, N., Khalil, A.A., Khalilian, A., Khamesipour, F., Khan, A., Khan, A., Khan, G., Khan, I., Khan, I.A., Khan, M.N., Khan, M., Khan, M.J., Khan, M.A.B., Khan, Z.A., Khan suheb, M.Z., Khanmohammadi, S., Khatab, K., Khatami, F., Khatatbeh, H., Khatatbeh, M.M., Khavandegar, A., Khayat Kashani, H.R., Khidri, F.F., Khodadoust, E., Khorgamphar, M., Khormali, M., Khorrami, Z., Khosravi, A., Khosravi, M.A., Kifle, Z.D., Kim, G., Kim, J., Kim, K., Kim, M.S., Kim, Y.J., Kimokoti, R.W., Kinzel, K.E., Kisa, A., Kisa, S., Klu, D., Knudsen, A.K.S., Kocarnik, J.M., Kochhar, S., Kocsis, T., Koh, D.S.Q., Kolahi, A.-A., Kolves, K., Kompani, F., Koren, G., Kosen, S., Kostev, K., Koul, P.A., Koulmane Laxminarayana, S.L., Krishan, K., Krishna, H., Krishna, V., Krishnamoorthy, V., Krishnamoorthy, Y., Krohn, K.J., Kuate Defo, B., Kucuk Bicer, B., Kuddus, M.A., Kuddus, M., Kuitunen, I., Kulimbet, M., Kulkarni, V., Kumar, A., Kumar, A., Kumar, H., Kumar, M., Kumar, R., Kumari, M., Kumie, F.T., Kundu, S., Kurmi, O.P., Kusnali, A., Kusuma, D., Kwarteng, A., Kyriopoulos, I., Kyu, H.H., La Vecchia, C., Lacey, B., Ladan, M.A., Laflamme, L., Lagat, A.K., Lager, A.C.J., Lahmar, A., Lai, D.T.C., Lal, D.K., Lalloo, R., Lallukka, T., Lam, H., Lám, J., Landrum, K.R., Lanfranchi, F., Lang, J.J., Langguth, B., Lansingh, V.C., Laplante-Lévesque, A., Larijani, B., Larsson, A.O., Lasrado, S., Lassi, Z.S., Latief, K., Latifinaibin, K., Lauriola, P., Le, N.H.H., Le, T.T.T., Le, T.D.T., Ledda, C., Ledesma, J.R., Lee, M., Lee, P.H., Lee, S.W., Lee, S.W.H., Lee, W.-C., Lee, Y.H., LeGrand, K.E., Leigh, J., Leong, E., Lerango, T.L., Li, M.-C., Li, W., Li, X., Li, Y., Li, Z., Ligade, V.S., Likaka, A.T.M., Lim, L.-L., Lim, S.S., Lindstrom, M., Linehan, C., Liu, C., Liu, G., Liu, J., Liu, R., Liu, S., Liu, X., Liu, X., Llanaj, E., Loftus, M.J., López-Bueno, R., Lopukhov, P.D., Loreche, A.M., Lorkowski, S., Lotufo, P.A., Lozano, R., Lubinda, J., Lucchetti, G., Lugo, A., Lunevicius, R., Ma, Z.F., Maass, K.L., Machairas, N., Machoy, M., Madadizadeh, F., Madsen, C., Madureira-Carvalho, Á.M., Maghazachi, A.A., Maharaj, S.B., Mahjoub, S., Mahmoud, M.A., Mahmoudi, A., Mahmoudi, E., Mahmoudi, R., Majeed, A., Makhdoom, I.F., Malakan Rad, E., Maled, V., Malekzadeh, R., Malhotra, A.K., Malhotra, K., Malik, A.A., Malik, I., Malta, D.C., Mamun, A.A., Mansouri, P., Mansournia, M.A., Mantovani, L.G., Maqsood, S., Marasini, B.P., Marateb, H.R., Maravilla, J.C., Marconi, A.M., Mardi, P., Marino, M., Marjani, A., Martinez, G., Martinez-Guerra, B.A., Martinez-Piedra, R., Martini, D., Martini, S., Martins-Melo, F.R., Martorell, M., Marx, W., Maryam, S., Marzo, R.R., Masaka, A., Masrie, A., Mathieson, S., Mathioudakis, A.G., Mathur, M.R., Mattumpuram, J., Matzopoulos, R., Maude, R.J., Maugeri, A., Maulik, P.K., Mayeli, M., Mazaheri, M., Mazidi, M., McGrath, J.J., McKee, M., McKowen, A.L.W., McLaughlin, S.A., McPhail, S.M., Mechili, E.A., Medina, J.R.C., Mediratta, R.P., Meena, J.K., Mehra, R., Mehrabani-Zeinabad, K., Mehrabi Nasab, E., Mekene Meto, T., Meles, G.G., Mendez-Lopez, M.A.M., Mendoza, W., Menezes, R.G., Mengist, B., Mentis, A.-F.A., Meo, S.A., Meresa, H.A., Meretoja, A., Meretoja, T.J., Mersha, A.M., Mesfin, B.A., Mestrovic, T., Mettananda, K.C.D., Mettananda, S., Meylakhs, P., Mhlanga, A., Mhlanga, L., Mi, T., Miazgowski, T., Micha, G., Michalek, I.M., Miller, T.R., Mills, E.J., Minh, L.H.N., Mini, G.K., Mir Mohammad Sadeghi, P., Mirica, A., Mirijello, A., Mirrakhimov, E.M., Mirutse, M.K., Mirzaei, M., Misganaw, A., Mishra, A., Misra, S., Mitchell, P.B., Mithra, P., Mittal, C., Mobayen, M., Moberg, M.E., Mohamadkhani, A., Mohamed, J., Mohamed, M.F.H., Mohamed, N.S., Mohammad-Alizadeh-Charandabi, S., Mohammadi, S., Mohammadian-Hafshejani, A., Mohammadifard, N., Mohammed, H., Mohammed, H., Mohammed, M., Mohammed, S., Mohammed, S., Mohan, V., Mojiri-Forushani, H., Mokari, A., Mokdad, A.H.,

Molinaro, S., Molokhia, M., Momtazmanesh, S., Monasta, L., Mondello, S., Moni, M.A., Moodi Ghalibaf, A., Moradi, M., Moradi, Y., Moradi-Lakeh, M., Moradzadeh, M., Moraga, P., Morawska, L., Moreira, R.S., Morovatdar, N., Morrison, S.D., Morze, J., Mosser, J.F., Motappa, R., Mougin, V., Mouodi, S., Mousavi, P., Mousavi, S.E., Mousavi Khaneghah, A., Mpolya, E.A., Mrejen, M., Mubarik, S., Muccioli, L., Mueller, U.O., Mughal, F., Mukherjee, S., Mulita, F., Munjal, K., Murillo-Zamora, E., Musaigwa, F., Musallam, K.M., Mustafa, A., Mustafa, G., Muthupandian, S., Muthusamy, R., Muzaffar, M., Myung, W., Nagarajan, A.J., Nagel, G., Naghavi, P., Naheed, A., Naik, G.R., Naik, G., Nainu, F., Nair, S., Najmuldeen, H.H.R., Nakhostin Ansari, N., Nangia, V., Naqvi, A.A., Narasimha Swamy, S., Narayana, A.I., Nargus, S., Nascimento, B.R., Nascimento, G.G., Nasehi, S., Nashwan, A.J., Natto, Z.S., Nauman, J., Naveed, M., Nayak, B.P., Nayak, V.C., Nazri-Panjaki, A., Ndejjo, R., Nduaguba, S.O., Negash, H., Negoi, I., Negoi, R.I., Negru, S.M., Nejadghaderi, S.A., Nejjari, C., Nena, E., Nepal, S., Ng, M., Nggada, H.A., Nguefack-Tsague, G., Ngunjiri, J.W., Nguyen, A.H., Nguyen, D.H., Nguyen, H.T.H., Nguyen, P.T., Nguyen, V.T., Niazi, R.K., Nielsen, K.R., Nigatu, Y.T., Nikolouzakis, T.K., Nikoobar, A., Nikoomanesh, F., Nikpoor, A.R., Ningrum, D.N.A., Nnaji, C.A., Nnyanzi, L.A., Noman, E.A., Nomura, S., Noreen, M., Noroozi, N., Norrving, B., Noubiap, J.J., Novotney, A., Nri-Ezedi, C.A., Ntaios, G., Ntsekhe, M., Nuñez-Samudio, V., Nurrika, D., Nutor, J.J., Oancea, B., Obamiro, K.O., Oboh, M.A., Odetokun, I.A., Odogwu, N.M., O'Donnell, M.J., Oduro, M.S., Ofakunrin, A.O.D., Ogunkoya, A., Oguntade, A.S., Oh, I.-H., Okati-Aliabad, H., Okeke, S.R., Okekunle, A.P., Okonji, O.C., Olagunju, A.T., Olaiya, M.T., Olatubi, M.I., Oliveira, G.M.M., Olufadewa, I.I., Olusanya, B.O., Olusanya, J.O., Oluwafemi, Y.D., Omar, H.A., Omar Bali, A., Omer, G.L., Ondayo, M.A., Ong, S., Onwujekwe, O.E., Onyedibe, K.I., Ordak, M., Orisakwe, O.E., Orish, V.N., Ortega-Altamirano, D.V., Ortiz, A., Osman, W.M.S., Ostroff, S.M., Osuagwu, U.L., Otoiu, A., Otstavnov, N., Otstavnov, S.S., Ouyahia, A., Ouyang, G., Owolabi, M.O., Ozten, Y., P A, M.P., Padron-Monedero, A., Padubidri, J.R., Pal, P.K., Palicz, T., Palladino, C., Palladino, R., Palma-Alvarez, R.F., Pan, F., Pan, H.-F., Pana, A., Panda, P., Panda-Jonas, S., Pandi-Perumal, S.R., Pangaribuan, H.U., Panos, G.D., Panos, L.D., Pantazopoulos, I., Pantea Stoian, A.M., Papadopoulou, P., Parikh, R.R., Park, S., Parthasarathi, A., Pashaei, A., Pasovic, M., Passera, R., Pasupula, D.K., Patel, H.M., Patel, J., Patel, S.K., Patil, S., Patoulias, D., Patthipati, V.S., Paudel, U., Pazoki Toroudi, H., Pease, S.A., Peden, A.E., Pedersini, P., Pensato, U., Pepito, V.C.F., Peprah, E.K., Peprah, P., Perdigão, J., Pereira, M., Peres, M.F.P., Perianayagam, A., Perico, N., Pestell, R.G., Pesudovs, K., Petermann-Rocha, F.E., Petri, W.A., Pham, H.T., Philip, A.K., Phillips, M.R., Pierannunzio, D., Pigeolet, M., Pigott, D.M., Pilgrim, T., Piracha, Z.Z., Piradov, M.A., Pirouzpanah, S., Plakkal, N., Plotnikov, E., Podder, V., Poddighe, D., Polinder, S., Polkinghorne, K.R., Poluru, R., Ponkilainen, V.T., Porru, F., Postma, M.J., Poudel, G.R., Pourshams, A., Pourtaheri, N., Prada, S.I., Pradhan, P.M.S., Prakasham, T.N., Prasad, M., Prashant, A., Prates, E.J.S., Prieto Alhambra, D., Priscilla, T., Pritchett, N., Purohit, B.M., Puvvula, J., Qasim, N.H., Qattea, I., Qazi, A.S., Qian, G., Qiu, S., Qureshi, M.F., Rabiee Rad, M., Radfar, A., Radhakrishnan, R.A., Radhakrishnan, V., Raeisi Shahraki, H., Rafferty, Q., Raggi, A., Raghav, P.R., Raheem, N., Rahim, F., Rahim, M.J., Rahimi-Movaghar, V., Rahman, M.M., Rahman, M.H.U., Rahman, M., Rahman, M.A., Rahmani, A.M., Rahmani, S., Rahmanian, V., Rajaa, S., Rajput, P., Rakovac, I., Ramasamy, S.K., Ramazanu, S., Rana, K., Ranabhat, C.L., Rancic, N., Rane, A., Rao, C.R., Rao, I.R., Rao, M., Rao, S.J., Rasali, D.P., Rasella, D., Rashedi, S., Rashedi, V., Rashidi, M.-M., Rasouli-Saravani, A., Rasul, A., Rathnaiah Babu, G., Rauniyar, S.K., Ravangard, R., Ravikumar, N., Rawaf, D.L., Rawaf, S., Rawal, L., Rawassizadeh, R., Rawlley, B., Raza, R.Z., Razo, C., Redwan, E.M.M., Rehman, F.U., Reifels, L., Reiner Jr, R.C., Remuzzi, G., Reyes, L.F., Rezaei, M., Rezaei, N., Rezaei, N., Rezaeian, M., Rhee, T.G., Riaz, M.A., Ribeiro, A.L.P., Rickard, J., Riva, H.R., Robinson-Oden, H.E., Rodrigues, C.F., Rodrigues, M., Roever, L., Rogowski, E.L.B., Rohloff, P., Romadlon, D.S., Romero-Rodríguez, E., Romoli, M., Ronfani, L., Roshandel, G., Roth, G.A., Rout, H.S., Roy, N., Roy, P., Rubagotti, E., Ruela, G.d.A., Rumisha, S.F., Runghien, T., Rwegerera, G.M., Rynkiewicz, A., S N, C., Saad, A.M.A., Saadatian, Z., Saber, K., Saber-Ayad, M.M., SaberiKamarposhti, M., Sabour, S., Sacco, S., Sachdev, P.S., Sachdeva, R., Saddik, B., Saddler, A., Sadee, B.A., Sadeghi, E., Sadeghi, E., Sadeghian, F., Saeb, M.R., Saeed, U., Safaeinejad, F., Safi, S.Z., Sagar, R., Saghazadeh, A., Sagoe, D., Saheb Sharif-Askari, F., Saheb Sharif-Askari, N., Sahebkar, A., Sahoo, S.S., Sahoo, U., Sahu, M., Saif, Z., Sajid, M.R., Sakshaug, J.W., Salam, N., Salamati, P., Salami, A.A., Salaroli, L.B., Saleh, M.A., Salehi, S., Salem, M.R., Salem, M.Z.Y., Salimi, S., Samadi Kafil, H., Samadzadeh, S., Samargandy, S., Samodra, Y.L., Samy, A.M., Sanabria, J., Sanna, F., Santomauro, D.F., Santos, I.S., Santric-Milicevic,

M.M., Sao Jose, B.P., Sarasmita, M.A., Saraswathy, S.Y.I., Saravanan, A., Saravi, B., Sarikhani, Y., Sarkar, T., Sarmiento-Suárez, R., Sarode, G.S., Sarode, S.C., Sarveazad, A., Sathian, B., Sathish, T., Satpathy, M., Sayeed, A., Sayeed, M.A., Saylan, M., Sayyah, M., Scarmeas, N., Schaarschmidt, B.M., Schlaich, M.P., Schlee, W., Schmidt, M.I., Schneider, I.J.C., Schuermans, A., Schumacher, A.E., Schutte, A.E., Schwarzinger, M., Schwebel, D.C., Schwendicke, F., Šekerija, M., Selvaraj, S., Senapati, S., Senthilkumaran, S., Sepanlou, S.G., Serban, D., Sethi, Y., Sha, F., Shabany, M., Shafaat, A., Shafie, M., Shah, N.S., Shah, P.A., Shah, S.M., Shahabi, S., Shahbandi, A., Shahid, I., Shahid, S., Shahid, W., Shahsavari, H.R., Shahwan, M.J., Shaikh, A., Shaikh, M.A., Shakeri, A., Shalash, A.S., Sham, S., Shamim, M.A., Shams-Beyranvand, M., Shamshad, H., Shamsi, M.A., Shanawaz, M., Shankar, A., Sharfaei, S., Sharifan, A., Sharifi-Rad, J., Sharma, R., Sharma, S., Sharma, U., Sharma, V., Shastry, R.P., Shavandi, A., Shayan, M., Shehabeldine, A.M.E., Sheikh, A., Sheikhi, R.A., Shen, J., Shetty, A., Shetty, B.S.K., Shetty, P.H., Shi, P., Shibuya, K., Shiferaw, D., Shigematsu, M., Shin, M.-J., Shin, Y.H., Shiri, R., Shirkoohi, R., Shitaye, N.A., Shittu, A., Shiue, I., Shivakumar, K.M., Shivarov, V., Shokraneh, F., Shokri, A., Shool, S., Shorofi, S.A., Shrestha, S., Shuval, K., Siddig, E.E., Silva, J.P., Silva, L.M.L.R., Silva, S., Simpson, C.R., Singal, A., Singh, A., Singh, B.B., Singh, G., Singh, J., Singh, N.P., Singh, P., Singh, S., Sinha, D.N., Sinto, R., Siraj, M.S., Sirota, S.B., Sitas, F., Sivakumar, S., Skryabin, V.Y., Skryabina, A.A., Sleet, D.A., Socea, B., Sokhan, A., Solanki, R., Solanki, S., Soleimani, H., Soliman, S.S.M., Song, S., Song, Y., Sorensen, R.J.D., Soriano, J.B., Soyiri, I.N., Spartalis, M., Spearman, S., Sreeramareddy, C.T., Srivastava, V.K., Stanaway, J.D., Stanikzai, M.H., Stark, B.A., Starnes, J.R., Starodubova, A.V., Stein, C., Stein, D.J., Steinbeis, F., Steiner, C., Steinmetz, J.D., Steiropoulos, P., Stevanović, A., Stockfelt, L., Stokes, M.A., Stortecky, S., Subramaniyan, V., Suleman, M., Suliankatchi Abdulkader, R., Sultana, A., Sun, H.Z., Sun, J., Sundström, J., Sunkersing, D., Sunnerhagen, K.S., Swain, C.K., Szarpak, L., Szeto, M.D., Szócska, M., Tabaee Damavandi, P., Tabarés-Seisdedos, R., Tabatabaei, S.M., Tabatabaei Malazy, O., Tabatabaeizadeh, S.-A., Tabatabai, S., Tabish, M., Tadakamadla, J., Tadakamadla, S.K., Taheri Abkenar, Y., Taheri Soodejani, M., Taiba, J., Takahashi, K., Talaat, I.M., Talukder, A., Tampa, M., Tamuzi, J.L., Tan, K.-K., Tandukar, S., Tang, H., Tang, H.K., Tarigan, I.U., Tariku, M.K., Tariqujjaman, M., Tarkang, E.E., Tavakoli Oliaee, R., Tavangar, S.M., Taveira, N., Tefera, Y.M., Temsah, M.-H., Temsah, R.M.H., Teramoto, M., Tesler, R., Teye-Kwadjo, E., Thakur, R., Thangaraju, P., Thankappan, K.R., Tharwat, S., Thayakaran, R., Thomas, N., Thomas, N.K., Thomson, A.M., Thrift, A.G., Thum, C.C.C., Thygesen, L.C., Tian, J., Tichopad, A., Ticoalu, J.H.V., Tillawi, T., Tiruye, T.Y., Titova, M.V., Tonelli, M., Topor-Madry, R., Toriola, A.T., Torre, A.E., Touvier, M., Tovani-Palone, M.R., Tran, J.T., Tran, N.M., Trico, D., Tromans, S.J., Truyen, T.T.T.T., Tsatsakis, A., Tsegay, G.M., Tsermpini, E.E., Tumurkhuu, M., Tung, K., Tyrovolas, S., Uddin, S.M.N., Udoakang, A.J., Udoh, A., Ullah, A., Ullah, I., Ullah, S., Ullah, S., Umakanthan, S., Umeokonkwo, C.D., Unim, B., Unnikrishnan, B., Unsworth, C.A., Upadhyay, E., Urso, D., Usman, J.S., Vahabi, S.M., Vaithinathan, A.G., Valizadeh, R., Van de Velde, S.M., Van den Eynde, J., Varga, O., Vart, P., Varthya, S.B., Vasankari, T.J., Vasic, M., Vaziri, S., Vellingiri, B., Venketasubramanian, N., Verghese, N.A., Verma, M., Veroux, M., Verras, G.-I., Vervoort, D., Villafañe, J.H., Villanueva, G.I., Vinayak, M., Violante, F.S., Viskadourou, M., Vladimirov, S.K., Vlassov, V., Vo, B., Vollset, S.E., Vongpradith, A., Vos, T., Vujcic, I.S., Vukovic, R., Wafa, H.A., Waheed, Y., Wamai, R.G., Wang, C., Wang, N., Wang, S., Wang, S., Wang, Y., Wang, Y.-P., Waqas, M., Ward, P., Wassie, E.G., Watson, S., Watson, S.L.W., Weerakoon, K.G., Wei, M.Y., Weintraub, R.G., Weiss, D.J., Westerman, R., Whisnant, J.L., Wiangkham, T., Wickramasinghe, D.P., Wickramasinghe, N.D., Wilandika, A., Wilkerson, C., Willeit, P., Wilson, S., Wojewodzic, M.W., Woldegebreal, D.H., Wolf, A.W., Wolfe, C.D.A., Wondimagegene, Y.A., Wong, Y.J., Wongsin, U., Wu, A.-M., Wu, C., Wu, F., Wu, X., Wu, Z., Xia, J., Xiao, H., Xie, Y., Xu, S., Xu, W.-D., Xu, X., Xu, Y.Y., Yadollahpour, A., Yamagishi, K., Yang, D., Yang, L., Yano, Y., Yao, Y., Yaribeygi, H., Ye, P., Yehualashet, S.S., Yesiltepe, M., Yesuf, S.A., Yezli, S., Yi, S., Yigezu, A., Yiğit, A., Yiğit, V., Yip, P., Yismaw, M.B., Yismaw, Y., Yon, D.K., Yonemoto, N., Yoon, S.-J., You, Y., Younis, M.Z., Yousefi, Z., Yu, C., Yu, Y., Yuh, F.H., Zadey, S., Zadnik, V., Zafari, N., Zakham, F., Zaki, N., Zaman, S.B., Zamora, N., Zand, R., Zangiabadian, M., Zar, H.J., Zare, I., Zarrintan, A., Zeariya, M.G.M., Zeinali, Z., Zhang, H., Zhang, J., Zhang, J., Zhang, L., Zhang, Y., Zhang, Z.-J., Zhao, H., Zhong, C., Zhou, J., Zhu, B., Zhu, L., Ziafati, M., Zielińska, M., Zitoun, O.A., Zoladl, M., Zou, Z., Zuhlke, L.J., Zumla, A., Zweck, E., Zyoud, S.H., Wool, E.E., Murray, C.J.L., 2024. Global burden of 288 causes of death and life expectancy decomposition in 204 countries

and territories and 811 subnational locations, 1990-2021: a systematic analysis for the Global Burden of Disease Study 2021. The Lancet 403, 2100-2132.
Nimmerjahn, A., Kirchhoff, F., Helmchen, F., 2005. Resting Microglial Cells Are Highly Dynamic Surveillants of Brain Parenchyma in Vivo. Science 308, 1314-1318.
Nishino, H., Hida, H., Kumazaki, M., Shimano, Y., Nakajima, K., Shimizu, H., Ooiwa, T., Baba, H., 2000. The Striatum Is the Most Vulnerable Region in the Brain to Mitochondrial Energy Compromise: A Hypothesis to Explain Its Specific Vulnerability. Journal of Neurotrauma 17, 251-260.
Oliveira, A.V., Vilaça, R., Santos, C.N., Costa, V., Menezes, R., 2017. Exploring the power of yeast to model aging and age-related neurodegenerative disorders. Biogerontology 18, 3-34.
Paxinos, G., Watson, C., 2007. The Rat Brain in Stereotaxic Coordinates. Elsevier.
Pearson-Leary, J., Eacret, D., Chen, R., Takano, H., Nicholas, B., Bhatnagar, S., 2017. Inflammation and vascular remodeling in the ventral hippocampus contributes to vulnerability to stress. Translational Psychiatry 7, e1160-e1160.
Pelvig, D.P., Pakkenberg, H., Stark, A.K., Pakkenberg, B., 2008. Neocortical glial cell numbers in human brains. Neurobiology of Aging 29, 1754-1762.
Perkins, A.E., Piazza, M.K., Deak, T., 2018. Stereological Analysis of Microglia in Aged Male and Female Fischer 344 Rats in Socially Relevant Brain Regions. Neuroscience 377, 40-52.
Perry, V.H., Holmes, C., 2014. Microglial priming in neurodegenerative disease. Nat Rev Neurol 10, 217-224.
Perry, V.H., Matyszak, M.K., Fearn, S., 1993. Altered antigen expression of microglia in the aged rodent CNS. Glia 7, 60-67.
Peruffo, A., Corain, L., Bombardi, C., Centelleghe, C., Grisan, E., Graïc, J.-M., Bontempi, P., Grandis, A., Cozzi, B., 2019. The motor cortex of the sheep: laminar organization, projections and diffusion tensor imaging of the intracranial pyramidal and extrapyramidal tracts. Brain Structure and Function 224, 1933-1946.
Philippens, I.H., Ormel, P.R., Baarends, G., Johansson, M., Remarque, E.J., Doverskog, M., 2017. Acceleration of Amyloidosis by Inflammation in the Amyloid-Beta Marmoset Monkey Model of Alzheimer's Disease. J Alzheimers Dis 55, 101-113.
Reid, S.J., McKean, N.E., Henty, K., Portelius, E., Blennow, K., Rudiger, S.R., Bawden, C.S., Handley, R.R., Verma, P.J., Faull, R.L.M., Waldvogel, H.J., Zetterberg, H., Snell, R.G., 2017. Alzheimer's disease markers in the aged sheep (Ovis aries). Neurobiol Aging 58, 112-119.
Rozovsky, I., Finch, C.E., Morgan, T.E., 1998. Age-Related Activation of Microglia and Astrocytes: In Vitro Studies Show Persistent Phenotypes of Aging, Increased Proliferation, and Resistance to Down-Regulation. Neurobiology of Aging 19, 97-103.
Schneider, C.A., Rasband, W.S., Eliceiri, K.W., 2012. NIH Image to ImageJ: 25 years of image analysis. Nature Methods 9, 671-675.
Schwarz, J.M., Sholar, P.W., Bilbo, S.D., 2012. Sex differences in microglial colonization of the developing rat brain. J Neurochem 120, 948-963.
Sengupta, P., 2013. The Laboratory Rat: Relating Its Age With Human's. Int J Prev Med 4, 624-630.
Shah, F., Hume, S.P., Pike, V.W., Ashworth, S., McDermott, J., 1994. Synthesis of the enantiomers of [N-methyl-11C]PK 11195 and comparison of their behaviours as radioligands for PK binding sites in rats. Nuclear Medicine and Biology 21, 573-581.
Sharaf, A., Krieglstein, K., Spittau, B., 2013. Distribution of microglia in the postnatal murine nigrostriatal system. Cell and Tissue Research 351, 373-382.
Sharma, K., Bisht, K., Eyo, U.B., 2021. A Comparative Biology of Microglia Across Species. Front Cell Dev Biol 9, 652748.
Sheffield, L.G., Berman, N.E.J., 1998. Microglial Expression of MHC Class II Increases in Normal Aging of Nonhuman Primates. Neurobiology of Aging 19, 47-55.
Sorby-Adams, A.J., Vink, R., Turner, R.J., 2018. Large animal models of stroke and traumatic brain injury as translational tools. American Journal of Physiology-Regulatory, Integrative and Comparative Physiology 315, R165-R190.
Sun, M., McDonald, S.J., Brady, R.D., Collins-Praino, L., Yamakawa, G.R., Monif, M., O'Brien, T.J., Cloud, G.C., Sobey, C.G., Mychasiuk, R., Loane, D.J., Shultz, S.R., 2020. The need to incorporate aged animals into the preclinical modeling of neurological conditions. Neuroscience & Biobehavioral Reviews 109, 114-128.

Takagi, S., Furube, E., Nakano, Y., Morita, M., Miyata, S., 2019. Microglia are continuously activated in the circumventricular organs of mouse brain. Journal of Neuroimmunology 331, 74-86.
Torres-Platas, S.G., Comeau, S., Rachalski, A., Bo, G.D., Cruceanu, C., Turecki, G., Giros, B., Mechawar, N., 2014. Morphometric characterization of microglial phenotypes in human cerebral cortex. J Neuroinflammation 11, 12.
Troncoso-Escudero, P., Parra, A., Nassif, M., Vidal, R.L., 2018. Outside in: Unraveling the Role of Neuroinflammation in the Progression of Parkinson's Disease. Frontiers in Neurology 9.
Turner, R.J., Farr, T.D., 2024. Climbing the STAIRs to SPAN the Clinical Translation Gap: Recent Advances in Multicenter Preclinical Stroke Trials. Stroke 55, 2366-2369.
Vaughan, D.W., Peters, A., 1974. Neuroglial cells in the cerebral cortex of rats from young adulthood to old age: an electron microscope study. J Neurocytol 3, 405-429.
Viana, L.C., Lima, C.M., Oliveira, M.A., Borges, R.P., Cardoso, T.T., Almeida, I.N.F., Diniz, D.G., Bento-Torres, J., Pereira, A., Batista-de-Oliveira, M., Lopes, A.A.C., Silva, R.F.M., Abadie-Guedes, R., Amâncio dos Santos, A., Lima, D.S.C., Vasconcelos, P.F.C., Cunningham, C., Guedes, R.C.A., Picanço-Diniz, C.W., 2013. Litter size, age-related memory impairments, and microglial changes in rat dentate gyrus: Stereological analysis and three dimensional morphometry. Neuroscience 238, 280-296.
Vidal-Itriago, A., Radford, R.A.W., Aramideh, J.A., Maurel, C., Scherer, N.M., Don, E.K., Lee, A., Chung, R.S., Graeber, M.B., Morsch, M., 2022. Microglia morphophysiological diversity and its implications for the CNS. Front Immunol 13, 997786.
Ward, T.H., Cummings, J., Dean, E., Greystoke, A., Hou, J.M., Backen, A., Ranson, M., Dive, C., 2008. Biomarkers of apoptosis. Br J Cancer 99, 841-846.
Wu, X., Wan, T., Gao, X., Fu, M., Duan, Y., Shen, X., Guo, W., 2022. Microglia Pyroptosis: A Candidate Target for Neurological Diseases Treatment. Frontiers in Neuroscience 16.
Xu, N., LaGrow, T.J., Anumba, N., Lee, A., Zhang, X., Yousefi, B., Bassil, Y., Clavijo, G.P., Khalilzad Sharghi, V., Maltbie, E., Meyer-Baese, L., Nezafati, M., Pan, W.J., Keilholz, S., 2022. Functional Connectivity of the Brain Across Rodents and Humans. Front Neurosci 16, 816331.
Xu, P., Zhang, X., Liu, Q., Xie, Y., Shi, X., Chen, J., Li, Y., Guo, H., Sun, R., Hong, Y., Liu, X., Xu, G., 2019. Microglial TREM-1 receptor mediates neuroinflammatory injury via interaction with SYK in experimental ischemic stroke. Cell Death Dis 10, 555.
Youm, Y.-H., Grant, Ryan W., McCabe, Laura R., Albarado, Diana C., Nguyen, Kim Y., Ravussin, A., Pistell, P., Newman, S., Carter, R., Laque, A., Münzberg, H., Rosen, Clifford J., Ingram, Donald K., Salbaum, J.M., Dixit, Vishwa D., 2013. Canonical Nlrp3 Inflammasome Links Systemic Low-Grade Inflammation to Functional Decline in Aging. Cell Metab 18, 519-532.
Żakowski, W., 2020. Animal Use in Neurobiological Research. Neuroscience 433, 1-10.
Zhang, W., Xiao, D., Mao, Q., Xia, H., 2023. Role of neuroinflammation in neurodegeneration development. Signal Transduction and Targeted Therapy 8, 267.
Zhou, J., Qiu, J., Song, Y., Liang, T., Liu, S., Ren, C., Song, X., Cui, L., Sun, Y., 2023. Pyroptosis and degenerative diseases of the elderly. Cell Death & Disease 14, 94.
Zhou, K.Q., Bennet, L., Wassink, G., McDouall, A., Curtis, M.A., Highet, B., Stevenson, T.J., Gunn, A.J., Davidson, J.O., 2022. Persistent cortical and white matter inflammation after therapeutic hypothermia for ischemia in near-term fetal sheep. J Neuroinflammation 19, 139.

4.9 Supporting Information

Cross-Species Characterisation of Microglial Morphology and Proliferation During Ageing

Laura M. Carr[1], Shannon Stuckey[1], Isabella Bilecki[1], Sanam Mustafa[1], Renée J. Turner[1], Lyndsey E. Collins-Praino[1]

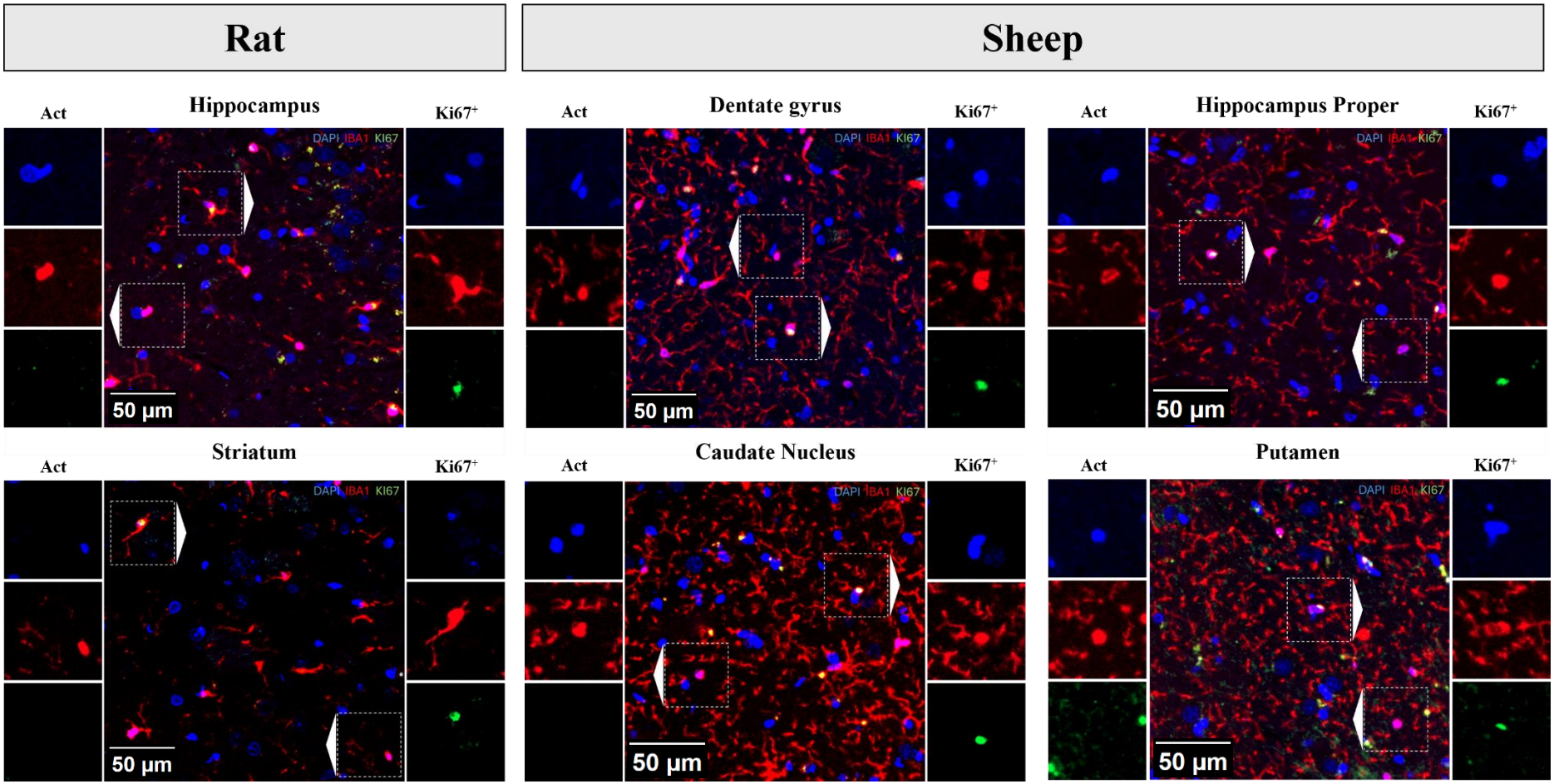
[1]School of Biomedicine, University of Adelaide, Adelaide, Australia
[2]School of Life Sciences, University of Technology Sydney, Sydney, Australia

A/Professor Lyndsey Collins-Praino
Email: Lyndsey.collins-praino@adelaide.edu.au

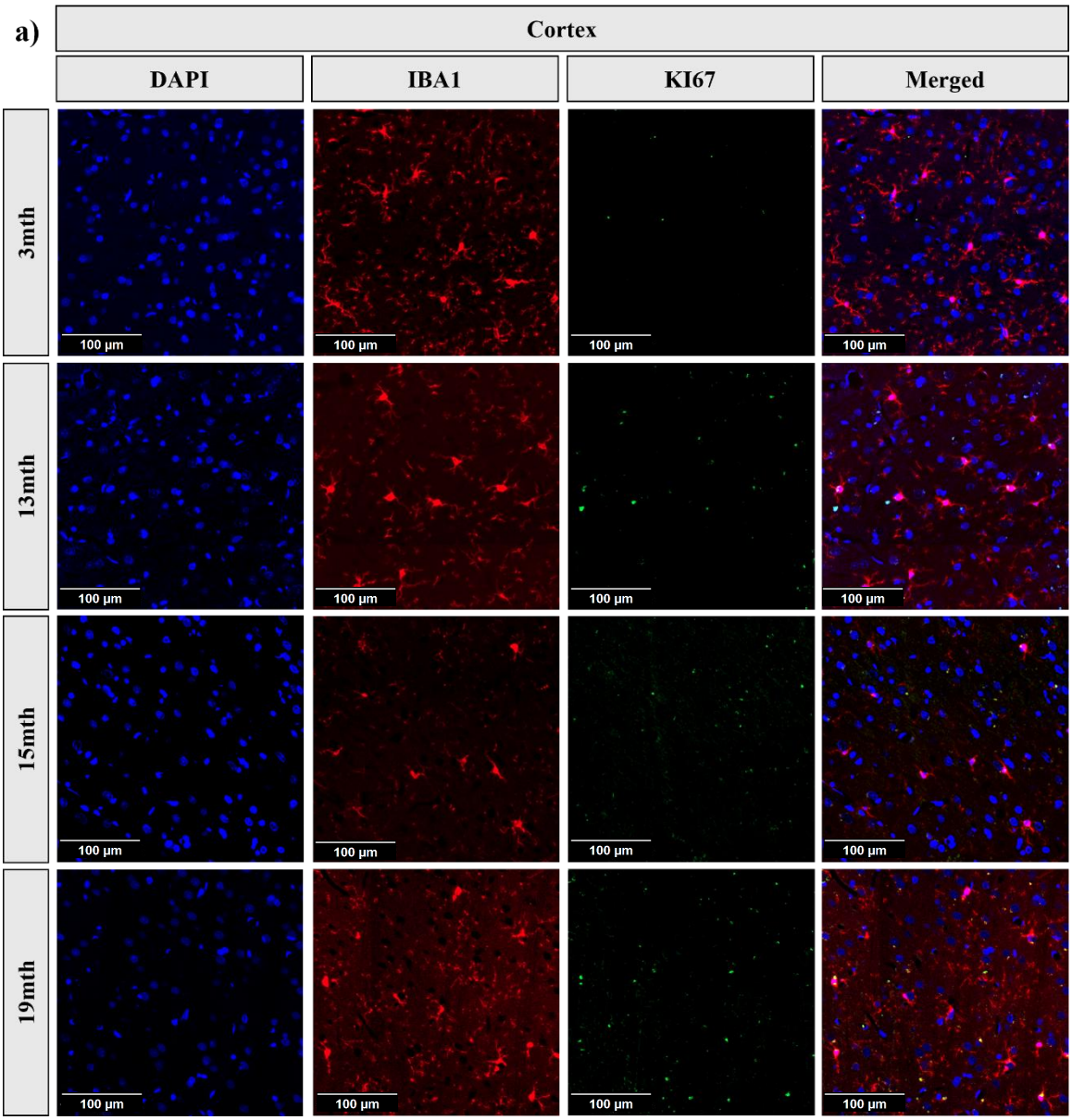
This document includes

Figures S4.1-S4.10

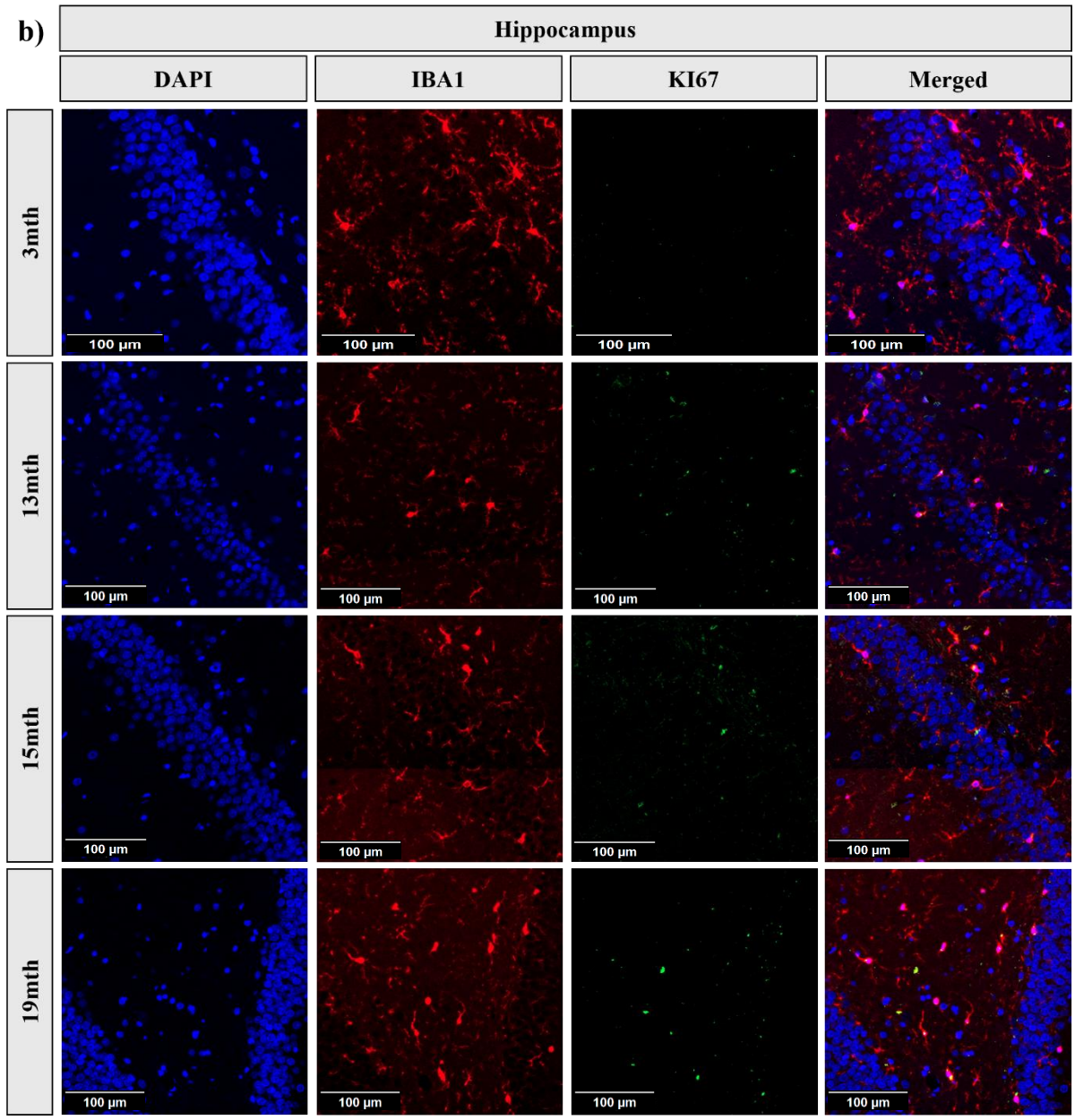
Tables S4.1-S4.3



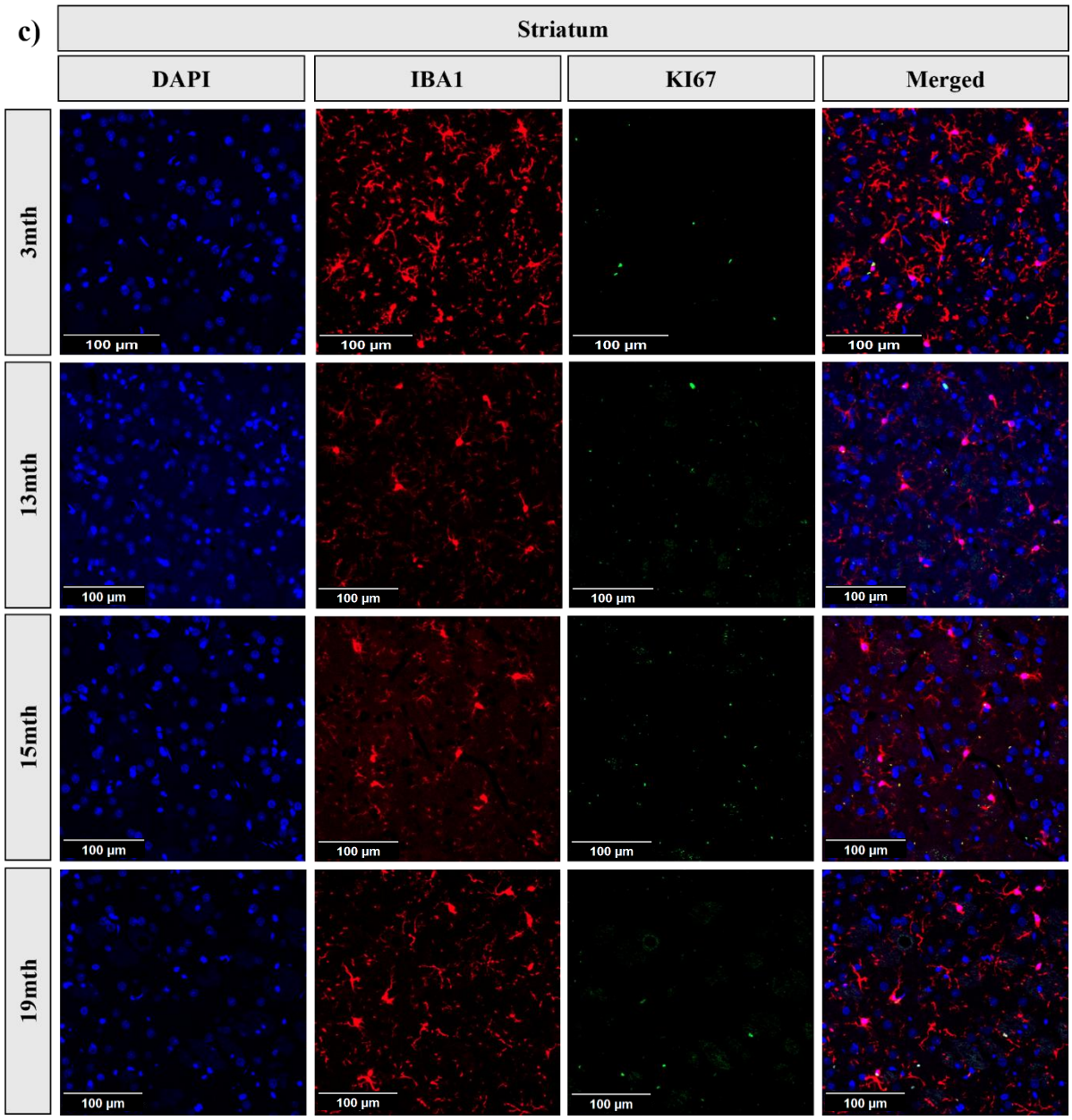
Supplementary Figure S 4.4 Representative images of immunofluorescent staining in old rat and sheep brains in hippocampal and striatal regions. Microglia were counted by identifying colocalised DAPI and IBA1. Microglia with an amoeboid morphology were classified as activated (Act) (left columns). Microglia were classified as Ki67$^+$ when both DAPI, IBA1 and Ki67 signal overlapped (right columns). Number of non-activated, activated and Ki67$^+$ microglia were counted manually



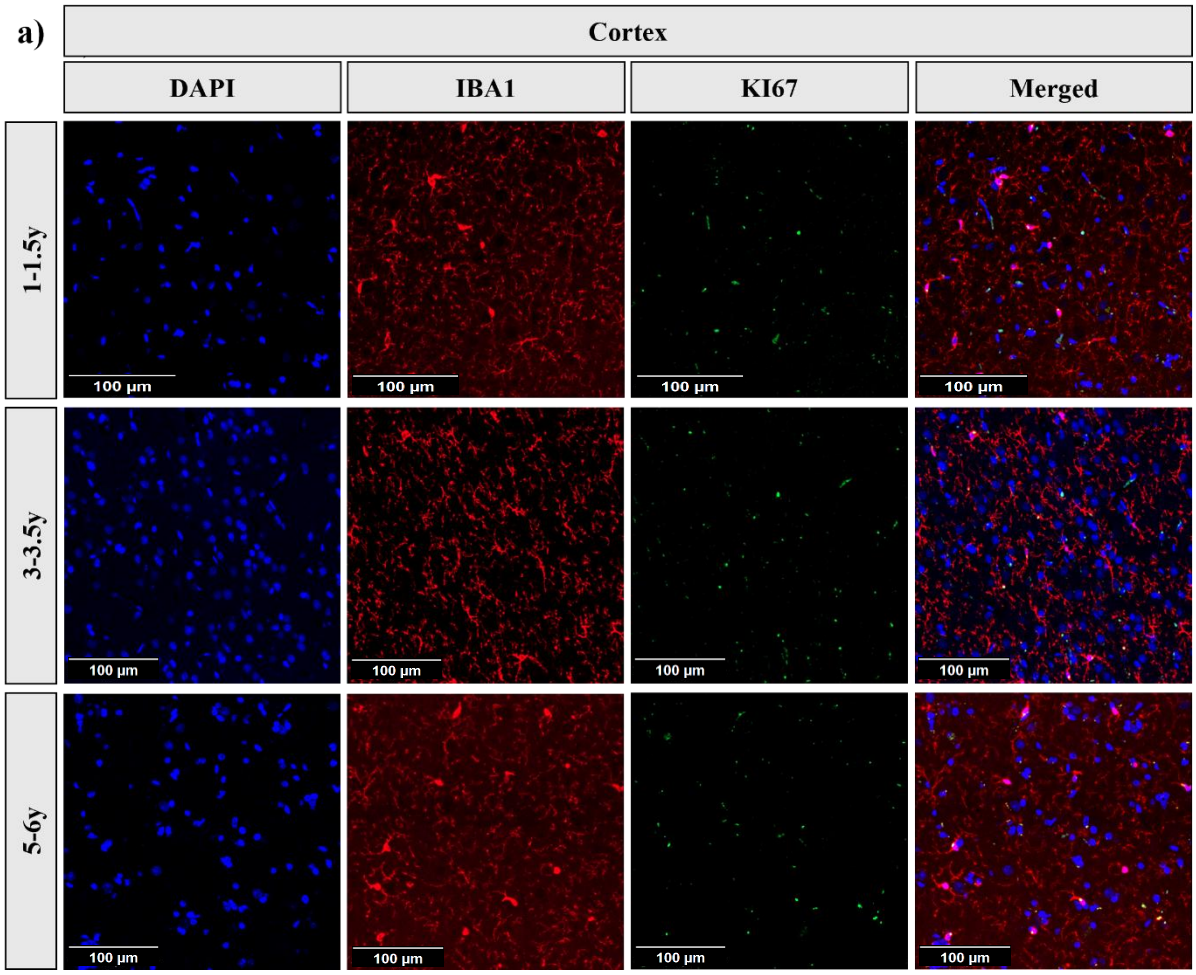
Supplementary Figure S 4.2 Individual channels for representative images in Fig 4.3a. Microglia were stained for IBA1 (red) in the rat cortex at each age. IBA1^{+} cells with a strong Ki67 signal (green) were classified as Ki67^{+} microglia. Nuclei were visualized using DAPI (blue).



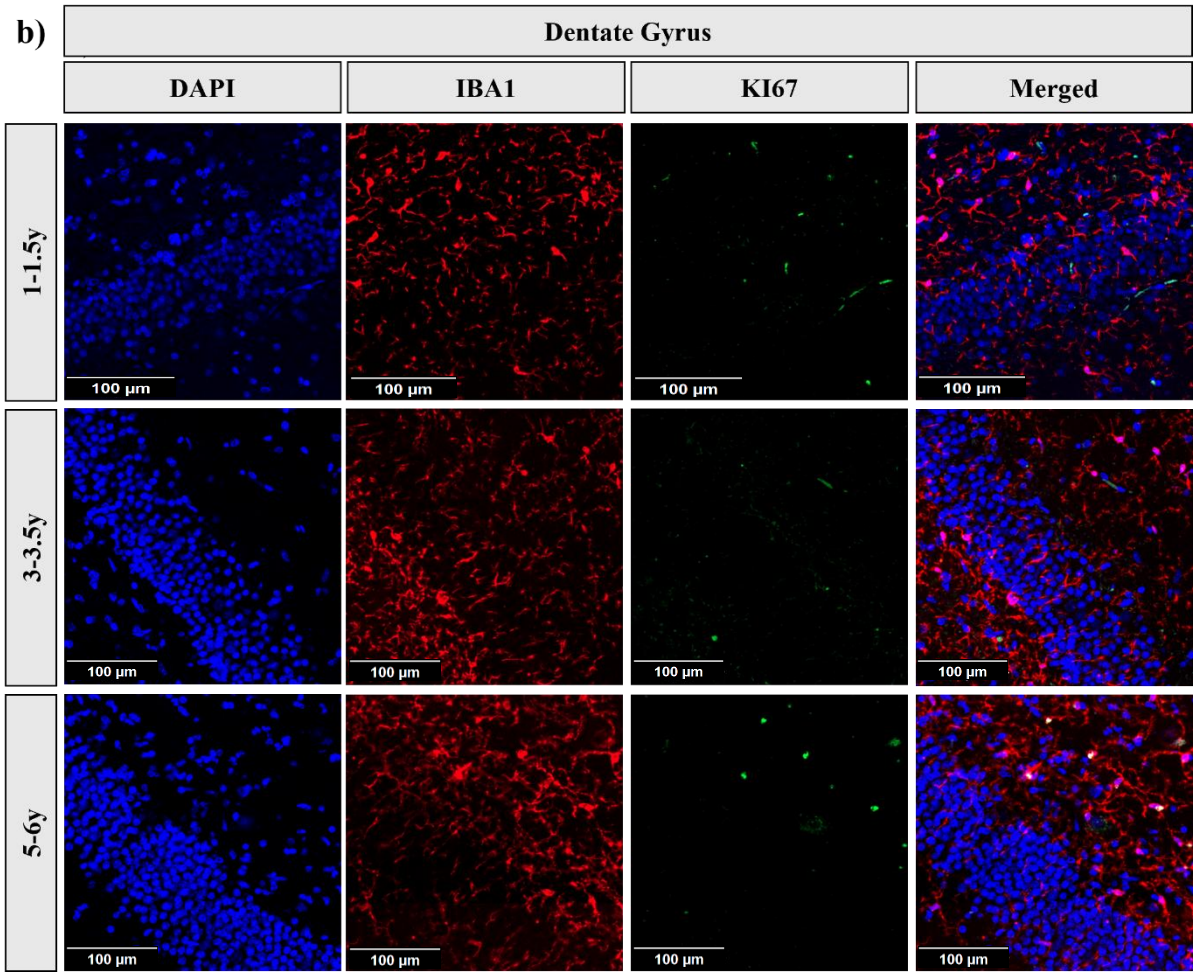
Supplementary Figure S 4.1.1 Individual channels for representative images in Fig 4.3a. Microglia were stained for IBA1 (red) in the rat Hippocampus at each age. IBA1$^+$ cells with a strong Ki67 signal (green) were classified as Ki67$^+$ microglia. Nuclei were visualized using DAPI (blue).



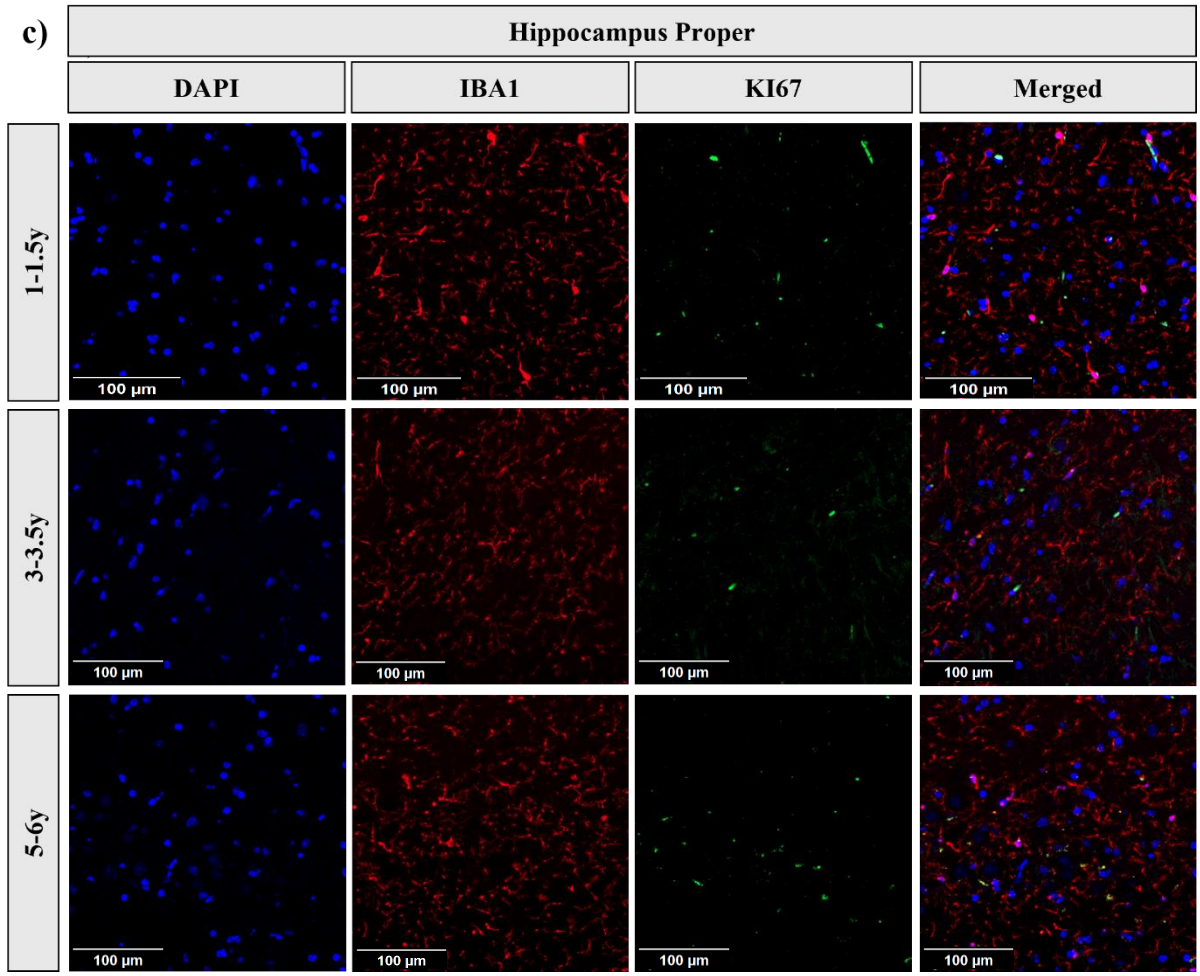
Supplementary Figure S4.1.2 Individual channels for representative images in Fig 4.3aMicroglia were stained for IBA1 (red) in the rat Striatum at each age. IBA1^{+} cells with a strong Ki67 signal (green) were classified as Ki67^{+} microglia. Nuclei were visualized using DAPI (blue).



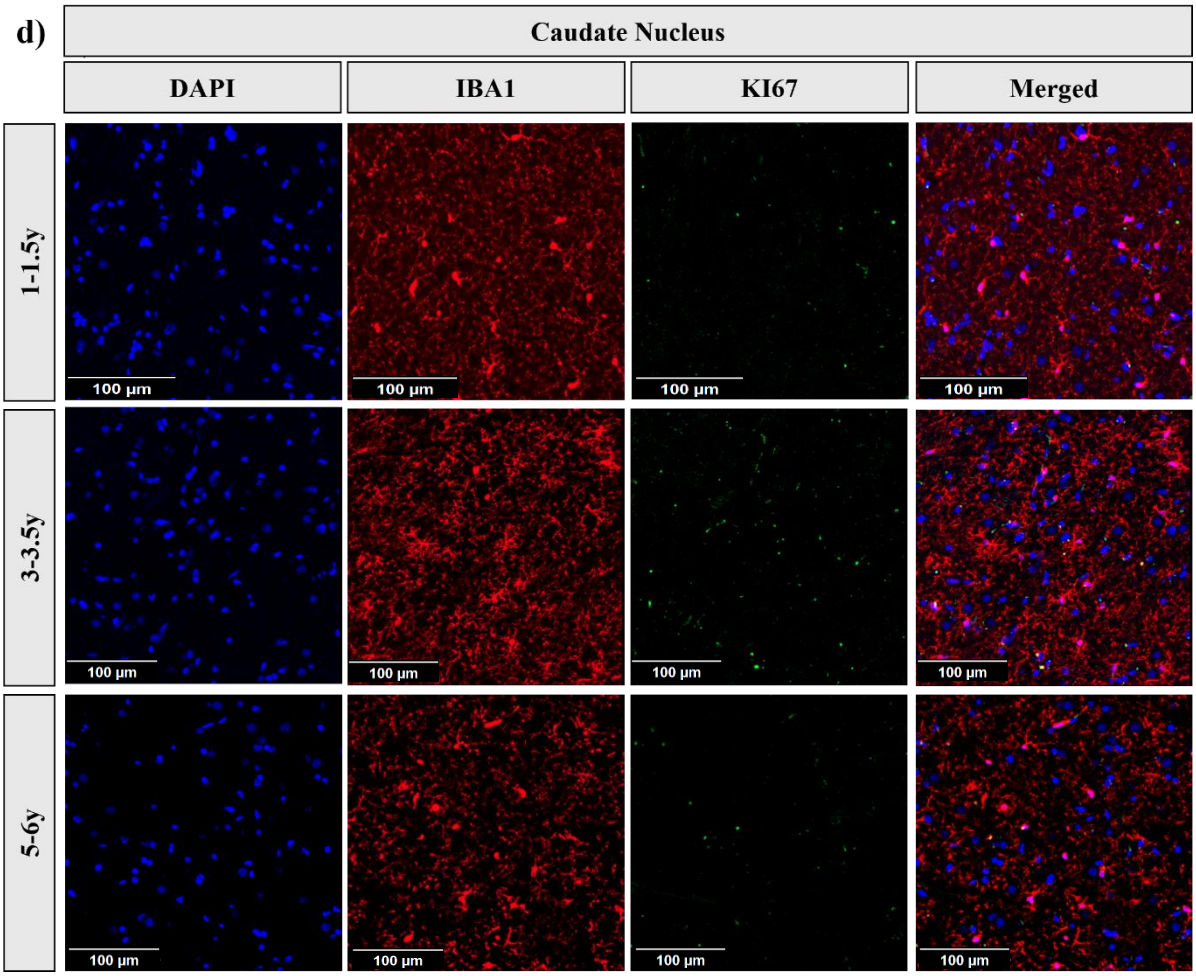
Supplementary Figure S 4.1.3 Individual channels for representative images in Fig 4.3a. Microglia were stained for IBA1 (red) in the sheep cortex at each age. $IBA1^+$ cells with a strong Ki67 signal (green) were classified as $Ki67^+$ microglia. Nuclei were visualized using DAPI (blue).



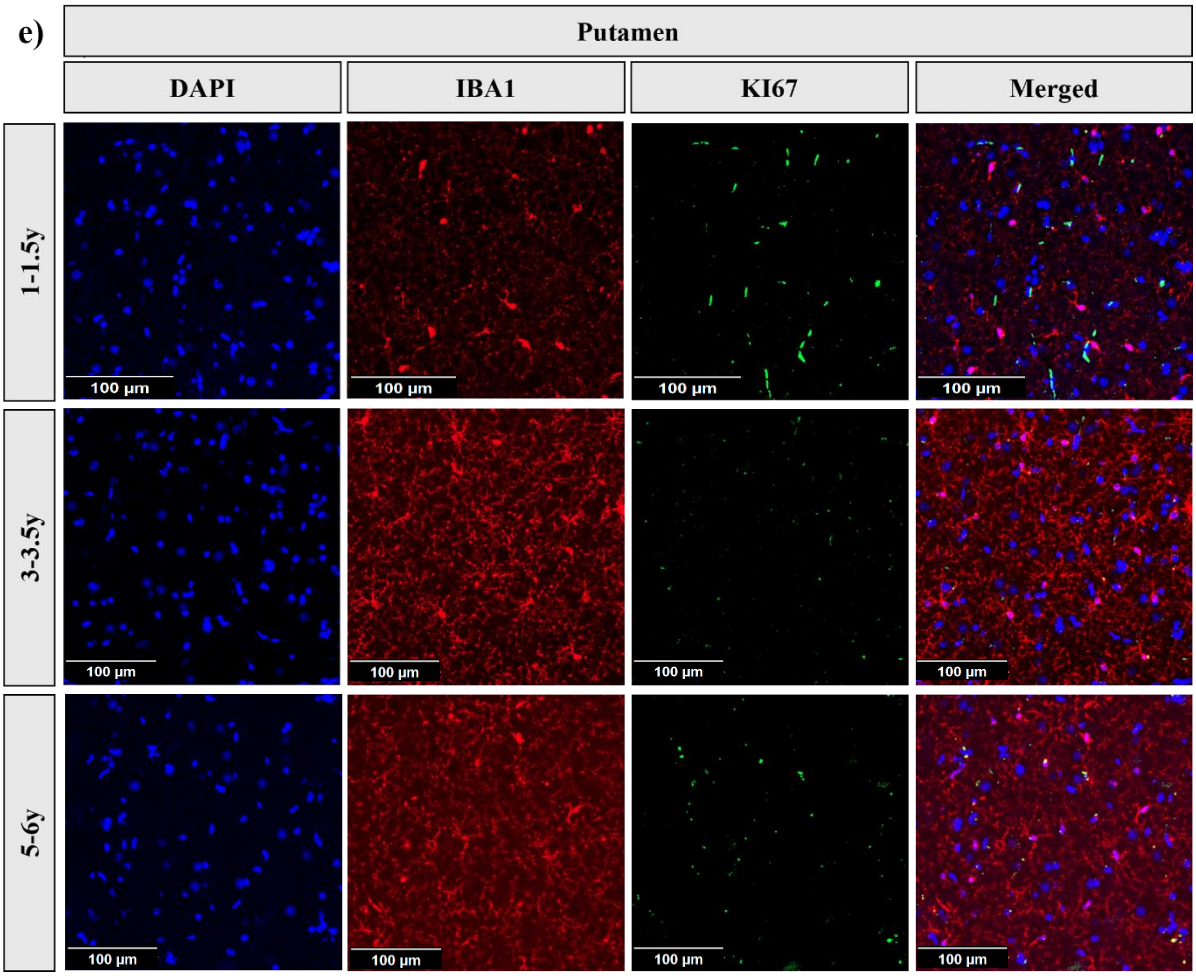
Supplementary Figure S 4.1.4 Individual channels for representative images in Fig 4.3a. Microglia were stained for IBA1 (red) in the sheep Dentate Gyrus at each age. IBA1^{+} cells with a strong Ki67 signal (green) were classified as Ki67^{+} microglia. Nuclei were visualized using DAPI (blue).



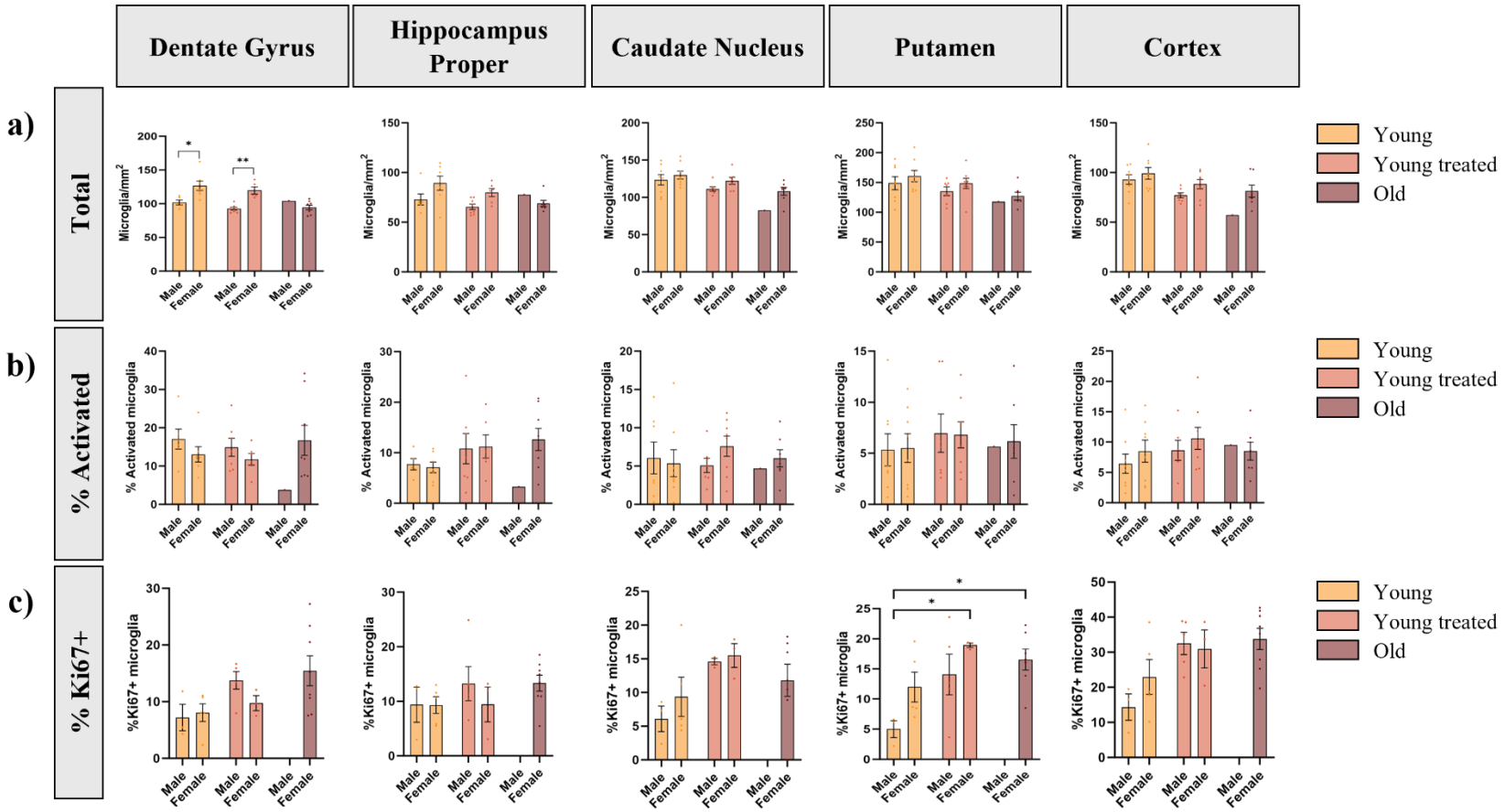
Supplementary Figure S 4.1.5 Individual channels for representative images in Fig 4.3a. Microglia were stained for IBA1 (red) in the sheep hippocampus proper at each age. IBA1^{+} cells with a strong Ki67 signal (green) were classified as Ki67^{+} microglia. Nuclei were visualized using DAPI (blue).



Supplementary Figure S 4.1.6 Individual channels for representative images in Fig 4.3a. Microglia were stained for IBA1 (red) in the sheep caudate nucleus at each age. IBA1^{+} cells with a strong Ki67 signal (green) were classified as Ki67^{+} microglia. Nuclei were visualized using DAPI (blue).



Supplementary Figure S 4.1.7 Individual channels for representative images in Fig 4.3a. Microglia were stained for IBA1 (red) in the sheep putamen at each age. IBA1$^+$ cells with a strong Ki67 signal (green) were classified as Ki67$^+$ microglia. Nuclei were visualized using DAPI (blue).



Supplementary Figure S 4.1.8 Microglia in the sheep brain, grouped by age and sex. a) total number of microglia detected by manual counting. n = 1-1.5y (8M:8F), 3-3.5y (8M:8F), 5-6y (1M:8F) b) % activated microglia detected by manual counting. n = 1-1.5y (8M:8F), 3-3.5y (8M:8F), 5-6y (1M:8F). c) number of Ki67+ microglia detected by manual counting. n = 1-1.5y (3M:5F), 3-3.5y (5M:3F), 5-6y (0M:8F). Data are graphed as mean±SEM. Significant differences were determined by two-way ANOVA (results presented in table S1). * = p<0.05, ** = p<0.01

Supplementary Table S4.1.1: Results from tukey post hoc testing conducted on sheep microglia data stratified into male and female groups. For total counts a significant interaction effect was observed in the DG, and main effects of sex were seen in the DG, CN and cortex. For Ki67 counts an effect of sex was seen in the PUT. Due to the low absence of males in the aged cohort for Ki67 counts, interaction effects could not be assessed.

		DG	HP	CN	PUT	Cortex
Total	Age	F (2, 28) = 2.796, P=0.0781	F (2, 29) = 1.674, P=0.2050	**F (2, 32) = 7.025, P=0.0030**	F (2, 33) = 2.850, P=0.0722	**F (2, 33) = 7.090, P=0.0027**
	Sex	**F (1, 28) = 7.355, P=0.0113**	F (1, 29) = 1.847, P=0.1846	**F (1, 32) = 5.155, P=0.0300**	F (1, 33) = 1.183, P=0.2846	**F (1, 33) = 5.486, P=0.0253**
	Interaction	**F (2, 28) = 3.707, P=0.0373**	F (2, 29) = 1.503, P=0.2393	F (2, 32) = 0.6261, P=0.5411	F (2, 33) = 0.009815, P=0.9902	F (2, 33) = 0.6261, P=0.5409
% activated	Age	F (2, 29) = 0.6332, P=0.5380	F (2, 28) = 1.378, P=0.2688	F (2, 32) = 0.1338, P=0.8753	F (2, 33) = 0.4607, P=0.6349	F (2, 32) = 0.8292, P=0.4456
	Sex	F (1, 29) = 0.3692, P=0.5482	F (1, 28) = 1.515, P=0.2286	F (1, 32) = 0.3470, P=0.5599	F (1, 33) = 0.009047, P=0.9248	F (1, 32) = 0.2548, P=0.6172
	Interaction	F (2, 29) = 2.010, P=0.1522	F (2, 28) = 1.136, P=0.3353	F (2, 32) = 0.5615, P=0.5759	F (2, 33) = 0.01198, P=0.9881	F (2, 32) = 0.1676, P=0.8464
Ki67+ *	Age	**F (2, 20) = 4.453, P=0.0251**	F (2, 20) = 1.572, P=0.2321	F (2, 17) = 3.244, P=0.0640	**F (2, 19) = 4.896, P=0.0193**	**F (2, 20) = 5.688, P=0.0111**
	Sex	F (1, 20) = 0.3375, P=0.5678	F (1, 20) = 0.5651, P=0.4610	F (1, 17) = 0.6135, P=0.4443	**F (1, 19) = 5.063, P=0.0365**	F (1, 20) = 0.5948, P=0.4496

Supplementary Table S4.1.2: Area analysed in microglial analysis in rat tissue.

Rat dataset												
	Cortex				Striatum				Hippocampus			
	3mth	13mth	15mth	19mth	3mth	13mth	15mth	19mth	3mth	13mth	15mth	19mth
# of sections	6		2		3		1-2		3		1	
Frame size	0.5mm^2				0.5mm^2				Entire visible hippocampus			
# of frames	6		12		6		6		3 x left 3 x right		1 x left 1 x right	
Av. Total area	3mm^2		6mm^2		3mm^2		3mm^2		8.65mm^2		6.66mm^2	
Av total cells counted	144.3	169	149	143.8	132.2	136.8	102.8	100.8	549.8	450.5	278	521.6

Supplementary Table S4.1.3: Area analysed in microglial analysis in sheep tissue.

Sheep dataset															
	Cortex			Dentate gyrus			Hippocampus Proper			Caudate nucleus			Putamen		
	1-1.5y	3-3.5y	5-6y	1-1.5y	3-3.5y	5-6y	1-1.5y	3-3.5y	5-6y	1-1.5y	3-3.5y	5-6y	1-1.5y	3-3.5y	5-6y
# of sections	1			1			1			1			1		
Frame size	0.95mm^2			Entire visible dentate gyrus			0.5mm^2			0.9mm^2			0.9mm^2		
# of frames	6			1x anterior, 1x posterior			6			3			3		
Av. Total area	5.7mm^2			7.01mm^2	10.24mm^2	9.39mm^2	3mm^2			2.7mm^2			2.7mm^2		
Av total cells counted	547.5	473.4	446	704.3	930	820.1	255	173.3	383.4	361.1	352.3	299	402.8	397.4	343

Contextual statement: Chapter 5

Chapter 5 is prepared in publication format. Chapter 4 highlighted the difficulties in aged animal research and the need to understand human disease by comparing results across species. Chapter 5 therefore utilises a publicly available database containing RNA-Seq data to assess microglial related gene expression across ageing, Alzheimer's Disease (AD), and Traumatic Brain Injury (TBI) in human post-mortem tissue. Specifically aiming to understand which pathways change in microglia across human ageing and if the presence of AD or TBI exacerbated these changes. Using the Allen Brain Atlas databases a panel of microglial related genes were assessed spanning microglial cell surface markers, pro-inflammatory cytokines and microglial signalling pathway genes. Additionally, Klotho, an ageing suppressor gene, was assessed in these cohorts as an established marker of ageing. Results from this analysis highlight key regions where microglia mRNA expression is altered, providing context for the results presented in chapter 4 where similar regions were assessed in pre-clinical models. Moreover, these results demonstrate potential areas for future research to focus on with regard to microglial ageing.

Statement of Authorship

Title of Paper	Characterising the Inflammatory mRNA Profile of Microglia Across Healthy Ageing, Neurodegeneration and Traumatic Brain Injury using the Allen Brain Atlas
Publication Status	☐ Published ☐ Accepted for Publication ☐ Submitted for Publication ☑ Unpublished and Unsubmitted w ork w ritten in manuscript style
Publication Details	

Principal Author

Name of Principal Author (Candidate)	Laura Carr		
Contribution to the Paper	First author and main contributor. Concept, writer and formulation of manuscript. Reviewed prepared final draft following inputs from co-authors.		
Overall percentage (%)	70%		
Certification:	This paper reports on original research I conducted during the period of my Higher Degree by Research candidature and is not subject to any obligations or contractual agreements with a third party that would constrain its inclusion in this thesis. I am the primary author of this paper.		
Signature		Date	25/11/2024

Co-Author Contributions

By signing the Statement of Authorship, each author certifies that:

i. the candidate's stated contribution to the publication is accurate (as detailed above);
ii. permission is granted for the candidate in include the publication in the thesis; and
iii. the sum of all co-author contributions is equal to 100% less the candidate's stated contribution.

Name of Co-Author	Aline Kunnel		
Contribution to the Paper	Statistical analysis, reviewed and edited manuscript		
Signature		Date	26/11/24

Name of Co-Author	Sanam Mustafa
Contribution to the Paper	Reviewed and edited manuscript, project supervision

Signature		Date	4/12/24

Name of Co-Author	Lyndsey E. Collins-Praino		
Contribution to the Paper	Conceptualisation, reviewed and edited manuscript, project supervision		
Signature		Date	2/12/24

Please cut and paste additional co-author panels here as required.

Chapter 5 : Characterising the Inflammatory mRNA Profile of Microglia Across Healthy Ageing, Neurodegeneration and Traumatic Brain Injury using the Allen Brain Atlas

Laura M. Carr[1], Aline Kunnel[2], Sanam Mustafa[1,3,4], Lyndsey E Collins-Praino[1]

[1] School of Biomedicine, University of Adelaide, Adelaide, Australia
[2]Womens and Kids Theme, South Australian Health and Medical Research Institute, South Australia, Australia
[3]Australian Research Council Centre of Excellence for Nanoscale Biophotonics, The University of Adelaide, Adelaide, SA, Australia
[4]Davies Livestock Research Centre, The University of Adelaide, Roseworthy, SA, Australia

5.1 Abstract

Microglia are the major immune cell in the central nervous system (CNS) and are critical in regulating the immune responses in the brain. Activation of microglia in response to injury or to pathology is important however, this response can become dysregulated, particularly during ageing and in certain neurological conditions. Chronic microglial activation has previously been linked to Alzheimer's Disease (AD) and traumatic brain injury (TBI), where pro-inflammatory factors secreted by microglia can exacerbate pathology and impede tissue repair. While the cytokines involved in this response are well-characterised, the upstream mechanisms of microglial activation in these conditions are not well understood. The present study aimed to characterise changes in expression of microglial related genes across healthy ageing (n=30), AD (n=30) and TBI (n=26), compared to young control cases (n=6), using an existing publicly available human gene database, the Allen Brain Atlas (ABA). Additionally, changes in Klotho, an ageing suppressor gene, were investigated to uncover potential neuroprotective mechanisms at play in these conditions. Supervised clustering analysis revealed distinct clustering of hippocampus samples compared to cortical regions in all cohorts of interest. Differential gene expression analysis identified 15 genes differentially expressed between groups. Of the groups of genes investigated, those related to cell surface marker expression in microglia were the most dysregulated, showing increases in the hippocampus of all groups compared to young controls and decreases in the temporal cortex compared to young controls almost exclusively in the TBI group. Minimal changes in microglial signalling pathways were observed in the hippocampus, with no changes seen in cortical

regions. Additionally, in all groups, Klotho expression decreased in the temporal cortex and increased in the hippocampus compared to young controls These results suggest that at the mRNA level, changes in microglia with age are not further exacerbated by disease or injury. However, further analysis of downstream effects of mRNA alterations with age is needed to uncover the effects of microglial ageing within these conditions.

5.2 Introduction

Microglia are the major immune cell in the brain and are critical in regulating inflammatory responses in the CNS (Yaqubi et al., 2023). In early life, microglia are important for facilitating the correct development of the CNS, including supporting neurogenesis, formation of neural pathways, synaptogenesis and gliogenesis (Menassa et al., 2022). At all stages of life, microglia have critical roles in immune system processes; however, regulation of stress responses is enriched during teenage years and beyond, indicating enhanced immune functions for microglia post-adolescence (Yaqubi et al., 2023). During this time, microglia are highly ramified in morphology and constantly survey the surrounding environment for pathogens, debris and immunological threats (Vidal-Itriago et al., 2022). Microglia become activated when a threat is detected, characterised by retraction of their processes and increased production of inflammatory cytokines (Vidal-Itriago et al., 2022). Under physiological conditions, this activation results in an initial pro-inflammatory response to combat the threat, followed by an anti-inflammatory response to promote tissue repair (Smith et al., 2012). With advanced age, however, microglia have lower thresholds for activation and an enhanced pro-inflammatory response (Norden and Godbout, 2013). As evidence of this, in C57BL/6J mice deficient in the DNA repair protein Ercc1, a model of accelerated ageing, have been used to assess microglial responses following peripheral administration by intraperitoneal (IP) injection with 1mg/kg of the endotoxin lipopolysaccharide (LPS). Microglia isolated from whole brains had an exaggerated response characterised by increased expression of the pro-inflammatory cytokines *IL-1β, TNF,* and *IL6* mRNA compared to WT controls (Raj et al., 2014). Similarly, an exaggerated expression of pro-inflammatory *IL-1β* mRNA, as well as increased *IL-10* mRNA expression, was reported within the cortex of naturally aged 18- to 20-month old (mo) BALB/c mice compared to 3- to 4-mo mice following IP injection with 0.33mg/kg of LPS challenge (Henry et al., 2009). While this finding was not specific to microglia, it highlights an increase in neuroinflammatory responses with age and when microglia were isolated from this region, those positive for Major Histocompatibility complex II (MHCII) showed the most prominent *IL1β* expression, indicating that activated microglia are the major contributors to the increased proinflammatory cytokine expression observed in the aged mouse cortex.

Microglia also undergo significant alterations in neurodegenerative diseases (ND), including Alzheimer's Disease (AD), with increases in microglial activation shown to occur both in pre-clinical rodent (Cao et al., 2021; McLarnon et al., 2006) and non-human primate (Jiang et al., 2024) models of AD, as well as in post-mortem assessment of human AD brains (see systematic review: (Hopperton et al., 2018)). As age is the number one risk factor for developing AD (Hou et al., 2019), disease-related changes may be exacerbated by the changes that occur as a result of physiological ageing (Norden et al., 2015). In line with this, microglial responses to ND pathology have been shown to be dysregulated with increased age. Interestingly, however, contrary to the increase in pro-inflammatory cytokine production seen with physiological ageing (Henry et al., 2009; Raj et al., 2014) microglia isolated from 18-mo C57BL/6 mice showed a decreased capacity to phagocytose amyloid-β (Aβ) and a decreased expression of pro-inflammatory cytokine genes following Aβ administration *in vitro* compared to microglia from 3-mo mice (Thomas et al., 2022), suggesting that the response of aged microglia to AD pathology is altered. In support of this, findings from microarray analysis of aged and AD human post-mortem tissue from the hippocampus have shown altered responses in AD brains compared to healthy aged brains. When young (20-59-years-old (yo)), aged (60-99-yo) and AD brains (74-95-yo) were analysed for expression of inflammatory genes, AD samples were observed to have higher expression of certain immune related genes (*IL-6* and *IL-10*) compared to the aged group, although this effect was not consistently seen for all markers, with no differences between AD and ageing noted for either *IL-1β* or *TNF* (Cribbs et al., 2012). These results are in conflict with mouse studies described above using isolated microglia, suggesting that aged mouse microglia may respond in a different manner to microglia in human microglia from AD brains however this could also be a result of methodological differences rather than representing a true biological discrepancy. These results suggest that there may be potentially distinct changes in microglial inflammatory pathways in AD compared to healthy ageing, which differ in humans compared to mice.

Beyond neurodegenerative disease, dysregulated neuroinflammation has also been shown to occur across multiple other neurological conditions, including traumatic brain injury (TBI). Interestingly, TBI is also hypothesised to trigger accelerated brain ageing (Gan et al., 2021) and is known to increase the risk of dementia (Fann et al., 2018; Gardner et al., 2023). The mechanisms responsible for this are poorly understood; however, TBI induced by controlled cortical impact (CCI) in 18-mo male C57BL/6 mice has recently been shown to accelerate the onset of ageing-related changes in microglia, which, in turn, are associated with increased phagocytosis of neurons and myelin and subsequent neurodegeneration (Ritzel et al., 2023). Notably, these microglial changes persisted for up to 1-year post-injury, suggesting that they may play a critical role in the increased risk of ND development following TBI. Advances in techniques to assess neuroinflammation following TBI have been recently reviewed and discussed in relation to the need to more thoroughly consider neuroinflammation as a consequence of TBI both acutely and chronically (Zheng et al., 2022). Neuroinflammation in the acute timeframe following TBI is characterised by increased release of pro-inflammatory cytokines, including TNF, IL-6, interferon-γ, and IL-1β, which peaks within 48 hours of injury (Frugier et al., 2010; Simon et al., 2017). However, of growing concern are the long-term effects of TBI, specifically the sustained activation of glial cells such as microglia. Microglial activation as measured by an increase in amoeboid and $CD68^+$ cells has been observed in approximately 28% of cases more than year up following TBI (Johnson et al., 2013). Further, high levels of Nod-like receptor (NLR) pyrin domain containing 3 (NLRP3) inflammasome, components (NLRP3, caspase-1 and apoptosis-associated speck-like protein containing a CARD (ASC)) have been detected in the cerebrospinal fluid (CSF) of moderate-severe TBI survivors who presented with an unfavourable Glasgow Outcome Scale (GOS) score 5-months following injury (Adamczak et al., 2012). Microglia strongly express the NLRP3 inflammasome in the CNS (Chiarini et al., 2023), the chronic upregulation of NLRP3 components following TBI suggests an association between heightened pro-inflammatory microglial activation and worsened cognitive outcomes at chronic timepoints following injury. This is in line with previous hypotheses that ageing induces changes in microglia that make the brain more vulnerable to the development of ND (Bickford et al., 2017). Critically, enhanced expression of ageing suppressor genes, such as *Klotho*, can reduce microglial activation and hyperphosphorylated tau pathology in the APP/PS1 model of AD (Zhao et al.,

2020). While not yet investigated in TBI, *Klotho* also appears to be neuroprotective in another model of neurotrauma, cerebral ischemia induced by common carotid occlusion (Long et al., 2018). It is currently unclear how *Klotho* and other ageing-related suppressor genes reduce microglial activation, but it may interfere with classical pattern recognition receptor (PRR) pathways of microglial activation.

PRR pathways are critical in triggering microglial activation in disease and injury (Glezer et al., 2007). PRRs include Toll-like receptors (TLRs), NLRs and Rig-like receptors (RLRs) which are activated by damage- or pathogen-associated molecular patterns (DAMPs/PAMPs) (Kigerl et al., 2014). Pathology, such as the presence of Aβ in AD (Jana et al., 2008) or cell death (Balança et al., 2021) induced following TBI, can cause activation of these pathways. Activation of these signalling pathways leads to the production and release of inflammatory factors, further promoting inflammation in the brain (Kigerl et al., 2014). This response is thought to be exaggerated during physiological ageing (Letiembre et al., 2007), although the specific molecular changes within microglia that may drive this are unclear. Nuclear factor Kappa B (NF-KB) (O'Neill and Kaltschmidt, 1997), Fyn kinase (Panicker et al., 2015) and induction of the NLRP3 inflammasome (Liang et al., 2024) are all key upstream signalling mechanisms that play a role in driving the production and release of pro-inflammatory factors during microglial activation, but how these change with healthy ageing, compared to in ND or following neurotrauma, is still a matter of debate.

Thus, the current study utilised the publicly available human gene database, the Allen Brain Atlas (ABA), to investigate how genes associated with microglia, cytokines and key intracellular signalling pathways change with age, compared to alterations seen in AD or following TBI. Additionally, changes in *Klotho* were investigated in these conditions, in order to uncover potential associations between *Klotho* expression and microglial activation. Taken together, these results will contribute to understanding of how microglial gene expression varies across brain regions with age and whether this differs further with disease or injury, elucidating potential involvement of microglial ageing in AD and TBI.

5.3 Materials and Methods

5.3.1 Data Sources

Gene expression data from brain regions of interest (Table 5.1) were downloaded from the ABA database. Gene expression data were extracted for the temporal cortex (TCx), parietal cortex (PCx) and hippocampus, regions selected due to their known involvement in ageing (Cheng et al., 2020; Jao et al., 2020; Raz et al., 2004), AD (Foster et al., 1984; Jack et al., 1998; Thompson et al., 2004; Thompson et al., 2001) and TBI (Bielefeld et al., 2024; Xue et al., 2022). Young control data were obtained from the Human Brain Atlas (HBA) (Allen Institute for Brain Science, 2024d) and experimental cohort data were obtained from the Aging, Dementia and TBI study (ADTS) (Allen Institute for Brain Science, 2024c). Cohort details and tissue collection and processing procedures for each dataset are available below, with further information available in the ABA white paper documentation (HBA: (Allen Institute for Brain Science, 2024b), ADTS: (Allen Institute for Brain Science, 2024a)). Tissue collection was conducted with informed consent from the patients' next of kin and was conducted with approval from the Human Investigation Committees and Institutional Ethics Committees of the University of Maryland. Demographic data for each cohort is presented in Table 5.2.

Table 5.1: Regions of interest and sub structures included in analysis

Temporal cortex structures	Parietal cortex structures	Hippocampus structures
Fusiform gyrus	Angular gyrus	CA1
Inferior temporal gyrus	Anterior paracentral lobule	CA2
Planum temporale	Posterior paracentral lobule	CA3
Superior temporal gyrus	Post-central gyrus	Dentate gyrus
Temporal pole	Precuneus	Subiculum
Transverse gyri	Superior parietal lobe	
	Supramarginal gyrus	

5.3.2 Human Brain Atlas Database

Data for the young control group were obtained from the HBA RNAseq transcriptome data. Briefly, the brains of six individuals, aged 24-57 years old, with no known pathology were obtained from independent tissue branks by the Allen Institute and anatomical regions of interest were processed for analysis by RNAseq. Data were normalised to an internal control and incorporated into the HBA

dataset. Z-score data for genes of interest (GOI) were extracted for each of the subregions of interest within Table 5.1 and a composite value for each ROI was used for subsequent analyses.

5.3.3 Aging, Dementia and TBI study cohort

Data for aged, AD and TBI cohorts were obtained from the ADTS RNAseq transcriptome data. Briefly, the brains of 107 participants were obtained by the University of Washington Neuropathology Core as part of the Adult Changes in Thought (ACT) study and sections from the hippocampus, parietal lobe and temporal lobe were sent to the Allen Institute for RNAseq analysis. Data were normalised to an internal control and incorporated into the ADTS dataset. Subjects with a Diagnostic and Statistical Manual of mental disorders-IV (DSM-IV) diagnosis of multiple aetiologies, other medical condition, vascular dementia, or other causes of dementia were excluded from the current study (n=21). Subjects with no history of TBI and no dementia diagnosis were included as the aged control group (n=30). Subjects with a history of one or more TBIs and a DSM-IV diagnosis of no dementia were included as the TBI group (n=26). Subjects with a DSM-IV diagnosis of AD-type dementia comprised the AD group (n=30). The AD group also included those with both an AD diagnosis and a history of TBI. Of note, DSM-IV diagnosis was utilised over a national Institute of Neurological and Communicative disorders and Stroke (NINCDS) and Alzheimer's Disease and Related Disorders Association (ADRDA) (NINCDS-ADRDA) diagnosis of probable AD in order to maintain statistical power. Z-score data for GOI were extracted for each of the overall ROIs in Table 5.1 (TCx, PCx, HIP) and used in subsequent analyses. In table 5.2 injury severity in the TBI and AD groups were classified based on longest loss of consciousness (LOC) duration as follows. Mild (<10 minutes LOC), moderate (10 minutes to 1 hour LOC), severe (>1hour LOC) or unknown. Injury severity and Braak staging was not accounted for in grouping.

Table 5.2: Demographic information for control and experimental groups

Group	N	Age (years)	Sex	Num subjects with TBI	Time since first TBI (years)	Injury severity (n of cases)	Braak stage
Young control	6	Range: 24-57 Median: 44	5M:1F	0	N/A		N/A

Aged control	30	Range: 78-97 Median: 89	15M:14F	0	N/A		Range: 0-5 Median: 3 Mean±SD: 2.65±1.26
Alzheimer's Disease (AD)	30	Range: 78-100 Median: 88.5	16M:14F	14	Range: 4-90 Median: 38 Mean±SD: 41.71±31.11	Unknown: 2 Mild: 8 Moderate: 2 Severe: 2	Range: 0-6 Median: 5 Mean±SD: 4.23±1.85
Traumatic Brain Injury (TBI)	26	Range: 78-100 Median: 90.5	19M:7F	26	Range: 2-85 Median: 56 Mean±SD: 45.07±30.05	Unknown: 2 Mild: 16 Moderate: 4 Severe: 4	Range: 0-6 Median: 3 Mean±SD: 3±1.76

5.3.4 Genes of interest

21 GOIs were selected for investigation. Based on previous literature, these genes can be categorised into one of four groups of interest: ageing-related, microglial cell surface markers, inflammatory cytokines and cytokine receptors, and microglial signalling pathways. Probe IDs varied between HBA and ADTS datasets, but corresponded to the same GOI and Entrez ID. Specific GOIs and the respective probes used for analysis are presented in Table 5.3.

Table 5.3: GOI, Entrez ID and gene probe IDs used in the HBA and ADTS.

GOI	ABBR.	Entrez ID	HBA probe ID	ADTS probe ID
Ageing related genes				
Klotho	KL	9365	1048676	499337340
Klotho beta	KLB	152831	1034281	499316273
Microglial cell surface marker genes				
Allograft inflammatory factor 1	AIF1	199	1059297	499321143
CD68 molecule	CD68	968	1021849	499344129
Triggering receptor expressed on myeloid cells 2	TREM2	54209	1042976	499321451
Purinergic receptor P2Y, G-protein coupled, 12	P2RY12	64805	1023078	499315054
Transmembrane protein 119	TMEM119	338773	1032073	499336504
Inflammatory cytokine and receptor genes				
Interleukin 6	IL6	3569	1055072	499323373
Interleukin 6 receptor	IL6R	3570	1055070	499307536
Interleukin 1, beta	IL1B	3553	1055098	499311184
Tumor necrosis factor	TNF	7124	1050713	499321138
Tumor necrosis factor receptor superfamily, member 1A	TNFRSF1A	7132	1050701	499334745

Microglial signalling pathway genes				
FYN proto-oncogene, Src family tyrosine kinase	FYN	2534	1029625	499322245
Nuclear factor of kappa light polypeptide gene enhancer in B-cells 1	NFKB1	4790	1053731	499317002
NLR family, pyrin domain containing 3	NLRP3	114548	1017159	499309291
Toll-like receptor 4	TLR4	7099	1029986	499329240
Caspase 1, apoptosis-related cysteine peptidase*	CASP1	834	1026236	499334048
Protein kinase C, delta*	PRKCD	5580	1030581	499313862
PYD and CARD domain containing*	PYCARD	29108	1044291	499342838
Mitogen-activated protein kinase 3*	MAPK3	5595	1052670	499342773
Mitogen-activated protein kinase 14*	MAPK14	1432	1057918	499321360

**Genes in bold were not included in differential expression analysis*

5.3.5 Statistical analysis

Statistical analyses were conducted using R (version 4.4.1) (Dalgaard, 2010), with the level of statistical significance set at 0.05.

5.3.5.1 Supervised Clustering Analysis

Supervised clustering using partial least squares-discriminant analysis (PLS-DA) and Sparse PLS-DA was applied to cluster the samples according to brain region, and to identify the markers playing the most important role in determining cluster membership. This process was applied to the young control group, aged control group, AD group and TBI group separately. PLS-DA and Sparse least squares-discriminant analysis were performed using mixOmics package (González et al., 2012; Lê Cao et al., 2009; Rohart et al., 2017).

Each component describes a linear combination of samples that best distinguished between the three brain regions (TCx, PCx, HIP). For each component, 5-fold cross validation repeated 10 times was used to evaluate the PLS-DA classification performance and its ability to correctly classify 'new' samples into their brain region category using repeated cross-validation. It was found that the error rate reached a minimum from 2-3 components for each group, respectively, and was optimal.

5.3.5.2 Differential Gene Expression Analysis

Following clustering, the gene panel for microglia signalling pathways was reduced to only the main upstream markers of key pro-inflammatory signalling pathways (*NLRP3, FYN, TLR4* and *NF-KB)* to conduct differential gene expression analysis. Bolded genes in Table 5.3 were not included in this

analysis. The *limma* package (Ritchie et al., 2015) was used to test for differential expression using linear models. This package uses empirical Bayes methods to shrink variances towards a common value and allows adjustment for multiple comparisons. In determining statistical significance, multiple-comparisons adjustment was undertaken to control the Family-Wise Error Rate at < 0.05. Linear models were fitted for each region separately. Log fold change (LogFC) estimates with 95% confidence intervals were reported for each marker. All pairwise comparisons were reported, with p-values adjusted for multiple tests using the Bonferroni correction. Expression data were visualised using version 10.0.0 for Windows (GraphPad Software, San Diego, California USA).

5.4 Results

5.4.1 The hippocampus has a distinct gene profile in aged, AD and TBI brains, with a similar but less distinct pattern present in young controls

Supervised cluster analysis was conducted to identify components that best separated the brain regions and the genes that contributed most to these components. Distinct profiles were observed between cortical clusters (PCx and TCx regions) and the HIP cluster in all four cohorts. In young controls, there was distinct clustering of all 3 brain regions, with the first component explaining 44% of the variance and the second component explaining 12% of the variance (Fig 5.1a). Nevertheless, due to the small sample size (n = 6), clustering for this cohort should be interpreted with caution. PLS-DA component 1 was able to successfully discriminate HIP from PCx and TCx in aged control (Fig 5.1b), AD (Fig 5.1c), and TBI (Fig 5.1d) groups.

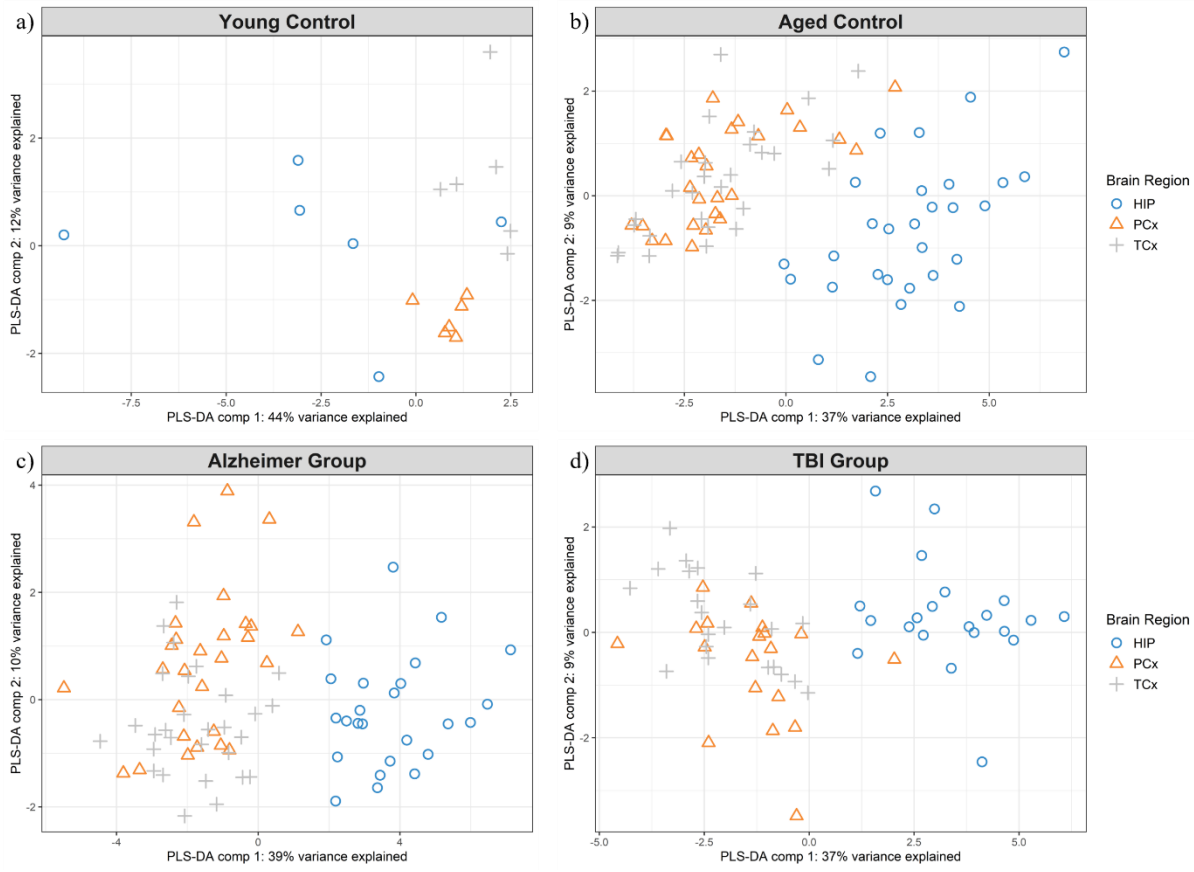


Figure 5.1: PLS-DA plot of samples in control and experimental groups. Samples are projected into the space spanned by the first two components and are coloured by brain region. a)young controlsamples: component 1 explains 44% of variance and component 2 explains 12% of variance. b) aged control samples: component 1 explains 37% of variance and component 2 explains 9% of variance. c) AD samples: component 1 explains 39% of variance and component 2 explains 10% of variance. d) TBI samples: component 1 explains 37% of variance and component 2 explains 9% of variance.

5.4.2 Microglial cell surface markers are upregulated in the hippocampus, but downregulated in the TCx, with age

To identify differentially expressed genes (DEGs), linear regression models were fitted for each region separately. For brevity, only significant statistical results for regression models are presented in Table 5.4. For all results from linear regression models, see Supplementary Tables S5.1-S5.3. Six DEGs were identified in the TCx, seven in the HIP and two in the PCx. These changes were mainly associated with the expression of microglial cell surface marker genes and *Klotho*, with only minor changes noted for microglial signalling pathway genes. No changes in the expression of any inflammatory cytokine and cytokine receptor genes were observed (Supplementary Figure S5.1).

Table 5.4: Significant results from multiple comparison tests

TCx				
Gene	**LogFC (95%CI)**	**Ave Expr**	**P-val**	**Adj.P-val**
Aged Control vs Young Control				
KL	-0.484 (-0.744, -0.224)	-0.412	0.000	0.000
TREM2	-0.878 (-1.384, -0.371)	-0.503	0.001	0.016
TMEM119	-0.890 (-1.430, -0.351)	-0.482	0.001	0.016
CD68	-0.920 (-1.515, -0.324)	-0.516	0.003	0.048
AD vs Young Control				
KL	-0.488 (-0.747, -0.229)	-0.412	0.000	0.000
TMEM119	-0.864 (-1.402, -0.326)	-0.482	0.002	0.032
TBI vs Young Control				
KL	-0.523 (-0.789, -0.257)	-0.412	0.000	0.000
P2RY12	-0.930 (-1.541, -0.320)	-0.251	0.003	0.048
AIF1	-1.077 (-1.755, -0.399)	-0.300	0.002	0.032
TREM2	-1.061 (-1.580, -0.542)	-0.503	0.000	0.000
TMEM119	-1.416 (-1.968, -0.863)	-0.482	0.000	0.000
CD68	-1.133 (-1.742, -0.523)	-0.516	0.000	0.000
TBI vs AD				
TMEM119	-0.552 (-0.891, -0.212)	-0.482	0.002	0.032
TBI vs Aged Control				
TMEM119	-0.525 (-0.867, -0.183)	-0.482	0.003	0.048

PCx				
Gene	**LogFC (95%CI)**	**Ave Expr**	**P-val**	**Adj.P-val**
TBI vs Young Control				
CD68	-0.880 (-1.455, -0.306)	-0.484	0.003	0.048
P2RY12	-0.920 (-1.479, -0.360)	-0.274	0.002	0.032
HIP				
Gene	**LogFC (95%CI)**	**Ave Expr**	**P-val**	**Adj.P-val**
Aged Control vs Young Control				
KL	1.687 (1.014, 2.361)	1.440	0.000	0.000
P2RY12	1.091 (0.405, 1.777)	0.605	0.002	0.032
TREM2	1.128 (0.523, 1.733)	0.728	0.000	0.000
TLR4	1.149 (0.426, 1.871)	0.791	0.002	0.032
TMEM119	1.103 (0.431, 1.775)	0.675	0.001	0.016
CD68	1.382 (0.747, 2.016)	0.729	0.000	0.000
AD vs Young Control				
KL	1.340 (0.657, 2.022)	1.440	0.000	0.000
P2RY12	1.167 (0.472, 1.863)	0.605	0.001	0.016
TREM2	1.368 (0.755, 1.981)	0.728	0.000	0.000
FYN	1.023 (0.355, 1.691)	0.751	0.003	0.048
TLR4	1.282 (0.549, 2.014)	0.791	0.001	0.016
TMEM119	1.296 (0.615, 1.977)	0.675	0.000	0.000
CD68	1.524 (0.881, 2.168)	0.729	0.000	0.000
TBI vs Young Control				
KL	1.368 (0.673, 2.063)	1.440	0.000	0.000
P2RY12	1.130 (0.422, 1.838)	0.605	0.002	0.032
TREM2	1.067 (0.443, 1.692)	0.728	0.001	0.016
CD68	1.407 (0.752, 2.062)	0.729	0.000	0.000

Five microglia cell surface markers were assessed covering both general markers (*AIF1*, *P2RY12*, and *TMEM119)*, and markers of activation (*CD68* and *TREM2)*. The majority of these showed at least some change in differential expression with age. Visualisations of microglial cell surface marker expression in the TCx, HIP and PCx are displayed in Figure 5.2a, b, and c, respectively. Expression of the microglial marker *P2RY12* was altered in all brain regions, increasing in the TBI group in the HIP *($p = 0.032$),* but decreasing in both the PCx *($p = 0.032$)* and TCx *($p = 0.048$),* compared to young control.

P2RY12 in the HIP also increased in aged control *(p = 0.032)* and AD *(p = 0.016)* compared to young control, but not in either the PCx or TCx ($p > 0.05$).

Other microglial cell surface markers were also increased in the HIP in aged control compared to young control(*TREM2*: *p = <0.001, TMEM119*: *p = 0.016*, *CD68*: *p = <0.001*), AD compared to young control(*TREM2*: *p = <0.001*, *TMEM119*: *p = <0.001*, *CD68*: *p = <0.001*), and in TBI compared to young control (*TREM2*: *p = 0.016*, *CD68*: *p = <0.001*). Conversely, in the TCx, several microglial markers were decreased in aged control compared to young control (*TREM2*: *p = 0.016*, *TMEM119*: *p = 0.016, CD68: p= 0.048*), AD compared to young control (*TMEM119*: *p = 0.032*), and in TBI compared to young control (*AIF1*: p = 0.032, *TREM2*: p = <0.001, *TMEM119*: p = <0.001, *CD68*: *p = <0.001*). For the PCx, the only significant changes in microglial cell surface marker expression noted were between TBI and young control (*P2RY12*: *p = 0.032*, *CD68*: *p = 0.048*), where a significance decrease in expression was noted for both markers in the TBI group.

Notably, the only microglial cell surface marker that significantly differed between aged cohorts was *TMEM119*, with its expression reduced in the TCx in TBI compared to both AD (*p = 0.036)* and aged control *(p= 0.048)*.

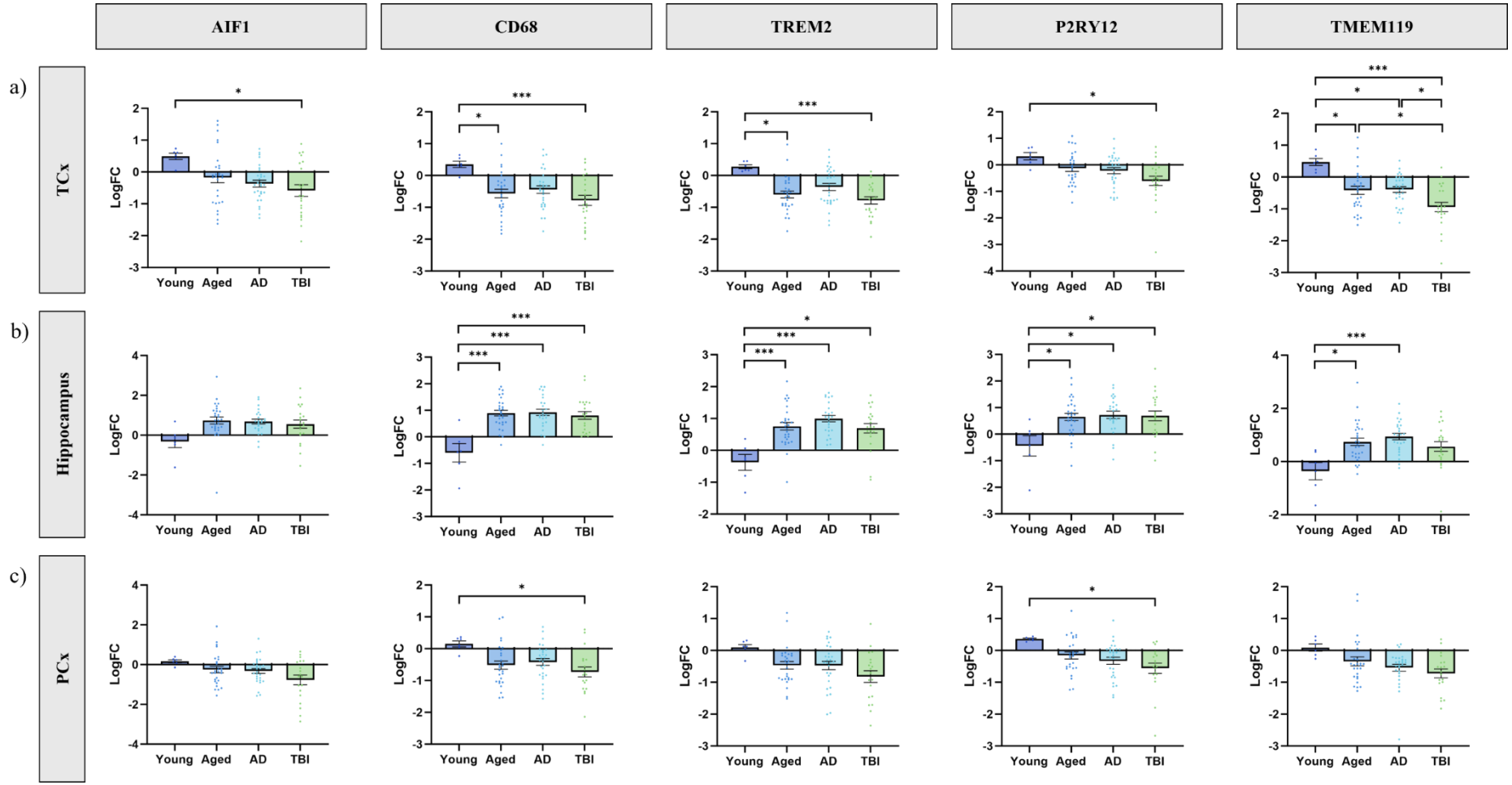


Figure 5.2: Gene expression of microglial markers in the human brain. Cohorts showed significant differences in gene expression of microglial cell surface markers *P2RY12*, *TREM2*, *TMEM119*, *CD68* and *AIF1* in a) the TCx, b) the HIP and c) the PCx. Differences were identified by linear regression with p-values adjusted by Bonferroni correction for multiple comparisons. * = p <0.05, ** = p <0.01, *** = p <0.001

5.4.3 The hippocampus, but not cortex, shows significant alterations in differential patterns of expression of FYN and TLR4 in ageing and AD

The differential expression of 4 markers related to major microglial intracellular signalling pathways was assessed: *TLR4, FYN, NFKB1* and *NLRP3.* Limited changes were seen in expression of these markers in the HIPP in aged control and AD (Table 5.4; Figure 5.3b). Specifically, in the HIP, *TLR4* gene expression was upregulated in both aged control *($p = 0.032$)* and AD *($p = 0.016$)* compared to young control, with *FYN* expression also significantly upregulated in AD compared to young control (*$p = 0.048$)*. This effect was not seen in the HIPP in TBI compared to young control (*$p > 0.05$)*. Of note, however, no significant differences in the expression pattern of microglial signalling pathway genes were found between aged control and either AD or TBI (*$p > 0.05$)*. Further, the cortical expression pattern of microglial signalling pathway genes did not significantly differ in any of the aged cohorts compared to young control (Figure 5.3a, c).

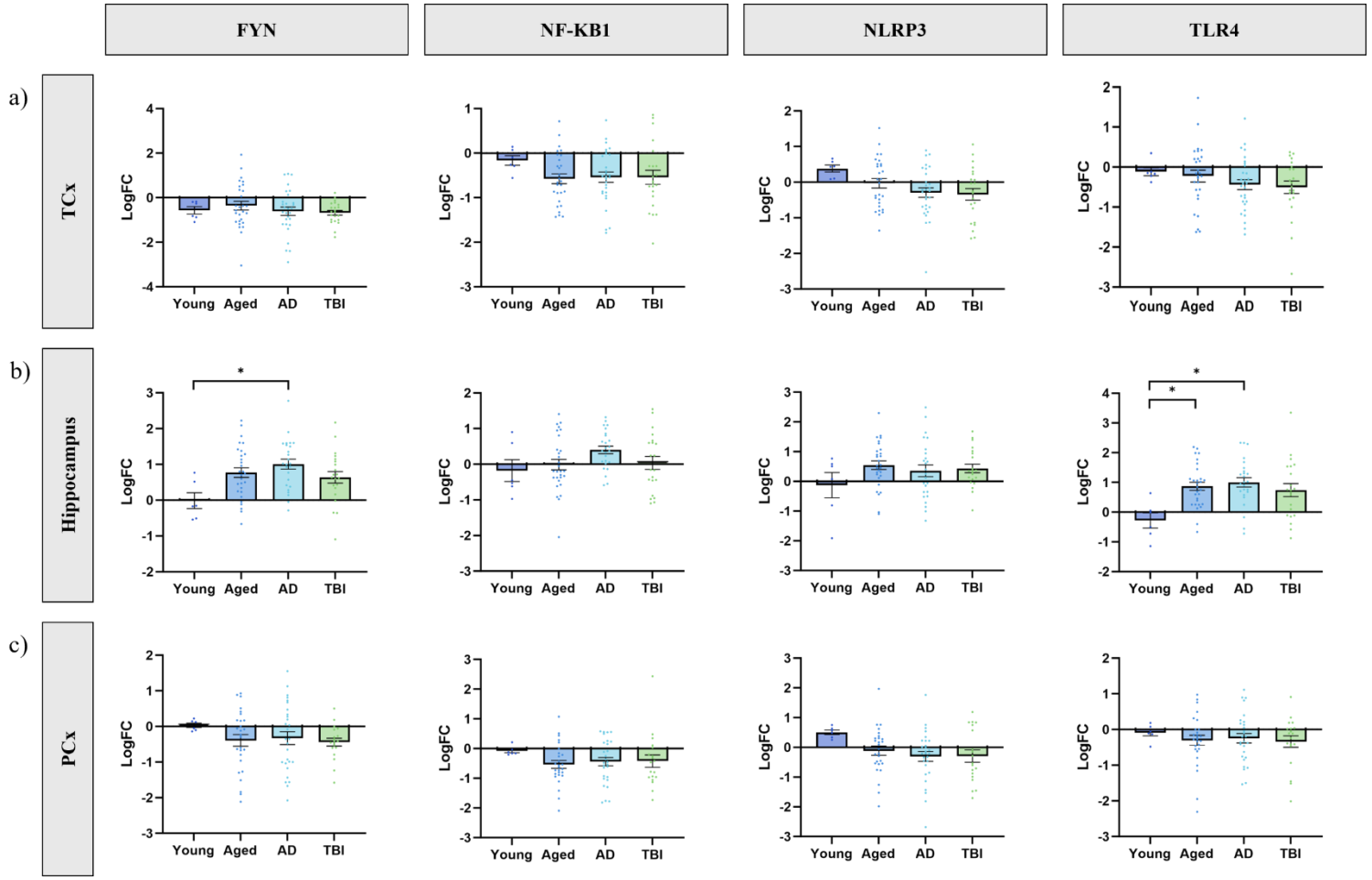


Figure 5.3: Gene expression of microglial signalling genes in the human brain. Cohorts showed significant differences in gene expression of microglial signaling genes *FYN* and *TLR4* in b) the HIP. Differences were identified by linear regression with p-values adjusted by Bonferroni correction for multiple comparisons. * = p <0.05, ** = p <0.01, *** = p <0.001

5.4.4 Differential expression of the ageing suppressor gene Klotho is upregulated in the hippocampus and downregulated in the TCx with age.

Expression of *Klotho* in the TCx, HIP and PCx is displayed in Figure 5.4a, b, and c, respectively. In the TCx, Klotho expression was downregulated compared to young control in all three aged cohorts: aged control *($p = <0.001$)*, AD *($p = <0.001$)* and TBI *($p = <0.001$) (*Figure 5.4a). Conversely, *Klotho* in the HIP showed the opposite pattern, with upregulated expression compared to young control in all groups (aged control *($p = <0.001$)*, AD *($p = <0.001$)*, and TBI *($p = <0.001$) (*Figure 5.4b)*)*. None of the aged groups significantly differed from one another in differential expression of Klotho (*$p > 0.05$)*. No changes in *Klotho* expression were seen in the PCx (Figure 5.4c) and no changes in *Klotho-β* were seen in any region analysed *($p>0.05$).*

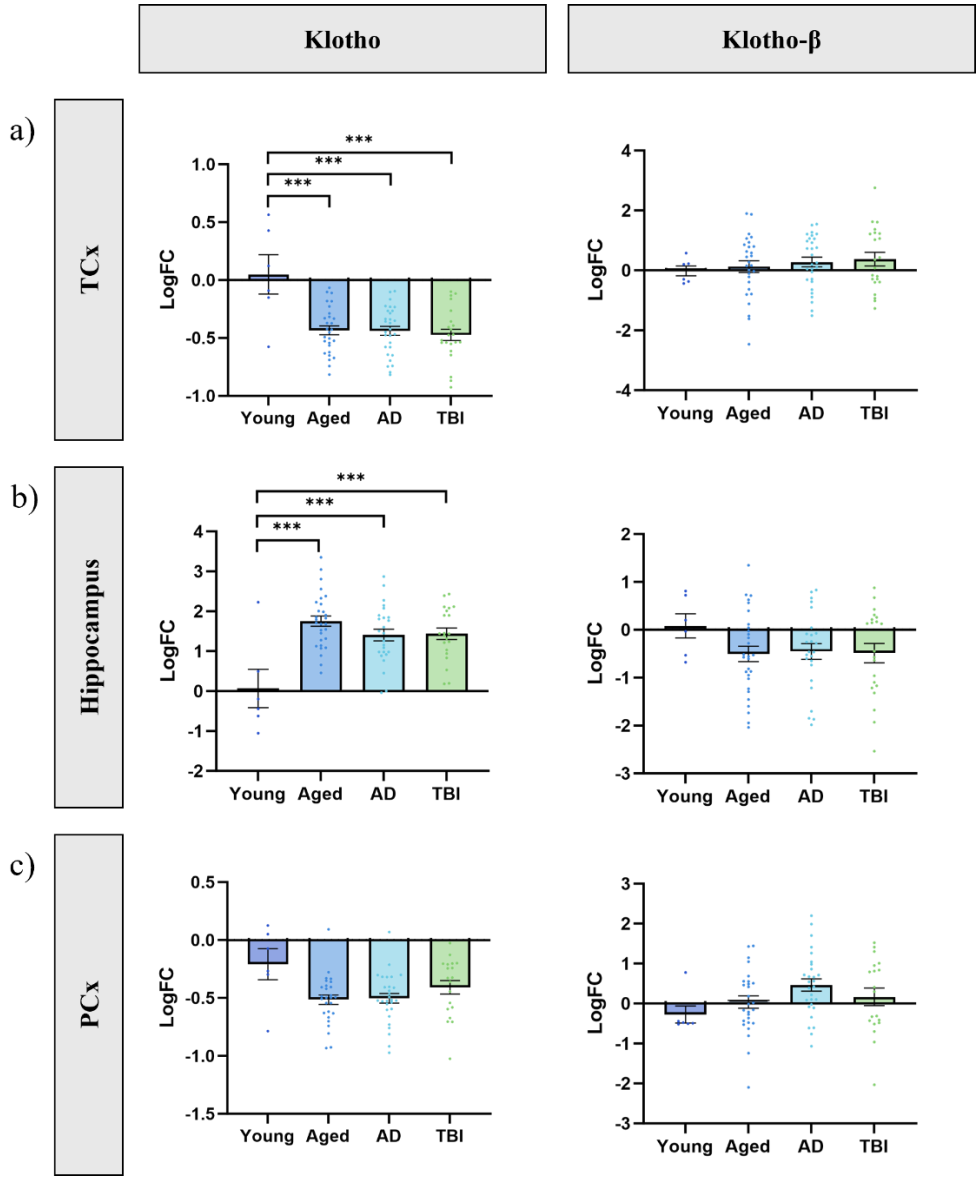


Figure 5.4: Expression of Klotho and Klotho-β in the human brain during ageing, AD and TBI. Cohorts showed significant differences in *Klotho* gene expression in a) the TCx b) the HIP. Differences were identified by linear regression with p-values adjusted by Bonferroni correction for multiple comparisons. * = p <0.05, ** = p <0.01, *** = p <0.001

Table 5.5: Summary of changes seen in GOI across ageing, AD and TBI. Red text indicates decreased expression, blue text indicates increased expression. All changes are relative to young control except where indicated by: * = compared to aged control and # = compared to AD.

GOI.	Ageing	AD	TBI
Ageing related genes			
KL	↓TCx ↑HIP	↓TCx ↑HIP	↓TCx ↑HIP
KLB	-	-	-
Microglial cell surface marker genes			
AIF1	-	-	↓TCx
CD68	↑HIP ↓TCx	↑HIP	↑HIP ↓TCx ↓PCx
TREM2	↑HIP ↓TCx	↑HIP	↑HIP ↓TCx
P2RY12	↑HIP	↑HIP	↑HIP ↓PCx ↓TCx
TMEM119	↑HIP ↓TCx	↑HIP ↓TCx	↓TCx #↓TCx *↓TCx
Inflammatory cytokine and receptor genes			
IL6	-	-	-
IL6R	-	-	-
IL1B	-	-	-
TNF	-	-	-
TNFRSF1A	-	-	-
Microglial signalling pathway genes			
NLRP3	-	-	-
FYN	-	↑HIP	-
NFKB1	-	-	-
TLR4	↑HIP	↑HIP	-

5.5 Discussion

Understanding the link between microglial ageing and other neurological conditions is critical in unravelling the immune contribution to disease. Thus, the current study sought to characterise the expression of microglia related genes across human ageing, as well as in both AD and TBI, by using publicly available RNAseq datasets from the ABA (Allen Institute for Brain Science, 2024d). A summary of significant changes in gene expression are shown in Table 5.5. Across healthy ageing (young control n=6 compared to aged control n=30), microglial cell surface markers were the most differentially expressed genes, with both general and activation-specific markers increasing in the hippocampus but decreasing in the TCx. The pattern of differential expression of these markers was largely similar to aged control in both AD (n=30) and in those with a history of TBI (n=26), although more markers were significantly downregulated in the cortex of the TBI group compared to the other two. Interestingly, however, very few significant differences were observed between groups, suggesting that age itself, and not disease state, is the primary factor contributing to changes in microglial expression identified. Also of note, while significant differences in cell surface marker expression were noted with age, relatively minimal changes were seen in microglial signalling pathways, and no changes were noted in inflammatory cytokine or receptor gene expression, suggesting that while cell number or activation state might be altered with age, this is not necessarily associated with significant changes in gene expression of microglial signalling pathway initiators. Finally, differential expression of the ageing suppressor gene *Klotho* was observed in the hippocampus and TCx in all groups compared to young controls. This altered expression was a pattern of decrease in the TCx and increase in the hippocampus.

The hippocampus and cortex show distinct patterns of change in both microglial-related and *Klotho* gene expression, as highlighted by supervised cluster analysis where the hippocampus was distinguishable from other regions, in all experimental cohorts (Fig 5.1.) However, it is important to note key limitations in the supervised clustering approach employed here. Supervised clustering analysis was applied to each cohort separately, meaning that the components identified in each group are specific to that dataset. As a result, the first component in one cohort may represent a different linear combination of genes compared to the first component of other cohorts. This cohort specific nature

prevents direct quantitative comparisons of clustering structures between groups and limits conclusions regarding relative differences in gene expression patterns across conditions. Additionally, due to the small sample size in the young control cohort (n = 6), which is reflective of the difficulty associated with sourcing postmortem brain tissue from healthy young donors (Rush et al., 2024), the results of the clustering analysis in this group should be interpreted with particular caution. Despite these constraints, the distinct profile of expression observed in the hippocampus relative to cortical regions is interesting, given the connection between memory impairment and the conditions investigated in this study. The hippocampus, critical for normal memory function (for review, see: (Bird and Burgess, 2008; Voss et al., 2017)), is strongly implicated in AD, a disease characterised by its progressive memory impairment (DeTure and Dickson, 2019), with rapid atrophy occurring in this region even in early disease stages (Jack et al., 1998). Similarly, both memory impairment and hippocampal atrophy are known to occur following TBI (Bielefeld et al., 2024) and during normal ageing (Raz et al., 2004). While cortical structure and function changes have also been shown to occur both in healthy ageing (Cheng et al., 2020; Jao et al., 2020) and in the context of AD (Foster et al., 1984; Thompson et al., 2004; Thompson et al., 2001) and TBI (Xue et al., 2022), these tend to be, at least to some extent, regionally specific (Bakkour et al., 2013; Koenig et al., 2022; Warner et al., 2010). Thus, it is possible that the results of our cluster analysis may have differed if individual subregions of either the parietal or temporal cortices were examined, which was not possible with the available data.

Overall, the distinct expression patterns noted between the hippocampus and cortex highlight that considering regional specificity is critical when looking at alterations in microglial gene expression patterns. This is in line with previous literature suggesting that the brain response to inflammatory challenge is region specific, with different patterns of pro-inflammatory gene expression measured by Bulk RNA-Seq noted in the cortex, as well as the striatum and thalamus, compared to the hippocampus and cerebellum (Süß et al., 2020). Similarly, in a genome-wide analysis of mouse microglia, regional differences in the ageing of microglia were reported, with the cerebellum and hippocampus being most susceptible to transcriptomic changes at 22-months-old compared to 4-months-old (Grabert et al., 2016). Although, in that study, in contrast with the results seen here, hippocampal microglia showed a

less distinct phenotype with age, with decreased expression of several genes related to immunoregulation and interaction with the environment, which may reflect species-specific differences (Masuda et al., 2019). Given this, future research should seek to further investigate regional differences in the impact of ageing on human microglial gene expression from a wider selection of brain regions, including the cerebellum.

Of the categories of genes explored within this study, those related to microglial cell surface markers were the most differentially expressed, with all genes in this group demonstrating some degree of alteration between groups. Interestingly, a different pattern of expression changes was noted in the hippocampus relative to the cortex, with microglial markers generally up-regulated in the hippocampus and down-regulated in the cortex (particularly the TCx) relative to young controls. Previous studies have suggested that the hippocampus is particularly vulnerable to the effects of inflammation (Colasanti et al., 2016; Davidson and Stevenson, 2024; Jung et al., 2022), and that inflammation is a critical driver of memory impairment (Chen et al., 2008; d'Avila et al., 2018; Lopez-Rodriguez et al., 2021), which, as noted above, is known to occur in the context of healthy ageing, as well as in both AD and following TBI. Thus, it is not surprising that microglial cell surface markers genes were altered in this region, including both general microglial markers (i.e. *TMEM119* (Bennett et al., 2016; Ruan et al., 2020) and *P2RY12 (Gómez Morillas et al., 2021)*) and those specific to microglial activation, such as *CD68*, a marker of lysosomal and phagocytic activity (Hendrickx et al., 2017), and *TREM2*, a surface PRR expressed on microglia (Tagliatti et al., 2024). What is unexpected, however, is that both markers related to microglia homeostasis and activation specific markers showed an up-regulation in this region. While some previous studies have reported an upregulation of *TMEM119* mRNA expression in the context of microglial activation (Mercurio et al., 2022; Satoh et al., 2016), multiple others have suggested reduced levels (Keren-Shaul et al., 2017; Krasemann et al., 2017; Li et al., 2018; Masuda et al., 2020; van Wageningen et al., 2019). Similarly, while resting microglia generally express high levels of *P2RY12* expression (Rivera et al., 2016), which plays a critical role in microglial motility and migration (see (Gómez Morillas et al., 2021) for review), upon microglial activation, expression levels drop as microglia switch to a more phagocytic phenotype (Haynes et al., 2006; Mildner et al., 2017;

Moore et al., 2015). In line with this, a reduction in *P2RY12* expression is seen across multiple diseases involving persistent neuroinflammation (Mildner et al., 2017), including AD (Sanchez-Mejias et al., 2016; Walker et al., 2020), as well as with healthy ageing (Crain et al., 2009; Galatro et al., 2017). Thus, the fact that a similar dissociation between homeostatic and activation genes was not observed here is difficult to explain. Interestingly, however, in a controlled cortical impact model in mice, Mercurio and colleagues (2022) demonstrated that while *TMEM119* mRNA expression was upregulated in active microglia, TMEM119 protein levels were actually decreased, suggesting a potential impairment in mRNA translation due to post-transcriptional modifications (Mercurio et al., 2022). Given that protein values are not available within the ABA, future research should pair mRNA and protein level analysis in order to investigate whether the upregulation in expression of these genes translated to increased protein levels within the hippocampus. While many studies have combined mRNA and protein analysis (for example: (Hickman et al., 2013; Pandey et al., 2018)), this should be more widespread as relying solely on mRNA data may not accurately reflect functional changes in microglia. This approach has been utilised previously by Williams et al., 2022 who applied an integrated approach using the YC cohort from the ABA database. Differentially expressed genes identified in microarray data were mapped to known protein interaction networks using the STRING protein-protein interaction database (Williams et al., 2022). While this study did not specifically examine microglia or age-related changes, it demonstrates how an integrated approach can provide deeper insights into molecular relationships within the ABA dataset. Further, investigation of whether microglia specifically are expressing these markers may shed light on this discrepancy, as CD68, AIF1, and TREM2 are expressed by both macrophages and microglia. Given that ageing, AD and TBI all feature some level of BBB dysfunction (Cash and Theus, 2020; Deo et al., 2014; Montagne et al., 2015) and macrophage infiltration (Gate et al., 2010; Hsieh et al., 2013; Wolfe et al., 2018), the presence of these cells may account for some expression of these non-specific markers.

In contrast to the significant up-regulation of microglial-related genes (and more modest changes in microglial signalling pathway gene expression) seen in the hippocampus, the cortex showed the opposite pattern, although this down-regulation was largely contained within the TCx and

disproportionately seen in the TBI group. This contrasting pattern of expression may reflect regional variation in microglial responses, which, as discussed above, previous literature has highlighted. Literature has additionally reported regional differences in microglial density (Lawson et al., 1990) and activation (Grabert et al., 2016) across the brain. The only microglial marker to show down-regulation in the TCx in comparison to young control across all three groups was *TMEM119*, with a down-regulation of the microglial activation markers *TREM2* and *CD68* also noted in the aged control group. Conversely, in the TBI group, a significant down-regulation in the TCx compared to young control was observed for every microglial gene assessed, including both general markers (*AIF1, P2RY12* and *TMEM119*) and those associated with microglial activation (*TREM2* and *CD68*). Additionally, a significant down-regulation in expression was noted in the PCx for *P2RY12* and *CD68* in this group. While the downregulation of both homeostatic and activation markers may seem counterintuitive given their inverse relationship, this highlights the possibility of suppression of microglial activity as a whole in cortical regions compared to other regions of the brain, which may disproportionately affect those with a history of TBI (with levels of TMEM119 significantly decreased in the TCx in this group relative to both aged control and AD). This could potentially reflect a compensatory response to TBI, characterised by decreases in microglia and suppression of inflammatory gene expression, in order to limit further inflammatory damage. It is important to note, however, that similar changes were not seen in the hippocampus, nor were there concomitant changes in the expression profiles of either cytokine or microglial signalling pathway genes in the TBI group compared to young control, so the functional significance of this cortical downregulation is unclear. Further, it is important to note that there was an extremely broad range of time since injury in the TBI group, 2 to 85 years, which may further complicate the interpretation of these results, due to potential alterations in microglial phenotype at different timepoints post-injury (Donat et al., 2017). Additionally, in the ABA database, beyond the total number of TBIs and whether these featured a loss of consciousness there is no measure of injury severity, limiting the ability to assess this variable and further contributing to the heterogeneity of results. It would thus be interesting to investigate the acute effect of TBI on microglial expression in older adults, in order to investigate how the injury itself may interact with ageing.

In the current study, significant upregulation of expression of microglial signalling pathway markers was noted, with the same general trend observed between aged groups. Specifically, significantly increased *FYN* signalling was seen in the hippocampus in AD, with hippocampal up-regulation of *TLR4* also noted in this group, as well as in the aged control group. While not reaching statistical significance, the TBI group also showed the same pattern of upregulation for these markers. TLR4 is an important PRR expressed on microglia and activation of these receptors can lead to the recruitment of Fyn (Panicker et al., 2015), an Src family tyrosine kinase involved in pro-inflammatory signalling (Guglietti et al., 2021). TLR4 expression has previously been shown to be enhanced in both ageing and AD (for review see: (Kim et al., 2023)). In line with this, in long-term cultures of hippocampal neurons, an *in vitro* model of ageing, both age and amyloid beta oligomers were shown to enhance TLR4 expression and neuronal cell death (Calvo-Rodríguez et al., 2017). Notably, TLR4 activation can subsequently mediate the activation of Fyn, which is thought to occur via interactions with adapter proteins such as myeloid differentiation primary response protein 88 (MyD88) and TIR-domain-containing adapter-inducing interferon-β (TRIF), leading to phosphorylation events that potentiate downstream signalling cascades, including activation of MAPK and Akt pathways. Recruitment of Fyn can amplify inflammatory responses and has been implicated in synaptic dysfunction and pathology in AD (Guglietti et al., 2021). For example, dysregulated Fyn activity has been linked to Aβ pathology via Fyn phosphorylation of Tau (Lee et al., 2004). Further, activity of Fyn disrupts NMDA receptor function and synaptic stability, thereby contributing to cognitive decline in AD (Trepanier et al., 2012). To date, however, age-related changes in Fyn are less well characterised. Interestingly, while the upregulation in *TLR4* and *FYN* in the hippocampus were in line with what might be expected given the upregulation of microglial cell surface marker genes in this region, other microglial signalling pathway markers, including *NFKB1* and *NLRP3* were not similarly affected. *FYN* in particular is a key mediator of inflammatory pathways including the activation of NF-κB *via* TLR4 signalling (Guglietti et al., 2021) however the absence of upregulation in *NFKB1* suggests that downstream components of these pathways may be regulated independently. Alternatively, while mRNA upregulation is observed, this

may not be effectively translated to Fyn protein expression or TLR4 receptors, thereby not initiating these pathways. In the case of TLR4, glycosylation is an important post-translational modification necessary for translocation of TLR4 to the membrane surface (da Silva Correia and Ulevitch, 2002). Alterations in many glycans and decreased glycosylation efficiency has been demonstrated with age (reviewed: (Paton et al., 2021)) and impacts the ability of cells to express factors dependent on this process such as TLR4. Similarly, mRNA expression of *FYN* requires lipidation in order to direct Fyn action on downstream targets (Koegl et al., 1994). The dysregulation of post-translational mechanisms with age (reviewed: (Santos and Lindner, 2017)) may therefore have impacted the ability of upregulated genes in the current study to act on downstream pathways, leading to no detectable upregulation of these targets.

Despite the significant up-regulation in the expression of genes related to microglial activation seen in the hippocampus, this was not accompanied by a concomitant increase in expression of inflammatory-cytokine related genes. This finding contrasts with previous findings where age related increases in pro-inflammatory cytokine expression and release have been seen during ageing and are further upregulated in AD compared to age matched controls. For example, p7.*2fms*-EGFP mutant mice on a C57BL6/6XCBA background which have green fluorescent protein (GFP) expressing microglia and macrophages, have shown an increase in *IL-6, TNF* and *IL-1β* mRNA at 18-months-old compared to 2-months-old (Sierra et al., 2007). Similarly, increases in TNF and IL-1β have been seen in the brains of 20- to 22-month-old male C57BL/6J mice compared to 3-months-old in both protein levels and in gene expression (Ritzel et al., 2015). These results suggest that at both the protein and mRNA level, pro-inflammatory cytokines increase with age in mouse models of ageing. Comparatively, in the current study no changes in mRNA cytokine expression were observed which may be explained by the concurrent lack of upstream signalling expression. NF-κB is the major initiator of TNF, IL-1β and IL-6 transcription during microglial activation and in the current study this pathway showed no alterations with age. Similarly, no increased expression of NLRP3 was observed, which aligns with the lack of *IL-1β* expression as these factors are strongly linked. The disparity between the results seen in the current study and the increase in pro-inflammatory cytokines with ageing and disease detailed throughout the

literature is unexpected. One potential explanation for this may be the advanced age and disease state at which the samples were analysed. The experimental groups (AC, AD or TBI) consisted of individuals aged 70 years and older, with some exceeding 100 years at the time of sample collection. It is possible that the heightened cytokine levels typically observed in earlier disease staged had diminished overtime, rendering them undetectable at the mRNA level. Additionally, inconsistencies may be more obvious when comparing between mRNA studies in rodents and human studies due to the region specificity. In the above two studies, the brain region samples were taken from was not specified whereas in the current study, analysis was conducted on multiple regions allowing for a more specific measurement. Thus, while overall levels of cytokines in the brain may increase in rodent studies, these results may not translate into human studies focused on specific regional expression of cytokines. In the current study a composite value for the hippocampus was used, which included multiple regions within the hippocampus (dentate gyrus, CA1, CA2, CA3 and subiculum). While this is a more targeted strategy, it is important to note that some sub-regions within the hippocampus show particularly high microglial activation relative to other sub-regions (Perkins et al., 2018; Viana et al., 2013). Therefore, an aggregated technique may not be truly representative of changes within these regions.

Contrary to our hypothesis, there were largely no significant differences noted between the aged control, AD and TBI groups for any of the microglia, cytokine or microglial signalling genes assessed in the current study. The only exception to this was a significant reduction in the TCx of the TBI group in *TMEM119* expression relative to both aged control and AD. This suggests that most of the gene expression changes noted in the current study are likely a function of age, and not a result of disease pathology. This is particularly surprising, given that the existing literature consistently documents microglial changes in AD and TBI compared to age-matched human controls (Johnson et al., 2013; Morimoto et al., 2011). These changes are often characterised by upregulation of microglial activation markers and pro-inflammatory cytokines, putting the results of the current study in direct opposition to the literature. For example, AD pathology is frequently associated with increased microglial activation and inflammatory signalling particularly in response to Aβ plaques (Bolmont et al., 2008) and Tau tangles (Perea et al., 2020; Perea et al., 2018). Similarly, TBI often leads to persistent

neuroinflammation, including at chronic timepoints following injury (Simon et al., 2017). Of note, nearly half (14/30) of individuals within the AD group had a prior history of TBI, making it difficult to truly assess the impact of injury compared to AD. This is higher than that reported in previous studies, with one population-based observational cohort study reporting that ~5% of individuals with dementia included in that study had a prior history of TBI (Fann et al., 2018). Despite this, TBI is a well-recognised risk factor for dementia, with TBI resulting in a 1.6-to-3.7-fold increase in dementia risk (Gardner et al., 2014; Raj et al., 2017) and with 5-15% of cases of dementia thought to be attributable to TBI (Shively et al., 2012). Thus, future analyses should compare expression levels in individuals with AD with and without a past history of TBI, which was not possible here due to the limited sample size.

In addition to assessing microglia specific pathways, here, the expression of the ageing suppressor gene *Klotho* was investigated. Levels of Klotho are known to decline with age. In a study examining levels of Klotho in the serum 181 healthy volunteers, children expressed significantly higher levels of Klotho than adult volunteers (Yamazaki et al., 2010). Prior to this, *Klotho* expression in the white matter of Rhesus Macaques was found to be increased in aged animals >20-years-old compared to young adult animals at 4- to 7-years-old (Duce et al., 2008). In the current study, in line with this previous literature, the expected pattern of decline in *Klotho* expression was observed within the TCx in all three aged groups compared to young controls suggesting a loss of ageing suppression and likely emergence of ageing in the TCx. This decrease was associated with decreases in expression of microglia related genes (both homeostatic and activation markers) but no changes in microglial signalling. However, this effect was not observed in the PCx, suggesting that there is regional variability in the regulation of ageing in the brain. This variability is further supported by the significant upregulation of *Klotho* within the hippocampus which was associated with increased expression of microglia-related genes across all three aged groups (as well as more limited up-regulation of *FYN* and *TLR4*). This may represent a compensatory mechanism of upregulating *Klotho* for its neuroprotective properties (Colasanti et al., 2016; Davidson and Stevenson, 2024; Jung et al., 2022). Demonstrating this neuroprotective effect in the hippocampus, upregulation of Klotho in 7-month-old male $APP^{SWE}/PS1^{dE9}$ mice by

intracerebroventricular injection of lentiviral vector encoding of full-length mouse *Klotho* cDNA has shown amelioration of long-term working memory deficits (Zeng et al., 2019). The combined results here therefore suggest region specific actions of Klotho and necessitating future work in order to understand the exact relationship between *Klotho* expression and potential neuroprotection in vulnerable regions of the brain such as the hippocampus.

The current study has several key issues which limit the interpretability of results. The relatively small number of samples, particularly for the young control group (n=6) limits the generalisability of the results. Increasing this number would greatly assist in improving this; however, may be difficult to achieve in practice due to the challenges associated with obtaining young, healthy control postmortem brain tissue. Many post-mortem ND studies also suffer from this limitation and contain either a small young control cohort or no young comparison tissue at all, suggesting that results should be interpreted with caution. For example, one study demonstrated an increase in *IL-1β* mRNA in the TCx of AD brains compared to low pathology non-dementia controls, but no change in *IL-6* of *TNF* expression (Morimoto et al., 2011). However, this study contained only n=10 per group and, importantly, no young control group, thus limiting the ability to assess an effect of age on cytokine mRNA expression (Morimoto et al., 2011). This highlights the need for consistent use of young controls in human ageing and ND research and a guideline for what constitutes classification as young or aged in research, as the classification of an old adult is inconsistent between studies. This classification would contribute to mediating the heterogeneity in post-mortem ageing cohorts where currently the age range included in studies as elderly is variable. For example, someone over 60 years old is classified as an older adult by the United Nations (Nations, 2024). However, it has been suggested that this be increased due to improved health and functional capacity (Jacobs et al., 2012; Orimo et al., 2006) or instead measured based on biological rather than chronological age (Mitnitski et al., 2002). This may account for variation between previous literature, as studies may use a wide range of ages as was the case here (79 years to >100 years) which further contributed to the heterogeneity of the cohort within the current study. Further heterogeneity can be observed specifically in the young control group, where only one of the six cases was female, potentially skewing the data toward expression of a male genetic phenotypes in

this group. Similar to other genetic studies due to difficulty obtaining true young, healthy control brain tissue (Rush et al., 2024), the young controls are potentially problematic. This is particularly the case when studying neuroinflammatory conditions, as spontaneous deaths in healthy young people often have a neuroinflammatory component, for example during motor vehicle accidents where TBI may occur (Kumar et al., 2008). In order to combat these common issues faced by researchers, effort should be made to facilitate broader access to biobanked samples and improving communication between researchers and biorepositories. Finally, the use of mRNA data in the current study provides valuable insight into transcriptional regulation but does not provide insight into whether these factors are expressed at the protein level. Future work should seek to characterise both mRNA expression and protein level expression of genes since, as discussed above in the context of pro-inflammatory cytokines, changes in mRNA expression do not always lead to altered expression of these factors at the protein level.

5.6 Conclusions

The current study supports the idea of microglial dysregulation in the hippocampus and cortex in ageing, AD and TBI, highlighting the region-specific vulnerability of the hippocampus to neuroinflammatory changes. While no significant group differences were observed to suggest an increased effect of disease or injury on microglial ageing, the findings underscore the role of dysregulated microglia in shaping immune dysregulation in the brain. This suggests that understanding microglial dynamics, particularly in the early stages of disease, is critical in uncovering mechanisms which contribute to the onset and progression of neurodegenerative processes. However, a key limitation is the inability to assess whether these mRNA changes translate to functional protein level alterations. This thus remains a vital area of future research. Addressing this gap, potentially by employing transcriptomic databases with single cell resolution to investigate microglia across a wide range of brain regions, will be crucial in understanding variation in functional changes of microglia throughout the brain. Finally, opposing changes in *Klotho* expression were seen in the current study between regions, which differed from what literature would suggest with age. Understanding how changes in this key ageing suppression gene are associated with alterations in microglia is key in uncovering how Klotho contributes to declines in the immune system

in the brain. Overall, this work contributes to a growing body of evidence regarding the impacts of dysregulated microglia during ageing and their potential impacts on neurodegeneration.

5.7 References

Adamczak, S., Dale, G., de Rivero Vaccari, J.P., Bullock, M.R., Dietrich, W.D., Keane, R.W., 2012. Inflammasome proteins in cerebrospinal fluid of brain-injured patients as biomarkers of functional outcome: clinical article. J Neurosurg 117, 1119-1125.

Allen Institute for Brain Science, 2024a. Allen Brain Atlas Community: Aging, Dementia, and TBI How-To. Allen Institute for Brain Science,.

Allen Institute for Brain Science, 2024b. Allen Brain Atlas Community: Human Atlas How-To. Allen Institute for Brain Science,.

Allen Institute for Brain Science, 2024c. Allen Brain Atlas: Aging, Dementia, and TBI. Allen Institute for Brain Science,.

Allen Institute for Brain Science, 2024d. Allen Human Brain Atlas. Allen Institute for Brain Science,.

Bakkour, A., Morris, J.C., Wolk, D.A., Dickerson, B.C., 2013. The effects of aging and Alzheimer's disease on cerebral cortical anatomy: specificity and differential relationships with cognition. Neuroimage 76, 332-344.

Balança, B., Desmurs, L., Grelier, J., Perret-Liaudet, A., Lukaszewicz, A.C., 2021. DAMPs and RAGE Pathophysiology at the Acute Phase of Brain Injury: An Overview. Int J Mol Sci 22.

Bennett, M.L., Bennett, F.C., Liddelow, S.A., Ajami, B., Zamanian, J.L., Fernhoff, N.B., Mulinyawe, S.B., Bohlen, C.J., Adil, A., Tucker, A., Weissman, I.L., Chang, E.F., Li, G., Grant, G.A., Hayden Gephart, M.G., Barres, B.A., 2016. New tools for studying microglia in the mouse and human CNS. Proc Natl Acad Sci U S A 113, E1738-1746.

Bickford, P.C., Flowers, A., Grimmig, B., 2017. Aging leads to altered microglial function that reduces brain resiliency increasing vulnerability to neurodegenerative diseases. Experimental Gerontology 94, 4-8.

Bielefeld, P., Martirosyan, A., Martín-Suárez, S., Apresyan, A., Meerhoff, G.F., Pestana, F., Poovathingal, S., Reijner, N., Koning, W., Clement, R.A., Van der Veen, I., Toledo, E.M., Polzer, O., Durá, I., Hovhannisyan, S., Nilges, B.S., Bogdoll, A., Kashikar, N.D., Lucassen, P.J., Belgard, T.G., Encinas, J.M., Holt, M.G., Fitzsimons, C.P., 2024. Traumatic brain injury promotes neurogenesis at the cost of astrogliogenesis in the adult hippocampus of male mice. Nature Communications 15, 5222.

Bird, C.M., Burgess, N., 2008. The hippocampus and memory: insights from spatial processing. Nature Reviews Neuroscience 9, 182-194.

Bolmont, T., Haiss, F., Eicke, D., Radde, R., Mathis, C.A., Klunk, W.E., Kohsaka, S., Jucker, M., Calhoun, M.E., 2008. Dynamics of the microglial/amyloid interaction indicate a role in plaque maintenance. J Neurosci 28, 4283-4292.

Calvo-Rodríguez, M., de la Fuente, C., García-Durillo, M., García-Rodríguez, C., Villalobos, C., Núñez, L., 2017. Aging and amyloid β oligomers enhance TLR4 expression, LPS-induced Ca2+ responses, and neuron cell death in cultured rat hippocampal neurons. J Neuroinflammation 14, 24.

Cao, S., Fisher, D.W., Rodriguez, G., Yu, T., Dong, H., 2021. Comparisons of neuroinflammation, microglial activation, and degeneration of the locus coeruleus-norepinephrine system in APP/PS1 and aging mice. J Neuroinflammation 18, 10.

Cash, A., Theus, M.H., 2020. Mechanisms of Blood-Brain Barrier Dysfunction in Traumatic Brain Injury. Int J Mol Sci 21.

Chen, J., Buchanan, J.B., Sparkman, N.L., Godbout, J.P., Freund, G.G., Johnson, R.W., 2008. Neuroinflammation and disruption in working memory in aged mice after acute stimulation of the peripheral innate immune system. Brain Behav Immun 22, 301-311.

Cheng, D.T., Katzenelson, A.M., Faulkner, M.L., Disterhoft, J.F., Power, J.M., Desmond, J.E., 2020. Contingency awareness, aging, and the parietal lobe. Neurobiol Aging 91, 125-135.

Chiarini, A., Gui, L., Viviani, C., Armato, U., Dal Prà, I., 2023. NLRP3 Inflammasome's Activation in Acute and Chronic Brain Diseases-An Update on Pathogenetic Mechanisms and Therapeutic Perspectives with Respect to Other Inflammasomes. Biomedicines 11.

Colasanti, A., Guo, Q., Giannetti, P., Wall, M.B., Newbould, R.D., Bishop, C., Onega, M., Nicholas, R., Ciccarelli, O., Muraro, P.A., Malik, O., Owen, D.R., Young, A.H., Gunn, R.N., Piccini, P., Matthews, P.M., Rabiner, E.A., 2016. Hippocampal Neuroinflammation, Functional Connectivity, and Depressive Symptoms in Multiple Sclerosis. Biol Psychiatry 80, 62-72.

Crain, J.M., Nikodemova, M., Watters, J.J., 2009. Expression of P2 nucleotide receptors varies with age and sex in murine brain microglia. J Neuroinflammation 6, 24.

Cribbs, D.H., Berchtold, N.C., Perreau, V., Coleman, P.D., Rogers, J., Tenner, A.J., Cotman, C.W., 2012. Extensive innate immune gene activation accompanies brain aging, increasing vulnerability to cognitive decline and neurodegeneration: a microarray study. J Neuroinflammation 9, 179.

d'Avila, J.C., Siqueira, L.D., Mazeraud, A., Azevedo, E.P., Foguel, D., Castro-Faria-Neto, H.C., Sharshar, T., Chrétien, F., Bozza, F.A., 2018. Age-related cognitive impairment is associated with long-term neuroinflammation and oxidative stress in a mouse model of episodic systemic inflammation. J Neuroinflammation 15, 28.

da Silva Correia, J., Ulevitch, R.J., 2002. MD-2 and TLR4 N-Linked Glycosylations Are Important for a Functional Lipopolysaccharide Receptor *. Journal of Biological Chemistry 277, 1845-1854.

Dalgaard, P., 2010. R Development Core Team (2010): R: A language and environment for statistical computing.

Davidson, T.L., Stevenson, R.J., 2024. Vulnerability of the Hippocampus to Insults: Links to Blood–Brain Barrier Dysfunction. International Journal of Molecular Sciences.

Deo, A.K., Borson, S., Link, J.M., Domino, K., Eary, J.F., Ke, B., Richards, T.L., Mankoff, D.A., Minoshima, S., O'Sullivan, F., Eyal, S., Hsiao, P., Maravilla, K., Unadkat, J.D., 2014. Activity of P-Glycoprotein, a β-Amyloid Transporter at the Blood-Brain Barrier, Is Compromised in Patients with Mild Alzheimer Disease. J Nucl Med 55, 1106-1111.

DeTure, M.A., Dickson, D.W., 2019. The neuropathological diagnosis of Alzheimer’s disease. Molecular Neurodegeneration 14, 32.

Donat, C.K., Scott, G., Gentleman, S.M., Sastre, M., 2017. Microglial Activation in Traumatic Brain Injury. Front Aging Neurosci 9, 208.

Duce, J.A., Podvin, S., Hollander, W., Kipling, D., Rosene, D.L., Abraham, C.R., 2008. Gene profile analysis implicates Klotho as an important contributor to aging changes in brain white matter of the rhesus monkey. Glia 56, 106-117.

Fann, J.R., Ribe, A.R., Pedersen, H.S., Fenger-Grøn, M., Christensen, J., Benros, M.E., Vestergaard, M., 2018. Long-term risk of dementia among people with traumatic brain injury in Denmark: a population-based observational cohort study. The Lancet Psychiatry 5, 424-431.

Foster, N.L., Chase, T.N., Mansi, L., Brooks, R., Fedio, P., Patronas, N.J., Di Chiro, G., 1984. Cortical abnormalities in Alzheimer's disease. Annals of Neurology 16, 649-654.

Frugier, T., Morganti-Kossmann, M.C., O'Reilly, D., McLean, C.A., 2010. In situ detection of inflammatory mediators in post mortem human brain tissue after traumatic injury. J Neurotrauma 27, 497-507.

Galatro, T.F., Holtman, I.R., Lerario, A.M., Vainchtein, I.D., Brouwer, N., Sola, P.R., Veras, M.M., Pereira, T.F., Leite, R.E.P., Möller, T., Wes, P.D., Sogayar, M.C., Laman, J.D., den Dunnen, W.,

Pasqualucci, C.A., Oba-Shinjo, S.M., Boddeke, E., Marie, S.K.N., Eggen, B.J.L., 2017. Transcriptomic analysis of purified human cortical microglia reveals age-associated changes. Nat Neurosci 20, 1162-1171.

Gan, S., Shi, W., Wang, S., Sun, Y., Yin, B., Bai, G., Jia, X., Sun, C., Niu, X., Wang, Z., Jiang, X., Liu, J., Zhang, M., Bai, L., 2021. Accelerated Brain Aging in Mild Traumatic Brain Injury: Longitudinal Pattern Recognition with White Matter Integrity. Journal of Neurotrauma 38, 2549-2559.

Gardner, R.C., Bahorik, A., Kornblith, E.S., Allen, I.E., Plassman, B.L., Yaffe, K., 2023. Systematic Review, Meta-Analysis, and Population Attributable Risk of Dementia Associated with Traumatic Brain Injury in Civilians and Veterans. J Neurotrauma 40, 620-634.

Gardner, R.C., Burke, J.F., Nettiksimmons, J., Kaup, A., Barnes, D.E., Yaffe, K., 2014. Dementia risk after traumatic brain injury vs nonbrain trauma: the role of age and severity. JAMA Neurol 71, 1490-1497.

Gate, D., Rezai-Zadeh, K., Jodry, D., Rentsendorj, A., Town, T., 2010. Macrophages in Alzheimer's disease: the blood-borne identity. J Neural Transm (Vienna) 117, 961-970.

Glezer, I., Simard, A.R., Rivest, S., 2007. Neuroprotective role of the innate immune system by microglia. Neuroscience 147, 867-883.

Gómez Morillas, A., Besson, V.C., Lerouet, D., 2021. Microglia and Neuroinflammation: What Place for P2RY12? Int J Mol Sci 22.

González, I., Cao, K.-A.L., Davis, M.J., Déjean, S., 2012. Visualising associations between paired ‘omics’ data sets. BioData Mining 5, 19.

Grabert, K., Michoel, T., Karavolos, M.H., Clohisey, S., Baillie, J.K., Stevens, M.P., Freeman, T.C., Summers, K.M., McColl, B.W., 2016. Microglial brain region-dependent diversity and selective regional sensitivities to aging. Nat Neurosci 19, 504-516.

Guglietti, B., Sivasankar, S., Mustafa, S., Corrigan, F., Collins-Praino, L.E., 2021. Fyn Kinase Activity and Its Role in Neurodegenerative Disease Pathology: a Potential Universal Target? Mol Neurobiol 58, 5986-6005.

Haynes, S.E., Hollopeter, G., Yang, G., Kurpius, D., Dailey, M.E., Gan, W.B., Julius, D., 2006. The P2Y12 receptor regulates microglial activation by extracellular nucleotides. Nat Neurosci 9, 1512-1519.

Hendrickx, D.A.E., van Eden, C.G., Schuurman, K.G., Hamann, J., Huitinga, I., 2017. Staining of HLA-DR, Iba1 and CD68 in human microglia reveals partially overlapping expression depending on cellular morphology and pathology. Journal of Neuroimmunology 309, 12-22.

Henry, C.J., Huang, Y., Wynne, A.M., Godbout, J.P., 2009. Peripheral lipopolysaccharide (LPS) challenge promotes microglial hyperactivity in aged mice that is associated with exaggerated induction of both pro-inflammatory IL-1beta and anti-inflammatory IL-10 cytokines. Brain Behav Immun 23, 309-317.

Hickman, S.E., Kingery, N.D., Ohsumi, T.K., Borowsky, M.L., Wang, L.C., Means, T.K., El Khoury, J., 2013. The microglial sensome revealed by direct RNA sequencing. Nat Neurosci 16, 1896-1905.

Hopperton, K.E., Mohammad, D., Trépanier, M.O., Giuliano, V., Bazinet, R.P., 2018. Markers of microglia in post-mortem brain samples from patients with Alzheimer's disease: a systematic review. Mol Psychiatry 23, 177-198.

Hou, Y., Dan, X., Babbar, M., Wei, Y., Hasselbalch, S.G., Croteau, D.L., Bohr, V.A., 2019. Ageing as a risk factor for neurodegenerative disease. Nature Reviews Neurology 15, 565-581.

Hsieh, C.L., Kim, C.C., Ryba, B.E., Niemi, E.C., Bando, J.K., Locksley, R.M., Liu, J., Nakamura, M.C., Seaman, W.E., 2013. Traumatic brain injury induces macrophage subsets in the brain. Eur J Immunol 43, 2010-2022.

Jack, C.R., Petersen, R.C., Xu, Y., O'Brien, P.C., Smith, G.E., Ivnik, R.J., Tangalos, E.G., Kokmen, E., 1998. Rate of medial temporal lobe atrophy in typical aging and Alzheimer's disease. Neurology 51, 993-999.

Jacobs, J.M., Maaravi, Y., Cohen, A., Bursztyn, M., Ein-Mor, E., Stessman, J., 2012. Changing Profile of Health and Function from Age 70 to 85 Years. Gerontology 58, 313-321.

Jana, M., Palencia, C.A., Pahan, K., 2008. Fibrillar amyloid-beta peptides activate microglia via TLR2: implications for Alzheimer's disease. J Immunol 181, 7254-7262.

Jao, C.W., Yeh, J.H., Wu, Y.T., Lien, L.M., Tsai, Y.F., Chu, K.E., Hsiao, C.Y., Wang, P.S., Lau, C.I., 2020. Alteration of the Intra- and Inter-Lobe Connectivity of the Brain Structural Network in Normal Aging. Entropy (Basel) 22.

Jiang, Z., Wang, J., Qin, Y., Liu, S., Luo, B., Bai, F., Wei, H., Zhang, S., Wei, J., Ding, G., Ma, L., He, S., Chen, R., Sun, Y., Chen, Y., Wang, L., Xu, H., Wang, X., Chen, G., Lei, W., 2024. A nonhuman primate model with Alzheimer's disease-like pathology induced by hippocampal overexpression of human tau. Alzheimer's Research & Therapy 16, 22.

Johnson, V.E., Stewart, J.E., Begbie, F.D., Trojanowski, J.Q., Smith, D.H., Stewart, W., 2013. Inflammation and white matter degeneration persist for years after a single traumatic brain injury. Brain 136, 28-42.

Jung, H., Lee, H., Kim, D., Cheong, E., Hyun, Y.M., Yu, J.W., Um, J.W., 2022. Differential Regional Vulnerability of the Brain to Mild Neuroinflammation Induced by Systemic LPS Treatment in Mice. J Inflamm Res 15, 3053-3063.

Keren-Shaul, H., Spinrad, A., Weiner, A., Matcovitch-Natan, O., Dvir-Szternfeld, R., Ulland, T.K., David, E., Baruch, K., Lara-Astaiso, D., Toth, B., Itzkovitz, S., Colonna, M., Schwartz, M., Amit, I., 2017. A Unique Microglia Type Associated with Restricting Development of Alzheimer's Disease. Cell 169, 1276-1290.e1217.

Kigerl, K.A., de Rivero Vaccari, J.P., Dietrich, W.D., Popovich, P.G., Keane, R.W., 2014. Pattern recognition receptors and central nervous system repair. Exp Neurol 258, 5-16.

Kim, H.-J., Kim, H., Lee, J.-H., Hwangbo, C., 2023. Toll-like receptor 4 (TLR4): new insight immune and aging. Immunity & Ageing 20, 67.

Koegl, M., Zlatkine, P., Ley, S.C., Courtneidge, S.A., Magee, A.I., 1994. Palmitoylation of multiple Src-family kinases at a homologous N-terminal motif. Biochem J 303 (Pt 3), 749-753.

Koenig, L.N., LaMontagne, P., Glasser, M.F., Bateman, R., Holtzman, D., Yakushev, I., Chhatwal, J., Day, G.S., Jack, C., Mummery, C., Perrin, R.J., Gordon, B.A., Morris, J.C., Shimony, J.S., Benzinger, T.L.S., 2022. Regional age-related atrophy after screening for preclinical alzheimer disease. Neurobiol Aging 109, 43-51.

Krasemann, S., Madore, C., Cialic, R., Baufeld, C., Calcagno, N., El Fatimy, R., Beckers, L., O'Loughlin, E., Xu, Y., Fanek, Z., Greco, D.J., Smith, S.T., Tweet, G., Humulock, Z., Zrzavy, T., Conde-Sanroman, P., Gacias, M., Weng, Z., Chen, H., Tjon, E., Mazaheri, F., Hartmann, K., Madi, A., Ulrich, J.D., Glatzel, M., Worthmann, A., Heeren, J., Budnik, B., Lemere, C., Ikezu, T., Heppner, F.L., Litvak, V., Holtzman, D.M., Lassmann, H., Weiner, H.L., Ochando, J., Haass, C., Butovsky, O., 2017. The TREM2-APOE Pathway Drives the Transcriptional Phenotype of Dysfunctional Microglia in Neurodegenerative Diseases. Immunity 47, 566-581.e569.

Kumar, A., Lalwani, S., Agrawal, D., Rautji, R., Dogra, T.D., 2008. Fatal road traffic accidents and their relationship with head injuries: An epidemiological survey of five years. The Indian Journal of Neurotrauma 5, 63-67.

Lawson, L.J., Perry, V.H., Dri, P., Gordon, S., 1990. Heterogeneity in the distribution and morphology of microglia in the normal adult mouse brain. Neuroscience 39, 151-170.

Lê Cao, K.-A., González, I., Déjean, S., 2009. integrOmics: an R package to unravel relationships between two omics datasets. Bioinformatics 25, 2855-2856.

Lee, G., Thangavel, R., Sharma, V.M., Litersky, J.M., Bhaskar, K., Fang, S.M., Do, L.H., Andreadis, A., Van Hoesen, G., Ksiezak-Reding, H., 2004. Phosphorylation of tau by fyn: implications for Alzheimer's disease. J Neurosci 24, 2304-2312.

Letiembre, M., Hao, W., Liu, Y., Walter, S., Mihaljevic, I., Rivest, S., Hartmann, T., Fassbender, K., 2007. Innate immune receptor expression in normal brain aging. Neuroscience 146, 248-254.

Li, Q., Lan, X., Han, X., Wang, J., 2018. Expression of Tmem119/Sall1 and Ccr2/CD69 in FACS-Sorted Microglia- and Monocyte/Macrophage-Enriched Cell Populations After Intracerebral Hemorrhage. Front Cell Neurosci 12, 520.

Liang, R., Qi, X., Cai, Q., Niu, L., Huang, X., Zhang, D., Ling, J., Wu, Y., Chen, Y., Yang, P., Liu, J., Zhang, J., Yu, P., 2024. The role of NLRP3 inflammasome in aging and age-related diseases. Immun Ageing 21, 14.

Long, F.-Y., Shi, M.-Q., Zhou, H.-J., Liu, D.-L., Sang, N., Du, J.-R., 2018. Klotho upregulation contributes to the neuroprotection of ligustilide against cerebral ischemic injury in mice. European Journal of Pharmacology 820, 198-205.

Lopez-Rodriguez, A.B., Hennessy, E., Murray, C.L., Nazmi, A., Delaney, H.J., Healy, D., Fagan, S.G., Rooney, M., Stewart, E., Lewis, A., de Barra, N., Scarry, P., Riggs-Miller, L., Boche, D., Cunningham, M.O., Cunningham, C., 2021. Acute systemic inflammation exacerbates neuroinflammation in Alzheimer's disease: IL-1β drives amplified responses in primed astrocytes and neuronal network dysfunction. Alzheimers Dement 17, 1735-1755.

Masuda, T., Amann, L., Sankowski, R., Staszewski, O., Lenz, M., P, D.E., Snaidero, N., Costa Jordão, M.J., Böttcher, C., Kierdorf, K., Jung, S., Priller, J., Misgeld, T., Vlachos, A., Meyer-Luehmann, M., Knobeloch, K.P., Prinz, M., 2020. Novel Hexb-based tools for studying microglia in the CNS. Nat Immunol 21, 802-815.

Masuda, T., Sankowski, R., Staszewski, O., Böttcher, C., Amann, L., Sagar, Scheiwe, C., Nessler, S., Kunz, P., van Loo, G., Coenen, V.A., Reinacher, P.C., Michel, A., Sure, U., Gold, R., Grün, D., Priller, J., Stadelmann, C., Prinz, M., 2019. Spatial and temporal heterogeneity of mouse and human microglia at single-cell resolution. Nature 566, 388-392.

McLarnon, J.G., Ryu, J.K., Walker, D.G., Choi, H.B., 2006. Upregulated Expression of Purinergic P2X7 Receptor in Alzheimer Disease and Amyloid-β Peptide-Treated Microglia and in Peptide-Injected Rat Hippocampus. Journal of Neuropathology & Experimental Neurology 65, 1090-1097.

Menassa, D.A., Muntslag, T.A.O., Martin-Estebané, M., Barry-Carroll, L., Chapman, M.A., Adorjan, I., Tyler, T., Turnbull, B., Rose-Zerilli, M.J.J., Nicoll, J.A.R., Krsnik, Z., Kostovic, I., Gomez-Nicola, D., 2022. The spatiotemporal dynamics of microglia across the human lifespan. Developmental Cell 57, 2127-2139.e2126.

Mercurio, D., Fumagalli, S., Schafer, M.K.H., Pedragosa, J., Ngassam, L.D.C., Wilhelmi, V., Winterberg, S., Planas, A.M., Weihe, E., De Simoni, M.-G., 2022. Protein Expression of the Microglial Marker Tmem119 Decreases in Association With Morphological Changes and Location in a Mouse Model of Traumatic Brain Injury. Frontiers in Cellular Neuroscience 16.

Mildner, A., Huang, H., Radke, J., Stenzel, W., Priller, J., 2017. P2Y(12) receptor is expressed on human microglia under physiological conditions throughout development and is sensitive to neuroinflammatory diseases. Glia 65, 375-387.

Mitnitski, A.B., Graham, J.E., Mogilner, A.J., Rockwood, K., 2002. Frailty, fitness and late-life mortality in relation to chronological and biological age. BMC Geriatr 2, 1.

Montagne, A., Barnes, Samuel R., Sweeney, Melanie D., Halliday, Matthew R., Sagare, Abhay P., Zhao, Z., Toga, Arthur W., Jacobs, Russell E., Liu, Collin Y., Amezcua, L., Harrington, Michael G., Chui, Helena C., Law, M., Zlokovic, Berislav V., 2015. Blood-Brain Barrier Breakdown in the Aging Human Hippocampus. Neuron 85, 296-302.

Moore, C.S., Ase, A.R., Kinsara, A., Rao, V.T., Michell-Robinson, M., Leong, S.Y., Butovsky, O., Ludwin, S.K., Séguéla, P., Bar-Or, A., Antel, J.P., 2015. P2Y12 expression and function in alternatively activated human microglia. Neurol Neuroimmunol Neuroinflamm 2, e80.

Morimoto, K., Horio, J., Satoh, H., Sue, L., Beach, T., Arita, S., Tooyama, I., Konishi, Y., 2011. Expression profiles of cytokines in the brains of Alzheimer's disease (AD) patients compared to the brains of non-demented patients with and without increasing AD pathology. J Alzheimers Dis 25, 59-76.

Nations, U., 2024. Persons at Risk: Older persons.

Norden, D.M., Godbout, J.P., 2013. Review: microglia of the aged brain: primed to be activated and resistant to regulation. Neuropathol Appl Neurobiol 39, 19-34.

Norden, D.M., Muccigrosso, M.M., Godbout, J.P., 2015. Microglial priming and enhanced reactivity to secondary insult in aging, and traumatic CNS injury, and neurodegenerative disease. Neuropharmacology 96, 29-41.

O'Neill, L.A.J., Kaltschmidt, C., 1997. NF-kB: a crucial transcription factor for glial and neuronal cell function. Trends in Neurosciences 20, 252-258.

Orimo, H., Ito, H., Suzuki, T., Araki, A., Hosoi, T., Sawabe, M., 2006. Reviewing the definition of “elderly”. Geriatrics & Gerontology International 6, 149-158.

Pandey, G.N., Rizavi, H.S., Zhang, H., Ren, X., 2018. Abnormal gene and protein expression of inflammatory cytokines in the postmortem brain of schizophrenia patients. Schizophrenia Research 192, 247-254.

Panicker, N., Saminathan, H., Jin, H., Neal, M., Harischandra, D.S., Gordon, R., Kanthasamy, K., Lawana, V., Sarkar, S., Luo, J., Anantharam, V., Kanthasamy, A.G., Kanthasamy, A., 2015. Fyn Kinase Regulates Microglial Neuroinflammatory Responses in Cell Culture and Animal Models of Parkinson's Disease. J Neurosci 35, 10058-10077.

Paton, B., Suarez, M., Herrero, P., Canela, N., 2021. Glycosylation Biomarkers Associated with Age-Related Diseases and Current Methods for Glycan Analysis. Int J Mol Sci 22.

Perea, J.R., Bolós, M., Avila, J., 2020. Microglia in Alzheimer's Disease in the Context of Tau Pathology. Biomolecules 10.

Perea, J.R., Llorens-Martín, M., Ávila, J., Bolós, M., 2018. The Role of Microglia in the Spread of Tau: Relevance for Tauopathies. Frontiers in Cellular Neuroscience 12.

Perkins, A.E., Piazza, M.K., Deak, T., 2018. Stereological Analysis of Microglia in Aged Male and Female Fischer 344 Rats in Socially Relevant Brain Regions. Neuroscience 377, 40-52.

Raj, D.D.A., Jaarsma, D., Holtman, I.R., Olah, M., Ferreira, F.M., Schaafsma, W., Brouwer, N., Meijer, M.M., de Waard, M.C., van der Pluijm, I., Brandt, R., Kreft, K.L., Laman, J.D., de Haan, G., Biber, K.P.H., Hoeijmakers, J.H.J., Eggen, B.J.L., Boddeke, H.W.G.M., 2014. Priming of microglia in a DNA-repair deficient model of accelerated aging. Neurobiology of Aging 35, 2147-2160.

Raj, R., Kaprio, J., Korja, M., Mikkonen, E.D., Jousilahti, P., Siironen, J., 2017. Risk of hospitalization with neurodegenerative disease after moderate-to-severe traumatic brain injury in the working-age population: A retrospective cohort study using the Finnish national health registries. PLoS Med 14, e1002316.

Raz, N., Rodrigue, K.M., Head, D., Kennedy, K.M., Acker, J.D., 2004. Differential aging of the medial temporal lobe. Neurology 62, 433-438.

Ritchie, M.E., Phipson, B., Wu, D., Hu, Y., Law, C.W., Shi, W., Smyth, G.K., 2015. limma powers differential expression analyses for RNA-sequencing and microarray studies. Nucleic Acids Res 43, e47-e47.

Ritzel, R.M., Li, Y., Jiao, Y., Lei, Z., Doran, S.J., He, J., Shahror, R.A., Henry, R.J., Khan, R., Tan, C., Liu, S., Stoica, B.A., Faden, A.I., Szeto, G., Loane, D.J., Wu, J., 2023. Brain injury accelerates the onset of a reversible age-related microglial phenotype associated with inflammatory neurodegeneration. Sci Adv 9, eadd1101.

Ritzel, R.M., Patel, A.R., Pan, S., Crapser, J., Hammond, M., Jellison, E., McCullough, L.D., 2015. Age- and location-related changes in microglial function. Neurobiology of Aging 36, 2153-2163.

Rivera, A., Vanzulli, I., Butt, A.M., 2016. A Central Role for ATP Signalling in Glial Interactions in the CNS. Curr Drug Targets 17, 1829-1833.

Rohart, F., Gautier, B., Singh, A., Lê Cao, K.-A., 2017. mixOmics: An R package for 'omics feature selection and multiple data integration. PLOS Computational Biology 13, e1005752.

Ruan, C., Sun, L., Kroshilina, A., Beckers, L., De Jager, P., Bradshaw, E.M., Hasson, S.A., Yang, G., Elyaman, W., 2020. A novel Tmem119-tdTomato reporter mouse model for studying microglia in the central nervous system. Brain, Behavior, and Immunity 83, 180-191.

Rush, A., Weil, C., Siminoff, L., Griffin, C., Paul, C.L., Mahadevan, A., Sutherland, G., 2024. The Experts Speak: Challenges in Banking Brain Tissue for Research. Biopreservation and Biobanking 22, 179-184.

Sanchez-Mejias, E., Navarro, V., Jimenez, S., Sanchez-Mico, M., Sanchez-Varo, R., Nuñez-Diaz, C., Trujillo-Estrada, L., Davila, J.C., Vizuete, M., Gutierrez, A., Vitorica, J., 2016. Soluble phospho-tau from Alzheimer's disease hippocampus drives microglial degeneration. Acta Neuropathol 132, 897-916.

Santos, A.L., Lindner, A.B., 2017. Protein Posttranslational Modifications: Roles in Aging and Age-Related Disease. Oxid Med Cell Longev 2017, 5716409.

Satoh, J., Kino, Y., Asahina, N., Takitani, M., Miyoshi, J., Ishida, T., Saito, Y., 2016. TMEM119 marks a subset of microglia in the human brain. Neuropathology 36, 39-49.

Shively, S., Scher, A.I., Perl, D.P., Diaz-Arrastia, R., 2012. Dementia resulting from traumatic brain injury: what is the pathology? Arch Neurol 69, 1245-1251.

Sierra, A., Gottfried-Blackmore, A.C., McEwen, B.S., Bulloch, K., 2007. Microglia derived from aging mice exhibit an altered inflammatory profile. Glia 55, 412-424.

Simon, D.W., McGeachy, M.J., Bayır, H., Clark, R.S.B., Loane, D.J., Kochanek, P.M., 2017. The far-reaching scope of neuroinflammation after traumatic brain injury. Nature Reviews Neurology 13, 171-191.

Smith, J.A., Das, A., Ray, S.K., Banik, N.L., 2012. Role of pro-inflammatory cytokines released from microglia in neurodegenerative diseases. Brain Research Bulletin 87, 10-20.

Süß, P., Hoffmann, A., Rothe, T., Ouyang, Z., Baum, W., Staszewski, O., Schett, G., Prinz, M., Krönke, G., Glass, C.K., Winkler, J., Schlachetzki, J.C.M., 2020. Chronic Peripheral Inflammation Causes a Region-Specific Myeloid Response in the Central Nervous System. Cell Reports 30, 4082-4095.e4086.

Tagliatti, E., Desiato, G., Mancinelli, S., Bizzotto, M., Gagliani, M.C., Faggiani, E., Hernández-Soto, R., Cugurra, A., Poliseno, P., Miotto, M., Argüello, R.J., Filipello, F., Cortese, K., Morini, R., Lodato, S., Matteoli, M., 2024. Trem2 expression in microglia is required to maintain normal neuronal bioenergetics during development. Immunity 57, 86-105.e109.

Thomas, A.L., Lehn, M.A., Janssen, E.M., Hildeman, D.A., Chougnet, C.A., 2022. Naturally-aged microglia exhibit phagocytic dysfunction accompanied by gene expression changes reflective of underlying neurologic disease. Sci Rep 12, 19471.

Thompson, P.M., Hayashi, K.M., Sowell, E.R., Gogtay, N., Giedd, J.N., Rapoport, J.L., de Zubicaray, G.I., Janke, A.L., Rose, S.E., Semple, J., Doddrell, D.M., Wang, Y., van Erp, T.G.M., Cannon, T.D., Toga, A.W., 2004. Mapping cortical change in Alzheimer's disease, brain development, and schizophrenia. NeuroImage 23, S2-S18.

Thompson, P.M., Mega, M.S., Woods, R.P., Zoumalan, C.I., Lindshield, C.J., Blanton, R.E., Moussai, J., Holmes, C.J., Cummings, J.L., Toga, A.W., 2001. Cortical Change in Alzheimer's Disease Detected with a Disease-specific Population-based Brain Atlas. Cerebral Cortex 11, 1-16.

Trepanier, C.H., Jackson, M.F., MacDonald, J.F., 2012. Regulation of NMDA receptors by the tyrosine kinase Fyn. The FEBS Journal 279, 12-19.

van Wageningen, T.A., Vlaar, E., Kooij, G., Jongenelen, C.A.M., Geurts, J.J.G., van Dam, A.M., 2019. Regulation of microglial TMEM119 and P2RY12 immunoreactivity in multiple sclerosis white and grey matter lesions is dependent on their inflammatory environment. Acta Neuropathol Commun 7, 206.

Viana, L.C., Lima, C.M., Oliveira, M.A., Borges, R.P., Cardoso, T.T., Almeida, I.N.F., Diniz, D.G., Bento-Torres, J., Pereira, A., Batista-de-Oliveira, M., Lopes, A.A.C., Silva, R.F.M., Abadie-Guedes, R., Amâncio dos Santos, A., Lima, D.S.C., Vasconcelos, P.F.C., Cunningham, C., Guedes, R.C.A., Picanço-Diniz, C.W., 2013. Litter size, age-related memory impairments, and microglial changes in rat dentate gyrus: Stereological analysis and three dimensional morphometry. Neuroscience 238, 280-296.

Vidal-Itriago, A., Radford, R.A.W., Aramideh, J.A., Maurel, C., Scherer, N.M., Don, E.K., Lee, A., Chung, R.S., Graeber, M.B., Morsch, M., 2022. Microglia morphophysiological diversity and its implications for the CNS. Front Immunol 13, 997786.

Voss, J.L., Bridge, D.J., Cohen, N.J., Walker, J.A., 2017. A Closer Look at the Hippocampus and Memory. Trends Cogn Sci 21, 577-588.

Walker, D.G., Tang, T.M., Mendsaikhan, A., Tooyama, I., Serrano, G.E., Sue, L.I., Beach, T.G., Lue, L.F., 2020. Patterns of Expression of Purinergic Receptor P2RY12, a Putative Marker for Non-Activated Microglia, in Aged and Alzheimer's Disease Brains. Int J Mol Sci 21.

Warner, M.A., Youn, T.S., Davis, T., Chandra, A., Marquez de la Plata, C., Moore, C., Harper, C., Madden, C.J., Spence, J., McColl, R., Devous, M., King, R.D., Diaz-Arrastia, R., 2010. Regionally Selective Atrophy After Traumatic Axonal Injury. Archives of Neurology 67, 1336-1344.

Williams, J.A., Burgess, S., Suckling, J., Lalousis, P.A., Batool, F., Griffiths, S.L., Palmer, E., Karwath, A., Barsky, A., Gkoutos, G.V., Wood, S., Barnes, N.M., David, A.S., Donohoe, G., Neill, J.C., Deakin, B., Khandaker, G.M., Upthegrove, R., Collaboration, P., 2022. Inflammation and Brain Structure in Schizophrenia and Other Neuropsychiatric Disorders: A Mendelian Randomization Study. JAMA Psychiatry 79, 498-507.

Wolfe, H., Minogue, A.M., Rooney, S., Lynch, M.A., 2018. Infiltrating macrophages contribute to age-related neuroinflammation in C57/BL6 mice. Mech Ageing Dev 173, 84-91.

Xue, Q., Wang, L., Zhao, Y., Tong, W., Wang, J., Li, G., Cheng, W., Gao, L., Dong, Y., 2022. Cortical and Subcortical Alterations and Clinical Correlates after Traumatic Brain Injury. J Clin Med 11.

Yamazaki, Y., Imura, A., Urakawa, I., Shimada, T., Murakami, J., Aono, Y., Hasegawa, H., Yamashita, T., Nakatani, K., Saito, Y., Okamoto, N., Kurumatani, N., Namba, N., Kitaoka, T., Ozono, K., Sakai, T., Hataya, H., Ichikawa, S., Imel, E.A., Econs, M.J., Nabeshima, Y.-i., 2010. Establishment of sandwich ELISA for soluble alpha-Klotho measurement: Age-dependent change of soluble alpha-

Klotho levels in healthy subjects. Biochemical and Biophysical Research Communications 398, 513-518.

Yaqubi, M., Groh, A.M.R., Dorion, M.-F., Afanasiev, E., Luo, J.X.X., Hashemi, H., Sinha, S., Kieran, N.W., Blain, M., Cui, Q.-L., Biernaskie, J., Srour, M., Dudley, R., Hall, J.A., Sonnen, J.A., Arbour, N., Prat, A., Stratton, J.A., Antel, J., Healy, L.M., 2023. Analysis of the microglia transcriptome across the human lifespan using single cell RNA sequencing. J Neuroinflammation 20, 132.

Zeng, C.-Y., Yang, T.-T., Zhou, H.-J., Zhao, Y., Kuang, X., Duan, W., Du, J.-R., 2019. Lentiviral vector–mediated overexpression of Klotho in the brain improves Alzheimer's disease–like pathology and cognitive deficits in mice. Neurobiology of Aging 78, 18-28.

Zhao, Y., Zeng, C.-Y., Li, X.-H., Yang, T.-T., Kuang, X., Du, J.-R., 2020. Klotho overexpression improves amyloid-β clearance and cognition in the APP/PS1 mouse model of Alzheimer's disease. Aging Cell 19, e13239.

Zheng, R.Z., Lee, K.Y., Qi, Z.X., Wang, Z., Xu, Z.Y., Wu, X.H., Mao, Y., 2022. Neuroinflammation Following Traumatic Brain Injury: Take It Seriously or Not. Front Immunol 13, 855701.

5.8 Supporting Information

Characterising the Inflammatory mRNA Profile of Microglia Across Healthy Ageing, Neurodegeneration and Traumatic Brain Injury using the Allen Brain Atlas

Laura M. Carr[1], Aline Kunnel[2], Sanam Mustafa[1,3,4], Lyndsey E. Collins-Praino[1]

[1] School of Biomedicine, University of Adelaide, Adelaide, Australia
[2]Womens and Kids Theme, South Australian Health and Medical Research Institute, South Australia, Australia
[3]Australian Research Council Centre of Excellence for Nanoscale Biophotonics, The University of Adelaide, Adelaide, SA, Australia
[4]Davies Livestock Research Centre, The University of Adelaide, Roseworthy, SA, Australia

A/Professor Lyndsey Collins-Praino
Email: Lyndsey.collins-praino@adelaide.edu.au

This section includes

Tables S5.1-5.3

Supplementary Table S 5.0.1 All statistical results from linear regression models in the TCx.

TCx				
Gene	**LogFC (95% CI)**	**Ave Expr**	**P-val**	**Adj.P-val**
Aged control vs young control				
KLB	0.144 (-0.694, 0.982)	0.233	0.733	1
KL	**-0.484 (-0.744, -0.224)**	**-0.412**	**0.000**	**0**
IL6R	-0.596 (-1.197, 0.004)	-0.367	0.052	0.832
NLRP3	0.413 (-1.041, 0.215)	-0.171	0.195	1
IL1B	-0.468 -1.141, 0.205)	0.051	0.171	1
P2RY12	-0.454 (-1.050, 0.142)	-0.251	0.134	1
NFKB1	-0.410 (-0.969, 0.149)	-0.526	0.149	1
TNF	0.127 (-0.569, 0.823)	0.270	0.718	1
AIF1	-0.668 (-1.330, -0.006)	-0.300	0.048	0.768
TREM2	**-0.878 (-1.384, -0.371)**	**-0.503**	**0.001**	**0.016**
FYN	0.210 (-0.560, 0.979)	-0.544	0.590	1
IL6	-0.250 (-0.895, 0.395)	-0.037	0.444	1
TLR4	-0.110 (-0.742, 0.521)	-0.363	0.729	1
TNFRSF1A	-0.781 (-1.530, -0.031)	-0.550	0.041	0.656
TMEM119	**-0.890 (-1.430, -0.351)**	**-0.482**	**0.001**	**0.016**
CD68	**-0.920 (-1.515, -0.324)**	**-0.516**	**0.003**	**0.048**
Alzheimer's vs young control				
KLB	0.293 (-0.542, 1.129)	0.233	0.487	1
KL	**-0.488 (-0.747, -0.229)**	**-0.412**	**0.000**	**0**
IL6R	-0.882 (-1.481, -0.283)	-0.367	0.004	0.064
NLRP3	-0.675 (-1.301, -0.049)	-0.171	0.035	0.56
IL1B	-0.381 (-1.052, 0.290)	0.051	0.262	1
P2RY12	-0.543 (-1.138, 0.051)	-0.251	0.073	1
NFKB1	-0.376 (-0.933, 0.182)	-0.526	0.184	1
TNF	0.421 (-0.273, 1.116)	0.270	0.231	1
AIF1	-0.860 (-1.520, -0.200)	-0.300	0.011	0.176
TREM2	-0.638 (-1.143, -0.133)	-0.503	0.014	0.224
FYN	-0.043 (-0.810, 0.724)	-0.544	0.912	1
IL6	-0.328 (-0.971, 0.315)	-0.037	0.314	1
TLR4	-0.326 (-0.956, 0.304)	-0.363	0.306	1
TNFRSF1A	-0.910 (-1.658, -0.163)	-0.550	0.017	0.272
TMEM119	**-0.864 (-1.402, -0.326)**	**-0.482**	**0.002**	**0.032**

CD68	-0.796 (-1.389, -0.202)	-0.516	0.009	0.144
TBI vs young control				
KLB	0.392 (-0.466, 1.250)	0.233	0.367	1
KL	**-0.523 (-0.789, -0.257)**	**-0.412**	**0.000**	**0**
IL6R	-0.542 (-1.158, 0.073)	-0.367	0.083	1
NLRP3	-0.726 (-1.369, -0.083)	-0.171	0.027	0.432
IL1B	-0.367 (-1.056, 0.322)	0.051	0.293	1
P2RY12	**-0.930 (-1.541, -0.320)**	**-0.251**	**0.003**	**0.048**
NFKB1	-0.377 (-0.949, 0.196)	-0.526	0.195	1
TNF	0.420 (-0.293, 1.133)	0.270	0.245	1
AIF1	**-1.077 (-1.755, -0.399)**	**-0.300**	**0.002**	**0.032**
TREM2	**-1.061 (-1.580, -0.542)**	**-0.503**	**0.000**	**0**
FYN	-0.109 (-0.897, 0.679)	-0.544	0.784	1
IL6	-0.203 (-0.863, 0.458)	-0.037	0.544	1
TLR4	-0.392 (-1.039, 0.255)	-0.363	0.232	1
TNFRSF1A	-0.797 (-1.565, -0.030)	-0.550	0.042	0.672
TMEM119	**-1.416 (-1.968, -0.863)**	**-0.482**	**0.000**	**0**
CD68	**-1.133 (-1.742, -0.523)**	**-0.516**	**0.000**	**0**
Alzheimer's vs aged control				
KLB	0.149 (-0.344, 0.643)	0.233	0.549	1
KL	-0.004 (-0.157, 0.149)	-0.412	0.963	1
IL6R	-0.285 (-0.639, 0.068)	-0.367	0.113	1
NLRP3	-0.262 (-0.632, 0.108)	-0.171	0.163	1
IL1B	0.087 (-0.309, 0.483)	0.051	0.664	1
P2RY12	-0.090 (-0.441, 0.262)	-0.251	0.614	1
NFKB1	0.034 (-0.295, 0.364)	-0.526	0.836	1
TNF	0.294 (-0.116, 0.705)	0.270	0.157	1
AIF1	-0.193 (-0.582, 0.197)	-0.300	0.329	1
TREM2	0.240 (-0.059, 0.538)	-0.503	0.114	1
FYN	-0.252 (-0.706, 0.201)	-0.544	0.271	1
IL6	-0.078 (-0.458, 0.302)	-0.037	0.684	1
TLR4	-0.216 (-0.588, 0.156)	-0.363	0.253	1
TNFRSF1A	-0.130 (-0.571, 0.312)	-0.550	0.561	1
TMEM119	0.027 (-0.291, 0.345)	-0.482	0.868	1
CD68	0.124 (-0.226, 0.474)	-0.516	0.484	1
TBI vs Alzheimer's				

KLB	0.098 (-0.429, 0.625)	0.233	0.712	1
KL	-0.035 (-0.199, 0.128)	-0.412	0.668	1
IL6R	0.339 (-0.038, 0.717)	-0.367	0.078	1
NLRP3	-0.051 (-0.446, 0.344)	-0.171	0.798	1
IL1B	0.014 (-0.409, 0.437)	0.051	0.947	1
P2RY12	-0.387 (-0.762, -0.012)	-0.251	0.043	0.688
NFKB1	-0.001 (-0.353, 0.351)	-0.526	0.995	1
TNF	-0.002 (-0.439, 0.436)	0.270	0.994	1
AIF1	-0.217 (-0.633, 0.200)	-0.300	0.304	1
TREM2	-0.423 (-0.742, -0.105)	-0.503	0.010	0.16
FYN	-0.066 (-0.550, 0.418)	-0.544	0.787	1
IL6	0.125 (-0.280, 0.531)	-0.037	0.541	1
TLR4	-0.066 (-0.463, 0.331)	-0.363	0.743	1
TNFRSF1A	0.113 (-0.358, 0.584)	-0.550	0.634	1
TMEM119	**-0.552 (-0.891, -0.212)**	**-0.482**	**0.002**	**0.032**
CD68	-0.337 (-0.711, 0.037)	-0.516	0.077	1
TBI vs aged control				
KLB	0.247 (-0.283, 0.778)	0.233	0.357	1
KL	-0.039 (-0.203, 0.126)	-0.412	0.639	1
IL6R	0.054 (-0.327, 0.434)	-0.367	0.779	1
NLRP3	-0.313 (-0.711, 0.085)	-0.171	0.121	1
IL1B	0.101 (-0.325, 0.527)	0.051	0.639	1
P2RY12	-0.477 (-0.854, -0.099)	-0.251	0.014	0.224
NFKB1	0.033 (-0.321, 0.388)	-0.526	0.852	1
TNF	0.293 (-0.148, 0.734)	0.270	0.191	1
AIF1	-0.409 (-0.828, 0.010)	-0.300	0.056	0.896
TREM2	-0.183 (-0.504, 0.137)	-0.503	0.259	1
FYN	-0.318 (-0.806, 0.169)	-0.544	0.198	1
IL6	0.047 (-0.361, 0.456)	-0.037	0.819	1
TLR4	-0.281 (-0.681, 0.119)	-0.363	0.166	1
TNFRSF1A	-0.017 (-0.491, 0.458)	-0.550	0.945	1
TMEM119	**-0.525 (-0.867, -0.183)**	**-0.482**	**0.003**	**0.048**
CD68	-0.213 (-0.590, 0.164)	-0.516	0.264	1

Table displays the LogFC estimates, 95% confidence interval. P-values are adjusted for multiple comparisons using the Bonferroni correction. Significant comparisons where $p<0.05$ are bolded.

Supplementary Table S 5.0.2 All statistical results from linear regression models in the PCx.

PCx				
Gene	**LogFC (95% CI)**	**Ave Expr**	**P-val**	**Adj.P-val**
Aged control vs young control				
KLB	0.315 (-0.412, 1.042)	0.195	0.391	1
KL	-0.306 (-0.573, -0.039)	-0.462	0.025	0.4
IL6R	-0.357 (-1.087, 0.373)	-0.213	0.333	1
NLRP3	-0.622 (-1.352, 0.107)	-0.179	0.094	1
IL1B	-0.537 (-1.251, 0.176)	0.167	0.138	1
P2RY12	-0.517 (-1.057, 0.022)	-0.274	0.060	0.96
NFKB1	-0.455 (-1.115, 0.205)	-0.442	0.174	1
TNF	0.228 (-0.303, 0.760)	0.157	0.396	1
AIF1	-0.423 (-1.137, 0.291)	-0.370	0.242	1
TREM2	-0.562 (-1.167, 0.043)	-0.513	0.068	1
FYN	-0.425 (-1.128, 0.279)	-0.350	0.233	1
IL6	0.312 (-0.555, 1.180)	0.137	0.476	1
TLR4	-0.216 (-0.836, 0.404)	-0.274	0.491	1
TNFRSF1A	-0.380 (-1.059, 0.300)	-0.335	0.270	1
TMEM119	-0.434 (-0.999, 0.131)	-0.472	0.131	1
CD68	-0.669 (-1.223, -0.115)	-0.484	0.019	0.304
Alzheimer's vs young control				
KLB	0.741 (0.016, 1.466)	0.195	0.045	0.72
KL	-0.294 (-0.561, -0.028)	-0.462	0.031	0.496
IL6R	-0.487 (-1.214, 0.241)	-0.213	0.187	1
NLRP3	-0.815 (-1.542, -0.088)	-0.179	0.029	0.464
IL1B	-0.032 (-0.744, 0.679)	0.167	0.928	1
P2RY12	-0.686 (-1.223, -0.148)	-0.274	0.013	0.208
NFKB1	-0.363 (-1.020, 0.295)	-0.442	0.276	1
TNF	0.238 (-0.292, 0.768)	0.157	0.374	1
AIF1	-0.482 (-1.194, 0.230)	-0.370	0.182	1
TREM2	-0.568 (-1.171, 0.035)	-0.513	0.064	1
FYN	-0.362 (-1.063, 0.340)	-0.350	0.308	1
IL6	0.610 (-0.255, 1.474)	0.137	0.165	1
TLR4	-0.160 (-0.778, 0.459)	-0.274	0.608	1
TNFRSF1A	-0.509 (-1.186, 0.168)	-0.335	0.139	1

TMEM119	-0.633 (-1.197, -0.070)	-0.472	0.028	0.448
CD68	-0.568 (-1.120, -0.016)	-0.484	0.044	0.704
TBI vs young control				
KLB	0.444 (-0.311, 1.199)	0.195	0.246	1
KL	-0.199 (-0.476, 0.078)	-0.462	0.158	1
IL6R	-0.285 (-1.042, 0.472)	-0.213	0.456	1
NLRP3	-0.804 (-1.561, -0.047)	-0.179	0.038	0.608
IL1B	-0.325 (-1.065, 0.415)	0.167	0.385	1
P2RY12	**-0.920 (-1.479, -0.360)**	**-0.274**	**0.002**	**0.032**
NFKB1	-0.344 (-1.029, 0.341)	-0.442	0.321	1
TNF	0.273 (-0.279, 0.825)	0.157	0.328	1
AIF1	-0.938 (-1.679, -0.197)	-0.370	0.014	0.224
TREM2	-0.916 (-1.544, -0.289)	-0.513	0.005	0.08
FYN	-0.473 (-1.203, 0.257)	-0.350	0.201	1
IL6	0.651 (-0.249, 1.552)	0.137	0.154	1
TLR4	-0.253 (-0.896, 0.391)	-0.274	0.437	1
TNFRSF1A	-0.571 (-1.275, 0.134)	-0.335	0.111	1
TMEM119	-0.813 (-1.400, -0.227)	-0.472	0.007	0.112
CD68	**-0.880 (-1.455, -0.306)**	**-0.484**	**0.003**	**0.048**
Alzheimer's vs aged control				
KLB	0.426 (-0.009, 0.861)	0.195	0.055	0.88
KL	0.012 (-0.148, 0.172)	-0.462	0.883	1
IL6R	-0.129 (-0.565, 0.307)	-0.213	0.557	1
NLRP3	-0.193 (-0.629, 0.243)	-0.179	0.382	1
IL1B	0.505 (0.079, 0.931)	0.167	0.021	0.336
P2RY12	-0.168 (-0.491, 0.154)	-0.274	0.302	1
NFKB1	0.093 (-0.302, 0.487)	-0.442	0.642	1
TNF	0.010 (-0.308, 0.328)	0.157	0.950	1
AIF1	-0.059 (-0.486, 0.368)	-0.370	0.784	1
TREM2	-0.006 (-0.368, 0.355)	-0.513	0.972	1
FYN	0.063 (-0.357, 0.484)	-0.350	0.766	1
IL6	0.297 (-0.221, 0.816)	0.137	0.258	1
TLR4	0.056 (-0.315, 0.427)	-0.274	0.764	1
TNFRSF1A	-0.130 (-0.535, 0.276)	-0.335	0.527	1
TMEM119	-0.199 (-0.537, 0.139)	-0.472	0.245	1
CD68	0.101 (-0.230, 0.432)	-0.484	0.546	1

TBI vs Alzheimer's				
KLB	-0.297 (-0.776, 0.182)	0.195	0.220	1
KL	0.095 (-0.081, 0.271)	-0.462	0.284	1
IL6R	0.201 (-0.279, 0.682)	-0.213	0.407	1
NLRP3	0.011 (-0.470, 0.491)	-0.179	0.965	1
IL1B	-0.292 (-0.762, 0.178)	0.167	0.219	1
P2RY12	-0.234 (-0.589, 0.121)	-0.274	0.194	1
NFKB1	0.019 (-0.416, 0.453)	-0.442	0.932	1
TNF	0.035 (-0.315, 0.385)	0.157	0.844	1
AIF1	-0.456 (-0.926, 0.015)	-0.370	0.057	0.912
TREM2	-0.348 (-0.746, 0.050)	-0.513	0.086	1
FYN	-0.112 (-0.575, 0.352)	-0.350	0.633	1
IL6	0.042 (-0.530, 0.613)	0.137	0.885	1
TLR4	-0.093 (-0.501, 0.316)	-0.274	0.653	1
TNFRSF1A	-0.062 (-0.509, 0.386)	-0.335	0.785	1
TMEM119	-0.180 (-0.553, 0.192)	-0.472	0.338	1
CD68	-0.312 (-0.677, 0.052)	-0.484	0.092	1
TBI vs aged control				
KLB	0.129 (-0.354, 0.611)	0.195	0.597	1
KL	0.107 (-0.070, 0.284)	-0.462	0.233	1
IL6R	0.072 (-0.412, 0.556)	-0.213	0.768	1
NLRP3	-0.182 (-0.666, 0.302)	-0.179	0.457	1
IL1B	0.213 (-0.261, 0.686)	0.167	0.374	1
P2RY12	-0.402 (-0.760, -0.045)	-0.274	0.028	0.448
NFKB1	0.111 (-0.326, 0.549)	-0.442	0.614	1
TNF	0.045 (-0.308, 0.398)	0.157	0.801	1
AIF1	-0.515 (-0.989, -0.041)	-0.370	0.034	0.544
TREM2	-0.354 (-0.755, 0.047)	-0.513	0.083	1
FYN	-0.048 (-0.515, 0.418)	-0.350	0.837	1
IL6	0.339 (-0.237, 0.915)	0.137	0.245	1
TLR4	-0.037 (-0.448, 0.375)	-0.274	0.860	1
TNFRSF1A	-0.191 (-0.642, 0.259)	-0.335	0.401	1
TMEM119	-0.379 (-0.754, -0.004)	-0.472	0.048	0.768
CD68	-0.212 (-0.579, 0.156)	-0.484	0.256	1

Table displays the LogFC estimates, 95% confidence interval. P-values are adjusted for multiple comparisons using the Bonferroni correction. Significant comparisons where $p<0.05$ are bolded.

Supplementary Table S 5.0.3 All statistical results from linear regression models in the HIP

HIP				
Gene	**LogFC (95% CI)**	**Ave Expr**	**P-val**	**Adj.P-val**
Aged control vs young control				
KLB	-0.587 (-1.328, 0.153)	-0.441	0.119	1
KL	**1.687 (1.014, 2.361)**	**1.440**	**0.000**	**0**
IL6R	0.742 (0.032, 1.453)	0.270	0.041	0.656
NLRP3	0.674 (-0.059, 1.406)	0.408	0.071	1
IL1B	0.495 (-0.315, 1.306)	0.308	0.229	1
P2RY12	**1.091 (0.405, 1.777)**	**0.605**	**0.002**	**0.032**
NFKB1	0.170 (-0.496, 0.835)	0.117	0.615	1
TNF	0.498 (-0.381, 1.378)	0.490	0.264	1
AIF1	1.053 (0.321, 1.784)	0.595	0.005	0.08
TREM2	**1.128 (0.523, 1.733)**	**0.728**	**0.000**	**0**
FYN	0.787 (0.127, 1.446)	0.751	0.020	0.32
IL6	0.412 (-0.359, 1.183)	0.010	0.292	1
TLR4	**1.149 (0.426, 1.871)**	**0.791**	**0.002**	**0.032**
TNFRSF1A	0.932 (0.286, 1.579)	0.753	0.005	0.08
TMEM119	**1.103 (0.431, 1.775)**	**0.675**	**0.001**	**0.016**
CD68	**1.382 (0.747, 2.016)**	**0.729**	**0.000**	**0**
Alzheimer's vs young control				
KLB	-0.536 (-1.286, 0.215)	-0.441	0.160	1
KL	**1.340 (0.657, 2.022)**	**1.440**	**0.000**	**0**
IL6R	0.847 (0.127, 1.567)	0.270	0.022	0.352
NLRP3	0.484 (-0.258, 1.227)	0.408	0.199	1
IL1B	0.800 (-0.022, 1.622)	0.308	0.056	0.896
P2RY12	**1.167 (0.472, 1.863)**	**0.605**	**0.001**	**0.016**
NFKB1	0.581 (-0.094, 1.255)	0.117	0.091	1
TNF	0.478 (-0.414, 1.369)	0.490	0.291	1
AIF1	0.997 (0.255, 1.738)	0.595	0.009	0.144
TREM2	**1.368 (0.755, 1.981)**	**0.728**	**0.000**	**0**
FYN	**1.023 (0.355, 1.691)**	**0.751**	**0.003**	**0.048**
IL6	0.495 (-0.287, 1.276)	0.010	0.213	1
TLR4	**1.282 (0.549, 2.014)**	**0.791**	**0.001**	**0.016**
TNFRSF1A	0.945 (0.289, 1.600)	0.753	0.005	0.08

TMEM119	**1.296 (0.615, 1.977)**	**0.675**	**0.000**	**0**
CD68	**1.524 (0.881, 2.168)**	**0.729**	**0.000**	**0**
TBI vs young control				
KLB	-0.570 (-1.334, 0.195)	-0.441	0.143	1
KL	**1.368 (0.673, 2.063)**	**1.440**	**0.000**	**0**
IL6R	0.829 (0.096, 1.562)	0.270	0.027	0.432
NLRP3	0.566 (-0.191, 1.322)	0.408	0.141	1
IL1B	0.768 (-0.068, 1.605)	0.308	0.072	1
P2RY12	**1.130 (0.422, 1.838)**	**0.605**	**0.002**	**0.032**
NFKB1	0.217 (-0.470, 0.904)	0.117	0.533	1
TNF	0.855 (-0.053, 1.763)	0.490	0.065	1
AIF1	0.870 (0.115, 1.625)	0.595	0.024	0.384
TREM2	**1.067 (0.443, 1.692)**	**0.728**	**0.001**	**0.016**
FYN	0.653 (-0.028, 1.333)	0.751	0.060	0.96
IL6	0.441 (-0.355, 1.236)	0.010	0.275	1
TLR4	1.021 (0.276, 1.767)	0.791	0.008	0.128
TNFRSF1A	0.811 (0.143, 1.478)	0.753	0.018	0.288
TMEM119	0.924 (0.231, 1.618)	0.675	0.009	0.144
CD68	**1.407 (0.752, 2.062)**	**0.729**	**0.000**	**0**
Alzheimer's vs aged control				
KLB	0.052 (-0.399, 0.502)	-0.441	0.821	1
KL	-0.347 (-0.757, 0.062)	1.440	0.096	1
IL6R	0.104 (-0.328, 0.537)	0.270	0.634	1
NLRP3	-0.189 (-0.635, 0.257)	0.408	0.402	1
IL1B	0.305 (-0.188, 0.798)	0.308	0.223	1
P2RY12	0.077 (-0.341, 0.494)	0.605	0.717	1
NFKB1	0.411 (0.006, 0.816)	0.117	0.047	0.752
TNF	-0.021 (-0.556, 0.515)	0.490	0.939	1
AIF1	-0.056 (-0.501, 0.389)	0.595	0.804	1
TREM2	0.240 (-0.128, 0.608)	0.728	0.199	1
FYN	0.236 (-0.165, 0.637)	0.751	0.246	1
IL6	0.083 (-0.386, 0.552)	0.010	0.728	1
TLR4	0.133 (-0.307, 0.572)	0.791	0.551	1
TNFRSF1A	0.012 (-0.381, 0.406)	0.753	0.951	1
TMEM119	0.193 (-0.216, 0.602)	0.675	0.352	1
CD68	0.143 (-0.243, 0.529)	0.729	0.465	1

TBI vs Alzheimer's				
KLB	-0.034 (-0.523, 0.455)	-0.441	0.891	1
KL	0.028 (-0.416, 0.473)	1.440	0.899	1
IL6R	-0.018 (-0.487, 0.451)	0.270	0.939	1
NLRP3	0.081 (-0.402, 0.565)	0.408	0.740	1
IL1B	-0.032 (-0.567, 0.503)	0.308	0.907	1
P2RY12	-0.037 (-0.490, 0.416)	0.605	0.872	1
NFKB1	-0.364 (-0.803, 0.075)	0.117	0.104	1
TNF	0.378 (-0.203, 0.958)	0.490	0.200	1
AIF1	-0.127 (-0.609, 0.356)	0.595	0.604	1
TREM2	-0.301 (-0.700, 0.099)	0.728	0.139	1
FYN	-0.370 (-0.805, 0.065)	0.751	0.095	1
IL6	-0.054 (-0.562, 0.455)	0.010	0.835	1
TLR4	-0.260 (-0.737, 0.216)	0.791	0.282	1
TNFRSF1A	-0.134 (-0.561, 0.293)	0.753	0.535	1
TMEM119	-0.372 (-0.815, 0.072)	0.675	0.100	1
CD68	-0.117 (-0.536, 0.302)	0.729	0.581	1
TBI vs aged control				
KLB	0.018 (-0.455, 0.491)	-0.441	0.941	1
KL	-0.319 (-0.749, 0.111)	1.440	0.145	1
IL6R	0.086 (-0.368, 0.540)	0.270	0.708	1
NLRP3	-0.108 (-0.576, 0.360)	0.408	0.649	1
IL1B	0.273 (-0.245, 0.791)	0.308	0.298	1
P2RY12	0.039 (-0.399, 0.478)	0.605	0.859	1
NFKB1	0.047 (-0.378, 0.472)	0.117	0.826	1
TNF	0.357 (-0.205, 0.919)	0.490	0.211	1
AIF1	-0.183 (-0.650, 0.285)	0.595	0.441	1
TREM2	-0.061 (-0.447, 0.326)	0.728	0.757	1
FYN	-0.134 (-0.555, 0.287)	0.751	0.530	1
IL6	0.029 (-0.464, 0.521)	0.010	0.908	1
TLR4	-0.128 (-0.589, 0.334)	0.791	0.585	1
TNFRSF1A	-0.122 (-0.535, 0.291)	0.753	0.561	1
TMEM119	-0.179 (-0.608, 0.251)	0.675	0.412	1
CD68	0.026 (-0.380, 0.431)	0.729	0.900	1

Table displays the LogFC estimates, 95% confidence interval. P-values are adjusted for multiple comparisons using the Bonferroni correction. Significant comparisons where $p<0.05$ are bolded.

Contextual statement: Chapter 6

Chapter 6 is an experimental chapter prepared in as a manuscript with the intention to submit for publication. In accordance with the research pipeline outlined in chapter 1, ways to assess microglial ageing *in vitro* were also investigated in this thesis. Chapter 6 presents the development of an *in vitro* model of ageing microglia in the immortalised BV2 cell line. Cell culture studies for neurodegenerative disease are critical in uncovering molecular basis of disease and ageing in addition to being used for screening of treatments prior to *in vivo* administration. Therefore, in fitting with the theme of this thesis, which is to improve translatability of results, we believe that research models must best reflect the environment of the target disease. This is particularly important when investigating the responses of immune cells in the ND brain such as microglia which have altered immune responses during ageing. Serial passage of primary cells in culture induces cell cycle arrest and cellular senescence however while immortalised cell lines present with phenotypic changes with increasing passage, it is unknown if these changes are reflective of a senescent state. Thus chapter 6 aimed to investigate this and serially passage BV2 cell lines to induce changes in markers of aged microglia. The validation of such a model would represent a significant and widely available tool to conduct investigations into how aged microglia respond to potential treatments before moving into animal studies.

Statement of Authorship

Title of Paper	Examining the Potential of an Immortalised Glial cell Line as an In Vitro Model of Cellular Senescence
Publication Status	☐ Published ☐ Accepted for Publication ☐ Submitted for Publication ☑ Unpublished and Unsubmitted work written in manuscript style
Publication Details	

Principal Author

Name of Principal Author (Candidate)	Laura Carr		
Contribution to the Paper	First author and main contributor. Conducted cell culture experiments and majority subsequent analysis. Concept, writer and formulation of manuscript. Reviewed prepared final draft following inputs from co-authors.		
Overall percentage (%)	70%		
Certification:	This paper reports on original research I conducted during the period of my Higher Degree by Research candidature and is not subject to any obligations or contractual agreements with a third party that would constrain its inclusion in this thesis. I am the primary author of this paper.		
Signature		Date	10/11/2024

Co-Author Contributions

By signing the Statement of Authorship, each author certifies that:

i. the candidate's stated contribution to the publication is accurate (as detailed above);
ii. permission is granted for the candidate in include the publication in the thesis; and
iii. the sum of all co-author contributions is equal to 100% less the candidate's stated contribution.

Name of Co-Author	Gustavo Bracho		
Contribution to the Paper	Conducted cell imaging and image analysis. Reviewed and edited manuscript methods.		
Signature		Date	14/11/2024

Name of Co-Author	Claire Rennie

Contribution to the Paper	Conducted TNF cytokine analysis, reviewed manuscript		
Signature		Date	27/11/2024

Name of Co-Author	Andrew Care		
Contribution to the Paper	Assisted with TNF cytokine analysis, reviewed and edited manuscript, Project supervision		
Signature		Date	27/11/2024

Name of Co-Author	Ian Musgrave		
Contribution to the Paper	Experimental advice, Reviewed and edited manuscript, Project supervision		
Signature		Date	22/11/24

Name of Co-Author	Sanam Mustafa		
Contribution to the Paper	Conceptualised paper, provided experimental support and advice, reviewed and edited manuscript, Project supervision		
Signature		Date	01/12/24

Name of Co-Author	Lyndsey E. Collins-Praino		
Contribution to the Paper	Conceptualised paper, provided experimental support and advice, reviewed and edited manuscript, Project supervision		
Signature		Date	22/11/24

Please cut and paste additional co-author panels here as required.

Chapter 6 : Examining The Potential of an Immortalised Glial Cell Line as an *In Vitro* Model of Cellular Senescence

Laura M. Carr[1], Gustavo Bracho[2], Claire Rennie[3], Andrew Care[3], Ian Musgrave[1], Sanam Mustafa[1,4], Lyndsey E. Collins-Praino[1]

[1]School of Biomedicine, University of Adelaide, Adelaide, SA, Australia
[2] College of Medicine and Public Health, Flinders University, Adelaide, South Australia
[3]School of Life Sciences, University of Technology Sydney, Sydney, NSW, Australia
[4]Australian Research Council Centre of Excellence for Nanoscale Biophotonics, The University of Adelaide, Adelaide, SA, Australia

6.1 Abstract

Neurodegenerative diseases (NDs), including Alzheimer's disease (AD) and Parkinson's disease (PD), are amongst the most common causes of disability in the over 75 population [1]. Currently, translation of ND research is difficult, due in part to the lack of models which accurately recapitulate the aged CNS environment, particularly in the early *in vitro* stages of research. Immortalised cell lines are used often in ND research and are known to show phenotypic changes with increasing passage, though these changes vary between cell lines and are largely uncharacterised. Here, we investigate the extent to which the phenotypic changes in a commonly used microglial-like cell line (BV2) following multiple passages reflect those seen in aged cells.

BV2 cells were cultured from 7 to >90 passages, and cells at either end of this range were assessed for markers of cellular senescence. High passage BV2 cells demonstrated an increased growth rate and decreased cytokine release in response to inflammatory stimuli, the opposite of what is expected with age. Additionally, high passage cells show an increase in uptake, aggregation and ubiquitination of $A\beta^{1-42}$, and morphological changes associated with activation.

These results indicate that high passage BV2 cells do not completely capture the aged microglial phenotype but may recapitulate the dysregulated proteostasis of microglial ageing. Though these results suggest that replicative senescence is not fully inducible in the BV2 cell line, other methods to age cells in culture may provide a more feasible alternative to induce an aged phenotype in immortalised cell lines.

6.2 Introduction

Neurodegenerative diseases (NDs), including Alzheimer's Disease (AD) and Parkinson's Disease (PD), currently affect millions of people globally, with both diseases among the top 20 causes of Disability-Adjusted Life Years in those over the age of 75 according to the 2019 Global Burden of Disease Study (GBD) (Vos et al., 2020). Although the exact cause of these diseases is yet to be elucidated, it is well understood that the most significant risk factor for developing a neurodegenerative disease is increased age (Hou et al., 2019), with both diseases emerging around 65 years of age (Oliveira et al., 2017). Currently, treatments for these diseases provide only symptomatic relief, and safe and effective disease modifying treatments are lacking (Ricci, 2024). This is due, in part, to the poor translation of treatments from pre-clinical research to a clinical setting (Zeiss, 2017).

In particular, current research models do not adequately recapitulate the ageing background on which NDs occur (Johnson, 2015). In fact, despite the clear link between NDs and ageing, age is rarely considered in current research models, an oversight which has been well documented in recent reviews (Carr et al., 2024; Johnson, 2015; Sun et al., 2020; Wallace and Howlett, 2016). This is critical to consider, as age-related changes in the immune system and drug metabolism can have an impact on the effectiveness of treatments. In line with this, older patients have been known to respond differently to treatment administration, with hospitalisations due to adverse drug reactions four times higher in the elderly population than for younger patients (Beijer and de Blaey, 2002). Additionally, drug metabolism is altered during ageing, with multiple members of the cytochromes P450 family of drug metabolising enzymes known to have altered inducibility during ageing, leading to differences in pharmacokinetic profiles in older patients (Kinirons and O'Mahony, 2004). Thus, accurately modelling the aged environment is key in developing effective and safe treatments and improving translation of treatments from bench to bedside.

The *in vitro* screening of therapeutic interventions is critical to understand the safety and tolerability of treatments (Zhao, 2023). When ageing cells *in vitro,* culturing cells to their proliferative end is widely employed, due to the long-established understanding that continued replication causes ageing-like changes. This is termed replicative senescence and was first demonstrated by Leonard Hayflick in 1965,

who showed that human diploid cells have a limited lifespan in culture (Hayflick, 1965). Since then, characteristics of cells which have undergone replicative senescence have been further described, and this method is utilised as a model of ageing in peripheral cells (James et al., 2016; Krtolica et al., 2001; Schloesser et al., 2023), but rarely in CNS cells (Pontén and Macintyre, 1968) (Cohen and Torres, 2019). Consequently, the use of *in vitro* models of aged CNS cells is scarce. To model CNS ageing specifically, iPSCs derived from fibroblasts from aged donors can be differentiated CNS cells (Strässler et al., 2018; Zheng et al., 2018). However, the major drawback of this method is the conversion of cells to pluripotency, which resets many cellular properties, erasing the aged phenotype of interest (Aversano et al., 2022). Alternatively, primary CNS cells can be derived from animal samples (Milner et al., 2022; Vijaya et al., 2023). Notably, protocols to skip the induction to pluripotency and directly convert donor cells to CNS cells have been developed for both neurons (Huh et al., 2016; Vierbuchen et al., 2010) and astrocytes (Gatto et al., 2021). However, while primary cultures may be able to capture some elements of aging, they have low yield and high variability between studies, with the limited lifespan of primary cells constraining longer term experiments (Hayflick, 1965).

Currently, immortalised cell lines remain one of the most commonly used methods for *in vitro* screening of treatments (Cetin et al., 2022). Immortalised CNS cell types including SHSY-5Y neuroblastoma (Biedler et al., 1978), C6 astroglioma cells (Benda et al., 1968), BV2 (Blasi et al., 1990) and CG4 (Louis et al., 1992) derived from both human and animal brains, are widely commercially available, affordable and easy to culture (Chalak et al., 2024). While they are the cell type most often used in *in vitro* ND studies due to their suitability to high throughput research, in particular for drug screening (Cetin et al., 2022), they have been considered inappropriate to use in a model of ageing due to their indefinite proliferative capacity and thus are assumed to be unable to undergo replicative senescence (Bunc et al., 2019). However, immortalised cell lines are known to undergo phenotypic changes following multiple passages, and for this reason, are often not used beyond passage 20 (Weiskirchen et al., 2023), although the exact suggested number varies between cell lines (Abdul-Hamid et al., 2019). This supposed phenotypic shift includes the presentation of genomic, epigenetic and functional changes in these cells following multiple passages, which could potentially impact study outcomes and accuracy of results

(Hughes et al., 2007; Weiskirchen et al., 2023). While these changes are widely reported to occur, this is an area that is not well considered in the literature, and further study of the phenotypes of late passage cell lines would greatly contribute to the understanding of these cells (He et al., 2023; Hughes et al., 2007).

In particular, it is important to probe whether immortalised cell lines undergo phenotypic changes associated with physiological ageing with increased passage number. There are a host of hallmarks of ageing, including increased inflammation and altered intercellular communication (López-Otín et al., 2023); however, cellular senescence is the most relevant to modelling age *in vitro* and has been well described since the early studies describing the Hayflick limit, where human cells in culture were described to have a proliferative limit (Hayflick, 1965; Hayflick L Fau - Moorhead and Moorhead, 1961). Dysregulated proteostasis is also seen in senescent cells, with decreased protein degradation and increased accumulation of proteins identified as a hallmark of ageing (Trigo et al., 2019). In particular, dysregulation of the ubiquitin proteasome pathway (UPP) has been demonstrated to occur during ageing (Löw, 2011), which has been suggested to contribute to the accumulation of misfolded intracellular proteins seen in NDs (Hegde et al., 2023). One of the most profound cellular changes with age is the development of the senescence associated secretory phenotype (SASP), which drives the increase in pro-inflammatory cytokine release seen with ageing (Budamagunta et al.). This is of particular importance in the brain and neurodegeneration, where chronic neuroinflammation has a known link to neurodegenerative disease (Kwon and Koh, 2020). This inflammatory phenotype in CNS glial cells, including microglia and astrocytes in particular contributes to reduced injury response (Finger et al., 2022), loss of blood brain barrier integrity (Kang et al., 2020) and an uncontrolled pro-inflammatory environment (Kwon and Koh, 2020). However, as microglia are the divers of the CNS immune response (Ginhoux et al., 2013), modelling changes in these cells with age is critical in understanding potential responses to treatments. Aged microglia are known to acquire a pro-inflammatory phenotype, characterised by an increased release of pro-inflammatory cytokines such as IL-6 and TNF at rest (Coppé et al., 2008). Additionally, the microglial response to inflammatory stimulation becomes more robust, with aged microglia becoming primed to respond in a pro-inflammatory manner (Nikodemova

et al., 2016) and take a longer time to resolve immune responses following stimulation (Wasserman et al., 2008). In addition to increased release of cytokines, aged microglia display increased levels of oxidative stress, characterised by increased generation of reactive oxygen species (ROS) as opposed to other oxidative products which have been seen in microglia isolated from C57BL/6 mice at 12-months-old exposed to 0.5mg/kg of LPS *via* intraperitoneal injection (Tichauer et al., 2014). Microglia isolated from aged LPS treated mice demonstrated an induction of ROS following administration of 1µg/ml of LPS to cultures whereas microglia isolated from young LPS exposed mice (2-months-old) showed increases in nitric oxide (NO) instead (Tichauer et al., 2014). Thus, age predisposes primed microglia to release ROS over NO in response to further immune stimulation. Considering the damaging effects of ROS (Gu et al., 2011) compared to the antioxidant effects of NO (Džoljić et al., 2015), this suggests that aged microglia will have higher levels of oxidative stress and less antioxidant capacity compared to younger microglia.

Previous studies have characterised hallmarks of the aged phenotype in a number of studies utilising primary cells, both peripheral (Fan et al., 2024; Jung et al., 2009) and CNS derived (Karabag et al., 2023; Windener et al., 2024). However, the applicability of this to immortalised cell lines has not previously been described, and to our knowledge, no model of ageing in immortalised cell CNS lines exists. Thus, there exists a clear gap in the current understanding of how immortalised cell lines change with passage, and what effect these specific changes have on cell function. Therefore, the current study utilised BV2 cells, a commonly used microglia-like cell line, to understand whether the phenotypic changes observed following multiple passages in these cells were reflective of those seen during cellular senescence.

6.3 Methods

6.3.1 Cell culture

Mouse microglia-like cells (BV2), kindly provided by Professor Mark Hutchinson (Adelaide, Australia), were cultured from 7 to >90 passages. Culture media was Dulbecco's Modified Eagle's Medium (DMEM): high-glucose (Gibco, Thermofisher, Victoria, Australia) with 10% foetal bovine serum (FBS), 2mM L-Glutamine, 50U/ml Penicillin-Streptomycin and 100µg/ml Normocin

(InvivoGen, San Diego, USA). Cells were grown in a humidified incubator at 37°C in 5% CO_2. Every 10 passages, a batch of cells was frozen in culture media with 10% DMSO and stored in liquid nitrogen for later use. Cells from each end of the passage range were used in experiments and classified as either young cells (<20 passages) or old cells (>90 passages).

6.3.2 Tracking cell growth rate

Cells were passaged every three days at around 70 to 80% confluency. At each passage cells were counted and seeded at $3x10^5$ cells in T75 flasks. The growth rate of cells was calculated by counting cells at each passage using trypan blue and an automated cell counter (Bio-Rad, CA, USA, TC20 Automated Cell Counter). Viability of passaged cells was >90% as measured by the cell counter. Cumulative population doubling (CPD) was calculated using equation 1 (Phipps et al., 2007). A = number of cells seeded at the beginning of the growth period, B = number of cells counted after growth period, C = previous population doubling, n = the largest number that satisfies the equation $A(2^n) \leq B$. The CPD was divided by the growth period to calculate population doubling/day, which was averaged for each passage from at least 2 replicate flasks.

Equation 1:

$$PD = \mathrm{C} + \mathrm{n} + [\frac{B - A(2^n)}{A(2^{n+1}) - A(2^n)}]$$

6.3.3 Cell treatments

To investigate changes in BV2 cells, young or old cells were seeded in T75 flasks allowed to adhere and grow for 24 hours. Flasks were then treated with either 50ng/ml of LPS (InvivoGen, San Diego, USA, Cat: trl-3pelps) or 0.5µM Amyloid-Beta$^{1-42}$ ($A\beta^{1-42}$) (rPeptide, Cat: A-1002-2) for 4-, 24- and 48-hours. Additionally, young and old cells were seeded as above and treated with 5µM of the proteasome inhibitor MG132 (Sigma-Aldrich, Cat: M7449) for 4-hours as, based on previous results from our laboratory, MG132 is toxic to cells beyond 5-hours. Dose for LPS and MG132 treatments was based on previous literature (LPS: (Kim et al., 2016; McCarron et al., 2015), MG132: (D'Souza et al., 2013; Lee et al., 2021) and previous experiments conducted in our laboratory. A range of concentrations were tested to confirm optimal $A\beta^{1-42}$ dose from previous literature which used $A\beta^{1-42}$ peptide with

immortalised cell lines (Schaeffer et al., 2008). Supernatant from each treatment was collected and stored at -20°C and cells were harvested and washed 3 times with PBS, with $2.5x10^6$ cells snap frozen in liquid nitrogen and stored at -80ºC until lysed using the appropriate buffer as described for the assays below.

6.3.4 MTT assay

Viability and metabolic activity were assessed using the MTT (3-(4,5-dimethylthiazol-2-yl)-2,5-diphenyltetrazolium bromide) assay across three experimental replicates (Invitrogen, California, United States, #M6494). Young and old BV2 cells were seeded at 2000 cells per well in 96-well plates and treated with the same reagents as for inflammatory treatments above. Controls containing equal amounts of buffer for each treatment were included at each timepoint; LPS control = 1% PBS, $A\beta^{1-42}$ control = 0.3% ammonium hydroxide, MG132 control = 0.05% DMSO). The MTT assay was performed using the "quick protocol" in accordance with the manufacturer's instructions. In brief, 2.4mg MTT powder was mixed with 10mL serum-free media before incubation for 4hrs. Following this, media was replaced with 50µl 100% dimethyl sulfoxide (DMSO) and incubated at 37°C for 10-minutes, before reading absorbance on a Synergy Mx plate reader (BioTek Instruments, Inc., Synergy Mx Gen 5, version 2.09, Winooski, Vermont, USA) at 570nm. Cell viability was calculated as a percentage of the positive control (young BV2 cells at baseline).

6.3.5 IL-6 ELISA

Enzyme-linked immunosorbent assay (ELISA) was performed using cell supernatant to measure IL-6 release across three experimental replicates. Samples and standards were performed in triplicate wells. ELISA kit (Mouse IL-6, #555240) and equivalent reagent set (Reagent set B #550534) were obtained from BD Biosciences (California, United States). Assays were performed in 96-well half area plates, according to a modified protocol. Briefly, plates were coated with 50µl of the provided capture antibody overnight at 4ºC, following which plates were washed 3x in provided wash buffer and blocked in assay diluent for an hour at room temperature. Following 3x washes in wash buffer, 50µl of sample and standards (0- to 1000 pg/ml) were added to plates and incubated overnight at 4°C. The following day, wells were washed 5x in wash buffer and incubated in 50µl of working detector for one hour at room

temperature. Following 7x 1-minute washes, 50µl of substrate solution was added to wells for 30-minutes, with plates protected from light. 25µl of stop solution was then added and absorbance read within 30-minutes on a Synergy Mx plate reader (BioTek Instruments, Inc., Synergy Mx Gen 5, version 2.09, Winooski, Vermont, USA) at 450nm and 570nm. For wavelength correction, readings at 570nm were subtracted from 450nm readings. The standard curve was plotted using excel, with the amount of IL-6 per well (pg/ml) calculated based on this curve.

6.3.6 CBA assay for TNF release

TNF release was measured using a flow-cytometry based assay. A Cytometric Bead Array (CBA) set (Mouse TNF Flex Set, #558299) and equivalent protein buffer kit (Mouse/Rat Soluble Protein Master Buffer Kit, #558266) were purchased from BD Biosciences (California, United States). Briefly, a mixed capture bead stock was prepared and incubated at room temperature for 15-minutes. 100µl of wash buffer was added and then removed from a 96-well round-bottom plate, after which 10µl of sample or standard was added to the wells. Following this, 10µl of mixed capture bead solution was then added to wells and the plate was shaken at 500rpm for 5-minutes. The plate was then incubated at room temperature for an hour protected from light. 10µl of prepared detection reagent was added to each well, with the plate shaken at 500rpm for 5-minutes before being incubated at room temperature for 2-hours. Following incubation, 120µl of wash buffer was added and the plate was shaken at 400rpm for 10-minutes. Calibration and compensation beads were prepared, and plates transferred to the flow cytometer (BD LSR Fortessa X20) for acquisition. Readings from samples were plotted against the standard curve and the amount of TNF (pg/ml) was calculated.

6.3.7 BCA assay for protein determination

Protein estimations were performed on snap frozen pellets of $2x10^6$ BV2 cells at young and old timepoints (n=3 per age) following cell lysis as specified for each assay below. Briefly, 25µl of standard (0.04mg/ml – 1mg/ml) was added to duplicate wells of a 96 well plate. 23µl of milli-q water was added to lysis buffer and sample wells. 2µl of lysis buffer or sample were added to lysis buffer or sample wells respectively. Samples were assayed in triplicate wells. Assay solution was made up by mixing the provided part A and part B reagents at a ratio of 50:1, and 200µl of solution was added to all sample,

standard and lysis buffer wells. Plates were then incubated in 37°C oven for 20 minutes following which absorbance was read at 540nm on a Synergy Mx plate reader (BioTek Instruments, Inc., Synergy Mx Gen 5, version 2.09, Winooski, Vermont, USA). Standard curve was plotted using excel and protein concentrations (mg/ml) were calculated.

6.3.8 Thiobarbituric acid reactive substances (TBARS) assay

Thiobarbituric acid (TBA) reactive substances (TBARS) are formed as a by-product of lipid peroxidation and measurement of these products is considered an indicator of oxidative stress response (Del Rio et al., 2005). A Lipid Peroxidation (MDA) Assay kit (ab118970, Abcam, Australia) was used to measure malondialdehyde (MDA), formed through lipid peroxidation. Cells treated with 50ng/ml of LPS were used as a positive control for MDA at each age and timepoint (4-, 24-, and 48- hours). TBA lysis buffer with butylated hydroxytoluene was added to $2.5x10^6$ cells which had been snap frozen and stored at -80°C and a sample was taken for protein estimation using a Pierce BCA assay kit as above (Thermofisher Scientific Inc., #23227). TBA solution was added to samples and standards and incubated at 95°C for 60-minutes. Samples were then spun down, supernatant was transferred to a 96-well plate, and absorbance read on a Synergy Mx plate reader (BioTek Instruments, Inc., Synergy Mx Gen 5, version 2.09, Winooski, Vermont, USA) at 532 nm. The standard curve was plotted and ng of MDA/mg of protein was calculated for each sample.

6.3.9 Oxygen Radical Absorbance Capacity assay

Oxygen radical absorbance capacity (ORAC) Assay Kit (ab233473) was used to measure antioxidant capacity. Cells were lysed by sonication (3x 10 second bursts at 400W). A sample was taken for protein estimation using a Pierce BCA assay kit (Thermofisher Scientific Inc., #23227). Briefly, 25ul of either cell supernatant or Trolox standard was added to the provided microplate. Fluorescein solution was added to wells containing samples and standards and mixed, before being incubated at 37°C for 30 minutes. Free radical initiator solution was added and read immediately with a fluorescent microplate reader (BMG Labtech, CLARIOstar plate reader, Ortenberg, Germany) at 480nm excitation/520 nm emission at 5-minute increments for a total of 60 minutes. The area under the curve was calculated and Trolox equivalents (TE) as a percentage of young BV2 cells at baseline was plotted.

6.3.10 Western blot

Western blot analysis was performed using the standard milk method to assess levels of caspase-1, a component of the NLRP3 inflammasome (Song et al., 2017), and K48-linked ubiquitination, a form of protein ubiquitination liked specifically to degradation by the 26S proteasome (Grice and Nathan, 2016). Briefly, 25ug of cell lysate was added to 4x Blot LDS sample buffer, 10x Bolt reducing agent and dH20 for a total volume of 40ul. Samples were heated at 99°C for 10 minutes and gel electrophoresis was performed using Bolt 4-12% Bis-Tris gels (Invitrogen, California, United States, NW04122BOX) run at 120 V for 1-hour and 45-minutes. Following this, gels were transferred to a PVDF membrane using the iBlot 2 Dry Blotting System (Thermofisher scientific Inc., Waltham, MA, USA). Membranes underwent 3 x 5-minute washes in 1x tris-buffered saline with 0.1 Tween® 20 detergent (TBS-T), before staining with Ponceau S red solution (Sigma-Aldrich, P7172-1L) for 5-minutes to ensure even protein loading between wells. Membranes were then washed with TBS-T until all traces of the Ponceau stain was removed. Membranes were subsequently blocked for 2-hours in 5% w/v powdered skim milk (SMP) in TBS-T (SMP-TBS-T), before overnight incubation at 4°C with K48-linked ubiquitin antibody in 2% SMP-TBS-T. Incubation was performed separately for housekeeper and K48-ubiquitin antibody to avoid antibody interactions whereby a clean housekeeper band could not be obtained. Table 6.1 summarises the antibodies used in this analysis and respective concentrations.

Following overnight incubation, antibody solution was removed and membranes were washed in TBS-T (3x 5-minute washes) and incubated in 2% SMP-TBS-T and secondary antibody 1 for 2-hours at room temperature protected from light. Each membrane was then washed in TBS-T (3x 5-minute washes) and visualised using an Odyssey CLx Imaging System (Image Studio V5.2 (LI-COR, Inc.)) at a resolution of 169um. Membranes then underwent 3x 5-minute washes in TBS-T before overnight incubation at 4°C in 2% SMP-TBS-T and the housekeeper GAPDH. Following overnight incubation, membranes were washed in TBS-T (3x 5-minute washes) and incubated in 2% SMP-TBS-T and secondary antibody 2 (, LI-COR, Inc., 1:10,000) for 2-hours at room temperature protected from light. Following incubation, membranes were washed 3 times in TBS-T for 5-minutes and visualised as above.

Blots were then assessed for levels of caspase-1. First, membranes previously stained with anti-ubiquitin antibody and anti-GAPDH were incubated for 30-minutes in NewBlot™ Nitrocellulose stripping buffer (LI-COR, cat# 928-40030) and visualised to confirm correct stripping of the antibodies. Following this, membranes were blocked for 2-hours in 5% SMP-TBS-T, before overnight incubation at 4°C with caspase-1 and GAPDH antibodies in 2% SMP-TBS-T. The following day, membranes were washed in TBS-T (3x 5-minute washes) and incubated in 2% SMP-TBS-T and both secondary antibodies for 2-hours at room temperature protected from light. Membranes were then washed 3 times in TBS-T for 5-minutes and visualised as above. Analysis of all blots was conducted using Empiria Studio software (LI-COR, Inc, Version 2.2.0.141) to visualise target and housekeeper band signals. Target signal was normalised to the housekeeper GAPDH signal and presented as relative density.

Table 6.1: Antibodies and concentrations used for Western blots.

Antibody	Host species	Source	Concentration
Primary antibodies			
Anti-ubiquitin (linkage-specific K48)	Rabbit	Abcam: ab140601	1:1000
Anti-GAPDH	Chicken	Abcam: ab83956	1:1000
Anti-Caspase-1	Rabbit	Abcam: ab138483	1:750
Secondary antibodies			
1: donkey anti-rabbit IRDye 800CW	Donkey	LI-COR, Inc: 926-32213	1:10,000
2: donkey anti-chicken IRDye 680CW	Donkey	LI-COR, Inc: 926-68075	1:10,000

6.3.11 Phagocytosis assay

BV2 phagocytosis was measured using the Vybrant Phagocytosis Assay (Molecular Probes, Eugene, OR, USA) according to the manufacturer's protocols. Briefly, BV2 cells were seeded at 1,750 cells per well in a 96-well plate and treated with LPS, FIT-C tagged $A\beta^{1-42}$ (rPeptide, Cat: A-1119r-1) or MG132, as described above. Wells containing only FIT-C tagged $A\beta^{1-42}$ were included and used to obtain background $A\beta^{1-42}$ fluorescence in treatment wells. The provided fluorescent BioParticle solution was prepared according to manufacturers instructions. 500µl of 10x concentrated Hank's balanced salt solution (HBSS) was mixed with 5mg of fluorescein-labelled *Escherichia coli* K-12 BioParticles and sonicated for 1-minute. The solution was then added to 4.5mL of deionized water and sonicated until

homogeneous. Following treatments, BV2 cells were incubated for 2-hours at 37°C with 100µl of the fluorescent BioParticle solution. The provided Trypan Blue suspension was mixed with 4mL of deionized water. Following incubation, the BioParticle solution was aspirated and 100µl of the Trypan Blue suspension was added to the wells for 1-minute at room temperature before being aspirated. The plate was then transferred to a fluorescent microplate reader (BioTek Instruments, Inc., Synergy Mx Gen 5, version 2.09, Winooski, Vermont, USA) and wells were read at 480nm excitation/520 nm emission. Phagocytic responses of experimental conditions were expressed as a percent of the positive control wells (i.e. young BV2 cells at baseline).

6.3.12 Preparation of cells for imaging

Visualisation of BV2 cells was carried out to investigate changes in BV2 morphology and uptake of $A\beta^{1-42}$. Cells were seeded at 1,750 cells per well in 96-well black walled clear bottom plates (PhenoPlate, PerkinElmer) and treated as for phagocytosis assays above. Additionally, co-treatments of LPS+$A\beta^{1-42}$ and MG132+$A\beta^{1-42}$ were included to investigate the effects of inflammation and proteasome inhibition on $A\beta^{1-42}$ uptake. Following treatment, plates were removed from incubator and placed on ice. Culture media was aspirated, and cells were washed twice with 200µl of PBS. Cells were then fixed by 30-minute incubation in neutral buffered formalin (NBF) with 5% sucrose. Following incubation, cells were again washed twice and stored in PBS at 4°C for a maximum of 14 days before undergoing staining. Wells were incubated overnight at 4°C with 50µl of the primary antibody (anti-ubiquitin (linkage-specific K48), 1:500, ab140601, Abcam) diluted in PBS. Following this, cells were washed twice with PBS and incubated with 50µl of the secondary antibody (Goat anti-Rabbit IgG (H+L) Alexa Fluor Plus 647, Thermofisher: A21244, 1:1000), DAPI (Sigma-Aldrich, D9542, 1:1000) and TRIT-C Phalloidin (Sigma-Aldrich, P1951, 1:2000) diluted in PBS for 1-hour at room temperature protected from light. Cells were washed twice with PBS, leaving 50µl in the wells so they did not dry out. Plates were stored at 4ºC protected from light until imaging.

6.3.13 High throughput microscopy

Following cell fixation and staining, the plates were imaged on an Operetta high-content imaging system coupled with a robotic arm (Cell::Explorer, Revvity), using Harmony 4.1 software (Revvity).

Signals for each of the fluorescent dyes were optimised and are presented in Table 6.2. Images were taken at 20x magnification for analysis of ubiquitination, $A\beta^{1-42}$ uptake and cell morphology, and at 40x magnification using a high numerical aperture lens for analysis of processes. Twenty-five fields of views at the same plane were captured for each well and images were transferred to a dedicated server for analysis.

Table 6.2: Optimised signals for each of the fluorescent dyes used in imaging experiments

Target	Fluorophore	Excitation wavelength (nm)	Emission wavelength (nm)	Exposition time (ms)
Nucleus	DAPI	360-400	410-480	50
Actin Cytoskeleton	TRITC Phalloidin	520-550	560-630	100
K48-linked ubiquitin	Alexa Fluor 647 antibody	620-640	650-760	300
$A\beta^{1-42}$	FITC tagged Dis$A\beta^{1-42}$	460-480	500-550	150

All images were processed in batch with the same analysis algorithms using a Columbus 2.0 software (Revvity) running on an Omero 4.0 and Acapella 3.2 image analysis server. Briefly, cells were localised using DAPI nuclear counterstaining. After discarding cells on the edges of the image, the cytoplasm, membrane and cytoskeleton was segmented for every cell individually using the Phalloidin staining. Several morphological properties were calculated including area and shape for both cell and nuclei. Regions and spots with detectable signals on the FITC ($A\beta^{1-42}$ regions) and Alexa Fluor 647 (K48-linked ubiquitin) regions were identified in the cell cytoplasm. The number of spots and relative intensity was calculated for these regions. A similar approach was used to identify and quantify FITC regions but using the previously identified Alexa fluor 647 regions of interest, to assess colocalization of Aβ spots within the K48-linked ubiquitin regions.

For process morphology analysis, the membrane regions of the cell were resized and used as the region of interest. The processes detection algorithm was adjusted to the TRITC Phalloidin channel and used to calculate the number of processes, branches and total processes length.

Data for each individual cell was then exported to CSV files and files from each plate were merged into a single file using a Python script (Python 3.11). Data handling and analysis was carried out using Spotfire desktop 10.8 (TIBCO). Results are presented as an average and standard deviation per well calculated from measurements from all individual cells in the well.

6.3.14 Statistical analysis

Statistical analysis was conducted using R (version 1.4.1717) (Dalgaard, 2010). Three-way ANOVA, with Tukey post-hoc where significant ($p < 0.05$) effects were present, was used to determine the effects of age, treatment and time on BV2 cells. As the current study was interested in the effects of age within treatment groups, only significant interactions of age:treatment and three-way interaction effects are probed further in the main text. Significant effects of treatment are stated in the main text where appropriate to validate treatment controls. Supplementary data S1 contains the significant effects from all three-way ANOVAs. Data were plotted using GraphPad Prism version 10.0.0 for Windows (GraphPad Software, San Diego, California USA). Graphing for imaging data was performed using Spotfire desktop 10.8 (TIBCO).

6.4 Results

6.4.1 Growth rate and Metabolic activity

BV2 growth rate, as measured by population doubling per day, increased with passage number. An independent samples t-test showed that old BV2 cells had higher population doublings per day *(1.57±0.35)* than young BV2 cells *(1.3±0.14), (t(69) = 4.174, p = <0.0001)* (Fig 6.1a). Metabolic activity of BV2 cells was assessed using an MTT assay which also allows for assessment of cell viability and analysis of effects of treatment controls (TC). Three-way ANOVA detected no interaction of age, treatment and time on metabolic activity measured by MTT assay *(F(8,56)=0.150, p=0.996)*. A significant main effect of treatment was, however, observed *(F(6,59)=7.788, p=<0.0001)* and probed further to ensure that TC were not decreasing the viability of cells. Tukey-post hoc showed a significant decrease in metabolic activity in $A\beta^{1-42}$ treated BV2 cells (*69±22.7)* compared to the TC BV2 cells treated with 0.3% ammonia *(108±14.8, p=<0.0001)* and compared to untreated BV2 cells *(107±15.7, p=<0.0001)* (Fig 6.1d). This was the only significant difference observed between treatment and relative treatment control. A significant decrease in MG132 treated BV2 cells *(72.8±19.2)* was also seen in comparison to untreated BV2 cells *(p=0.017)* (Fig 6.1e). Additionally, a significant main effect of age was seen *(F(1,59)=10.377, p=0.002)* with Tukey post-hoc showing that young cells *(88.4±23.6)* overall had lower metabolic activity than old cells *(104±25.9, p=0.002)*.

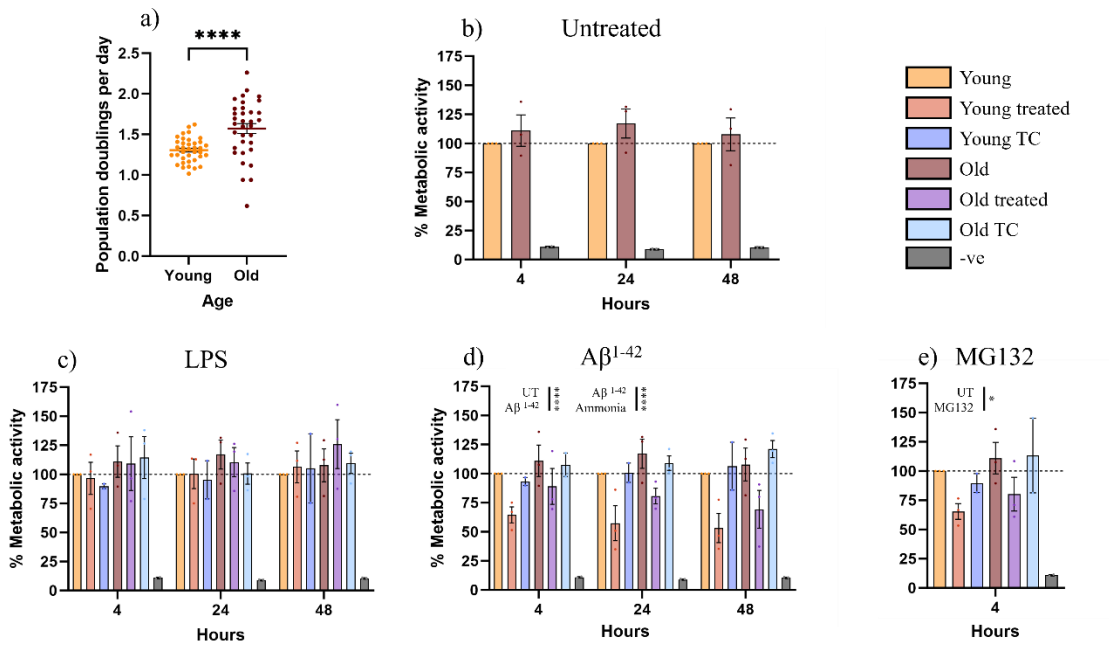


Figure 6.1: Growth rate and metabolic activity of BV2 cells. a) Growth rate as population doubling per day. b-e) Metabolic activity of BV2 cells measured by MTT assay at b) baseline and following treatment with b) 50ng/ml LPS, c) 0.5µM Aβ$^{1-42}$ for 4, 24 or 48 hours or d) 5µM of MG132 for 4 hours. Values are presented as a percentage of untreated BV2 cells and graphed as mean±SEM. Treatment controls (TC) containing an equal amount of buffer for each condition were included at each timepoint (LPS control = 1% PBS, Aβ$^{1-42}$ control = 0.3% ammonium hydroxide, MG132 control = 0.05% DMSO). No significant interaction effects were seen. * = p<0.05, **** = p<0.0001

6.4.2 Inflammatory profile and oxidative stress of BV2 cells

BV2 inflammatory profile was measured by analysing release of inflammatory cytokines IL-6 (Fig 6.2a) and TNF (Fig 6.2b) both at baseline and following administration of LPS, Aβ$^{1-42}$ or MG132. Further, we assessed both cell oxidative stress (Fig 6.2c) and antioxidant capacity (Fig 6.2d). Three-way ANOVAs were performed to assess if BV2 response to treatment changed with age and time.

6.4.3 IL-6 release

A significant main effect of age was seen in IL-6 release *(F(1,39)=24.519, p= <0.0001)* (Fig 6.2a) where Tukey post-hoc detected lower IL-6 release in old cells *(522±1401)* than in young cells *(3716±7437, p=0.02)*. Additionally, a significant three-way interaction effect on IL-6 release was detected by ANOVA *(F(4,39)=2.916, p=0.033)*. This effect was shown by Tukey post-hoc to be a significantly decreased IL-6 response by aged BV2 cells at both 24- *(Young: 16741±4616 vs Old: 1782±2198, p = 0.007)* and 48-hours *(Young: 2844±1414 vs Old: 31.3±0, p = 0.032)* following LPS administration. Of note, at 48-hours following LPS treatment, IL-6 levels in old cells were below the limit of detection of the assay (31.3ng/ml). Young BV2 cells released some IL-6 following Aβ$^{1-42}$

administration (*104±103)* particularly at the 24-hour timepoint (*202±130)*; however, no statistically significant differences were detected in young, treated cells compared to young untreated cells (31.3±*0)*.

6.4.4 TNF release

A significant main effect of age was seen in TNF release (*F(1,40)=184.638, p= <0.0001)* (Fig 6.2b) however Tukey post-hoc detected no differences in TNF release in old cells (*604±1059)* compared to in young cells *(1142±1475, p=>0.05).* Additionally, a significant three-way interaction effect on TNF release was detected *(F(4,40)=2.672, p=0.045).* Statistical results of post-hoc tests are presented in Table 6.3. Tukey post-hoc test showed a decreased release of TNF at baseline by old BV2 cells compared to young cells at 4-, 24-, and 48-hours. Additionally, old cells showed a decreased response to both LPS administration and $A\beta^{1-42}$ administration at all timepoints. Old cells also showed a decreased TNF release following MG132 treatment for 4-hours.

Table 6.3: Results of Tukey post-hoc tests following three-way ANOVA of TNF dataSignificance was set at <0.05.

	Young mean±SD	***Old mean±SD***	***p-value***
Untreated (4hrs)	*5.22 ± 0.41*	*3.05 ± 0.29*	***0.001***
Untreated (24hrs)	17.6 ± *1.85*	11.7 ± *1.47*	***0.012***
Untreated (48hrs)	34.8 ± *3.95*	16 ± *7.23*	***0.017***
LPS (4hrs)	4110 ± *250*	3228 ± *442*	***0.039***
LPS (24hrs)	3516 ± *106*	1856 ± *361*	***0.001***
LPS (48hrs)	1834 ± *15.9*	588 ± *130*	***0.000***
$A\beta^{1-42}$ (4hrs)	397 ± *96.8*	101 ± *26.9*	***0.006***
$A\beta^{1-42}$ (24hrs)	978 ± *113*	138 ± *52.8*	***0.000***
$A\beta^{1-42}$ (48hrs)	509 ± *164*	91.8 ± *8*	***0.012***
MG132 (4hrs)	18.3 ± *4.13*	6.72 ± *2.06*	***0.012***

6.4.5 Oxidative stress response and antioxidant capacity

No significant interaction effects were seen detected by three-way ANOVA on either oxidative stress response *(Age:Treatment:Time = F(4,39) = 1.298, p=0.287)* (Fig 6.2c) or antioxidant capacity *(Age:Treatment:Time = F(4,40) = 0.761, p=0.556)* (Fig 6.2d).

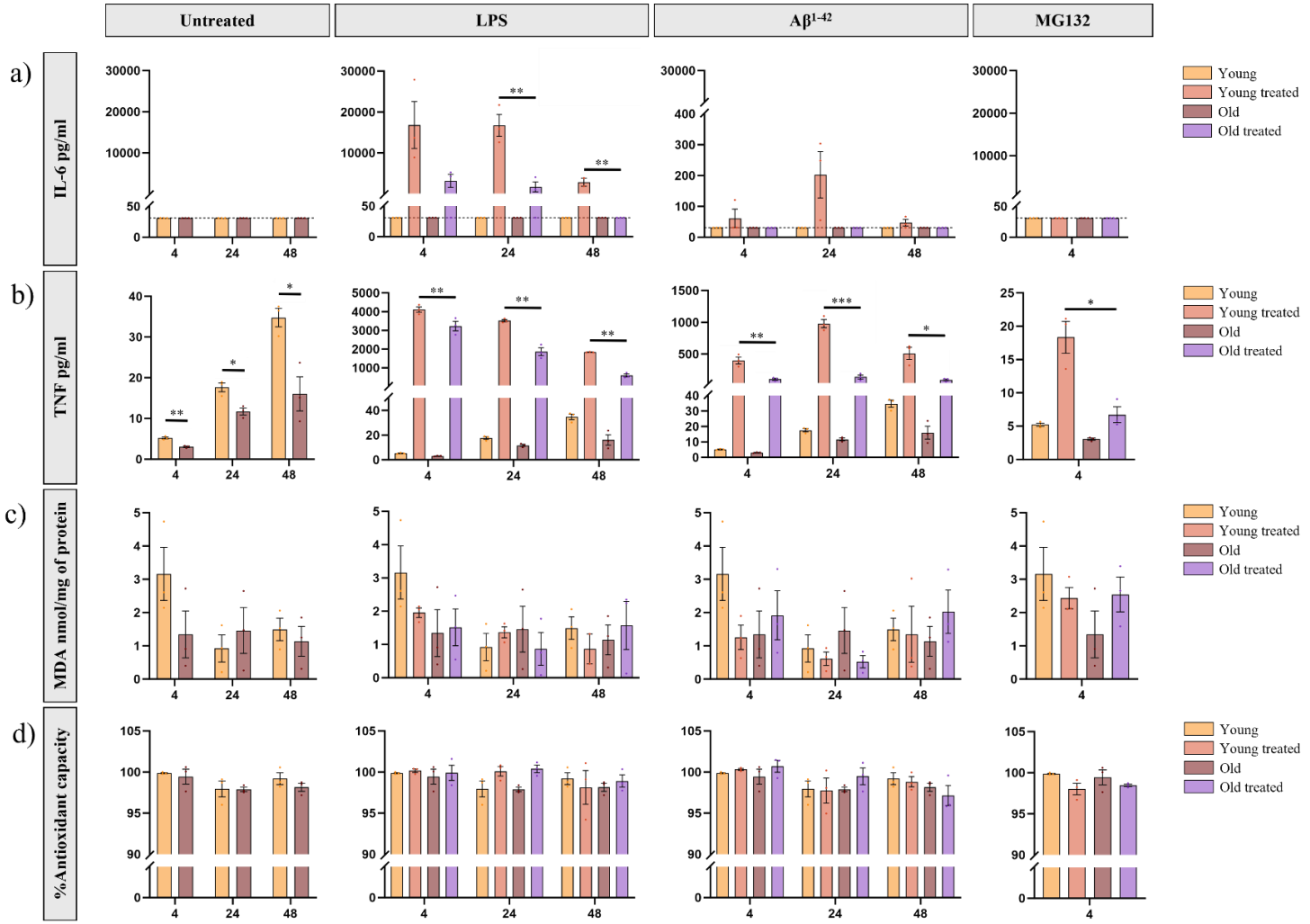


Figure 6.2: Inflammatory profile of BV2 cells. a) IL-6 and b) TNF release by BV2 cells at baseline and following treatment with 50ng/ml LPS or 0.5uM Aβ$^{1-42}$ for 4, 24 or 48 hours; or 5uM MG132 for 4 hours. c) Oxidative stress measured by MDA production in BV2 cells at baseline and following treatment as above. d) Antioxidant capacity of BV2 cells at baseline and following treatment as above. Mean±SEM are plotted and significant effects of age as determined by three-way ANOVA with Tukey post-hoc are shown. * = p<0.05, ** = p<0.01, *** = p<0.001

6.4.6 Caspase-1 Western blot

Caspase-1 is a key component of NLRP3 inflammasome activation in microglia (Song et al., 2017). Levels of caspase-1 in BV2 lysates were analysed by Western blot and representative images can be seen in Figure 6.3 (a-c), with graphical results in Figure 6.3 (d-g). Using Empiria studio, signal of bands at 45kDa were measured and normalised to the housekeeper GAPDH signal. No significant main effect of age was seen by three-way ANOVA *(F(1,29)=2.256, p= 0.143).* Additionally, no significant three way interaction effect of age, treatment and time was seen in caspase-1 activity in BV2 cells *(F(4,29) = 0.320, p=0.862).* However, an effect of treatment was seen *(F(3,29) = 7.864, p=<0.001),* with Tukey post-hoc showing that MG132 treated cells had increased levels of caspase-1 (*112±40.9)* compared to untreated cells *(74.4±27.7, p = 0.048)* (Fig 6.3g), LPS treated cells *(67.2±29.4, p = 0.015)* (Fig 6.3e) and Aβ$^{1-42}$ treated cells *(59.6±20.2, p = 0.002)* (Fig 6.3f).

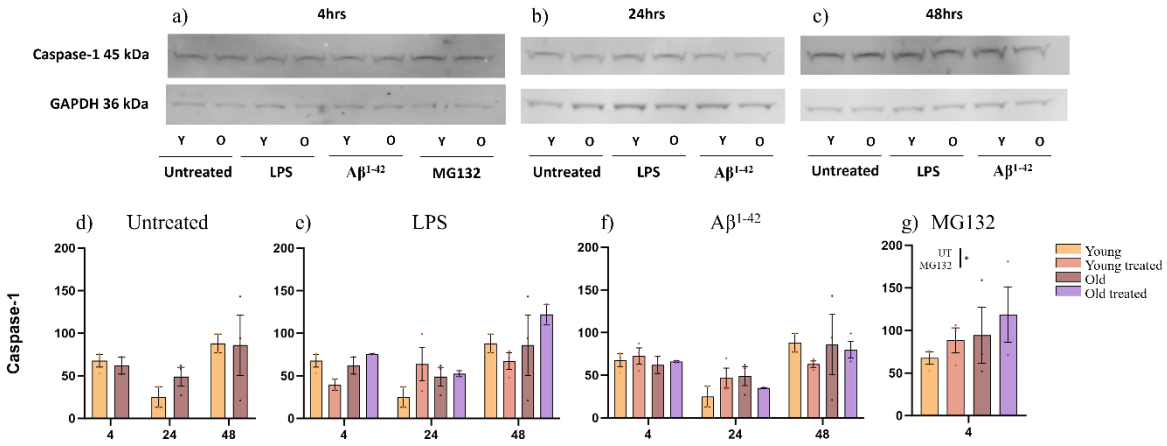


Figure 6.3: Caspase-1 in BV2 cells analysed by Western blot. a-c) representative images of blots from a) 4hr samples, b) 24hr samples, c) 48hr samples. Levels of Caspase-1 in BV2 cells at d) baseline, and following treatment with e) LPS, f) Aβ$^{1-42}$, g) MG132. Mean±SEM are plotted and significant effects of age as determined by three-way ANOVA with Tukey post-hoc are shown. * = p<0.05

6.4.7 K-48 linked ubiquitination

Levels of K48 ubiquitin in BV2 lysates were analysed by Western blot to assess levels of polyubiquitinated proteins marked for degradation by the 26S proteasome and representative images can be seen in Figure 6.4 (a-c), with graphical results in Figure 6.4 (d-g). Using Empiria studio, the entire lane above 37kDa was measured, in order to focus on polyubiquitin chains and to avoid low molecular weight signal which may include higher levels of monoubiquitin chains and free ubiquitin (Seyfried et al., 2008). No significant main effect of age was seen by three-way ANOVA

(F(1,29)=0.784, p= 0.383)., Additionally, no significant three way interaction effect of age, treatment and time was seen in K48 ubiquitination in BV2 cells *(F(4,29) = 0.760, p=0.560)*. However, an effect of treatment was seen *(F(3,29) = 37.012, p=0.0001),* where Tukey post-hoc showed that MG132 treated cells (*270±78.7)* had increased levels of K48 ubiquitin compared to untreated cells *(83.2±26, p = >0.0001)* (Fig 6.4g), LPS treated cells *(62.7±27.6, p = >0.0001)* (Fig 6.4e), and $A\beta^{1-42}$ treated cells *(74±34.5, p = >0.0001)* (Fig 6.4f).

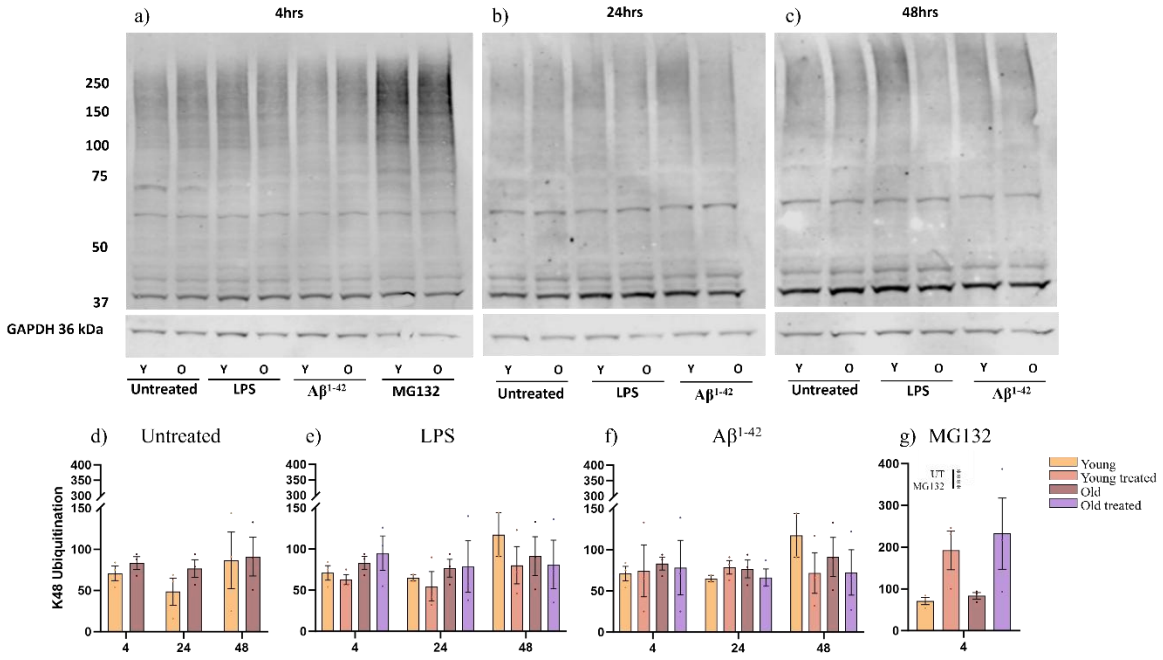


Figure 6.4: K48 linked ubiquitination in BV2 cells analysed by Western blot. a-c) representative images of blots from a) 4hr samples, b) 24hr samples, c) 48hr samples. Levels of K48 ubiquitination in BV2 cells at d) baseline, and following treatment with e) LPS, f) $A\beta^{1-42}$ or g) MG132. Mean±SEM are plotted and significant effects of age as determined by three-way ANOVA with Tukey post-hoc are shown. **** = p<0.0001

6.4.8 Phagocytic capacity

No significant main effect of age was seen by three-way ANOVA *(F(1,40)=2.394, p= 0.129).* Additionally, no significant three way interaction effect of age, treatment and time was seen in phagocytic capacity of BV2 cells *(F(4,40) = 0.629, p=0.644)*. However, an effect of treatment was seen *(F(3,40) = 4.565, p=0.007),* with Tukey post-hoc showing that $A\beta^{1-42}$ treated cells had decreased phagocytic capacity compared to untreated cells *(63.5±67.5 vs 143±96.5, p = 0.009)* (Fig 6.5c).

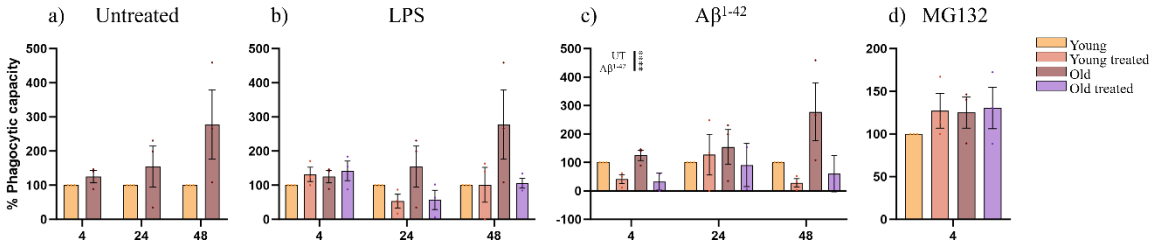


Figure 6.5: Phagocytic activity of BV2 cells analysed by Vybrant Phagocytosis assay. Phagocytic capacity is expressed as a % of the young untreated cells at that timepoint. a) baseline phagocytic capacity of young and old BV2 cells. Phagocytic capacity of BV2 cells following treatment with b) LPS, c) Aβ$^{1-42}$, and d) MG132. Mean±SEM are plotted and significant effects of age as determined by three-way ANOVA with Tukey post-hoc are shown. **** = p<0.0001

6.4.9 BV2 morphology

BV2 cells were seeded to 96-well plates, imaged and analysed for morphological changes at 4-, 24-, and 48-hours following treatment. Figure 6.6 shows representative images of BV2 cells 4-hours following administration of each treatment. Representative images of cells at 24- and 48-hours are shown in Supplementary data S6.2. Analysis of whole cell area, cell roundness, nucleus area and nucleus:cell size ratio was conducted at 20x magnification (Fig 6.7). For improved visualisation, analysis of total number of processes, total process length and number of branches per process were assessed at 40x magnification (Fig 6.8).

Three-way ANOVA detected a main effect of age on cell area *(F(1,224)=225.344, p= <0.0001))* (Fig 6.7a), cell roundness *(F(1,224)=556.891, p= <0.0001))* (Fig 6.7b), nucleus area *(F(1,224)=68.305, p= <0.0001))* (Fig 6.7c), and nucleus:cell ratio *(F(1,224)=320.2, p= <0.0001)* (Fig 6.7d). Tukey post-hoc tests showed that young cells were larger than old cells *(334±46.3 vs 272±33.9, p = <0.0001))* and had larger nuclei than old cells *(122±16.3 vs 108±15.6, p = <0.0001),* but old cells were rounder than young cells *(0.795±0.011 vs 0.770±0.014, p = <0.0001)* and had a bigger nucleus:cell size ratio *(0.395±0.018 vs 0.366±0.016, p = <0.0001).* No main effect of age was seen for number of processes per cell *(F(1,222) = 0.994, p= 0.319),* total process length *(F(1,222) = 0.901, p= 0.343)* or number of branches per process *(F(1,222) = 0.312, p= 0.577).*

A significant three-way interaction was seen in nucleus:cell ratio *(F(6,224) = 2.961, p= 0.008)* (Fig 6.7d). Tukey post-hoc tests revealed that young BV2 cells had a smaller nucleus:cell ratio than old cells at every timepoint in every treatment. Statistical results from this analysis are presented in Table 6.4.

No significant interaction of age, treatment and hours on cell area *(F(6,224) = 0.362, p= 0.902),* cell roundness *(F(6,224) = 0.621, p= 0.713),* nucleus area *(F(6,224) = 0.553, p= 0.767),* number of processes per cell *(F(6,222) = 2.041, p= 0.061)* (Fig 6.8a), total process length *(F(6,222) = 2.062, p= 0.058)* (Fig 6.8b) or number of branches per process *(F(6,222) = 1.926, p= 0.077)* (Fig 6.8c).

Table 6.4: Statistical results from Tukey post-hoc tests following three-way ANOVA of nucleus:cell ratio data.Significance was set at <0.05

	Young mean±SD	***Old mean±SD***	***p-value***
Untreated (4hrs)	*0.382±0.007*	*0.397±0.018*	***0.033***
Untreated (24hrs)	0.388±*0.011*	0.409±*0.012*	***0.002***
Untreated (48hrs)	0.386±*0.009*	0.408±*0.019*	***0.007***
LPS (4hrs)	0.376±*0.007*	0.394±*0.017*	***0.011***
LPS (24hrs)	0.360±*0.007*	0.389±*0.009*	***0.000***
LPS (48hrs)	0.359±*0.017*	0.411±*0.013*	***0.000***
Aβ$^{1-42}$ (4hrs)	0.364±*0.006*	0.386±*0.014*	***0.000***
Aβ$^{1-42}$ (24hrs)	0.363±*0.014*	0.378±*0.007*	***0.010***
Aβ$^{1-42}$ (48hrs)	0.364±*0.011*	0.407±*0.012*	***0.000***
Aβ$^{1-42}$ + LPS (4hrs)	0.380±*0.006*	0.394±*0.016*	***0.037***
Aβ$^{1-42}$ + LPS (24hrs)	0.357±*0.013*	0.369±*0.007*	***0.027***
Aβ$^{1-42}$ + LPS (48hrs)	0.352±*0.017*	0.409±*0.012*	***0.000***
Aβ$^{1-42}$ + MG132 (4hrs)	0.349±*0.009*	0.393±*0.011*	***0.000***
MG132 (4hrs)	0.350±*0.006*	0.379±*0.011*	***0.000***

Additionally, a significant interaction between treatment and age was detected on cell roundness *(F(5,224) = 5.297, p= 0.0001).* Tukey post-hoc test showed that young cells were less round than old cells at baseline *(0.773±0.009 vs 0.796±0.008, p = <0.0001)* and when treated with LPS *(0.761±0.009 vs 0.790±0.009, p = <0.0001),* Aβ$^{1-42}$ *(0.770±0.006 vs 0.798±0.007, p = <0.0001),* MG132 *(0.796±0.002 vs 0.810±0.012, p = 0.003),* Aβ$^{1-42}$ + MG132 *(0.797±0.008 vs 0.808±0.009, p = 0.021),* and Aβ$^{1-42}$ + LPS *(63.5±67.5 vs 143±96.5, p = <0.0001).*

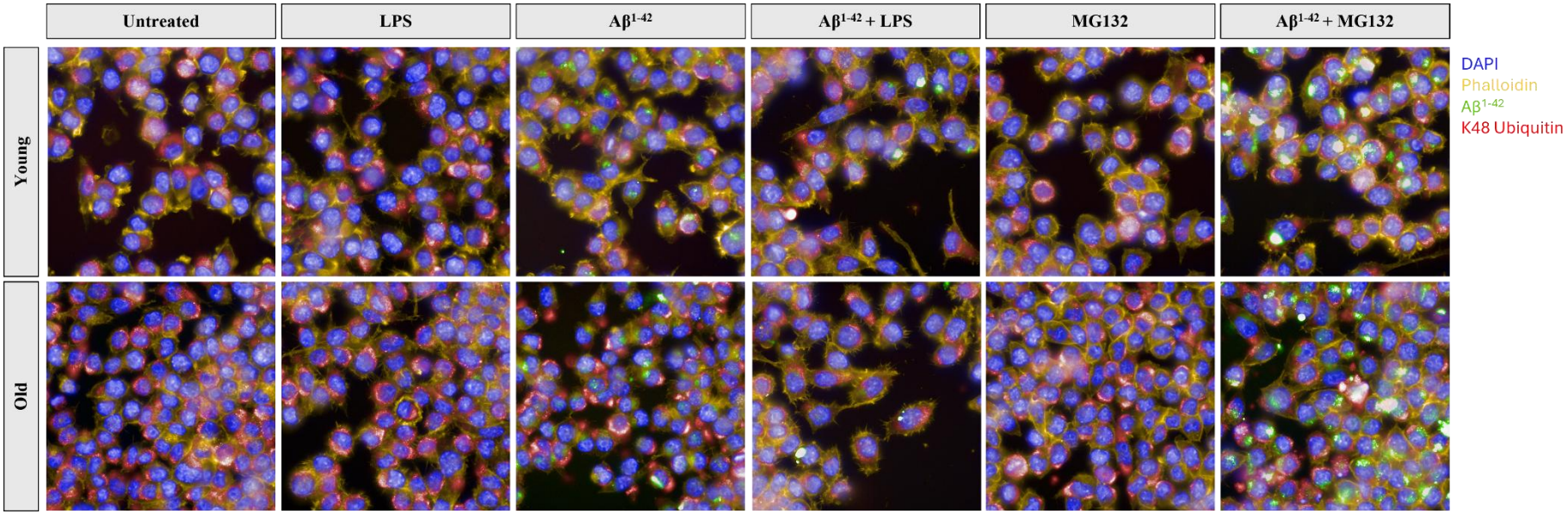


Figure 6.6: Representative images of young and old BV2 cells at 4 hours following treatments. Cells were stained with DAPI (blue), phalloidin (yellow), and anti-K48 ubiquitin (red). FITC tagged $A\beta^{1-42}$ was used to treat cells and can be seen in green. Images were taken at 40x magnification.

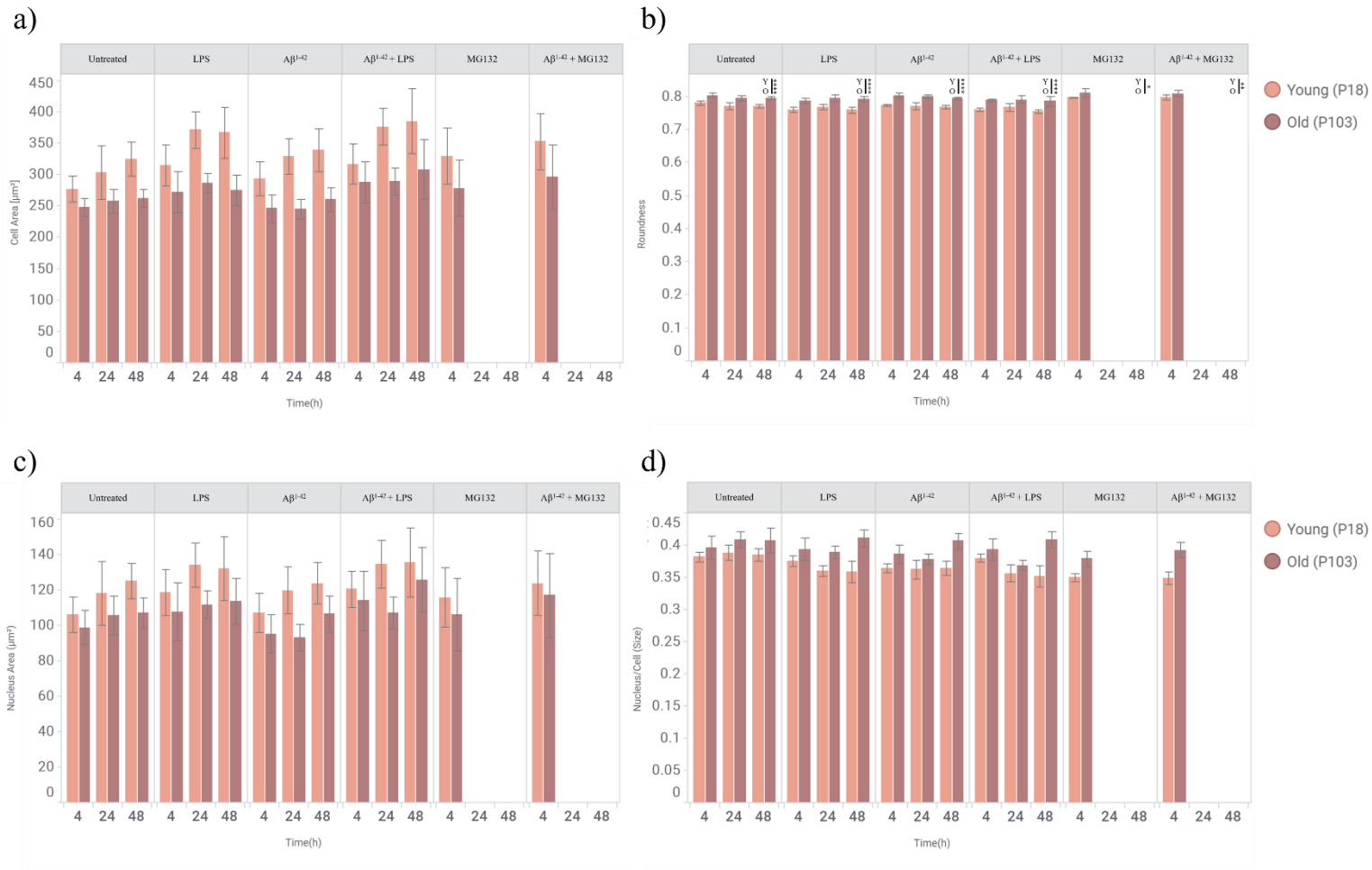


Figure 6.7: Morphological analysis conducted at 20x magnification of BV2 cells 4-, 24-, and 48-hours following treatments. a) total cell area, b) cell roundness, c) nucleus area, and d) nucleus size to cell size ratio are plotted as mean±SD. Significant differences as determined by three-way ANOVA and Tukey post-hoc are shown. * = p<0.05, ** = p<0.01, *** = p<0.001, **** = p<0.0001.

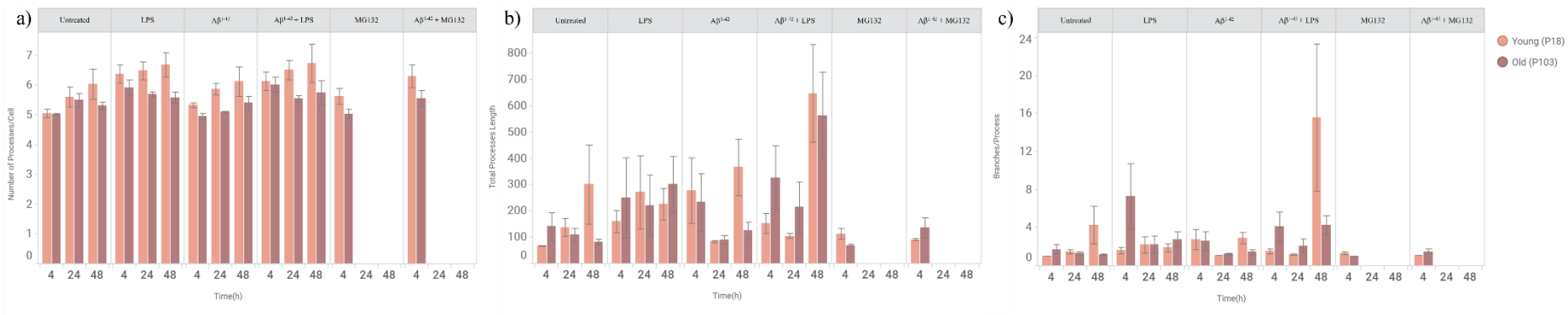


Figure 6.8: Morphological analysis conducted at 40x magnification for adequate visualisation of BV2 processes 4-, 24-, and 48-hours following treatments. a) number of processes, b) total process length per well, c) number of branches per process are plotted as mean±SD. No significant interactions effects were detected by three-way ANOVA.

6.4.10 K48-linked ubiquitination and Aβ$^{1-42}$ uptake

BV2 cells were seeded to 96-well plates, imaged and analysed for K48-linked ubiquitination (Fig 6.9d) and uptake of Aβ$^{1-42}$ (Fig 6.9a) by measuring fluorescence intensity. The number of K48 ubiquitin aggregates (Fig 6.9e) and Aβ$^{1-42}$ aggregates (Fig 6.9b) were assessed by quantifying the number of spots. Ubiquitination of Aβ$^{1-42}$ was assessed by counting the number of Aβ$^{1-42}$ spots within the K48 ubiquitin area (Fig 6.9c).

Three-way ANOVA detected a main effect of age on K48-linked ubiquitin intensity *(F(1,222)=5.663, p= 0.018)* (Fig 6.9d), K48-linked ubiquitin spots *(F(1,222)=25.537, p= <0.0001)* (Fig 6.9e), Aβ$^{1-42}$ spots *(F(1,112)=8.755, p= 0.003)* (Fig 6.9b), and ubiquitinated Aβ$^{1-42}$ *(F(1,224)=320.2, p= <0.0001)* (Fig 6.9c). Tukey post-hoc tests showed that young cells had more K48 ubiquitin signal than old cells *(3105±1018 vs 2813±1009, p = 0.023)* but less K48 ubiquitin aggregates than old cells *(6205±2966 vs 8234±3705, p =<0.0001)*. Additionally, old cells accumulated more Aβ$^{1-42}$ spots than young cells *(2705±2631 vs 1898±1376, p = 0.033)* and more ubiquitinated Aβ$^{1-42}$ spots than young cells *(3733±3257 vs 2698±1884, p =0.030)*.

Further, a significant main effect of treatment was observed in the number of K48 ubiquitin spots*(F(5,222)=4.099, p= 0.001),* Aβ$^{1-42}$ intensity *(F(2,112)=25.022, p= <0.0001)* (Fig 6.9a), the number of Aβ$^{1-42}$ spots *(F(2,112)=46.499, p= <0.0001),* and the number of ubiquitinated Aβ$^{1-42}$ spots *(F(2,112)=29.246, p= <0.0001)*. Tukey post-hoc tests showed that cells treated with Aβ$^{1-42}$ and LPS simultaneously had less K48 ubiquitin spots *(6029±3717)* than untreated cells *(8003±2933, p = 0.037)* and Aβ$^{1-42}$ treated cells *(8410±3871, p = 0.004)*. Additionally, cells treated with Aβ$^{1-42}$ and LPS simultaneously had higher Aβ$^{1-42}$ intensity *(4635±1129)* than cells treated with Aβ$^{1-42}$ and MG132 *(3218±166, p = <0.0001)* and Aβ$^{1-42}$ treated cells *(3962±938, p = 0.001)*, and Aβ$^{1-42}$ treated cells had higher Aβ$^{1-42}$ intensity than cells treated with Aβ$^{1-42}$ and MG132 *(p = 0.014)*. Further, cells treated with Aβ$^{1-42}$ and LPS simultaneously had less Aβ$^{1-42}$ spots *(1355±1101)* than cells treated with Aβ$^{1-42}$ and MG132 *(5366±3424, p = <0.0001)* and Aβ$^{1-42}$ treated cells *(2226±1345, p = 0.024)*, and Aβ$^{1-42}$ treated cells had less Aβ$^{1-42}$ spots than cells treated with Aβ$^{1-42}$ and MG132 *(p = <0.0001)*. Finally, cells treated with Aβ$^{1-42}$ and MG132 simultaneously had more ubiquitinated Aβ$^{1-42}$ spots *(6481±3933)* than cells

treated with $A\beta^{1-42}$ and LPS *(2097±1560, p = <0.0001)* and $A\beta^{1-42}$ treated cells *(3246±2214, p = <0.0001)*, and $A\beta^{1-42}$ treated cells had more ubiquitinated $A\beta^{1-42}$ spots than cells treated with $A\beta^{1-42}$ and LPS *(p = 0.028).*

No significant interactions of age, treatment and time were detected by three-way ANOVA when analysing $A\beta^{1-42}$ intensity*(F(2,112) = 0.738, p= 0.480),* K48 ubiquitin intensity *(F(6,222) = 0.899, p= 0.496),* number of $A\beta^{1-42}$ spots *(F(2,112) = 0.367, p= 0.693),* number of K48 ubiquitin spots *(F(6,222) = 0.742, p= 0.616),* or ubiquitinated $A\beta^{1-42}$ spots *(F(2,112) = 0.384, p= 0.682)*. Significant interactions of age and treatment were, however, detected in the number of K48 spots *(F(5,222) = 2.577, p= 0.023),* the number of $A\beta^{1-42}$ spots *(F(2,112) = 8.025, p= <0.001)* and the amount of ubiquitinated $A\beta^{1-42}$ *(F(2,112) = 4.855, p= 0.009).* Tukey post-hoc tests showed that old BV2 cells had higher levels of K48 ubiquitin aggregates than young cells following treatment both with $A\beta^{1-42}$ *(10609±3525 vs 6211±2483, p = <0.0001)* and with MG132 *(8863±3158 vs 5277±1879, p = 0.009)*. Additionally, old cells had more $A\beta^{1-42}$ aggregates than young cells *(2772±1500vs 1680±905, p = 0.002)* and more ubiquitination of $A\beta^{1-42}$ aggregates *(4043±2487 vs 2449±1577, p = 0.006)* following treatment with $A\beta^{1-42}$.

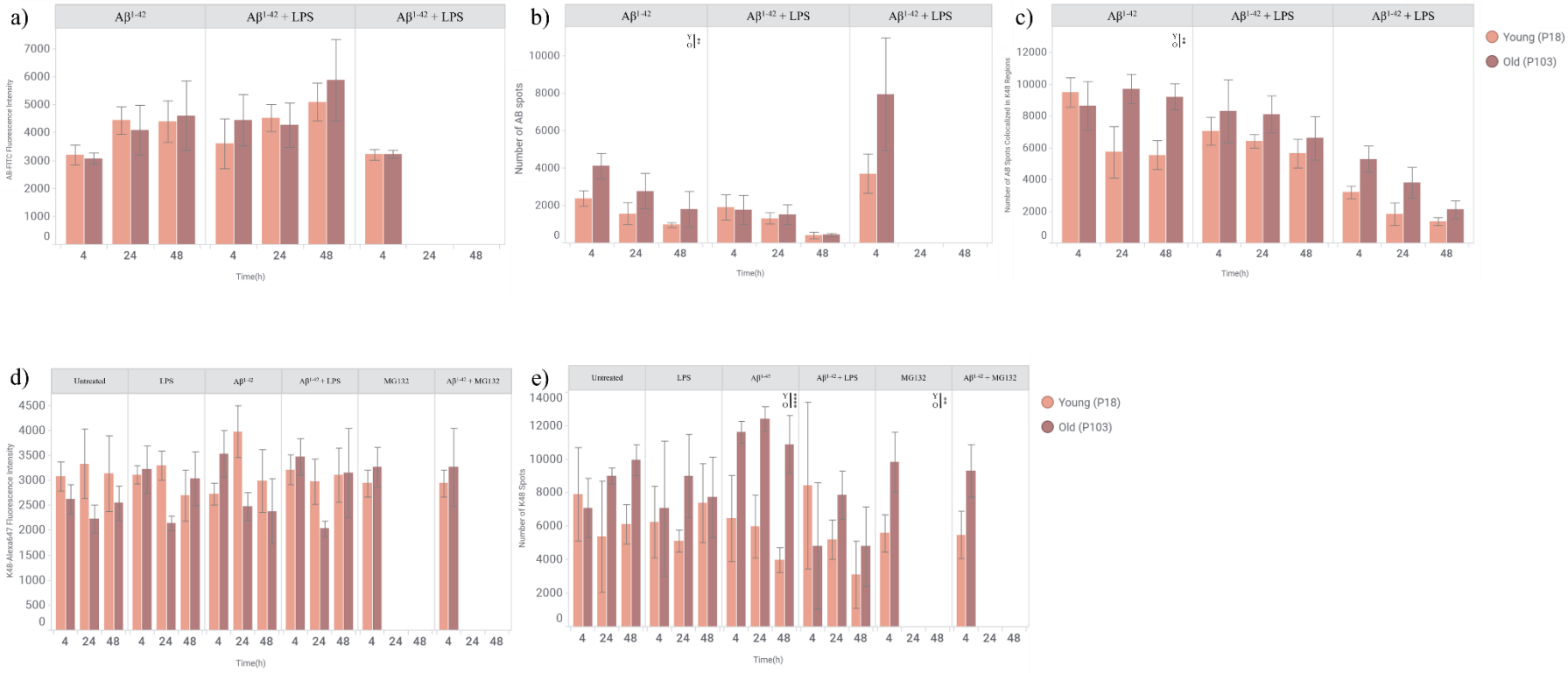


Figure 6.9: Image analysis conducted at 20x magnification of BV2 cells 4-, 24-, and 48-hours following treatments. a) Intensity of FITC tagged $A\beta^{1-42}$, b) number of $A\beta^{1-42}$ spots, c) the number of $A\beta^{1-42}$ spots colocalised with K48 ubiquitin, d) intensity of K48 ubiquitin and e) number of K48 ubiquitin spots are plotted as mean±SD. Significant effects of age and treatment as determined by three-way ANOVA and Tukey post-hoc are shown. ** = p<0.01, **** = p<0.0001.

Table 6.5: Summary of changes in high passage BV2 cells compared to low passage BV2 cells in each marker assessed in the current study

	Baseline	50ng/ml LPS	0.5µM Aβ1-42	5µM MG132	0.5µM Aβ1-42 + 50ng/ml LPS	0.5µM Aβ1-42 + 5µM MG132
Growth rate	↑	N/A	N/A	N/A	N/A	N/A
Metabolic activity	-	-	-	-	N/A	N/A
Il-6 release		↓ release at 24- and 48-hours			N/A	N/A
TNF release	↓ release at all timepoints	↓ release at all timepoints	↓ release at all timepoints	↓ release at all timepoints	N/A	N/A
Oxidative stress	-	-	-	-	N/A	N/A
Antioxidant capacity	-	-	-	-	N/A	N/A
Phagocytosis	-	-	-	-	N/A	N/A
Caspase-1	-	-	-	-	N/A	N/A
K48-ubiquitination (WB)	-	-	-	-	N/A	N/A
K48-ubiquitination (Imaging)	-	-	↑ number of aggregates	↑ number of aggregates	-	-
Aβ1-42 uptake	N/A	N/A	↑ number of aggregates and number of ubiquitinated aggregates	-	-	-
Cell area	-	-	-	-	-	-

Cell roundness	↑	↑	↑	↑	↑	↑
Nucleus area	-	-	-	-	-	-
Nucleus:cell ratio	↑ at all timepoints	↑ at all timepoints	↑ at all timepoints	↑ at all timepoints	↑ at all timepoints	↑ at all timepoints
Number processes	-	-	-	-	-	-
Process length	-	-	-	-	-	-
Number of branches	-	-	-	-	-	-

1

6.5 Discussion

The current study presents, to our knowledge, the first evaluation of phenotypic changes in the microglial-like BV2 line with increased number of passages (from 7 to >90 passages). Here, we demonstrate that BV2 cells show increased growth rate, decreased cytokine responses and alterations in protein homeostasis and cell morphology (namely, increases in cell roundness and nucleus:cell size ratio) with increasing passage. Critically, while high passage BV2 cells did not display an overall aged phenotype, they did nevertheless capture the characteristic dysregulated protein degradation seen with microglial ageing. It has been estimated that the microglial population undergoes renewal at a rate of ~28% per year (Réu et al., 2017), equating to around 20 cycles of renewal over an 80-year lifespan. Comparatively, 90 passages in culture represents significantly more divisions than would occur in the human brain. However, the aim of the current study was to establish a method for ageing immortalised cells which are expected to have a greater replicative capacity than their non-immortalised counterparts.

A key regulator of proteostasis is the ubiquitin proteasome pathway (UPP) (Jansen et al., 2014) and while proteins can also be degraded by lysosomal proteolysis (Shang and Taylor, 2011), the UPP is the main pathway by which proteins are degraded in microglia. With increased age, there is a decrease in the efficiency of protein degradation within the UPP (Vernace et al., 2007) and an increase in the presence of polyubiquitin chains (Davidson and Pickering, 2023), which can lead to an accumulation of intracellular proteins and cause disrupted cellular functioning. In the present study, K48-linked ubiquitination, specific to degradation by the 26S proteasome (Grice and Nathan, 2016) which is a major component of the UPP (Türker et al., 2021), was used as a measure of intracellular proteostasis in BV2 cells and investigated using two different techniques, Western blot and fluorescence microscopy. Of note, the fluorophore FITC was utilised in cell treatments which exhibits reduced emission under acidic conditions. However, the presence of phenol red as a pH indicator allowed visual monitoring of pH stability where media retained a red coloration (indicating a pH of ~7.4), indicating that fluorescence was unlikely to be significantly affected by pH fluctuations. When the proteasome was inhibited by MG132 administration, as expected, BV2 cells showed heightened levels of ubiquitin protein. However, this did not differ between “young” and “old” cells. Additionally, the presence of

$A\beta^{1-42}$ did not cause changes in ubiquitination from baseline, indicating that the decrease in phagocytic capacity observed in response to $A\beta^{1-42}$ was not a result of alterations in ubiquitination within these cells but instead potentially a result of dysfunctional lysosomal degradation pathways which are also known to be impaired in AD (Zhang et al., 2022). In contrast, when investigating ubiquitin at a single cell level using fluorescence microscopy, image analysis demonstrated an increase in the number of ubiquitin aggregates in "old" BV2 cells compared to "young" cells following both $A\beta^{1-42}$ and MG132 treatment. This point of difference is likely to be due to the ability of image analysis to detect specifically aggregated ubiquitin as opposed to quantification of total amount of ubiquitin using Western blot (Mortati et al., 2022). Previous studies suggest that with age the ubiquitination of certain proteins in the brain increases, such as with ferroportin-1, a protein supporting iron transport, which has been shown to be highly polyubiquitinated in the cortex of 22-month-old female UM-HET3 mice compared to mice at 4 months old (Sato et al., 2022). However, limited studies have looked at overall ubiquitination in the brain with regard to overall protein control mechanisms with age and to our knowledge no study has investigated changes with ubiquitination in microglia with age. Thus, this study demonstrated that while Western blot is the most common way to assess ubiquitination in samples, it may not be sensitive enough to detect changes in total ubiquitination in microglia. Interestingly, microscopy analysis also did not detect any changes in overall levels of ubiquitin, indicating that how proteins are ubiquitinated (mono- or poly-ubiquitination) and if the ubiquitin aggregates is altered in microglia with age, rather than the overall amount of ubiquitin. Additionally, while age-related changes in ubiquitination have not been specifically investigated in microglia previously, it has been suggested that polyubiquitination of proteins *via* K48-linked ubiquitin chain in glial cells overall is higher than in neurons. Further, this difference has been proposed to be key in the aggregation of pathological proteins in NDs (Tydlacka et al., 2008).

Providing support for this idea, in the current study, "old" BV2 cells accumulated more ubiquitinated $A\beta^{1-42}$ aggregates than young cells, suggesting that the accumulation of pathological proteins within these high passage cells may be due not to impaired ubiquitination, but rather reduced function of the 26S proteasome itself to degrade polyubiquitinated proteins. During ageing, decreased proteasomal

capacity is known to occur in microglia. For example, proteasomal subunits PSMB4, PSMA6, and PSMC1 have been found to be downregulated in microglia isolated from 20- to 24-month-old mice compared to cells isolated from 3- to 5-month-old mice (Flowers et al., 2017). Thus, high passage (i.e. "aged") BV2 cells do appear to display this specific element of microglial ageing, which suggests that this may be an appropriate model system for studying alterations in protein degradation with age and in NDs, as well as for screening therapeutic strategies targeting proteasome function. Interestingly, BV2 cells treated with $A\beta^{1-42}$ and LPS simultaneously did not show any changes in ubiquitination of $A\beta^{1-42}$, nor did cells treated with $A\beta^{1-42}$ and MG132. The pro-inflammatory effects of LPS may have a beneficial effect on the ability of BV2 cells to degrade ubiquitinated $A\beta^{1-42}$, as previous studies have demonstrated that activation of microglia in culture enhances the activity of alternative proteolytic pathways. RAW264.7 cells when treated with 100ng/ml of LPS had enhanced expression of autophagosomes, indicating an increase in LPS induced autophagy (Xu et al., 2007). Similarly, inhibition of the proteasome by MG132 is known to activate the unfolded protein response (UPR) and redirect ubiquitinated proteins toward autophagic pathways to maintain viability and function (Hetz, 2012). While treatment with MG132 inhibited proteasomal degradation of ubiquitinated $A\beta^{1-42}$, no effect of age was seen on BV2 accumulation of these proteins, suggesting that the UPR is unaffected by passage. Together, these results suggest an overall difference in how proteins are ubiquitinated and degraded in high passage BV2 cells which represents a potentially viable method to model age-related dysfunctional proteostasis in cultured microglia.

In addition to changes in microglial function noted above, the morphology of BV2 cells was altered with increased passage number in the current study. With age, microglia are known to take on a dystrophic phenotype characterised by an enlarged cell body and fragmented or swollen processes (Neumann et al., 2023). Here, "old" BV2 cells had a significantly increased nucleus:cell size ratio compared to "young" cells at all timepoints and across all conditions, although the magnitude of this change was small. Additionally, "old" BV2 cells were overall rounder than "young" BV2 cells. Together, this suggests a slight shift towards an amoeboid shape, which is more reminiscent of activated microglia than the dystrophic morphology characteristic of aged microglia. However, it is important to

note that the activated microglial morphology also features an increase in cell size (Parakalan et al., 2012) and no changes in cell size were observed here between groups. In fact, "young" cells appeared to have larger overall cell and nucleus size than "old" cells, although this did not reach statistical significance. This may be due, at least in part, to changes in process dynamics, with "young" cells exhibiting a pattern of increased process number, length and branching compared to "old" cells, although this also did not reach statistical significance. Similarly, it must be acknowledged that the typical resting morphology of BV2 cells is different to that of microglia seen *in vivo.* In tissue, microglia at rest are highly ramified and motile, switching to an amoeboid phagocytic shape when activated (Reddaway et al., 2023). However, BV2 cells typically display an elongated morphology at rest and are constantly undergoing replication in culture (Sarkar et al., 2018), meaning that rather than an indicator of activation, an increase in amoeboid BV2 cells may instead represent actively dividing cells. In line with this, a significantly increased growth rate was observed in high passage BV2 cells, supporting the idea that there is likely a higher number of dividing cells in these samples.

However, while high passage BV2 morphology corresponds to potentially phagocytic cells, in the current study, the phagocytic capacity of BV2 cells was decreased in response to administration of $A\beta^{1-42}$ but no changes with age were seen. This decrease in the presence of pathology is in line with a previous study which reported that administration of 50μM of $A\beta^{1-42}$ impaired the phagocytic ability of microglia isolated from 6-month-old C57BL/6 mice (Floden and Combs, 2011).However, the lack of changes with age in the current study contrasts with previous literature which has shown that the phagocytic capacity of microglia increases with physiological ageing (Koellhoffer et al., 2017). This is likely due to the immortalisation of BV2 cells where the continuous division may sustain cellular processes such as phagocytosis. This has previously been observed in the RAW264.7 macrophage cell line where the phagocytic abilities of RAW cells between passages 10-30 was variable however no changes were observed at passage 50 compared to passage 5 cells, indicating that beyond passage 30, these cells stabilise and maintain their phagocytic abilities (Taciak et al., 2018).

Another surprising result was the significant decrease in pro-inflammatory cytokine production observed in response to stimulation with increased passage number in BV2 cells. The SASP is one of

the most commonly assessed elements of senescence and is particularly well characterised in microglia, as they are responsible for the initiation of inflammatory responses in the CNS (Greenwood and Brown, 2021). The SASP is characterised by an increased production and release of pro-inflammatory factors, including cytokines and chemokines, both during resting state and following an immune challenge (Rim et al., 2024). When pro-inflammatory cytokines were investigated in p7.2*fms*-EGFP mice on a C57Bl6/6X CBA background, a transgenic model causing GFP expression in microglia/macrophages (Sasmono et al., 2003), microglia from 18-month-old mice showed an increase in mRNA expression of TNF, IL-1β and Il-6 compared to microglia from 2-month-old mice at baseline (Sierra et al., 2007). Expression of these cytokines was further increased in mice which had been exposed to 1mg/kg of LPS by intraperitoneal injection 3-hours prior to sacrifice (Sierra et al., 2007). In contrast, here, the levels of TNF released by "old" cells at baseline were significantly lower than in "young" cells at all timepoints assessed, with no difference observed between groups for IL-6.

Additionally, in aged microglia, there is a decreased ability to resolve the immune response following activation by neurotrauma (Norden et al., 2015). For example, in the hippocampus of male C57BL/6 mice at 24-months-old, markers of microglial activation, measured by mRNA expression of CD11b and IBA1, remained elevated compared to levels in mice at 5- to 6-months-old at 3-, 7-, 14-, and 28-days following controlled cortical impact (Sandhir et al., 2008). Further, following intracerebral haemorrhage induced by collagenase injection to the striatum, the microglial response in male Sprague-Dawley rats at 22-months-old was prolonged compared to 3- to 4-month-old rats following injury (Wasserman et al., 2008). Here, however, "old" BV2 cells exhibited a dampened IL-6 response to LPS administration compared to "young" cells at both the 24- and 48-hour timepoints, with no detectable IL-6 release in response to $A\beta^{1-42}$ administration. Similar differences were observed in TNF release following both LPS and $A\beta^{1-42}$ administration, with "young" cells displaying a more robust response than "old" cells at all timepoints. Notably, while no differences were seen between groups over time in response to LPS stimulation, "old" BV2 cells showed similar levels of TNF release across all timepoints in response to $A\beta^{1-42}$. This is in contrast to "young" cells, where a declining pattern of release was seen

at 48-hours compared to 24-hours, which may suggest that high passage BV2 cells have a dampened TNF response, but a decreased ability to resolve this response.

While at first surprising, these results are nevertheless in line with several previous studies, which have also demonstrated decreased cytokine production in microglia isolated from aged mice suggesting that dysregulated microglial cytokine production is a feature of aged microglia. For example, microglia isolated from aged (24-months old) BALB/c mice treated with LPS (dose not provided) demonstrated a decreased IL-6 response compared to microglia isolated from both 3- to 6-month-old and 7-day-old mice (Ye and Johnson, 1999). This response has also been observed in peripheral macrophages isolated from aged (22- to 24-month-old) and adult (3- to 4-month-old) BALB/c and C57Bl/6J mice, with aged macrophages displaying a 3-fold lower release of TNF and IL-6 in response to a single dose of 1µg/ml of LPS in culture (Chelvarajan et al., 2005). Similar results have also been reported in response to $A\beta^{1-42}$ stimulation. In line with this, when microglia isolated from 1- to 2-day-old mice aged for 16 days in culture (i.e. "aged" microglia), they exhibited lower levels of mRNA expression of TNF and IL-6 at both baseline and in response to 24-hour incubation with 1000nM $A\beta^{1-42}$, along with decreased expression of TLR4 and TLR2 (Caldeira et al., 2017). Interestingly, within that study, there were varying differences in the expression of NLRP3 inflammasome components with age. "Aged" microglia demonstrated decreased IL-1β expression compared to non-aged microglia, but "aged" cells were still able to express IL-1β mRNA in response to $A\beta^{1-42}$ administration however to a lesser extent than non-aged cells. Further, IL-18 and NLRP3 were expressed at lower levels in "aged" microglia compared to non-aged microglia and both markers were not expressed following $A\beta^{1-42}$ administration in "aged" cells. This study demonstrates limited capacity of high passage microglia to activate the NLRP3 inflammasome following an inflammatory stimulus with minimal expression of these components at baseline compared to young cells. Conversely, our Western blot results, showed no changes in protein levels of caspase-1, which is a key initiator of NLRP3 activation (Song et al., 2017), however mRNA levels were not assessed in the current study which limits the ability to compare results to other studies as mRNA expression does not always correlate with protein or cytokine production (Shebl et al., 2010). Such discrepancies in the literature highlight the need for consistencies in cytokine assessment across

studies, as previous references describing the SASP in aged microglia above also utilise mRNA expression of pro-inflammatory markers to assess microglial activation in tissue samples (Sandhir et al., 2008; Sierra et al., 2007). In order to adequately compare results, a combination of mRNA and cytokine/protein expression should be undertaken to fully capture the changes seen in these studies (Shebl et al., 2010). The reliance on mRNA expression in *in vivo* studies is likely due to the fact that analysis of cytokine levels in tissue is not specific to microglia and thus limits the inferences that can be made based on these results. These results should in future be paired together in order to understand the contribution of microglia to levels of released cytokines (Shebl et al., 2010). Thus, additional studies focused on characterisation of the inflammatory response of aged microglia using this approach are needed in order to better understand results obtained *in vitro* through measurement of directly released cytokines, relative to those from pre-clinical *in vivo* models, where analysis of mRNA is the primary method of cytokine analysis.

Interestingly, although changes in inflammatory cytokine release were observed in "old" BV2 cells, indicating an activated pro-inflammatory state, no concomitant changes in either oxidative stress response or antioxidant capacity were detected. This is surprising, as microglia are known to release ROS upon activation, leading to increased oxidative stress (Gu et al., 2011). Microglial activation during ageing is typically associated with increased levels of ROS rather than other less harmful antioxidants (Gu et al., 2011). This has been previously demonstrated in microglia isolated from C57BL/6 mice at 12-months-old that had been exposed to 0.5mg/kg of LPS *via* intraperitoneal injection (Gu et al., 2011). This study demonstrated that, following further stimulation by 1 µg/ml of LPS in culture, microglia isolated from aged animals (12-months-old) produced higher levels of ROS rather than NO whereas in microglia from young animals (2-months-old) produced a NO response over ROS (Gu et al., 2011). Therefore, in the current study, it was expected that old cells would display higher levels of oxidative stress and have less antioxidant capacity, due to the lower levels of NO release, than young cells. However, this was not the case; in fact, despite this previous literature (Fang et al., 2022), no induction of oxidative stress was seen in the current study. The assay utilised here measures MDA, a product generated following lipid peroxidation which also occurs at baseline as cells are constantly

generating ROS under homeostatic conditions (Smith et al., 2022). The levels of MDA in samples from the current study remained unchanged and were below the limit of detection of the assay (4µg/well) however the assay plates demonstrated a colour change between samples, indicating the presence of MDA in sample wells, particularly in $A\beta^{1-42}$ at 24-hours. Images of plates can be found in Supplementary Figure S6.5. Nevertheless, increased ROS have been demonstrated previously in BV2 microglia following 1hr incubation with 100ng/ml LPS (Kim et al., 2019) which indicates that a higher dose may have been needed to see profound effects of LPS on ROS generation and downstream oxidative stress compared to baseline. Overall, the lack of detection of oxidative stress or antioxidant capacity suggests that much like phagocytosis, these functions remain stable across passage and potentially BV2 cells require a longer timepoint and/or higher dose to induce detectable levels of oxidative stress following inflammatory treatment.

The current study additionally tracked the growth rate of BV2 cells across the passage range to assess whether these cells showed any indication of a decline in replicative capacity with passage. Contrary to our expectations, the growth rate of BV2 cells did not decline, but instead increased with passage number. Further, no changes in metabolic activity were observed in high passage cells either at baseline or following treatment with LPS, $A\beta^{1-42}$ or MG132. The lack of decline in replicative capacity and metabolism is likely due to the stable cell cycle resulting from the immortalisation process of BV2 cells, induced using a v-*raf/v-myc* oncogene carrying retrovirus (Blasi et al., 1990). The use of the *v-myc* oncogene causes immortalisation by inactivating cell cycle regulators and tumour suppressors, including p16, p21 and p53, thus enabling cells to divide indefinitely (de Bardet et al., 2023). These cell cycle regulators are often used as markers of senescent cells however the and the inactivation of these markers allows cells to proliferate indefinitely. Without these key regulators of the cell cycle the integrity of critical checkpoints is compromised, resulting in greater genomic instability with increasing passage (Liu et al., 2014). In fact, the loss of p53 and p21 has been linked with increase proliferation in the human colon carcinoma cell line, HCT116, where the absence of p53 and p21 in mutant cells caused increases in proliferation measured by Ki67 activity (Uxa et al., 2021), which could provide an explanation for the increase in growth rate observed in the current study.

Currently, due to the phenotypic changes occurring in immortalised cells, the recommended limit for use of cell lines is around 20 passages (Weiskirchen et al., 2023). Given that BV2 cells are largely utilised in studies of inflammatory responses in the brain (Stansley et al., 2012), it is important to keep this limit in mind when utilising this cell line, as increasing passage appears to have a significant impact on BV2 cytokine responses. Further, the results of the current study demonstrate that, overall, multiple passages do not induce a universal aged phenotype in BV2 cells. Nevertheless, there were some advantages associated with the current model. Specifically, high passage BV2 cells appeared to replicate the dysregulated proteostasis seen in ageing, which may be beneficial when studying the effect of pathological proteins on microglia in age-related NDs. The use of immortalised cell lines, such as BV2 cells, also demonstrate advantages over primary cells in regard to workflow and feasibility for long term experiments. Thus, it is worthwhile to explore if these cells can be altered to make them a more suitable model of ageing. In line with this, a previous study used repeated LPS exposure (10ng/ml of LPS for 4-hours either 3 times at 48-hour intervals or 6 times at 24-hour intervals) to induce inflammatory ageing in BV2 cells based on the idea of microglial priming (Yu et al., 2012). This resulted in the induction of several markers of senescence, including increased senescence associated heterochromatin foci, increased SA-β-Gal, and increased expression of p53.

Further study of methods to induce ageing in immortalised cells should be investigated, potentially by the creation of stable aged cell lines that can be easily utilised without the need for continual passage or administration of inflammatory agents to induce ageing. As an example, a stable BV2 cell line overexpressing hypoxia-inducible factor 1-α (Hif1α), a transcription factor associated with increased phagocytosis that is increased in aged microglia, has been previously created (Grubman et al., 2021). The role of Hif1α in microglial Aβ phagocytosis was then explored using this cell line, where Hif1α activity in mutant BV2 cells corresponded to increased phagocytic activity (Grubman et al., 2021). While this presents a promising start to study the effects of ageing on microglial phagocytosis, the identification of genes which potentially drive an aged phenotype in microglia would greatly contribute to the development of a stable *in vitro* model of aged microglia. However, prior to this a fundamental

understanding of what changes are present in physiologically aged microglia would greatly benefit the ability of researchers to validate these *in vitro* models.

6.6 Conclusions

Adequately replicating the aged brain in *in vitro* studies of NDs is critical in improving the translatability of results into an aged environment. Complex *in vitro* models of the CNS are still in early stages of development and, until they are available for widespread use, it is important that we utilise and make the most of the tools that we have, which are likely to translate well across research groups. The present study investigated whether multiple passages of a microglial cell line were able to recapitulate features of ageing in microglia. The changes in proteostasis in BV2 cells at high passage observed here are akin to changes seen in this pathway during ageing and in NDs. However, the inflammatory changes observed were in opposition to the increase in inflammatory cytokine release which typically occurs during microglial ageing (although not all previous literature is in agreement). Thus, while the model of BV2 ageing presented here represents a valuable method to investigate age-related protein dysregulation in relation to NDs, it may have limited utility outside of this purpose. Instead, alternative methods to induce ageing in this cell line should be further investigated. Taken together the results of the current study provide a foundation for understanding how cell lines can model aspects of ageing and how this may be used to explore specific elements of aged microglia, namely dysregulated proteostasis, in BV2 cells. By utilising the unique attributes of BV2 cells, the current study highlights the usefulness of immortalised cell lines more broadly in ND and particularly in ageing research which should continue to be explored.

6.7 References

Abdul-Hamid, N.A., Abas, F., Maulidiani, M., Ismail, I.S., Tham, C.L., Swarup, S., Umashankar, S., 2019. NMR metabolomics for evaluating passage number and harvesting effects on mammalian cell metabolome. Analytical Biochemistry 576, 20-32.

Aversano, S., Caiazza, C., Caiazzo, M., 2022. Induced pluripotent stem cell-derived and directly reprogrammed neurons to study neurodegenerative diseases: The impact of aging signatures. Frontiers in Aging Neuroscience 14.

Beijer, H.J., de Blaey, C.J., 2002. Hospitalisations caused by adverse drug reactions (ADR): a meta-analysis of observational studies. Pharm World Sci 24, 46-54.

Benda, P., Lightbody, J., Sato, G., Levine, L., Sweet, W., 1968. Differentiated Rat Glial Cell Strain in Tissue Culture. Science 161, 370-371.

Biedler, J.L., Roffler-Tarlov, S., Schachner, M., Freedman, L.S., 1978. Multiple neurotransmitter synthesis by human neuroblastoma cell lines and clones. Cancer Res 38, 3751-3757.

Blasi, E., Barluzzi, R., Bocchini, V., Mazzolla, R., Bistoni, F., 1990. Immortalization of murine microglial cells by a v-raf / v-myc carrying retrovirus. Journal of Neuroimmunology 27, 229-237.

Budamagunta, V., Manohar-Sindhu, S., Yang, Y., He, Y., Traktuev, D.O., Foster, T.C., Zhou, D., Senescence-associated hyper-activation to inflammatory stimuli in vitro. Aging (Albany NY) 13, 19088-19107.

Bunc, M., Hanning, S., Prieto, J., Kristl, J., Orlu, M., 2019. Characterisation of an in vitro aged cell culture model. Farmacia 67.

Caldeira, C., Cunha, C., Vaz, A.R., Falcão, A.S., Barateiro, A., Seixas, E., Fernandes, A., Brites, D., 2017. Key Aging-Associated Alterations in Primary Microglia Response to Beta-Amyloid Stimulation. Front Aging Neurosci 9, 277.

Carr, L.M., Mustafa, S., Care, A., Collins-Praino, L.E., 2024. More than a number: Incorporating the aged phenotype to improve in vitro and in vivo modeling of neurodegenerative disease. Brain, Behavior, and Immunity 119, 554-571.

Cetin, S., Knez, D., Gobec, S., Kos, J., Pišlar, A., 2022. Cell models for Alzheimer's and Parkinson's disease: At the interface of biology and drug discovery. Biomedicine & Pharmacotherapy 149, 112924.

Chalak, M., Hesaraki, M., Mirbahari, S.N., Yeganeh, M., Abdi, S., Rajabi, S., Hemmatzadeh, F., 2024. Cell Immortality: In Vitro Effective Techniques to Achieve and Investigate Its Applications and Challenges. Life.

Chelvarajan, R.L., Collins, S.M., Van Willigen, J.M., Bondada, S., 2005. The unresponsiveness of aged mice to polysaccharide antigens is a result of a defect in macrophage function. Journal of Leukocyte Biology 77, 503-512.

Cohen, J., Torres, C., 2019. Astrocyte senescence: Evidence and significance. Aging Cell 18, e12937.

Coppé, J.-P., Patil, C.K., Rodier, F., Sun, Y., Muñoz, D.P., Goldstein, J., Nelson, P.S., Desprez, P.-Y., Campisi, J., 2008. Senescence-Associated Secretory Phenotypes Reveal Cell-Nonautonomous Functions of Oncogenic RAS and the p53 Tumor Suppressor. PLOS Biology 6, e301.

D'Souza, A.J., Desai, S.D., Rudner, X.L., Kelly, M.N., Ruan, S., Shellito, J.E., 2013. Suppression of the Macrophage Proteasome by Ethanol Impairs MHC Class I Antigen Processing and Presentation. PLOS ONE 8, e56890.

Dalgaard, P., 2010. R Development Core Team (2010): R: A language and environment for statistical computing.

Davidson, K., Pickering, A.M., 2023. The proteasome: A key modulator of nervous system function, brain aging, and neurodegenerative disease. Front Cell Dev Biol 11, 1124907.

de Bardet, J.C., Cardentey, C.R., González, B.L., Patrone, D., Mulet, I.L., Siniscalco, D., Robinson-Agramonte, M.L.A., 2023. Cell Immortalization: In Vivo Molecular Bases and In Vitro Techniques for Obtention. BioTech (Basel) 12.

Del Rio, D., Stewart, A.J., Pellegrini, N., 2005. A review of recent studies on malondialdehyde as toxic molecule and biological marker of oxidative stress. Nutrition, Metabolism and Cardiovascular Diseases 15, 316-328.

Džoljić, E., Grbatinić, I., Kostić, V., 2015. Why is nitric oxide important for our brain? Funct Neurol 30, 159-163.

Fan, Y., Zhang, W., Huang, X., Fan, M., Shi, C., Zhao, L., Pi, G., Zhang, H., Ni, S., 2024. Senescent-like macrophages mediate angiogenesis for endplate sclerosis via IL-10 secretion in male mice. Nature Communications 15, 2939.
Fang, J., She, J., Lin, F., Wu, J.-C., Han, R., Sheng, R., Wang, G., Qin, Z.-H., 2022. RRx-001 Exerts Neuroprotection Against LPS-Induced Microglia Activation and Neuroinflammation Through Disturbing the TLR4 Pathway. Frontiers in Pharmacology 13.
Finger, C.E., Moreno-Gonzalez, I., Gutierrez, A., Moruno-Manchon, J.F., McCullough, L.D., 2022. Age-related immune alterations and cerebrovascular inflammation. Molecular Psychiatry 27, 803-818.
Floden, A.M., Combs, C.K., 2011. Microglia Demonstrate Age-Dependent Interaction with Amyloid-β Fibrils. Journal of Alzheimer's Disease 25, 279-293.
Flowers, A., Bell-Temin, H., Jalloh, A., Stevens, S.M., Bickford, P.C., 2017. Proteomic analysis of aged microglia: shifts in transcription, bioenergetics, and nutrient response. J Neuroinflammation 14, 96.
Gatto, N., Dos Santos Souza, C., Shaw, A.C., Bell, S.M., Myszczynska, M.A., Powers, S., Meyer, K., Castelli, L.M., Karyka, E., Mortiboys, H., Azzouz, M., Hautbergue, G.M., Márkus, N.M., Shaw, P.J., Ferraiuolo, L., 2021. Directly converted astrocytes retain the ageing features of the donor fibroblasts and elucidate the astrocytic contribution to human CNS health and disease. Aging Cell 20, e13281.
Ginhoux, F., Lim, S., Hoeffel, G., Low, D., Huber, T., 2013. Origin and differentiation of microglia. Frontiers in Cellular Neuroscience 7.
Greenwood, E.K., Brown, D.R., 2021. Senescent Microglia: The Key to the Ageing Brain? , International Journal of Molecular Sciences.
Grice, G.L., Nathan, J.A., 2016. The recognition of ubiquitinated proteins by the proteasome. Cell Mol Life Sci 73, 3497-3506.
Grubman, A., Choo, X.Y., Chew, G., Ouyang, J.F., Sun, G., Croft, N.P., Rossello, F.J., Simmons, R., Buckberry, S., Landin, D.V., Pflueger, J., Vandekolk, T.H., Abay, Z., Zhou, Y., Liu, X., Chen, J., Larcombe, M., Haynes, J.M., McLean, C., Williams, S., Chai, S.Y., Wilson, T., Lister, R., Pouton, C.W., Purcell, A.W., Rackham, O.J.L., Petretto, E., Polo, J.M., 2021. Transcriptional signature in microglia associated with Aβ plaque phagocytosis. Nat Commun 12, 3015.
Gu, Y., Dee, C.M., Shen, J., 2011. Interaction of free radicals, matrix metalloproteinases and caveolin-1 impacts blood-brain barrier permeability. FBS 3, 1216-1231.
Hayflick, L., 1965. The limited in vitro lifetime of human diploid cell strains. Experimental Cell Research 37, 614-636.
Hayflick L Fau - Moorhead, P.S., Moorhead, P.S., 1961. The serial cultivation of human diploid cell strains.
He, Z., Wilson, A., Rich, F., Kenwright, D., Stevens, A., Low, Y.S., Thunders, M., 2023. Chromosomal instability and its effect on cell lines. Cancer Rep (Hoboken) 6, e1822.
Hegde, A.N., Duke, L.M., Timm, L.E., Nobles, H., 2023. The Proteasome and Ageing. In: Harris, J.R., Korolchuk, V.I. (Eds.), Biochemistry and Cell Biology of Ageing: Part III Biomedical Science. Springer International Publishing, Cham, pp. 99-112.
Hetz, C., 2012. The unfolded protein response: controlling cell fate decisions under ER stress and beyond. Nature Reviews Molecular Cell Biology 13, 89-102.
Hou, Y., Dan, X., Babbar, M., Wei, Y., Hasselbalch, S.G., Croteau, D.L., Bohr, V.A., 2019. Ageing as a risk factor for neurodegenerative disease. Nature Reviews Neurology 15, 565-581.
Hughes, P., Marshall, D., Reid, Y., Parkes, H., Gelber, C., 2007. The costs of using unauthenticated, over-passaged cell lines: how much more data do we need? BioTechniques 43, 575-586.
Huh, C.J., Zhang, B., Victor, M.B., Dahiya, S., Batista, L.F.Z., Horvath, S., Yoo, A.S., 2016. Maintenance of age in human neurons generated by microRNA-based neuronal conversion of fibroblasts. Elife 5, e18648.
James, E.L., Lane, J.A.E., Michalek, R.D., Karoly, E.D., Parkinson, E.K., 2016. Replicatively senescent human fibroblasts reveal a distinct intracellular metabolic profile with alterations in NAD+ and nicotinamide metabolism. Scientific Reports 6, 38489.
Jansen, A.H., Reits, E.A., Hol, E.M., 2014. The ubiquitin proteasome system in glia and its role in neurodegenerative diseases. Front Mol Neurosci 7, 73.
Johnson, I.P., 2015. Age-related neurodegenerative disease research needs aging models. Frontiers in Aging Neuroscience 7.

Jung, T., Höhn, A., Catalgol, B., Grune, T., 2009. Age-related differences in oxidative protein-damage in young and senescent fibroblasts. Archives of Biochemistry and Biophysics 483, 127-135.
Kang, R., Gamdzyk, M., Lenahan, C., Tang, J., Tan, S., Zhang, J.H., 2020. The Dual Role of Microglia in Blood-Brain Barrier Dysfunction after Stroke. Curr Neuropharmacol 18, 1237-1249.
Karabag, D., Scheiblich, H., Griep, A., Santarelli, F., Schwartz, S., Heneka, M.T., Ising, C., 2023. Characterizing microglial senescence: Tau as a key player. J Neurochem 166, 517-533.
Kim, B.-W., More, S.V., Yun, Y.-S., Ko, H.-M., Kwak, J.-H., Lee, H., Suk, K., Kim, I.-S., Choi, D.-K., 2016. A novel synthetic compound MCAP suppresses LPS-induced murine microglial activation in vitro via inhibiting NF-kB and p38 MAPK pathways. Acta Pharmacologica Sinica 37, 334-343.
Kim, S.Y., Jin, C.Y., Kim, C.H., Yoo, Y.H., Choi, S.H., Kim, G.Y., Yoon, H.M., Park, H.T., Choi, Y.H., 2019. Isorhamnetin alleviates lipopolysaccharide-induced inflammatory responses in BV2 microglia by inactivating NF-κB, blocking the TLR4 pathway and reducing ROS generation. Int J Mol Med 43, 682-692.
Kinirons, M.T., O'Mahony, M.S., 2004. Drug metabolism and ageing. Br J Clin Pharmacol 57, 540-544.
Koellhoffer, E.C., McCullough, L.D., Ritzel, R.M., 2017. Old Maids: Aging and Its Impact on Microglia Function. Int J Mol Sci 18.
Krtolica, A., Parrinello, S., Lockett, S., Desprez, P.-Y., Campisi, J., 2001. Senescent fibroblasts promote epithelial cell growth and tumorigenesis: A link between cancer and aging. Proceedings of the National Academy of Sciences 98, 12072-12077.
Kwon, H.S., Koh, S.-H., 2020. Neuroinflammation in neurodegenerative disorders: the roles of microglia and astrocytes. Translational Neurodegeneration 9, 42.
Lee, H.K., Park, S.-H., Nam, M.J., 2021. Proteasome inhibitor MG132 induces apoptosis in human osteosarcoma U2OS cells. Human & Experimental Toxicology 40, 1985-1997.
Liu, P., Kaplan, A., Yuan, B., Hanna, J.H., Lupski, J.R., Reiner, O., 2014. Passage number is a major contributor to genomic structural variations in mouse iPSCs. Stem Cells 32, 2657-2667.
López-Otín, C., Blasco, M.A., Partridge, L., Serrano, M., Kroemer, G., 2023. Hallmarks of aging: An expanding universe. Cell 186, 243-278.
Louis, J.C., Magal, E., Muir, D., Manthorpe, M., Varon, S., 1992. CG-4, a new bipotential glial cell line from rat brain, is capable of differentiating in vitro into either mature oligodendrocytes or type-2 astrocytes. J Neurosci Res 31, 193-204.
Löw, P., 2011. The role of ubiquitin–proteasome system in ageing. General and Comparative Endocrinology 172, 39-43.
McCarron, E.P., Williams, D.P., Antoine, D.J., Kipar, A., Lemm, J., Stehr, S., Welters, I.D., 2015. Exploring the translational disconnect between the murine and human inflammatory response: analysis of LPS dose-response relationship in murine versus human cell lines and implications for translation into murine models of sepsis. J Inflamm Res 8, 201-209.
Milner, M.T., Lawrence, G.M., Holley, C.L., Bodea, L.G., Götz, J., Burgener, S.S., Schroder, K., 2022. Isolation and culture of pure adult mouse microglia and astrocytes for in vitro characterization and analyses. STAR Protoc 3, 101295.
Mortati, L., Pergolizzi, B., Panuzzo, C., Bracco, E., 2022. Present and Future Opportunities in Imaging the Ubiquitin System (Ub-System). Biophysica, pp. 174-183.
Neumann, P., Lenz, D.E., Streit, W.J., Bechmann, I., 2023. Is microglial dystrophy a form of cellular senescence? An analysis of senescence markers in the aged human brain. Glia 71, 377-390.
Nikodemova, M., Small, A.L., Kimyon, R.S., Watters, J.J., 2016. Age-dependent differences in microglial responses to systemic inflammation are evident as early as middle age. Physiol Genomics 48, 336-344.
Norden, D.M., Muccigrosso, M.M., Godbout, J.P., 2015. Microglial priming and enhanced reactivity to secondary insult in aging, and traumatic CNS injury, and neurodegenerative disease. Neuropharmacology 96, 29-41.
Oliveira, A.V., Vilaça, R., Santos, C.N., Costa, V., Menezes, R., 2017. Exploring the power of yeast to model aging and age-related neurodegenerative disorders. Biogerontology 18, 3-34.
Parakalan, R., Jiang, B., Nimmi, B., Janani, M., Jayapal, M., Lu, J., Tay, S.S., Ling, E.A., Dheen, S.T., 2012. Transcriptome analysis of amoeboid and ramified microglia isolated from the corpus callosum of rat brain. BMC Neurosci 13, 64.

Phipps, S.M.O., Berletch, J.B., Andrews, L.G., Tollefsbol, T.O., 2007. Aging cell culture: methods and observations. Methods Mol Biol 371, 9-19.
Pontén, J., Macintyre, E.H., 1968. Long term culture of normal and neoplastic human glia. Acta Pathol Microbiol Scand 74, 465-486.
Reddaway, J., Richardson, P.E., Bevan, R.J., Stoneman, J., Palombo, M., 2023. Microglial morphometric analysis: so many options, so little consistency. Frontiers in Neuroinformatics 17.
Réu, P., Khosravi, A., Bernard, S., Mold, J.E., Salehpour, M., Alkass, K., Perl, S., Tisdale, J., Possnert, G., Druid, H., Frisén, J., 2017. The Lifespan and Turnover of Microglia in the Human Brain. Cell Rep 20, 779-784.
Ricci, C., 2024. Neurodegenerative Disease: From Molecular Basis to Therapy. Int J Mol Sci 25.
Rim, C., You, M.-J., Nahm, M., Kwon, M.-S., 2024. Emerging role of senescent microglia in brain aging-related neurodegenerative diseases. Translational Neurodegeneration 13, 10.
Sandhir, R., Onyszchuk, G., Berman, N.E., 2008. Exacerbated glial response in the aged mouse hippocampus following controlled cortical impact injury. Exp Neurol 213, 372-380.
Sarkar, S., Malovic, E., Sarda, D., Lawana, V., Rokad, D., Jin, H., Anantharam, V., Kanthasamy, A., Kanthasamy, A.G., 2018. Characterization and comparative analysis of a new mouse microglial cell model for studying neuroinflammatory mechanisms during neurotoxic insults. Neurotoxicology 67, 129-140.
Sasmono, R.T., Oceandy, D., Pollard, J.W., Tong, W., Pavli, P., Wainwright, B.J., Ostrowski, M.C., Himes, S.R., Hume, D.A., 2003. A macrophage colony-stimulating factor receptor–green fluorescent protein transgene is expressed throughout the mononuclear phagocyte system of the mouse. Blood 101, 1155-1163.
Sato, T., Shapiro, J.S., Chang, H.-C., Miller, R.A., Ardehali, H., 2022. Aging is associated with increased brain iron through cortex-derived hepcidin expression. Elife 11, e73456.
Schaeffer, V., Meyer, L., Patte-Mensah, C., Eckert, A., Mensah-Nyagan, A.G., 2008. Dose-dependent and sequence-sensitive effects of amyloid-β peptide on neurosteroidogenesis in human neuroblastoma cells. Neurochemistry International 52, 948-955.
Schloesser, D., Lindenthal, L., Sauer, J., Chung, K.J., Chavakis, T., Griesser, E., Baskaran, P., Maier-Habelsberger, U., Fundel-Clemens, K., Schlotthauer, I., Watson, C.K., Swee, L.K., Igney, F., Park, J.E., Huber-Lang, M.S., Thomas, M.J., El Kasmi, K.C., Murray, P.J., 2023. Senescent cells suppress macrophage-mediated corpse removal via upregulation of the CD47-QPCT/L axis. J Cell Biol 222.
Seyfried, N.T., Xu, P., Duong, D.M., Cheng, D., Hanfelt, J., Peng, J., 2008. Systematic approach for validating the ubiquitinated proteome. Anal Chem 80, 4161-4169.
Shang, F., Taylor, A., 2011. Ubiquitin–proteasome pathway and cellular responses to oxidative stress. Free Radical Biology and Medicine 51, 5-16.
Shebl, F.M., Pinto, L.A., García-Piñeres, A., Lempicki, R., Williams, M., Harro, C., Hildesheim, A., 2010. Comparison of mRNA and protein measures of cytokines following vaccination with human papillomavirus-16 L1 virus-like particles. Cancer Epidemiol Biomarkers Prev 19, 978-981.
Sierra, A., Gottfried-Blackmore, A.C., McEwen, B.S., Bulloch, K., 2007. Microglia derived from aging mice exhibit an altered inflammatory profile. Glia 55, 412-424.
Smith, A.N., Shaughness, M., Collier, S., Hopkins, D., Byrnes, K.R., 2022. Therapeutic targeting of microglia mediated oxidative stress after neurotrauma. Frontiers in Medicine 9.
Song, L., Pei, L., Yao, S., Wu, Y., Shang, Y., 2017. NLRP3 Inflammasome in Neurological Diseases, from Functions to Therapies. Frontiers in Cellular Neuroscience 11.
Stansley, B., Post, J., Hensley, K., 2012. A comparative review of cell culture systems for the study of microglial biology in Alzheimer's disease. J Neuroinflammation 9, 115.
Strässler, E.T., Aalto-Setälä, K., Kiamehr, M., Landmesser, U., Kränkel, N., 2018. Age Is Relative-Impact of Donor Age on Induced Pluripotent Stem Cell-Derived Cell Functionality. Front Cardiovasc Med 5, 4.
Sun, M., McDonald, S.J., Brady, R.D., Collins-Praino, L., Yamakawa, G.R., Monif, M., O'Brien, T.J., Cloud, G.C., Sobey, C.G., Mychasiuk, R., Loane, D.J., Shultz, S.R., 2020. The need to incorporate aged animals into the preclinical modeling of neurological conditions. Neuroscience & Biobehavioral Reviews 109, 114-128.

Taciak, B., Białasek, M., Braniewska, A., Sas, Z., Sawicka, P., Kiraga, Ł., Rygiel, T., Król, M., 2018. Evaluation of phenotypic and functional stability of RAW 264.7 cell line through serial passages. PLoS One 13, e0198943.
Tichauer, J.E., Flores, B., Soler, B., Eugenín-von Bernhardi, L., Ramírez, G., von Bernhardi, R., 2014. Age-dependent changes on TGFβ1 Smad3 pathway modify the pattern of microglial cell activation. Brain, Behavior, and Immunity 37, 187-196.
Trigo, D., Nadais, A., da Cruz e Silva, O.A.B., 2019. Unravelling protein aggregation as an ageing related process or a neuropathological response. Ageing Research Reviews 51, 67-77.
Türker, F., Cook, E.K., Margolis, S.S., 2021. The proteasome and its role in the nervous system. Cell Chemical Biology 28, 903-917.
Tydlacka, S., Wang, C.E., Wang, X., Li, S., Li, X.J., 2008. Differential activities of the ubiquitin-proteasome system in neurons versus glia may account for the preferential accumulation of misfolded proteins in neurons. J Neurosci 28, 13285-13295.
Uxa, S., Castillo-Binder, P., Kohler, R., Stangner, K., Müller, G.A., Engeland, K., 2021. Ki-67 gene expression. Cell Death Differ 28, 3357-3370.
Vernace, V.A., Schmidt-Glenewinkel, T., Figueiredo-Pereira, M.E., 2007. Aging and regulated protein degradation: who has the UPPer hand? Aging Cell 6, 599-606.
Vierbuchen, T., Ostermeier, A., Pang, Z.P., Kokubu, Y., Südhof, T.C., Wernig, M., 2010. Direct conversion of fibroblasts to functional neurons by defined factors. Nature 463, 1035-1041.
Vijaya, A.K., Iešmantaitė, M., Mela, V., Baltriukienė, D., Burokas, A., 2023. Microglia isolation from aging mice for cell culture: A beginner's guide. Front Cell Neurosci 17, 1082180.
Vos, T., Lim, S.S., Abbafati, C., Abbas, K.M., Abbasi, M., Abbasifard, M., Abbasi-Kangevari, M., Abbastabar, H., Abd-Allah, F., Abdelalim, A., Abdollahi, M., Abdollahpour, I., Abolhassani, H., Aboyans, V., Abrams, E.M., Abreu, L.G., Abrigo, M.R.M., Abu-Raddad, L.J., Abushouk, A.I., Acebedo, A., Ackerman, I.N., Adabi, M., Adamu, A.A., Adebayo, O.M., Adekanmbi, V., Adelson, J.D., Adetokunboh, O.O., Adham, D., Afshari, M., Afshin, A., Agardh, E.E., Agarwal, G., Agesa, K.M., Aghaali, M., Aghamir, S.M.K., Agrawal, A., Ahmad, T., Ahmadi, A., Ahmadi, M., Ahmadieh, H., Ahmadpour, E., Akalu, T.Y., Akinyemi, R.O., Akinyemiju, T., Akombi, B., Al-Aly, Z., Alam, K., Alam, N., Alam, S., Alam, T., Alanzi, T.M., Albertson, S.B., Alcalde-Rabanal, J.E., Alema, N.M., Ali, M., Ali, S., Alicandro, G., Alijanzadeh, M., Alinia, C., Alipour, V., Aljunid, S.M., Alla, F., Allebeck, P., Almasi-Hashiani, A., Alonso, J., Al-Raddadi, R.M., Altirkawi, K.A., Alvis-Guzman, N., Alvis-Zakzuk, N.J., Amini, S., Amini-Rarani, M., Aminorroaya, A., Amiri, F., Amit, A.M.L., Amugsi, D.A., Amul, G.G.H., Anderlini, D., Andrei, C.L., Andrei, T., Anjomshoa, M., Ansari, F., Ansari, I., Ansari-Moghaddam, A., Antonio, C.A.T., Antony, C.M., Antriyandarti, E., Anvari, D., Anwer, R., Arabloo, J., Arab-Zozani, M., Aravkin, A.Y., Ariani, F., Ärnlöv, J., Aryal, K.K., Arzani, A., Asadi-Aliabadi, M., Asadi-Pooya, A.A., Asghari, B., Ashbaugh, C., Atnafu, D.D., Atre, S.R., Ausloos, F., Ausloos, M., Ayala Quintanilla, B.P., Ayano, G., Ayanore, M.A., Aynalem, Y.A., Azari, S., Azarian, G., Azene, Z.N., Babaee, E., Badawi, A., Bagherzadeh, M., Bakhshaei, M.H., Bakhtiari, A., Balakrishnan, S., Balalla, S., Balassyano, S., Banach, M., Banik, P.C., Bannick, M.S., Bante, A.B., Baraki, A.G., Barboza, M.A., Barker-Collo, S.L., Barthelemy, C.M., Barua, L., Barzegar, A., Basu, S., Baune, B.T., Bayati, M., Bazmandegan, G., Bedi, N., Beghi, E., Béjot, Y., Bello, A.K., Bender, R.G., Bennett, D.A., Bennitt, F.B., Bensenor, I.M., Benziger, C.P., Berhe, K., Bernabe, E., Bertolacci, G.J., Bhageerathy, R., Bhala, N., Bhandari, D., Bhardwaj, P., Bhattacharyya, K., Bhutta, Z.A., Bibi, S., Biehl, M.H., Bikbov, B., Bin Sayeed, M.S., Biondi, A., Birihane, B.M., Bisanzio, D., Bisignano, C., Biswas, R.K., Bohlouli, S., Bohluli, M., Bolla, S.R.R., Boloor, A., Boon-Dooley, A.S., Borges, G., Borzì, A.M., Bourne, R., Brady, O.J., Brauer, M., Brayne, C., Breitborde, N.J.K., Brenner, H., Briant, P.S., Briggs, A.M., Briko, N.I., Britton, G.B., Bryazka, D., Buchbinder, R., Bumgarner, B.R., Busse, R., Butt, Z.A., Caetano dos Santos, F.L., Cámera, L.L.A.A., Campos-Nonato, I.R., Car, J., Cárdenas, R., Carreras, G., Carrero, J.J., Carvalho, F., Castaldelli-Maia, J.M., Castañeda-Orjuela, C.A., Castelpietra, G., Castle, C.D., Castro, F., Catalá-López, F., Causey, K., Cederroth, C.R., Cercy, K.M., Cerin, E., Chandan, J.S., Chang, A.R., Charlson, F.J., Chattu, V.K., Chaturvedi, S., Chimed-Ochir, O., Chin, K.L., Cho, D.Y., Christensen, H., Chu, D.-T., Chung, M.T., Cicuttini, F.M., Ciobanu, L.G., Cirillo, M., Collins, E.L., Compton, K., Conti, S., Cortesi, P.A., Costa, V.M., Cousin, E., Cowden, R.G., Cowie, B.C., Cromwell, E.A., Cross, D.H., Crowe, C.S., Cruz, J.A., Cunningham, M., Dahlawi, S.M.A., Damiani, G., Dandona, L., Dandona, R., Darwesh, A.M., Daryani, A., Das, J.K., Das Gupta, R., das Neves, J., Dávila-Cervantes, C.A., Davletov,

K., De Leo, D., Dean, F.E., DeCleene, N.K., Deen, A., Degenhardt, L., Dellavalle, R.P., Demeke, F.M., Demsie, D.G., Denova-Gutiérrez, E., Dereje, N.D., Dervenis, N., Desai, R., Desalew, A., Dessie, G.A., Dharmaratne, S.D., Dhungana, G.P., Dianatinasab, M., Diaz, D., Dibaji Forooshani, Z.S., Dingels, Z.V., Dirac, M.A., Djalalinia, S., Do, H.T., Dokova, K., Dorostkar, F., Doshi, C.P., Doshmangir, L., Douiri, A., Doxey, M.C., Driscoll, T.R., Dunachie, S.J., Duncan, B.B., Duraes, A.R., Eagan, A.W., Ebrahimi Kalan, M., Edvardsson, D., Ehrlich, J.R., El Nahas, N., El Sayed, I., El Tantawi, M., Elbarazi, I., Elgendy, I.Y., Elhabashy, H.R., El-Jaafary, S.I., Elyazar, I.R.F., Emamian, M.H., Emmons-Bell, S., Erskine, H.E., Eshrati, B., Eskandarieh, S., Esmaeilnejad, S., Esmaeilzadeh, F., Esteghamati, A., Estep, K., Etemadi, A., Etisso, A.E., Farahmand, M., Faraj, A., Fareed, M., Faridnia, R., Farinha, C.S.e.S., Farioli, A., Faro, A., Faruque, M., Farzadfar, F., Fattahi, N., Fazlzadeh, M., Feigin, V.L., Feldman, R., Fereshtehnejad, S.-M., Fernandes, E., Ferrari, A.J., Ferreira, M.L., Filip, I., Fischer, F., Fisher, J.L., Fitzgerald, R., Flohr, C., Flor, L.S., Foigt, N.A., Folayan, M.O., Force, L.M., Fornari, C., Foroutan, M., Fox, J.T., Freitas, M., Fu, W., Fukumoto, T., Furtado, J.M., Gad, M.M., Gakidou, E., Galles, N.C., Gallus, S., Gamkrelidze, A., Garcia-Basteiro, A.L., Gardner, W.M., Geberemariyam, B.S., Gebrehiwot, A.M., Gebremedhin, K.B., Gebreslassie, A.A.A.A., Gershberg Hayoon, A., Gething, P.W., Ghadimi, M., Ghadiri, K., Ghafourifard, M., Ghajar, A., Ghamari, F., Ghashghaee, A., Ghiasvand, H., Ghith, N., Gholamian, A., Gilani, S.A., Gill, P.S., Gitimoghaddam, M., Giussani, G., Goli, S., Gomez, R.S., Gopalani, S.V., Gorini, G., Gorman, T.M., Gottlich, H.C., Goudarzi, H., Goulart, A.C., Goulart, B.N.G., Grada, A., Grivna, M., Grosso, G., Gubari, M.I.M., Gugnani, H.C., Guimaraes, A.L.S., Guimarães, R.A., Guled, R.A., Guo, G., Guo, Y., Gupta, R., Haagsma, J.A., Haddock, B., Hafezi-Nejad, N., Hafiz, A., Hagins, H., Haile, L.M., Hall, B.J., Halvaei, I., Hamadeh, R.R., Hamagharib Abdullah, K., Hamilton, E.B., Han, C., Han, H., Hankey, G.J., Haro, J.M., Harvey, J.D., Hasaballah, A.I., Hasanzadeh, A., Hashemian, M., Hassanipour, S., Hassankhani, H., Havmoeller, R.J., Hay, R.J., Hay, S.I., Hayat, K., Heidari, B., Heidari, G., Heidari-Soureshjani, R., Hendrie, D., Henrikson, H.J., Henry, N.J., Herteliu, C., Heydarpour, F., Hird, T.R., Hoek, H.W., Hole, M.K., Holla, R., Hoogar, P., Hosgood, H.D., Hosseinzadeh, M., Hostiuc, M., Hostiuc, S., Househ, M., Hoy, D.G., Hsairi, M., Hsieh, V.C.-r., Hu, G., Huda, T.M., Hugo, F.N., Huynh, C.K., Hwang, B.-F., Iannucci, V.C., Ibitoye, S.E., Ikuta, K.S., Ilesanmi, O.S., Ilic, I.M., Ilic, M.D., Inbaraj, L.R., Ippolito, H., Irvani, S.S.N., Islam, M.M., Islam, M., Islam, S.M.S., Islami, F., Iso, H., Ivers, R.Q., Iwu, C.C.D., Iyamu, I.O., Jaafari, J., Jacobsen, K.H., Jadidi-Niaragh, F., Jafari, H., Jafarinia, M., Jahagirdar, D., Jahani, M.A., Jahanmehr, N., Jakovljevic, M., Jalali, A., Jalilian, F., James, S.L., Janjani, H., Janodia, M.D., Jayatilleke, A.U., Jeemon, P., Jenabi, E., Jha, R.P., Jha, V., Ji, J.S., Jia, P., John, O., John-Akinola, Y.O., Johnson, C.O., Johnson, S.C., Jonas, J.B., Joo, T., Joshi, A., Jozwiak, J.J., Jürisson, M., Kabir, A., Kabir, Z., Kalani, H., Kalani, R., Kalankesh, L.R., Kalhor, R., Kamiab, Z., Kanchan, T., Karami Matin, B., Karch, A., Karim, M.A., Karimi, S.E., Kassa, G.M., Kassebaum, N.J., Katikireddi, S.V., Kawakami, N., Kayode, G.A., Keddie, S.H., Keller, C., Kereselidze, M., Khafaie, M.A., Khalid, N., Khan, M., Khatab, K., Khater, M.M., Khatib, M.N., Khayamzadeh, M., Khodayari, M.T., Khundkar, R., Kianipour, N., Kieling, C., Kim, D., Kim, Y.-E., Kim, Y.J., Kimokoti, R.W., Kisa, A., Kisa, S., Kissimova-Skarbek, K., Kivimäki, M., Kneib, C.J., Knudsen, A.K.S., Kocarnik, J.M., Kolola, T., Kopec, J.A., Kosen, S., Koul, P.A., Koyanagi, A., Kravchenko, M.A., Krishan, K., Krohn, K.J., Kuate Defo, B., Kucuk Bicer, B., Kumar, G.A., Kumar, M., Kumar, P., Kumar, V., Kumaresh, G., Kurmi, O.P., Kusuma, D., Kyu, H.H., La Vecchia, C., Lacey, B., Lal, D.K., Lalloo, R., Lam, J.O., Lami, F.H., Landires, I., Lang, J.J., Lansingh, V.C., Larson, S.L., Larsson, A.O., Lasrado, S., Lassi, Z.S., Lau, K.M.-M., Lavados, P.M., Lazarus, J.V., Ledesma, J.R., Lee, P.H., Lee, S.W.H., LeGrand, K.E., Leigh, J., Leonardi, M., Lescinsky, H., Leung, J., Levi, M., Lewington, S., Li, S., Lim, L.-L., Lin, C., Lin, R.-T., Linehan, C., Linn, S., Liu, H.-C., Liu, S., Liu, Z., Looker, K.J., Lopez, A.D., Lopukhov, P.D., Lorkowski, S., Lotufo, P.A., Lucas, T.C.D., Lugo, A., Lunevicius, R., Lyons, R.A., Ma, J., MacLachlan, J.H., Maddison, E.R., Maddison, R., Madotto, F., Mahasha, P.W., Mai, H.T., Majeed, A., Maled, V., Maleki, S., Malekzadeh, R., Malta, D.C., Mamun, A.A., Manafi, A., Manafi, N., Manguerra, H., Mansouri, B., Mansournia, M.A., Mantilla Herrera, A.M., Maravilla, J.C., Marks, A., Martins-Melo, F.R., Martopullo, I., Masoumi, S.Z., Massano, J., Massenburg, B.B., Mathur, M.R., Maulik, P.K., McAlinden, C., McGrath, J.J., McKee, M., Mehndiratta, M.M., Mehri, F., Mehta, K.M., Meitei, W.B., Memiah, P.T.N., Mendoza, W., Menezes, R.G., Mengesha, E.W., Mengesha, M.B., Mereke, A., Meretoja, A., Meretoja, T.J., Mestrovic, T., Miazgowski, B., Miazgowski, T., Michalek, I.M., Mihretie, K.M., Miller, T.R., Mills, E.J., Mirica, A., Mirrakhimov, E.M., Mirzaei, H., Mirzaei, M., Mirzaei-Alavijeh, M., Misganaw, A.T., Mithra, P.,

Moazen, B., Moghadaszadeh, M., Mohamadi, E., Mohammad, D.K., Mohammad, Y., Mohammad Gholi Mezerji, N., Mohammadian-Hafshejani, A., Mohammadifard, N., Mohammadpourhodki, R., Mohammed, S., Mokdad, A.H., Molokhia, M., Momen, N.C., Monasta, L., Mondello, S., Mooney, M.D., Moosazadeh, M., Moradi, G., Moradi, M., Moradi-Lakeh, M., Moradzadeh, R., Moraga, P., Morales, L., Morawska, L., Moreno Velásquez, I., Morgado-da-Costa, J., Morrison, S.D., Mosser, J.F., Mouodi, S., Mousavi, S.M., Mousavi Khaneghah, A., Mueller, U.O., Munro, S.B., Muriithi, M.K., Musa, K.I., Muthupandian, S., Naderi, M., Nagarajan, A.J., Nagel, G., Naghshtabrizi, B., Nair, S., Nandi, A.K., Nangia, V., Nansseu, J.R., Nayak, V.C., Nazari, J., Negoi, I., Negoi, R.I., Netsere, H.B.N., Ngunjiri, J.W., Nguyen, C.T., Nguyen, J., Nguyen, M., Nguyen, M., Nichols, E., Nigatu, D., Nigatu, Y.T., Nikbakhsh, R., Nixon, M.R., Nnaji, C.A., Nomura, S., Norrving, B., Noubiap, J.J., Nowak, C., Nunez-Samudio, V., Oţoiu, A., Oancea, B., Odell, C.M., Ogbo, F.A., Oh, I.-H., Okunga, E.W., Oladnabi, M., Olagunju, A.T., Olusanya, B.O., Olusanya, J.O., Oluwasanu, M.M., Omar Bali, A., Omer, M.O., Ong, K.L., Onwujekwe, O.E., Orji, A.U., Orpana, H.M., Ortiz, A., Ostroff, S.M., Otstavnov, N., Otstavnov, S.S., Øverland, S., Owolabi, M.O., P A, M., Padubidri, J.R., Pakhare, A.P., Palladino, R., Pana, A., Panda-Jonas, S., Pandey, A., Park, E.-K., Parmar, P.G.K., Pasupula, D.K., Patel, S.K., Paternina-Caicedo, A.J., Pathak, A., Pathak, M., Patten, S.B., Patton, G.C., Paudel, D., Pazoki Toroudi, H., Peden, A.E., Pennini, A., Pepito, V.C.F., Peprah, E.K., Pereira, A., Pereira, D.M., Perico, N., Pham, H.Q., Phillips, M.R., Pigott, D.M., Pilgrim, T., Pilz, T.M., Pirsaheb, M., Plana-Ripoll, O., Plass, D., Pokhrel, K.N., Polibin, R.V., Polinder, S., Polkinghorne, K.R., Postma, M.J., Pourjafar, H., Pourmalek, F., Pourmirza Kalhori, R., Pourshams, A., Poznańska, A., Prada, S.I., Prakash, V., Pribadi, D.R.A., Pupillo, E., Quazi Syed, Z., Rabiee, M., Rabiee, N., Radfar, A., Rafiee, A., Rafiei, A., Raggi, A., Rahimi-Movaghar, A., Rahman, M.A., Rajabpour-Sanati, A., Rajati, F., Ramezanzadeh, K., Ranabhat, C.L., Rao, P.C., Rao, S.J., Rasella, D., Rastogi, P., Rathi, P., Rawaf, D.L., Rawaf, S., Rawal, L., Razo, C., Redford, S.B., Reiner, R.C., Jr., Reinig, N., Reitsma, M.B., Remuzzi, G., Renjith, V., Renzaho, A.M.N., Resnikoff, S., Rezaei, N., Rezai, M.s., Rezapour, A., Rhinehart, P.-A., Riahi, S.M., Ribeiro, A.L.P., Ribeiro, D.C., Ribeiro, D., Rickard, J., Roberts, N.L.S., Roberts, S., Robinson, S.R., Roever, L., Rolfe, S., Ronfani, L., Roshandel, G., Roth, G.A., Rubagotti, E., Rumisha, S.F., Sabour, S., Sachdev, P.S., Saddik, B., Sadeghi, E., Sadeghi, M., Saeidi, S., Safi, S., Safiri, S., Sagar, R., Sahebkar, A., Sahraian, M.A., Sajadi, S.M., Salahshoor, M.R., Salamati, P., Salehi Zahabi, S., Salem, H., Salem, M.R.R., Salimzadeh, H., Salomon, J.A., Salz, I., Samad, Z., Samy, A.M., Sanabria, J., Santomauro, D.F., Santos, I.S., Santos, J.V., Santric-Milicevic, M.M., Saraswathy, S.Y.I., Sarmiento-Suárez, R., Sarrafzadegan, N., Sartorius, B., Sarveazad, A., Sathian, B., Sathish, T., Sattin, D., Sbarra, A.N., Schaeffer, L.E., Schiavolin, S., Schmidt, M.I., Schutte, A.E., Schwebel, D.C., Schwendicke, F., Senbeta, A.M., Senthilkumaran, S., Sepanlou, S.G., Shackelford, K.A., Shadid, J., Shahabi, S., Shaheen, A.A., Shaikh, M.A., Shalash, A.S., Shams-Beyranvand, M., Shamsizadeh, M., Shannawaz, M., Sharafi, K., Sharara, F., Sheena, B.S., Sheikhtaheri, A., Shetty, R.S., Shibuya, K., Shiferaw, W.S., Shigematsu, M., Shin, J.I., Shiri, R., Shirkoohi, R., Shrime, M.G., Shuval, K., Siabani, S., Sigfusdottir, I.D., Sigurvinsdottir, R., Silva, J.P., Simpson, K.E., Singh, A., Singh, J.A., Skiadaresi, E., Skou, S.T., Skryabin, V.Y., Sobngwi, E., Sokhan, A., Soltani, S., Sorensen, R.J.D., Soriano, J.B., Sorrie, M.B., Soyiri, I.N., Sreeramareddy, C.T., Stanaway, J.D., Stark, B.A., Ştefan, S.C., Stein, C., Steiner, C., Steiner, T.J., Stokes, M.A., Stovner, L.J., Stubbs, J.L., Sudaryanto, A., Sufiyan, M.a.B., Sulo, G., Sultan, I., Sykes, B.L., Sylte, D.O., Szócska, M., Tabarés-Seisdedos, R., Tabb, K.M., Tadakamadla, S.K., Taherkhani, A., Tajdini, M., Takahashi, K., Taveira, N., Teagle, W.L., Teame, H., Tehrani-Banihashemi, A., Teklehaimanot, B.F., Terrason, S., Tessema, Z.T., Thankappan, K.R., Thomson, A.M., Tohidinik, H.R., Tonelli, M., Topor-Madry, R., Torre, A.E., Touvier, M., Tovani-Palone, M.R.R., Tran, B.X., Travillian, R., Troeger, C.E., Truelsen, T.C., Tsai, A.C., Tsatsakis, A., Tudor Car, L., Tyrovolas, S., Uddin, R., Ullah, S., Undurraga, E.A., Unnikrishnan, B., Vacante, M., Vakilian, A., Valdez, P.R., Varughese, S., Vasankari, T.J., Vasseghian, Y., Venketasubramanian, N., Violante, F.S., Vlassov, V., Vollset, S.E., Vongpradith, A., Vukovic, A., Vukovic, R., Waheed, Y., Walters, M.K., Wang, J., Wang, Y., Wang, Y.-P., Ward, J.L., Watson, A., Wei, J., Weintraub, R.G., Weiss, D.J., Weiss, J., Westerman, R., Whisnant, J.L., Whiteford, H.A., Wiangkham, T., Wiens, K.E., Wijeratne, T., Wilner, L.B., Wilson, S., Wojtyniak, B., Wolfe, C.D.A., Wool, E.E., Wu, A.-M., Wulf Hanson, S., Wunrow, H.Y., Xu, G., Xu, R., Yadgir, S., Yahyazadeh Jabbari, S.H., Yamagishi, K., Yaminfirooz, M., Yano, Y., Yaya, S., Yazdi-Feyzabadi, V., Yearwood, J.A., Yeheyis, T.Y., Yeshitila, Y.G., Yip, P., Yonemoto, N., Yoon, S.-J., Yoosefi Lebni, J., Younis, M.Z., Younker, T.P., Yousefi, Z., Yousefifard,

M., Yousefinezhadi, T., Yousuf, A.Y., Yu, C., Yusefzadeh, H., Zahirian Moghadam, T., Zaki, L., Zaman, S.B., Zamani, M., Zamanian, M., Zandian, H., Zangeneh, A., Zastrozhin, M.S., Zewdie, K.A., Zhang, Y., Zhang, Z.-J., Zhao, J.T., Zhao, Y., Zheng, P., Zhou, M., Ziapour, A., Zimsen, S.R.M., Naghavi, M., Murray, C.J.L., 2020. Global burden of 369 diseases and injuries in 204 countries and territories, 1990-2019: a systematic analysis for the Global Burden of Disease Study 2019. The Lancet 396, 1204-1222.
Wallace, L.M.K., Howlett, S.E., 2016. Commentary: Age-related neurodegenerative disease research needs aging models. Frontiers in Aging Neuroscience 8.
Wasserman, J.K., Yang, H., Schlichter, L.C., 2008. Glial responses, neuron death and lesion resolution after intracerebral hemorrhage in young vs. aged rats. European Journal of Neuroscience 28, 1316-1328.
Weiskirchen, S., Schröder, S.K., Buhl, E.M., Weiskirchen, R., 2023. A Beginner's Guide to Cell Culture: Practical Advice for Preventing Needless Problems. Cells.
Windener, F., Grewing, L., Thomas, C., Dorion, M.-F., Otteken, M., Kular, L., Jagodic, M., Antel, J., Albrecht, S., Kuhlmann, T., 2024. Physiological aging and inflammation-induced cellular senescence may contribute to oligodendroglial dysfunction in MS. Acta Neuropathologica 147, 82.
Xu, Y., Jagannath, C., Liu, X.D., Sharafkhaneh, A., Kolodziejska, K.E., Eissa, N.T., 2007. Toll-like receptor 4 is a sensor for autophagy associated with innate immunity. Immunity 27, 135-144.
Ye, S.-M., Johnson, R.W., 1999. Increased interleukin-6 expression by microglia from brain of aged mice. Journal of Neuroimmunology 93, 139-148.
Yu, H.-M., Zhao, Y.-M., Luo, X.-G., Feng, Y., Ren, Y., Shang, H., He, Z.-Y., Luo, X.-M., Chen, S.-D., Wang, X.-Y., 2012. Repeated Lipopolysaccharide Stimulation Induces Cellular Senescence in BV2 Cells. Neuroimmunomodulation 19, 131-136.
Zeiss, C.J., 2017. From Reproducibility to Translation in Neurodegenerative Disease. ILAR Journal 58, 106-114.
Zhang, W., Xu, C., Sun, J., Shen, H.-M., Wang, J., Yang, C., 2022. Impairment of the autophagy–lysosomal pathway in Alzheimer's diseases: Pathogenic mechanisms and therapeutic potential. Acta Pharmaceutica Sinica B 12, 1019-1040.
Zhao, C., 2023. Cell culture: in vitro model system and a promising path to in vivo applications. Journal of Histotechnology 46, 1-4.
Zheng, W., Li, Q., Zhao, C., Da, Y., Zhang, H.-L., Chen, Z., 2018. Differentiation of Glial Cells From hiPSCs: Potential Applications in Neurological Diseases and Cell Replacement Therapy. Frontiers in Cellular Neuroscience 12.

6.8 Supporting Information

Examining the potential of an immortalised glial cell line as an *in vitro* model of cellular senescence

Laura M. Carr[1], Gustavo Bracho[2], Claire Rennie[3], Andrew Care[3], Ian Musgrave[1], Sanam Mustafa[1,4], Lyndsey E. Collins-Praino[1]

[1]School of Biomedicine, University of Adelaide, Adelaide, SA, Australia
[2] College of Medicine and Public Health, Flinders University, Adelaide, South Australia
[3]School of Life Sciences, University of Technology Sydney, Sydney, NSW, Australia
[4]Australian Research Council Centre of Excellence for Nanoscale Biophotonics, The University of Adelaide, Adelaide, SA, Australia

A/Professor Lyndsey Collins-Praino
Email: Lyndsey.collins-praino@adelaide.edu.au

This section includes

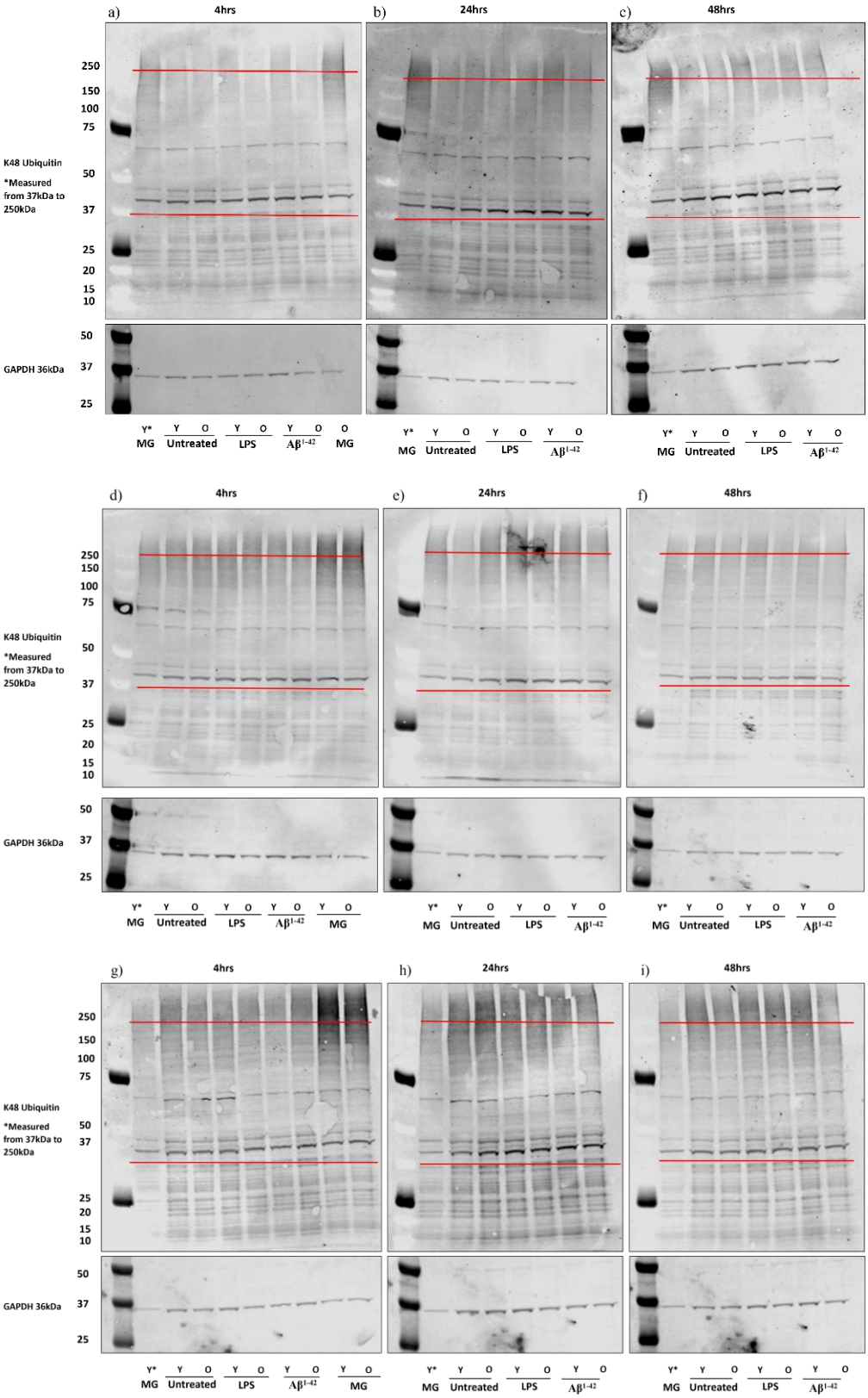
Supplementary Table S6.1
Supplementary Figures S6.1-6.5

Supplementary Table S 6.1 Significant main effects and two-way interaction effects seen for each marker.

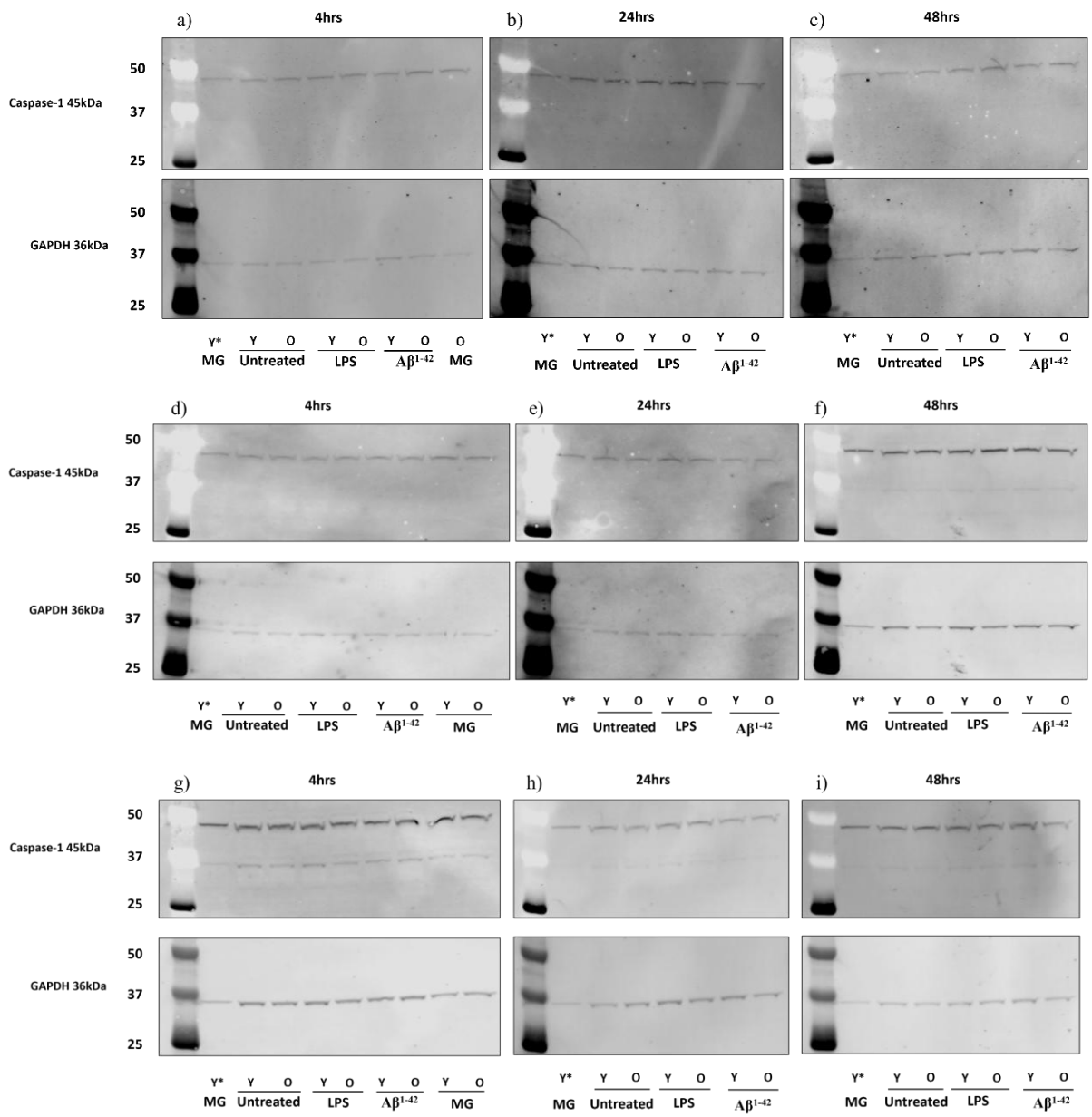
	Age	Treatment	Time	Age:Treatment	Age:Time	Treatment:Time
Metabolic activity	***(F(1,59)=10.377, p=0.002)***	***(F(6,59)=7.788, p=<0.0001)***				
IL-6	***F(1,39)=24.519, p= <0.0001***	*F(3,39)=29.812, p= <0.0001*	*F(2,39)=5.359, p= 0.008*	*F(3,39)=19.216, p= <0.0001*		*F(4,39)=4.882, p= 0.002*
TNF	***F(1,40)=184.638, p= <0.0001***	*F(3,40)=1009.869, p= <0.0001*	*F(2,40)=128.976, p= <0.0001*	*F(3,40)=57.293, p= <0.0001*	*F(2,40)=9.527, p= 0.0004*	*F(4,40)=134.307, p= <0.0001*
Oxidative stress			*F(2,39)=4.283, p= 0.020*			
Antioxidant capacity			*F(2,40)=5.326, p= 0.008*			
Phagocytosis		***F(3,40)=4.565, p= 0.007***				*F(4,40)=3.121, p= 0.02*
Caspase-1		***F(3,29)=7.864, p= 0.0005***	*F(2,29)=11.954, p= 0.0001*			
K48 ubiquitination (WB)		***F(3,29)=37.012, p= <0.0001***				
K48 ubiquitin intensity	***F(1,222)=5.663, p= 0.018***				*F(2,222)=9.182, p= 0.0001*	
K48 ubiquitin spots	***F(1,222)=25.537, p= <0.0001***	***F(5,222)=4.099, p= 0.001***		*F(5,222)=2.577, p= 0.027*		
Aβ intensity		***F(2,112)=25.022, p= <0.0001***	*F(2,112)=29.754, p= <0.0001*			*F(2,112)=3.262, p= 0.042*

Aβ spots	***F(1,112)=8.755, p= 0.003***	***F(2,112)=46.499, p= <0.0001***	*F(2,112)=5.736, p= 0.004*	*F(2,112)=8.025, p= <0.0001*		
Aβ spots in ubiquitin area	***F(1,112)=7.615, p= 0.006***	***F(2,112)=29.246, p= <0.0001***	*F(2,112)=8.227, p= 0.0004*	*F(2,112)=4.855, p= 0.009*		
Cell area	***F(1,224)=225.344, p= <0.0001***	*F(5,224)=17.741, p= <0.0001*	*F(2,224)=20.020, p= <0.0001*		*F(2,224)=8.761, p= <0.0001*	
Cell roundness	***F(1,224)=556.891, p= <0.0001***	*F(5,224)=62.588, p= <0.0001*	*F(2,224)=7.623, p= <0.0001*	***F(5,224)=5.297, p= <0.0001***		*F(6,224)=3.184, p= 0.001*
Nucleus area	***F(1,224)=68.305, p= <0.0001***	*F(5,224)=9.635, p= <0.0001*	*F(2,224)=14.537, p= <0.0001*		*F(2,224)=3.916, p= 0.021*	
Nucleuss:cell ratio	***F(1,224)=320.2, p= <0.0001***	*F(5,224)=24.169, p= <0.0001*	*F(2,224)=12.737, p= <0.0001*	*F(5,224)=3.246, p= 0.007*	*F(2,224)=24.523, p= <0.0001*	*F(6,224)=6.268, p= <0.0001*
Process number		*F(5,222)=3.006, p= 0.012*	*F(2,222)=4.964, p= 0.007*		*F(2,222)=5.777, p= 0.003*	*F(6,222)=3.508, p= 0.002*
Process length		*F(5,222)=2.994, p= 0.012*	*F(2,222)=5.090, p= 0.006*		*F(2,222)=5.809, p= 0.003*	*F(6,222)=3.562, p= 0.002*
Number of branches		*F(5,222)=2.824, p= 0.017*	*F(2,222)=4.777, p= 0.009*		*F(2,222)=6.055, p= 0.002*	*F(6,222)=3.416, p= 0.003*

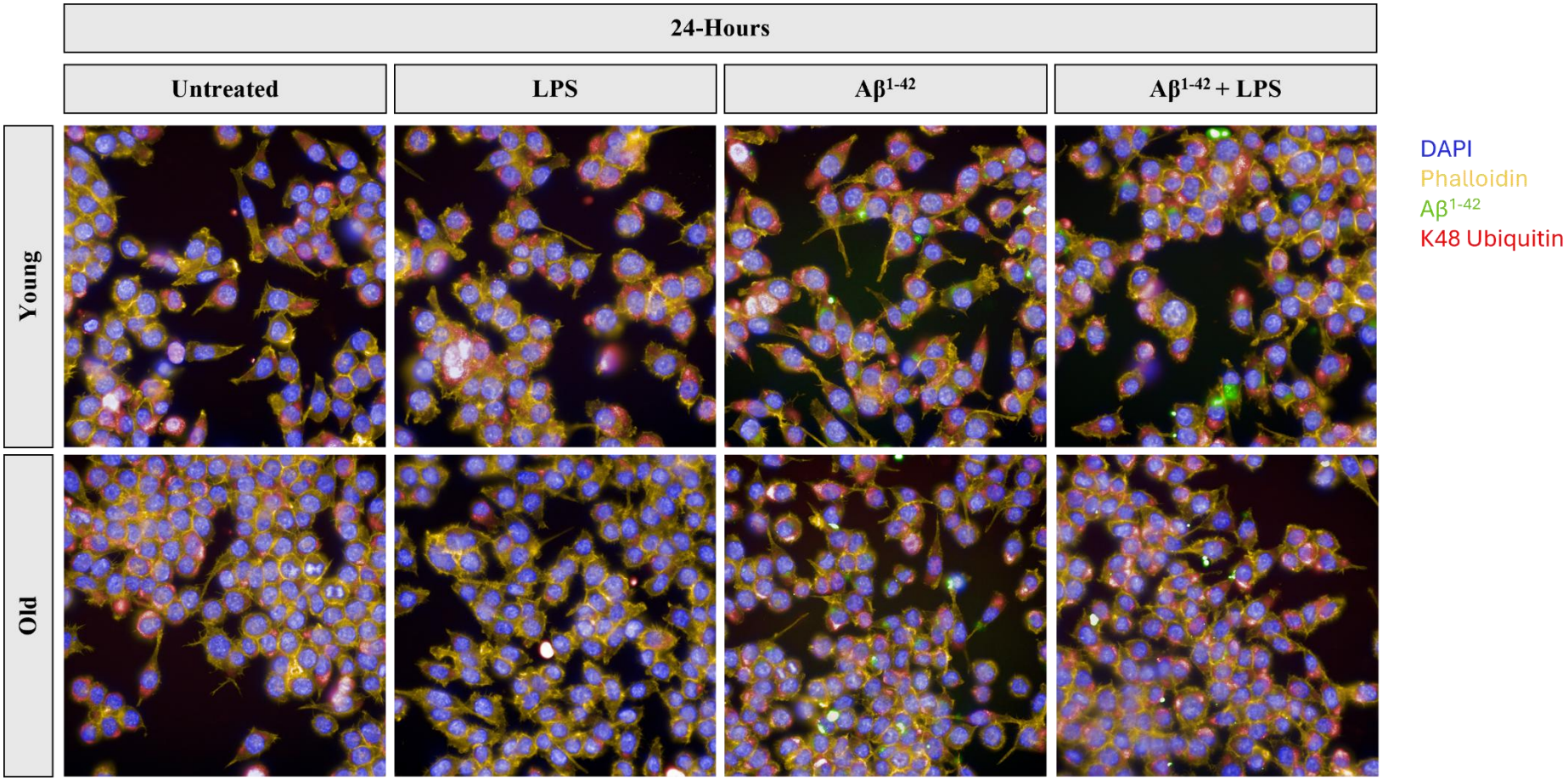
Any three-way interaction effects are presented in the main text. Only significant effects (p=<0.05) are presented in this table. Bolded effects are also presented in the main text.



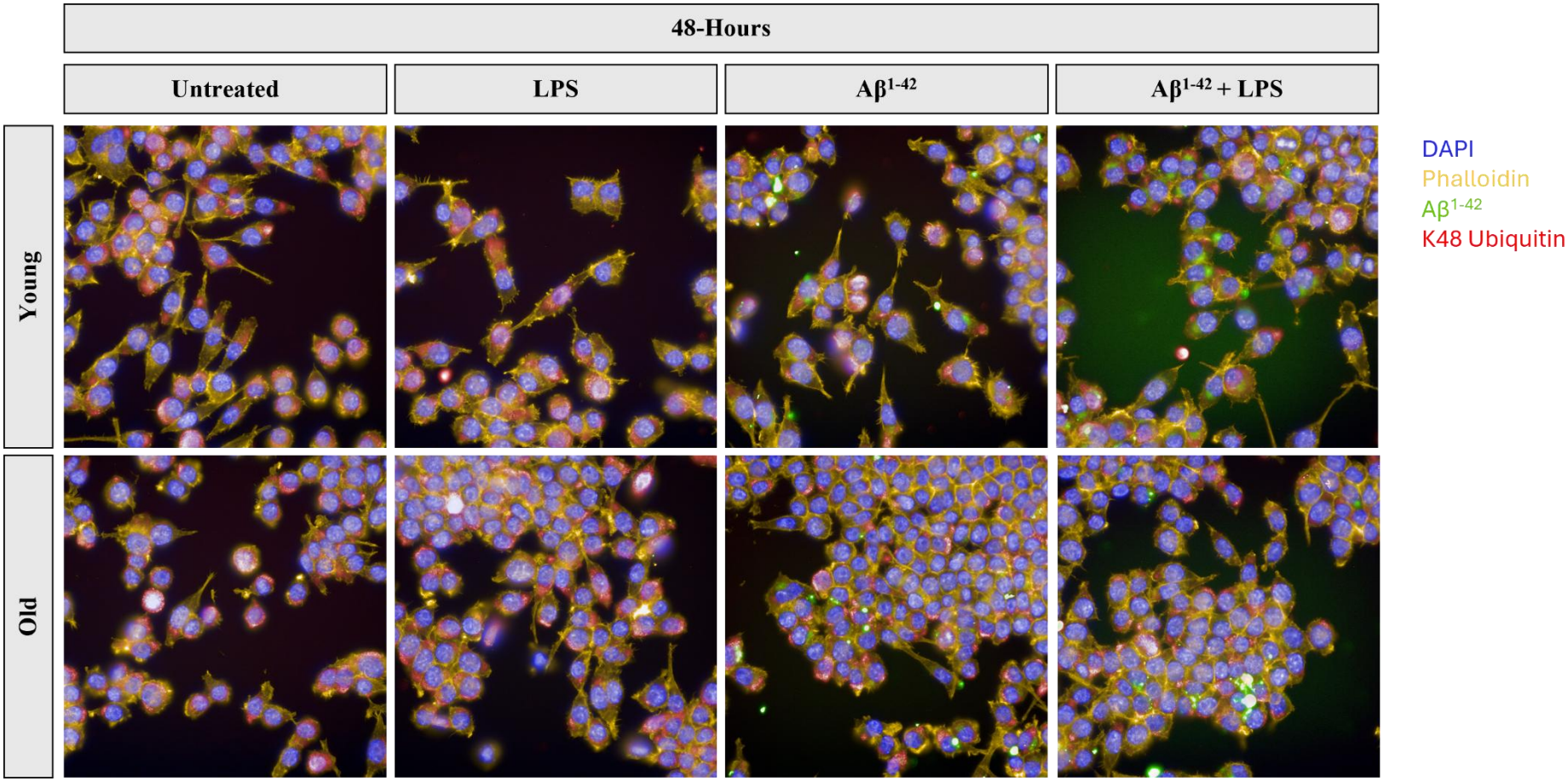
Supplementary Figure S 6.1 Western blot replicates of K48-linked ubiquitination. a-c) samples from replicate 1, d-f) samples from replicate 2, g-i) samples from replicate 3. Blots were analysed using Empiria studio. K48 measurement was performed using signal from 37 kDa to 250 kDa shown by red lines on figure above. Signal was calculated as relative amount compared to the GAPDH signal for each sample and normalized to the control sample in lane one of each blot (young MG132* treated sample).



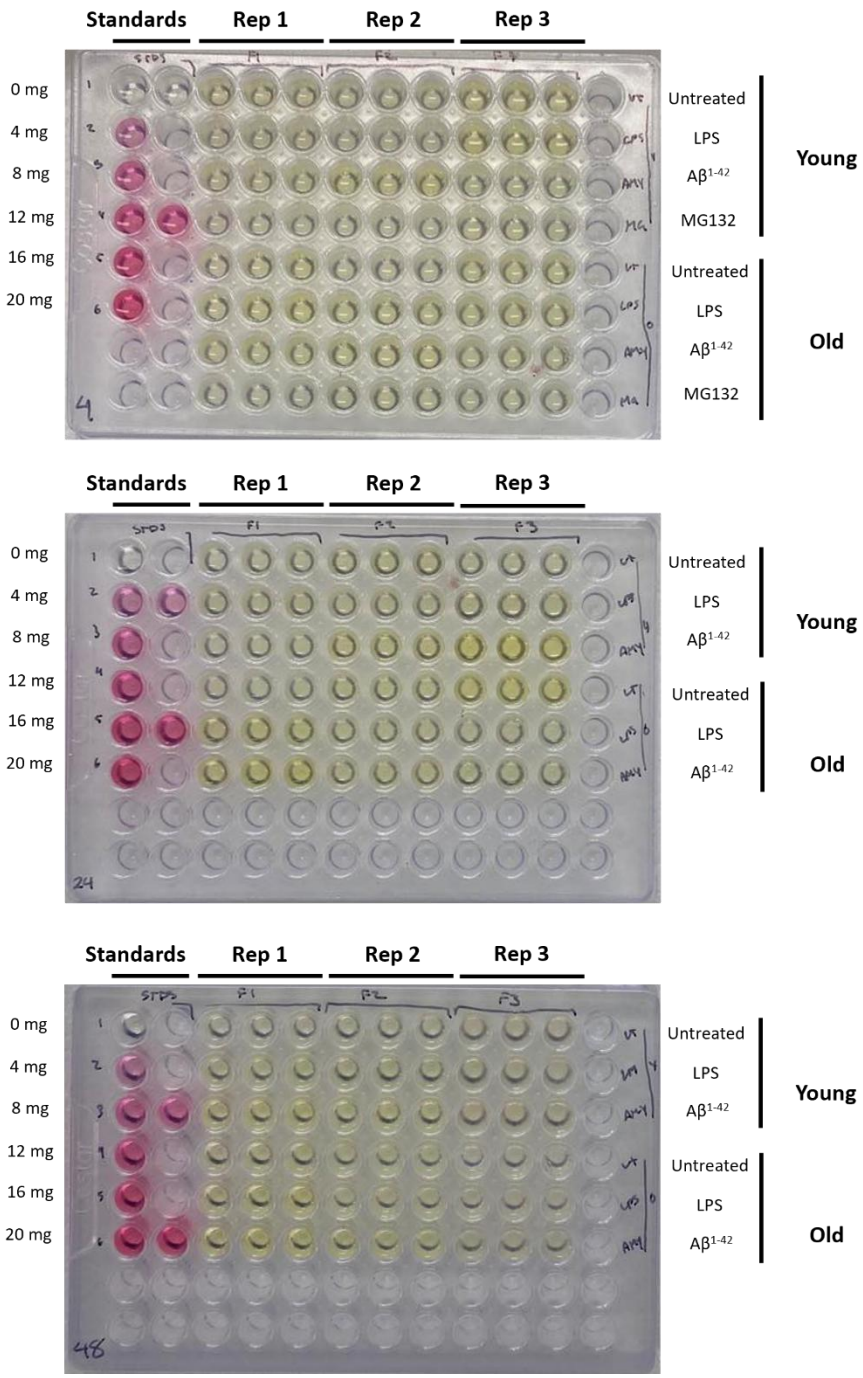
Supplementary Figure S 6.2 Western blot replicates of Caspase-1. a-c) samples from replicate 1, d-f) samples from replicate 2, g-i) samples from replicate 3. Blots were analysed using Empiria studio. Caspase measurement was performed using signal from 45 kDa. Signal was calculated as relative amount compared to the GAPDH signal for each sample and normalized to the control sample in lane one of each blot (young MG132* treated sample)



Supplementary Figure S 6.3 Representative images of immunofluorescent staining in BV2 cells after 24-hour incubation with treatments. Cells were stained with DAPI (blue), phalloidin (yellow), and anti-K48 ubiquitin (red). FITC tagged $A\beta^{1-42}$ was used to treat cells and can be seen in green. Images were taken at 40x magnification



Supplementary Figure S 6.4 Representative images of immunofluorescent staining in BV2 cellsafter 48-hour incubation with treatments.Cells were stained with DAPI (blue), phalloidin (yellow), and anti-K48 ubiquitin (red). FITC tagged $A\beta^{1-42}$ was used to treat cells and can be seen in green. Images were taken at 40x magnification



Supplementary Figure S 6.5 Photographs of MDA assay plates demonstrating intensity of colour change relative to standards. Visual differences in intensity of yellow colour change were observed however this did not result in statistically significant change as per data in the main text

Chapter 7 : Thesis General Discussion and Future considerations

7.1 Research Summary and Significance

Age-related Neurodegenerative Diseases (NDs), such as Alzheimer's Disease (AD) and Parkinson's Disease (PD), have become a mounting global issue driven largely by population ageing. Due to scientific advances, life expectancy increased by 9.8% between 2000 and 2019 (Cao and Ho, 2020), and the number of people in the >60 age group is further expected to double by 2050 (Rudnicka et al., 2020). AD and PD are typically diagnosed around 60-65 years of age (Oliveira et al., 2017) and thus increasing age is the number one risk factor for developing these diseases. These trends in global ageing predict an increase in the percentage of the population in the most at-risk age group for age-related NDs and thus a rise in cases, emphasising the need for improved treatment and disease management. Currently, treatment of NDs is symptom focused, with a clear lack of effective disease modifying treatments (Kalia and Lang, 2015; Yiannopoulou and Papageorgiou, 2020). Translation of ND treatments from bench to bedside is notoriously slow, exemplified by the failure of 99.6% of clinical trials for AD (Asher and Priefer, 2022). This poor translation is contributed to by the lack of appropriate models for disease conditions, specifically, the oversight in inclusion of age in pre-clinical models (Carr et al., 2024; Sun et al., 2020). Accounting for age is critical to understand the effect of potential treatments on the aged brain, where there are likely to be differences in immune responses and treatment efficacy. Aged individuals report adverse drug reactions twice as frequently as younger patients (Beijer and de Blaey, 2002) and have alterations in drug metabolism which may alter treatment efficacy (Kinirons and O'Mahony, 2004), further solidifying the importance of considering age in research models of NDs. Despite a decade of publications calling for age to be incorporated into ND research (Farooqui and Farooqui, 2009; Johnson, 2015; Sun et al., 2020; Wallace and Howlett, 2016), this is still lacking, due to both the difficulty in replicating such complex interactions *in vitro,* and the poor characterisation of brain ageing at the cellular and molecular levels (Carr et al., 2024). Understanding and replicating the brain's immune response is particularly critical in evaluating treatment safety and feasibility. Microglia are the main immune cell in the brain and are important in both initiating and regulating the central nervous system (CNS) immune response (Ginhoux et al., 2013). Despite their

importance in maintaining a healthy CNS, however, beyond a general increase in pro-inflammatory phenotypes with increased age, microglial ageing is largely uncharacterised.

In the current PhD thesis, the research presented aimed to address the gaps in our knowledge of microglial ageing, by conducting a comprehensive analysis of microglia across ageing and in various pre-clinical models. In the first instance, a comprehensive review of models of ageing in NDs was conducted to understand at which stages of research age can be better incorporated **(Chapter 1)**. This review made specific recommendations around including ageing at both *in vitro* and *in vivo* stages of research, further suggesting that before age can be widely included in ND research, models of the aged brain itself need to be improved. A second review of the literature was then conducted to focus specifically on how microglia change with age beyond inflammatory phenotypes and with reference to established hallmarks of ageing (López-Otín et al., 2023) **(Chapter 2)**. The findings of this review suggested that although the inflammatory changes in microglia with age have been well studied, investigation of other molecular hallmarks of ageing, including genomic instability, proteostasis, and alterations in inter- and intra-cellular signalling, in microglia is scarcely conducted and inconsistently reported. Additionally, this review highlighted that what is known about changes in these markers comes largely from mouse models and studies using post-mortem human tissue, the latter of which often include a small sample size and no young healthy comparison group, making it difficult to conclude which alterations are related to physiological ageing specifically. Identification of these gaps in the literature highlighted weaknesses in how microglial ageing is currently investigated, which we then aimed to fill in the subsequent chapters. In the first instance, due to the fact that that methods to count and characterise microglial activation need improvement, we used a novel software platform (Halo Microglial Activation Module, Indica Labs, Albuquerque, New Mexico, USA) to quantify and characterise microglia in comparison to both the gold-standard manual assessment and an established protocol using open-source software (ImageJ) **(Chapter 3)**. The results suggested that the Halo platform performs similarly to other automated methods and is comparable to manual assessment when it comes to quantifying microglia. However, when assessing activation, in comparison to manual assessment, both Halo and ImageJ do not classify microglia accurately relative to manual counting. This research

further highlights the inaccuracy of classifying microglia as activated based on an amoeboid appearance and suggests that a detailed consideration of how microglial morphology relates to functional state is needed at a single cell level. Next, a cross-species comparison of microglial ageing was conducted using archival rat and sheep tissue **(Chapter 4)**. This research aimed to fill two gaps identified in previous chapters, firstly to conduct a more detailed investigation into microglial morphological changes with age on a single cell level, and second, to gain insight into how translatable results from small animal models are to a larger gyrencephalic brain. Results of this study support the notion that microglial proliferation increases with age, and that they acquire an altered morphological phenotype, characterised by enlarged cell size and elongated processes. These changes were preserved across species; however, the location of these changes differed between the rat and sheep brain, with rat microglia showing changes in the cortex, and sheep microglia changing more in subcortical regions. These differences highlight the importance of gyrencephalic pre-clinical models, which are likely to be more translatable to humans than rodent models due to their similar structure. Additionally, these animals were roughly equivalent to a 55-year-old human, allowing insight into how the microglial response changes at middle-aged timepoints, a critical period for understanding when age-related changes may first begin to manifest. Therapeutic options are limited once neurodegenerative processes are underway, and therefore identifying those at risk for heightened neuroinflammatory responses during this period opens the door for new therapeutic interventions. Unfortunately, we were not able to obtain postmortem tissue from enough healthy young and aged cases in order to allow for investigation of such changes in humans. Thus, given the differences in microglia from lissencephalic rats to gyrencephalic sheep, the next chapter moved into human gene expression data, in order to assess microglial pathways which may be altered during human brain ageing **(Chapter 5)**. Utilising the publicly available Allen Brain Atlas database, this study investigated expression of microglia-related genes across healthy ageing (young controls compared to aged, non-neurologically impaired brains) and assessed if the presence of either AD or history of traumatic brain injury (TBI) influenced these changes. Genes related to microglial cell surface markers were the most altered with ageing, but showed opposing changes between regions, with an increase in these markers noted in the hippocampus of aged individuals across groups and a decrease seen in the temporal cortex (TCx) in a subset of individuals.

Interestingly, changes in the TCx were largely confined to aged individuals with a history of TBI (with the exception of *TMEM119,* which showed a decrease in all aged groups and *TREM2*, which showed a decrease in both the healthy aged and TBI groups), however no differences were observed between ageing, AD and TBI groups, suggesting that disease and injury do not further alter age related microglial changes. Interestingly, in all groups, there was limited changes in innate immune signalling pathways, despite upregulation in *TLR4* expression in aged controls and AD, and in *FYN* expression solely in the AD group, compared to young controls, but no differences in inflammatory cytokine expression. The upregulation of upstream inflammatory pathways without induction of cytokines alludes to other mechanisms at play potentially regulating these pathways and suggests that action of Fyn and TLR4 may should be investigated further during these conditions to understand these changes. Finally, immortalised microglia-like BV2 cells were investigated as a potential model of *in vitro* ageing **(Chapter 6)**. As no particular markers stood out as altered in the previous chapter **(Chapter 5)**, a broad range of markers were assessed. The majority of changes observed in BV2 cells following multiple passages were limited and showed opposing changes to those known to occur with age. The observation of increased aggregation and ubiquitination of administered $A\beta^{1-42}$ suggests that with passage BV2 cells demonstrate altered proteostasis mechanisms, potentially reflecting similar mechanisms observed in microglia during ageing. These results demonstrate that while phenotypic changes do occur in these immortalised cells after 90+ passages, they are not reflective of the aged phenotype more broadly, BV2 cells at high passage instead show a decreased capacity to respond to immune stimulation and should therefore be avoided when conducting screening of potential treatments. Primary microglia, while more reflective of *in vivo* responses, have a limited lifespan in culture which limits the capacity for long term experimentation. Additionally, iPSCs present challenges for ageing research specifically when cells from aged donors, as the induction to pluripotency resets the ageing phenotype observed in the original donor cell (Tang et al., 2017). With this in mind, best efforts should be made to utilise the *in vitro* tools which are currently in widespread use such as immortalised cell lines for which other methods of ageing beyond serial passage, including repeated inflammatory stimulation, genetic modifications and induction of epigenetic alterations, are promising. Taken together, the results of this thesis highlight that ageing in microglia is multifaceted characterised by region- and species-specific changes with age.

The molecular basis of this has thus far been difficult to uncover due to the heavy reliance on rodent models and underrepresentation of large animal research, which may be more translatable to humans. The current literature is lacking in consistency regarding microglial phenotypes themselves and how this presents during ageing. This makes developing more complex models of aged microglia for ND research difficult. Nevertheless, the current thesis highlights a path forward for standardisation and more thorough research in this area to address this critical need.

7.2 The need for consistency in the analysis of microglial morphology in tissue

Morphological assessment of microglia is a staple in studies of NDs, currently done by both classifying microglia based on morphology and assessing molecular markers to gain insight into function (Green and Rowe, 2024). The literature is moving away from simple active/resting classifications of microglia and towards a spectrum of microglial phenotypes encompassing variations in resting functions (surveillant) and activation states (immune activation, disease associated activation or intermediate/transitional states) (Paolicelli et al., 2022). However, there is significant inconsistency in how these states are currently classified and in the morphological nomenclature used between studies (Reddaway et al., 2023). Additionally, various methods to analyse microglia in tissue exist across the literature and the most popular programs are outlined in Table 7.1. The method used can have inherent limitations, particularly when used with inappropriate samples (blurry images for example) and by inexperienced users, both of which can affect the results of the analysis (Green et al., 2022). **Chapter 3** demonstrates the utility of automated methods for quantifying total numbers of microglia, whilst highlighting the inconsistencies between methods when classifying these cells as active/resting. Manual counting of microglia by an experienced assessor was utilised as a benchmark for accurate analysis of microglial number and activation state as it is the current gold standard method within the literature (Gallego and de Gracia, 2016) and was compared to automated analysis on ImageJ and on the novel Halo software platform. Total numbers were comparable to manual quantification; however, a high degree of variability was present for the activation analysis. This suggests that the use of a wide range of automated methods to assess microglial activation states may cause difficulty comparing across

studies. An abundance of programs to assess microglia are currently used across the literature and include using open-source programs, such as ImageJ (Clarke et al., 2021; Khakpour et al., 2022; Young and Morrison, 2018), or specialised software, including Imaris (Althammer et al., 2020; García-Magro et al., 2020) or the Halo platform (Guglietti et al., 2024; Krieg et al., 2023). Each have advantages and disadvantages which are highlighted in Table 7.1 along with further available software to conduct microglial analysis, but the general inconsistency of which programs are used, owing to the different resources available to different research groups (for example the financial barriers to using programs such as Imaris or Neurolucida) is an issue which plagues the field of microglial morphological classification (Reddaway et al., 2023). Indeed, this discrepancy was noted in a 2024 review, which discussed the variability of current methods to assess microglial morphology and warns against comparing results of such analyses across laboratories, as findings are often variable and difficult to reproduce (Green and Rowe, 2024). Additionally, in their 2022 paper, these same authors suggest that classification of microglia by automated methods based on morphology is better conducted at a single cell level, rather than across tissue sections, as whole tissue analysis often fails to capture morphological changes observed at the single cell level (Green et al., 2022). This reflects the current direction of the literature regarding microglial analysis, whereby classification as activated or non-activated is being replaced by grouping cells into phenotypes along a morphological spectrum based on their morphology.

Table 7.1: Features, advantages and disadvantages of popular methods of *in vivo* microglia analysis. Bolded techniques were utilised in the current thesis, cost estimates for Imaris and Neurolucida were obtained through the Q&A section on ResearchGate and other science community forums

Program	Main uses	Accuracy	Cost for setup	Sample compatibility	Ease of use	Support
QuPath (Bankhead et al., 2017)	Multitude of uses • Manual counting • Single cell morphology analysis • Automated analysis • Area quantification • Cell detection and segmentation	Accuracy of automated segmentation analysis depends on: • Method of analysis • Image/stain quality	Free	Compatible with IHC/IF stained tissue of any thickness Supports whole slide imaging	Moderate learning curve Requires scripting knowledge for automated analysis	Strong community and documentation Active online forums
ImageJ/Fiji (Arganda-Carreras et al., 2010; Arshadi et al., 2021)	Highly versatile • Single cell analysis and cell counting • Additional functionality with plugins • Automated analysis	Accuracy of automated segmentation analysis depends on: • Method of analysis • Image/stain quality • Parameters/plugin settings Most plugins/methods widely validated Wide range of protocols make consistency between studies/laboratories difficult	Free	Compatible with IHC/IF stained tissue of any thickness Works with most 2D image formats	Simple for basic processing and analysis Steep learning curve for advanced analysis Requires scripting for automated analysis	Strong community and documentation Active online forums Extensive video tutorials
Cell Profiler (Stirling et al., 2021)	High throughput image analysis • Cell counting and morphology analysis • Batch processing capabilities	Highly validated segmentation Optimisation improves accuracy	Free	Compatible with IHC/IF stained tissue of any thickness Works with most 2D image formats	Moderate learning curve Requires optimisation	Strong community support and documentation
TREES Toolbox (Cuntz et al., 2010)	Advanced branching analysis well suited for single-cell morphology studies	Widely validated topological analysis for neurons and adaptable for microglia	Free	Requires MATLAB Good for 3D confocal imaging data Limited compatibility with IHC/IF without extensive pre-processing of images	Steep learning curve for non-MATLAB users	Limited community support

3D Morph (York et al., 2018)	Detailed 3D morphological analysis • Branching dynamics/ramification • Soma and cell measurements	Validated for 3D morphology Relies on high quality imaging	Free	Compatible with confocal/light sheet microscopy Can handle 3D IF-stained tissue but not IHC Requires MATLAB	Moderate learning curve User friendly	Moderate support available but fewer community resources
Halo (Indica Labs, 2024)	Whole-tissue microglial analysis • Automated cell counting • Morphology metrics	Depends on input parameters and image quality but comparable to manual methods of cell detection	$10,000 - $20,000 USD	Compatible with stained tissue of any thickness • IHC and IF require different modules specific to the stain type	User friendly Minimal training needed for basic tasks	Comprehensive documentation provided with module Responsive technical support No online community support
Imaris (Instruments, 2024)	3D visualisation and analysis • Branching, volume and connectivity	Validated for 3D studies of cells but requires optimised imaging for best results	>$15,000 USD	Works with multiple image formats but best with high-resolution 3D data Not designed for IHC, works best with IF tissue	Steep learning curve Requires training for high level analysis	Strong technical support and user community
Neurolucida (Bioscience, 2024)	Detailed single-cell tracing and 3D reconstruction of cells	Extensively validated	>$20,000 USD	Compatible with most 3D imaging formats Best with confocal and light microscopy data Limited capacity for IHC analysis, fully compatible with IF tissue	Steep learning curve Requires significant training	Strong technical support and documentation

Chapter 2 touches on these phenotypes and their supposed functions; however, these are highly debated and a major issue with this classification is consistency in the use of terms across studies. For example, the terms “bushy microglia” and “hyper-ramified microglia” have been used interchangeably in some studies (Reddaway et al., 2023; Ziebell et al., 2015). Further, the definition of a given morphological phenotype can differ between studies. In line with this, a 2014 review by Ziebell et al., describes both bushy and hyper-ramified microglia as a surveillant state characterised by retracting of processes and thickening in appearance (Ziebell et al., 2015). Contrastingly, a 2017 study investigating microglial morphology in a rat model of neuroinflammation induced by single injection of neuraminidase to the right left ventricle described bushy microglia as having short and poorly ramified processes with swollen cell bodies (Fernández-Arjona et al., 2017). Even more confusingly, a more recent review, focusing on the inconsistencies of microglial analysis, describes hyper-ramified/bushy cells as having an increased process length, volume and branching complexity associated with an intermediate state following activation, citing the above study by Ziebell and colleagues amongst others for this statement (Reddaway et al., 2023). Therefore, it is clear that the field has yet to agree upon a specific definition for each of the recognised microglial phenotypes. Figure 7.1a provides visual examples of what is classified as bushy/hyper-ramified in the above studies which are numbered as study 1, 2 and 3. Notably, although the microglia from study 1 are visually similar to those from study 2, their description in the text using the term hyper-ramified is more similar to the description provided in study 3 which is visually distinct from the microglia in studies 1 and 2. Based on the representative images and descriptions from the studies in Figure 7.1a, the term bushy should be utilised to describe microglia with a large cell body and many shortened/retracted processes, as is pictured in studies 1 and 2. ‘Hyper-ramified’ should refer to microglia with lots of highly ramified, long branching processes, as is pictured in study 3. Additionally, this inconsistency can be seen for the classification of rod and rod-like microglia, which are typically associated with infection or injury (Taylor et al., 2014). A 2021 study by Leyh and colleagues aimed at improving the classification of microglia described rod-like microglia as having a narrow soma and non-planar processes (Leyh et al., 2021). Comparatively, rod microglia have been described in another study by Taylor and colleagues as presenting with a sausage-like soma and describe specific ratios for rod microglia soma (2.5 times longer than wide). This study additionally

suggested that trains of rod microglia with retraction of planar processes 7-days following TBI (Taylor et al., 2014). Further, they describe chains of rod microglia oriented perpendicular to the pial surface of the brain. The provided example of these microglia shows a structural organisation of microglia which is described as unique to rod microglia. Finally, a 2019 review summarising the literature on rod microglia (Holloway et al., 2019) describes them as having absent planar processes and a narrow cell and soma. These descriptions are all similar, describing lack of processes and a narrow soma however the examples given by the 2021 study vary in comparison to the other two as shown in figure 7.1b. The latter review (study 3 under Fig 7.1b) highlights that the description of rod microglia should never include microglia in healthy brain tissue but is only used to describe the rod-shaped cells which form alongside neuronal pathology, in order to definitively distinguish from bipolar microglia in white matter tracts which likely do not exhibit the same functional phenotype (Holloway et al., 2019). Given the suggested unknown but likely important roles of rod microglia in disease and injury repair (Giordano et al., 2021), it is critical that this morphology be consistently classified within the literature and clearly distinguish states of rod microglia (for example a distinguishing classification for the trains of microglia seen in TBI). Additionally, based on the examples presented in Figure 7.1b, the term rod microglia should be utilised to describe microglia with an elongated or 'sausage-like' soma and bipolar processes extending along a single axis. Microglia with an elongated soma but multi-directional or highly ramified processes should not be classified under this term.

It is critical that these morphologies be clearly defined and adhered to in order to be able to compare results across literature. However, such analysis is complicated and a detailed characterisation of microglial morphology alongside functional markers at a single cell level would likely be beneficial in defining a set of criteria for wider application across the literature. Therefore, in **Chapter 4**, we characterised microglial activation based on morphology and conducted single cell morphological analysis using several methods commonly applied using ImageJ throughout the literature. Of note, the specific parameters (i.e. cell size, soma size, process length, number of processes and process complexity) investigated in this chapter are not an exhaustive list, and in order to more fully define characteristics of specific subtypes of microglia, additional analyses should be undertaken. Additional

analysis on ImageJ may include span ratio, dimensionality or spatial distribution analysis, and where possible, 3D reconstruction and analysis would provide more accurate measures (Green et al., 2022; York et al., 2018). For more details on this, see the “Future directions” subsection below.

Overall, although it is unlikely that one method will be agreed upon for all microglia analysis moving forward, laboratory groups should endeavour to be detailed and consistent across studies to promote reproducibility of results. To this end, the field would highly benefit from a detailed research framework of how to consistently classify and assess microglial morphological phenotypes. Further, investigation of microglial phenotype needs to move beyond morphology alone and also focus on associated functional changes.

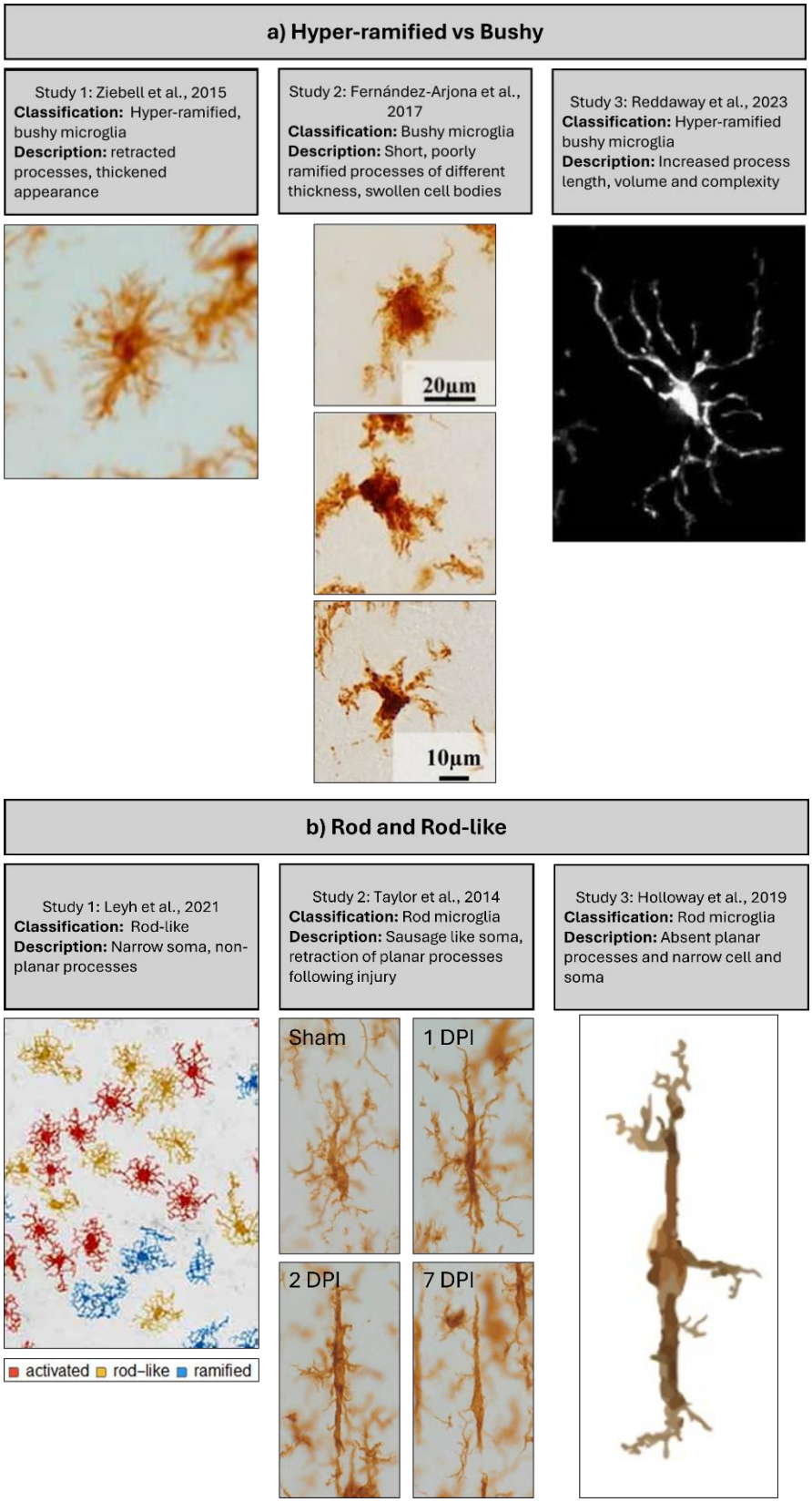


Figure 7.1: Examples of microglia provided by studies highlighting differences in description and visual examples provided by authors. a) bushy/hyper-ramified microglia Study 1: excerpt from (Ziebell et al., 2015) figure 1 panel B. Study 2: excerpts from (Fernández-Arjona et al., 2017) figure 3 panels F, Q and R (top to bottom). Scale bar was not provided on panel Q. Study 3: excerpt from (Reddaway et al., 2023) figure 1 panel D. b) rod and rod-like microglia. Study 1: excerpts from (Leyh et al., 2021) figure 6 panel B. Panel was rotated and shows what was classified as rod microglia in yellow. Study 2: excerpts from (Taylor et al., 2014) figure 2. Study 3: excerpt from (Holloway et al.,

2019) figure 2. Panels were screenshotted and pasted into the current figure, panel labels (a, b, c etc.) were removed to avoid confusion.

7.3 Using multiple methods to assess microglia during ageing

An array of methods to investigate microglial function exist within the literature. In **chapter 2**, the current state of the literature on hallmarks of ageing in microglia was reviewed. Within the literature, there is a reliance on gene expression in microglia in order to identify differentially regulated pathways with age. Specifically, studies often isolate microglia from pre-clinical animal models through flow-cytometry and use RNAseq to assess differential gene expression across experimental groups (DePaula-Silva et al., 2019; Noristani et al., 2017). Specifically, many studies use mRNA expression to determine changes in cytokine release, an indicator of microglial function. In fact, many of the studies which have reported elevated levels of pro-inflammatory cytokines in aged microglia used elevated mRNA expression to come to this conclusion (Henry et al., 2009). In the current thesis, differing methods were used to assess microglia across chapters, including the assessment of markers related to both structure and function. In **Chapter 5**, we used a similar approach of analysing mRNA expression to identify alterations in key microglial pathways in aged human brain tissue. Utilising existing microarray data from the publicly available Allen Brain Atlas (ABA) databases (Allen Institute for Brain Science, 2024a, b), general markers of ageing, microglia and immune signalling pathways were investigated. Moving beyond cytokine expression alone and incorporating the expression of key downstream signalling pathways provided the ability to determine whether cytokine transcription levels were associated with concomitant activation of related immune signalling mechanisms. Interestingly, although this analysis uncovered age-related changes in the pattern of expression of microglial cell surface markers, there was largely no concomitant change in the expression of either inflammatory cytokine genes or relevant immune signalling pathways observed, with the exception of an increase in the hippocampal expression of *TLR4* expression in the healthy aged and AD groups (but not the TBI group) and of *FYN* solely in the AD group. As TLR4 can mediate action of Fyn *via* recruitment of myeloid differentiation primary response protein 88 (MyD88) and TIR-domain-containing adapter-inducing interferon-β (TRIF) to activate downstream pro-inflammatory signalling, the results from this chapter suggest that with ageing alone TLR4 recruitment of Fyn is not altered however in AD, *FYN*

signalling is increased from baseline levels in young controls. Combined with the lack of pro-inflammatory signalling in all groups, this suggests that the pro-inflammatory signalling pathways in microglia are altered, and in order to further understand these changes studies must investigate downstream activity beyond mRNA expression.

Although isolation and study of cellular gene expression provides robust, high throughput data (Sorokin et al., 2020), it is not without limitations. Notably, although increased mRNA expression of a given gene may lead to release of the associated pro-inflammatory cytokine, such release is often dependent on post-translational modifications, as is the case with IL-1β (Schindler et al., 1990), which are in turn dependent on successful activation of relevant signalling pathways (Shebl et al., 2010). Thus, there may be a disconnect between mRNA expression and the actual functional readout (i.e. cytokine release on the protein level) of microglia. Thus, in **Chapters 4** and **6**, we aimed to move beyond gene expression to study alterations in microglia at the molecular level. Specifically, in **Chapter 4**, a single cell approach was taken by isolating microglia from regions of interest that were previously used for cell counts and conducting a series of analyses using ImageJ. This provides a more detailed insight into the morphology of microglia; however, as noted above, changes in microglial morphology should not be used as the sole metric of microglial activation, but instead as a proxy marker to guide further analysis. For example, an amoeboid morphology is associated with activation (Reddaway et al., 2023), but may also reflect a cell undergoing proliferation (Vidal-Itriago et al., 2022). Thus, simply classifying microglia as 'activated' does not provide any insight into the specific functional phenotype of those microglia.

In order to overcome this, studies using microglial morphology should also be paired with assessment of objective markers of microglial function such as CD206 or IL-10 for anti-inflammatory activation and MHCII or CD68 for pro-inflammatory activation (Jurga et al., 2020). A review of markers of specific microglial phenotypes has been recently published and summarises both pro- and anti-inflammatory markers of microglia (Jurga et al., 2020). In **Chapter 4**, we initially intended to analyse MHCII as a marker of microglial activation. However, we experienced difficulties optimising MHCII antibodies for these datasets and financial constraints prevented this from being further explored within the timeframe of the thesis. Given these challenges, we instead chose to utilise Ki67 to assess how

changes in microglial numbers related to the proliferative state of the population. While an increase in Ki67 was observed in both rat and sheep brain tissue, increases in microglial population were only seen in sheep. The increase in proliferation noted in the rat tissue, in the absence of a concomitant change in absolute microglial numbers, could be due to a number of events occurring within the population at this time. For example, increased cell death may occur in conjunction with increased proliferation, leading to a stable microglial population with high replicative activity (Askew et al., 2017). In order to assess this, Ki67 analysis could be paired with assessment of apoptotic markers, such as cleaved caspase-3 or cytokeratin-18 (Ward et al., 2008), or a terminal deoxynucleotidyl transferase dUTP nick end labelling (TUNEL) assay (Mitsui et al., 2023), in order to assess whether cell death may be occurring in these regions, an outcome that is unlikely, given the age of the animals and lack of any gross tissue pathology. Further, it would be beneficial to double label cells with both Ki67 and markers of microglial activation (e.g. MHCII), in order to assess whether proliferating microglia also show a pro-inflammatory activation state. While this was our original intention, it was unfortunately not able to be achieved due to the methodological limitations noted above. It would also be beneficial to study the phagocytic capacity of these microglia *in vivo* using techniques such as flow cytometry to measure microglial uptake of fluorescently labelled pathological proteins (e.g. amyloid beta (Lau et al., 2021; Murinello et al., 2016)) or dual colour imaging of microglia and apoptotic neurons (Kamei and Okabe, 2023), Given the archival nature of formalin-fixed paraffin-embedded (FFPE) tissue available for the current analysis, however, such investigations were not feasible. Further, future studies should directly assess how well age-related changes observed at the structural/functional protein level are reflected in mRNA gene expression data.

7.4 Assessment of microglial ageing across species and models

As discussed in **Chapter 1** (Carr et al., 2024), ageing must be incorporated at each stage of the research pipeline. Interpretation of results should then take species specific differences into account when assessing the translation of results. Cross-species comparisons are critical to understand how changes seen in animal models reflect those seen in humans (Geirsdottir et al., 2019). Humans and mice share ~90% of their genes (Paigen, 1995), however differences in immune systems have been noted and

summarised by Mestas and Hughes (Mestas and Hughes, 2004), including differences in TLRs and expression of T cell MHCII. In a study comparing the mouse and human neuroinflammatory responses the brain, 58% of cytokine interactions have been found to be unique to humans (Kodamullil et al., 2017). These differences highlights that it is important to consider how changes seen in animal models replicate those seen with physiological ageing in humans. Currently, however, our understanding of the phenotype of aged microglia in humans is lacking. **Chapter 2** highlights that the majority of our knowledge on this topic is drawn from mouse and rat models, which may differ from microglial ageing in humans. Aside from the major neuroanatomical differences between rodents and humans (lissencephalic vs gyrencephalic, size and, weight), differences in neuroimmune responses are prominent. Therefore, a major aim of the current thesis was to assess microglial ageing phenotypes across *in vivo* pre-clinical models.

A comprehensive comparison of microglia across 18 different species has previously been conducted in a landmark 2019 paper by Geirsdottir and colleagues, which demonstrated that parenchymal microglia display a largely conserved morphology across evolution, with similar dendrite length, number of branching segments, terminal points and volume observed between humans and multiple other species, including both rodents and sheep (Geirsdottir et al., 2019). Further, single cell RNA-seq across a subset of species showed that the expression of a core set of microglial genes is mainly conserved from rodents to humans. Nevertheless, some differences were noted, with humans having greater heterogeneity in microglial phenotype (as opposed to most species, which showed a dominant transcriptional state), as well as differences in several groups of genes (e.g. DNA repair, complement, phagocytosis) in rodents compared to primates. As this study did not incorporate an investigation of the changes that occur with microglial ageing, however, in **Chapter 4**, we assessed changes in microglial morphology and proliferation in two species commonly used in neurological research- rate and sheep. A key difference between these species is that sheep have gyrencephalic brains that are similar in organisation to humans, while rats have lissencephalic brains that contain a lower proportion of white matter (Sorby-Adams et al., 2018). In line with this, we found that sheep and rats showed differential vulnerability of brain regions to microglial change with ageing, with changes appearing in the cortex in

rats as opposed to the subcortical regions in sheep. In rats, the majority of changes at the oldest timepoint occurred in microglia from the cortex and hippocampus, including decreased activation and increased proliferation of microglia. In contrast, sheep exhibited limited changes in the cortex, with microglial proliferation being the only significant difference in this region, while morphological changes were instead localised to the striatum, suggesting that this region may be particularly vulnerable to the effects of ageing in this large animal model. These morphological changes included an increase in cell area, soma area, which potentially indicates a shift toward a more reactive state, although an increase in branch length was also noted. Additionally, we observed changes in the sheep hippocampus specifically in the dentate gyrus, where a decrease in total numbers and an increase in proliferation was observed. This change is consistent with results from the literature showing localised microglial change in the dentate gyrus rather than other hippocampal regions in both rodent (Long et al., 1998) and human studies (Bachstetter et al., 2015). In rats, in addition to the morphological changes noted in sheep, decreases in branch number and complexity were also seen, further supporting a transition towards a more activated state. These findings highlight how different brain regions may be differentially vulnerable to microglial ageing across species, emphasising the importance of considering brain anatomy and function in cross-species studies. Additionally, this highlights that microglial morphology is highly diverse between both regions of the brain and between species, and this is critical to consider when attempting to compare activation states defined by morphology as they will likely lead to differential results.

The findings of **Chapter 4**, however, need to be interpreted in the light of several limitations. Firstly, the lack of female animals in this cohort should be noted, as across the literature, changes in microglial responses are consistently observed in studies of female, but not male, rats (Pelvig et al., 2008; Perkins et al., 2018; Viana et al., 2013). This effect is seen more broadly in neuroinflammation in general, where females have a more robust immune response to inflammatory stimuli (Bekhbat and Neigh, 2018). Thus, sex is an important factor to consider when investigating microglial changes with age; however, due to the use of archival data from male rats, this was limited in the current study. Second, the age of animals could explain some of the variation compared to the literature. Rats at 19 months were used in

Chapter 4, whereas studies typically look at aged rats 23 months and beyond (Perry et al., 1993; Vaughan and Peters, 1974; Viana et al., 2013). The timepoint assessed here is thus more reflective of a human around 55 years old, rather than an older adult, which the literature more typically defines as beyond 60 (Nations, 2024) although some studies suggest this should be increased to beyond 70 due to increased health and lifespan (Jacobs et al., 2012; Orimo et al., 2006). Similarly, the oldest timepoint in the sheep cohort was 6 years, also equivalent to around 50-60 in humans. Thus, it may be that our results underestimate the full impact of age on microglia and are instead more reflective of changes seen during middle-age. This suggests that our results do not truly represent an aged phenotype of microglia but rather the dynamic nature of these cells at middle-aged timepoints. Future work should seek to replicate our analyses in tissue collected from older animals, but we acknowledge the difficulty in obtaining tissue from animals within these age ranges, particularly for groups where access to aged rodent colonies is not readily available and studying large animals such as sheep presents additional financial difficulties (Mitchell et al., 2023). Further, it is difficult to understand whether the changes that we observe here are reflective of changes seen in middle-aged humans, as it is challenging to obtain human postmortem tissue from healthy older adults within this age range (Rush et al., 2024).

Overall, microglial ageing in pre-clinical animal models is difficult to assess relative to human microglial ageing. Despite these limitations, which are elaborated on further below, in **Chapter 5**, publicly available microarray data was utilised to assess the gene expression of microglia-related genes in the cortex and hippocampus of young (24-57-years-old) versus older adults (78-100-years-old). This analysis revealed distinct genetic profiles in the hippocampus compared to cortical regions in all groups assessed, but this as most clear in healthy, age-matched AD-patients and age-matched individuals, perhaps due to the reduced sample size and imbalance of sex (5M:1F) in the young control group. Notably, the gene expression levels of several cell surface markers of both total and activated microglia were increased in the hippocampus of all three aged groups, regardless of whether they had a history of AD or TBI. Conversely, these markers were decreased in the temporal cortex, particularly in the TBI group. This contrasted with the results seen in **Chapter 4**, where decreases were noted in both the cortex and hippocampus for the percent of activated microglia in the oldest group (i.e. 19-months) of rats, with

a decrease in total number of microglia seen in the dentate gyrus in the oldest group (i.e. 6 years) of sheep. At the single cell level, as noted above, no changes were seen in microglial morphology in the hippocampus in the oldest age group for either the rats or sheep, although an increase in soma area and branch length, and a decrease in the number of branches and branching complexity, was noted in the cortex of 19-month-old rats. While this may suggest that the age-related changes seen in these pre-clinical models are not reflective of those seen in humans, these findings should be interpreted with caution and in the context of the limitations outlined above. Specifically, while the median age of the individuals included in the analysis in **Chapter 5** was ~89 years old, as discussed above, the sheep and rat tissue used for the current analyses were sourced from middle-aged animals (~55 years of age). Instead, it would be more appropriate to compare the results of the ABA analysis to those obtained from older animals, but this was unfortunately not possible for the current work. Additionally, as the rodent cohort included only male animals, it can be difficult to directly compare the results to those obtained for either the sheep cohort in **Chapter 4** or the human data from **Chapter 5**, given the known sex differences in immune response (Pelvig et al., 2008; Perkins et al., 2018; Rozovsky et al., 1998; Viana et al., 2013). Additionally, the number of samples was low for all cohorts of interest, particularly the young healthy control cohort in the ABA analysis in **Chapter 4**, so results may have been influenced by reduced statistical power. Further, in the ABA analysis, we were confined to analysis of brain regions available in that dataset (namely, the hippocampus and cortex) and were not able to analyse other regions of interest, such as the striatum, which may show age-related change based on the sheep data in **Chapter 4**. Previous literature has demonstrated specific ageing changes in the striatum of human brains using MRI assessments undertaken 5 years apart. It was found that atrophy of the caudate nucleus and putamen occurred with age and interestingly the globus pallidus remained stable (Raz et al., 2003). Further, in C57Bl/6J mice, the caudate/putamen region showed the most pronounced decreases in D2 receptors, measured by decreased binding of the positron emission tomography (PET) tracer [^{11}C]Raclopride, when assessed longitudinally at 12-, 18- and 24-months-old (Giacobbo et al., 2022). These findings highlight the striatum as an area of interest to assess microglia with age, particularly in understanding the potential susceptibility to change in this region during PD (Medina-Luque et al., 2024). Given the links between microglia driven neuroinflammation in the striatum in PD

(Imamura et al., 2003; Zhang et al., 2024), understanding how microglial ageing may contribute to striatal vulnerability is critical. Studies should therefore aim to include the striatum in microglial analysis moving forward for histological, genetic, and molecular analyses, as currently there is little consideration of this region with regard to microglial ageing.

The combination of pre-clinical and human data throughout this thesis demonstrates how these methods can complement one another to enhance our understanding of microglial ageing. Given the similarities between the human brain and the sheep brain in terms of structure and organisation, it would be expected that they would show similar patterns of change with regard to where these changes first emerge. Indeed both, **Chapters 4** and **5** highlight subcortical regions, such as the hippocampus and striatum, where microglia seem to be particularly vulnerable to changes with age in gyrencephalic brains. These findings highlight the value of an integrated approach using multiple models and species to better understand the complexities of microglial ageing and its implications for NDs.

7.5 The effect of injury on ageing phenotypes

It has been proposed that injury and disease can have an accelerating effect on ageing mechanisms. Specifically, TBI is thought to accelerate brain ageing, with a single TBI after age 60 accelerating brain ageing by approximately 10 years (Amgalan et al., 2022). Pre-clinically, TBI induced by a controlled cortical impact (CCI) in male C57BL/6 mice leads to accelerated ageing in microglia which persists up to 1-year post injury in 18-mo mice (Ritzel et al., 2023). The notion of TBI as accelerated brain ageing suggests a potential mechanism to explain the increased risk of developing NDs following a TBI (Fann et al., 2018; Gardner et al., 2023) as age is the number one risk factor for developing an ND (Oliveira et al., 2017). Additionally supporting the link between accelerated ageing and ND development, ageing as measured by loss of electrical connectivity, has been observed in the early stages of AD in mouse models (Leparulo et al., 2022). These studies highlight the potential links between two major risk factors of NDs, TBI and ageing, which warrants further investigation. In the current thesis, **Chapter 5** sought to characterise changes in gene expression not only in ageing, but also in AD and TBI. As described above, the hippocampus and cortex displayed a unique signature across all three aged groups in comparison to young controls, with almost no significant differences noted between the aged groups

for any marker assessed. Further, contrary to our expectations, AD did not have a significant effect on the expression of microglia-related genes beyond those seen with ageing itself in either cortical or hippocampal regions. While this may seem surprising, several factors within the cohorts may provide an explanation for this. Firstly, approximately 50% of the AD cohort also had a history of TBI which confounds results and limits interpretation of data. Recent publications have highlighted the importance of accounting for history of TBI when investigating AD (D'Souza et al., 2024) which unfortunately was not possible in the current thesis in order to maintain statistical power. Further, the young cohort had a large age range, low numbers and only a single female case. This inherently limits the interpretation as microglia during early adulthood and middle-age are known to be diverse and dynamic. This limitation reflects a larger difficulty in obtaining young control tissue for human post-mortem work, which has been expanded on previously in the current chapter. Interestingly, however, in the TBI group, analysis of differentially expressed genes revealed decreased expression of microglial cell surface marker genes for both total and activated microglia in the temporal cortex compared to young controls, effects that were largely not seen in either the aged controls or in AD. Additionally, *TMEM119* was significantly decreased in the temporal cortex in TBI brains compared to AD and aged control brains. Notably, however, no changes were seen to support that accelerated ageing in the TBI group, with the ageing suppressor gene, *Klotho*, showing significant increases in the hippocampus and decreases in the cortex across all three groups. Klotho is a relatively newly investigated gene target for AD, with only 104 PubMed search results since 2009 for "Klotho and Alzheimer's disease" and has not been previously investigated in TBI. Therefore, the mechanisms behind these region-specific changes are difficult to uncover as many of the current studies investigate the neuroprotective effects of Klotho as an AD treatment rather than investigating regional expression of Klotho itself. However, given the previously demonstrated protective capabilities of Klotho on cognitive deficits in mice (Zeng et al., 2019), the results seen in **Chapter 5** may be reflective of a compensatory mechanism in an attempt to exert neuroprotection on the hippocampus, a particularly vulnerable brain region (Colasanti et al., 2016; Davidson and Stevenson, 2024; Jung et al., 2022). Taken together, the results of this analysis suggest that age itself is the largest contributor to changes seen microglial expression, even in the face of injury or underlying pathology, further emphasising the need to account for ageing when modelling NDs.

While the other chapters in this thesis did not directly assess this potential interaction between disease and ageing on microglial phenotype, in **Chapter 6** we investigated whether "ageing" in our BV2 model was associated with changes in response to amyloid-beta stimulation or in alterations in amyloid-beta uptake. The results of these investigations have potential implications for AD, given the critical role of amyloid beta aggregation in that condition (Hampel et al., 2021). While no effect of age was observed on BV2 phagocytic capacity, dysregulated proteostasis was seen in $A\beta^{1-42}$ treated cells, specifically increased aggregation of $A\beta^{1-42}$ was observed and increased ubiquitinated $A\beta^{1-42}$ aggregates in the aged cells. This suggests that in the presence of pathology, aged microglia do not correctly degrade pathological proteins. Given that increased passage number did not fully replicate the aged phenotype in immortalised BV2 cells, however, future work should seek to replicate these experiments in an alternative model, such as a model of repetitive inflammatory stimulation which is expanded on below in the "Future Directions" section, in order to more fully understand how increased age may interact with presence of disease-related pathology to alter microglial phenotype. Further, future work should incorporate the investigation of additional pathological proteins known to be implicated in NDs, such as hyperphosphorylated tau (AD (Gong and Iqbal, 2008) and PD (Zhang et al., 2018)), alpha synuclein (PD (Stefanis, 2012)) and TDP43 (motor neurone disease (Suk and Rousseaux, 2020)), to assess if the impact on microglial phenotype differs as a function of specific proteins. Similarly, the archival tissue used in **Chapters 3** and **4** was sourced from several larger studies investigating the effects of TBI in 12-month-old rats (**Chapter 3**) and stroke in 15- and 18-month rats and in aged sheep, with both TBI and stroke previously, shown to be associated with increased risk of dementia development (Fann et al., 2018; Gardner et al., 2014; Kuźma et al., 2018) **(Chapter 4)**. As the focus of this thesis was primarily on the effects of ageing, we elected not to include injury comparison groups for the cross-species comparison in **Chapter 4**. Future work, however, could assess whether injury interacts synergistically with age to exacerbate effects on the microglial phenotype and plays a role in either perpetuating worsened functional outcomes post-injury or increasing risk of ND development. This would be in line with the literature suggesting that TBI is associated with accelerated brain ageing (Amgalan et al., 2022; Ritzel et al., 2023), as discussed above, as well as with studies supporting that age is known to increase the risk of stroke (Rajati et al., 2023) and adversely affect stroke outcomes (Yoo et al., 2020).

7.6 Investigating the untapped potential of immortalised cells for ageing research

In ageing and ND research, *in vitro* studies are critical in understanding the brain in further detail than can be achieved through animal models alone. Although complex *in vitro* models of the brain are in development, they are not widely available at many research facilities. In searching for ways to incorporate ageing into *in vitro* ND research, for now, we should seek to maximise those tools which are most widely available and in use, until the technology develops to age more complex *in vitro* models, such as brain organoids. Previously, ageing *in vitro* has been conducted using primary cells either isolated from aged donors or cells aged over time in culture, often referred to as Days *In Vitro* (DIV). Primary cell use offers many advantages, including higher biological relevance, preserved molecular properties, maintenance of original donor genome and higher relevance for *in vivo* experiments compared to immortalised cell lines (Richter et al., 2021). However, there are also a number of limits to using these cell types in ageing research. Isolation of primary microglia from mice is extensively described (Vijaya et al., 2023) and is one of the most straightforward methods to study microglia *in vitro.* This provides a more biologically relevant model compared to immortalised cells which have undergone alterations and likely diverge from the original cell origin (Stansley et al., 2012). However, the short time primary cells can be maintained in culture limits the ability to perform long term experiments, which are particularly relevant when studying ageing and NDs which have a long disease time course (Richter et al., 2021). Further, in order to understand how human cells act in culture, human samples must be utilised. For CNS cells, this can be achieved through the use of iPSC technology, by converting cells from aged donors to pluripotent stem cells, and further differentiating them to the desired cell type. However as highlighted in **Chapter 1**, conversion to pluripotency has been known to erase the aged phenotype of original donor cells, a key limitation when studying ageing (Lapasset et al., 2011; Ocampo et al., 2016).

In contrast, immortalised cell lines are widely available and utilised across laboratories. While previously they have been considered unfit as an ageing model due to their capacity for indefinite replication and divergence from original cell phenotypes (Bunc et al., 2019), their potential to replicate

features of aged cells should not be overlooked. In fact, at least one previous study has utilised such a cell line to demonstrate aspects of aged microglia. The BV2 microglial-like cell line has been shown to display increased accumulation of senescence associated heterochromatin foci, increased senescence associated β-Galactosidase activity and increased cell cycle regulators (p53) following repeated administration of LPS (Yu et al., 2012). These changes were induced by 4-hour incubations with 100uM LPS either 3x once every 48-hours or 6x once every 24hours. This suggests that multiple exposures to inflammatory stimuli may induce ageing-like features in microglia and also supports that BV2 cells are capable of expressing markers of senescence. Given this**, Chapter 6** focused on inducing "ageing" in an immortalised microglial cell line through multiple passages. Although a complete aged phenotype was not observed in BV2 cells, dysregulated proteostasis was induced in these cells in the presence of $A\beta^{1-42}$. This effect likely reflects the decreased capacity of high passage BV2 cells to manage pathological protein loads, an effect that is observed during ageing (Madore et al., 2020) and relevant to the progression of NDs (McFarland and Chakrabarty, 2022). This model therefore offers a potential tool for understanding age-related changes in proteostasis in the context of pathology and for evaluating treatments targeting this specific mechanism, which in the short term is useful in elucidating underlying disease processes. It is unlikely, however, to have utility for studying other age-related changes which, looking long term, is necessary to progress ageing and ND knowledge.

This approach to induce senescence was taken as cell lines are known to undergo a number of functional and genetic changes with increasing passage (Hughes et al., 2007; Weiskirchen et al., 2023), although the exact nature of these changes remains largely uncharacterised. Interestingly, in contrast to the previous study by Yu and colleagues (Yu et al., 2012), the phenotype of BV2 cells at high passage was in opposition to that expected for senescent cells, with old BV2s showing a decreased cytokine response to LPS and $A\beta^{1-42}$ stimulation, rather than the exaggerated inflammatory response associated with senescence (Rim et al., 2024). Nevertheless, cells displayed dysregulation of proteostasis in the presence of $A\beta^{1-42}$, as occurs with microglial ageing (López-Otín et al., 2023).Thus, BV2 cells appear to be uniquely sensitive to protein stressors such as $A\beta^{1-42}$ suggesting that high passage BV2 cells may be useful for studying alterations in proteostasis, such as those that occur in NDs (Tydlacka et al., 2008),

as well as how to pharmacologically target such changes. Additionally, coupled with the results of the Yu et al. (2012) study, these results indicate that further investigation on how to best induce an aged phenotype in immortalised cells is warranted, with some potential ways to do so considered further in the "Future directions" subsection below.

Beyond this, the results of **Chapter 6**, despite demonstrating stability in metabolism and oxidative stress, demonstrated a number of key alterations in the responses of BV2 cells to inflammatory stimulation. These results challenge the belief that immortalised cell lines are highly stable, a major reason for their popularity across research groups (Richter et al., 2021). Indeed, Stansley and colleagues (Stansley et al., 2012) have also challenged this, citing inconsistencies in results across different laboratories and attributing these to phenotypic drift that occurs in cell lines over time. This emphasises the need for better standardisation and reporting of procedures and conditions for culturing these cell lines, in order to improve the ability to draw conclusions across studies. For example, one variable factor that is not reported in many *in vitro* studies is passage number. This is critical to report, as even cells provided directly from the manufacturer can be initially obtained at high passage number. As an example, in our laboratory, we purchased the SHSY-5Y neuroblastoma cell line from a major supplier for a previous study. This cell line arrived at passage 13 from the manufacturer, meaning that once thawed and ready for experiments, there were only a few passages possible before reaching the generally suggested 20 passage limit for use (Weiskirchen et al., 2023). Thus, it is critical that researchers be aware of the passage number at which cells are received, as well as the maximum recommended passage number for a particular cell subtype, and that this information be routinely reported in publications, in order to aid in interpretation of results. Thus, *in vitro* models of ageing must be improved, with several suggestions for achieving this offered in **Chapter 1** including developing more sophisticated *in vitro* models and assessing ageing cell models in the context of an established ageing panel of markers such as that developed by Hartmann and colleagues (Hartmann et al., 2023). Of the markers in this panel only the expression of pro-inflammatory cytokines was evaluated in **Chapter 6**. The use of this panel would have been useful to replicate in this chapter however this was not possible, as the experiments for **Chapter 6** were conducted prior to the publication of the AgeScore

panel study. The benefits of improving *in vitro* models, rather than relying solely on results from *in vivo* studies, are clear, as it limits the need to rely on the use of animals in research and allows for dosages to be optimised prior to extensive *in vivo* testing, saving the research time and money.

7.7 Future directions

While the current thesis addresses gaps in the literature surrounding the inconsistencies of microglial analysis and incorporating ageing into current *in vitro* models, a number of directions for future research can be identified from these results. Figure 7.2 summarises these future directions in relation to three overarching themes: improved consistency in morphological classification of microglia, use of a multi-species approach and integration of multiple methods of analysis, and improved *in vitro* modelling and characterisation.

In the first instance, morphological phenotypes of microglia need to be better defined, as described in **Chapter 2**. Researchers must agree on correct terminology going forward and studies should seek to be as consistent as possible with this usage. In order to do so, a detailed characterisation of microglia in tissue should be conducted to group cells based on specific morphological parameters (Fig 7.2a). In particular, process dynamics are critical to define as these are a key discriminating feature between currently classified phenotypes (Vidal-Itriago et al., 2022). Process length, thickness and number of branches are key points of difference in distinguishing morphological phenotypes. For example, hyper-ramified microglia are classified as having thin complex branching structures (Vidal-Itriago et al., 2022), whereas bushy microglia are characterised by thickened processes with less complex branching (Wicks et al., 2022). These two phenotypes, as described above, are often used interchangeably; however, as Figure 7.1 shows, the cells described look vastly different across studies. Additionally, classifying the cell soma and nucleus morphology are also important in determining the phenotype of microglia. There are numerous protocols for understanding microglial morphology available on ImageJ, with such open-source software being particularly useful in order to provide the most accessible classification methods (Green et al., 2022). Thus, in order to improve consistency in microglial analysis, the field would greatly benefit from a study characterising and outlining specific parameters for microglial morphological classification. Defining classification parameters of morphological

phenotypes of microglia has been conducted using machine learning in the cortex and hippocampus of C57BL/6J mice by Leyh and colleagues (Leyh et al., 2021). However, as discussed above and highlighted in Figure 7.1b, this study only considers 4 classifications of microglia: amoeboid, activated, rod-like and ramified. Further, their classification of rod-like microglia is in contrast to other studies on rod and rod-like microglia and thus is an example of the inconsistent terminology across studies. Therefore, a thorough assessment of microglial phenotypes and classifications is necessary to ensure consistency across studies, and further, this should account for different morphologies present in grey versus white matter which present with distinct morphological phenotypes, (extended and complex processes in grey matter compared to bipolar cells in white matter) (Taylor et al., 2014; Vidal-Itriago et al., 2022).

Conducting further characterisation of microglial ageing in both small rodent and large animal models by elaborating on the markers assessed in **Chapter 4** will further contribute to the overall understanding of human microglia throughout ageing. Focusing on characterising microglia, and more broadly CNS ageing, in large gyrencephalic models, such as sheep or pigs, is particularly critical for improving translational research. Specifically, conducting analysis of morphology in conjunction with a more detailed immunofluorescent panel of markers will allow for greater understanding on how microglial morphology and function differ with ageing within and across species. This panel should reflect key functions of microglia in order to understand the full phenotype. This should include markers of immune activation (MHCII, CD68), phagocytosis (CD209), proliferation (Ki67), apoptosis (cleaved caspase-3, TUNEL staining), and markers of pro-inflammatory cytokines (IL-6, TNF, IL-1β). Further, analysis of microglia in this same level of detail should be conducted in human post-mortem tissue obtained from various aged individuals. This will likely prove difficult, given the challenges in obtaining healthy young and age-matched control postmortem tissue that already plague the ND field; however, it is a critical step for understanding microglia, and the brain as a whole, at these stages of life. Additionally, both human post-mortem studies and pre-clinical animal models should seek to conduct gene expression analysis. If fresh tissue is not available to conduct this through standard methods, methods to conduct spatiotemporal transcriptomic analysis are becoming more readily available, although these are

currently expensive to conduct (Williams et al., 2022). Technological advantages in PET imaging have also allowed for investigation of CNS cells by using TSPO ligands, which bind to activated microglia and astrocytes and can be used as a measure of neuroinflammation (Lee et al., 2020). This has been conducted using the ligand [^{18}F]-FEPPA in a cohort of 33 healthy individuals aged 20-85-yo for the investigation of neuroinflammation with age where it was found that [^{18}F]-FEPPA binding was not associated with age (Suridjan et al., 2014). Such advancements will allow for better understanding of microglia across human ageing and assist in assessing the translatability of current pre-clinical models. The characterisation of microglial ageing across rodent, large animal and human studies is critical in advancing our understanding of the contribution of microglia to ND development and progression. This knowledge will further allow us to develop translational models of ageing for ND research.

With consideration of *in* vitro models in particular, in **Chapter 6**, a potential model of ageing in immortalised cells was investigated and it was found that multiple passages of immortalised cells induced dysregulated proteostasis to a degree in BV2 microglia. This, coupled with findings that repeated LPS is capable of inducing senescence-related markers in BV2 cells, encourages further study of methods to induce ageing in immortalised cells. Stable BV2 cell lines overexpressing age associated genes have previously been created, including the overexpression of hypoxia-inducible factor 1-α (Hif1α), which is increased in ageing microglia and associated with increased phagocytosis (Grubman et al., 2021). This cell line was used to uncover the role of Hif1α in Aβ phagocytosis by microglia, where it was found that Hif1α activity was involved in increased phagocytic activity of BV2 cells (Grubman et al., 2021). This study additionally identified genes associated with an ageing trajectory in microglia isolated from 5xFAD mice overexpressing mutant APP. Of these genes, Defa17 and Defa24 appear to be the most associated with microglial ageing. Thus, a similar method to overexpress the Defa17 or Defa24 genes in BV2 cells may promote an ageing signature which would not require long term passaging to setup experiments and may more accurately reflect the aged phenotype. Additional methods to induce ageing in immortalised cell lines is not well researched; however, other drivers of ageing, including increased oxidative stress and epigenetic changes such as altered histone modification, may provide potential avenues to drive an aged phenotype in these cells. In fact,

H3k27me3, suggested as a marker of ageing to determine the AgeScore by Hartmann and colleagues, has been the target of a previous study to induce senescence by repressing EZH2, a component of the enzyme responsible for deposition of the H3k27me3 mark. This study demonstrated downregulation of EZH2 promotes the loss of H3k27me3 which induces expression of p16 and SASP genes in LF1 cells (Ito et al., 2018). While not specific to H3k27me3 or investigated in microglia, this study provides evidence that the loss of H3k27me3 is a potential avenue to induce senescence in culture which could be applied to microglial cel lines. Further, inducing oxidative stress has been shown to induce premature senescence in the NIH 3T3 mouse fibroblast cell line by administration of subtoxic levels of hydrogen peroxide (150μM). This phenotype was assessed by characterisation of a senescent morphology (enlarged, flattened cells) and positive SA-β-Gal staining (Volonte et al., 2002). While these methods have not been investigated in microglia specifically, they present new avenues for potential ageing models *in vitro*. If successful in inducing an aged phenotype in immortalised microglial cell lines, these could be combined in mixed co-cultures to create a more complex model of cell-cell interactions in the CNS. For example, differentiated SHSY-5Y neurons could be cultured alongside “aged” BV2 microglia and an astrocyte cell line, in order to model complex tetrapartite synapse interactions as has been done using primary cells (Goshi et al., 2020) which may more adequately replicate the aged CNS.

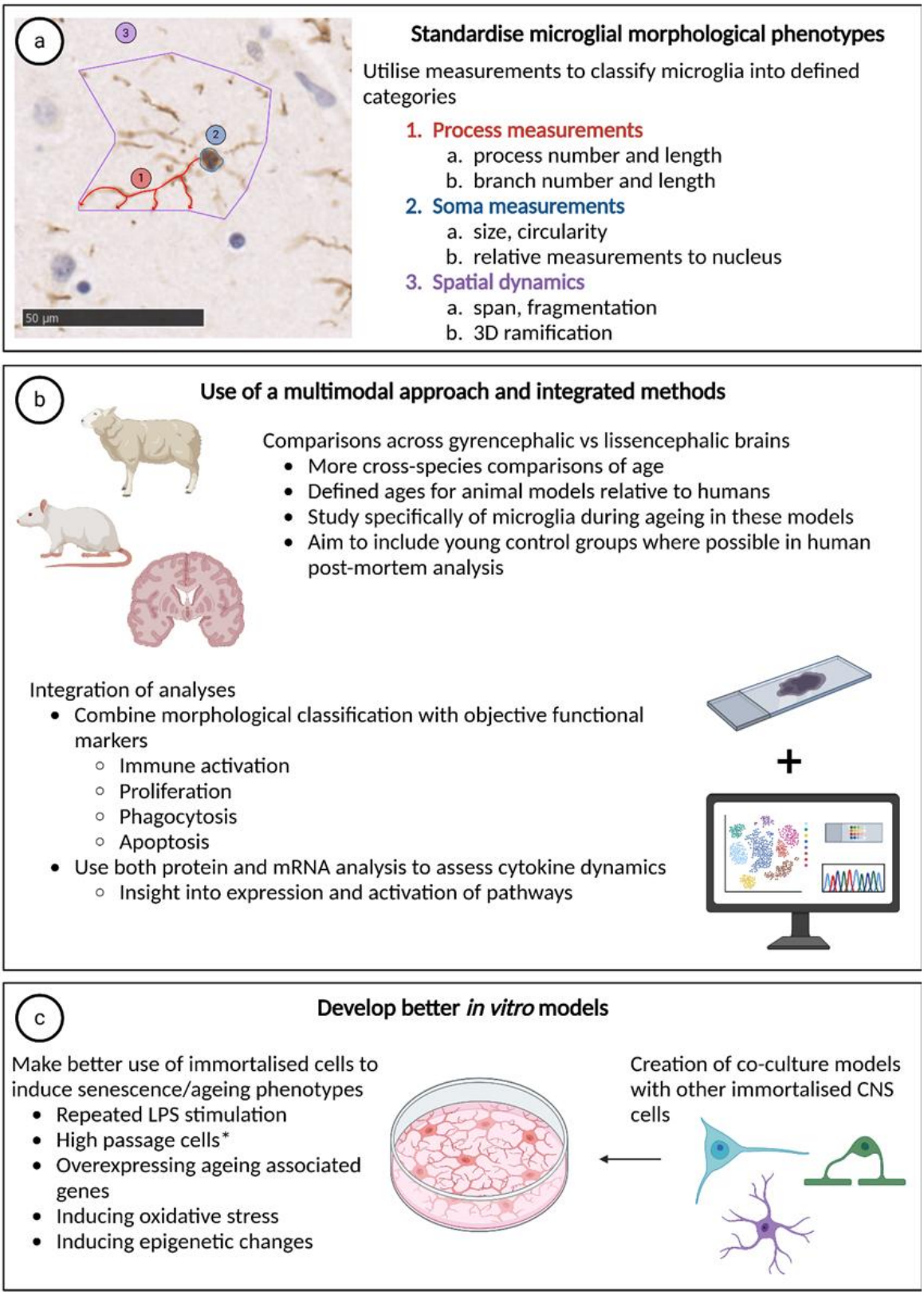


Figure 7.2: Considerations and future directions for microglial analysis. a) improves consistency of microglial morphological classifications. b) enhancing translatability by conducting cross species studies utilising integrated analyses. c) further development of novel *in vitro* models of the aged CNS

7.8 Thesis conclusions

Taken together, the results of this thesis highlight the critical importance of considering microglial ageing and provide a path forward for more consistent characterisation and analysis of microglia in pre-clinical models and human post-mortem tissue. Microglial morphological analysis as a whole suffers from a lack of consistency across research groups, which the use of automated analysis programs, such as the Halo analysis platform assessed in the current thesis, may be able to alleviate. However, guidelines for characterisation of morphological phenotypes will allow for greater consistency between studies and will ultimately improve our understanding of how morphology reflects function. This thesis utilised both morphological and functional analysis of microglia across species, finding key differences between the location and timing of microglial changes across ageing in rodent, sheep and human microglia. Importantly, the current thesis highlights that microglial ageing is a spectrum, with distinct changes emerging at different stages of the lifespan and varying between species. By comparing rodent, sheep and human data, this work highlights both conserved and species-specific aspects of microglial ageing. Notably, that while small animal models provide valuable mechanistic insights, they may not fully capture the complex changes in the human gyrencephalic brain. Larger animal models, such as sheep, may better reflect these aspects of microglial ageing relevant to human pathology. Future investigations should seek to integrate data from multiple species and age groups to refine our understanding of microglial ageing and enhance translational value of experimental models. In investigating potential models of ageing, this thesis sought to understand whether multiple passages of a microglial-like cell line (BV2) induced ageing phenotypes in culture. This analysis discovered that while these cells do not replicate the pro-inflammatory ageing phenotype in microglia referred to throughout the literature, dysregulated proteostasis developed in these cells in the presence of pathological proteins. This is promising, as immortalised cell lines are easily accessible, making inducing ageing in these cells desirable as a simple *in vitro* model of aged microglia through the use of the aforementioned potential avenues in the prior “Future Directions” section. Thus, while the current thesis represents an important effort to investigate microglial ageing using multiple methods and across

several species, further work in this area is necessary in order to fully understand the molecular changes that drive microglial alterations with ageing in both humans and relevant pre-clinical models.

7.9 References

Allen Institute for Brain Science, 2024a. Allen Brain Atlas: Aging, Dementia, and TBI. Allen Institute for Brain Science,.

Allen Institute for Brain Science, 2024b. Allen Human Brain Atlas. Allen Institute for Brain Science,.

Althammer, F., Ferreira-Neto, H.C., Rubaharan, M., Roy, R.K., Patel, A.A., Murphy, A., Cox, D.N., Stern, J.E., 2020. Three-dimensional morphometric analysis reveals time-dependent structural changes in microglia and astrocytes in the central amygdala and hypothalamic paraventricular nucleus of heart failure rats. J Neuroinflammation 17, 221.

Amgalan, A., Maher, A.S., Ghosh, S., Chui, H.C., Bogdan, P., Irimia, A., 2022. Brain age estimation reveals older adults' accelerated senescence after traumatic brain injury. GeroScience 44, 2509-2525.

Arganda-Carreras, I., Fernández-González, R., Muñoz-Barrutia, A., Ortiz-De-Solorzano, C., 2010. 3D reconstruction of histological sections: Application to mammary gland tissue. Microscopy Research and Technique 73, 1019-1029.

Arshadi, C., Günther, U., Eddison, M., Harrington, K.I.S., Ferreira, T.A., 2021. SNT: a unifying toolbox for quantification of neuronal anatomy. Nature Methods 18, 374-377.

Asher, S., Priefer, R., 2022. Alzheimer's disease failed clinical trials. Life Sciences 306, 120861.

Askew, K., Li, K., Olmos-Alonso, A., Garcia-Moreno, F., Liang, Y., Richardson, P., Tipton, T., Chapman, M.A., Riecken, K., Beccari, S., Sierra, A., Molnár, Z., Cragg, M.S., Garaschuk, O., Perry, V.H., Gomez-Nicola, D., 2017. Coupled Proliferation and Apoptosis Maintain the Rapid Turnover of Microglia in the Adult Brain. Cell Reports 18, 391-405.

Bachstetter, A.D., Van Eldik, L.J., Schmitt, F.A., Neltner, J.H., Ighodaro, E.T., Webster, S.J., Patel, E., Abner, E.L., Kryscio, R.J., Nelson, P.T., 2015. Disease-related microglia heterogeneity in the hippocampus of Alzheimer's disease, dementia with Lewy bodies, and hippocampal sclerosis of aging. Acta Neuropathologica Communications 3, 32.

Bankhead, P., Loughrey, M.B., Fernández, J.A., Dombrowski, Y., McArt, D.G., Dunne, P.D., McQuaid, S., Gray, R.T., Murray, L.J., Coleman, H.G., James, J.A., Salto-Tellez, M., Hamilton, P.W., 2017. QuPath: Open source software for digital pathology image analysis. Scientific Reports 7, 16878.

Beijer, H.J., de Blaey, C.J., 2002. Hospitalisations caused by adverse drug reactions (ADR): a meta-analysis of observational studies. Pharm World Sci 24, 46-54.

Bekhbat, M., Neigh, G.N., 2018. Sex differences in the neuro-immune consequences of stress: Focus on depression and anxiety. Brain Behav Immun 67, 1-12.

Bioscience, M., 2024. Neurolucida.

Bunc, M., Hanning, S., Prieto, J., Kristl, J., Orlu, M., 2019. Characterisation of an in vitro aged cell culture model. Farmacia 67.

Cao, B., Ho, J., 2020. WHO methods and data sources for life tables 1990-2019. World Health Organization (WHO), Geneva.

Carr, L.M., Mustafa, S., Care, A., Collins-Praino, L.E., 2024. More than a number: Incorporating the aged phenotype to improve in vitro and in vivo modeling of neurodegenerative disease. Brain, Behavior, and Immunity 119, 554-571.

Clarke, D., Crombag, H.S., Hall, C.N., 2021. An open-source pipeline for analysing changes in microglial morphology. Open Biol 11, 210045.

Colasanti, A., Guo, Q., Giannetti, P., Wall, M.B., Newbould, R.D., Bishop, C., Onega, M., Nicholas, R., Ciccarelli, O., Muraro, P.A., Malik, O., Owen, D.R., Young, A.H., Gunn, R.N., Piccini, P., Matthews, P.M., Rabiner, E.A., 2016. Hippocampal Neuroinflammation, Functional Connectivity, and Depressive Symptoms in Multiple Sclerosis. Biol Psychiatry 80, 62-72.

Cuntz, H., Forstner, F., Borst, A., Häusser, M., 2010. One Rule to Grow Them All: A General Theory of Neuronal Branching and Its Practical Application. PLOS Computational Biology 6, e1000877.

D'Souza, G.M., Churchill, N.W., Guan, D.X., Khoury, M.A., Graham, S.J., Kumar, S., Fischer, C.E., Schweizer, T.A., 2024. Interaction of Alzheimer Disease and Traumatic Brain Injury on Cortical Thickness. Alzheimer Disease & Associated Disorders 38.

Davidson, T.L., Stevenson, R.J., 2024. Vulnerability of the Hippocampus to Insults: Links to Blood–Brain Barrier Dysfunction. International Journal of Molecular Sciences.

DePaula-Silva, A.B., Gorbea, C., Doty, D.J., Libbey, J.E., Sanchez, J.M.S., Hanak, T.J., Cazalla, D., Fujinami, R.S., 2019. Differential transcriptional profiles identify microglial- and macrophage-specific gene markers expressed during virus-induced neuroinflammation. J Neuroinflammation 16, 152.
Fann, J.R., Ribe, A.R., Pedersen, H.S., Fenger-Grøn, M., Christensen, J., Benros, M.E., Vestergaard, M., 2018. Long-term risk of dementia among people with traumatic brain injury in Denmark: a population-based observational cohort study. The Lancet Psychiatry 5, 424-431.
Farooqui, T., Farooqui, A.A., 2009. Aging: An important factor for the pathogenesis of neurodegenerative diseases. Mechanisms of Ageing and Development 130, 203-215.
Fernández-Arjona, M.d.M., Grondona, J.M., Granados-Durán, P., Fernández-Llebrez, P., López-Ávalos, M.D., 2017. Microglia Morphological Categorization in a Rat Model of Neuroinflammation by Hierarchical Cluster and Principal Components Analysis. Frontiers in Cellular Neuroscience 11, 235.
Gallego, B.I., de Gracia, P., 2016. Automatic counting of microglial cell activation and its applications. Neural Regen Res 11, 1212-1215.
García-Magro, N., Martin, Y.B., Palomino-Antolin, A., Egea, J., Negredo, P., Avendaño, C., 2020. Multiple Morphometric Assessment of Microglial Cells in Deafferented Spinal Trigeminal Nucleus. Frontiers in Neuroanatomy 13.
Gardner, R.C., Bahorik, A., Kornblith, E.S., Allen, I.E., Plassman, B.L., Yaffe, K., 2023. Systematic Review, Meta-Analysis, and Population Attributable Risk of Dementia Associated with Traumatic Brain Injury in Civilians and Veterans. J Neurotrauma 40, 620-634.
Gardner, R.C., Burke, J.F., Nettiksimmons, J., Kaup, A., Barnes, D.E., Yaffe, K., 2014. Dementia risk after traumatic brain injury vs nonbrain trauma: the role of age and severity. JAMA Neurol 71, 1490-1497.
Geirsdottir, L., David, E., Keren-Shaul, H., Weiner, A., Bohlen, S.C., Neuber, J., Balic, A., Giladi, A., Sheban, F., Dutertre, C.-A., Pfeifle, C., Peri, F., Raffo-Romero, A., Vizioli, J., Matiasek, K., Scheiwe, C., Meckel, S., Mätz-Rensing, K., van der Meer, F., Thormodsson, F.R., Stadelmann, C., Zilkha, N., Kimchi, T., Ginhoux, F., Ulitsky, I., Erny, D., Amit, I., Prinz, M., 2019. Cross-Species Single-Cell Analysis Reveals Divergence of the Primate Microglia Program. Cell 179, 1609-1622.e1616.
Giacobbo, B.L., Özalay, Ö., Mediavilla, T., Ericsson, M., Axelsson, J., Rieckmann, A., Sultan, F., Marcellino, D., 2022. The Aged Striatum: Evidence of Molecular and Structural Changes Using a Longitudinal Multimodal Approach in Mice. Frontiers in Aging Neuroscience 14.
Ginhoux, F., Lim, S., Hoeffel, G., Low, D., Huber, T., 2013. Origin and differentiation of microglia. Frontiers in Cellular Neuroscience 7.
Giordano, K.R., Denman, C.R., Dubisch, P.S., Akhter, M., Lifshitz, J., 2021. An update on the rod microglia variant in experimental and clinical brain injury and disease. Brain Commun 3, fcaa227.
Gong, C.X., Iqbal, K., 2008. Hyperphosphorylation of microtubule-associated protein tau: a promising therapeutic target for Alzheimer disease. Curr Med Chem 15, 2321-2328.
Goshi, N., Morgan, R.K., Lein, P.J., Seker, E., 2020. A primary neural cell culture model to study neuron, astrocyte, and microglia interactions in neuroinflammation. J Neuroinflammation 17, 155.
Green, T.R.F., Murphy, S.M., Rowe, R.K., 2022. Comparisons of quantitative approaches for assessing microglial morphology reveal inconsistencies, ecological fallacy, and a need for standardization. Sci Rep 12, 18196.
Green, T.R.F., Rowe, R.K., 2024. Quantifying microglial morphology: an insight into function. Clinical and Experimental Immunology 216, 221-229.
Grubman, A., Choo, X.Y., Chew, G., Ouyang, J.F., Sun, G., Croft, N.P., Rossello, F.J., Simmons, R., Buckberry, S., Landin, D.V., Pflueger, J., Vandekolk, T.H., Abay, Z., Zhou, Y., Liu, X., Chen, J., Larcombe, M., Haynes, J.M., McLean, C., Williams, S., Chai, S.Y., Wilson, T., Lister, R., Pouton, C.W., Purcell, A.W., Rackham, O.J.L., Petretto, E., Polo, J.M., 2021. Transcriptional signature in microglia associated with Aβ plaque phagocytosis. Nat Commun 12, 3015.
Guglietti, B., Mustafa, S., Corrigan, F., Collins-Praino, L.E., 2024. Anatomical distribution of Fyn kinase in the human brain in Parkinson's disease. Parkinsonism & Related Disorders 118.
Hampel, H., Hardy, J., Blennow, K., Chen, C., Perry, G., Kim, S.H., Villemagne, V.L., Aisen, P., Vendruscolo, M., Iwatsubo, T., Masters, C.L., Cho, M., Lannfelt, L., Cummings, J.L., Vergallo, A., 2021. The Amyloid-β Pathway in Alzheimer's Disease. Molecular Psychiatry 26, 5481-5503.

Hartmann, C., Herling, L., Hartmann, A., Köckritz, V., Fuellen, G., Walter, M., Hermann, A., 2023. Systematic estimation of biological age of in vitro cell culture systems by an age-associated marker panel. Frontiers in Aging 4.
Henry, C.J., Huang, Y., Wynne, A.M., Godbout, J.P., 2009. Peripheral lipopolysaccharide (LPS) challenge promotes microglial hyperactivity in aged mice that is associated with exaggerated induction of both pro-inflammatory IL-1beta and anti-inflammatory IL-10 cytokines. Brain Behav Immun 23, 309-317.
Holloway, O.G., Canty, A.J., King, A.E., Ziebell, J.M., 2019. Rod microglia and their role in neurological diseases. Seminars in Cell & Developmental Biology 94, 96-103.
Hughes, P., Marshall, D., Reid, Y., Parkes, H., Gelber, C., 2007. The costs of using unauthenticated, over-passaged cell lines: how much more data do we need? BioTechniques 43, 575-586.
Imamura, K., Hishikawa, N., Sawada, M., Nagatsu, T., Yoshida, M., Hashizume, Y., 2003. Distribution of major histocompatibility complex class II-positive microglia and cytokine profile of Parkinson's disease brains. Acta Neuropathologica 106, 518-526.
Indica Labs, I., 2024. HALO Microglial Activation Module.
Instruments, O., 2024. Imaris 10.2.
Ito, T., Teo, Y.V., Evans, S.A., Neretti, N., Sedivy, J.M., 2018. Regulation of Cellular Senescence by Polycomb Chromatin Modifiers through Distinct DNA Damage- and Histone Methylation-Dependent Pathways. Cell Rep 22, 3480-3492.
Jacobs, J.M., Maaravi, Y., Cohen, A., Bursztyn, M., Ein-Mor, E., Stessman, J., 2012. Changing Profile of Health and Function from Age 70 to 85 Years. Gerontology 58, 313-321.
Johnson, I.P., 2015. Age-related neurodegenerative disease research needs aging models. Frontiers in Aging Neuroscience 7.
Jung, H., Lee, H., Kim, D., Cheong, E., Hyun, Y.M., Yu, J.W., Um, J.W., 2022. Differential Regional Vulnerability of the Brain to Mild Neuroinflammation Induced by Systemic LPS Treatment in Mice. J Inflamm Res 15, 3053-3063.
Jurga, A.M., Paleczna, M., Kuter, K.Z., 2020. Overview of General and Discriminating Markers of Differential Microglia Phenotypes. Front Cell Neurosci 14, 198.
Kalia, L.V., Lang, A.E., 2015. Parkinson's disease. The Lancet 386, 896-912.
Kamei, R., Okabe, S., 2023. In vivo imaging of the phagocytic dynamics underlying efficient clearance of adult-born hippocampal granule cells by ramified microglia. Glia 71, 2005-2023.
Khakpour, M., Ibáñez, F.G., Bordeleau, M., Picard, K., McKee-Reid, L., Ben-Azu, B., Maggi, L., Tremblay, M.-È., 2022. Manual versus automatic analysis of microglial density and distribution: a comparison in the hippocampus of healthy and lipopolysaccharide-challenged mature male mice. Micron 161, 103334.
Kinirons, M.T., O'Mahony, M.S., 2004. Drug metabolism and ageing. Br J Clin Pharmacol 57, 540-544.
Kodamullil, A.T., Iyappan, A., Karki, R., Madan, S., Younesi, E., Hofmann-Apitius, M., 2017. Of Mice and Men: Comparative Analysis of Neuro-Inflammatory Mechanisms in Human and Mouse Using Cause-and-Effect Models. J Alzheimers Dis 59, 1045-1055.
Krieg, J.L., Leonard, A.V., Tuner, R.J., Corrigan, F., 2023. Characterization of Traumatic Brain Injury in a Gyrencephalic Ferret Model Using the Novel Closed Head Injury Model of Engineered Rotational Acceleration (CHIMERA). Neurotrauma Reports 4, 761-780.
Kuźma, E., Lourida, I., Moore, S.F., Levine, D.A., Ukoumunne, O.C., Llewellyn, D.J., 2018. Stroke and dementia risk: A systematic review and meta-analysis. Alzheimers Dement 14, 1416-1426.
Lapasset, L., Milhavet, O., Prieur, A., Besnard, E., Babled, A., Aït-Hamou, N., Leschik, J., Pellestor, F., Ramirez, J.M., De Vos, J., Lehmann, S., Lemaitre, J.M., 2011. Rejuvenating senescent and centenarian human cells by reprogramming through the pluripotent state. Genes Dev 25, 2248-2253.
Lau, S.F., Wu, W., Seo, H., Fu, A.K.Y., Ip, N.Y., 2021. Quantitative in vivo assessment of amyloid-beta phagocytic capacity in an Alzheimer's disease mouse model. STAR Protoc 2, 100265.
Lee, Y., Park, Y., Nam, H., Lee, J.W., Yu, S.W., 2020. Translocator protein (TSPO): the new story of the old protein in neuroinflammation. BMB Rep 53, 20-27.
Leparulo, A., Bisio, M., Redolfi, N., Pozzan, T., Vassanelli, S., Fasolato, C., 2022. Accelerated Aging Characterizes the Early Stage of Alzheimer's Disease. Cells 11.

Leyh, J., Paeschke, S., Mages, B., Michalski, D., Nowicki, M., Bechmann, I., Winter, K., 2021. Classification of Microglial Morphological Phenotypes Using Machine Learning. Frontiers in Cellular Neuroscience 15.
Long, J.M., Kalehua, A.N., Muth, N.J., Calhoun, M.E., Jucker, M., Hengemihle, J.M., Ingram, D.K., Mouton, P.R., 1998. Stereological analysis of astrocyte and microglia in aging mouse hippocampus. Neurobiology of Aging 19, 497-503.
López-Otín, C., Blasco, M.A., Partridge, L., Serrano, M., Kroemer, G., 2023. Hallmarks of aging: An expanding universe. Cell 186, 243-278.
Madore, C., Yin, Z., Leibowitz, J., Butovsky, O., 2020. Microglia, Lifestyle Stress, and Neurodegeneration. Immunity 52, 222-240.
McFarland, K.N., Chakrabarty, P., 2022. Microglia in Alzheimer's Disease: a Key Player in the Transition Between Homeostasis and Pathogenesis. Neurotherapeutics 19, 186-208.
Medina-Luque, J., Piechocinski, P., Feyen, P., Sgobio, C., Herms, J., 2024. Striatal dopamine neurotransmission is altered in age- and region-specific manner in a Parkinson's disease transgenic mouse. Scientific Reports 14, 164.
Mestas, J., Hughes, C.C.W., 2004. Of Mice and Not Men: Differences between Mouse and Human Immunology. The Journal of Immunology 172, 2731.
Mitchell, S.J., MacArthur, M.R., Kane, A.E., 2023. Optimizing preclinical models of ageing for translation to clinical trials. British Journal of Clinical Pharmacology n/a.
Mitsui, S., Yamaguchi, J., Suzuki, C., Uchiyama, Y., Tanida, I., 2023. TUNEL-positive structures in activated microglia and SQSTM1/p62-positive structures in activated astrocytes in the neurodegenerative brain of a CLN10 mouse model. Glia 71, 2753-2769.
Murinello, S., Moreno, S.K., Macauley, M.S., Sakimoto, S., Westenskow, P.D., Friedlander, M., 2016. Assessing Retinal Microglial Phagocytic Function In Vivo Using a Flow Cytometry-based Assay. J Vis Exp.
Nations, U., 2024. Persons at Risk: Older persons.
Noristani, H.N., Gerber, Y.N., Sabourin, J.-C., Le Corre, M., Lonjon, N., Mestre-Frances, N., Hirbec, H.E., Perrin, F.E., 2017. RNA-Seq Analysis of Microglia Reveals Time-Dependent Activation of Specific Genetic Programs following Spinal Cord Injury. Frontiers in Molecular Neuroscience 10.
Ocampo, A., Reddy, P., Martinez-Redondo, P., Platero-Luengo, A., Hatanaka, F., Hishida, T., Li, M., Lam, D., Kurita, M., Beyret, E., Araoka, T., Vazquez-Ferrer, E., Donoso, D., Roman, J.L., Xu, J., Rodriguez Esteban, C., Nuñez, G., Nuñez Delicado, E., Campistol, J.M., Guillen, I., Guillen, P., Izpisua Belmonte, J.C., 2016. In Vivo Amelioration of Age-Associated Hallmarks by Partial Reprogramming. Cell 167, 1719-1733.e1712.
Oliveira, A.V., Vilaça, R., Santos, C.N., Costa, V., Menezes, R., 2017. Exploring the power of yeast to model aging and age-related neurodegenerative disorders. Biogerontology 18, 3-34.
Orimo, H., Ito, H., Suzuki, T., Araki, A., Hosoi, T., Sawabe, M., 2006. Reviewing the definition of "elderly". Geriatrics & Gerontology International 6, 149-158.
Paigen, K., 1995. A miracle enough: the power of mice. Nature Medicine 1, 215-220.
Paolicelli, R.C., Sierra, A., Stevens, B., Tremblay, M.-E., Aguzzi, A., Ajami, B., Amit, I., Audinat, E., Bechmann, I., Bennett, M., Bennett, F., Bessis, A., Biber, K., Bilbo, S., Blurton-Jones, M., Boddeke, E., Brites, D., Brône, B., Brown, G.C., Butovsky, O., Carson, M.J., Castellano, B., Colonna, M., Cowley, S.A., Cunningham, C., Davalos, D., De Jager, P.L., de Strooper, B., Denes, A., Eggen, B.J.L., Eyo, U., Galea, E., Garel, S., Ginhoux, F., Glass, C.K., Gokce, O., Gomez-Nicola, D., González, B., Gordon, S., Graeber, M.B., Greenhalgh, A.D., Gressens, P., Greter, M., Gutmann, D.H., Haass, C., Heneka, M.T., Heppner, F.L., Hong, S., Hume, D.A., Jung, S., Kettenmann, H., Kipnis, J., Koyama, R., Lemke, G., Lynch, M., Majewska, A., Malcangio, M., Malm, T., Mancuso, R., Masuda, T., Matteoli, M., McColl, B.W., Miron, V.E., Molofsky, A.V., Monje, M., Mracsko, E., Nadjar, A., Neher, J.J., Neniskyte, U., Neumann, H., Noda, M., Peng, B., Peri, F., Perry, V.H., Popovich, P.G., Pridans, C., Priller, J., Prinz, M., Ragozzino, D., Ransohoff, R.M., Salter, M.W., Schaefer, A., Schafer, D.P., Schwartz, M., Simons, M., Smith, C.J., Streit, W.J., Tay, T.L., Tsai, L.-H., Verkhratsky, A., von Bernhardi, R., Wake, H., Wittamer, V., Wolf, S.A., Wu, L.-J., Wyss-Coray, T., 2022. Microglia states and nomenclature: A field at its crossroads. Neuron 110, 3458-3483.
Pelvig, D.P., Pakkenberg, H., Stark, A.K., Pakkenberg, B., 2008. Neocortical glial cell numbers in human brains. Neurobiology of Aging 29, 1754-1762.

Perkins, A.E., Piazza, M.K., Deak, T., 2018. Stereological Analysis of Microglia in Aged Male and Female Fischer 344 Rats in Socially Relevant Brain Regions. Neuroscience 377, 40-52.
Perry, V.H., Matyszak, M.K., Fearn, S., 1993. Altered antigen expression of microglia in the aged rodent CNS. Glia 7, 60-67.
Rajati, F., Rajati, M., Rasulehvandi, R., Kazeminia, M., 2023. Prevalence of stroke in the elderly: A systematic review and meta-analysis. Interdisciplinary Neurosurgery 32, 101746.
Raz, N., Rodrigue, K.M., Kennedy, K.M., Head, D., Gunning-Dixon, F., Acker, J.D., 2003. Differential aging of the human striatum: longitudinal evidence. AJNR Am J Neuroradiol 24, 1849-1856.
Reddaway, J., Richardson, P.E., Bevan, R.J., Stoneman, J., Palombo, M., 2023. Microglial morphometric analysis: so many options, so little consistency. Frontiers in Neuroinformatics 17.
Richter, M., Piwocka, O., Musielak, M., Piotrowski, I., Suchorska, W.M., Trzeciak, T., 2021. From Donor to the Lab: A Fascinating Journey of Primary Cell Lines. Frontiers in Cell and Developmental Biology 9.
Rim, C., You, M.-J., Nahm, M., Kwon, M.-S., 2024. Emerging role of senescent microglia in brain aging-related neurodegenerative diseases. Translational Neurodegeneration 13, 10.
Ritzel, R.M., Li, Y., Jiao, Y., Lei, Z., Doran, S.J., He, J., Shahror, R.A., Henry, R.J., Khan, R., Tan, C., Liu, S., Stoica, B.A., Faden, A.I., Szeto, G., Loane, D.J., Wu, J., 2023. Brain injury accelerates the onset of a reversible age-related microglial phenotype associated with inflammatory neurodegeneration. Sci Adv 9, eadd1101.
Rozovsky, I., Finch, C.E., Morgan, T.E., 1998. Age-Related Activation of Microglia and Astrocytes: In Vitro Studies Show Persistent Phenotypes of Aging, Increased Proliferation, and Resistance to Down-Regulation. Neurobiology of Aging 19, 97-103.
Rudnicka, E., Napierała, P., Podfigurna, A., Męczekalski, B., Smolarczyk, R., Grymowicz, M., 2020. The World Health Organization (WHO) approach to healthy ageing. Maturitas 139, 6-11.
Rush, A., Weil, C., Siminoff, L., Griffin, C., Paul, C.L., Mahadevan, A., Sutherland, G., 2024. The Experts Speak: Challenges in Banking Brain Tissue for Research. Biopreservation and Biobanking 22, 179-184.
Schindler, R., Clark, B.D., Dinarello, C.A., 1990. Dissociation between interleukin-1 beta mRNA and protein synthesis in human peripheral blood mononuclear cells. Journal of Biological Chemistry 265, 10232-10237.
Shebl, F.M., Pinto, L.A., García-Piñeres, A., Lempicki, R., Williams, M., Harro, C., Hildesheim, A., 2010. Comparison of mRNA and protein measures of cytokines following vaccination with human papillomavirus-16 L1 virus-like particles. Cancer Epidemiol Biomarkers Prev 19, 978-981.
Sorby-Adams, A.J., Vink, R., Turner, R.J., 2018. Large animal models of stroke and traumatic brain injury as translational tools. American Journal of Physiology-Regulatory, Integrative and Comparative Physiology 315, R165-R190.
Sorokin, M., Ignatev, K., Poddubskaya, E., Vladimirova, U., Gaifullin, N., Lantsov, D., Garazha, A., Allina, D., Suntsova, M., Barbara, V., Buzdin, A., 2020. RNA Sequencing in Comparison to Immunohistochemistry for Measuring Cancer Biomarkers in Breast Cancer and Lung Cancer Specimens. Biomedicines 8.
Stansley, B., Post, J., Hensley, K., 2012. A comparative review of cell culture systems for the study of microglial biology in Alzheimer's disease. J Neuroinflammation 9, 115.
Stefanis, L., 2012. α-Synuclein in Parkinson's disease. Cold Spring Harb Perspect Med 2, a009399.
Stirling, D.R., Swain-Bowden, M.J., Lucas, A.M., Carpenter, A.E., Cimini, B.A., Goodman, A., 2021. CellProfiler 4: improvements in speed, utility and usability. BMC Bioinformatics 22, 433.
Suk, T.R., Rousseaux, M.W.C., 2020. The role of TDP-43 mislocalization in amyotrophic lateral sclerosis. Molecular Neurodegeneration 15, 45.
Sun, M., McDonald, S.J., Brady, R.D., Collins-Praino, L., Yamakawa, G.R., Monif, M., O'Brien, T.J., Cloud, G.C., Sobey, C.G., Mychasiuk, R., Loane, D.J., Shultz, S.R., 2020. The need to incorporate aged animals into the preclinical modeling of neurological conditions. Neuroscience & Biobehavioral Reviews 109, 114-128.
Suridjan, I., Rusjan, P.M., Voineskos, A.N., Selvanathan, T., Setiawan, E., Strafella, A.P., Wilson, A.A., Meyer, J.H., Houle, S., Mizrahi, R., 2014. Neuroinflammation in healthy aging: A PET study using a novel Translocator Protein 18kDa (TSPO) radioligand, [18F]-FEPPA. NeuroImage 84, 868-875.

Tang, Y., Liu, M.L., Zang, T., Zhang, C.L., 2017. Direct Reprogramming Rather than iPSC-Based Reprogramming Maintains Aging Hallmarks in Human Motor Neurons. Front Mol Neurosci 10, 359.
Taylor, S.E., Morganti-Kossmann, C., Lifshitz, J., Ziebell, J.M., 2014. Rod Microglia: A Morphological Definition. PLOS ONE 9, e97096.
Tydlacka, S., Wang, C.E., Wang, X., Li, S., Li, X.J., 2008. Differential activities of the ubiquitin-proteasome system in neurons versus glia may account for the preferential accumulation of misfolded proteins in neurons. J Neurosci 28, 13285-13295.
Vaughan, D.W., Peters, A., 1974. Neuroglial cells in the cerebral cortex of rats from young adulthood to old age: an electron microscope study. J Neurocytol 3, 405-429.
Viana, L.C., Lima, C.M., Oliveira, M.A., Borges, R.P., Cardoso, T.T., Almeida, I.N.F., Diniz, D.G., Bento-Torres, J., Pereira, A., Batista-de-Oliveira, M., Lopes, A.A.C., Silva, R.F.M., Abadie-Guedes, R., Amâncio dos Santos, A., Lima, D.S.C., Vasconcelos, P.F.C., Cunningham, C., Guedes, R.C.A., Picanço-Diniz, C.W., 2013. Litter size, age-related memory impairments, and microglial changes in rat dentate gyrus: Stereological analysis and three dimensional morphometry. Neuroscience 238, 280-296.
Vidal-Itriago, A., Radford, R.A.W., Aramideh, J.A., Maurel, C., Scherer, N.M., Don, E.K., Lee, A., Chung, R.S., Graeber, M.B., Morsch, M., 2022. Microglia morphophysiological diversity and its implications for the CNS. Front Immunol 13, 997786.
Vijaya, A.K., Iešmantaitė, M., Mela, V., Baltriukienė, D., Burokas, A., 2023. Microglia isolation from aging mice for cell culture: A beginner's guide. Front Cell Neurosci 17, 1082180.
Volonte, D., Zhang, K., Lisanti, M.P., Galbiati, F., 2002. Expression of Caveolin-1 Induces Premature Cellular Senescence in Primary Cultures of Murine Fibroblasts. Molecular Biology of the Cell 13, 2502-2517.
Wallace, L.M.K., Howlett, S.E., 2016. Commentary: Age-related neurodegenerative disease research needs aging models. Frontiers in Aging Neuroscience 8.
Ward, T.H., Cummings, J., Dean, E., Greystoke, A., Hou, J.M., Backen, A., Ranson, M., Dive, C., 2008. Biomarkers of apoptosis. Br J Cancer 99, 841-846.
Weiskirchen, S., Schröder, S.K., Buhl, E.M., Weiskirchen, R., 2023. A Beginner's Guide to Cell Culture: Practical Advice for Preventing Needless Problems. Cells.
Wicks, E.E., Ran, K.R., Kim, J.E., Xu, R., Lee, R.P., Jackson, C.M., 2022. The Translational Potential of Microglia and Monocyte-Derived Macrophages in Ischemic Stroke. Frontiers in Immunology 13.
Williams, C.G., Lee, H.J., Asatsuma, T., Vento-Tormo, R., Haque, A., 2022. An introduction to spatial transcriptomics for biomedical research. Genome Medicine 14, 68.
Yiannopoulou, K.G., Papageorgiou, S.G., 2020. Current and Future Treatments in Alzheimer Disease: An Update. J Cent Nerv Syst Dis 12, 1179573520907397-1179573520907397.
Yoo, J.W., Hong, B.Y., Jo, L., Kim, J.S., Park, J.G., Shin, B.K., Lim, S.H., 2020. Effects of Age on Long-Term Functional Recovery in Patients with Stroke. Medicina (Kaunas) 56.
York, E.M., LeDue, J.M., Bernier, L.P., MacVicar, B.A., 2018. 3DMorph Automatic Analysis of Microglial Morphology in Three Dimensions from Ex Vivo and In Vivo Imaging. eNeuro 5.
Young, K., Morrison, H., 2018. Quantifying Microglia Morphology from Photomicrographs of Immunohistochemistry Prepared Tissue Using ImageJ. J Vis Exp.
Yu, H.-M., Zhao, Y.-M., Luo, X.-G., Feng, Y., Ren, Y., Shang, H., He, Z.-Y., Luo, X.-M., Chen, S.-D., Wang, X.-Y., 2012. Repeated Lipopolysaccharide Stimulation Induces Cellular Senescence in BV2 Cells. Neuroimmunomodulation 19, 131-136.
Zeng, C.-Y., Yang, T.-T., Zhou, H.-J., Zhao, Y., Kuang, X., Duan, W., Du, J.-R., 2019. Lentiviral vector–mediated overexpression of Klotho in the brain improves Alzheimer's disease–like pathology and cognitive deficits in mice. Neurobiology of Aging 78, 18-28.
Zhang, X., Gao, F., Wang, D., Li, C., Fu, Y., He, W., Zhang, J., 2018. Tau Pathology in Parkinson's Disease. Front Neurol 9, 809.
Zhang, X., Shen, Z.-L., Ji, Y.-W., Yin, C., Xiao, C., Zhou, C., 2024. Activation and polarization of striatal microglia and astrocytes are involved in bradykinesia and allodynia in early-stage parkinsonian mice. Fundamental Research 4, 806-819.
Ziebell, J.M., Adelson, P.D., Lifshitz, J., 2015. Microglia: dismantling and rebuilding circuits after acute neurological injury. Metab Brain Dis 30, 393-400.

Brain, Behavior, and Immunity 119 (2024) 554–571

Contents lists available at ScienceDirect

Brain Behavior and Immunity

journal homepage: www.elsevier.com/locate/ybrbi

More than a number: Incorporating the aged phenotype to improve *in vitro* and *in vivo* modeling of neurodegenerative disease

Laura M. Carr [a], Sanam Mustafa [a,b,c], Andrew Care [d], Lyndsey E Collins-Praino [a,b,*]

[a] School of Biomedicine, University of Adelaide, Adelaide, SA, Australia
[b] Australian Research Council Centre of Excellence for Nanoscale Biophotonics, The University of Adelaide, Adelaide, SA, Australia
[c] Davies Livestock Research Centre, The University of Adelaide, Roseworthy, SA, Australia
[d] School of Life Sciences, University of Technology Sydney, Sydney, NSW, Australia

ARTICLE INFO

Keywords:
Central nervous system ageing
In vitro models
Mouse models
Senescence
Neurodegenerative disease
Parkinson's disease
Alzheimer's disease
Ageing neuron

ABSTRACT

Age is the number one risk factor for developing a neurodegenerative disease (ND), such as Alzheimer's disease (AD) or Parkinson's disease (PD). With our rapidly ageing world population, there will be an increased burden of ND and need for disease-modifying treatments. Currently, however, translation of research from bench to bedside in NDs is poor. This may be due, at least in part, to the failure to account for the potential effect of ageing in preclinical modelling of NDs. While ageing can impact upon physiological response in multiple ways, only a limited number of preclinical studies of ND have incorporated ageing as a factor of interest. Here, we evaluate the aged phenotype and highlight the critical, but unmet, need to incorporate aspects of this phenotype into both the *in vitro* and *in vivo* models used in ND research. Given technological advances in the field over the past several years, we discuss how these could be harnessed to create novel models of ND that more readily incorporate aspects of the aged phenotype. This includes a recently described *in vitro* panel of ageing markers, which could help lead to more standardised models and improve reproducibility across studies. Importantly, we cannot assume that young cells or animals yield the same responses as seen in the context of ageing; thus, an improved understanding of the biology of ageing, and how to appropriately incorporate this into the modelling of ND, will ensure the best chance for successful translation of new therapies to the aged patient.

1. Introduction

1.1. Global ageing: Implications for neurodegenerative disease

Substantial scientific advancements have resulted in longer life expectancies. Global average life expectancy in 2019 was 9.8 % higher than in 2000 and further increases are predicted, resulting in a significant aged population (Cao and Ho, 2020). For example, in Sweden, more than 50 % of the 50,000 babies born in 2007 are expected to become centenarians, compared to ~750 people who turned 100 in 2007 (Vaupel, 2010). Concerningly, however, *healthy* average life expectancy (HALE) has not maintained this pace. In 2019, global HALE was 63.7, compared to the overall life expectancy of 73.4 years (Cao and Ho, 2020). This means that, while individuals may be living longer, they are not necessarily maintaining their health for this full period, resulting in increased prevalence of age-related diseases and demand for healthcare services (Chang et al., 2019). Particularly, incidence of neurodegenerative diseases (NDs), including Alzheimer's disease (AD) and Parkinson's disease (PD), which are highly prevalent in the >65 population, has increased dramatically (Hou et al., 2019).

This is significant, as these age-related NDs have long-term cumulative societal and economic impacts (Arafah et al., 2023). Analysis of the global burden of disease study 2019 revealed AD was responsible for 25.3 million disability adjusted life years (DALYs) and PD 6.2 million in 2019 (Ding et al., 2022). This represents a 161 % and 128 % increase in DALYs caused by AD and PD, respectively, since 1990 (Ding et al., 2022). Additionally, AD has an annual treatment cost of $305 billion USD (Wong, 2020) and PD around $52 billion (Yang et al., 2020a), with costs set to rise with the number of diagnoses. Current management focuses solely on symptomatic relief, as disease-modifying therapeutics are lacking (Kalia and Lang, 2015; Yiannopoulou and Papageorgiou, 2020). While symptomatic relief is critical for improving patient's daily lives, this does not address the underlying brain mechanisms of the disease, ultimately resulting in increased healthcare burden as the

* Corresponding author at: SG31, Helen Mayo South, The University of Adelaide, Adelaide, SA 5005 Australia.
E-mail address: Lyndsey.collins-praino@adelaide.edu.au (L.E. Collins-Praino).

https://doi.org/10.1016/j.bbi.2024.04.023
Received 22 May 2023; Received in revised form 4 March 2024; Accepted 22 April 2024
Available online 23 April 2024
0889-1591/© 2024 The Author(s). Published by Elsevier Inc. This is an open access article under the CC BY license (http://creativecommons.org/licenses/by/4.0/).

disease continues to progress and comorbidities arise (Arafah et al., 2023).

To develop disease-modifying treatments for NDs, there needs to be a better understanding not only of disease-specific pathophysiology, but also, the shared contribution of ageing across NDs (Mayne et al., 2020). Age is the primary risk for developing NDs (Hou et al., 2019), and it is well documented that age-related cellular changes can impact physiological function and exacerbate disease pathology (González-Gualda et al., 2021). Despite this, while there are exceptions (DiMarco et al., 2023; Muñoz-Manchado et al., 2016), many preclinical ND studies are still conducted in young animals and *in vitro* studies are rarely carried out on the background of ageing. While this may be appropriate for certain study designs, for example where the focus is specifically on finding potential prophylactic therapeutic options for NDs (Yang et al., 2020b), this is nevertheless a considerable shortcoming for many investigations in the field. Assuming responses in young cohorts are reflective of older populations is inaccurate (Sun et al., 2020) and has the potential to impact translation of findings from preclinical therapeutic investigations to aged patients. With this in mind, here we first introduce the aged phenotype in mammals and then discuss how aspects of this phenotype may be better incorporated into both *in vitro* and *in vivo* modelling of NDs.

1.2. The aged phenotype

As ageing characterised by decline in function and is often described as a pathophysiological process, there is debate as to whether healthy ageing truly exists (Faragher, 2015). For this review, healthy ageing refers to the biological changes that occur in an organism later in life, after the growth and development period has ended and advanced adulthood has begun, and which are not associated with a diagnosed condition. There are a number of visible features commonly associated with natural ageing (Fig. 1A) which define an individual as aged. These include hair greying, skin changes (Halliwell and Dittmar, 2003) and musculoskeletal changes, including muscle wasting, joint immobility and decreased bone density (Azzolino et al., 2021). Functionally, ageing corresponds to changes in multiple systems, including digestive (Bhutto and Morley, 2008), reproductive (Kaufman et al., 2019; Shirasuna and Iwata, 2017), circulatory (Strait and Lakatta, 2012) and immunity (Wang et al., 2022), with the latter two contributing to increased vulnerability to infections and diseases (Strait and Lakatta, 2012). Cognitive function is also affected with natural ageing, with declines

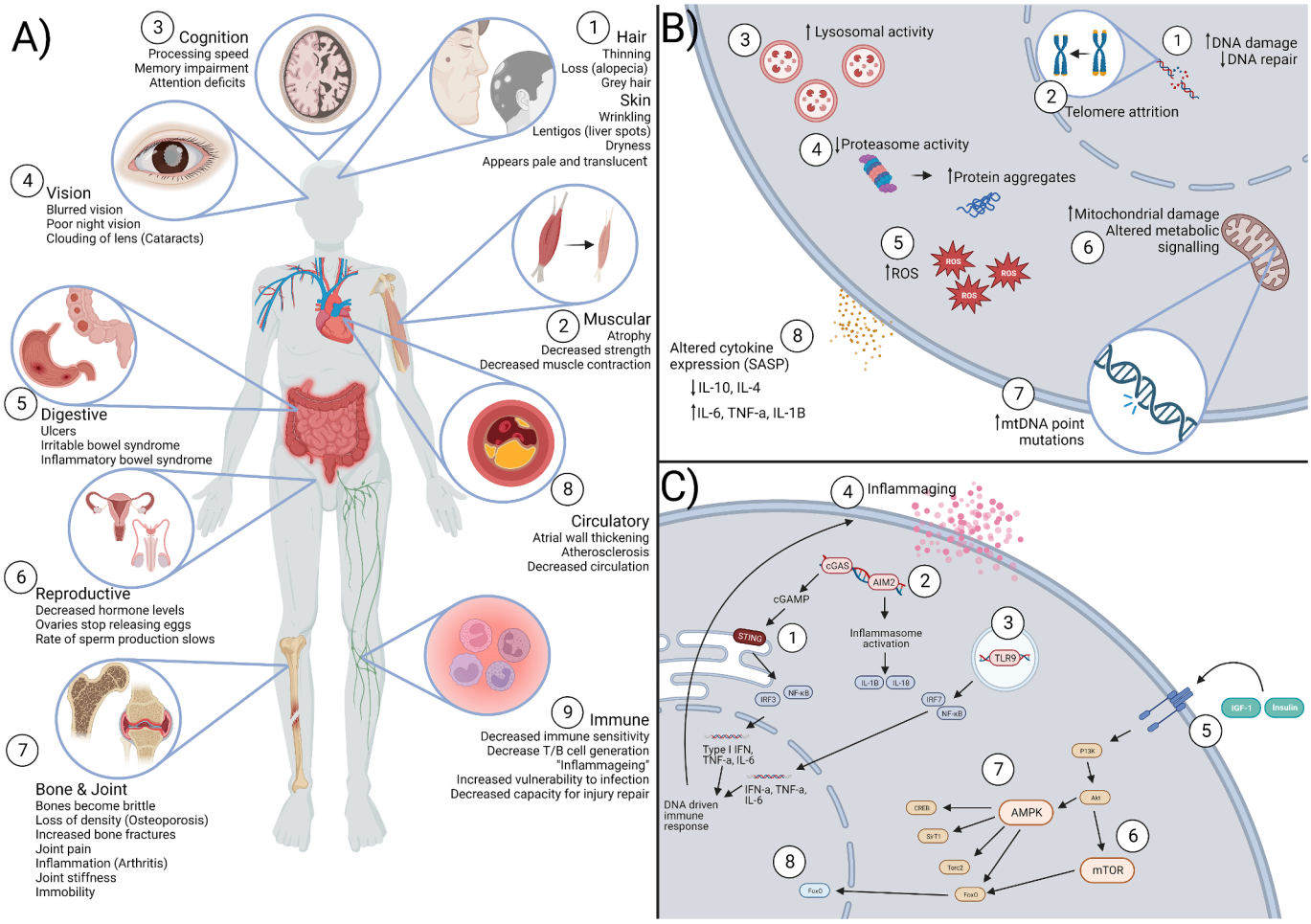


Fig. 1. Biological ageing A) whole-body distinguishing features including changes in (1) hair and skin (2) muscle, (3) cognition, (4) vision, (5) digestion, (6) reproduction, (7) bones and joints, (8) circulation and (9) immunity. B) cells display aged/senescent features including (1) increased DNA damage and decreased DNA repair, (2) telomere shortening, (3) increased lysosomal presence and activity, (4) decreased proteasome activity causing an increase in intracellular protein aggregates, (5) increased production of reactive oxygen species (ROS), (6) mitochondrial damage, (7) increased mitochondrial DNA mutations and (8) the development of the senescence-associated secretory phenotype (SASP). C) functional changes to inflammation and metabolism driven by cell signalling changes with an increase in the DNA driven immune response influenced by the (1) cGAS-STING pathway, (2) AIM2 pathway and (3) the TLR9 pathway which all contribute to (4) increased inflammation termed 'inflammageing'. Metabolic signalling pathways are also altered with (5) altered insulin/IGF-1 binding and (6) mitochondrial damage both influencing changes in the (7) mTOR and (8) AMPK pathways. Both pathways can regulate transcription of factors important for cell cycle regulation, metabolism, and apoptosis such as (9) FoxO.

seen in several domains, including memory, processing speed and reasoning ability, although these changes are not as pronounced as mild cognitive impairment or AD (Moreira et al., 2019). Conversely, other aspects of cognition, such as vocabulary, are resistant to the effects of ageing and even increase until individuals are 60^{+} years old (Hartshorne and Germine, 2015). Given the multiple systems impacted, ageing is clearly multifactorial, reflected by several theories being put forward to explain mechanisms of ageing (reviewed: (da Costa et al., 2016)). This has led to the formulation of 12 hallmarks of ageing by López-Otín and colleagues (López-Otín et al., 2023): genomic instability, telomere shortening, epigenetic alterations, loss of proteostasis, disabled macroautophagy, dysregulated nutrient sensing, mitochondrial dysfunction, cellular senescence, stem cell exhaustion, alterations in intracellular communication, chronic inflammation and dysbiosis. While an in-depth consideration of all of these hallmarks is outside the scope of the current work, below we discuss markers of ageing in the context of a senescent phenotype specifically those relevant to brain ageing. We direct the reader to López-Otín and colleagues excellent review on the topic (López-Otín et al., 2023) for further reading on the additional markers not discussed here. The markers discussed in aged cellular phenotype below are critical to take into account for age-related neurodegenerative diseases.

Central to ageing mechanisms are the defining features of a senescent cell, (Fig. 1B) with cellular senescence named as one of the hallmarks of ageing (López-Otín et al., 2023). Senescent cells are often physically distinguishable, with enlarged and flattened morphology compared to young cells (González-Gualda et al., 2021). A characteristic feature of cellular senescence is cell cycle arrest, with loss of proliferative capacity. Cellular senescence is commonly assessed by evaluating levels of cell cycle regulators, including P16 and P21, kinases which play crucial roles in the transition from G1 to S phase of the cell cycle and are upregulated in G1-phase cell cycle arrest (Serrano et al., 1997). DNA damage, measured by DNA double strand breaks (DSBs), and telomere shortening (Fig. 1B (1–2)) are considered major drivers of cell cycle arrest and consequent senescent phenotype (Fumagalli et al., 2012), and accordingly were listed as two of the 12 hallmarks of ageing (López-Otín et al., 2023). Normally, the DNA damage response (DDR) counteracts DNA damage by either repairing damage or initiating apoptosis if the damage is beyond repair (reviewed: (Chatterjee and Walker, 2017). However, with ageing, rate of DNA damage overwhelms the capacity of the DDR, resulting in accumulated damage in both mitochondrial (mtDNA) and nuclear DNA, with subsequent altered gene expression, impaired cellular function and senescence (Victorelli et al., 2023).

Increased lysosome activity (Fig. 1B (3)), measured by senescence-associated-beta-galactosidase (SA-β-gal) staining, is one of the most common markers of a senescent cell (López-Otín et al., 2023). While SA-β-gal increases have been shown in ageing cells, including mammalian neurons (Jurk et al., 2012) and fibroblasts (Yang and Hu, 2005), the presence of SA-β-gal is not exclusive to, or required for, senescence (de Mera-Rodríguez et al., 2021). In fact, SA-β-gal has been found to be upregulated in PD CSF (van Dijk et al., 2013) and AD plasma samples (Magini et al., 2015) compared to aged controls, indicating the presence of ND-related lysosomal dysfunction beyond ageing alone (van Dijk et al., 2013). A decrease in proteasome activity with age (Fig. 1B (4)) is also widely reported (Ferrington et al., 2005; Kelmer Sacramento et al., 2020; Ponnappan et al., 1999), with dysfunctional proteostasis, identified as one of the 12 hallmarks of ageing (López-Otín et al., 2023), acting as a potential contributor to pathological protein accumulation in NDs (Kelmer Sacramento et al., 2020). Similarly, mitochondrial dysfunction is a major contributor to the senescent phenotype (Fig. 1B (5)), leading to an altered metabolic phenotype (López-Otín et al., 2023). Damaged or dysfunctional mitochondria are a hallmark of ageing (López-Otín et al., 2023) and are major contributors to increased reactive oxygen species (ROS) production (Fig. 1B (6)), which has been linked to both senescence (Nelson et al., 2018) and NDs (Gao et al., 2020). Increased ROS contributes to mitochondrial stress and damage, thereby exacerbating the senescent phenotype (Chakrabarti et al., 2011).

Inflamm-aging was a term first devised by Franceschi et al in 2000 to describe the concurrent decline in immune function and development of a chronic pro-inflammatory state with increasing age, in the absence of any external immune stimulation (Franceschi et al., 2000) and has since become a prominent theory of ageing (Xia et al., 2016). Fittingly, chronic inflammation is described as a hallmark of ageing (López-Otín et al., 2023) and is thought to be driven by the development of the senescence associated secretory phenotype (SASP) (Olivieri et al., 2018) (Fig. 1B (8)), which is a key element of senescence discussed by López-Otín and colleagues (López-Otín et al., 2023). The SASP was observed to occur in multiple cell lines and *in vivo* in 2008 as a response to DNA damage (Coppé et al., 2008). This phenotype features high ongoing production of pro-inflammatory cytokines, such as interleukins (IL-6, IL-8, IL-1β) and Tumour Necrosis Factor (TNF, formerly known as TNF-α (Grimstad, 2016)), which contribute to further immune activation (Coppé et al., 2008). In the brain, microglia are thought to be responsible for the emergence of this damaging inflammation in NDs and the SASP (Hu et al., 2021), with specific microglial pathways implicated in this process.

The shift toward an inflammatory phenotype in the brain is associated with changes in major signalling pathways involved in DNA-driven immune recognition responses (Gulen et al., 2023) (Fig. 1C). For example, cyclic GMP-AMP synthase (cGAS) is a cytosolic DNA sensor, which, upon binding to DNA in the cytosol, initiates cyclic GMP-AMP (cGAMP) to bind with the stimulator of interferon genes (STING) located on the endoplasmic reticulum (Fig. 1C (1)). This binding induces a signalling cascade leading to production of type-1 interferons and pro-inflammatory cytokines (Sun et al., 2013). During ageing, cGAS recognition of cytosolic DNA danger signals increases, potentially due to increased nuclear and mitochondrial damage, as outlined in Fig. 1B (1–2 and 5)) (Gulen et al., 2023). The resulting increase in activation of this pathway is hypothesised to drive the ongoing low-grade inflammatory state seen in ageing(Gulen et al., 2023), a state which is also linked to neurodegenerative diseases (Guzman-Martinez et al., 2019) (Fig. 1C (4)).

Similarly, dysregulated intracellular metabolic processes are one of the hallmarks of ageing (López-Otín et al., 2023) and thus are critical in cellular and systems ageing. Key regulators of metabolism are insulin and insulin-like growth factor-1 (IGF-1), which both decline with age, as does binding to insulin/IGF-1 receptors (Fig. 1C (5)) (Toth et al., 2022). Not only does decreased insulin/IGF-1 signalling impair cerebral blood flow and contribute to neuronal dysfunction (Toth et al., 2022), it also causes dysregulation in the mechanistic target of rapamycin (mTOR) and AMP-activated protein kinase (AMPK) metabolic pathways (Yang et al., 2018)(Fig. 1C (6–8)). The mTOR and AMPK pathways are major regulators of cell metabolism, mitochondrial function, cell growth and cell survival (Kazyken et al., 2019), and of the many signalling pathways involved in metabolism, these are the best described and most closely linked to biological ageing (Morita et al., 2013). With age, there is a loss of sensitivity of the AMPK pathway, which normally has an inhibitory effect on mTOR signalling (Gwinn et al., 2008). This subsequently leads to an increase in mTOR signalling, which has been linked to the manifestation of age-related disorders (Bitto et al., 2016). Additionally, both AMPK and mTOR pathways induce transcription of genes related to mitochondrial function, in particular transcription of forkhead box class 0 (Fox0), a regulator of mitochondrial homeostasis (Davila et al., 2012). Dysregulation of these pathways with age may thus further exacerbate mitochondrial dysfunction. Interestingly, there is conflicting evidence regarding whether activation of the mTOR and AMPK pathways confers neuroprotective or damaging effects in ND (reviewed: (Querfurth and Lee, 2021)). Overall, however, it is evident that ND pathophysiology does not occur in isolation, but rather is concomitant with the complex and multifactorial physiological changes of ageing. It is thus imperative to consider these changes when modelling ND preclinically.

1.3. The aged phenotype may not only affect pathophysiology, but also directly influence drug response

Given that there is no single causative gene or pathway controlling ageing, but rather many changes contributing to the ageing process, results obtained in "young" models may not be translatable within an aged context. In fact, age-related differences in drug responses are widely recognised, with adverse drug reactions in elderly patients being twice as common compared to younger patients, particularly with drugs targeting the CNS (Beijer and de Blaey, 2002).

Further, age-associated alterations have been reported for multiple (but not all) members of the cytochromes P450 family of drug-metabolising enzymes (CYPs) (reviewed: (Kinirons and O'Mahony, 2004)), suggesting that drug pharmacokinetics are altered in natural ageing. In line with this, a study that looked at the mRNA expression profile of 101 xenobiotic-processing genes in mice found that 44 % of genes were altered with age in male mice and 64 % changed with age in female mice (Zidong Donna et al., 2012). Interestingly, although it would be reasonable to hypothesise that these changes would be further exacerbated in NDs, to date, this has yet to be explored in the literature (Wu and Lin, 2019).

Although CYPs are abundantly expressed and studied in the liver, the primary site of drug metabolism, CYPs are also widely expressed in the brain, with some forms, such as CYP2D4 and CYP2D18, expressed exclusively, or at much higher levels, here than in other tissues (Kawashima and Strobel, 1995; Komori, 1993). Importantly, brain CYPs play a role in metabolising many drugs that act on the CNS (for review, see (Miksys and Tyndale, 2013)) and can alter response to CNS-acting drugs (Khokhar and Tyndale, 2011). This may have implications for the treatment of CNS disorders, including NDs. Intriguingly, there is great inter-individual variation in brain expression levels of CYP levels, and this can be affected by multiple factors, including age. For example, in humans, brain levels of the neuroprotective enzyme CYP2D6 gradually increase with age, reaching their highest levels in those aged 65+ (Mann et al., 2012). This gives further support to the idea that the response to centrally acting drugs may differ in younger versus older adults. This response may be further altered in those with NDs. In line with this, those with PD were shown to have ~40 % lower levels of CYP2D6 within several brain regions, including the frontal cortex, cerebellum and hippocampus (although, interestingly, not in the substantia nigra or caudate), compared to age-matched controls (Mann et al., 2012).

These effects may be due, at least in part, to the increases in inflammation seen both with natural ageing (i.e. inflammageing) (Franceschi and Campisi, 2014) and in NDs (Guzman-Martinez et al., 2019). In support of this, pro-inflammatory factors are known to correspond to reduced activity of many drug metabolising enzymes (Aitken et al., 2008), including CYPs (reviewed: (de Jong et al., 2020)). A systematic review of 218 studies in adults by Lenoir et al. (2021) demonstrated that inflammation modulates the activity of multiple CYPs and thus alters drug pharmacokinetics, although the effect is dependent on the particular CYP isoform and source of inflammation considered (Lenoir et al., 2021). While the exact implications of this for understanding drug response in younger versus older individuals, as well as in individuals with a ND, remain to be explored, it nevertheless highlights that when testing potential therapeutics for NDs, either in *in vitro* or *in vivo* models, it is critical to account for the potential impact of age, in order to improve the translational relevance of the findings.

2. Laboratory models of the aged phenotype

The mechanisms underpinning ageing are multifactorial and thus make modelling age-related NDs complex. In the following section, key laboratory models of ageing are described and critically examined for their applicability to NDs.

2.1. In vitro models of CNS ageing: relevance for ND research

2.1.1. Cells derived from aged donors

In vitro studies are a critical tool in understanding how the aged brain functions at the cellular level. Primary cells from aged individuals are understandably regarded as one of the most accurate models, as they can capture the features of an aged cell and retain the genetic characteristics of the donor when harvested using specific techniques. However, for the human CNS, obtaining such cells directly can be difficult, relying on cultures produced from post-mortem brains or tissue removed during brain surgery. The advent of human induced pluripotent stem cells (iPSCs) in 2006 (Takahashi and Yamanaka, 2006) resolved some of these difficulties, allowing somatic cells to be induced to become pluripotent by expression of four reprogramming factors known as OKSM factors or Yamanaka factors (Takahashi and Yamanaka, 2006). These iPSCs can then be differentiated into CNS cells and used to model neurological disorders.

Using this method, both neurons (Miller et al., 2013) and glial cells (Abud et al., 2017; Voulgaris et al., 2022) derived from iPSCs have successfully been used as models of AD and PD (reviewed: (Pandey et al., 2022)). For example, utilising iPSCs derived from somatic cells of patients with familial PD, it is possible to generate dopaminergic neurons that express pathological PD mutations and show PD-like pathology in culture, including increased pathological α-synuclein aggregates (Kouroupi et al., 2017), neurite degeneration (Sánchez-Danés et al., 2012) and dysregulated dopamine pathways (Jiang et al., 2012). Cultures derived from iPSCs obtained from individuals with idiopathic PD also display PD-like impairment of neurite formation (Sánchez-Danés et al., 2012) and increased autophagy and mitophagy (Hsieh et al., 2016). Similarly, neurons derived from iPSCs of AD patients carrying the APP mutation display short fragments of amyloid-beta (Aβ) and increased Aβ42:40 ratios. Importantly, however, when using iPSCs to model ageing, studies have shown that the developmental reset induced by treatment of the somatic cells with Yamanaka transcription factors erases senescent features in these cells (Kim et al., 2018; Tang et al., 2017). Table 1 summarises several studies where reset of the ageing phenotype has been demonstrated in iPSC-derived neurons and glia. Reset of telomeres, heterochromatin levels, mitochondrial health, nuclear organisation, and protein damage is widely thought to occur during induction to pluripotency (Miller et al., 2013) and has been reported across multiple studies on ageing iPSCs (Lapasset et al., 2011; Ocampo et al., 2016) (Prigione et al., 2011; Suhr et al., 2009). While iPSC technology has great potential for regenerative therapy in ND treatment (Limone et al., 2022), simply utilising iPSCs derived from older individuals may be insufficient to accurately replicate the aged phenotype of CNS cells.

Alternative to iPSCs, directly induced neurons (iNs) aim to achieve control over the phenotype of the induced cells. These are derived from somatic cells by lentiviral or microRNA-based expression of "BAM" factors and neurogenesis factors, such as NeuroD1 and Ngn2, similar to the expression of Yamanaka factors in the reprogramming iPSCs, but bypassing the need to become pluripotent before differentiation (Vierbuchen et al., 2010). Promisingly, these cells display retention of age after differentiation, with epigenetic age of the original donor cell, measured by DNA methylation, displaying a high correlation with epigenetic age of the iN (Huh et al., 2016). Additionally, iNs derived from idiopathic PD patients maintain age-associated genetic signatures and α-syn pathology, which is not present in iPSC-neurons derived from these same patients (Drouin-Ouellet et al., 2022). Similarly, directly converted neural progenitor cells display ageing when further differentiated to astrocytes, with changes summarised in Table 1 (Gatto et al., 2021). Thus, skipping induction to pluripotency through direct conversion appears to avoid the senescence reset, allowing for a more robust model of ageing (Huh et al., 2016), as well as retention of sporadic neurodegenerative pathology (Drouin-Ouellet et al., 2022). While promising, protocols for direct cellular reprogramming into brain cells

Table 1
Strengths and weaknesses of *in vitro* methods to model CNS ageing.

Method of ageing	Model	Time to achieve phenotype	Aspects of the aged phenotype induced	Strengths	Weaknesses
Human donor derived cells	iPSC derived CNS cells	3wk-1mth	Astrocytes: Markers of mature astrocytes (GFAP, AQP4, ALDH1L1), presence of glutamate transporters, functional glutamate uptake (Voulgaris et al., 2022) Neurons: ↓γH2AX, ↓SA-B-gal, no impairment of nuclear organisation (Tang et al., 2017)	Reflective of primary cells from patients and of CNS origin Potential in regenerative therapy	Induction to pluripotency resets ageing Complex to establish Low production efficiency Single cells not complex model
	Induced neurons	4–6 wks	Impaired mitochondrial function, ↓oxidative phosphorylation (Kim et al., 2018) ↑γH2AX, ↑SA-B-gal, impaired nuclear organisation and compartmentalisation (Tang et al., 2017)	Reflective of primary cells from patients and of CNS origin Cells retain ageing and neurodegenerative pathology Preservation of epigenetic factors Potential in regenerative therapy	Limited time to be sustained in culture Complex to establish Low production efficiency Single cells not complex model
Replicative senescence	Primary cells (of peripheral or CNS origin)	40–60 population doublings 50–60 passages 10–20 days in culture	↑SA-B-gal (Boraldi et al., 2015; Caldeira et al., 2014; Deng et al., 2023; Kurz et al., 2000), ↑lysosomal mass (Kurz et al., 2000) Activated morphology, ↑Matrix Metalloproteinase (MMP)-2, ↓NF-kB, ↓MMP-9, ↓TLR-2, ↓TLR-4, ↓autophagy, ↓migration and phagocytic capacity(Caldeira et al., 2014) Enlarged cells, vacuolated cytoplasm, aHDF: longer growth periods than nHDF (Boraldi et al., 2015) Enlarged nuclei, ↓proliferation, ↑P16/P21, ↑γH2AX, ↑uPAR, SASP (Deng et al., 2023)	Ageing is not biased by manipulating a specific pathway Simple model to establish and maintain Insight into basic cell changes	N/A for post-mitotic cells e.g., neurons. Not practical for long term experiments. Variability in measurement of age Highly variable phenotype between cell populations Inconsistent markers assessed between studies makes it hard to compare results Not well understood in immortalised cell lines Single cells not complex model
Complex models	Co-culture primary neurons and glia	27 days	↑SA-B-gal, ↑γH2AX, ↑oxidative stress, ↑pro-inflammatory cytokine production (Bigagli et al., 2016)	Shows microRNA signature reflecting pathological ageing More complexity than single monolayer culture	difficult to establish successful co-cultures
	Organoid models	45 days	SASP (↑IL-1β, TNF-a), ↑P16, P21 (Ao et al., 2022)	Resembles the brain environment Demonstrates ageing phenotype without manipulating pathways	Complex to establish Stem cells have a young cellular phenotype inconsistent with ageing

have been less extensively described than those for iPSCs. Additionally, there is a need for further validation regarding the neuronal phenotypes induced from differing cellular origin (Chouchane et al., 2017) and potential risks involved in using iNs for regenerative therapy (Kim et al., 2021).

Overall, it is important to note that the donor age does not consistently affect the lifespan of primary cells *in vitro* (Cristofalo et al., 1998; Kaji et al., 2009). This is exemplified from cultures generated from participants in the Baltimore Longitudinal Study of Ageing. This study compared the proliferative capacity of fibroblasts collected from young donors (20–29 years) versus old donors (65^{+}years) both cross-sectionally and longitudinally, with donor matched biopsies up to nine years apart (Smith et al., 2002). No difference in lifespan of fibroblasts was observed cross-sectionally, except when derived from female donors (Smith et al., 2002), where a reduced proliferative potential correlated with donor age. Comparison of cells from the same donor longitudinally demonstrated a trend to decrease in proliferative potential over time, but this was not statistically significant, potentially on account of considerable variation between cell lifespan from different donors (Smith et al., 2002). Conversely, a study comparing fibroblasts from donors aged 21–36 versus donors aged 63^{+} reported significant effect of donor age on the proliferative potential of cells in culture (Schneider and Mitsui, 1976), although large variability and overlapping data points between age groups was observed. These studies highlight that *in vivo* chronological age may not directly translate to reduced proliferative capacity and senescence *in vitro*, with variation between donors, combined with variations in cell isolation and culture protocols, leading to challenges in reproducibility (Qadan et al., 2018). While simply generating iPSCs or iNs from aged donor cells may not fully encapsulate an aged phenotype in the sense of proliferative capacity, the potential utility of these cells in ND research and therapy should not be understated. Further, other markers in addition to proliferation can be used to assess age and determine the age of a culture, as discussed in more detail below.

2.1.2. Replicative senescence

Other than utilising cells from aged donors, the most prominent method of inducing senescence *in vitro* is by culturing cells to a proliferative limit, termed replicative senescence, first proposed by Leonard Hayflick in 1965 (Hayflick, 1965). In these early studies, primary cells were cultured from human foetal tissue continually for up to 11mths or 55 passages. The “Hayflick limit” is widely accepted and is the basis for characterising serially cultured cells as a model of cellular ageing (Phipps et al., 2007). Passaging cells to this limit produces the characteristic cell cycle arrest and SASP seen in senescent cells, without researchers intentionally altering specific cellular pathways (Hayflick, 1965) and thus may result in a more translationally relevant aged phenotype. In line with this, studies using peripheral cells (presented in table 1), including dermal fibroblasts and umbilical vein endothelial cells, display a senescent phenotype featuring the SASP (Deng et al., 2023), SA-β-gal (Boraldi et al., 2015; Caldeira et al., 2014; Kurz et al., 2000), increased cell cycle regulators (Deng et al., 2023), decreased proliferation (Boraldi et al., 2015) and increased markers of DNA damage (Deng et al., 2023), all key components of the aged phenotype (Fig. 1). When looking at CNS cells, similar results have been observed; however, the use of CNS cell types in studies of replicative senescence is sparce. Primary microglia have been shown to change from a reactive to a chronically active, age-like phenotype (Table 1) when kept in culture for a 16-day period (Caldeira et al., 2014). The lack of investigation of replicative senescence in neurons is due to the fact that they are post-mitotic, and thus do not replicate and cannot undergo replicative senescence (Hartmann et al., 2023), making this method less applicable for the modelling of NDs.

Replicative senescence as an *in vitro* model of ageing has been validated mostly in passaged primary cells, where replicative senescence occurs more readily than in immortalised cell lines. Recently, however, untransformed primary mouse T-cells have demonstrated the ability to continue to divide and remain functional in culture for 10 years, potentially challenging the idea of universal applicability of the Hayflick limit (Soerens et al., 2023). Additionally, a primary cell model of ageing is difficult to consistently reproduce due to variation between cell populations, presenting a challenge for widespread use and high throughput industry applications. Furthermore, there is limited capacity to conduct complex experiments or investigate long-term effects, due to the limited time primary cells can be sustained in culture (Hayflick, 1965). Alternatively, investigating passage number as a proxy for ageing in immortalised cell lines may offer the opportunity to study phenotypic or functional changes over time, rather than simply modelling cells at their proliferative end (Sapieha and Mallette, 2018). Although immortalised cells have been argued as unfit for a model of ageing due to their limitless proliferative capacity and resistance to replicative exhaustion (Bunc et al., 2019), it is a recommended laboratory practice to only culture cell lines for a limited passage range, beyond which the cells are assumed to have diverged from the original cell phenotype (Geraghty et al., 2014; Hughes et al., 2007). Exactly what changes are induced in these cells with passage is not well characterised (Hughes et al., 2007), and, potentially, these changes may mirror some of the changes associated with the aged phenotype. Of particular relevance for NDs, it would be useful to characterise the phenotypic changes that occur in both immortalised glial cell lines (e.g. BV2 cells) and in neuronal-like cell lines (e.g., both differentiated and undifferentiated SH-SY5Y neuroblastoma cells, an *in vitro* model of PD (Xicoy et al., 2017)). If such immortalised cell lines do show alterations consistent with the aged phenotype with increased passage numbers, then this has significant implications for how these cells might be used to more appropriately model ND on an aged background *in vitro*.

2.1.3. Emerging methods and future directions

While single monolayer cultures provide a basic way to induce the senescence-related molecular changes associated with ageing, these models lack the complexity of co-culture and organoid brain models. This is particularly relevant for NDs, which are multifaceted, heterogenous diseases that involve interactions between multiple brain cell types (Luchena et al., 2022). In recent years, these alternative culture methods have been developed that provide an avenue to improve modelling of NDs. The use of co-culture models, which involve simultaneous expression of neuronal and glial cells, allows for examination of cellular interactions at the level of the tetrapartite synapse. Co-culture is being used to improve modelling of NDs and provide critical insights into cellular interactions in these diseases (see Table 1). For example, in a 2D triple co-culture model of murine astrocytes, microglia and neurons, exposure to oligomeric amyloid beta resulted in neuroinflammation and synaptic loss, providing a model that is more reflective of pathological processes associated with AD (Luchena et al., 2022). Similarly, using a co-culture model of LPS-stimulated macrophages and SH-SY5Y cells (model for dopaminergic neurons), reactive macrophages were shown to induce oxidative stress and consequent increased alpha-synuclein nitration and cell death in the SH-SY5Y cells (Shavali et al., 2006).

While allowing for complex interactions to be captured, it remains to be seen how the aged phenotype might be best incorporated into such co-cultures. One promising study by Bigagli and colleagues (2016) maintained primary neuronal/glial co-cultures up to 27 days *in vitro* and demonstrated that these cultures displayed multiple signs of cellular senescence, including increased levels of SA-β-gal, γ-H2AX, oxidative stress and pro-inflammatory cytokines (Bigagli et al., 2016). Interestingly, however, analysis of 180 microRNAs showed a pattern of change more consistent with transgenic TgCRND8 mice (model of amyloid-β deposition) than with physiologically aged mice, suggesting that long-term maintenance of the co-culture model may more closely resemble the changes of pathological ageing than natural ageing. Nevertheless, this provides preliminary evidence that aspects of the aged phenotype can be incorporated in more complex co-culture models.

Similar to co-culture models, brain organoid models demonstrate potential to replicate the complexity of the aged brain. Organoid models are stem cell derived 3D tissue cultures comprised of multiple cell types aimed at recapitulating the complexity of whole systems, in a way that co-culture and single monolayer culture cannot (Shou et al., 2020). These models are generated by embedding embryoid bodies into extracellular matrix and inducing neural differentiation by supplementation with growth factors to support growth of specific brain structures (Shou et al., 2020). For NDs, these complex models have demonstrated utility in modelling ND pathology. Brain organoids have demonstrated pathological Aβ aggregation and Tau phosphorylation when derived from familial AD patients with cells overexpressing APP and PSEN1 (Choi et al., 2014; Raja et al., 2016). Similarly, organoids which have the LRRK2-G2019S mutations seen in familial PD display α-synuclein aggregation and altered neuronal morphology, as is seen in PD (Kim et al., 2019). Excitingly, organoids may also offer a way to incorporate an aged phenotype into models of ND. In support of this, a recent study by Ao and colleagues (2022) demonstrated that 45-day-old brain organoids show upregulation of key ageing markers, including cell cycle regulators and pro-inflammatory cytokines, in response to monocyte infiltration from aged patients compared to cultures infiltrated with young monocytes (Ao et al., 2022). Therefore, while embryonic stem cells, from which organoids are developed, naturally have a young cellular phenotype, with elongated telomeres not reflective of the senescent phenotype seen in the aged brain (Ao et al., 2022), long-term culture of organoids may produce a more translationally relevant model for studies of ND.

In addition to current model limitations, another major challenge in reproducing the aged phenotype *in vitro* is the inconsistency of markers used across studies, which can make it difficult to fully evaluate models. This was recently addressed by Hartmann and colleagues (2023), who validated a biomarker-based panel to assess age *in vitro* in fibroblast cultures (Hartmann et al., 2023). This panel included many ageing markers discussed above, including DNA damage, telomere attrition, SA-β-gal, SASP, cell cycle arrest and morphological changes, as well as additional markers, such as histone modification and changes in nuclear lamina protein: Lamin B. Using these markers, an 'AgeScore' was derived, which correlated well with chronological donor age in both healthy individuals and donors with progeroid syndromes (diseases associated with accelerated ageing) (Hartmann et al., 2023). While not yet investigated, this AgeScore may also be translatable to CNS cells. However, neuronal populations are post-mitotic, meaning cell cycle arrest, the defining feature of replicative senescence, cannot define an aged neuron (Hartmann et al., 2023). Despite this, a recent study investigating senescence 1wk following repeated mild traumatic brain injury induced by closed skull controlled cortical impact in C57BL/6 mice identified 15 clusters of neurons in injured mice, all expressing at least one marker of senescence (Schwab et al., 2022). This study provides evidence that, while neurons are post-mitotic, they can still demonstrate traditional markers of a senescent phenotype following traumatic brain injury, hypothesised to accelerate brain ageing (Cole et al., 2015). Thus, a modified version of the "AgeScore" may have utility even in evaluating neuronal cultures and subsequent standardisation of modelling ageing *in vitro* between studies.

Overall, while there is a multitude of research on inducing and characterising age in cell culture models (reviewed: (González-Gualda et al., 2021)), there has been less implementation of these models in ND research. This may be due to the difficulties in replicating results from primary culture across laboratories and across studies (Hirsch and Schildknecht, 2019) or the complexity of modelling disease alongside brain ageing. While research using standard models has and will continue to make significant contributions to the ND research field, given the critical role of age in the risk of ND development, incorporating aspects of the aged phenotype *in vitro* has the potential to lead to more translationally relevant models of ND. This will enhance our understanding of the pathophysiological mechanisms that drive ND emergence and lend insight into the therapeutic effects of putative treatments.

2.2. *In vivo models of ageing: Potential applications to ND research*

2.2.1. *Spontaneous and accelerated models of ageing*

To date, research incorporating aged animals has shown differences in motor performance, cognition and pathology following induction of neurodegenerative models. Recently, in an intracerebroventricularly injected streptozotocin model of sporadic AD, aged rats at 23 months old demonstrated increased p-Tau/Tau levels compared to controls whereas this increase was not displayed in young AD rats compared to controls (Gáspár et al., 2022). Additionally, these aged rats showed increased susceptibility to toxicity following induction of the model compared to young rats. Similarly, age impacted the effect of 6-hydroxydopamine lesion on skilled motor function and TH positive neuronal loss in the substantia nigra (Barata-Antunes et al., 2020). The results from these studies, and others discussed at length by Sun and colleagues (Sun et al., 2020), highlight the importance of including age in pre-clinical models of NDs in order to fully recapitulate a disease phenotype relevant to those seen in aged patients in the clinic.

A natural model of ageing would be most accurate in recapitulating all elements of this phenotype *in vivo*. The naked mole rat has a lifespan upwards of 37 years and low incidence of age-related neurodegeneration (Delaney et al., 2021). This species has provided insight into the mechanisms of natural ageing and disease resistance; however, due to their long lifespan, the utilisation of naked mole rats in laboratory research is impractical (Delaney et al., 2021). Additionally, given their resistance to age-related neurodegenerative pathology, genetic or experimental manipulation is required to make them a relevant model for ND research. Instead, for an estimated 80 % of ageing research, shorter lived rodent models are utilised (Andreollo et al., 2012), such as mice and rats, which live around 3 and 3.5 years, respectively, and, therefore, make it logistically feasible to house and obtain naturally aged animals within the time-frame of a reasonable research study (Andreollo et al., 2012).

Importantly, translating ageing across species is difficult due to differences in rate of maturation. In line with this, from birth to 1-month, mice mature approximately 150 times faster than humans, but this drops to 45 times faster in mice aged 1–6 months and to 25 times faster in mice aged 6-months or older (Flurkey et al., 2007). Despite this, some guidance has been put forward by Jackson Labs (Jackson Laboratory, 2020). In brief, based on survival analyses in a large cohort of C57BL/6J mice, the most commonly used inbred strain, the following life stages have been proposed: (1) mature adult from 3-6 months of age, roughly equivalent to 20–30 years of age in humans; (2) middle age from 10-15 months of age, which corresponds to approximately 38–47 years of age in humans and (3) old age from 18-24 months+, which is comparable to humans from 56 to 69 years of age (Jackson Laboratory, 2020). Interestingly, given that the old age period in mice is approximately equivalent to the period when age-related neurodegenerative diseases typically begin to arise in humans (Hou et al., 2019), while mice at 18–24 months old may not fully encapsulate the full aged phenotype of humans 70+ years of age, they can still provide valuable insights into the impact of ageing on disease pathophysiology and vulnerability to age-related diseases. It is important to investigate, however, how these age equivalents might vary as a factor of mouse strain, or indeed in other species, such as rats. In line with this, allele variation has been shown to result in both phenotypic differences (Simon et al., 2013) and disparities in response to an intervention (Liao et al., 2010), even in closely related strains.

Overall, the use of aged rodents comes with caveats, such as the presence of comorbidities, leading to many animals meeting ethical criteria for euthanasia prior to becoming aged (Brayton et al., 2012). While this may reflect population morbidities in humans, a portion of the study cohort is lost prior to reaching the experimental starting point

Table 2
Strengths and weaknesses of *in vivo* methods to model CNS ageing.

Method of ageing	Model	Age of phenotype presentation	Phenotype induced	Strengths	Weaknesses
Spontaneous accelerated ageing mice	SAMP8(Takeda et al., 1981)	6-16mths	Shortened lifespan, hair loss, skin pigment changes, ↓light phase activity, cataract development, amyloidosis, lordokyphosis (spine curvature) (Takeda et al., 1981) ↓spine density in hippocampus, ↑axonal dystrophy in hippocampus, astrogliosis (Kawamata et al., 1998), Aβ aggregates, ↑Tau phosphorylation (Takeda, 2009), ↑microglia, dysfunctional mitochondria(Kawamata et al., 1998), DA neuron degeneration in SN, noradrenergic neuron degeneration in LC (Takeda et al., 1981) Decreased anxiety-like behaviour, disrupted sleep cycle (Miyamoto, 1997), impaired memory and learning (Takeda et al., 1981)	Ageing is not biased by manipulating a specific pathway. Mice widely available for purchase Compatible with other genetic models of disease	Longer time to achieve ageing (10 mths +) Cognitive and behavioural changes may confound results for NDs
	SAMP10(Takeda et al., 1981)	6-16mths	Shortened lifespan, hair loss, skin pigment changes, ↓light phase activity, cataract development, amyloidosis, lordokyphosis (spine curvature) (Takeda et al., 1981) DNA damage (Shimada et al., 2002), cortical atrophy (Shimada et al., 1994), ↑microglial activation, ↑pro-inflammatory microglial signalling(Kumagai et al., 2007), ↑ubiquitinated inclusions (Shimada et al., 2008), ↓spine density and synapse density(Shimada et al., 2006) Depressive behaviour, emotional dysfunction (Miyamoto, 1997)		
	SAMP8-APP/PS1(Lok et al., 2013)	6–9 mth (3mth earlier than SAMP8 control)	Aβ accumulation, neuronal loss, abnormal movement, anxiety, learning and memory deficits		
WRN protein deficiency	129/Sv/Black Swiss WRN$^{\Delta hel/\Delta hel}$ (Lebel and Leder, 1998)	4–6 mths old	Develop features of metabolic syndrome (↑blood insulin, cholesterol and triglyceride), ↑cardiac fibrosis, ↑ROS levels (Massip et al., 2006) ↓motor activity/coordination, ↓perception and memory, ↑ repetitive behaviour, ↑hyper ramified microglia, ↑ neuronal oxidative stress in PFC (Hui et al., 2018)	Wide range of ageing changes displayed including brain relevant changes.	Cognitive and behavioural changes may confound results for NDs.
	Mixed genetic background Terc$^{-/-}$ WRN$^{-/-}$(Chang et al., 2004)	~7-mths old	Premature death, hair greying, alopecia, type-2 diabetes, osteoperosis, cataracts Cultured cells: ↑DNA damage markers, accelerated replicative senescence, ↑chromosomal instability		
LMNA mutation	C57BL/6 with HGS mutation: LMNA$^{G609G/G609G}$ Mice with HGS mutation: Tetop-LA^{G608G+}/Tetop-LA^{G608G-}	3 wks 16 mths	Growth retardation, ↑ cancer incidence, infertility, spine curvature Nuclear distortion, nuclear blebbing, nuclear invaginations No neurological deficits	No neurological deficits to confound results	Variable timeframe for ageing to be induced (3wkss-16mths)
Terc deficiency	Terc$^{-/-}$ C57BL/6J	4–5 mths	Spatial learning and memory deficits, loss of neurons, loss of synaptic density, ↑CD11b + microglia, ↑IBA1 + microglia, ↑microglial density Accelerated formation of a-synuclein aggregates in PD mice	Inflammatory ageing phenotype in the brain Compatible with other genetic ND models	Cognitive and behavioural changes may confound results for NDs
IL-10 deficiency	IL-10$^{-/-}$ C57BL/6J	10–15 mths	Alopecia, decreased muscle strength (Walston et al., 2008), ↑activation of pro-inflammatory pathways (IL-6, TNF-a, IL-1B) (Ko et al., 2012) ↑Tau phosphorylation following neuroinflammatory stimulus (Weston et al., 2021)	Brain relevant changes Impacts ND pathology	Long time to achieve ageing

(*continued on next page*)

Table 2 (*continued*)

Method of ageing	Model	Age of phenotype presentation	Phenotype induced	Strengths	Weaknesses
SIRT6 deficiency	SIRT6$^{-/-}$ C57BL/6J (Mostoslavsky et al., 2006)	4 wks	Genomic instability, development of altered glucose homeostasis, ↓body size, ↓B/T-cell generation Death at around 4 wks old	Brain specific KO does not significantly reduce lifespan and provides a short timeframe to achieve ageing	Overall KO causes significantly shortened lifespan. Cognitive and behavioural changes may confound results for NDs More reflective of an AD model than aged CNS model
	Brain specific SIRT6$^{-/-}$ C57BL/6J (Kaluski et al., 2017)	4 mths	Accumulated DNA damage, ↑hyperphosphorylated Tau, ↑locomotor activity, ↓non-associative learning		
Induced changes to the epigenome (ICE)	Targeted expression of an endonuclease I-Ppol (Yang et al., 2023)	10mths	↑muscle loss, alopecia, loss of skin pigment, ↑frailty, ↑glial activation in hippocampus	Visibly aged mice Can have direct control over ageing during studies	Long time to achieve ageing Neurological effects not characterised

(Toth, 2018). Further, the portion of the cohort that remains is arguably biased. In addition, long-term housing of rodents can often be prohibitively expensive and may be limited by potential space constraints of animal holding facilities. Additionally, when animals are housed long-term under so-called standard conditions, it can also lead to chronic stress, behavioural abnormalities and increased risk of health conditions (Cait et al., 2022; Pinelli et al., 2017), requiring alterations to conventional housing protocols when maintaining animals for months at a time. To counter these practical and ethical difficulties, inbred and genetic models of accelerated ageing have been developed and are discussed below as alternatives to naturally ageing animals in research. Such models, particularly when crossed with well-established genetic models of ND, such as the APP/PS1 mouse model of AD, may allow for accelerated investigations, overcoming the practical challenges associated with long-term rodent investigations, while also modelling disease pathophysiology on a more translationally relevant aged phenotype background.

Mice are the most common model of accelerated ageing, due to their well characterised ageing phenotype and genome (Cai et al., 2022). The senescence accelerated prone mouse (SAMP) model is widely used and was created by selectively inbreeding mice from the AKR/J strain that showed spontaneous age-related changes between 2 and 12mths, such as shortened lifespan and decreased activity, as well as physical features of ageing, including alopecia, cataracts and musculoskeletal changes (Takeda et al., 1981). One strength of SAMP mice is that, as opposed to genetically modified models, acquisition of the aged phenotype is spontaneous and not induced by manipulation of a specific gene or pathway. As biological ageing has no known single cause, inducing models via specific pathways may over-simplify the complexity of natural ageing. In this sense, the SAMP mouse model may be more reflective of the heterogenous nature of human ageing.

A number of sub-strains of the SAMP mouse were generated displaying different phenotypes, two of which (SAMP8 and SAMP10) are particularly relevant to ND (reviewed: (Takeda, 2009)). SAMP8 is widely utilised in AD research, as these mice display both the cognitive deficits seen in AD and AD-specific pathology. Behaviourally, SAMP8 mice have deficits in learning and memory and show decreased anxiety-like behaviours and disrupted sleep cycles (Miyamoto et al., 1992). Summarised in Table 2, the brains of these mice show age-related changes (Takeda et al., 1981), as well as amyloid beta aggregates and tau hyperphosphorylation (Takemura et al., 1993). Additionally, SAMP8 mice have shown evidence of a dysregulated immune response, which, as discussed above, has been linked to both ageing and neurodegeneration (Molina-Martínez et al., 2020). Thus, the SAMP8 mouse combines ageing with the presence of relevant neurodegenerative brain pathology (del Valle et al., 2010) and has been used to test the therapeutic potential of multiple agents, including lithium (Malerba et al., 2021; Toricelli et al., 2021), fatty acids (Vela et al., 2019), acupuncture (Wang et al., 2018; Zhang et al., 2013) and both natural (Igarashi et al., 2022; Kim et al., 2023; Shih et al., 2010) and conventional (Lian et al., 2021) medicines. In addition, SAMP8 mice have also furthered our understanding of the role that an array of factors may play in the pathophysiology of AD, including protein chaperones (Akbor et al., 2021b), protein (Liu et al., 2010) and histone deacetylases (Fontán-Lozano et al., 2008) and candidate AD genes, such as SLC24A4 polymorphism (Akbor et al., 2021a).

Interestingly, combining the SAMP8 mouse strain with a mouse model of AD may better represent both the natural ageing changes occurring in these mice, as well as disease pathology. In line with this, the SAMP8 mouse was crossed with the widely used APP/PS1 model of AD (SAMP8-APP/PS1) by Lok and colleagues in 2013 (Lok et al., 2013). The APP/PS1 transgenic model mimics amyloid pathology in the brain and the combined SAMP8-APP/PS1 model demonstrates earlier presentation of pathology, with Aβ immunoreactivity manifesting at 6-mths, compared to 9-mths in control mice. Further, an increased number of Aβ deposits were present in the hippocampus in SAMP8-APP/PS1

mice at 9-mths. Acquisition of the AD behavioural phenotype was also more pronounced in SAMP8-APP/PS1 mice, with more severe learning and memory deficits and decreased anxiety at 9-mths of age (Lok et al., 2013). While this suggests that it is feasible to generate a combined model to investigate AD in the context of an aged phenotype, outside of this initial report a decade ago, this model has not been used in further studies and no other combined models have been produced, representing a potential underutilised opportunity to more quickly and accurately model AD. Additionally, despite the presence of relevant pathology, including degeneration of DA neurons in the substantia nigra and noradrenergic neurons in the locus coeruleus in SAMP mice (Karasawa et al., 1997), SAMP8 mice are rarely used for PD research.

In contrast to SAMP8 mice, SAMP10 mice display primarily age-related changes in the brain and lack the Aβ deposition and tau hyperphosphorylation seen in SAMP8 (see Table 2). There are also behavioural differences between the two strains. While SAMP8 mice show a pronounced decrease in anxiety-like behaviour, SAMP10 mice display increased emotional dysfunction and depressive behaviour (Shimada and Hasegawa-Ishii, 2011). This is thought to be due to a number of changes in the dopamine and serotonin systems of SAMP10 mice, with changes in DA and serotonin receptor sensitivity (Onodera et al., 2000) and altered DA metabolism present in these mice (Takahashi et al., 2004). Interestingly, however, despite these observed changes in the dopaminergic pathway, SAMP10 mice are also underutilised as a model in PD research.

2.2.2. Genetic mouse models of ageing

In contrast to the spontaneous ageing models, genetic models, which involve knockout, mutation, or overexpression of particular genes, are widespread methods in many areas of research, including both ageing and ND. In the context of ageing research specifically, these models involve manipulating a specific pathway or factor to induce premature ageing, which allows for the study of how this pathway/factor contributes to the neurobiological process of natural ageing. An understanding of this is critical for understanding the mechanisms of normal ageing, which lays the foundation for how this may be further altered in the context of age-related ND. Mouse models of the aged CNS have been reviewed previously (Heng et al., 2017), including transgenic models based on genetic changes in progeroid syndromes and specific age-related pathways, including IL-10 and SIRT6. While multiple genetic models of ageing are available, Sharma et al., (2018) recommended the use of progeroid mouse models particularly to study AD, in order to combine the rapid ageing seen in the progeroid models with the disease phenotype induced by AD models (Sharma et al., 2018). Progeroid mouse models are based on accelerated ageing diseases with a known genetic cause, such as the LMNA gene in Hutchinson Gilford syndrome (HGS), which results in a partially processed pre-lamin A protein, termed progerin (Inesta-Vaquera et al., 2022), and the WRN gene in Werner syndrome (WS), which causes dysregulation in DNA repair systems (Massip et al., 2006). These progeroid syndromes are characterised by early onset of ageing and age-related disease (Ding and Shen, 2008). HGS mice with a mutation in the LMNA gene ($LMNA^{G609G/G609G}$) display ageing at three wks, including increased cancer incidence, infertility and curvature of the spine (Osorio et al., 2011). Importantly, however, the brains of these mice do not demonstrate neurodegenerative change, with neurons appearing to not be sensitive to increased progerin expression (Baek et al., 2015). In line with this, HGS mice do not display deficits on tests of reference or spatial memory (Baek et al., 2015) and individuals with HGS do not exhibit deficits in mental or intellectual abilities. This makes the HGS mouse model itself unsuitable for studying ND; however, it may have utility for crossing with established genetic models of ND (e.g., the APP/PS1 model of AD) to produce ND changes in combination with an accelerated aged phenotype.

In contrast, WS mice, which are deficient in part of the helicase domain of the WRN protein ($WRN^{\Delta hel/\Delta hel}$), show an ageing phenotype with onset at 5 mths, including insulin resistance, increased ROS, DNA damage and increased cancer incidence (Massip et al., 2006). Additionally, both motor (loss of activity and coordination) and cognitive (deficits in spatial and social novelty memory) changes, concomitant with signs of cellular ageing and enhanced oxidative stress and neuroinflammation, have been described in this model (Hui et al., 2018) (Table 2). This suggests that these mice may have utility in their own right for the study of ND, with studies needed to examine markers associated with neurodegenerative change (e.g., tau hyperphosphorylation). It is also important to note, however, that this potentially limits the ability to cross WRN mice with established genetic models of ND (e.g., the APP/PS1 model of AD) to produce mixed models, as the presence of such behavioural impairments may confound interpretation of results.

This has not, however, prevented the generation of a mouse model with a combined complete KO of both WRN and telomerase RNA component (Terc), a ribonucleoprotein polymerase that maintains telomere length, ($Terc^{-/-}WRN^{-/-}$) (Chang et al., 2004). $Terc^{-/-}$ mice display accelerated ageing at just 4–8 mths old, as well as upregulation of SASP related genes, increased oxidative stress response and apoptotic markers in the brain (Yang et al., 2022). To date, $Terc^{-/-}WRN^{-/-}$ mice have not been assessed for neurological or behavioural effects, but since both $Terc^{-/-}$ (Khan et al., 2015) and WRN modified ($WRN^{\Delta hel/\Delta hel}$) (Hui et al., 2018) mice have neurological impairments and cellular brain changes (Yang et al., 2022), it is reasonable to predict that $Terc^{-/-}WRN^{-/-}$ mice may display exacerbated behavioural change and a greater extent of age-related pathophysiological change, compared to either model alone. This may make this model particularly useful for ND research, although this has yet to be evaluated. Nevertheless, Terc knockout mice have previously been utilised to study PD. Scheffold and colleagues (2016) crossed C57/BL6/J $Terc^{-/-}$mice with C57/BL6/J mice expressing the human mutant α-synuclein (A3oP) to model PD in the context of telomere shortening (Scheffold et al., 2016). Results demonstrated that telomere shortening accelerated the formation of α-synuclein aggregates and impaired responses of brainstem microglia (Scheffold et al., 2016). This study provided evidence that age-related changes in the brain, such as telomere shortening, impact the progression of degenerative pathology in PD, further highlighting the importance of accounting for the effects of ageing when modelling ND.

In addition to progeroid and telomere shortening, genetic models based on inflammatory and metabolic theories of ageing have also been utilised, including IL-10 (Walston et al., 2008) and SIRT6 deficiency (Kaluski et al., 2017). Mice deficient in the anti-inflammatory cytokine IL-10 ($IL\text{-}10^{-/-}$) had previously been established as a model of human frailty, showing alopecia and decreased muscle strength at 11mths (Walston et al., 2008), low-grade activation of inflammatory signalling pathways, including IL-6, TNF-α and IL-1β, at 15mths (Ko et al., 2012), and increased neuroinflammation and Tau phosphorylation at 6mths old following an inflammatory stimulus (Weston et al., 2021). While $IL\text{-}10^{-/-}$ mice display brain changes similar to those in AD (Richwine et al., 2009), however, they are currently not widely used in ND research.

Similarly, SIRT6, a member of the Sirtuin family of signalling proteins, is important for maintaining normal DNA repair (Mostoslavsky et al., 2006) and has been the basis for modelling ageing in C57BL/6 mice (Mostoslavsky et al., 2006). $SIRT6^{-/-}$ mice demonstrated genomic instability, altered metabolic homeostasis and immune cell generation and decreased size (Mostoslavsky et al., 2006). While these changes demonstrate key elements of the mammalian aged phenotype discussed above, $SIRT6^{-/-}$ mice develop degenerative progeroid pathology and do not survive beyond 4wks (Mostoslavsky et al., 2006), limiting the ability of researchers to conduct experiments. However, mice with a neuronal specific SIRT6 deficiency survive longer and demonstrate ageing, measured by DNA damage and cell death, at 4mths of age (Kaluski et al., 2017) (Table 2). Considering the deficits in non-associative learning and increases in locomotor activity in this model are similar to those in AD models, and that SIRT6 expression in the brain

is reduced in AD patients compared to aged controls (Kaluski et al., 2017), SIRT6$^{-/-}$ mice may be useful for modelling AD in the context of an accelerated aged phenotype. Of note, SIRT6$^{-/-}$ embryonic stem cells have previously been used as an *in vitro* model of age-related cellular changes (Mostoslavsky et al., 2006) (Table 1).

Of potential relevance, a new genetic rodent model of ageing was reported in January 2023, the inducible changes to the epigenome (ICE) mouse. This mouse was created by tamoxifen-controlled expression of the endonuclease I-PpoI at 20 canonical sites in the mouse genome, causing DSBs without mutations in the genome (Yang et al., 2023). When I-Ppol was activated at 4-6mths, an aged phenotype was observed by 10-12mths. This featured muscle loss, alopecia, loss of skin pigment and premature frailty, similar to that of 24mo controls (Yang et al., 2023). Additionally, higher levels of activated glial cells in the hippocampus suggest potential applications in modelling the brain changes seen in NDs. The researchers additionally investigated the ability to reverse these changes by treatment with Yamanaka factors, which are used to differentiate somatic cells to iPSCs. Ageing changes observed in ICE mice were able to be reversed *in vitro*, demonstrating the potential usefulness of the Yamanaka factors beyond iPSC differentiation. It is important to note, however, that there have been a number of major issues identified with the design of this study (Timmons and Brenner, 2023), most notably that genotoxicity due to the expression of I-Ppol appears to potentially play a role in development of the ageing phenotype in ICE mice through p53 signalling (Kim et al., 2016), which has not been accounted for in controls of this study. However, while the specific mechanisms driving ageing in this model are yet to be fully validated, this method presents a potentially significant contribution to the research field by providing an inducible rodent model of ageing that could be crossed with established genetic models of ND disease. Regardless, further characterisation of the neurobiological changes in these mice needs to be undertaken to understand the utility of this model in age-related research, as well as for CNS research more generally.

While potentially promising, particularly with regard to their ability to overcome the practical challenges associated with the long-term investigations needed to investigate spontaneous ageing, it is important to note that accelerated ageing models are not without their own limitations and challenges. Namely, there are important questions about how closely these models mirror the changes associated with natural ageing. In line with this, it has been observed that the histopathologic lesions associated with these accelerated ageing models often don't overlap completely with those seen in natural ageing (Gurkar and Niedernhofer, 2015), and that accelerated ageing models often exhibit features not typical of normal ageing (Kõks et al., 2016). Similarly, none of the progeria models reviewed here are able to mimic all of the complex aspects associated with the aged phenotype in mammals due to the fact that they were created to specifically model the changes seen in certain diseases (Gurkar and Niedernhofer, 2015). It is also important to note that the morphologic changes observed in these models are often segmental in nature, meaning that multiple different models would be required in order to fully explore the complex changes that contribute to the aged phenotype within a particular tissue or organ system (Harkema et al., 2016).

3. Considering age in NDs moving forward- recommendations for researchers

A major gap in ND research currently is the lack of consideration given in current disease models to the typical changes associated with the aged phenotype that occur alongside disease-specific pathology. Fig. 2 outlines a proposed research pipeline to integrate ageing into ND research both *in vitro* and *in vivo* using currently available models. First, the aged phenotype is induced in either a relevant cell or animal model (Fig. 2 step1), in order to simulate the complex cellular environment present in the aged individual. Once this has been established, a disease model can then be induced on this background using an inflammatory (Hoban et al., 2013; Mutemberezi et al., 2018), chemical (Sherer et al., 2003) or protein stimulus *in vitro (*Ross et al., 2020*)* and, additionally, genetic (Flood et al., 2002) or neurotoxic methods (Ungerstedt, 1968) *in vivo* (Fig. 2 step 2). This more translationally relevant model can then be used to undertake the desired investigations (Fig. 2 step 3). The incorporation of this pipeline would benefit both the understanding of disease pathogenesis, by providing insight into the contribution of biological ageing to NDs, and additionally would assist in the development of disease treatments by providing more accurate screening of potential therapies. Major drawbacks of this pipeline include not only the time needed to establish the combined ageing and ND model, but that the complexity of the generated model introduces the need for extra validation and requires a more multifaceted interpretation of results. To address the issue of time, utilising the accelerated *in vivo* ageing models reviewed here would alleviate some of this cost compared to using naturally ageing animals; however, none of these models individually can capture all the age-related changes described above. Establishing such models *in vitro* is far less costly and time consuming; for example, inducing replicative senescence in primary cells, which have a limited lifespan, would be considerably faster and cheaper than housing mice for 18 months or longer. Modelling the complex processes seen in both ageing and NDs presents significant challenges for researchers both *in vitro* and *in vivo*. Below, we present a discussion of these challenges, and in Table 3, we offer some recommendations to consider when designing both *in vitro* and *in vivo* ND studies.

As reviewed above, despite the array of techniques used to induce and quantify ageing *in vitro* and *in vivo,* there is yet untapped potential for incorporating the aged phenotype in preclinical ND research. First, when it comes to *in vitro* work, current models are often over-simplified and fail to recapitulate the complex 3D interactions amongst different types of brain cells in the tetrapartite synapse. Moving forward, use of co-culture and organoid models kept for longer periods of time in culture (i.e. 27 day old co-cultures (Bigagli et al., 2016) or 45 day old brain organoids (Ao et al., 2022) displaying ageing markers) can be drawn upon, in combination with iN technology, to produce sophisticated "aged" *in vitro* models that allow for investigation of disease mechanisms or treatment efficacy in more representative models. In order to validate such models, use of a standardised "aged phenotype" marker panel, inspired by the 'AgeScore' panel of Hartmann and colleagues (2023) (Hartmann et al., 2023), should be developed and consistently applied across studies in order to improve reproducibility and allow for more ready comparison between labs. By utilising cells which meet a minimum criterion on this panel, or a minimum 'AgeScore', ageing can be equally accounted for across experiments and between lab groups. While this panel needs further validation across cell types, we suggest that for a culture to be considered 'aged,' cells must show changes in major cellular ageing markers discussed as part of the aged cellular phenotype above and identified as a hallmark of ageing. For ND models, the acquisition of the SASP is particularly important, as chronic inflammation has well established links to neurodegenerative pathology (Guzman-Martinez et al., 2019) and ageing (Franceschi and Campisi, 2014) and should serve as a major marker of ageing in any potential aged ND model. This could serve a similar function to the ARRIVE guidelines (Animal Research: Reporting of *In Vivo* Experiments), which have sought to improve reporting of research in animal studies (Percie du Sert et al., 2020), and could also be used for validation of *in vivo* models. The generation of such well-validated, sophisticated "aged" *in vitro* models will provide a powerful tool on which to model ND and could be used in combination with exciting advances in bioengineering technologies, such as microfluidic devices (Fernandes et al., 2016) (e.g. brain-on chip) and 3D tissue engineering (Lam et al., 2019) (e.g. extracellular matrix decellularization) to take our understanding of disease mechanisms and drug development to new heights.

From an *in vivo* perspective, despite recent improvements in animal models of ageing, there is an overall lack of consideration of age in ND study design. In a survey of 297 researchers on the use of rodents in

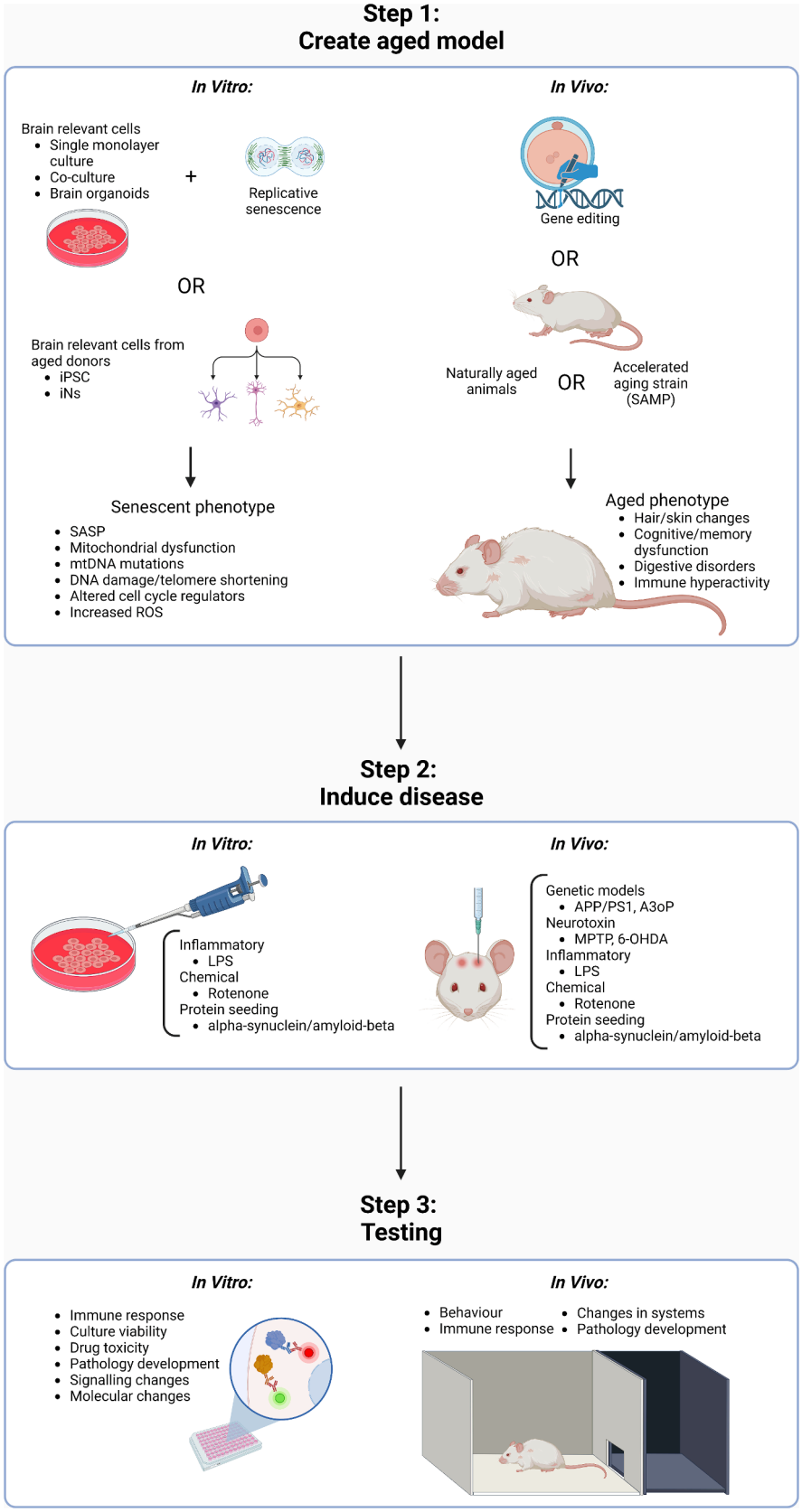


Fig. 2. Pipeline for the incorporation of age into ND research models. **Step 1**: Either *in vitro* or *in vivo*, studies need to induce the senescent phenotype in cells or ageing in animals. **Step 2:** Once ageing has been induced, disease can then be modelled within those animals/cultures. Types of models to induce disease include genetic, inflammatory, seeding, or neurotoxic models **Step 3:** biological responses of cells/tissue and behavioural responses of animals can then be tested to develop treatments and understand disease pathology.

Table 3
Summary of recommendations for improving the modelling of age both *in vitro* and *in vivo*.

***In vitro* recommendations**
Develop more sophisticated *in vitro* models as a background on which to model NDs using advances in co-culture and organoid technology
Validate "aged" models using a standard marker panel and use this to develop reporting guidelines (in line with the ARRIVE guidelines for *in vivo* research
Harness advances from bioengineering (e.g. brain on a chip and extracellular metric decellularization) to use in combination with aged *in vitro* models in order to allow for deeper investigation of disease mechanisms
***In vivo* recommendations**
When designing studies, utilise models which include changes relevant to the disease of interest (e.g. pathological protein deposition in ND studies)
Advocate for improvements in the availability and accessibility of aged animals, including better commercial availability, local/national networks for aged animal sharing or improved banking of tissues or findings into biobanks and data repositories for secondary analyses
Educate governmental and philanthropic bodies about the importance of incorporating aged animals into research and the need for increased funding to allow for this, where justified
Develop guidelines for animal care and use specifically tailored towards older animals that also account for strain-specific differences
Work closely with laboratory animal services and veterinary staff when designing experiments, in order to anticipate challenges that may arise and develop strategies to manage these.
Adhere to the ARRIVE guidelines for the appropriate reporting of animal age in peer-reviewed literature, reporting both summary statistics for each experimental group and, where possible, age data for individual animals in the supplementary data
Utilise tools developed to determine human equivalent age when selecting the age of animals to be used in a given study, in order to facilitate the development of a field-specific consensus about age of animals to be used in a given model moving forward

biomedical research conducted by the National Centre for the Replacement, Refinement and Reduction of Animals in Research (NC3R), the most common age of use is 8–12 weeks (Jackson et al., 2017) (with 6–20 weeks being reported as "adult" animals). This is problematic, as this is a stage in which many developmental processes are still ongoing, including, importantly, both development of the immune system (Holladay and Smialowicz, 2000) and brain maturation (Downes and Mullins, 2014) and myelination (Fu et al., 2013). Further, as discussed extensively above, the physiological changes that occur with ageing differ significantly in young versus old animals. Concerningly, however, only ten percent of respondents to the survey reported using rodents over 16 weeks of age, with just 24 % of these in in rats (Jackson et al., 2017). This is regardless of whether age is a significant risk factor for the disease being modelled (e.g. NDs) and in spite of a growing number of studies showing the moderating effect of age on disease presentation and pathophysiology (e.g. older rats have increased susceptibility (Yager and Thornhill, 1997) to and take longer to recover from (Brown et al., 2003) ischaemic insults).

To improve upon this, animal age must be carefully considered when designing studies. For NDs, this means planning for either the long-term use of animals (i.e. 18-months or longer) or the use of an accelerated ageing model, such as those reviewed above. In selecting an accelerated ageing model, particularly those based on progeroid syndromes, researchers must consider the different pathophysiological changes that occur in each model, when these changes occur and how this may impact their interpretation of findings (e.g. cognitive impairment seen in WRN mice may confound behavioural results in a mixed model of AD). Due to the difficulties in interpretation of results and the limited hallmarks of ageing displayed by any one accelerated model, using naturally aged animals is the ideal base model to use in step 1 (Fig. 2). However, when using naturally aged animals, there are important financial and practical difficulties associated with maintaining rodent colonies long term. For example, a comparison by NC3R of the cost of obtaining animals at six versus 12-weeks of age from a major commercial supplier in the US and UK demonstrated that 12-week animals cost at least 50 % more per animal, and sometimes as much as 100 % more (Jackson et al., 2017), and this is without accounting for increases in agistment costs associated with ageing rodents in-house. Improvements in the availability and accessibility of aged animals, such as better commercial availability, local/national networks for aged animal sharing or improved banking of tissues or findings into biobanks/data repositories for secondary analyses, would help to offset the significant costs, challenges and, most importantly, variability associated with individual research groups housing animals for extended periods of time within their own housing facilities, in order to obtain aged cohorts. Some efforts have already been made in this direction via the Shared Ageing Research Models (ShARM) initiative (Duran et al., 2013) and the Aging Rodent Colonies project at the National Institute on Aging (Jackson et al., 2017). Additionally, researchers must work together to advocate to government and philanthropic bodies to provide adequate funding to allow for the increased costs associated with the use of aged animals within grant applications, where appropriately justified.

The field would also benefit from the development of guidelines for animal care and use specifically tailored towards older animals, given the unique challenges associated with these cohorts. For example, rats have been shown to develop multiple diseases and alterations in organ function in conjunction with ageing, including renal disease (Roncal-Jimenez et al., 2016), respiratory disease/infections (Carthew et al., 1989), increased tumour presentation (Sandusky et al., 1988) and atrophy of lumbar/hindlimb muscles (Ibebunjo et al., 2013). Further, such age-related changes may be strain specific, which also must be accounted for when working with aged animals. In support of this, C57BL/6J mice have missense mutation in the nicotinamide nucleotide transhydrogenase gene, which leads to impaired glucose tolerance (Toye et al., 2005) and age-related declines in mitochondrial function (Ghosh et al., 2014). Researchers would thus benefit from sharing experiences of working with aged cohorts and from working closely with laboratory animal servicers and veterinary staff at the time of experimental design, to anticipate challenges that may arise and appropriately plan how to manage these. Importantly, there are also several extraneous factors not discussed in this review which can influence ageing markers and potentially contribute to heterogeneity in human populations, including stress(Yegorov et al., 2020), exercise (Carapeto and Aguayo-Mazzucato, 2021) and diet (Longo et al., 2021); however, these factors need to be considered and controlled for in the study design phase, keeping in mind that the needs of older animals may not be equivalent to those of younger animals.

Finally, in accordance with 8a of the Essential 10 of the ARRIVE guidelines, increased emphasis needs to be placed on appropriate reporting of animal age. This includes both summary statistics (mean +/− SD, as well as range) for each experimental group and, importantly, values for individual animals in the supplementary materials (Percie du Sert et al., 2020). This is critical, given that animal age is often poorly reported, or even unreported, in preclinical studies, with poor justifications offered for age choices (e.g. monetary costs, supply/availability and maintaining comparability with historical data) (Jackson et al., 2017). This leads to wide discrepancy in the age of animals being used by different labs, with an investigation of this by NC3R showing that, within the same model paradigm, the age of the animal used could vary over a range of up to 20 weeks (Jackson et al., 2017). Such inconsistencies in age choice and reporting can lead to variability between animals within a given study, as well as between studies using the same

model from different laboratories, negatively impacting data quality and study outcomes (Jackson et al., 2017). Additionally, there needs to be greater consensus in the field about what constitutes specific age ranges of interest in a given species (e.g. younger adult versus middle-age versus older adult) and how this relates to human ageing.

To assist with this, as discussed above, recommendations have been put forward by the Jackson Laboratory, proposing three life stages in mice: mature adult from 3-6 months of age (~20–30 human years), middle age from 10-15 months of age (~38–47 human years) and old age from 18-24 months (~56–69 human years) (Jackson Laboratory, 2020). Researchers can use these as a guide when designing studies which utilise aged mice; however, potential strain and species differences also need to be considered. In order to facilitate this, additional tools have been developed to help determine equivalent human age in mice (Geifman and Rubin, 2013) and rats (Quinn, 2005), as well as other species (Clancy et al., 2007). Ideally, researchers should aim to utilise animals at the higher end of the defined "old age" range (e.g. 24-months of age in C57BL/6J mice), although potential health concerns for animals of this age, as well as practical and financial concerns associated with long-term housing, also need to be considered.

4. Conclusions

Overall, there is a critical need to incorporate ageing into studies of neurodegeneration, which is currently often overlooked by researchers, despite age being the most significant risk factor for ND development. Whilst we highlight that it is critical to include age in ND research to improve translatability, we acknowledge that all models have limitations and no one model can recapitulate all elements of human disease. ND research conducted without specific consideration of age still presents an invaluable contribution, as evidenced by the multiple advances made in the field to date. Nevertheless, moving forward, effort should be made to account for ageing in study design or consider it in the interpretation of results. This is particularly critical given how age may alter not only pathophysiology, but also potentially the response to therapeutic interventions. Therefore, whilst we also recognise the difficulties involved in analysing such convoluted data, the interactions between NDs and ageing make the diseases themselves complex. Thus, a complex model is more reflective of the naturally occurring disease environment. Here, we have summarised what constitutes the aged phenotype in humans and critically evaluated several major methods to induce ageing in a laboratory setting, with a particular focus on the significant underutilisation of these models to date in ND research. Emerging *in vitro* technologies could help to improve this, broadening the landscape of available models and allowing for more sophisticated investigations of disease mechanisms and therapeutic response in the context of a complex environment more reflective of the CNS. Similarly, the advent of *in vivo* models of ageing that are both inducible and reversible may help us to probe the contribution of ageing to the emergence of the ND-phenotype in a way never before possible. In spite of these advancements, however, it is critical that ND researchers prioritise including age as a critical component of their models moving forward. With this in mind, and in the spirit of overcoming current practical challenges, we have offered here specific recommendations for improving the incorporation of the aged phenotype into both *in vitro* and *in vivo* experimental models. Taken together, it is hoped that more widespread use of these models, in conjunction with our recommendations, will improve the quality and reproducibility of the data produced, ultimately helping to ensure that results can translate to effective treatments for neurodegeneration.

CRediT authorship contribution statement

Laura M. Carr: Writing – review & editing, Writing – original draft, Data curation, Conceptualization. **Sanam Mustafa:** Writing – review & editing, Supervision. **Andrew Care:** Writing – review & editing, Supervision, Funding acquisition. **Lyndsey E Collins-Praino:** Writing – review & editing, Writing – original draft, Funding acquisition, Conceptualization, Supervision.

Declaration of competing interest

The authors declare that they have no known competing financial interests or personal relationships that could have appeared to influence the work reported in this paper.

Data availability

No data was used for the research described in the article.

Acknowledgements

LC is supported by an Australian Government Research Training Program Scholarship provided by the Department of Education and Training, Canberra, Australia. This work was supported by grants to LCP and AC by the National Foundation for Medical Research and Innovation, Australia. Figures created in BioRender.

References

Abud, E.M., Ramirez, R.N., Martinez, E.S., Healy, L.M., Nguyen, C.H.H., Newman, S.A., Yeromin, A.V., Scarfone, V.M., Marsh, S.E., Fimbres, C., Caraway, C.A., Fote, G.M., Madany, A.M., Agrawal, A., Kayed, R., Gylys, K.H., Cahalan, M.D., Cummings, B.J., Antel, J.P., Mortazavi, A., Carson, M.J., Poon, W.W., Blurton-Jones, M., 2017. iPSC-derived human microglia-like cells to study neurological diseases. Neuron 94, 278–293.e279.

Aitken, A.E., Lee, C.M., Morgan, E.T., 2008. Roles of nitric oxide in inflammatory downregulation of human cytochromes P450. Free Radic. Biol. Med. 44, 1161–1168.

Akbor, M.M., Kim, J., Nomura, M., Sugioka, J., Kurosawa, N., Isobe, M., 2021a. A candidate gene of Alzheimer diseases was mutated in senescence-accelerated mouse prone (SAMP) 8 mice. Biochem. Biophys. Res. Commun. 572, 112–117.

Akbor, M.M., Kurosawa, N., Nakayama, H., Nakatani, A., Tomobe, K., Chiba, Y., Ueno, M., Tanaka, M., Nomura, Y., Isobe, M., 2021b. Polymorphic SERPINA3 prolongs oligomeric state of amyloid beta. PLoS One 16, e0248027.

Andreollo, N.A., Santos, E.F., Araújo, M.R., Lopes, L.R., 2012. Rat's age versus human's age: what is the relationship? Arq. Bras. Cir. Dig. 25, 49–51.

Ao, Z., Song, S., Tian, C., Cai, H., Li, X., Miao, Y., Wu, Z., Krzesniak, J., Ning, B., Gu, M., Lee, L.P., Guo, F., 2022. Understanding immune-driven brain aging by human brain organoid microphysiological analysis platform. Adv. Sci. 9, 2200475.

Arafah, A., Khatoon, S., Rasool, I., Khan, A., Rather, M.A., Abujabal, K.A., Faqih, Y.A.H., Rashid, H., Rashid, S.M., Bilal Ahmad, S., Alexiou, A., Rehman, M.U., 2023. The future of precision medicine in the cure of Alzheimer's disease. Biomedicines 11.

Azzolino, D., Spolidoro, G.C.I., Saporiti, E., Luchetti, C., Agostoni, C., Cesari, M., 2021. Musculoskeletal changes across the lifespan: nutrition and the life-course approach to prevention. Front. Med. 8.

Baek, J.H., Schmidt, E., Viceconte, N., Strandgren, C., Pernold, K., Richard, T.J., Van Leeuwen, F.W., Dantuma, N.P., Damberg, P., Hultenby, K., Ulfhake, B., Mugnaini, E., Rozell, B., Eriksson, M., 2015. Expression of progerin in aging mouse brains reveals structural nuclear abnormalities without detectible significant alterations in gene expression, hippocampal stem cells or behavior. Hum. Mol. Genet. 24, 1305–1321.

Barata-Antunes, S., Teixeira, F.G., Mendes-Pinheiro, B., Domingues, A.V., Vilaça-Faria, H., Marote, A., Silva, D., Sousa, R.A., Salgado, A.J., 2020. Impact of aging on the 6-OHDA-induced rat model of Parkinson's disease. Int. J. Mol. Sci.

Beijer, H.J., de Blaey, C.J., 2002. Hospitalisations caused by adverse drug reactions (ADR): a meta-analysis of observational studies. Pharm. World Sci. 24, 46–54.

Bhutto, A., Morley, J.E., 2008. The clinical significance of gastrointestinal changes with aging. Curr. Opin. Clin. Nutr. Metab. Care 11, 651–660.

Bigagli, E., Luceri, C., Scartabelli, T., Dolara, P., Casamenti, F., Pellegrini-Giampietro, D. E., Giovannelli, L., 2016. Long-term neuroglial cocultures as a brain aging model: hallmarks of senescence, MicroRNA expression profiles, and comparison with in vivo models. The Journals of Gerontology: Series A 71, 50–60.

Bitto, A., Ito, T.K., Pineda, V.V., LeTexier, N.J., Huang, H.Z., Sutlief, E., Tung, H., Vizzini, N., Chen, B., Smith, K., Meza, D., Yajima, M., Beyer, R.P., Kerr, K.F., Davis, D.J., Gillespie, C.H., Snyder, J.M., Treuting, P.M., Kaeberlein, M., 2016. Transient rapamycin treatment can increase lifespan and healthspan in middle-aged mice. Elife 5.

Boraldi, F., Bartolomeo, A., Di Bari, C., Cocconi, A., Quaglino, D., 2015. Donor's age and replicative senescence favour the in-vitro mineralization potential of human fibroblasts. Exp. Gerontol. 72, 218–226.

Brayton, C.F., Treuting, P.M., Ward, J.M., 2012. Pathobiology of aging mice and GEM: background strains and experimental design. Vet. Pathol. 49, 85–105.

Brown, A.W., Marlowe, K.J., Bjelke, B., 2003. Age effect on motor recovery in a post-acute animal stroke model. Neurobiol. Aging 24, 607–614.

Bunc, M., Hanning, S., Prieto, J., Kristl, J., Orlu, M., 2019. Characterisation of an in vitro aged cell culture model. Farmacia 67.

Cai, N., Wu, Y., Huang, Y., 2022. Induction of accelerated aging in a mouse model. Cells 11.
Cait, J., Cait, A., Scott, R.W., Winder, C.B., Mason, G.J., 2022. Conventional laboratory housing increases morbidity and mortality in research rodents: results of a meta-analysis. BMC Biol. 20, 15.
Caldeira, C., Oliveira, A.F., Cunha, C., Vaz, A.R., Falcão, A.S., Fernandes, A., Brites, D., 2014. Microglia change from a reactive to an age-like phenotype with the time in culture. Front. Cell. Neurosci. 8, 152.
Cao, B., Ho, J., 2020. WHO methods and data sources for life tables 1990-2019. World Health Organization (WHO), Geneva.
Carapeto, P.V., Aguayo-Mazzucato, C., 2021. Effects of exercise on cellular and tissue aging. Aging (Albany NY) 13, 14522–14543.
Carthew, P., Aldred, P., Hill, R.J., Riley, J., Edwards, R.E., 1989. Dyspnea in aging rats due to disseminated intravascular coagulation (DIC). Vet. Pathol. 26, 505–509.
Chakrabarti, S., Munshi, S., Banerjee, K., Thakurta, I.G., Sinha, M., Bagh, M.B., 2011. Mitochondrial dysfunction during brain aging: role of oxidative stress and modulation by antioxidant supplementation. Aging Dis. 2, 242–256.
Chang, S., Multani, A.S., Cabrera, N.G., Naylor, M.L., Laud, P., Lombard, D., Pathak, S., Guarente, L., DePinho, R.A., 2004. Essential role of limiting telomeres in the pathogenesis of Werner syndrome. Nat. Genet. 36, 877–882.
Chang, A.Y., Skirbekk, V.F., Tyrovolas, S., Kassebaum, N.J., Dieleman, J.L., 2019. Measuring population ageing: an analysis of the Global Burden of Disease Study 2017. Lancet Public Health 4, e159–e167.
Chatterjee, N., Walker, G.C., 2017. Mechanisms of DNA damage, repair, and mutagenesis. Environ. Mol. Mutagen. 58, 235–263.
Choi, S.H., Kim, Y.H., Hebisch, M., Sliwinski, C., Lee, S., D'Avanzo, C., Chen, H., Hooli, B., Asselin, C., Muffat, J., Klee, J.B., Zhang, C., Wainger, B.J., Peitz, M., Kovacs, D.M., Woolf, C.J., Wagner, S.L., Tanzi, R.E., Kim, D.Y., 2014. A three-dimensional human neural cell culture model of Alzheimer's disease. Nature 515, 274–278.
Chouchane, M., Melo de Farias, A.R., Moura, D.M.S., Hilscher, M.M., Schroeder, T., Leão, R.N., Costa, M.R., 2017. Lineage reprogramming of astroglial cells from different origins into distinct neuronal subtypes. Stem Cell Rep. 9, 162–176.
Clancy, B., Kersh, B., Hyde, J., Darlington, R.B., Anand, K.J., Finlay, B.L., 2007. Web-based method for translating neurodevelopment from laboratory species to humans. Neuroinformatics 5, 79–94.
Cole, J.H., Leech, R., Sharp, D.J., 2015. Prediction of brain age suggests accelerated atrophy after traumatic brain injury. Ann. Neurol. 77, 571–581.
Coppé, J.-P., Patil, C.K., Rodier, F., Sun, Y., Muñoz, D.P., Goldstein, J., Nelson, P.S., Desprez, P.-Y., Campisi, J., 2008. Senescence-associated secretory phenotypes reveal cell-nonautonomous functions of oncogenic RAS and the p53 tumor suppressor. PLoS Biol. 6, e301.
Cristofalo, V.J., Allen, R.G., Pignolo, R.J., Martin, B.G., Beck, J.C., 1998. Relationship between donor age and the replicative lifespan of human cells in culture: a reevaluation. PNAS 95, 10614–10619.
da Costa, J.P., Vitorino, R., Silva, G.M., Vogel, C., Duarte, A.C., Rocha-Santos, T., 2016. A synopsis on aging-Theories, mechanisms and future prospects. Ageing Res. Rev. 29, 90–112.
Davila, D., Connolly, N.M.C., Bonner, H., Weisová, P., Dussmann, H., Concannon, C.G., Huber, H.J., Prehn, J.H.M., 2012. Two-step activation of FOXO3 by AMPK generates a coherent feed-forward loop determining excitotoxic cell fate. Cell Death Differ. 19, 1677–1688.
de Jong, L.M., Jiskoot, W., Swen, J.J., Manson, M.L., 2020. Distinct Effects of Inflammation on Cytochrome P450 Regulation and Drug Metabolism: Lessons from Experimental Models and a Potential Role for Pharmacogenetics. Genes (Basel) 11.
de Mera-Rodríguez, J.A., Álvarez-Hernán, G., Gañán, Y., Martín-Partido, G., Rodríguez-León, J., Francisco-Morcillo, J., 2021. Is senescence-associated β-galactosidase a reliable in vivo marker of cellular senescence during embryonic development? Front. Cell Dev. Biol. 9, 36.
del Valle, J., Duran-Vilaregut, J., Manich, G., Casadesús, G., Smith, M.A., Camins, A., Pallàs, M., Pelegrí, C., Vilaplana, J., 2010. Early amyloid accumulation in the hippocampus of SAMP8 mice. J. Alzheimers Dis. 19, 1303–1315.
Delaney, M.A., Imai, D.M., Buffenstein, R., 2021. Spontaneous disease and pathology of naked mole-rats. In: Buffenstein, R., Park, T.J., Holmes, M.M. (Eds.), The Extraordinary Biology of the Naked Mole-Rat. Springer International Publishing, Cham, pp. 353–380.
Deng, W., Jo, J.-I., Morikuni, H., Sasayama, S., Hashimoto, Y., Matsumoto, N., Honda, Y., 2023. Senescence-associated secretory phenotypes in rat-derived dedifferentiated fat cells with replicative senescence. Dental Materials Journal Advpub.
DiMarco, G.M., Harris, B.N., Savonenko, A.V., Soto, P.L., 2023. Acute stressors do not impair short-term memory or attention in an aged mouse model of amyloidosis. Front. Behav. Neurosci. 17.
Ding, S.-L., Shen, C.-Y., 2008. Model of human aging: recent findings on Werner's and Hutchinson-Gilford progeria syndromes. Clin. Interv. Aging 3, 431–444.
Ding, C., Wu, Y., Chen, X., Chen, Y., Wu, Z., Lin, Z., Kang, D., Fang, W., Chen, F., 2022. Global, regional, and national burden and attributable risk factors of neurological disorders: The Global Burden of Disease study 1990–2019. Frontiers. Public Health 10.
Downes, N., Mullins, P., 2014. The development of myelin in the brain of the juvenile rat. Toxicol. Pathol. 42, 913–922.
Drouin-Ouellet, J., Legault, E.M., Nilsson, F., Pircs, K., Bouquety, J., Petit, F., Shrigley, S., Birtele, M., Pereira, M., Storm, P., Sharma, Y., Bruzelius, A., Vuono, R., Kele, M., Stoker, T.B., Ottosson, D.R., Falk, A., Jakobsson, J., Barker, R.A., Parmar, M., 2022. Age-related pathological impairments in directly reprogrammed dopaminergic neurons derived from patients with idiopathic Parkinson's disease. Stem Cell Rep. 17, 2203–2219.
Duran, A.L., Potter, P., Wells, S., Kirkwood, T., von Zglinicki, T., McArdle, A., Scudamore, C., Meng, Q.J., de Haan, G., Corcoran, A., Bellantuono, I., 2013. Shared Ageing Research Models (ShARM): a new facility to support ageing research. Biogerontology 14, 789–794.
Faragher, R.G., 2015. Should we treat aging as a disease? The consequences and dangers of miscategorisation. Front. Genet. 6, 171.
Fernandes, J.T., Chutna, O., Chu, V., Conde, J.P., Outeiro, T.F., 2016. A novel microfluidic cell co-culture platform for the study of the molecular mechanisms of Parkinson's disease and other synucleinopathies. Front. Neurosci. 10, 511.
Ferrington, D.A., Husom, A.D., Thompson, L.V., 2005. Altered proteasome structure, function, and oxidation in aged muscle. FASEB J. 19, 644–646.
Flood, D.G., Reaume, A.G., Dorfman, K.S., Lin, Y.G., Lang, D.M., Trusko, S.P., Savage, M. J., Annaert, W.G., De Strooper, B., Siman, R., Scott, R.W., 2002. FAD mutant PS-1 gene-targeted mice: increased A beta 42 and A beta deposition without APP overproduction. Neurobiol. Aging 23, 335–348.
Flurkey, K., M. Currer, J., Harrison, D.E., 2007. Chapter 20 - Mouse Models in Aging Research. In: Fox, J.G., Davisson, M.T., Quimby, F.W., Barthold, S.W., Newcomer, C. E., Smith, A.L. (Eds.), The Mouse in Biomedical Research (Second Edition). Academic Press, Burlington, pp. 637-672.
Fontán-Lozano, Á., Romero-Granados, R., Troncoso, J., Múnera, A., Delgado-García, J. M., Carrión, Á.M., 2008. Histone deacetylase inhibitors improve learning consolidation in young and in KA-induced-neurodegeneration and SAMP-8-mutant mice. Mol. Cell. Neurosci. 39, 193–201.
Franceschi, C., Campisi, J., 2014. Chronic inflammation (inflammaging) and its potential contribution to age-associated diseases. J. Gerontol. A Biol. Sci. Med. Sci. 69 (Suppl 1), S4–S9.
Franceschi, C., Bonafè, M., Valensin, S., Olivieri, F., De Luca, M., Ottaviani, E., De Benedictis, G., 2000. Inflamm-aging. An evolutionary perspective on immunosenescence. Ann. New York Acad. Sci., pp. 244-254.
Fu, Y., Rusznák, Z., Herculano-Houzel, S., Watson, C., Paxinos, G., 2013. Cellular composition characterizing postnatal development and maturation of the mouse brain and spinal cord. Brain Struct. Funct. 218, 1337–1354.
Fumagalli, M., Rossiello, F., Clerici, M., Barozzi, S., Cittaro, D., Kaplunov, J.M., Bucci, G., Dobreva, M., Matti, V., Beausejour, C.M., Herbig, U., Longhese, M.P., d'Adda di Fagagna, F., 2012. Telomeric DNA damage is irreparable and causes persistent DNA-damage-response activation. Nat. Cell Biol. 14, 355–365.
Gao, Y., Tu, D., Yang, R., Chu, C.H., Hong, J.S., Gao, H.M., 2020. Through Reducing ROS Production, IL-10 Suppresses Caspase-1-Dependent IL-1β Maturation, thereby Preventing Chronic Neuroinflammation and Neurodegeneration. Int. J. Mol. Sci. 21.
Gáspár, A., Hutka, B., Ernyey, A.J., Tajti, B.T., Varga, B.T., Zádori, Z.S., Gyertyán, I., 2022. Performance of the intracerebroventricularly injected streptozotocin Alzheimer's disease model in a translationally relevant, aged and experienced rat population. Sci. Rep. 12, 20247.
Gatto, N., Dos Santos Souza, C., Shaw, A.C., Bell, S.M., Myszczynska, M.A., Powers, S., Meyer, K., Castelli, L.M., Karyka, E., Mortiboys, H., Azzouz, M., Hautbergue, G.M., Márkus, N.M., Shaw, P.J., Ferraiuolo, L., 2021. Directly converted astrocytes retain the ageing features of the donor fibroblasts and elucidate the astrocytic contribution to human CNS health and disease. Aging Cell 20, e13281.
Geifman, N., Rubin, E., 2013. The mouse age phenome knowledgebase and disease-specific inter-species age mapping. PLoS One 8, e81114.
Geraghty, R.J., Capes-Davis, A., Davis, J.M., Downward, J., Freshney, R.I., Knezevic, I., Lovell-Badge, R., Masters, J.R., Meredith, J., Stacey, G.N., Thraves, P., Vias, M., 2014. Guidelines for the use of cell lines in biomedical research. Br. J. Cancer 111, 1021–1046.
Ghosh, D., Levault, K.R., Brewer, G.J., 2014. Relative importance of redox buffers GSH and NAD(P)H in age-related neurodegeneration and Alzheimer disease-like mouse neurons. Aging Cell 13, 631–640.
González-Gualda, E., Baker, A.G., Fruk, L., Muñoz-Espín, D., 2021. A guide to assessing cellular senescence in vitro and in vivo. FEBS J. 288, 56–80.
Grimstad, Ø., 2016. Tumor Necrosis Factor and the Tenacious α. JAMA Dermatol. 152, 557.
Gulen, M.F., Samson, N., Keller, A., Schwabenland, M., Liu, C., Glück, S., Thacker, V.V., Favre, L., Mangeat, B., Kroese, L.J., Krimpenfort, P., Prinz, M., Ablasser, A., 2023. cGAS–STING drives ageing-related inflammation and neurodegeneration. Nature 620, 374–380.
Gurkar, A.U., Niedernhofer, L.J., 2015. Comparison of mice with accelerated aging caused by distinct mechanisms. Exp. Gerontol. 68, 43–50.
Guzman-Martinez, L., Maccioni, R.B., Andrade, V., Navarrete, L.P., Pastor, M.G., Ramos-Escobar, N., 2019. Neuroinflammation as a Common Feature of Neurodegenerative Disorders. Front. Pharmacol. 10, 1008.
Gwinn, D.M., Shackelford, D.B., Egan, D.F., Mihaylova, M.M., Mery, A., Vasquez, D.S., Turk, B.E., Shaw, R.J., 2008. AMPK phosphorylation of raptor mediates a metabolic checkpoint. Mol. Cell 30, 214–226.
Halliwell, E., Dittmar, H., 2003. A qualitative investigation of women's and men's body image concerns and their attitudes toward aging. Sex Roles 49, 675–684.
Harkema, L., Youssef, S.A., de Bruin, A., 2016. Pathology of mouse models of accelerated aging. Vet. Pathol. 53, 366–389.
Hartmann, C., Herling, L., Hartmann, A., Köckritz, V., Fuellen, G., Walter, M., Hermann, A., 2023. Systematic estimation of biological age of in vitro cell culture systems by an age-associated marker panel. Frontiers. Aging 4.
Hartshorne, J.K., Germine, L.T., 2015. When does cognitive functioning peak? The asynchronous rise and fall of different cognitive abilities across the life span. Psychol. Sci. 26, 433–443.
Hayflick, L., 1965. The limited in vitro lifetime of human diploid cell strains. Exp. Cell Res. 37, 614–636.

Heng, Y., Eggen, B.J.L., Boddeke, E.W.G.M., Kooistra, S.M., 2017. Mouse models of central nervous system ageing. Drug Discov. Today Dis. Model. 25–26, 21–34.
Hirsch, C., Schildknecht, S., 2019. In vitro research reproducibility: keeping up high standards. Front. Pharmacol. 10.
Hoban, D.B., Connaughton, E., Connaughton, C., Hogan, G., Thornton, C., Mulcahy, P., Moloney, T.C., Dowd, E., 2013. Further characterisation of the LPS model of Parkinson's disease: a comparison of intra-nigral and intra-striatal lipopolysaccharide administration on motor function, microgliosis and nigrostriatal neurodegeneration in the rat. Brain Behav. Immun. 27, 91–100.
Holladay, S.D., Smialowicz, R.J., 2000. Development of the murine and human immune system: differential effects of immunotoxicants depend on time of exposure. Environ. Health Perspect. 108 (Suppl 3), 463–473.
Hou, Y., Dan, X., Babbar, M., Wei, Y., Hasselbalch, S.G., Croteau, D.L., Bohr, V.A., 2019. Ageing as a risk factor for neurodegenerative disease. Nat. Rev. Neurol. 15, 565–581.
Hsieh, C.H., Shaltouki, A., Gonzalez, A.E., Bettencourt da Cruz, A., Burbulla, L.F., St Lawrence, E., Schüle, B., Krainc, D., Palmer, T.D., Wang, X., 2016. Functional impairment in miro degradation and mitophagy is a shared feature in familial and sporadic Parkinson's disease. Cell Stem Cell 19, 709–724.
Hu, Y., Fryatt, G.L., Ghorbani, M., Obst, J., Menassa, D.A., Martin-Estebane, M., Muntslag, T.A.O., Olmos-Alonso, A., Guerrero-Carrasco, M., Thomas, D., Cragg, M. S., Gomez-Nicola, D., 2021. Replicative senescence dictates the emergence of disease-associated microglia and contributes to Aβ pathology. Cell Rep. 35.
Hughes, P., Marshall, D., Reid, Y., Parkes, H., Gelber, C., 2007. The costs of using unauthenticated, over-passaged cell lines: how much more data do we need? Biotechniques 43, 575–586.
Huh, C.J., Zhang, B., Victor, M.B., Dahiya, S., Batista, L.F.Z., Horvath, S., Yoo, A.S., 2016. Maintenance of age in human neurons generated by microRNA-based neuronal conversion of fibroblasts. Elife 5, e18648.
Hui, C.W., St-Pierre, M.-K., Detuncq, J., Aumailley, L., Dubois, M.-J., Couture, V., Skuk, D., Marette, A., Tremblay, J.P., Lebel, M., Tremblay, M.-È., 2018. Nonfunctional mutant Wrn protein leads to neurological deficits, neuronal stress, microglial alteration, and immune imbalance in a mouse model of Werner syndrome. Brain Behav. Immun. 73, 450–469.
Ibebunjo, C., Chick, J.M., Kendall, T., Eash, J.K., Li, C., Zhang, Y., Vickers, C., Wu, Z., Clarke, B.A., Shi, J., Cruz, J., Fournier, B., Brachat, S., Gutzwiller, S., Ma, Q., Markovits, J., Broome, M., Steinkrauss, M., Skuba, E., Galarneau, J.R., Gygi, S.P., Glass, D.J., 2013. Genomic and proteomic profiling reveals reduced mitochondrial function and disruption of the neuromuscular junction driving rat sarcopenia. Mol. Cell Biol. 33, 194–212.
Igarashi, K., Takagi, M., Fukushima, Y., 2022. The effects of matcha and decaffeinated matcha on learning, memory and proteomics of hippocampus in senescence-accelerated (SAMP8) mice. Nutrients 14.
Inesta-Vaquera, F., Weiland, F., Henderson, C.J., Wolf, C.R., 2022. In vivo stress reporters as early biomarkers of the cellular changes associated with progeria. J. Cell Mol. Med. 26, 5463–5472.
Jackson, S.J., Andrews, N., Ball, D., Bellantuono, I., Gray, J., Hachoumi, L., Holmes, A., Latcham, J., Petrie, A., Potter, P., Rice, A., Ritchie, A., Stewart, M., Strepka, C., Yeoman, M., Chapman, K., 2017. Does age matter? The impact of rodent age on study outcomes. Lab Anim. 51, 160–169.
Jackson Laboratory, T., 2020. Aged C57BL/6J Mice for Research Studies. Bar Harbor, Maine.
Jiang, H., Ren, Y., Yuen, E.Y., Zhong, P., Ghaedi, M., Hu, Z., Azabdaftari, G., Nakaso, K., Yan, Z., Feng, J., 2012. Parkin controls dopamine utilization in human midbrain dopaminergic neurons derived from induced pluripotent stem cells. Nat. Commun. 3, 668.
Jurk, D., Wang, C., Miwa, S., Maddick, M., Korolchuk, V., Tsolou, A., Gonos, E.S., Thrasivoulou, C., Saffrey, M.J., Cameron, K., von Zglinicki, T., 2012. Postmitotic neurons develop a p21-dependent senescence-like phenotype driven by a DNA damage response. Aging Cell 11, 996–1004.
Kaji, K., Ohta, T., Horie, N., Naru, E., Hasegawa, M., Kanda, N., 2009. Donor age reflects the replicative lifespan of human fibroblasts in culture. Hum. Cell 22, 38–42.
Kalia, L.V., Lang, A.E., 2015. Parkinson's disease. Lancet 386, 896–912.
Kaluski, S., Portillo, M., Besnard, A., Stein, D., Einav, M., Zhong, L., Ueberham, U., Arendt, T., Mostoslavsky, R., Sahay, A., Toiber, D., 2017. Neuroprotective functions for the histone deacetylase SIRT6. Cell Rep. 18, 3052–3062.
Karasawa, N., Nagatsu, I., Sakai, K., Nagatsu, T., Watanabe, K., Onozuka, M., 1997. Immunocytochemical study of catecholaminergic neurons in the senescence-accelerated mouse (SAM-P8) brain. J. Neural Transm. 104, 1267–1275.
Kaufman, J.-M., Lapauw, B., Mahmoud, A., T'Sjoen, G., Huhtaniemi, I.T., 2019. Aging and the male reproductive system. Endocr. Rev. 40, 906–972.
Kawamata, T., Akiguchi, I., Maeda, K., Tanaka, C., Higuchi, K., Hosokawa, M., Takeda, T., 1998. Age-related changes in the brains of senescence-accelerated mice (SAM): Association with glial and endothelial reactions. Microsc. Res. Tech. 43, 59–67.
Kawashima, H., Strobel, H.W., 1995. cDNA cloning of a novel rat brain cytochrome P450 belonging to the CYP2D subfamily. Biochem. Biophys. Res. Commun. 209, 535–540.
Kazyken, D., Magnuson, B., Bodur, C., Acosta-Jaquez, H.A., Zhang, D., Tong, X., Barnes, T.M., Steinl, G.K., Patterson, N.E., Altheim, C.H., Sharma, N., Inoki, K., Cartee, G.D., Bridges, D., Yin, L., Riddle, S.M., Fingar, D.C., 2019. AMPK directly activates mTORC2 to promote cell survival during acute energetic stress. Sci. Signal. 12.
Kelmer Sacramento, E., Kirkpatrick, J.M., Mazzetto, M., Baumgart, M., Bartolome, A., Di Sanzo, S., Caterino, C., Sanguanini, M., Papaevgeniou, N., Lefaki, M., Childs, D., Bagnoli, S., Terzibasi Tozzini, E., Di Fraia, D., Romanov, N., Sudmant, P.H., Huber, W., Chondrogianni, N., Vendruscolo, M., Cellerino, A., Ori, A., 2020. Reduced proteasome activity in the aging brain results in ribosome stoichiometry loss and aggregation. Mol. Syst. Biol. 16, e9596.
Khan, A.M., Babcock, A.A., Saeed, H., Myhre, C.L., Kassem, M., Finsen, B., 2015. Telomere dysfunction reduces microglial numbers without fully inducing an aging phenotype. Neurobiol. Aging 36, 2164–2175.
Khokhar, J.Y., Tyndale, R.F., 2011. Drug metabolism within the brain changes drug response: selective manipulation of brain CYP2B alters propofol effects. Neuropsychopharmacology 36, 692–700.
Kim, H.L., Lee, S.K., Min, D.E., Bastola, T., Chang, B.Y., Bae, J.H., Lee, D.R., 2023. Effects of scrophularia buergeriana extract (Brainon®) on aging-induced memory impairment in SAMP8 mice. Curr. Issues Mol. Biol. 1287–1305.
Kim, H., Park, H.J., Choi, H., Chang, Y., Park, H., Shin, J., Kim, J., Lengner, C.J., Lee, Y. K., Kim, J., 2019. Modeling G2019S-LRRK2 sporadic Parkinson's disease in 3D midbrain organoids. Stem Cell Rep. 12, 518–531.
Kim, J., Sturgill, D., Tran, A.D., Sinclair, D.A., Oberdoerffer, P., 2016. Controlled DNA double-strand break induction in mice reveals post-damage transcriptome stability. Nucleic Acids Res. 44, e64.
Kim, K.M., Thaqi, M., Peterson, D.A., Marr, R.A., 2021. Induced neurons for disease modeling and repair: A focus on non-fibroblastic cell sources in direct reprogramming. Front. Bioeng. Biotechnol. 9.
Kim, Y., Zheng, X., Ansari, Z., Bunnell, M.C., Herdy, J.R., Traxler, L., Lee, H., Paquola, A. C.M., Blithikioti, C., Ku, M., Schlachetzki, J.C.M., Winkler, J., Edenhofer, F., Glass, C. K., Paucar, A.A., Jaeger, B.N., Pham, S., Boyer, L., Campbell, B.C., Hunter, T., Mertens, J., Gage, F.H., 2018. Mitochondrial aging defects emerge in directly reprogrammed human neurons due to their metabolic profile. Cell Rep. 23, 2550–2558.
Kinirons, M.T., O'Mahony, M.S., 2004. Drug metabolism and ageing. Br. J. Clin. Pharmacol. 57, 540–544.
Ko, F., Yu, Q., Xue, Q.L., Yao, W., Brayton, C., Yang, H., Fedarko, N., Walston, J., 2012. Inflammation and mortality in a frail mouse model. Age (Dordr.) 34, 705–715.
Kõks, S., Dogan, S., Tuna, B.G., González-Navarro, H., Potter, P., Vandenbroucke, R.E., 2016. Mouse models of ageing and their relevance to disease. Mech. Ageing Dev. 160, 41–53.
Komori, M., 1993. A novel P450 expressed at the high level in rat brain. Biochem. Biophys. Res. Commun. 196, 721–728.
Kouroupi, G., Taoufik, E., Vlachos, I.S., Tsioras, K., Antoniou, N., Papastefanaki, F., Chroni-Tzartou, D., Wrasidlo, W., Bohl, D., Stellas, D., Politis, P.K., Vekrellis, K., Papadimitriou, D., Stefanis, L., Bregestovski, P., Hatzigeorgiou, A.G., Masliah, E., Matsas, R., 2017. Defective synaptic connectivity and axonal neuropathology in a human iPSC-based model of familial Parkinson's disease. PNAS 114, E3679–E3688.
Kumagai, N., Chiba, Y., Hosono, M., Fujii, M., Kawamura, N., Keino, H., Yoshikawa, K., Ishii, S., Saitoh, Y., Satoh, M., Shimada, A., Hosokawa, M., 2007. Involvement of pro-inflammatory cytokines and microglia in an age-associated neurodegeneration model, the SAMP10 mouse. Brain Res. 1185, 75–85.
Kurz, D.J., Decary, S., Hong, Y., Erusalimsky, J.D., 2000. Senescence-associated (beta)-galactosidase reflects an increase in lysosomal mass during replicative ageing of human endothelial cells. J. Cell Sci. 113, 3613–3622.
Lam, D., Enright, H.A., Cadena, J., Peters, S.K.G., Sales, A.P., Osburn, J.J., Soscia, D.A., Kulp, K.S., Wheeler, E.K., Fischer, N.O., 2019. Tissue-specific extracellular matrix accelerates the formation of neural networks and communities in a neuron-glia co-culture on a multi-electrode array. Sci. Rep. 9, 4159.
Lapasset, L., Milhavet, O., Prieur, A., Besnard, E., Babled, A., Aït-Hamou, N., Leschik, J., Pellestor, F., Ramirez, J.M., De Vos, J., Lehmann, S., Lemaitre, J.M., 2011. Rejuvenating senescent and centenarian human cells by reprogramming through the pluripotent state. Genes Dev. 25, 2248–2253.
Lebel, M., Leder, P., 1998. A deletion within the murine Werner syndrome helicase induces sensitivity to inhibitors of topoisomerase and loss of cellular proliferative capacity. Proc. Natl. Acad. Sci. 95, 13097–13102.
Lenoir, C, Rollason, V, Desmeules, JA, Samer, CF, 2021. Influence of Inflammation on Cytochromes P450 Activity in Adults: A Systematic Review of the Literature. Front. Pharmacol 12.
Lian, W.W., Zhou, W., Zhang, B.Y., Jia, H., Xu, L.J., Liu, A.L., Du, G.H., 2021. DL0410 ameliorates cognitive disorder in SAMP8 mice by promoting mitochondrial dynamics and the NMDAR-CREB-BDNF pathway. Acta Pharmacol. Sin. 42, 1055–1068.
Liao, C.Y., Rikke, B.A., Johnson, T.E., Diaz, V., Nelson, J.F., 2010. Genetic variation in the murine lifespan response to dietary restriction: from life extension to life shortening. Aging Cell 9, 92–95.
Limone, F., Klim, J.R., Mordes, D.A., 2022. Pluripotent stem cell strategies for rebuilding the human brain. Front. Aging Neurosci. 14, 1017299.
Liu, W., Liu, C., Zhu, J.X., Li, A.H., Zhao, Z.Q., Yin, B., Peng, X.Z., 2010. D-Tyr-tRNA(Tyr) deacylase, a new role in Alzheimer's-associated disease in SAMP8 mice. Chin. Med. Sci. J. 25, 90–94.
Lok, K., Zhao, H., Shen, H., Wang, Z., Gao, X., Zhao, W., Yin, M., 2013. Characterization of the APP/PS1 mouse model of Alzheimer's disease in senescence accelerated background. Neurosci. Lett. 557, 84–89.
Longo, V.D., Di Tano, M., Mattson, M.P., Guidi, N., 2021. Intermittent and periodic fasting, longevity and disease. Nature Aging 1, 47–59.
López-Otín, C., Blasco, M.A., Partridge, L., Serrano, M., Kroemer, G., 2023. Hallmarks of aging: An expanding universe. Cell 186, 243–278.
Luchena, C., Zuazo-Ibarra, J., Valero, J., Matute, C., Alberdi, E., Capetillo-Zarate, E., 2022. A Neuron, Microglia, and Astrocyte Triple Co-culture Model to Study Alzheimer's Disease. Frontiers in Aging Neuroscience 14.
Magini, A., Polchi, A., Tozzi, A., Tancini, B., Tantucci, M., Urbanelli, L., Borsello, T., Calabresi, P., Emiliani, C., 2015. Abnormal cortical lysosomal β-hexosaminidase and

β-galactosidase activity at post-synaptic sites during Alzheimer's disease progression. Int. J. Biochem. Cell Biol. 58, 62–70.
Malerba, H.N., Pereira, A.A.R., Pierrobon, M.F., Abrao, G.S., Toricelli, M., Akamine, E.H., Buck, H.S., Viel, T.A., 2021. Combined neuroprotective strategies blocked neurodegeneration and improved brain function in senescence-accelerated mice. Front. Aging Neurosci. 13, 681498.
Mann, A., Miksys, S.L., Gaedigk, A., Kish, S.J., Mash, D.C., Tyndale, R.F., 2012. The neuroprotective enzyme CYP2D6 increases in the brain with age and is lower in Parkinson's disease patients. Neurobiol. Aging 33, 2160–2171.
Massip, L., Garand, C., Turaga, R.V.N., Deschênes, F., Thorin, E., Lebel, M., 2006. Increased insulin, triglycerides, reactive oxygen species, and cardiac fibrosis in mice with a mutation in the helicase domain of the Werner syndrome gene homologue. Exp. Gerontol. 41, 157–168.
Mayne, K., White, J.A., McMurran, C.E., Rivera, F.J., de la Fuente, A.G., 2020. Aging and Neurodegenerative Disease: Is the Adaptive Immune System a Friend or Foe? Frontiers in Aging Neuroscience 12.
Miksys, S., Tyndale, R.F., 2013. Cytochrome P450-mediated drug metabolism in the brain. J. Psychiatry Neurosci. 38, 152–163.
Miller, J.D., Ganat, Y.M., Kishinevsky, S., Bowman, R.L., Liu, B., Tu, E.Y., Mandal, P.K., Vera, E., Shim, J.W., Kriks, S., Taldone, T., Fusaki, N., Tomishima, M.J., Krainc, D., Milner, T.A., Rossi, D.J., Studer, L., 2013. Human iPSC-based modeling of late-onset disease via progerin-induced aging. Cell Stem Cell 13, 691–705.
Miyamoto, M., 1997. Characteristics of age-related behavioral changes in senescence-accelerated mouse SAMP8 and SAMP10. Exp. Gerontol. 32, 139–148.
Miyamoto, M., Kiyota, Y., Nishiyama, M., Nagaoka, A., 1992. Senescence-accelerated mouse (SAM): age-related reduced anxiety-like behavior in the SAM-P/8 strain. Physiol. Behav. 51, 979–985.
Molina-Martínez, P., Corpas, R., García-Lara, E., Cosín-Tomás, M., Cristòfol, R., Kaliman, P., Solà, C., Molinuevo, J.L., Sánchez-Valle, R., Antonell, A., Lladó, A., Sanfeliu, C., 2020. Microglial hyperreactivity evolved to immunosuppression in the hippocampus of a mouse model of accelerated aging and Alzheimer's disease traits. Front. Aging Neurosci. 12, 622360.
Moreira, H.S., Costa, A.S., Machado, Á., Castro, S.L., Lima, C.F., Vicente, S.G., 2019. Distinguishing mild cognitive impairment from healthy aging and Alzheimer's Disease: The contribution of the INECO Frontal Screening (IFS). PLoS One 14, e0221873.
Morita, M., Gravel, S.-P., Chénard, V., Sikström, K., Zheng, L., Alain, T., Gandin, V., Avizonis, D., Arguello, M., Zakaria, C., McLaughlan, S., Nouet, Y., Pause, A., Pollak, M., Gottlieb, E., Larsson, O., St-Pierre, J., Topisirovic, I., Sonenberg, N., 2013. mTORC1 controls mitochondrial activity and biogenesis through 4E-BP-dependent translational regulation. Cell Metab. 18, 698–711.
Mostoslavsky, R., Chua, K.F., Lombard, D.B., Pang, W.W., Fischer, M.R., Gellon, L., Liu, P., Mostoslavsky, G., Franco, S., Murphy, M.M., Mills, K.D., Patel, P., Hsu, J.T., Hong, A.L., Ford, E., Cheng, H.-L., Kennedy, C., Nunez, N., Bronson, R., Frendewey, D., Auerbach, W., Valenzuela, D., Karow, M., Hottiger, M.O., Hursting, S., Barrett, J.C., Guarente, L., Mulligan, R., Demple, B., Yancopoulos, G.D., Alt, F.W., 2006. Genomic instability and aging-like phenotype in the absence of mammalian SIRT6. Cell 124, 315–329.
Muñoz-Manchado, A.B., Villadiego, J., Romo-Madero, S., Suárez-Luna, N., Bermejo-Navas, A., Rodríguez-Gómez, J.A., Garrido-Gil, P., Labandeira-García, J.L., Echevarría, M., López-Barneo, J., Toledo-Aral, J.J., 2016. Chronic and progressive Parkinson's disease MPTP model in adult and aged mice. J. Neurochem. 136, 373–387.
Mutemberezi, V., Buisseret, B., Masquelier, J., Guillemot-Legris, O., Alhouayek, M., Muccioli, G.G., 2018. Oxysterol levels and metabolism in the course of neuroinflammation: insights from in vitro and in vivo models. J. Neuroinflammation 15, 74.
Nelson, G., Kucheryavenko, O., Wordsworth, J., von Zglinicki, T., 2018. The senescent bystander effect is caused by ROS-activated NF-κB signalling. Mech. Ageing Dev. 170, 30–36.
Ocampo, A., Reddy, P., Martinez-Redondo, P., Platero-Luengo, A., Hatanaka, F., Hishida, T., Li, M., Lam, D., Kurita, M., Beyret, E., Araoka, T., Vazquez-Ferrer, E., Donoso, D., Roman, J.L., Xu, J., Rodriguez Esteban, C., Nuñez, G., Nuñez Delicado, E., Campistol, J.M., Guillen, I., Guillen, P., Izpisua Belmonte, J.C., 2016. In vivo amelioration of age-associated hallmarks by partial reprogramming. Cell 167, 1719–1733.e1712.
Olivieri, F., Prattichizzo, F., Grillari, J., Balistreri, C.R., 2018. Cellular senescence and inflammaging in age-related diseases. Mediators Inflamm. 2018, 9076485.
Onodera, T., Watanabe, R., Tha, K.K., Hayashi, Y., Murayama, T., Okuma, Y., Ono, C., Oketani, Y., Hosokawa, M., Nomura, Y., 2000. Depressive behavior and alterations in receptors for dopamine and 5-hydroxytryptamine in the brain of the senescence accelerated mouse (SAM)-P10. Jpn. J. Pharmacol. 83, 312–318.
Osorio, F.G., Navarro, C.L., Cadiñanos, J., López-Mejía, I.C., Quirós, P.M., Bartoli, C., Rivera, J., Tazi, J., Guzmán, G., Varela, I., Depetris, D., de Carlos, F., Cobo, J., Andrés, V., De Sandre-Giovannoli, A., Freije, J.M.P., Lévy, N., López-Otín, C., 2011. Splicing-directed therapy in a new mouse model of human accelerated aging. Sci. Transl. Med. 3, 106ra107-106ra107.
Pandey, S., Jirásko, M., Lochman, J., Chvátal, A., Chottova Dvorakova, M., Kučera, R., 2022. iPSCs in neurodegenerative disorders: a unique platform for clinical research and personalized medicine. J Pers Med 12.
Percie du Sert, N., Hurst, V., Ahluwalia, A., Alam, S., Avey, M.T., Baker, M., Browne, W. J., Clark, A., Cuthill, I.C., Dirnagl, U., Emerson, M., Garner, P., Holgate, S.T., Howells, D.W., Karp, N.A., Lazic, S.E., Lidster, K., MacCallum, C.J., Macleod, M., Pearl, E.J., Petersen, O.H., Rawle, F., Reynolds, P., Rooney, K., Sena, E.S., Silberberg, S.D., Steckler, T., Würbel, H., 2020. The ARRIVE guidelines 2.0: Updated guidelines for reporting animal research. PLoS Biol. 18, e3000410.
Phipps, S.M.O., Berletch, J.B., Andrews, L.G., Tollefsbol, T.O., 2007. Aging cell culture: methods and observations. Methods Mol. Biol. 371, 9–19.
Pinelli, C.J., Leri, F., Turner, P.V., 2017. Long term physiologic and behavioural effects of housing density and environmental resource provision for adult male and female sprague dawley rats. Animals (Basel) 7.
Ponnappan, U., Zhong, M., Trebilcock, G.U., 1999. Decreased proteasome-mediated degradation in T cells from the elderly: A role in immune senescence. Cell. Immunol. 192, 167–174.
Prigione, A., Hossini, A.M., Lichtner, B., Serin, A., Fauler, B., Megges, M., Lurz, R., Lehrach, H., Makrantonaki, E., Zouboulis, C.C., Adjaye, J., 2011. Mitochondrial-associated cell death mechanisms are reset to an embryonic-like state in aged donor-derived iPS cells harboring chromosomal aberrations. PLoS One 6, e27352.
Qadan, M.A., Piuzzi, N.S., Boehm, C., Bova, W., Moos Jr., M., Midura, R.J., Hascall, V.C., Malcuit, C., Muschler, G.F., 2018. Variation in primary and culture-expanded cells derived from connective tissue progenitors in human bone marrow space, bone trabecular surface and adipose tissue. Cytotherapy 20, 343–360.
Querfurth, H., Lee, H.-K., 2021. Mammalian/mechanistic target of rapamycin (mTOR) complexes in neurodegeneration. Mol. Neurodegener. 16, 44.
Quinn, R., 2005. Comparing rat's to human's age: how old is my rat in people years? Nutrition 21, 775–777.
Raja, W.K., Mungenast, A.E., Lin, Y.T., Ko, T., Abdurrob, F., Seo, J., Tsai, L.H., 2016. Self-organizing 3D human neural tissue derived from induced pluripotent stem cells recapitulate Alzheimer's disease phenotypes. PLoS One 11, e0161969.
Richwine, A.F., Sparkman, N.L., Dilger, R.N., Buchanan, J.B., Johnson, R.W., 2009. Cognitive deficits in interleukin-10-deficient mice after peripheral injection of lipopolysaccharide. Brain Behav. Immun. 23, 794–802.
Roncal-Jimenez, C.A., Ishimoto, T., Lanaspa, M.A., Milagres, T., Hernando, A.A., Jensen, T., Miyazaki, M., Doke, T., Hayasaki, T., Nakagawa, T., Marumaya, S., Long, D.A., Garcia, G.E., Kuwabara, M., Sánchez-Lozada, L.G., Kang, D.H., Johnson, R.J., 2016. Aging-associated renal disease in mice is fructokinase dependent. Am. J. Physiol. Renal Physiol. 311, F722–F730.
Ross, A., Xing, V., Wang, T.T., Bureau, S.C., Link, G.A., Fortin, T., Zhang, H., Hayley, S., Sun, H., 2020. Alleviating toxic α-Synuclein accumulation by membrane depolarization: evidence from an in vitro model of Parkinson's disease. Mol. Brain 13, 108.
Sánchez-Danés, A., Richaud-Patin, Y., Carballo-Carbajal, I., Jiménez-Delgado, S., Caig, C., Mora, S., Di Guglielmo, C., Ezquerra, M., Patel, B., Giralt, A., Canals, J.M., Memo, M., Alberch, J., López-Barneo, J., Vila, M., Cuervo, A.M., Tolosa, E., Consiglio, A., Raya, A., 2012. Disease-specific phenotypes in dopamine neurons from human iPS-based models of genetic and sporadic Parkinson's disease. EMBO Mol. Med. 4, 380–395.
Sandusky, G.E., Van Pelt, C.S., Todd, G.C., Wightman, K., 1988. An immunocytochemical study of pituitary adenomas and focal hyperplasia in old Sprague-Dawley and Fischer 344 rats. Toxicol. Pathol. 16, 376–380.
Sapieha, P., Mallette, F.A., 2018. Cellular senescence in postmitotic cells: beyond growth arrest. Trends Cell Biol. 28, 595–607.
Scheffold, A., Holtman, I.R., Dieni, S., Brouwer, N., Katz, S.-F., Jebaraj, B.M.C., Kahle, P. J., Hengerer, B., Lechel, A., Stilgenbauer, S., Boddeke, E.W.G.M., Eggen, B.J.L., Rudolph, K.-L., Biber, K., 2016. Telomere shortening leads to an acceleration of synucleinopathy and impaired microglia response in a genetic mouse model. Acta Neuropathol. Commun. 4, 87.
Schneider, E.L., Mitsui, Y., 1976. The relationship between in vitro cellular aging and in vivo human age. PNAS 73, 3584–3588.
Schwab, N., Taskina, D., Leung, E., Innes, B.T., Bader, G.D., Hazrati, L.-N., 2022. Neurons and glial cells acquire a senescent signature after repeated mild traumatic brain injury in a sex-dependent manner. Frontiers in Neuroscience 16.
Serrano, M., Lin, A.W., McCurrach, M.E., Beach, D., Lowe, S.W., 1997. Oncogenic ras provokes premature cell senescence associated with accumulation of p53 and p16INK4a. Cell 88, 593–602.
Sharma, K., Darvas, M., Keene, C.D., Niedernhofer, L.J., Ladiges, W., 2018. Modeling Alzheimer's disease in progeria mice. An age-related concept. Pathobiol Aging Age Relat Dis 8, 1524815.
Shavali, S., Combs, C.K., Ebadi, M., 2006. Reactive macrophages increase oxidative stress and alpha-synuclein nitration during death of dopaminergic neuronal cells in co-culture: relevance to Parkinson's disease. Neurochem. Res. 31, 85–94.
Sherer, T.B., Betarbet, R., Testa, C.M., Seo, B.B., Richardson, J.R., Kim, J.H., Miller, G.W., Yagi, T., Matsuno-Yagi, A., Greenamyre, J.T., 2003. Mechanism of toxicity in rotenone models of Parkinson's disease. J. Neurosci. 23, 10756–10764.
Shih, P.H., Chan, Y.C., Liao, J.W., Wang, M.F., Yen, G.C., 2010. Antioxidant and cognitive promotion effects of anthocyanin-rich mulberry (Morus atropurpurea L.) on senescence-accelerated mice and prevention of Alzheimer's disease. J. Nutr. Biochem. 21, 598–605.
Shimada, A., Hasegawa-Ishii, S., 2011. Senescence-accelerated Mice (SAMs) as a Model for Brain Aging and Immunosenescence. Aging Dis. 2, 414–435.
Shimada, A., Hosokawa, M., Ohta, A., Akiguchi, I., Takeda, T., 1994. Localization of atrophy-prone areas in the aging mouse brain: Comparison between the brain atrophy model SAM-P/10 and the normal control SAM-R/1. Neuroscience 59, 859–869.
Shimada, A., Keino, H., Satoh, M., Kishikawa, M., Seriu, N., Hosokawa, M., 2002. Age-related progressive neuronal DNA damage associated with cerebral degeneration in a mouse model of accelerated senescence. J. Gerontol.: Series A 57, B415–B421.
Shimada, A., Tsuzuki, M., Keino, H., Satoh, M., Chiba, Y., Saitoh, Y., Hosokawa, M., 2006. Apical vulnerability to dendritic retraction in prefrontal neurones of ageing SAMP10 mouse: a model of cerebral degeneration. Neuropathol. Appl. Neurobiol. 32, 1–14.

Shimada, A., Keino, H., Kawamura, N., Chiba, Y., Hosokawa, M., 2008. Limbic structures are prone to age-related impairments in proteasome activity and neuronal ubiquitinated inclusions in SAMP10 mouse: a model of cerebral degeneration. Neuropathol. Appl. Neurobiol. 34, 33–51.
Shirasuna, K., Iwata, H., 2017. Effect of aging on the female reproductive function. Contracept Reprod Med 2, 23.
Shou, Y., Liang, F., Xu, S., Li, X., 2020. The application of brain organoids: from neuronal development to neurological diseases. Front. Cell Dev. Biol. 8.
Simon, M.M., Greenaway, S., White, J.K., Fuchs, H., Gailus-Durner, V., Wells, S., Sorg, T., Wong, K., Bedu, E., Cartwright, E.J., Dacquin, R., Djebali, S., Estabel, J., Graw, J., Ingham, N.J., Jackson, I.J., Lengeling, A., Mandillo, S., Marvel, J., Meziane, H., Preitner, F., Puk, O., Roux, M., Adams, D.J., Atkins, S., Ayadi, A., Becker, L., Blake, A., Brooker, D., Cater, H., Champy, M.-F., Combe, R., Danecek, P., di Fenza, A., Gates, H., Gerdin, A.-K., Golini, E., Hancock, J.M., Hans, W., Hölter, S.M., Hough, T., Jurdic, P., Keane, T.M., Morgan, H., Müller, W., Neff, F., Nicholson, G., Pasche, B., Roberson, L.-A., Rozman, J., Sanderson, M., Santos, L., Selloum, M., Shannon, C., Southwell, A., Tocchini-Valentini, G.P., Vancollie, V.E., Westerberg, H., Wurst, W., Zi, M., Yalcin, B., Ramirez-Solis, R., Steel, K.P., Mallon, A.-M., de Angelis, M.H., Herault, Y., Brown, S.D.M., 2013. A comparative phenotypic and genomic analysis of C57BL/6J and C57BL/6N mouse strains. Genome Biol. 14, R82.
Smith, J.R., Venable, S., Roberts, T.W., Metter, E.J., Monticone, R., Schneider, E.L., 2002. Relationship between in vivo age and in vitro aging: assessment of 669 cell cultures derived from members of the Baltimore longitudinal study of aging. J. Gerontol.: Series A 57, B239–B246.
Soerens, A.G., Künzli, M., Quarnstrom, C.F., Scott, M.C., Swanson, L., Locquiao, J.J., Ghoneim, H.E., Zehn, D., Youngblood, B., Vezys, V., Masopust, D., 2023. Functional T cells are capable of supernumerary cell division and longevity. Nature 614, 762–766.
Strait, J.B., Lakatta, E.G., 2012. Aging-associated cardiovascular changes and their relationship to heart failure. Heart Fail. Clin. 8, 143–164.
Suhr, S.T., Chang, E.A., Rodriguez, R.M., Wang, K., Ross, P.J., Beyhan, Z., Murthy, S., Cibelli, J.B., 2009. Telomere dynamics in human cells reprogrammed to pluripotency. PLoS One 4, e8124.
Sun, M., McDonald, S.J., Brady, R.D., Collins-Praino, L., Yamakawa, G.R., Monif, M., O'Brien, T.J., Cloud, G.C., Sobey, C.G., Mychasiuk, R., Loane, D.J., Shultz, S.R., 2020. The need to incorporate aged animals into the preclinical modeling of neurological conditions. Neurosci. Biobehav. Rev. 109, 114–128.
Sun, L., Wu, J., Du, F., Chen, X., Chen, Z.J., 2013. Cyclic GMP-AMP synthase is a cytosolic DNA sensor that activates the type I interferon pathway. Science 339, 786–791.
Takahashi, H., Sakamoto, J., Ohta, H., Miyamoto, M., 2004. Age-related decrease in spontaneity observed in senescence-accelerated mice (SAMP10) and the involvement of the dopaminergic system in behavioral disorders. Int. Congr. Ser. 1260, 309–314.
Takahashi, K., Yamanaka, S., 2006. Induction of pluripotent stem cells from mouse embryonic and adult fibroblast cultures by defined factors. Cell 126, 663–676.
Takeda, T., 2009. Senescence-Accelerated Mouse (SAM) with Special References to Neurodegeneration Models, SAMP8 and SAMP10 Mice. Neurochem. Res. 34, 639–659.
Takeda, T., Hosokawa, M., Takeshita, S., Irino, M., Higuchi, K., Matsushita, T., Tomita, Y., Yasuhira, K., Hamamoto, H., Shimizu, K., Ishii, M., Yamamuro, T., 1981. A new murine model of accelerated senescence. Mech. Ageing Dev. 17, 183–194.
Takemura, M., Nakamura, S., Akiguchi, I., Ueno, M., Oka, N., Ishikawa, S., Shimada, A., Kimura, J., Takeda, T., 1993. Beta/A4 proteinlike immunoreactive granular structures in the brain of senescence-accelerated mouse. Am. J. Pathol. 142, 1887–1897.
Tang, Y., Liu, M.L., Zang, T., Zhang, C.L., 2017. Direct reprogramming rather than iPSC-based reprogramming maintains aging hallmarks in human motor neurons. Front. Mol. Neurosci. 10, 359.
Timmons, J., Brenner, C., 2023. Matters Arising: The Information Theory of Aging Has Not Been Tested.
Toricelli, M., Evangelista, S.R., Buck, H.S., Viel, T.A., 2021. Microdose lithium treatment reduced inflammatory factors and neurodegeneration in organotypic hippocampal culture of old SAMP-8 mice. Cell. Mol. Neurobiol. 41, 1509–1520.
Toth, L.A., 2018. Identifying and Implementing Endpoints for Geriatric Mice. Comp. Med. 68, 439–451.
Toth, L., Czigler, A., Hegedus, E., Komaromy, H., Amrein, K., Czeiter, E., Yabluchanskiy, A., Koller, A., Orsi, G., Perlaki, G., Schwarcz, A., Buki, A., Ungvari, Z., Toth, P.J., 2022. Age-related decline in circulating IGF-1 associates with impaired neurovascular coupling responses in older adults. GeroScience 44, 2771–2783.
Toye, A.A., Lippiat, J.D., Proks, P., Shimomura, K., Bentley, L., Hugill, A., Mijat, V., Goldsworthy, M., Moir, L., Haynes, A., Quarterman, J., Freeman, H.C., Ashcroft, F. M., Cox, R.D., 2005. A genetic and physiological study of impaired glucose homeostasis control in C57BL/6J mice. Diabetologia 48, 675–686.
Ungerstedt, U., 1968. 6-Hydroxy-dopamine induced degeneration of central monoamine neurons. Eur. J. Pharmacol. 5, 107–110.
van Dijk, K.D., Persichetti, E., Chiasserini, D., Eusebi, P., Beccari, T., Calabresi, P., Berendse, H.W., Parnetti, L., van de Berg, W.D., 2013. Changes in endolysosomal enzyme activities in cerebrospinal fluid of patients with Parkinson's disease. Mov. Disord. 28, 747–754.
Vaupel, J.W., 2010. Biodemography of human ageing. Nature 464, 536–542.
Vela, S., Sainz, N., Moreno-Aliaga, M.J., Solas, M., Ramirez, M.J., 2019. DHA selectively protects SAMP-8-associated cognitive deficits through inhibition of JNK. Mol. Neurobiol. 56, 1618–1627.
Victorelli, S., Salmonowicz, H., Chapman, J., Martini, H., Vizioli, M.G., Riley, J.S., Cloix, C., Hall-Younger, E., Machado Espindola-Netto, J., Jurk, D., Lagnado, A.B., Sales Gomez, L., Farr, J.N., Saul, D., Reed, R., Kelly, G., Eppard, M., Greaves, L.C., Dou, Z., Pirius, N., Szczepanowska, K., Porritt, R.A., Huang, H., Huang, T.Y., Mann, D.A., Masuda, C.A., Khosla, S., Dai, H., Kaufmann, S.H., Zacharioudakis, E., Gavathiotis, E., LeBrasseur, N.K., Lei, X., Sainz, A.G., Korolchuk, V.I., Adams, P.D., Shadel, G.S., Tait, S.W.G., Passos, J.F., 2023. Apoptotic stress causes mtDNA release during senescence and drives the SASP. Nature 622, 627–636.
Vierbuchen, T., Ostermeier, A., Pang, Z.P., Kokubu, Y., Südhof, T.C., Wernig, M., 2010. Direct conversion of fibroblasts to functional neurons by defined factors. Nature 463, 1035–1041.
Voulgaris, D., Nikolakopoulou, P., Herland, A., 2022. Generation of Human iPSC-Derived Astrocytes with a mature star-shaped phenotype for CNS modeling. Stem Cell Rev. Rep. 18, 2494–2512.
Walston, J., Fedarko, N., Yang, H., Leng, S., Beamer, B., Espinoza, S., Lipton, A., Zheng, H., Becker, K., 2008. The physical and biological characterization of a frail mouse model. J. Gerontol. A Biol. Sci. Med. Sci. 63, 391–398.
Wang, Y., Dong, C., Han, Y., Gu, Z., Sun, C., 2022. Immunosenescence, aging and successful aging. Front. Immunol. 13, 942796.
Wang, X., Wang, Y., Yu, S., Ren, L., 2018. Effect of electroacupuncture on levels of β-amyloid and neprilysin proteins in the cerebral cortex of Alzheimer's disease mice based on "mutual assistance of kidney and brain" theory. Zhen Ci Yan Jiu 43, 20–24.
Weston, L.L., Jiang, S., Chisholm, D., Jantzie, L.L., Bhaskar, K., 2021. Interleukin-10 deficiency exacerbates inflammation-induced tau pathology. J. Neuroinflammation 18, 161.
Wong, W., 2020. Economic burden of Alzheimer disease and managed care considerations. Am. J. Manag. Care 26, S177–S183.
Wu, K.-C., Lin, C.-J., 2019. The regulation of drug-metabolizing enzymes and membrane transporters by inflammation: Evidences in inflammatory diseases and age-related disorders. J. Food Drug Anal. 27, 48–59.
Xia, S., Zhang, X., Zheng, S., Khanabdali, R., Kalionis, B., Wu, J., Wan, W., Tai, X., 2016. An update on inflamm-aging: mechanisms, prevention, and treatment. J. Immunol. Res. 2016, 8426874.
Xicoy, H., Wieringa, B., Martens, G.J.M., 2017. The SH-SY5Y cell line in Parkinson's disease research: a systematic review. Mol. Neurodegener. 12, 10.
Yager, J.Y., Thornhill, J.A., 1997. The effect of age on susceptibility to hypoxic-ischemic brain damage. Neurosci. Biobehav. Rev. 21, 167–174.
Yang, W., Hamilton, J.L., Kopil, C., Beck, J.C., Tanner, C.M., Albin, R.L., Ray Dorsey, E., Dahodwala, N., Cintina, I., Hogan, P., Thompson, T., 2020a. Current and projected future economic burden of Parkinson's disease in the U.S. npj. Parkinson's Disease 6, 15.
Yang, J.-H., Hayano, M., Griffin, P.T., Amorim, J.A., Bonkowski, M.S., Apostolides, J.K., Salfati, E.L., Blanchette, M., Munding, E.M., Bhakta, M., Chew, Y.C., Guo, W., Yang, X., Maybury-Lewis, S., Tian, X., Ross, J.M., Coppotelli, G., Meer, M.V., Rogers-Hammond, R., Vera, D.L., Lu, Y.R., Pippin, J.W., Creswell, M.L., Dou, Z., Xu, C., Mitchell, S.J., Das, A., O'Connell, B.L., Thakur, S., Kane, A.E., Su, Q., Mohri, Y., Nishimura, E.K., Schaevitz, L., Garg, N., Balta, A.-M., Rego, M.A., Gregory-Ksander, M., Jakobs, T.C., Zhong, L., Wakimoto, H., El Andari, J., Grimm, D., Mostoslavsky, R., Wagers, A.J., Tsubota, K., Bonasera, S.J., Palmeira, C.M., Seidman, J.G., Seidman, C.E., Wolf, N.S., Kreiling, J.A., Sedivy, J.M., Murphy, G.F., Green, R.E., Garcia, B.A., Berger, S.L., Oberdoerffer, P., Shankland, S.J., Gladyshev, V.N., Ksander, B.R., Pfenning, A.R., Rajman, L.A., Sinclair, D.A., 2023. Loss of epigenetic information as a cause of mammalian aging. Cell 186, 305–326. e327.
Yang, Y., He, Z., Xing, Z., Zuo, Z., Yuan, L., Wu, Y., Jiang, M., Qi, F., Yao, Z., 2020b. Influenza vaccination in early Alzheimer's disease rescues amyloidosis and ameliorates cognitive deficits in APP/PS1 mice by inhibiting regulatory T cells. J. Neuroinflammation 17, 65.
Yang, N.-C., Hu, M.-L., 2005. The limitations and validities of senescence associated-β-galactosidase activity as an aging marker for human foreskin fibroblast Hs68 cells. Exp. Gerontol. 40, 813–819.
Yang, C., Pang, Y., Huang, Y., Ye, F., Chen, X., Gao, Y., Zhang, C., Yao, L., Gao, J., 2022. Single-cell transcriptomics identifies premature aging features of TERC-deficient mouse brain and bone marrow. Geroscience 44, 2139–2155.
Yang, M., Wen, T., Chen, H., Deng, J., Yang, C., Zhang, Z., 2018. Knockdown of insulin-like growth factor 1 exerts a protective effect on hypoxic injury of aged BM-MSCs: role of autophagy. Stem Cell Res Ther 9, 284.
Yegorov, Y.E., Poznyak, A.V., Nikiforov, N.G., Sobenin, I.A., Orekhov, A.N., 2020. The link between chronic stress and accelerated aging. Biomedicines 8.
Yiannopoulou, K.G., Papageorgiou, S.G., 2020. Current and future treatments in alzheimer disease: an update. J Cent Nerv Syst Dis 12, 1179573520907397–1179573520907397.
Zhang, Y.F., Yu, J.C., Zhang, X.Z., Han, J.X., 2013. Effect of acupuncture intervention on hippocampal neuron loss and astrocytosis in SAMP 8 mice. Zhen Ci Yan Jiu 38, 358–364.
Zidong Donna, F., Iván, L.C., Curtis, D.K., 2012. Effects of aging on mRNA profiles for drug-metabolizing enzymes and transporters in livers of male and female mice. Drug Metab. Dispos. 40, 1216.